

**CONTRIBUTIONS TO THE DEVELOPMENT OF ANTICANCER
METALLOTHERAPEUTICS – FROM METAL COMPOUNDS TO NANOMATERIALS**

Habilitationsschrift

zur Erlangung des akademischen Grades

Dr. rer. nat. habil.

vorgelegt der

Naturwissenschaftlichen Fakultät II – Chemie, Physik und Mathematik

der Martin-Luther-Universität Halle-Wittenberg

von

Dr. rer. nat. Goran N. Kaluđerović

geboren am 08. November 1975 in Cetinje, Montenegro

Gutachter:

1. Prof. Dr. Dirk Steinborn
2. Prof. Dr. Bernhard Lippert
3. Prof. Dr. Ferdinando Nicoletti

Halle (Saale), verteidigt am 22.05.2014

CONTENTS

ABBREVIATIONS	1
1. INTRODUCTION – METAL COMPLEXES IN CANCER TREATMENT	3
1.1. HISTORY – FROM CISPLATIN TO THE 3 RD GENERATION DRUGS AS ANTICANCER AGENTS.....	3
1.2. COMMENCING OF NONPLATINUM METAL COMPLEXES AS ANTITUMORAL AGENTS	6
1.3. NANODRUG DELIVERY SYSTEM FOR METAL COMPLEXES.....	7
1.4. GOALS OF THE WORK	9
2. METALLOCOMPOUNDS.....	10
2.1. SYNTHESIS AND CHARACTERIZATION	10
2.1.1. Platinum complexes containing R ₂ edda-type ligands	10
2.1.2. Palladium complexes containing R ₂ edda-type ligands	12
2.1.3. Titanocene and <i>ansa</i> -titanocene complexes	13
2.1.4. Organotin(IV) compounds	14
2.2. BIOLOGICAL ACTIVITY OF METALLOCOMPOUNDS.....	16
2.2.1. R ₂ edda-type platinum(II/IV) and palladium(II) complexes	16
2.2.1.1. Structure–activity relationships of R ₂ edda-type ligand precursors, corresponding platinum(II/IV) and palladium(II) complexes	17
2.2.1.2. Platinum(IV) complexes: drugs or prodrugs?	18
2.2.1.3. The cell type-specific mode of cell death induced with [Pt(R ₂ edda-type)Cl ₄] complexes	19
2.2.1.4. Mode of action of Pt1 and Pt26 on B16 melanoma cell line	23
2.2.1.5. Pt1 versus cisplatin: Enhancement of cytotoxicity and decreasement in side effects <i>in vivo</i>	24
2.2.2. Improvement of the antitumor efficacy of titanocene dichloride by variation of structure	25
2.2.2.1. Modification of Cp ligand	25
2.2.2.2. Substitution of chlorido with carboxylato or thiolato ligands	27
2.2.3. Organotin(IV) compounds	28
2.2.3.1. Organotin(IV) compounds against cisplatin: cytotoxicity and toxicity	28
2.2.3.2. Organotin(IV) compounds and mode of action on the tumor cells	30
2.3. CONCLUSIONS	31

3. NANOMATERIALS AS DRUG CARRIERS	35
3.1. PREPARATION OF NANOMATERIALS	35
3.1.1. Liposomal formulation of THP-C11	35
3.1.2. Mesoporous silica grafted with titanocene derivatives and organotin(IV) compounds	36
3.2. BIOLOGICAL ACTIVITY OF NOVEL MATERIALS CONTAINING METAL COMPOUNDS	36
3.2.1. Liposomes as drug carriers for water-insoluble platinum based drugs	37
3.2.1.1. Liposomal cytotoxicity	37
3.2.1.2. Liposomal toxicity	38
3.2.2. First steps in nanostructured mesoporous materials as anticancer drug carrier vehicles	38
3.2.2.1. Nanostructured mesoporous materials grafted with titanocene derivatives	39
3.2.2.2. Material and content-dependence on the final cytotoxicity of nanostructured mesoporous materials	40
3.2.2.3. Proposed mechanism of action of nanostructured mesoporous materials grafted with titanium(IV) complexes	41
3.2.2.4. Nanostructured mesoporous materials grafted with organotin(IV) compounds	42
3.2.2.5. Cytotoxicity of nanostructured mesoporous materials grafted with 3-(triphenylstannyl)propan-1-ol	43
3.2.2.6. Mechanism of action of SBA-15p grafted with 3-(triphenylstannyl)propan-1-ol	44
3.2.2.7. Cytotoxicity of nanostructured mesoporous materials SBA-15p grafted with 6-(triphenylstannyl)hexan-1-ol	45
3.2.2.8. The first <i>in vivo</i> study of nanomaterials grafted with 6-(triphenylstannyl)hexan-1-ol	46
3.2.2.9. Mechanisms of antimelanoma action of SBA-15 grafted with 6-(triphenylstannyl)hexan-1-ol	47
3.3. CONCLUSIONS	50
4. SUMMARY	53
5. REFERENCES	58
6. CONTRIBUTING REFERENCES RELATED TO HABILITATION THESIS	65
SUPPLEMENT	70

The cumulative form of the Habilitation Thesis is selected for the presentation of the results. Herein, in short, the essential results are presented. The appropriate personal papers related to the work contain the experimental data as well as a detailed discussion of the results. Those papers are cited within the work and selected publications are included in appendices.

ABBREVIATIONS

en'	ethylenediamine type ligands
PEG	polyethylene glycol
MCM-41	mesoporous molecular sieve MCM (No. 41)
SBA-15	mesoporous molecular sieve SBA (No. 15)
SBA-15p	SBA-15 modified with 3-chloropropyltriethoxysilane
H ₂ edda	ethylenediamine- <i>N,N'</i> -diacetic acid
H ₂ eddp	ethylenediamine- <i>N,N'</i> -di-3-propionic acid
(<i>S,S</i>)-H ₂ eddip	(<i>S,S</i>)-ethylenediamine- <i>N,N'</i> -di-2-propionic acid
(<i>S,S</i>)-H ₂ eddl	(<i>S,S</i>)-ethylenediamine- <i>N,N'</i> -di-2-(4-methyl)-pentanoic acid
(<i>S,S</i>)-H ₂ eddch	(<i>S,S</i>)-ethylenediamine- <i>N,N'</i> -di-2-(3-cyclohexyl)-propionic acid
R ₂ edda	esters of H ₂ edda
R ₂ edda-type	esters of H ₂ edda, H ₂ eddp, (<i>S,S</i>)-H ₂ eddip, (<i>S,S</i>)-H ₂ eddl, (<i>S,S</i>)-H ₂ eddch
LDH	lactate dehydrogenase
ROS	reactive oxygen species
PHA	phytohemagglutinin
Cell lines	
1411HP, H12.1	testicular germ cell tumors (TGCT)
518A2	human melanoma
8505C, SW1736	human anaplastic thyroid cancer
A253, FaDu	head and neck cancer
A2780	human ovarian cancer
A549	human lung carcinoma
B16	mouse melanoma
DLD-1, HT-29, HCT116	human colon cancer
Fem-x	human malignant melanoma
HeLa	human adenocarcinoma
K562	human myelogenous leukaemia
L929	mouse fibrosarcoma

ABBREVIATIONS

MCF-7	human breast adenocarcinoma
U251	human astrocytoma
Primary cells	
CLL	chronic lymphocytic leukemia
PBMC	normal healthy periferal blood mononuclear cells
fibroblasts, keratinocytes	non-transformed and non-malignant cells

1. INTRODUCTION – METAL COMPLEXES IN CANCER TREATMENT

For more information see references K1, K2 (Appendices 1 and 2)

1.1. History – from cisplatin to the 3rd generation drugs as anticancer agents

Barnett Rosenberg, in one of his investigations on the influence of the electric field on cell division of bacteria (1965), accidentally discovered antiproliferative activity of cisplatin (Figure 1)^[1;2]. He proved that cisplatin completely inhibited the development of the solid sarcoma-180 tumor in mice^[3]. Cisplatin entered in clinical trials in 1971^[4] and in 1978, clinical use was approved from the Food and Drug Administration (FDA)^[5] presenting a major landmark in the history of successful anticancer drugs. Cisplatin is used for a treatment of epithelial malignancies, testicular, ovaria, lung, head and neck, esophagus stomach, colon, bladder, cervix and uterus cancers.

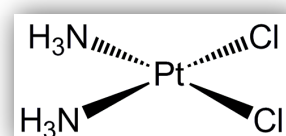


Figure 1. Cisplatin.

How does cisplatin work?

After administration, injection or infusion, blood stream is transporting cisplatin all over the body. Even the excess of chloride ions (~ 100 mM, that compensates ligand exchange reactions) present in blood stream or extracellular matrix few ligand substitutions are occurring. Formed hydrolysis products (Figure 2) in the blood are held responsible for acute toxicities (nephrotoxicity, neurotoxicity). Cisplatin enters the cells by the passive or even active transport binding temporary to one of the membrane components (e.g. phosphatidylserine)^[6;7].

Mechanistic studies on cisplatin firstly focused on DNA and its fragments as target molecules^[8]. It was found that guanosine (G) in comparison to adenine (A) or other bases binds thermodynamically more strongly to platinum^[9]. A much larger portion than statistically expected of platinum binds at GG (about two thirds)^[10]. From all interactions the adducts are mainly pGpG intrastrand cross-links (65%), compared to pApG intrastrand cross-links (22%), interstrand and/or intrastrand cross-links on pGpXpG sequences (13%) and monofunctional adducts (<1%). Beside DNA and water in cellular fluid, cisplatin might react with potential ligands such as phosphate, carbonate, glutathione and peptides (Figure 2)^[9].

1. INTRODUCTION – METAL COMPLEXES IN CANCER TREATMENT

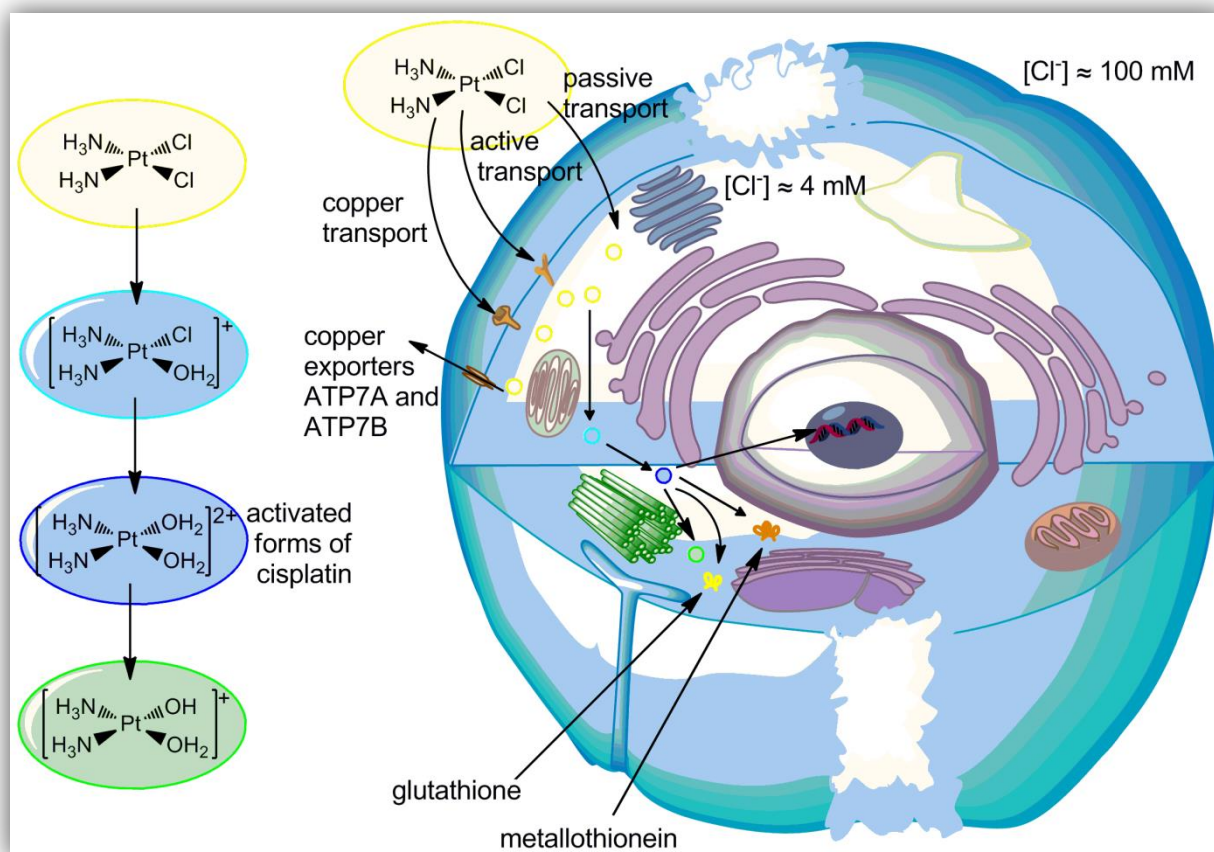


Figure 2. *In vivo* chemistry of cisplatin.

Cisplatin modulates a number of cell-type specific signalling pathways^[6]. As result, cisplatin-triggered changes in cell signalling activity of different transcription factors as well as DNA structure might conduct to cell cycle arrest or induction of caspase-dependent apoptosis through receptor dependent and/or independent pathways.

Second and third generation of anticancer drugs

Even though, one of the most effective and commonly used agents, cisplatin, causes severe side effects and resistance phenomena^[11]. Furthermore, the spectrum of cancers that can be treated with cisplatin is narrow. Effectiveness of cisplatin has been constrained by significantly unfavorable side effects like vomiting, nausea, hearing problems, nephrotoxicity, neurotoxicity, loss of balance and many other^[5;6;12]. Resistance against cisplatin could be developed from reduced platinum uptake, intracellular detoxification by glutathione, increased efflux, increased DNA repair, decreased mismatch repair, modulation of signalling pathways, defective apoptosis, or presence of quiescent non-cycling cells^[13;14]. In order to find suitable platinum complexes that specifically deal with some or even all of the resistance mechanisms a lot of com-

1. INTRODUCTION – METAL COMPLEXES IN CANCER TREATMENT

pounds have been synthesized. Consequently, much attention has been pointed to design new platinum-based complexes^[15–17].

Substitution of chlorido with other anionic ligands rised a second generation of platinum-based antitumor drugs, namely carboplatin and nedaplatin (Figure 3)^[18].

Carboplatin in vivo yields the same active component as cisplatin and forms the same DNA adducts^[17]. Hence, carboplatin is clinically only useful for the treatment of the same cancer types like cisplatin. From the side effects, carboplatin is causing bone marrow suppression, gastrointestinal toxicity, leukopenia, neutropenia and thrombocytopenia as the dose limiting toxicities.

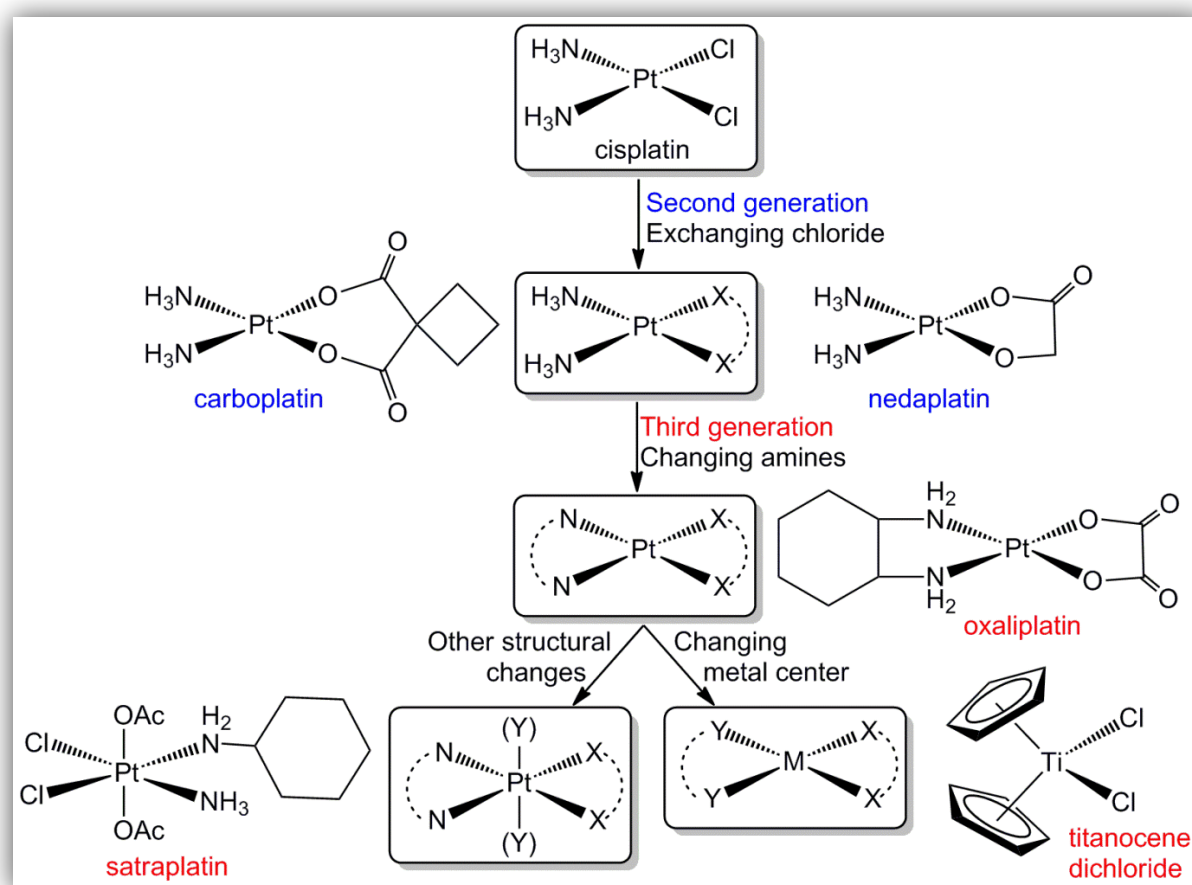


Figure 3. Milestones of the development of platinum and nonplatinum metal-based drugs.

Nedaplatin is used in Japan for the treatment of head and neck, cervical, testicular, ovarian, lung, non-small-cell lung cancer^[19]. Nevertheless, nedaplatin is triggering thrombocytopenia, but lower nephrotoxicity, neurotoxicity, and gastrointestinal toxicity than cisplatin^[20].

1. INTRODUCTION – METAL COMPLEXES IN CANCER TREATMENT

The third generation of platinum-based drugs is related to substitution of NH_3 molecules with different amine ligands (Figure 3)^[21]. From this generation, oxaliplatin appeared as the most promising agent. More kinetically inert compounds, obtained by a variation of oxidation state of platinum from +2 to +4, lead to potential drugs for oral application like satraplatin. Transplatinum complexes have been initially discharged as potential antitumor agents because of inactivity of cisplatin counter pair (transplatin). However, new approaches with aromatic or bulky amines *trans* configured around platinum center showed promising *in vitro* results, thus initiating reinvestigation of this class of compounds^[22]. In general, ideas for new compounds arise from mechanistic findings on previous generations of drugs.

Oxaliplatin is worldwide approved for the clinical treatment of adjuvant and metastatic colorectal cancers when used in combination with 5-fluorouracil and folinic acid^[23]. Still, oxaliplatin is causing side effects such as neurotoxicity, hematological toxicity and gastrointestinal toxicity. Oxalato ligand also greatly reduces the severity of the side effects of the drug compared with cisplatin.

Satraplatin is still a relatively new potential therapeutic in cancer treatment and is supposed to be the first orally administered platinum-based drug against prostate and metastatic breast cancer^[24;25]. It is too early to know all of the possible side effects, but until now vomiting, diarrhoea, nausea, anaemia are known.

BBR3464, *bis[trans-diamminechloridoplatinum(II)][μ -(trans-diamminedi-hexanediamine-*N,N'*)platinum(II)]* nitrate, is a leading agent from the multinuclear platinum(II) drugs^[26]. It is designed for a treatment of cisplatin-resistant tumors because of the high cellular uptake in astrocytoma, glioma, osteosarcoma, melanoma, neuroblastoma and cervical cancer cells (cytotoxicity at concentrations up to 1000-fold lower than cisplatin)^[27;28]. Phase I clinical trials relieved that BBR3464 is inducing severe systemic toxicity, neutropenia and gastro-intestinal toxicity^[29].

1.2. Commencing of nonplatinum metal complexes as antitumoral agents

The application of platinum complexes as anticancer agents has motivated and pointed research to the exploration of other active metal complexes (Figure 3) in cancer chemotherapy^[30]. Main objective in developing nonplatinum anticancer agents is to overcome a restricted range of activity, acquired primary and secondary resistance and severe toxicity. Nonplatinum metal-based compounds might demonstrate anti-

1. INTRODUCTION – METAL COMPLEXES IN CANCER TREATMENT

cancer activity and toxic side-effects distinctly asort from platinum-based onces. They are expected to have different chemical behaviour, hydrolytic rates and mechanism(s) of action^[31]. The most prominent biologically active compounds were found to be those containing ruthenium, gallium, titanium, tin and other metals^[32;33].

Titanium complexes

Titanium-based reagents have a significant potential against solid tumors^[34]. Two families of titanium(IV) complexes are used for biological applications: budotitane [*cis*-diethoxybis(1-phenylbutane-1,3-dionato)titanium(IV)] and titanocene dichloride (Figure 3)^[35–39]. Budotitane was the first nonplatinum complex that entered clinical trials, but was later discharged in Phase I clinical trials^[40]. Titanocene dichloride was abandoned after Phase II clinical trials because its efficacy in patients with metastatic renal cell carcinoma or metastatic breast cancer was too low to be pursued^[41;42].

Tin compounds

In the last few years, organotin compounds are considered as compounds with an promising position as anticancer metallotherapeutics^[43]. It has been established that organotin(IV) compounds are very important in cancer chemotherapy because of their apoptosis inducing character^[44–46]. Firstly, organotin compounds have been analyzed against murine leukaemia cell lines and also against different panels of human cancer cell lines. Beside high cytotoxicity, organotin(IV) complexes might also possess attractive properties such as increased water solubility, better body clearance, fewer side effects and lower general toxicity than platinum drugs^[43]. Significantly, unlike to cisplatin and its analogs, organotin complexes do not develop tumor drug tolerance^[47].

1.3. Nanodrug delivery system for metal complexes

Cancer treatment involving traditional therapeutic chemotherapy is characteristically accompanied by toxic side effects limiting the quantity of the drug that can be administered to a patient^[48]. Moreover, not all of the drug can reach the tumor tissues. The ability to deliver high-efficiency therapeutic compounds precisely to diseased sites is crucial for effective treating all human illnesses. Among many possible applications of nanotechnology in medicine^[49–56], drug delivery systems within the nanometer size regime can be developed to alter both pharmacological and therapeutic effects of

1. INTRODUCTION – METAL COMPLEXES IN CANCER TREATMENT

drug molecules. The use of nanocarriers such as liposomes and nanomaterials (Figure 4) can improve the pharmacological properties of chemotherapeutics.

Liposomes as drug carriers

Liposomes are investigated as vehicles for a variety of therapeutic agents, e.g. anticancer drugs (doxorubicin, cisplatin, paclitaxel, camptothecin)^[57–62] and antibiotic drugs (ciprofloxacin, amikacin, vancomycin), as well as biomolecules (anti-sense oligonucleotides, DNA)^[63–65]. A liposomal formulation of cisplatin, named lipoplatin, displays enhanced circulation in body fluids and evades immune surveillance by their coating with PEG^[66;67]. Additionally, lipoplatin due to small particle size (90–130 nm) and long circulation preferentially eliminates tumors through their compromised vasculature^[68]. Non-PEGylated liposomes are taken up by liver macrophages and destroyed with a half-life of 20 min in body fluids. On the other hand, PEGylated liposomes display a half-life of 5 days in body fluids^[69].

Nanostructured mesoporous materials as drug carriers

Current progress in nanostructured material synthesis and engineering has made an enormous influence on a number of fields including biomedical applications^[70–74]. Mesoporous particles of silicon dioxide are emerging as a new and promising class of nanoparticles that offers several attractive features for diagnostics and targeting of specific cell types in the context of drug delivery^[75–77]. For the first time, in 2001 mesoporous silicas were used as drug (ibuprofen) delivery systems^[78]. The studies related to cisplatin and nanomaterials based on hydroxyapatite were published in 2007. In that work, adsorption and release of cisplatin from nanomaterials were studied^[79]. Later on, the first studies on the antiproliferative activity of hydroxyapatite loaded with [Pt(en')Cl₂] were conducted (en' – ethylenediamine type ligands)^[80]. **MCM-41** (2D-hexagonal) particles displayed low cytotoxicity against HeLa cell line^[81].

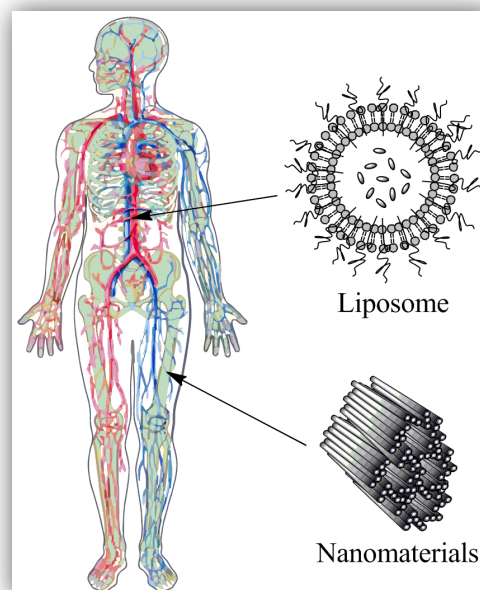


Figure 4. Pharmaceutical carriers applied in blood and bones.

1.4. Goals of the work

Various platinum and nonplatinum compounds have been investigated *in vitro* and *in vivo* as antitumor agents. In this work, investigated agents enclose conventional inorganic compounds, complexes with *N*, *O*, *S*- donor as well as *C*-donor ligands, as organometallic ligands. Because of expensive and time-intensive *in vitro* studies herein work is pointed on compounds of four different metal centres: 1) platinum(II/IV); 2) palladium(II); 3) titanium(IV) and 4) tin(IV). In the focus of the preparation of desired metal compounds were simple, frequently used synthetic methods allowing variation in the ligand sphere with respect to modulation of biological properties, following the proverb "*Doesn't matter if the cat is black or white as long as it catches mice*" (Deng Xiaoping). The main targets of the work will be to contribute to the development of the metal-based drugs as antitumor agents. Also, it was planned to develop new approaches in antitumoral treatment using water-insoluble cisplatin derivatives and some organometallic compounds. Based on published results following topics will be discussed:

1. Understanding of the bioactivity of R₂edda-type platinum(II), platinum(IV) and palladium(II) complexes.
2. Tuning the *in vitro* antitumoral activity of (*ansa*-)titanocene(IV) complexes.
3. Exploring the organotin(IV) compounds as potential antitumor drugs.
4. Efficiency of carrier molecules, liposomes and mesoporous nanomaterials, as drug shuttles.

2. METALLOCOMPOUNDS

The work is designed to contribute to the development of both platinum- and nonplatinum-based drugs. The synthesis and characterization of platinum(II/IV), palladium(II), titanium(IV) and tin(IV) compounds are discussed in this chapter. Furthermore, *in vitro* and *in vivo* antitumor activities are summarized.

2.1. Synthesis and characterization

2.1.1. Platinum complexes containing R₂edda-type ligands

For more information see references K3–K11 (Appendices 3–5).

Diverse R₂edda-type ligands (R₂edda = diesters of ethylenediamine-*N,N'*-diacetic acid, Figure 5.) were synthesized as hydrochloride salts by conventional method^[K3–K11]. Those ligands exhibit κ^2 -*N,N'*

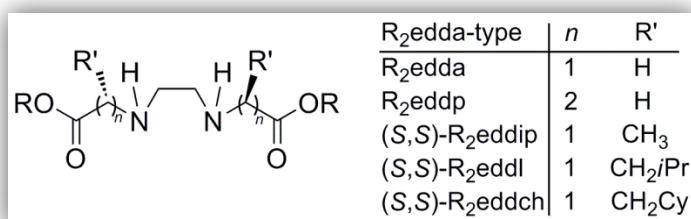


Figure 5. R₂edda-type ligands.

coordination to metal center. Various R₂edda-type platinum(II/IV) complexes have been prepared and this section summarizes, how they can be assembled from readily available precursors. The platinum(II) complexes belong to the class of square-planar d^8 [PtL₂Cl₂] coordination compounds having a bidentate L[∧]L = *N,N'*-R₂edda-type ligand with the other coordination sites occupied by chlorido ligands. On the other hand, platinum(IV) complexes are an octahedral d^6 system with general formula [Pt(R₂edda-type)Cl₄].

The first report on the preparation of a platinum(IV) complexes were published in 2004^{[82]*}. The synthesis and reactivity of R₂eddp·2HCl ligand precursors and K₂[PtCl₆] in the presence of base, LiOH, were described. The first two complexes of this class, [Pt(R₂eddp)Cl₄] (H₂eddp = ethylenediamine-*N,N'*-di-3-propionic acid; R = *n*Bu and *n*Pe), described in mentioned work, of a growing family of R₂edda-type platinum(IV)

* Work from PhD thesis references [82–85]; all other publications [K3–K11] related to habilitation thesis were performed by the author or under his supervision.

2. METALLOCOMPOUNDS

complexes are presented in Figure 6. Complexes of the $[\text{Pt}(\text{R}_2\text{edda-type})\text{Cl}_2]$ type were prepared by direct reaction of aqueous solutions of $\text{K}_2[\text{PtCl}_4]$ and $\text{R}_2\text{eddp}\cdot 2\text{HCl}$ ligand precursors in the presence of base.

A synthetic method for preparing $[\text{Pt}(\text{R}_2\text{edda-type})\text{Cl}_4]$ complexes differs in their starting materials and reaction conditions. In

Scheme 1 synthetic pathway is depicted. Platinum(II) complexes were prepared (Scheme 1) as reported for $[\text{Pt}(n\text{Bu}_2\text{eddp})\text{Cl}_2]$ ^[83]. Different series of the $[\text{Pt}(\text{R}_2\text{edda-type})\text{Cl}_4]$ complexes were synthesized using achiral $\text{R}_2\text{edda}\cdot 2\text{HCl}$ and $\text{R}_2\text{eddp}\cdot 2\text{HCl}$ as well as chiral $(S,S)\text{-R}_2\text{eddip}\cdot 2\text{HCl}$ [$(S,S)\text{-H}_2\text{eddip}$ = ethylenediamine- N,N' -di-2-propionic acid], $(S,S)\text{-R}_2\text{eddl}\cdot 2\text{HCl}$ [$(S,S)\text{-H}_2\text{eddl}$ = (S,S) -ethylenediamine- N,N' -di-2-(4-methyl)-pentanoic acid] and $(S,S)\text{-R}_2\text{eddch}\cdot 2\text{HCl}$ [$(S,S)\text{-H}_2\text{eddch}$ = ethylenediamine- N,N' -di-2-(3-cyclohexyl)-propionic acid] ligand precursors (Figure 7). In case of platinum(II), only complexes containing $(S,S)\text{-R}_2\text{eddip}$ and $(S,S)\text{-R}_2\text{eddl}$ ligands were prepared. All compounds were isolated in pure state and fully characterized by multinuclear NMR, IR spectroscopy and elemental analysis. Furthermore, for the several platinum(IV) compounds structures were additionally confirmed by X-ray diffraction measurements.

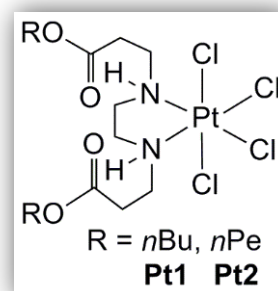
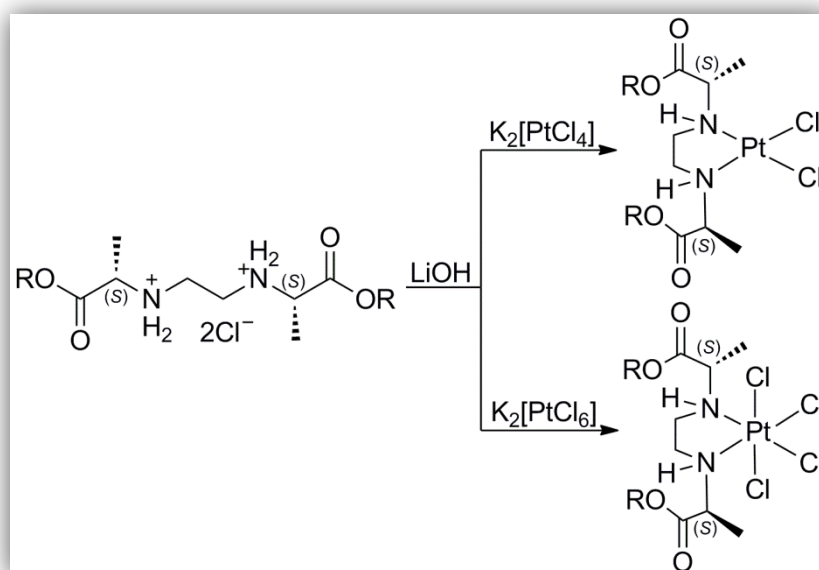


Figure 6. First examples of $\text{R}_2\text{edda-type}$ platinum compounds.



Scheme 1. General route for the synthesis of platinum(II/IV) complexes with $\text{R}_2\text{edda-type}$ ligands; shown is $(S,S)\text{-R}_2\text{eddip}$ ligand as example.

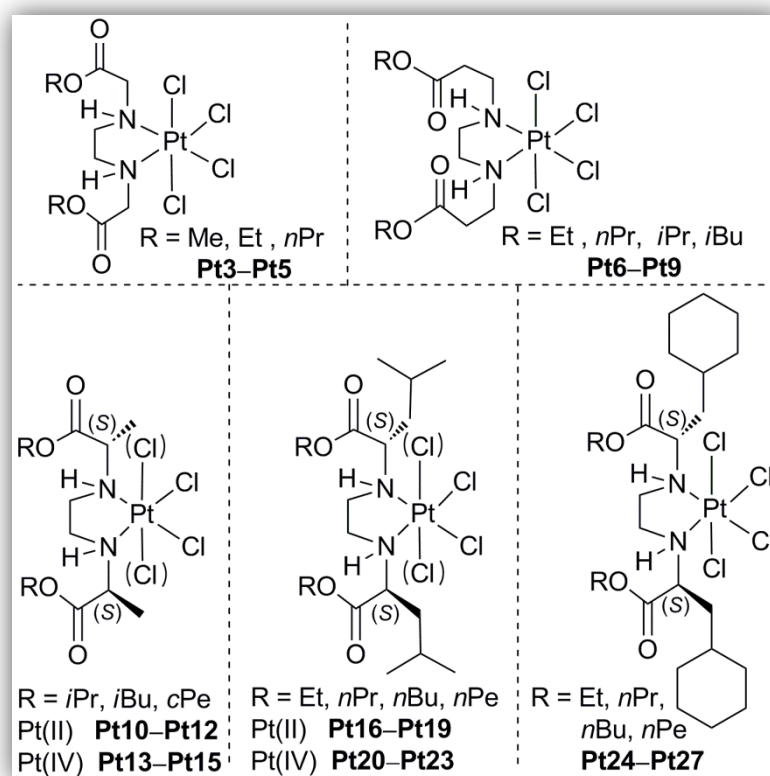


Figure 7. Prepared [Pt(R₂edda-type)Cl_n] (n = 2, 4) complexes, Pt3–Pt27.

2.1.2. Palladium complexes containing R₂edda-type ligands

For more information see references K12–K17.

Several dichloridopalladium(II) complexes containing chiral (S,S)-R₂edda-type ligands have been prepared by similar procedure as described for [Pt(R₂edda-type)Cl₂] (see Scheme 1). Compounds obtained were characterized by NMR (¹H, ¹³C), IR spectroscopy and elemental analysis. Complexes are presented in Figure 8.

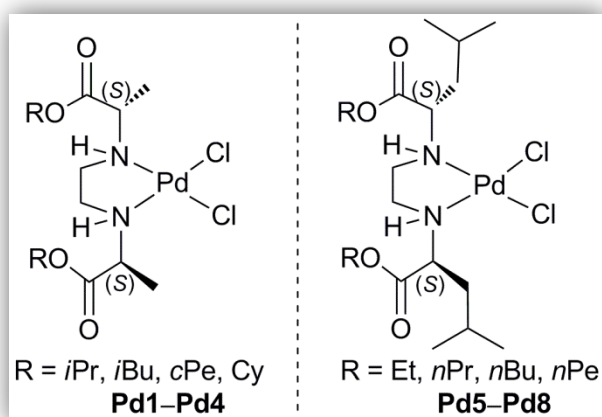


Figure 8. Prepared [Pd(R₂edda-type)Cl₂] (Pd1–Pd8) complexes.

2. METALLOCOMPOUNDS

2.1.3. Titanocene and *ansa*-titanocene complexes

For more information see references K18–K26 (Appendices 6–8).

A variety of substituted titanocene and *ansa*-titanocene complexes have been synthesized, and are depicted in Figure 9. The compounds were prepared by several reaction routes, some of them are presented by Scheme 2.

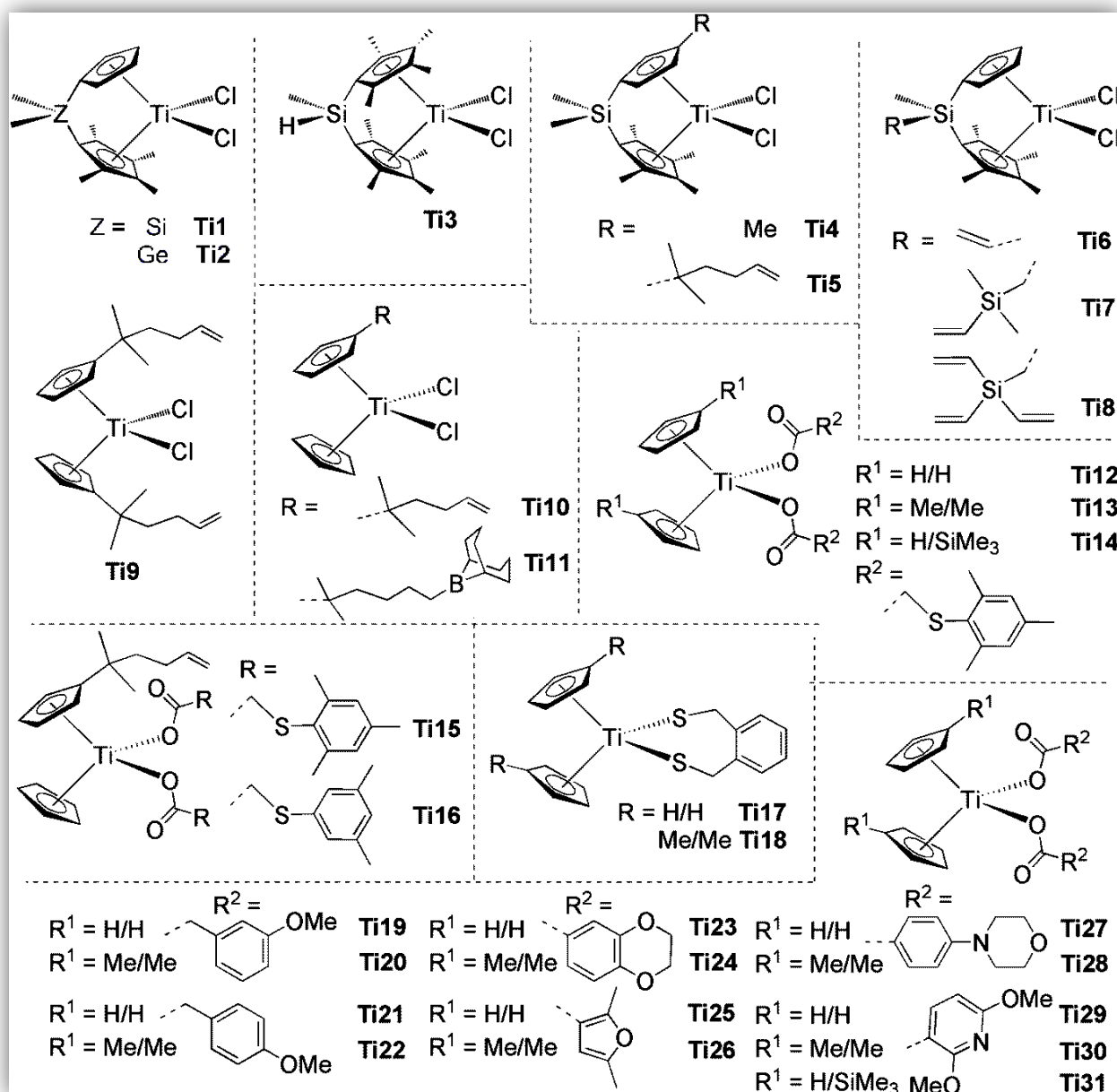
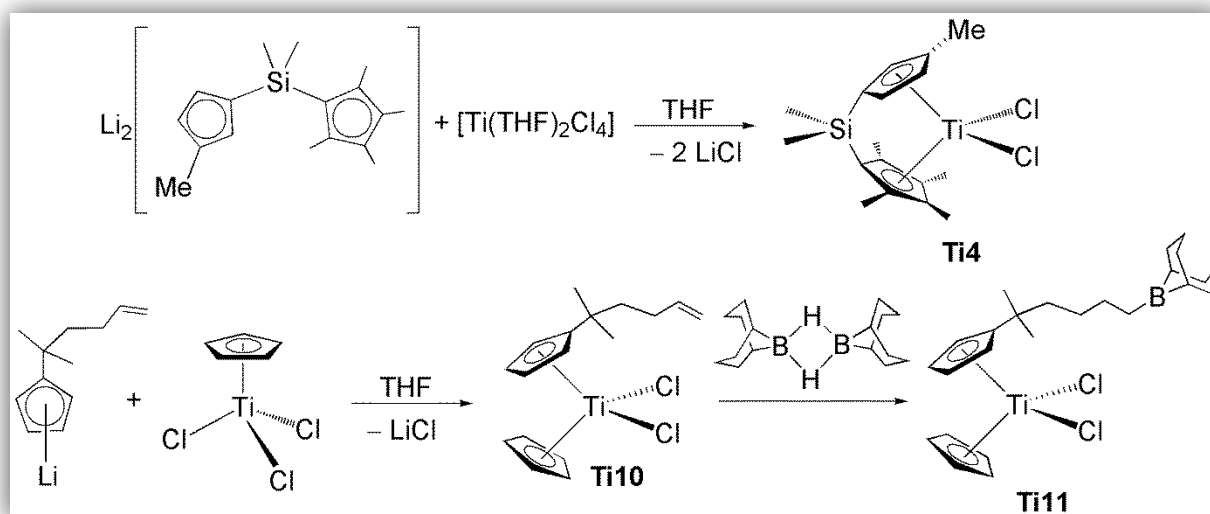


Figure 9. Synthesized titanocene and *ansa*-titanocene complexes, Ti1–Ti31.



Scheme 2. Some synthetic routes for the preparation of titanium(IV) complexes.

Titanocene complexes were obtained in the reaction of $[Ti(THF)_2Cl_4]$ or $[Ti(Cp')Cl_3]$ (Cp' = derivative of Cp) with lithium salts of Cp' . The *ansa*-titanocene complexes were prepared by the reaction of the corresponding dilithium salts of *ansa*-di-Cp derivatives with $[Ti(THF)_2Cl_4]$ (1:1). The compounds were characterized by multinuclear NMR spectroscopy, mass spectrometry, IR spectroscopy and elemental analysis. For some complexes, X-ray structural analyses confirmed proposed molecular structures.

2.1.4. Organotin(IV) compounds

For more information see references K23, K25 and K27–K31 (Appendices 9–11).

Four types of organotin(IV) compounds were prepared: neutral diphenyl- and triphenyltin(IV) carboxylates, (cyclopentadienyl)triphenyltin(IV), anionic triethylammonium (carboxylato)triphenyltin(IV) chlorides and polymeric (carboxylato)triphenyltin(IV) compounds (Figure 10). Neutral diphenyl- and triphenyltin(IV) carboxylates have been prepared by the reaction of carboxylic acid with triphenyltin(IV) chloride or diphenyltin(IV) dichloride in the presence of triethylamine. The preparation of (cyclopentadienyl)triphenyltin(IV) compounds were achieved *via* the reaction of the lithium cyclopentadienyl derivative with triphenyltin(IV) chloride. Triphenyltin(IV) chloride in the reaction with triethylammonium carboxylates yielded anionic tin(IV) compounds. In

2. METALLOCOMPOUNDS

the reaction of triphenyltin(IV) chloride with xyllylthioacetic/mesitylthioacetic acid polymeric triphenyltin(IV) carboxylates were obtained, as shown in Scheme 3.

The compounds were characterized by multinuclear NMR spectroscopy, mass spectrometry, IR spectroscopy and elemental analysis. X-ray diffraction analyses were used for the complexes obtained as single crystals. Among them, the triphenyltin(IV) anionic **Sn14**, from the trigonal-bipyramidal triphenyltin(IV) class of compounds, represent the first compound structurally characterized so far.

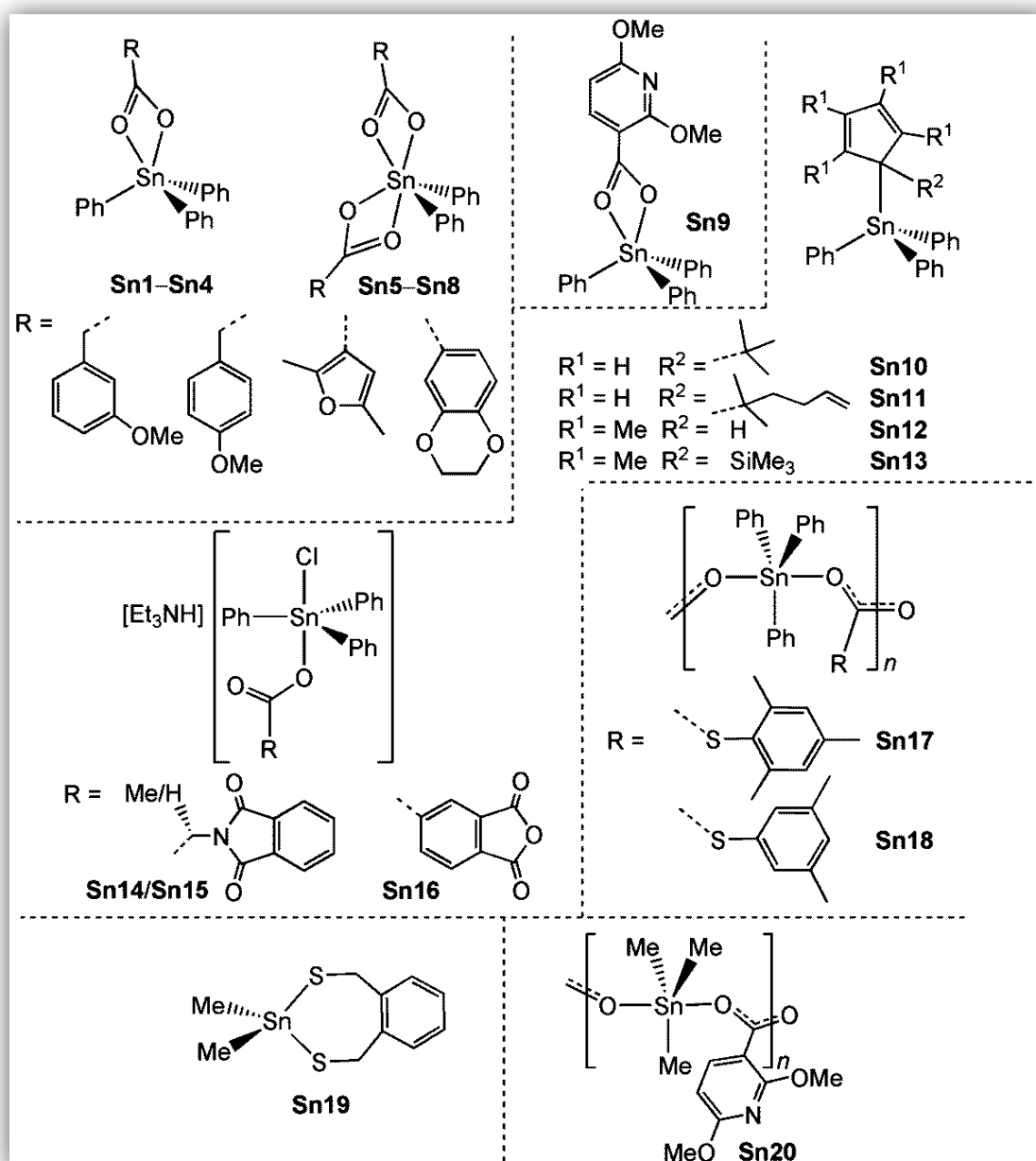
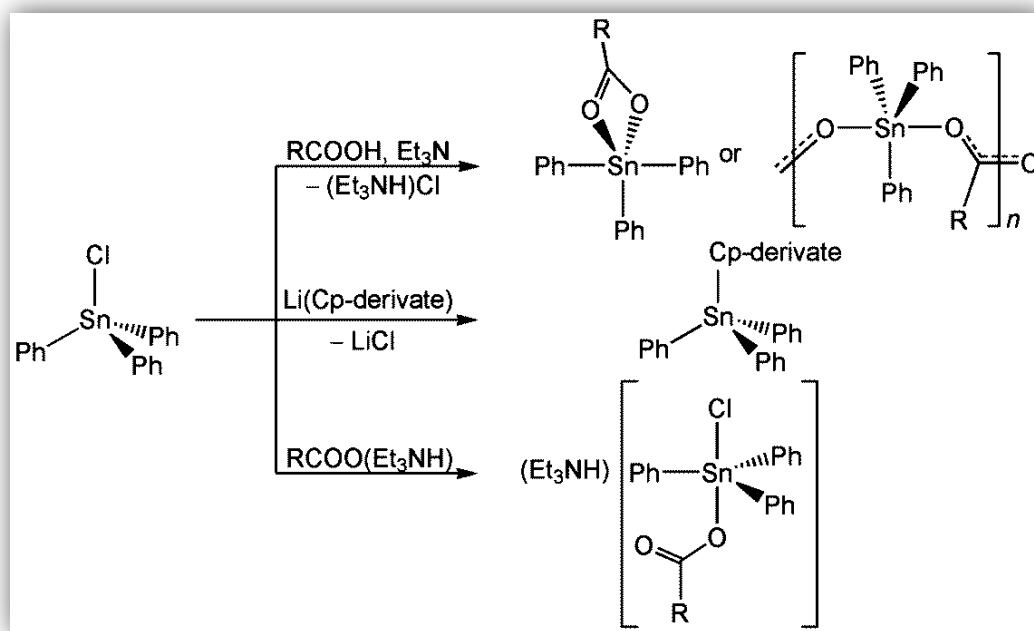


Figure 10. Synthesized organotin(IV) compounds, **Sn1-Sn20**.



Scheme 3. Synthetic routes for the preparation of organotin(IV) compounds.

2.2. Biological activity of metallocompounds

2.2.1. R₂edda-type platinum(II/IV) and palladium(II) complexes

Related publications: K3–K17 (Appendices 3–5).

The synthesis of [Pt(R₂edda-type)Cl_n] (*n* = 2, 4) complexes was initiated six years ago^[82–85]. These complexes have been designed in order to establish, how the type of the ester substituents, halogenido ligands and oxidation state of platinum affect *in vitro* antiproliferative activity against some tumor cell lines. Investigations showed that the most efficient complexes against human adenocarcinoma HeLa (*ca.* five times less active than cisplatin) and myelogenous leukaemia K562 cells (activity comparable with cisplatin) were the tetrachloridoplatinum(IV) complexes [Pt(R₂eddp)Cl₄] (R = *n*Bu, **Pt1**; *n*Pe, **Pt2**). **Pt1** and **Pt2** are inducing death of tumor cells activating apoptotic pathway^[83].

The cytotoxicity of **Pt1** and **Pt2** was found to be markedly higher than that of their platinum(II) counterparts and comparable to the antitumor action of cisplatin against mouse fibrosarcoma L929 and human astrocytoma U251 cell lines^[84]. These platinum(IV) complexes induced oxygen radical-mediated tumor cell necrosis, in contrast

to cisplatin which provoked oxidative stress-independent apoptotic cell death of tumor cells. The kinetics of tumor cell death caused by **Pt1** and **Pt2** were markedly faster than that of cisplatin.

As a contribution for a better understanding of structure–activity relationships of $[\text{Pt}(\text{R}_2\text{edda-type})\text{Cl}_n]$ complexes ($n = 2, 4$), new ligand precursors (less and more lipophilic) as well as corresponding platinum(II/IV) complexes and some palladium(II) complexes have been tested against various tumor cell lines^[K3–K11;K13;K15]. At first, the aim was to expand initial work regarding this class of compounds. Determination of the activity of ligand precursors, platinum(II), platinum(IV) and palladium(II) complexes should give structure–activity relationships. Furthermore, the aim was also to answer on some questions, such as “Are more lipophilic ligands improving cytotoxicity and are these complexes interacting with DNA?”. Additionally, for the most active compound the expansion of bioinvestigations to *in vivo* studies was scheduled. Using this model system, we sought to identify and characterize mechanisms that are recruited to produce cell-type specific responses to $[\text{Pt}(\text{R}_2\text{edda-type})\text{Cl}_4]$ complexes.

2.2.1.1. Structure–activity relationships of $\text{R}_2\text{edda-type}$ ligand precursors, corresponding platinum(II/IV) and palladium(II) complexes

Ligand precursors of $\text{R}_2\text{edda}\cdot 2\text{HCl}$ -type and related dichloridoplatinum(II), tetrachloridoplatinum(IV) and dichloridopalladium(II) complexes, $[\text{Pt}(\text{R}_2\text{edda-type})\text{Cl}_n]$ ($n = 2, 4$) and $[\text{Pd}(\text{R}_2\text{edda-type})\text{Cl}_2]$, were tested for *in vitro* antiproliferative activity against various tumor cell lines and normal primary cells (human peripheral blood mononuclear PBMC cells, keratinocytes, fibroblasts). Generally, it was shown that the *in vitro* activity is depending on the edda-type, R moiety as well as on the metal center $[\text{Pd}(\text{II}) \rightarrow \text{Pt}(\text{II/IV})]$ and oxidation state $[\text{Pt}(\text{II}) \rightarrow \text{Pt}(\text{IV})]$. Ligand precursors expressed lower *in vitro* antitumor activity, but within ligands activity increases with the lipophilicity of the compounds.

Metal complexes with lower efficiency against tumor cell lines are palladium(II) complexes. Platinum(II) complexes are expressing higher activity than ligand precursors and palladium(II) complexes. The agents with higher potential are found to be platinum(IV) complexes. Graphical interpretation of experimental findings are presented on Figure 11. These explorations gave new insights into the structure–activity relationships for investigated compounds against tumor cell lines.

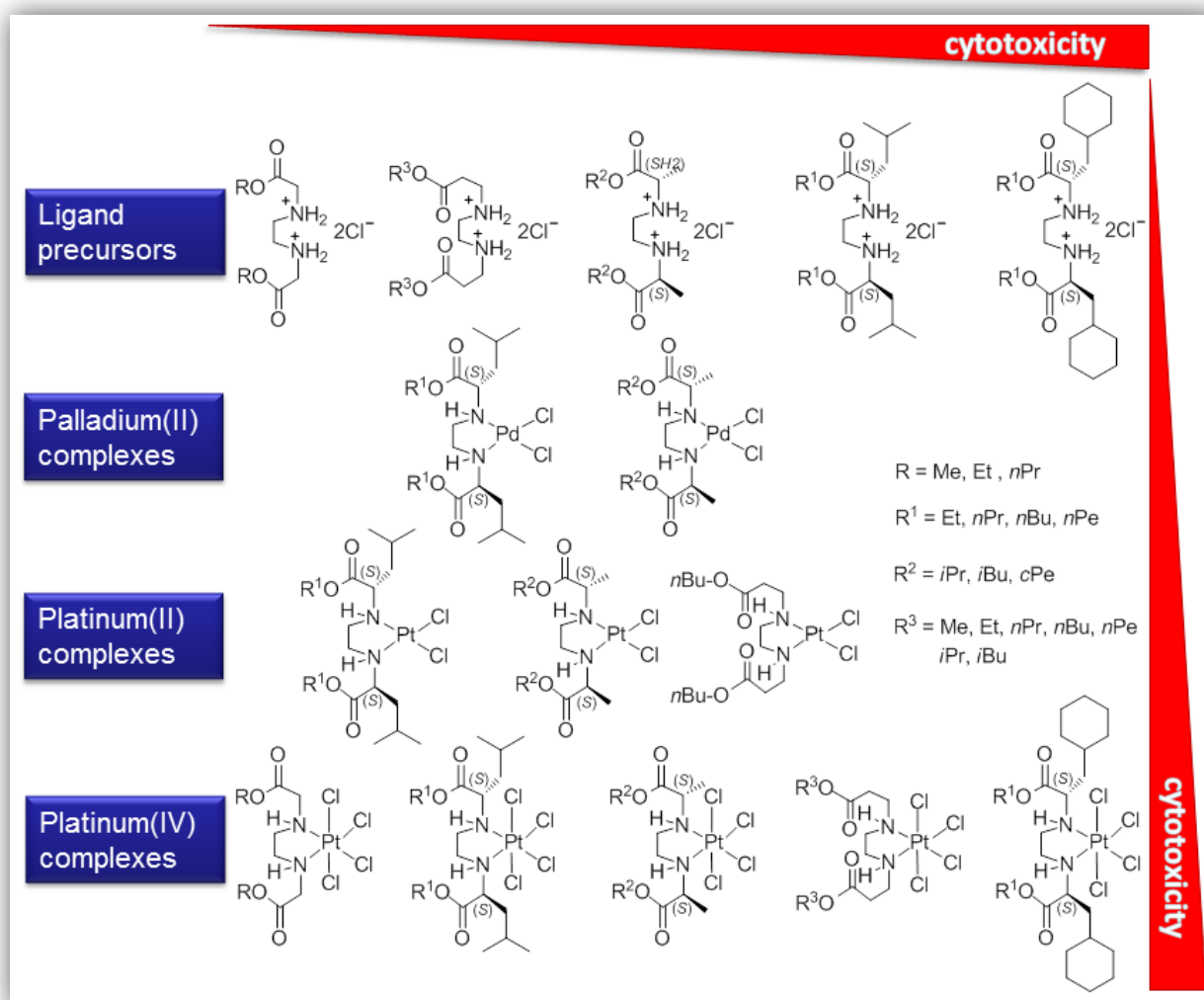


Figure 11. Structure–activity relationships.

An exception from this correlation is the activity of compounds against chronic lymphocytic leukaemia cells^[K8,K9,K15] in which platinum(IV) complexes were found to be less active than platinum(II) and palladium(II) complexes.

2.2.1.2. Platinum(IV) complexes: drugs or prodrugs?

Formerly, it has been generally accepted that reduction of platinum(IV) ions has to occur prior to binding to the target DNA^[86–88]. The platinum(IV) complexes are believed to represent relatively stable prodrugs able to compass the tumor tissue largely without being reduced in the bloodstream to enter the cell and to reach their target intact^[89;90]. Cellular reducing agents like ascorbic acid, thiol-containing species like metallothioneins and glutathione and some other may trigger an activation of platinum(IV) prodrugs^[91]. Electrochemical studies on **Pt6** and **Pt7** complexes demonstrat-

2. METALLOCOMPOUNDS

ed redox potentials^[K5] similar to that of satraplatin, a platinum(IV) complex (see Figure 3, page 5), or platinum(IV) complexes containing carbamates, suggesting that [Pt(R₂eddp)Cl₄] complexes should demonstrate stability in biological environment similar to those of satraplatin^[92].

Previous studies have shown that some platinum(IV) compounds may also react with DNA fragments^[9;93]. As model system, pBR322 plasmid DNA is usually involved in investigation in which is determined whether the platinum(IV) complex is acting as drug or prodrug^[94;95]. Analysis of electrophoretic mobility of pBR322 plasmid DNA (circular and supercoiled form) affected with platinum compound might give information if this drug acts as DNA–cleavage agent. The influence of platinum complexes **Pt6** and **Pt7** on pBR322 plasmid DNA was investigated^[K5]. Two sets of experiments were conducted. In one, it was investigated if [Pt(R₂eddp)Cl₄] complexes could interact with plasmid DNA without external reducing agents and in the other in the presence of ascorbic acid (cellular reducing agent). Results support both hypotheses, namely that this type of complexes may act both as drug and prodrug. However, because of similar redox potential to satraplatin, which is *in vivo* reduced to platinum(II) species^[5;9], the most likely [Pt(R₂eddp)Cl₄] complexes might also be reduced upon entering the cell. Thus, these complexes might act as prodrugs which are transformed *in vivo* into reactive platinum(II) species.

2.2.1.3. The cell type-specific mode of cell death induced with [Pt(R₂edda-type)Cl₄] complexes

Beside cytotoxicity, additional important information for evaluation of the compounds in preclinical studies are toxicity and mode of cell death. The next step in research was to improve cytotoxicity of the first synthesized compounds **Pt1** and **Pt2** by introducing more lipophilic group (e.g. *i*Pr, CH₂Cy) in amino acid backbone. The anti-tumoral activity depending on the introduced group could be improved by factor of around 10^[K7]. **Pt1** and **Pt2** complexes were found to be cell-type specific regarding mode of cell death, mostly inducing apoptosis^[83;84]. Derivatives of R₂edda·2HCl-type ligand precursors, R₂eddp·2HCl (R = *i*Pr, *n*Bu), (*S,S*)-R₂eddip·2HCl (R = *i*Pr, *i*Bu, *c*Pe) and (*S,S*)-R₂eddch·2HCl (R = Et, *n*Pr, *n*Bu, *n*Pe) as well as corresponding platinum complexes were investigated for the mode of cell death^[K7;K10]. The most active from each series on the selected tumor cell line will be discussed here.

2. METALLOCOMPOUNDS

Platinum complexes with R₂eddp and (S,S)-R₂eddip ligands

Platinum(II) and platinum(IV) complexes containing R₂eddp (R = *i*Pr, *n*Bu), (S,S)-R₂eddip ligands (R = *i*Pr, *i*Bu, *c*Pe) showed dose-dependent and cell-type specific activity^[K10]. Two examples with representative compounds in comparison to cisplatin against HCT116 cell lines (mainly higher activity than cisplatin, positive values = IC₅₀(cisplatin)/IC₅₀(compound)) and U251 (lower activity than cisplatin, negative values = IC₅₀(compound)/IC₅₀(cisplatin) multiplied by -1) are shown in Figure 12.

Viability of compounds on primary fibroblasts and keratinocytes (nontransformed and non-malignant cells) was minimally disturbed indicating that novel compounds are significantly less toxic to normal than tumor cells. The compounds [(S,S)-H₂cPe₂eddp]Cl₂ and **Pt8–Pt15** did not affect the increasement of lactate dehydrogenase (LDH) in culture supernatant (extracellular surrounding) of cisplatin-resistant colon carcinoma HCT116 cell line indicating that necrosis is not the primary mode of action of these derivatives. On the other hand, increased percentage of autophagosomes was detected in the cytoplasm after treatment. Autophagic cell death induced with **Pt8**, **Pt11** or **Pt15** contributes to decrease of HCT116 cell viability. Additionally, by simultaneous treatment of HCT116 with mentioned compounds and inhibitor of autophagy (3-methyladenine) cell viability was partly restored. Cell cycle analysis showed mainly substantial subG accumulation. In accordance to elevated subG compartment the presence of typical apoptotic cells with shrinkage of nucleus and apoptotic bodies upon the treatment with all tested drugs were microscopically visualized.

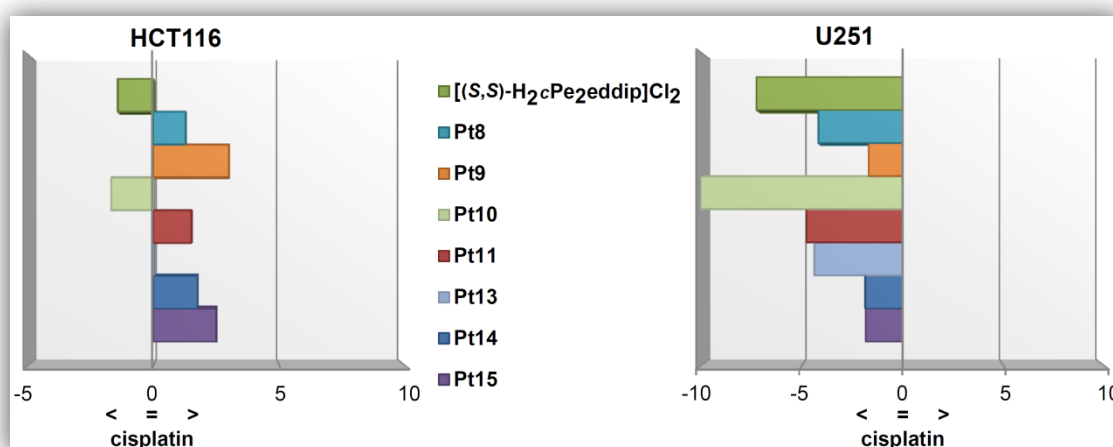


Figure 12. Relative cytotoxicity of ligand precursor and platinum(II/IV) complexes on HCT116 and U251 cell lines.

2. METALLOCOMPOUNDS

Furthermore, high activation of caspase 3 was observed, with exception in case of [(S,S)-H₂cPe₂eddip]Cl₂. Parallel treatment with compounds and pan-caspase inhibitor ZVAD resulted in a significant recovery of cell viability in cultures exposed to all compounds except [(S,S)-H₂cPe₂eddip]Cl₂ confirming the key role of caspases in apoptosis triggered by these drugs. In summary, compounds induced apoptosis as dominant mode of cell death.

Reactive oxygen and nitrogen species were generated in HCT116 cells when treated with investigated compounds, but by cotreatment with compounds and antioxidant (*N*-acetylcysteine) cell viability was not significantly restored (exception compound **Pt15**) indicating that regardless of intensive oxidative stress, ROS and RNS are not major mediators of drug toxicity.

Platinum complexes with (S,S)-R₂eddch ligands

Cytotoxicity of the first synthesized compounds, **Pt1** and **Pt2**, might be increased by introducing more lipophilic group (CH₂Cy) in amino acid backbone^[K7]. As discussed in previous Section (page 20), also here the compounds showed dose-dependent and cell-type specific activity. The highest activity was observed against U251 cell line and the mechanism of action of the two most potent compounds, ligand precursors and platinum(IV) complexes will be discussed here. Compared to previous platinum(IV) compounds (page 20), these complexes expressed higher activity against U251 cell line. The highest relative cytotoxicity is obtained in case of B16 cell line and is given in Figure 13.

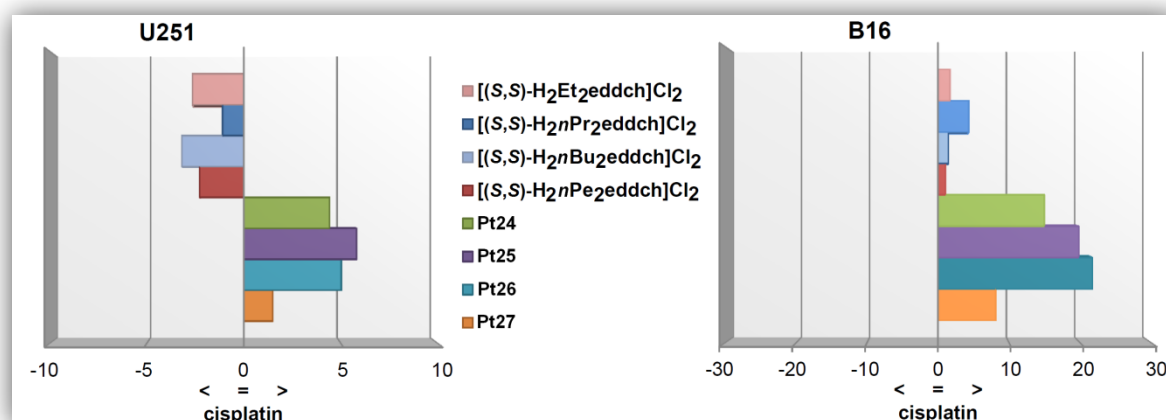


Figure 13. Relative cytotoxicity of ligand precursors and platinum(IV) complexes on U251 and B16 cell lines.

2. METALLOCOMPOUNDS

Contrary to cisplatin and platinum(IV) complexes containing $R_2\text{eddip}$ ($R = i\text{Pr}, n\text{Bu}$) and $(S,S)\text{-}R_2\text{eddip}$ ligands ($R = i\text{Pr}, i\text{Bu}, c\text{Pe}$), $[\text{Pt}\{(S,S)\text{-}R_2\text{eddch}\}\text{Cl}_4]$ complexes (**Pt24–Pt27**) are inducing different mode of cell death. Microscopical examinations showed differences in the cells after treatment with cisplatin, ligand precursor or corresponding platinum(IV) complex (Figure 14).

Explicitly, complexes **Pt24–Pt27** induced LDH release and no caspase 3 activation which is a characteristic of necrotic, rather than apoptotic cell death. Furthermore, it was found that this class of complexes is not able to bind to DNA and induced G0/G1 cell cycle arrest of the U251 cells. Cytotoxicity of $[\text{Pt}\{(S,S)\text{-}R_2\text{eddch}\}\text{Cl}_4]$ complexes is correlated with their ability to trigger production of ROS in U251 cells. Using antioxidant agent (*N*-acetylcysteine) viability was recovered, verifying the role of oxidative stress in the activity of $[\text{Pt}\{(S,S)\text{-}R_2\text{eddch}\}\text{Cl}_4]$ complexes.

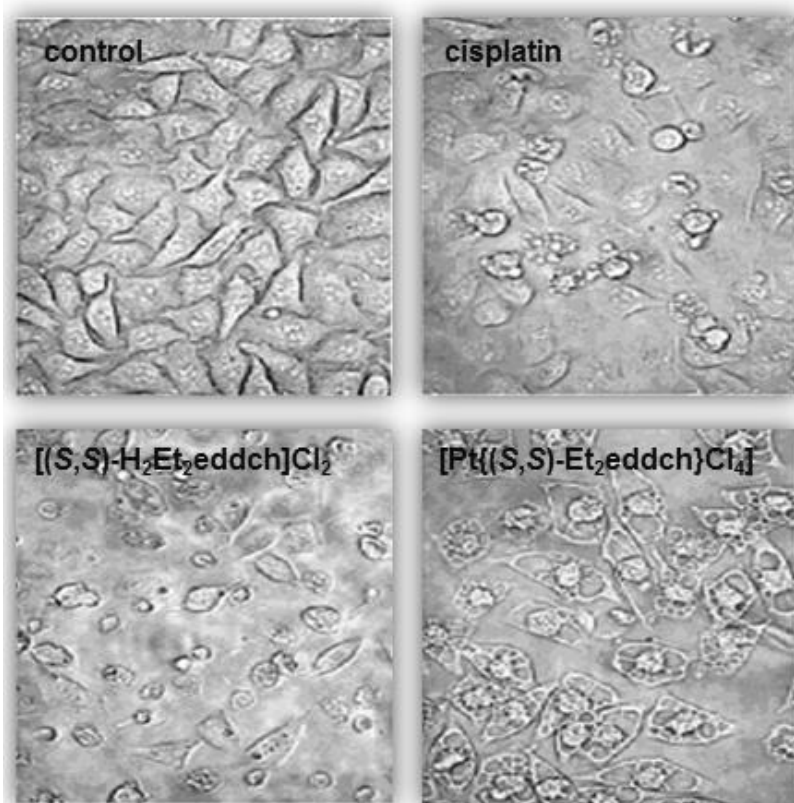


Figure 14. Microphotographs of the U251 cells treated with cisplatin, ligand precursor and corresponding platinum(IV) complex, respectively.

2.2.1.4. Mode of action of Pt1 and Pt26 on B16 melanoma cell line

Two platinum(IV) complexes **Pt1** and **Pt26** with lower and higher lipophilicity, respectively, were compared regarding the mechanism of action on B16 melanoma cells^[K7;K11] (Figure 15) to prove that structural changes might induce different mechanisms of action on the same tumor cell line.

Both complexes are inducing dose- and time-dependent cytotoxic effects with significantly higher activity than cisplatin against B16 melanoma cells. **Pt1** affects cell proliferation promoting both apoptotic and necrotic cell death^[K11], while **Pt26** is provoking necrotic mode of cell death^[K7]. Comparing the IC₅₀ values of **Pt1**, **Pt26** and cisplatin, **Pt26** is almost 10 times more active than **Pt1** and more than 20 times more active than cisplatin. But on the other hand, the main mechanism of action of **Pt26** is the induction of necrosis what is the unfavorable mode of cell death and because of that **Pt1** was used for further *in vivo* investigations.

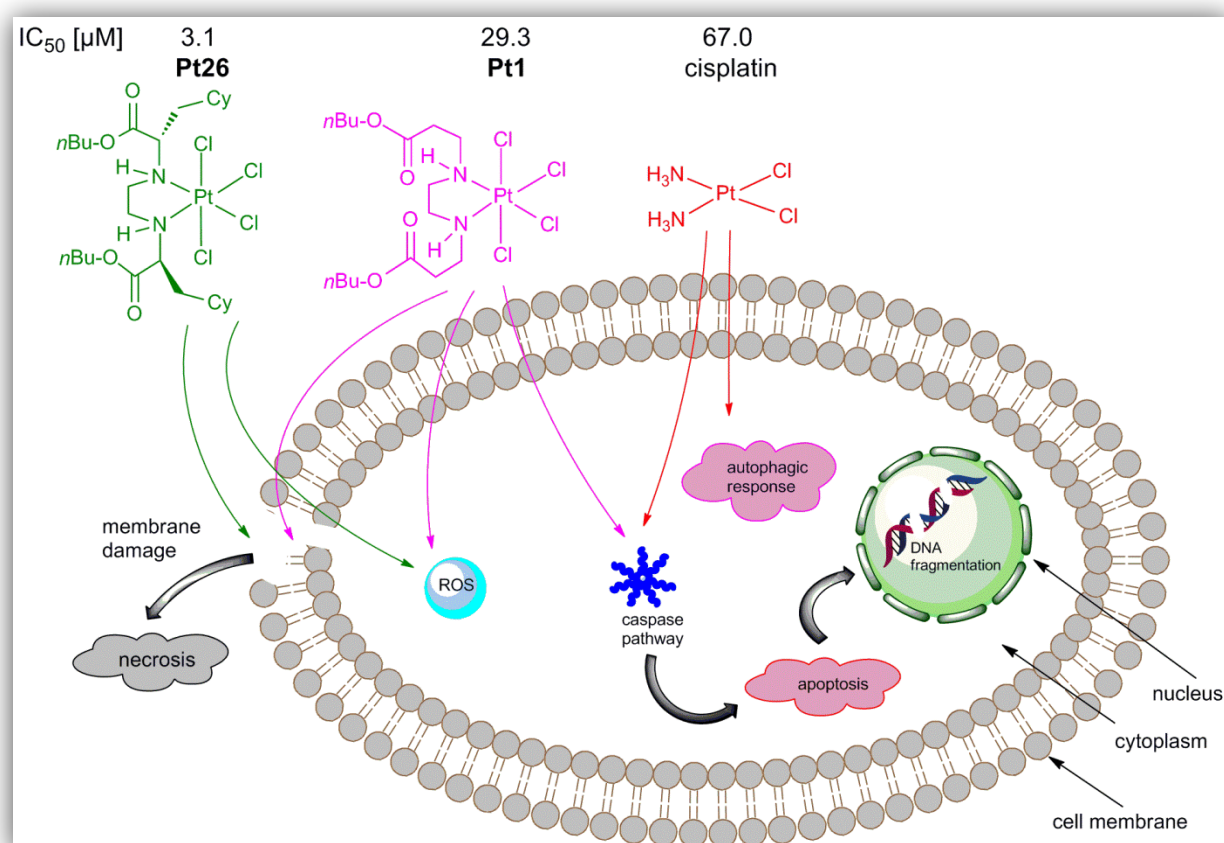


Figure 15. Mechanism of action of cisplatin and [Pt(R₂edda-type)Cl₄] complexes on B16 melanoma cell line.

2.2.1.5. Pt1 versus cisplatin: Enhancement of cytotoxicity and decrease in side effects *in vivo*

The most aggressive and treatment-resistant form of human cancer is melanoma^[96]. Despite recent advances, there is no successful agent in treatment of melanoma patients beside early surgical resection. Because of that we selected melanoma tumor model for the first *in vivo* investigations and **Pt1** from the [Pt(R₂edda-type)Cl₄] complexes^[K11]. The B16 melanoma tumor cells implanted in C57BL/6 mouse model was used for the assessment on the potency of the antitumoral activity of **Pt1**. In parallel, cisplatin has been used as positive control. From the 11th day after induction of the tumor, cisplatin (2 mg/kg) or **Pt1** (4 mg/kg) was administered to the animals every second day. Control animals received only PBS. On the 24th day, tumor volume in the control animal grow up to 2.000 mm³ and the mice were sacrificed. The tumor volume of control animals and those treated with cisplatin or **Pt1** are presented in Figure 16, left.

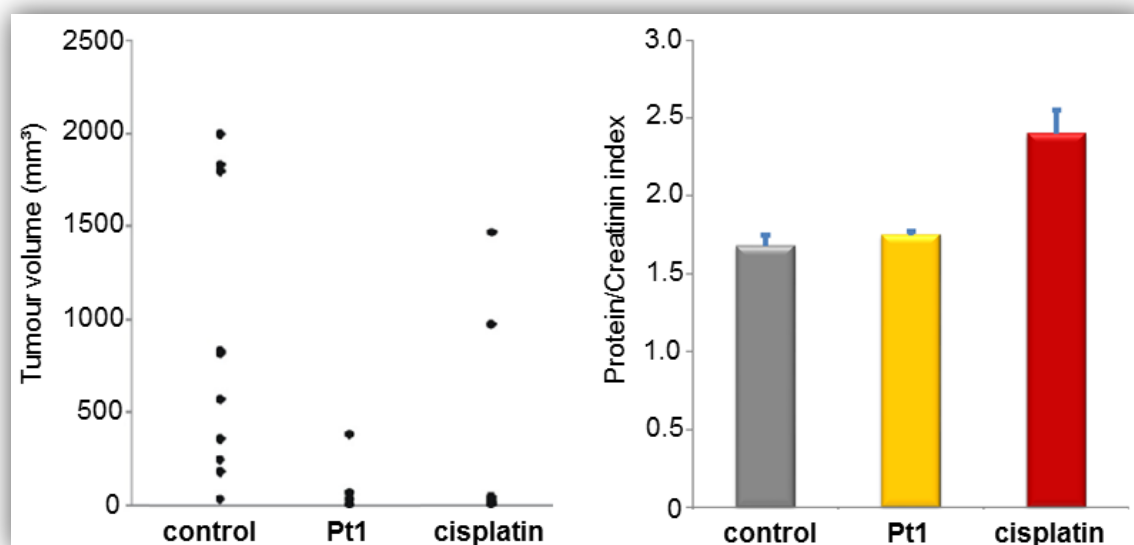


Figure 16. Tumor volume of B16 infected C57BL/6 mice after treatment with cisplatin or **Pt1** (left) and their nephrotoxicity (right, adapted from K11).

In vivo activity of **Pt1** is much higher against melanoma B16 tumor than cisplatin (**Pt1**: tumor volume 400 mm³; in cisplatin-treated group 3 animals died). Furthermore, protein/creatinine index indicates no presence of nephrotoxicity in case of **Pt1** (Figure 16, right). Contrarily, as already known from literature, cisplatin induced a higher protein/creatinine index indicating as side effect nephrotoxicity. **Pt1** is more efficient than

cisplatin *in vitro* and *in vivo* with absence of nephrotoxicity which is described by cisplatin. Mechanism of tumor destruction is essentially and visually different from cisplatin.

2.2.2. Improvement of the antitumor efficacy of titanocene dichloride by variation of structure

For more information see references K18–K26 (Appendices 6–8).

The aim was to investigate the influence of different substituents on the antiproliferative activity of the tumor cells^[K18–K26]. Namely, cyclopentadienyl ring was derivatized with different substituents (see Section 2.1.3.; pages 13, 14). Moreover, variation of substituent SiR₂ in *ansa*-bridge (including Si→Ge) was succeeded. As further variation of titanocene dichloride, chlorido ligands were exchanged with various carboxylato or thiolato ligands.

2.2.2.1. Modification of Cp ligand

Various titanocene complexes, **Ti1–Ti14**, were used in *in vitro* antitumoral studies against three different tumor cell lines and normal immunocompetent cells PBMC^[K18–K20]. The aim was to investigate influence of different substituents (cyclopentadienyl ring, SiR₂ in *ansa*-bridge) on the antiproliferative activity (Table 1).

Almost all complexes, with exception of **Ti8**, expressed higher cytotoxicity than reference compounds [Ti(Cp)₂Cl₂], [Ti(MeCp)₂Cl₂] and [Ti(Cp){Me₃Si(Cp)}Cl₂], but lower than cisplatin. Complex **Ti8** did not express cytotoxic activity (IC₅₀ > 200 μM) against investigated cell lines. Bulky alkenyl groups bonded to the silicon bridge atom seem to be responsible for the strong deactivation of the *in vitro* activity of **Ti1**. A marginal increase of activity was observed for the complex **Ti7** with a slightly less bulkier alkenyl group on the silicon bridge atom. Furthermore, decrease of the activity might be caused by the presence of a second steric demanding silyl group on the *ansa*-bridge (**Ti7** and **Ti8**, see Figure 9, page 13).

In **Ti10**, the presence of alkenyl group, –C(CH₃)₂CH₂CH₂CH=CH₂, increased *in vitro* activity as well as selectivity toward tumor cells. Further derivatization of **Ti10** with the boryl group (**Ti11**) decreased *in vitro* activity as well as selectivity toward tumor cells.

2. METALLOCOMPOUNDS

Exchanging the *ansa*-bridged silicon with germanium atom (**Ti1**→**Ti2**) led to similar cytotoxic activity on investigated tumor cell lines. Namely, the silicon analogue expressed slightly higher activity than germanium bridging atom on HeLa, K652 and Fem-x tumor cells. On the other hand, almost the same activity was found for both complexes against normal immunocompetent cells PBMC. Thus, it might be assumed that the bridge atom has no notable influence on the cytotoxic behaviour.

The presence of a tetramethylcyclopentadienyl ring instead of unsubstituted cyclopentadienyl ligand and hydrogen (**Ti3**) instead of the methyl group bonded to silicon (**Ti1**) has a similar effect on the antiproliferative activity against the tumor cell lines as substituting the methyl (**Ti1**) with an alkenyl group on silicon (**Ti6**).

Table 1. IC₅₀ [μM]^a for 72 h of action of the studied compounds and cisplatin determined by MTT test.

Compound \ Cell line	HeLa	K562	Fem-x	PBMC	PBMC+PHA
[Ti(Cp){(Me ₃ Si)Cp}Cl ₂]	>200	>200	>200	>200	>200
Ti8	>200	>200	nd ^b	nd	nd
[Ti(Cp) ₂ Cl ₂]	>200	>200	178 ± 5	>200	200 ± 10
[Ti(MeCp) ₂ Cl ₂]	>200	173 ± 6	199 ± 4	>200	181 ± 4
Ti7	189 ± 13	155 ± 9	>200	>200	195 ± 5
Ti11	166 ± 7	156 ± 5	168 ± 4	>200	>200
Ti2	154 ± 4	73 ± 1	106 ± 5	101 ± 6	83 ± 11
Ti10	149 ± 3	97 ± 3	134 ± 9	150 ± 3	142 ± 1
Ti12	142 ± 6	87 ± 1	165 ± 9	146 ± 4	148 ± 1
Ti13	139 ± 13	78 ± 1	191 ± 5	162 ± 4	156 ± 7
Ti1	135 ± 6	66 ± 6	96 ± 4	112 ± 7	77 ± 6
Ti4	117 ± 3	88 ± 4	101 ± 9	83 ± 10	82 ± 12
Ti3	109 ± 9	59 ± 8	116 ± 9	72 ± 2	87 ± 2
Ti14	107 ± 7	88 ± 4	90 ± 7	105 ± 5	117 ± 12
Ti6	79 ± 7	64 ± 9	134 ± 18	140 ± 1	151 ± 10
Ti9	86 ± 3	66 ± 4	99 ± 6	96 ± 3	101 ± 5
Ti5	84 ± 9	24 ± 3	89 ± 9	55 ± 8	70 ± 6
cisplatin	4.4 ± 0.3	5.7 ± 0.3	4.7 ± 0.3	33.6	26 ± 6

^a Mean value±SD from three to four experiments.

^b nd = not determined.

Derivatisation of cyclopentadienyl ring in **Ti1** with Me group (**Ti4**) yielded almost the same response of the tumor cell lines as when treated with **Ti1**, contrary substitution with -C(CH₃)₂CH₂CH₂CH=CH₂ group (**Ti5**) yielded the compound with the best activi-

2. METALLOCOMPOUNDS

ty against this tumor cell lines (e.g. against K562 $IC_{50} = 24 \pm 3 \mu M$). The complex **Ti9**, which has an alkenyl substituent, $-C(CH_3)_2CH_2CH_2CH=CH_2$, on each cyclopentadienyl ligand, showed lower cytotoxicity against K562 cell line (ca. 2.8 times) than **Ti5**.

2.2.2.2. Substitution of chlorido with carboxylato or thiolato ligands

Carboxylato complexes **Ti12–Ti14** containing mesitylthioacetato ligands^[K21] were found to be better agents for inhibition of cell proliferation than respective reference complexes $[Ti(Cp)_2Cl_2]$, $[Ti(MeCp)_2Cl_2]$ and $[Ti(Cp)\{Me_3Si(Cp)\}Cl_2]$ (Table 1). This indicates that the substitution of the chlorido by carboxylato ligands has a positive effect on the anticancer activity of the studied complexes (ca. 1.5–3 times more active). Substitution of one H atom on Cp ring with Me or SiMe₃ increased antitumoral activity in the mentioned order. Carboxylato complexes (or their corresponding hydrolysis products) might either possess higher affinity for the binding to transferrin or albumin^[97;98] or higher stability in the biological medium, which leads to a more effective antitumor agent. Worth to be mentioned, the *in vitro* activity of carboxylato complexes **Ti12–Ti14** is lower than that reported for oxali-titanocene derivatives^[99;100]. On the other hand, their activity is comparable to those described for other carboxylatotitanium(IV) complexes^[101;102]. The structure of complex **Ti10** has been modified by substitution of chlorido with mesitylthioacetato (**Ti15**) or xylylthioacetato ligands (**Ti16**)^[K22]. The complexes were found to be more active against tumor cells than titanocene dichloride, but, surprisingly, the cytotoxic activity of the carboxylato derivatives was lower than those of their corresponding titanocene dichloride (**Ti10**).

Changing both chlorido with two α,α' -dimercapto-o-xylene ligands in $[Ti(Cp)_2Cl_2]$ and $[Ti(MeCp)_2Cl_2]$ yielded in more *in vitro* active compounds **Ti17** and **Ti18**, respectively (exception **Ti17** against Fem-x cell line)^[K25]. **Ti18** was found to be more active than **Ti17** and comparable in activity with carboxylato complexes **Ti12–Ti14** against K562 cell line.

Carboxylato complexes **Ti19–Ti28** were tested against A2780 ovarian carcinoma cell line^[K26]. All complexes are much more active (IC_{50} from 40.5 ± 4.4 to $82.1 \pm 8.9 \mu M$) than reference compound $[Ti(Cp)_2Cl_2]$ ($IC_{50} = 124.8 \pm 4.6 \mu M$), but less than cisplatin ($IC_{50} = 0.55 \pm 0.03 \mu M$) indicating that the substitution of chlorido with carboxylato ligands leads to a significant increase in cytotoxic activity. The most active compounds **Ti25** and **Ti26** are found to be inactive against normal fibroblast cells ($IC_{50} >$

2. METALLOCOMPOUNDS

200 μM) indicating higher selectivity than cisplatin ($\text{IC}_{50} = 1.8 \pm 0.1 \mu\text{M}$) between normal and A2780 cells.

Generally, investigated titanocene complexes were found to be more active against K562 than against HeLa and Fem-x cells, with exception of **Ti8** (not active). Variations on cyclopentadienyl ring, *ansa*-bridged silicon atom or anionic ligands have different influence on the viability causing titanocene derivatives to be cell-type specific. This family of titanocene compounds is highly promising due to appreciable cytotoxic activity observed toward different tumor cell lines, which is higher than that of $[\text{Ti}(\text{Cp})_2\text{Cl}_2]$, $[\text{Ti}(\text{MeCp})_2\text{Cl}_2]$ and $[\text{Ti}(\text{Cp})\{\text{Me}_3\text{Si}(\text{Cp})\}\text{Cl}_2]$. Furthermore, cytotoxicity strongly depends on the structural features of the ligands. In addition, although all the analyzed complexes are less active than the reference compound cisplatin, a higher tolerance of relatively high titanium amounts in biological systems may be possible, pointing toward a potential applicability of the reported titanocene derivatives in cancer therapy.

2.2.3. Organotin(IV) compounds

For more information see references K23, K25 and K27–K31 (Appendices 9–11).

The cytotoxic properties of tin compounds have been recognized in 1929^[103;104] and they came into sight of potential biologically active metallopharmaceuticals. The organotin(IV) compounds became very important in cancer chemotherapy regarding their mechanism of action since they are inducing apoptosis^[105–1107]. However, the exact mechanism of antitumor action of organotin compounds has not yet been explored in detail. As contribution for better understanding the action of triphenyl, diphenyl, tetraorganyl, polymeric and anionic organotin compounds have been tested on various tumor and normal cells^[K23;K25;K27–K31] and on the most promising the mechanism of action have been examined and are discussed herein.

2.2.3.1. Organotin(IV) compounds against cisplatin: cytotoxicity and toxicity

Triphenyl (**Sn2–Sn4**) and diphenyltin(IV) compounds (**Sn5–Sn8**) containing different carboxylato ligands (see Section 2.1.4; pages 14–16) have been studied against tumor HeLa, K562, Fem-x and as well as normal healthy peripheral blood mononuclear cells without (PBMC) or with stimulation (PBMC+PHA)^[K27]. Generally, triphenyltin(IV) compounds were found to exhibit higher *in vitro* antiproliferative activity than corre-

2. METALLOCOMPOUNDS

sponding diphenyltin(IV) compounds. Moreover, cisplatin was found to be an agent less effective than triphenyl or diphenyl(IV) compounds. The most active compounds from both organotin(IV) families are presented in Figure 17. Corresponding carboxylic acid was found to be inactive against selected tumor cell lines. Cisplatin expressed 30–112 and 2.8–5.9 less activity than **Sn3** and **Sn7**, respectively. Mostly, organotin(IV) compounds are found to be more selective toward tumors than normal cells in comparison to cisplatin, especially diorganotin(IV) compounds (e.g. **Sn7** selectivity index >12.7, cisplatin 4.6–7.6).

Much higher activity against the same tumor cell lines induced triphenyltin(IV) compound containing 2,6-dimethoxynicotinato ligand, **Sn9**^[K31]. Also here, the ligand precursor was found to be inactive ($IC_{50} > 200 \mu\text{M}$). Compound **Sn9** possesses 68–124 higher *in vitro* activity than cisplatin (e.g. K562 cell line, IC_{50} : $46 \pm 4 \text{ nM}$, **Sn9**; $5.7 \pm 0.3 \mu\text{M}$, cisplatin).

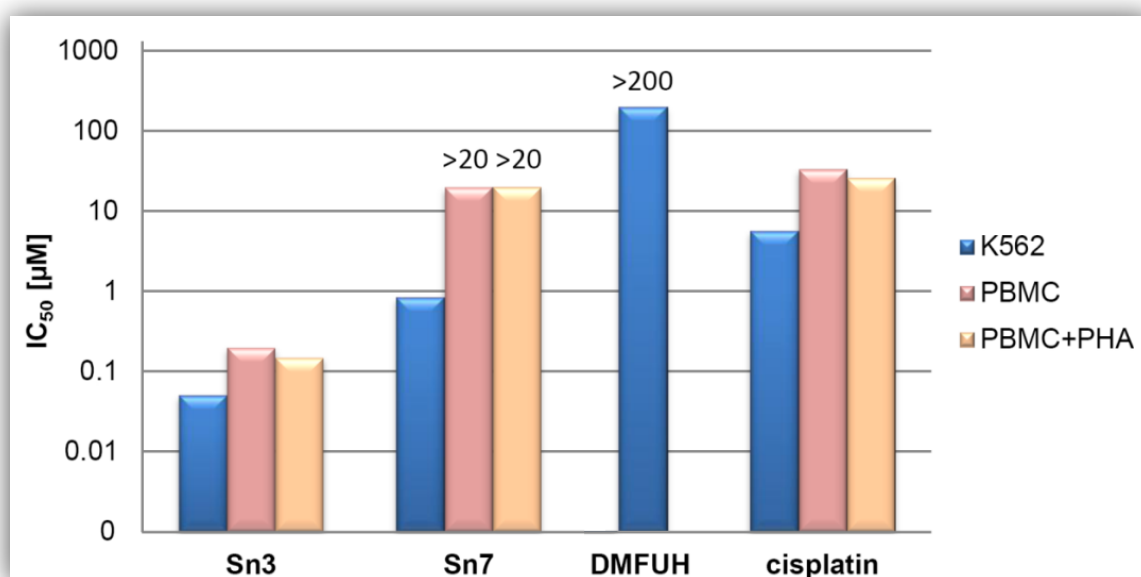


Figure 17. IC_{50} values [μM] of representative triphenyltin(IV), diphenyltin(IV) compounds and corresponding carboxylic acid (**Sn3**, **Sn7**, DMFUH[†], respectively) as well as cisplatin against selected cells.

Contrary to the results obtained with titanocene derivatives^[K18–K26] (IC_{50} values in μM range; see Sections 2.1.3. and 2.2.2.), triphenyltin(IV) compounds bearing cyclopentadienyl derivative substituents (**Sn10–Sn13**) showed higher *in vitro* activity (IC_{50} : 37–351 nM)^[K28]. Cyclopentadienyl(triphenyl)tin(IV) compounds were investigated on

[†] DMFUH not tested against rested and stimulated PBMC.

2. METALLOCOMPOUNDS

8505C, A253, A549, A2780 and DLD-1 tumor cell lines. Those compounds exhibited higher *in vitro* activity than cisplatin (IC_{50} : 0.5–5 μ M).

Trigonal bipyramidal configured anionic triphenyltin(IV) complexes containing *N*-phthaloylglycinato, *N*-phthaloyl-L-alaninato and 1,2,4-benzenetricarboxylato 1,2-anhydride ligands (**Sn14–Sn16**) were tested against 8505C, A253, A549, A2780, DLD-1, 518A2, SW1736, MCF-7, HT-29 and FaDu tumor cell lines^[K30,108]. The ammonium salts of used acids are not active against investigated cell lines ($IC_{50} > 100$ μ M). Compounds expressed high activity against cell lines with lower IC_{50} values (0.09–0.49 μ M) than cisplatin (0.55–5.14 μ M). The most active compound **Sn14** was found to be 50 times more active than cisplatin. Small structural changes on **Sn14**, replacement of H atom with Me group yielded the less active compound **Sn15**. The compounds preferably induce the death of the tumor cells compared to normal fibroblasts.

Polymeric organotin(IV) compounds (**Sn17** and **Sn18**) expressed higher activity^[K29] than titanocene compounds containing same ligands, xylylthioacetic or mesitylthioacetic acid (**Ti12–Ti16**)^[K21;K22], relatively to cisplatin. **Sn17** and **Sn18** were tested against 8505C, A253, A549 and DLD-1 tumor cell lines. Thus, similar antiproliferative activity of those compounds was found (IC_{50} : 0.081–0.178 μ M) with exception of DLD-1 cell line (IC_{50} : 0.060 ± 0.001 / 0.178 ± 0.002 μ M, **Sn17/Sn18**). However, stronger cytotoxicity of **Sn17** and **Sn18** over cisplatin (IC_{50} : 0.8–5.1 μ M) was determined.

Commonly, triphenyltin(IV) compounds are superior in the activity than diorganotin(IV) compounds, on the other side, cisplatin possesses lower activity than both triphenyl- and diorganotin(IV) compounds. Contrarily, dimethyltin(IV) (**Sn19**) and trimethyltin(IV) compounds (**Sn20**), known as very poisonous, expressed an activity that is at least two times lower than cisplatin, but higher than titanocene derivatives containing the same thiolato or carboxylato ligands (**Ti17**, **Ti18** or **Ti29–Ti31**).

2.2.3.2. Organotin(IV) compounds and mode of action on the tumor cells

Sn14 was found very active against cisplatin-resistant cell line DLD-1 and was used further for mechanistical studies on the mentioned cell line (Figure 18)^[K30]. **Sn14** is causing cell cycle perturbations shrinking the number of the cells in G1 and G2/M

2. METALLOCOMPOUNDS

phases (46 and 40%, respectively) associated with the increase of apoptotic cells in Sub-G1 phase. The compound **Sn14** was found to induce apoptosis faster than cisplatin within 6 h of action, but provoke a different apoptosis pathway. Cisplatin is activating mitochondrial (intrinsic) and cell death receptor apoptosis pathway. On the other hand, **Sn14** is inducing only the activation of cell death receptor apoptosis pathway on DLD-1 cell line.

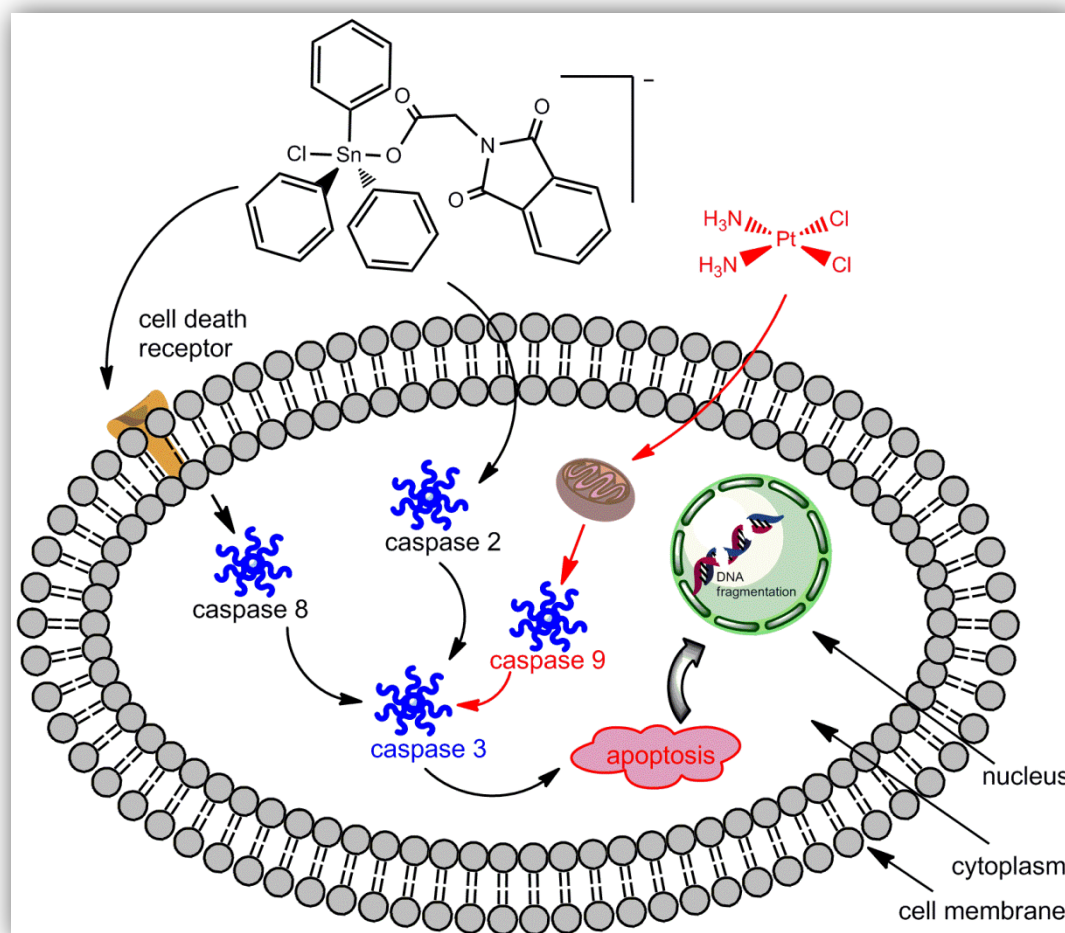


Figure 18. Induction of apoptosis by **Sn14** on DLD-1 cell line.

2.3. Conclusions

Different platinum(II), platinum(IV), palladium(II), titanium(IV) and tin(IV) compounds were synthesized and characterized. Platinum(II), platinum(IV) and palladium(II), complexes were obtained in the reaction of chloridoplatinates and chloridopalladates with respective ligand precursors. Titanium(IV) and tin(IV) compounds were obtained under inert conditions using different titanocene or organotin(IV) starting compounds

2. METALLOCOMPOUNDS

and various ligands. The constitution of the compounds has been proven by elemental analyses. The structure of the compounds has been determined using multinuclear NMR and IR spectroscopies, mass spectrometry as well as for some compounds with X-ray structural analyses.

Structure–activity relationships for R₂edda-type ligand precursors, platinum(II), platinum(IV) and palladium(II) complexes expressed some correlation. Substituent R, metal center (platinum, palladium) as well as the oxidation state [platinum(II) vs. platinum(IV)] remarkably influence the antitumoral activity. Mostly, the activity is increasing in the following order: R₂edda-type ligand precursors < palladium(II) complexes < platinum(II) complexes < platinum(IV) complexes. Within each group of compounds the activity is increasingly depending on ligand lipophilicity. Namely, the more lipophilic the ligand, the higher the cytotoxicity that is observed. Deviation from these findings are observed against chronic lymphocytic leukaemia cells, where platinum(II) complexes were found to be the most effective, followed by palladium(II) and platinum(IV) complexes. Investigations on non-malignant cells indicate that those compounds are significantly less toxic.

The biological activity of platinum(IV) complexes involves in most cases their reduction because platinum(IV) complexes might not bind directly to DNA or other biological targets, in contrast to their platinum(II) counterparts^[109]. Whereas in some cases binding of platinum(IV) to DNA or DNA fragments was proved^[93;110;111]. [Pt(R₂edda)Cl₄] complexes are expected to be stable enough in biological milieu similar to satraplatin, revealing their therapeutic potential for oral application. A higher antiproliferative effect of platinum(IV) complexes compared with corresponding platinum(II) complexes leads to the assumption that platinum in higher oxidation state in [Pt(R₂edda)Cl₄] complexes could have some additional *in vitro* activity. On the other side, similar redox potential to satraplatin, which is *in vivo* reduced to platinum(II) species^[5,9], indicates that these complexes act as prodrugs. Thus, it is therefore likely that [Pt(R₂edda)Cl₄] complexes require *in vivo* reduction to the kinetically more labile, and therefore reactive, platinum(II) species.

[Pt(R₂edda)Cl₄] complexes are inducing dose-dependent and cell-type specific *in vitro* activity. The key role of platinum complexes containing R₂eddp or (S,S)-R₂eddip ligands (from the group of **Pt6–Pt15**) in cell death of HCT116 cells is triggering the

2. METALLOCOMPOUNDS

caspase-dependent apoptotic pathway (e.g. **Pt8**, **Pt11** or **Pt15**). Also, those compounds are causing intensive oxidative stress and autophagy in HCT116 cells. These series of platinum(IV) complexes are found less active against human glioblastoma U251 or mouse malignant melanoma B16 cell lines than other complexes containing (S,S)-R₂eddch ligands (**Pt24–Pt27**). Cell death induced by compounds **Pt24–Pt27** is related to induction of the reactive oxygen species with characteristic signs of necrotic pathway.

Complex **Pt26** possesses greater *in vitro* inhibition in direct comparison with **Pt1** against melanoma B16 cell line. Furthermore, both complexes are more active than cisplatin by factor 2 (**Pt1**) and 10 (**Pt26**) against same cell line. On the other hand, the greater advantage of **Pt1** over **Pt26** is the induction of the favoured mode of cell death – apoptosis. Preferably, the *in vitro* properties of **Pt1** against cisplatin resistant B16 cell line, reflected in higher antitumor activity and higher selectivity toward tumor cells in comparison with cisplatin as well as induction of apoptosis, gave a promising candidate for further *in vivo* investigations.

Upon treatment of synergic C57BL/6 mouse model, in which the tumor was developed by implanting B16 melanoma cells with **Pt1**, some benefits were noticed. Thus, the tumor volume was reduced by 75% in comparison to control. On contrary, during *in vivo* investigations with cisplatin 3 animals died because of intoxication. Additionally, animals treated with **Pt1** did not show nephrotoxicity signs in contrast to cisplatin-treated animals. Along with improved antitumor activity and less side effects (such as nephrotoxicity) compared to cisplatin, complex **Pt1** represents the encouraging starting point for an upcoming exploration of this type of platinum complexes in cancer treatment. Although the present results show a significantly increased efficacy of **Pt1** in suppressing the growth of B16 tumor cells *in vivo* compared with cisplatin, it should be pointed out that the treatment of synergic C57BL/6 mouse model with **Pt1** did not result in the complete suppression of the tumor cells with the dose and schedules used in this study.

Titanocene and *ansa*-titanocene complexes are mainly (exception **Ti8**, not active) more active against human myelogenous leukaemia K562 than against human adenocarcinoma HeLa or malignant melanoma Fem-x cell lines. *In vitro* cytotoxic activity can be altered by modifying the cyclopentadienyl ring, substituents on silicon atom

2. METALLOCOMPOUNDS

(substitution pattern at *ansa*-bridge) or anionic ligands in the titanocene/*ansa*-titanocene dichloride complex. Titanocene derivatives are found to be cell type-specific. A modifying structure of the reference compounds $[\text{Ti}(\text{Cp})_2\text{Cl}_2]$, $[\text{Ti}(\text{MeCp})_2\text{Cl}_2]$ and $[\text{Ti}(\text{Cp})\{\text{Me}_3\text{Si}(\text{Cp})\}\text{Cl}_2]$, promising derivatives with regard to considerable cytotoxic activity, higher than that of reference compounds toward different tumor cell lines, were obtained. Due to the better tolerance of titanium(IV) over platinum(II) in the biological system and despite less antitumoral activity of titanium(IV) derivatives than cisplatin, these compounds seem to have a potential applicability in cancer therapy.

From organotin(IV) compounds, tetraorgano- and mononuclear or polynuclear triphenylstannanes (**Sn2–Sn4**, **Sn9–Sn18**) have been found as the most cytotoxic agents. Their superiority over diphenyl- (**Sn5–Sn8**), dimethyl- (**Sn19**) or trimethyltin(IV) (**Sn20**) resulted mainly in IC_{50} values in nM range, while compounds of other metals exhibited activity (IC_{50}) in mM range only. On the other hand, diphenyltin(IV) compounds showed greater selectivity toward normal and cancer cells. However, organotin(IV) compounds (with exception of compounds containing methyl groups, **Sn19** and **Sn20**) possess higher *in vitro* activity than cisplatin (IC_{50} cisplatin/ IC_{50} **Sn9** = 68–124). In direct comparison of organotin(IV) compounds and titanocene derivatives bearing the same ligand pattern in the light of anticancer activity superiority belongs to organotin(IV) compounds.

Further studies revealed that **Sn14** is causing apoptosis in cisplatin-resistant colon carcinoma DLD–1 cell line in a different mode than cisplatin. **Sn14** is affecting cell death receptor, while cisplatin affects mitochondrial apoptosis pathway.

3. NANOMATERIALS AS DRUG CARRIERS

Two different approaches were performed: a) incorporation of a water-insoluble platinum(II) complex into liposomes and b) functionalization of mesoporous silica with metal compounds (titanocene derivatives and organotin(IV) compounds).

3.1. Preparation of nanomaterials

3.1.1. Liposomal formulation of THP-C11

For more information see reference K32 (Appendix 12).

Formulation of a novel liposome delivery system formed from Lipoid S 75 and 2-[4-(tetrahydro-2H-pyran-2-yloxy)-undecyl]-propane-1,3-diamminedichloridoplatinum(II), **THP-C11** has been performed (Figure 19). Liposomes were prepared by conventional well-established lipid film method^[112]. The crude suspensions were extruded through polycarbonate membranes with 400 and 100 nm pore sizes. The **LipoTHP-C11** was characterized by light microscopy, dynamic light scattering and asymmetrical flow field-flow fractionation. The size of the liposomes in **LipoTHP-C11** was around 125 nm and for empty liposomes 118 nm. Stability studies showed that the new formulation was stable at 4 °C for more than two months.

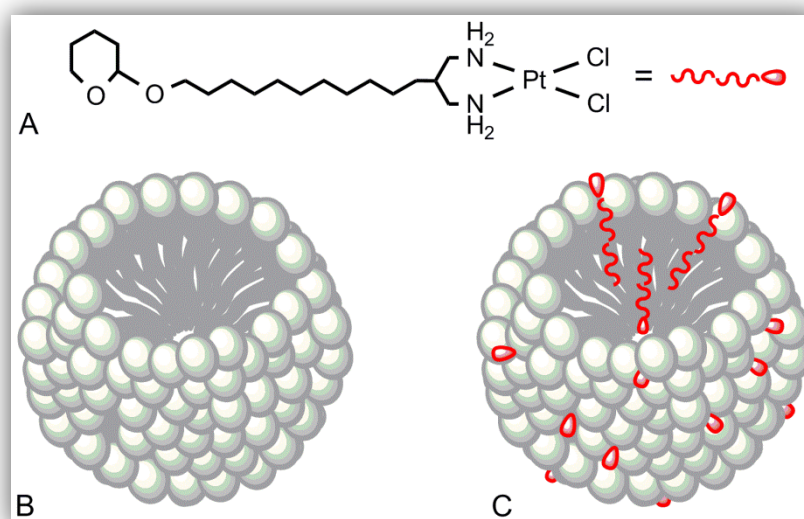


Figure 19. **THP-C11** (A), empty (B) and loaded liposomes (**LipoTHP-C11**, C).

3.1.2. Mesoporous silica grafted with titanocene derivatives and organotin(IV) compounds

For more information see references K33–K37 (Appendices 13, 14).

MCM-41 was prepared according to the method of Landau *et al.* using a hydrothermal crystallization^[113]. **SBA-15** was prepared using a poly(alkaline oxide) triblock copolymer surfactant in an acidic medium, according to the method of Zhao *et al.*^[114] **SBA-15p** was prepared by functionalization of **SBA-15** particles by covalent grafting with 3-chloropropyltriethoxysilane (CPTS). A solution of the metal compound was added to dehydroxylated mesoporous silica (**MCM-41**, **SBA-15** or **SBA-15p**). The novel nanomaterials (classified according to the literature^[115;116]; Figure 20) were characterized by powder X-ray diffraction analyses, X-ray fluorescence analyses, nitrogen gas sorption, multinuclear MAS NMR spectroscopy, SEM and TEM analyses.

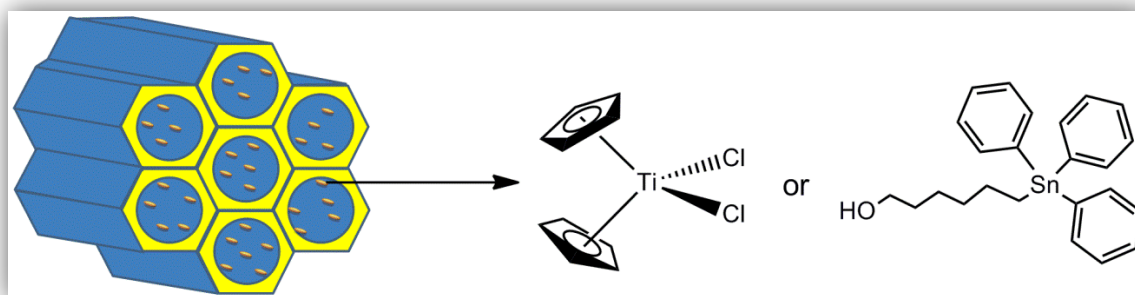


Figure 20. Mesoporous silica functionalized with metal compounds.

3.2. Biological activity of novel materials containing metal compounds

In recent years, nanomedicine (applied nanotechnology in medicine) has gained increasing attention, exclusively in treatment and diagnosis, monitoring, and control of biological systems^[117]. Within possible applications of nanomedicine the most prominent position deserves the use of various nanomaterials as drug delivery vehicles for RNA/DNA and imaging agents. The purpose of using nano-vehicles (liposomes, mesoporous silica, etc.) is to enhance the *in vivo* effectiveness of drugs (e.g. those with low solubility, availability, low selectivity). Liposomes as well as mesoporous silica were used as drug carrier within this study^[K32].

3.2.1. Liposomes as drug carriers for water-insoluble platinum based drugs

For more information see reference K32 (Appendix 12).

From the recent *in vitro* experiments was found that **THP-C11**, platinum(II) compound, is very active against testicular germ cell tumors (TGCT). Namely, **THP-C11** is able to overcome cisplatin resistance in TGCT cells^[118]. But the main limitation for examinations and consideration as potential antitumoral drug is the solubility of **THP-C11**. Namely, insolubility in water, but solubility in chloroform and dimethylformamide make this candidate not suitable for *in vivo* experiments even at a very low nonhepatotoxic dose of dimethylformamide^[119]. It has been shown that structural variations [shorter spacer between THP and *cis*-dichloridoplatinum(II) fragment, e. g. (CH₂)₄] led to *in vitro* deactivation of the **THP-C11** (Figure 19)^[118]. Thus, should be evaluated will liposomal formulation of the **THP-C11** overcome this problem.

3.2.1.1. Liposomal cytotoxicity

At first, the liposomal formulations (empty and **LipoTHP-C11**, Figure 19), along with cisplatin and **THP-C11** dissolved in DMF were *in vitro* tested against cisplatin-sensitive H12.1 and cisplatin-resistant 1411HP TGCT cell lines^[K32]. **THP-C11** and also **LipoTHP-C11** inhibit growth of the H12.1 and 1411HP TGCT cells faster than cisplatin within 2 h treatment. Thus, for 50% inhibition of H12.1 and 1411HP cell growth by 1.4 and 9.3 times lower concentration, respectively, of **LipoTHP-C11** (5.0 and 3.5 μ M) than cisplatin is needed. After 96 h of action, **LipoTHP-C11** expressed higher cytotoxicity than cisplatin (2.1 vs. 2.8 μ M) on cisplatin-resistant 1411HP TGCT cells. The cytotoxicity of **LipoTHP-C11** formulation is caused by the presence of the **THP-C11** since liposomes alone are not active.

To assess the cytotoxicity against several other cells lines from different histogenical tumors, empty and **LipoTHP-C11** liposomal formulations as well as cisplatin and **THP-C11** dissolved in DMF were tested against 518A2 (melanoma), A549 (lung carcinoma), HT-29 (human colonic adenocarcinoma), MCF-7 (human breast adenocarcinoma) and SW1736 (human anaplastic thyroid carcinoma)^[K32]. Also here should be mentioned that liposomes alone did not show activity against investigated cell lines. Alone **THP-C11** showed better activity than cisplatin against MCF-7 and SW1736 (0.5/2.0 μ M and 1.2/3.2 μ M, respectively), comparable against 518A2 and A549 (1.3–

1.5 μM), but lower on colonic adenocarcinoma HT-29 (1.2 vs. 0.6 μM). **LipoTHP-C11** had similar inhibition rates as **THP-C11** on A549 and SW1736. Contrarily, against 518A2, HT-29 and MCF-7 (2.0–2.5 μM) cell lines **LipoTHP-C11** was found to be less active than **THP-C11**. In direct comparison with cisplatin, **LipoTHP-C11** was found to be 2.6 times more active against anaplastic thyroid carcinoma SW1736 (1.1 μM), but similar activity against A549 and MCF-7 was observed. Lower activity than cisplatin was found when 518A2 and HT-29 cell lines were treated with **LipoTHP-C11**.

3.2.1.2. Liposomal toxicity

Furthermore, toxicity of the liposomal formulations as well as **THP-C11** and cisplatin on fibroblast normal cells (NF) has been determined (IC_{50} : 2.1 \pm 0.3 μM , **THP-C11**; 1.8 \pm 0.1 μM , cisplatin; 3.4 \pm 0.8 μM , **LipoTHP-C11**)^[K32]. Only in the case of HT-29 cell line higher selectivity of cisplatin than **LipoTHP-C11** and **THP-C11** has been observed (selectivity indices: 2.9 vs. 1.2 and 1.8, respectively). **LipoTHP-C11** and **THP-C11** expressed higher selectivity than cisplatin on other tumor cell lines than to fibroblasts (exception 518A2: **LipoTHP-C11** and cisplatin exhibited comparable selectivity). Cisplatin showed higher affinity to kill normal than SW1736 tumor cells, but in case of **LipoTHP-C11** (selectivity index: 2.8) and **THP-C11** (selectivity index: 1.8) the highest selectivity was found.

With this study, it is shown that for water-insoluble potential drugs an alternative than structural variation, namely, liposomal formulation might be very useful for the further consideration in *in vivo* testings, which are on the way under present investigations. This liposomal formulation of water-insoluble antitumor agents may retain both cytotoxic and toxic properties avoiding usage of solvents not allowed for *in vivo* experiments.

3.2.2. First steps in nanostructured mesoporous materials as anticancer drug carrier vehicles

For more information see references K33–K37 (Appendices 13, 14).

Unique features (ordered pore network, surface silanol groups that can be functionalized, high-pore volume and high-surface area) make mesoporous materials excellent

candidates for controlled drug–delivery systems^[78]. An intensive research has been carried out, mainly focussing on their possible application as carriers for the delivery of ibuprofen, nitrofurazone and gentamicin. Modification of mesoporous materials by the adsorption of some organic compounds led to the development of new biomaterials with cytotoxic application against human cancer cells^[120].

3.2.2.1. Nanostructured mesoporous materials grafted with titanocene derivatives

Novel research evaluates the cytotoxic activity of new materials^[K35] functionalized with $[\text{Ti}(\eta^5\text{-C}_5\text{H}_5)_2\text{Cl}_2]$ (**MCM-41M1**), $[\text{Ti}(\eta^5\text{-C}_5\text{H}_5)(\eta^5\text{-C}_5\text{H}_4\text{Pr}^i)\text{Cl}_2]$ (**MCM-41M2**), $[\text{Ti}(\eta^5\text{-C}_5\text{H}_5)(\eta^5\text{-C}_5\text{H}_4\text{Bu}^t)\text{Cl}_2]$ (**MCM-41M3**) and $[\text{Ti}(\eta^5\text{-C}_5\text{H}_5)\{\eta^5\text{-C}_5\text{H}_3(\text{SiMe}_3)_2\}\text{Cl}_2]$ (**MCM-41M4**) complexes (Figure 21)^[K34].

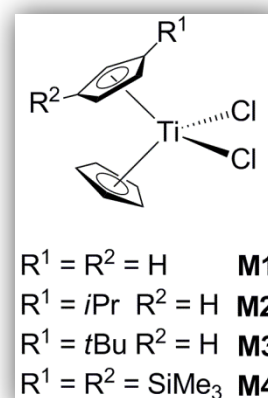


Figure 21. Titanocene derivatives grafted on **MCM-41**.

The mesoporous material **MCM-41** is not active against the studied human cancer cells (see Table 2). On the other hand, surfaces functionalized with titanocene derivatives, **MCM-41M1–MCM-41M4**, were active toward human cancer cell lines, such as adenocarcinoma HeLa, human myelogenous leukaemia K562 and human malignant melanoma Fem-x. Modification of **MCM-41** material by grafting with titanocene complexes led to a cytotoxic activity of modified surfaces being relatively higher to that reported previously for mesoporous materials modified with organic drugs^[120].

The cytotoxicity of the materials **MCM-41M1–MCM-41M3** was very similar on all the studied cancer cells, however, **MCM-41M4** showed M_{50} values that indicate the highest activity of all the studied materials, being two to three times more cytotoxic than **MCM-41M1–MCM-41M3**. The similar tendency was observed when the metal complexes **M1–M4** were analyzed, indicating that the cytotoxicity of the studied materials may be due to the release of the corresponding metal complex and is probably not due to the particle action.

3. NANOMATERIALS AS DRUG CARRIERS

Table 2. Cytotoxicity values $MC_{50}^{\ddagger}/IC_{50}$ of the titanocene derivates and corresponding functionalized materials against HeLa, K562, Fem-x, unstimulated and stimulated PBMC.

Cell line	HeLa	K562	Fem-x	PBMC-PHA	PBMC+PHA
Sample	MC_{50} [$\mu\text{g/ml}$]				
MCM-41M1	897 \pm 21	874 \pm 42	977 \pm 63	>1000	670 \pm 68
MCM-41M2	821 \pm 98	974 \pm 46	888 \pm 4	>1000	927 \pm 73
MCM-41M3	751 \pm 88	723 \pm 90	844 \pm 34	>1000	779 \pm 72
MCM-41M4	511 \pm 78	218 \pm 23	515 \pm 16	313 \pm 72	305 \pm 7
MCM-41	>1000	>1000	>1000	nd ^a	nd
	IC_{50} [μM]				
M1	>200	>200	177.7 \pm 4.9	>200	>200
M2, M3	>200	>200	>200	>200	>200
M4	15.3	10.5 \pm 1.9	59.8 \pm 4.1	10.5 \pm 2.0	8.2 \pm 0.8

^a nd = not determined.

3.2.2.2. Material and content-dependence on the final cytotoxicity of nanostructured mesoporous materials

Furthermore, titanocene(IV) complexes presented on Figure 22 have been used for the functionalization of the **MCM-41** and/or **SBA-15** mesoporous silica^[K35]. It was observed an increase of the functionalization rate (with ca. 3% wt Ti) by the incorporation of thiolato ligands with $-\text{Si}(\text{OMe})_3$ or $-\text{Si}(\text{OEt})_3$ groups in their structure. As mentioned above, unmodified **MCM-41** is not active against the studied human cancer cell lines; the functionalized surfaces **MCM-41M5** and **MCM-41M6** were active (Table 3).

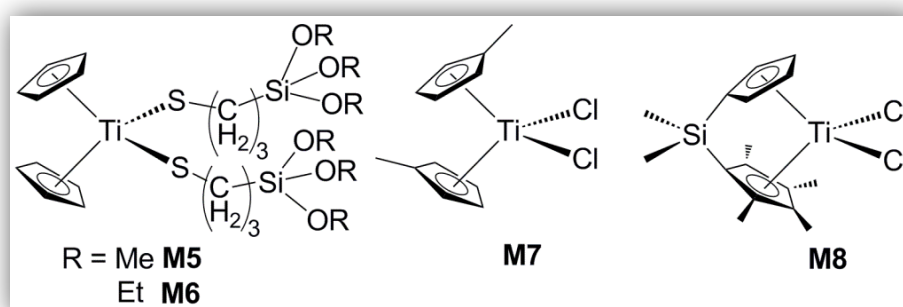


Figure 22. Titanocene derivates grafted on **MCM-41** (**MCM-41M5–MCM-41M8**) and on **SBA-15** (**SBA-15M7** and **SBA-15M8**).

[‡] Quantity of material in $\mu\text{g/ml}$ needed to inhibit normal cell growth by 50%.

3. NANOMATERIALS AS DRUG CARRIERS

Table 3. Cytotoxicity values, MC_{50} [$\mu\text{g/ml}$], of the **MCM-41** and **SBA-15** functionalized materials against HeLa, K562, Fem-x, unstimulated and stimulated PBMC.

Cell line Sample	HeLa	K562	Fem-x	PBMC-PHA	PBMC+PHA
MCM-41M5	743 \pm 44	784 \pm 19	631 \pm 51	>1000	>1000
MCM-41M6	685 \pm 60	704 \pm 30	573 \pm 76	>1000	>1000
MCM-41M7	912 \pm 10	683 \pm 50	555 \pm 77	>1000	>1000
SBA-15M7	508 \pm 63	338 \pm 18	328 \pm 18	>1000	457 \pm 40
MCM-41M8	861 \pm 18	536 \pm 51	464 \pm 52	>1000	918 \pm 130
SBA-15M8	671 \pm 48	456 \pm 36	309 \pm 42	>1000	934 \pm 178
SBA-15	>1000	>1000	>1000	nd ^a	nd
MCM-41	>1000	>1000	>1000	nd	nd

^a nd = not determined.

The cytotoxicity of **MCM-41M5** and **MCM-41M6** was very similar on all the studied cancer cells, however, **MCM-41M1** (1.1% wt Ti) showed MC_{50} values that indicated the lowest activity of all the analyzed materials on all the studied cells. Thus, a clear dependence of the titanium content of the functionalized **MCM-41** on the cytotoxic activity on human cancer cell lines has been reported^[K35].

Modification of materials **MCM-41** and **SBA-15** by grafting with titanocene complexes **M7** and **M8** led also to active materials when compared with unmodified ones. Surfaces **SBA-15M7** and **SBA-15M8** are the most active on all the human cancer cells. It was observed a slight selectivity of material **SBA-15M8** between tumor and normal human cells.

3.2.2.3. Proposed mechanism of action of nanostructured mesoporous materials grafted with titanium(IV) complexes

Two reasonable mechanisms of action of the novel materials are shown in Figure 23. Nanoparticles may enter the cell by endocytosis^[121;122] and inside the cells release of the titanocene derivative (or their hydrolysis product) may follow. On the other hand, in the extracellular matrix from the nanomaterials a leaking of the titanocene derivative (or its hydrolytic product) may occur. Both mechanisms are plausible and seem to occur (*vide infra* 3.2.2.6). In the extracellular matrix, after release and hydrolysis of

3. NANOMATERIALS AS DRUG CARRIERS

supported titanocene complexes, titanium hydrolytic species may reach the cells assisted by the major iron transport protein transferrin^[123–126].

Endosome action may release titanium hydrolytic species, which assisted with adenosine-5'-triphosphate (ATP), would reach the DNA in the cell nucleus (Figure 23)^[127]. However, DNA seems to be the biological target of titanium hydrolytic species released by these materials^[120–130]. The activity of grafted nanostructured mesoporous materials with titanocene derivatives might be related to that suggested for titanocene complexes in solution.

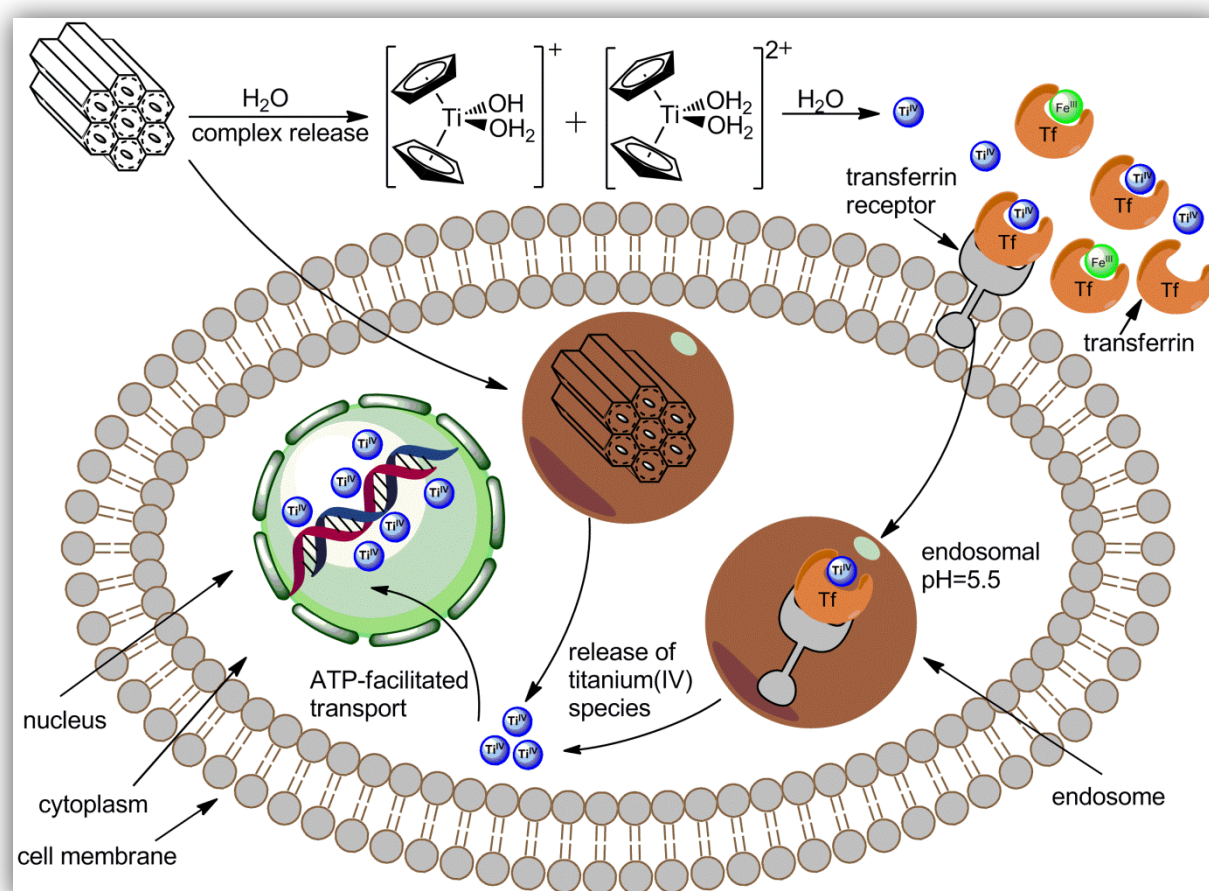


Figure 23. Possible mechanism of action of mesoporous silica grafted with titanocene derivatives.

3.2.2.4. Nanostructured mesoporous materials grafted with organotin(IV) compounds

Inspired by the recent results, on one hand, with mesoporous nanomaterials grafted with titanocene compounds, and on the other hand, with *in vitro* cytotoxicity and selectivity of organotin(IV) complexes, preliminary investigations on functionalized

SBA-15 materials grafted with 3-(triphenylstannyl)propan-1-ol (**M9**, Figure 24) were performed (**SBA-15pM9**)^[131]. Furthermore, 6-(triphenylstannyl)hexan-1-ol (**M10**, Figure 24)^[K37] was prepared as well as grafted on modified **SBA-15** mesoporous nano-materials (**SBA-15pM10**) and used for further *in vitro* and *in vivo* investigations.

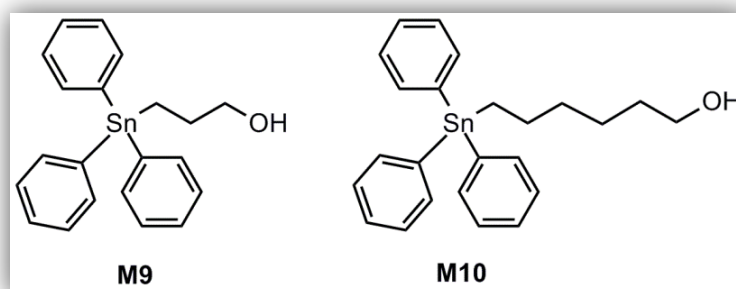


Figure 24. 3-(Triphenylstannyl)propan-1-ol (**M9**) and 6-(triphenylstannyl)hexan-1-ol (**M10**) compounds.

3.2.2.5. Cytotoxicity of nanostructured mesoporous materials grafted with 3-(triphenylstannyl)propan-1-ol

Mesoporous nanomaterial **SBA-15** was first functionalized with 3-chloropropyltriethoxysilane (**SBA-15p**) and then grafted with compound **M9**^[131]. In the first anti-tumoral experiments, the *in vitro* antiproliferative activity of **M9** as well as nanomaterials was investigated against two cisplatin-sensitive A549 (lung carcinoma) and A2780 (ovarian cancer) and one cisplatin-resistant DLD-1 (colon carcinoma) cell lines. Both, **SBA-15** and **SBA-15p**, were found inactive. Compound **M9** and nanomaterials **SBA-15pM9** exhibited dose-dependent activity and their cytotoxic results are presented in Table 4.

Table 4. Cytotoxicity values on A549, DLD-1 and A2780 of the organotin(IV) compound **M9** and functionalized materials. Given are values for **M9**: IC₅₀ in μM ; nanomaterials: M₅₀ in $\mu\text{g/ml}$; **M9**^a: IC₅₀ in nM.

Compound/Material	A549	DLD-1	A2780
M9 (molecular compound)	3.80 ± 0.01	3.67 ± 0.01	2.77 ± 0.01
SBA-15pM9	6.81 ± 0.09	9.73 ± 0.23	7.16 ± 1.42
M9^a (grafted compound)	0.25	0.36	0.26
Cisplatin	1.51 ± 0.02	5.14 ± 0.12	0.55 ± 0.03
SBA-15p	> 500	> 500	> 500
SBA-15	> 500	> 500	> 500

^a Recalculated from Sn quantity grafted on **SBA-15p** (experimental value).

M9 was found to be more effective against cisplatin-resistant cell line DLD-1, but lower activity was observed in case of cisplatin-sensitive A549 and A2780 cell lines. Astonishingly, cytotoxicity of the **SBA-15pM9** was found much higher than that of titanocene derivatives grafted on **SBA-15** or **MCM-41**.

3.2.2.6. Mechanism of action of SBA-15p grafted with 3-(triphenylstannyl)propan-1-ol

For answering questions related to mechanism of action, metal uptake study was performed^[131]. The A2780 cells were treated with **M9**, **SBA-15p** and **SBA-15pM9** and the cells were subjected to tin and silicon content determination. Proposed mechanism is shown in Figure 25.

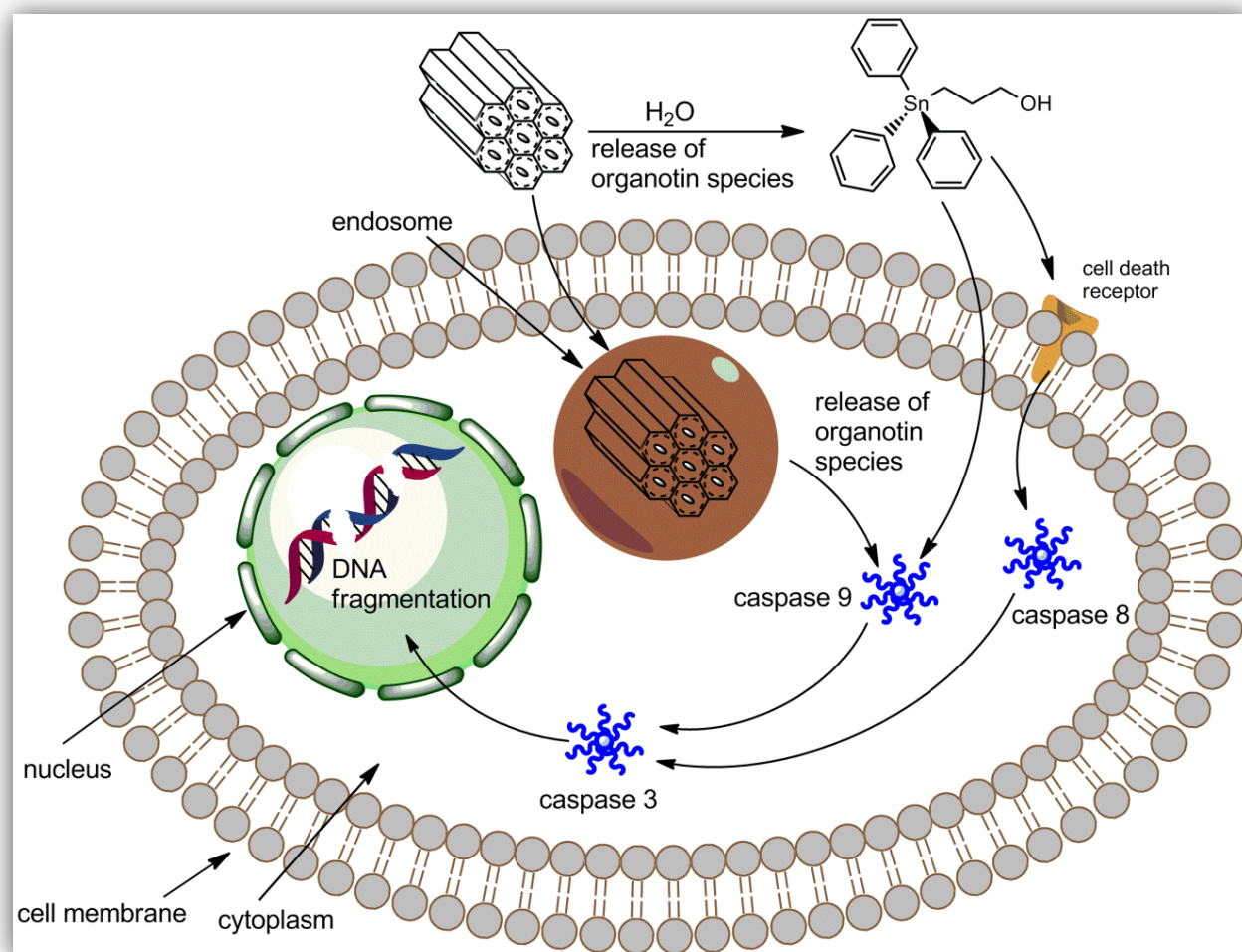


Figure 25. Proposed mechanism of action of **SBA-15pM9** on A2780 cell line.

The compound **M9** enters the cell in high concentration (tin uptake: 440 ppm). The cells treated with **SBA-15p** showed more than three times higher uptake of silicium (1500 ppm), while **SBA-15pM9**, even higher than **SBA-15p** (1900 ppm), strongly confirms that the nanomaterials are entering the cells. Furthermore, tin uptake experiment from the cells treated with **SBA-15pM9** (tin content: 120 ppm) indicates disagreement between the expected amount of tin (83 ppm, recalculated from tin content in **SBA-15pM9**) for around 30%. Thus, the release of **M9** from **SBA-15pM9** also occurs in extracellular matrix and free **M9** is entering the cell.

M9 and corresponding grafted nanomaterial are found to induce apoptotic mode of cell death (acridine orange/ethidium bromide assay) by inducing activation of caspase initiators 2, 8 and 9 as well as caspase executor 3 within 2 h of action, thus affecting cell death receptor and mitochondrion.

3.2.2.7. Cytotoxicity of nanostructured mesoporous materials **SBA-15p** grafted with 6-(triphenylstannyl)hexan-1-ol

Organotin(IV) compound **M10**, corresponding grafted mesoporous **SBA-15pM10** and precursor material **SBA-15p** were tested for cytotoxic activity against melanoma B16 cell line by MTT and CV tests (48 and 72 h; Figure 26)^[K37]. MTT assay measures mitochondrial respiration and CV DNA content in the cell. As shown in previous studies on A2780 cell line (see 3.2.2.5) it was also found that **SBA-15p** is inactive against melanoma B16 cell line. The proliferation of the B10 cells upon the treatment with **M10** or **SBA-15pM10** displayed a dose-dependent manner (Figure 26).

By examination of the IC_{50} values obtained from MTT and CV tests for **M10** disagreement between these two assays can be observed (IC_{50} : 20 μ M, MTT; 40 μ M, CV) indicating disturbance of mitochondrial respiration followed by reduction of cellular viability. B16 cells treated with **SBA-15pM10** showed quite good agreement between these two assays (IC_{50} : 2.0 μ g/ml, MTT; 2.6 μ g/ml CV). In this case, mitochondrial respiration is not targeted by **SBA-15pM10** and decrease of cell respiration is in correlation with number of viable cells. Both **M10** as well as **SBA-15pM10** are stronger cytotoxic agents than cisplatin (IC_{50} : 67 μ g/ml, MTT; 65 μ g/ml CV).

3. NANOMATERIALS AS DRUG CARRIERS

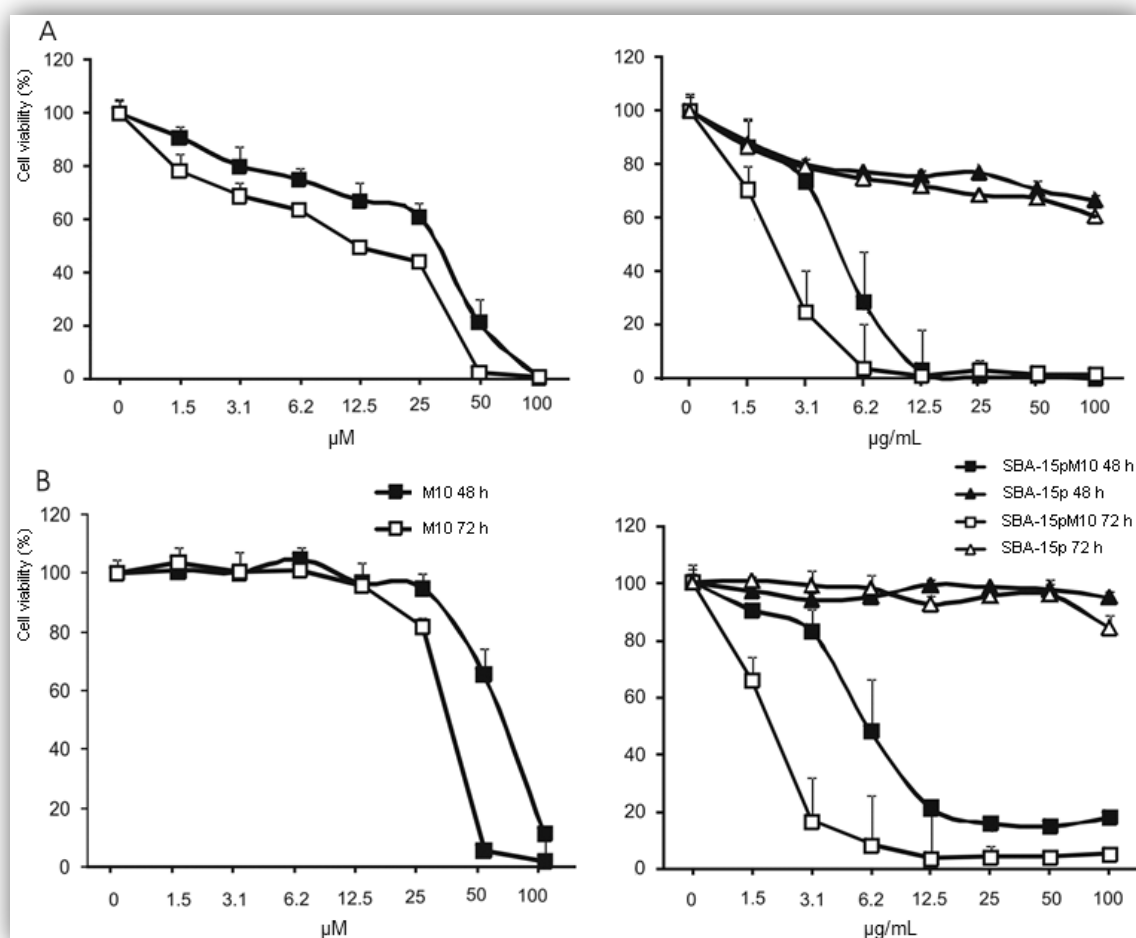


Figure 26. *In vitro* cytotoxicity of **M10**, **SBA-15p** and **SBA-15pM10** against mouse melanoma B16 cell line. The data are presented as mean from three independent experiments.

3.2.2.8. The first *in vivo* study of nanomaterials grafted with 6-(triphenylstannyl)hexan-1-ol

Melanoma tumor model was developed by inoculating B16 cells in syngeneic C57BL/6 mice and treatment was started when tumors were palpable (Figure 27)^[K37]. Mice were divided into four groups: 1. Control – received PBS; 2. **SBA-15p** – 8 mg/kg; 3. Cisplatin – 4 mg/kg; 4. **M10** – 8 mg/kg and 5. **SBA-15pM10** – 8 mg/kg (body weight). Within 28 days (at this time animals were sacrificed), in the control group the maximum allowed tumor volume developed in 4 of 5 animals.

Comparable tumor volume was observed in the group treated with **SBA-15p**. In cisplatin animals group – despite the fact that 2 animals died during the experiment – other 3 developed high tumor volume. Treatment with **M10** slightly diminished tumor

progression. Oppositely, in animals handled with **SBA-15pM10** tumor progression was almost completely abolished. Therefore, this trial indicated the strong therapeutic potential of **SBA-15pM10**.

Urine from tested animals was analyzed regarding possible toxic effects of used agents. As expected, only animals treated with cisplatin exhibited indications of nephrotoxicity implied with the occurrence of erythrocytes and leukocytes in urine. In addition, the level of the proteins in urine rose.

SBA-15pM10 possesses astonishingly higher activity than cisplatin *in vivo* eliminating tumor in syngeneic C57BL/6 mouse without visible side effects.

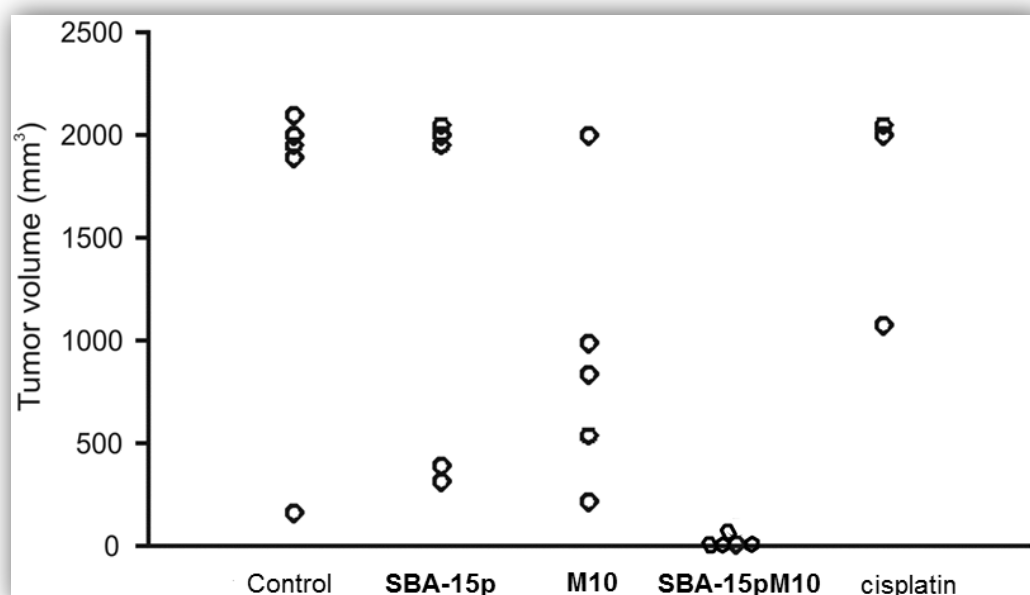


Figure 27. Efficiency of **M10** and **SBA-15pM10** against mouse melanoma *in vivo*.

3.2.2.9. Mechanisms of antimelanoma action of SBA-15 grafted with 6-(triphenylstannyl)hexan-1-ol

Motivated by results of highly promising *in vivo* studies the following step was to determine the mechanism of action of **SBA-15pM10** against B16 melanoma cell line (Figure 28)^[K37]. Melanoma cells treated with **M10** as well as with **SBA-15pM10** showed notably a higher quantity of hypodiploid cells. **SBA-15p** did not influence the distribution of the cells in different phases of cell cycle. Furthermore, **M10** and **SBA-15pM10** prompted early apoptosis (double staining by Ann/PI). On the other hand, **SBA-15p** just marginally raised early apoptotic cells. Intense caspase activation was

3. NANOMATERIALS AS DRUG CARRIERS

detected upon treatment with **M10** and **SBA-15pM10**, but not in **SBA-15p** treated melanoma cells. In addition, **SBA-15pM10** promoted a strong autophagy manifested by an increased number of autophagic vesicles. Autophagic response might be under some conditions dying pathway, but mainly it is the cytoprotective mechanism of the cells what was the case in treatments of B16 cells with **SBA-15pM10**.

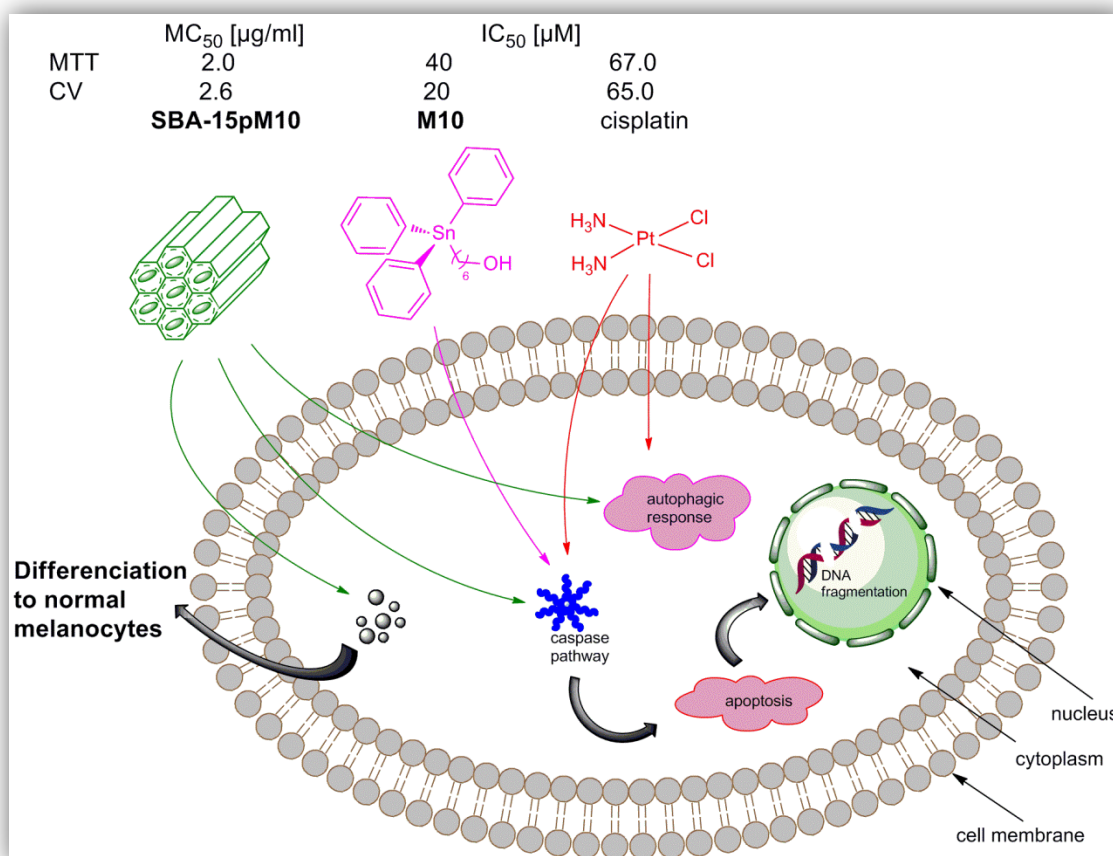


Figure 28. Proposed mechanism of action of **SBA-15pM10** on B16 cell line.

Morphology of the B16 cells treated with **M10** or **SBA-15pM10** was remarkably changed (Figure 29, upper microphotographs). Thus, round melanoma cells are being transformed into flat cells with enlarged cytoplasm volume accompanied by membrane growth resembling dendrits. All these morphological changes point toward differentiation process. Nevertheless, only cells treated with **SBA-15pM10** exhibited an enhanced granularity in cytoplasm implying that differentiation of the melanoma cells into primary melanocytes occurred. Similarly, diazepam and clonazepam (benzodiazepine drugs) are inducing changes in phenotype of B16 cells which are related to the loss of the malignancy. Upon treatment with those drugs the cells are morphologically

3. NANOMATERIALS AS DRUG CARRIERS

changed, the synthesis of melanine increased and activity of γ -glutamyl transpeptidase (enzyme related to metastatic potential of melanoma tumor) decreased^[132]. Furthermore, aloe emodin is also inducing transformation of melanoma B16 cells into primary melanocytes what is reflected by morphological changes (increase of the cytoplasm volume, presence of the high granularity in cytoplasm and membrane dendrits) as well as increased production of melanin and greater activity of tyrosinase (key enzyme in the synthesis of mentioned pigment)^[132–135].

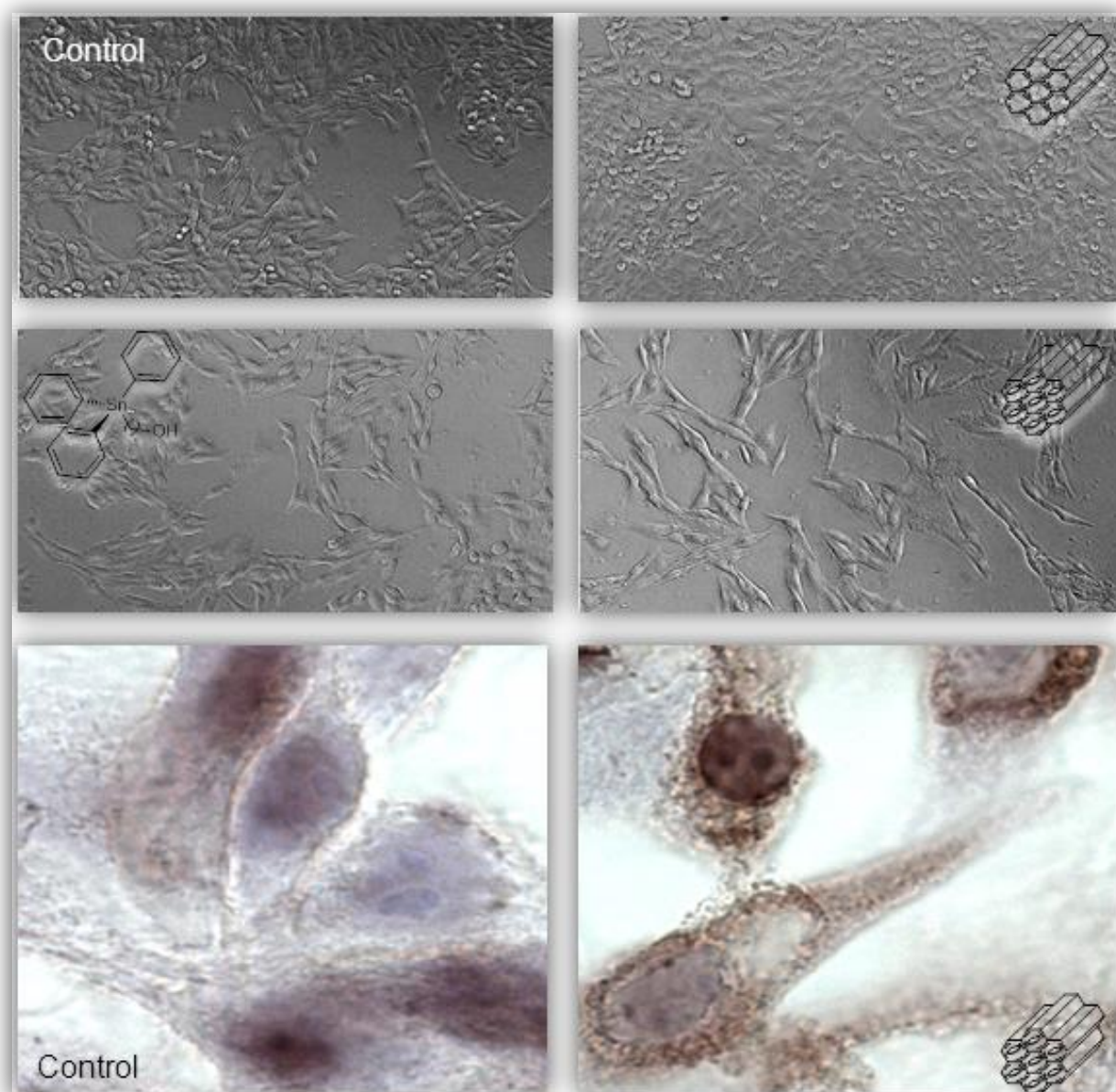


Figure 29. Differentiation of melanoma cells: Light microscopy microphotographs (upper), Mayer's haematoxylin stained cells (lower).

3. NANOMATERIALS AS DRUG CARRIERS

Likewise, **SBA-15pM10** strongly increased tyrosinase activity and raised melanin quantity in the cells. All these findings verified the assumption that enriched granularity is the result of the upregulated melanin synthesis. Additionally, numerous melanosomes (vesicular structures) and enriched quantity of melanin were found in treated cells (Figure 29, lower microphotographs).

SBA-15p or organotin(IV) compound **M10** did not affect the cell proliferation as strong as grafted **SBA-15p** with **M10** (**SBA-15pM10**)^[K39]. Thus, the novel materials exhibited more than the synergic sum of the cytotoxicity of the organotin(IV) compound and nanomaterial. Even preferred in the mechanism of action of antitumoral drugs, apoptosis may trigger “compensatory proliferation“ of surrounding cells initiating regeneration of tumor^[136]. Initially, **SBA-15pM10** is inducing apoptosis, but in the survived clones, which might develop resistance, stimulate an opposite process to malignant transformation namely cell differentiation. This reversion to normal phenotype is highly compatible with the surrounding tissue and presents the most appropriate and safe way of drug action.

3.3. Conclusions

Liposomal formulation **LipoTHP-C11** was prepared from Lipoid S 75 and **THP-C11**. Characterization was performed by light microscopy, dynamic light scattering and asymmetrical flow-field-flow fractionation determining the size around 125 nm. Mesoporous silica (**MCM-41** and **SBA-15**) were grafted with titanocene derivatives as well as (**SBA-15**) with organotin(IV) compounds. The novel materials were characterized by powder X-ray diffraction analysis, X-ray fluorescence analysis, nitrogen gas sorption, multinuclear MAS NMR spectroscopy, SEM and TEM analyses.

Using two different approaches, liposomes for water-insoluble potential platinum-based drug and mesoporous silica for nonplatinum-based agents, new strategies were achieved in terms of fight against cancer. The basic research gave some perspectives in retaining or, in some cases, in increasing the antitumor activity by using drug delivery vehicles.

Rather than searching for structural analogues which usually led in *in vitro* deactivation of potent antitumoral drug (**THP-C11**), as alternative, formulation of water-soluble

3. NANOMATERIALS AS DRUG CARRIERS

nanoparticles is shown to be a promising strategy. **LipoTHP-C11** retained quite well time-dependent cytotoxic property and slightly less final cytotoxicity of water-insoluble platinum(II) complex **THP-C11**. The total cytotoxicity of **LipoTHP-C11** is only due to the presence of **THP-C11**, since liposomes alone are not cytotoxic. On the other hand, toxic effect of the compound was reduced in liposomal formulation by 50%. Additionally, it is demonstrated that liposomes can be successfully used for delivery of water-insoluble anticancer drugs, such as **THP-C11**, to tumor cells in *in vitro* conditions. **LipoTHP-C11** is particularly effective against human anaplastic thyroid carcinoma SW1736 cell line.

The second approach of using mesoporous silica as drug shuttle contributes to the development of a totally new field within antitumor carrier species. Initial research concerning mesoporous silica gave unexpected results. Thus, materials resulted from functionalization of **MCM-41** or **SBA-15** mesoporous silica with titanocene derivatives showed an increase in *in vitro* antiproliferative activity. Notably, carrier molecules do not possess any cytotoxicity against neither tumor nor normal cells. As shown for titanocene derivatives (**T1-Ti18**), also novel nanomaterials are more active against human myelogenous leukaemia K562 than human adenocarcinoma HeLa or malignant melanoma Fem-x cell lines. Cytotoxic activity depends on the quantity of grafted titanocene derivative on **MCM-41**, the higher titanium amount causes higher anti-tumor activity. In addition, the type of mesoporous silica also influences the *in vitro* activity. Higher activity of **SBA-15** than **MCM-41** functionalized nanomaterials containing the same titanocene derivatives (**M7** and **M8**) was observed. From the functionalized nanomaterials titanocene derivatives may possibly leak in extracellular matrix and then enter the cell. Alternatively, materials could be internalized in the cell and in intracellular matrix leaking of titanocene derivatives might occur. Within both mechanisms it is expected that hydrolysis of titanocene derivatives may take place, followed by the interaction of titanium(IV) hydrolytic products with biomolecules. Both mechanisms of action are rational and expected to occur *in vitro*.

Considering that functionalized nanomaterials **SBA-15** are shown to be superior than functionalized **MCM-41** in cytotoxicity, for novel materials containing organotin(IV) compounds an **SBA-15** modification as carrier molecule was selected. Initially, **SBA-15** was functionalized with 3-chloropropyltriethoxysilane (**SBA-15p**) and then with

3. NANOMATERIALS AS DRUG CARRIERS

organotin(IV) compounds (**M9** or **M10**). Amazingly, this functionalization resulted at least in 100 times higher cytotoxic nanomaterials, compared to those containing titanocene derivatives. Depending on the cell line, organotin(IV) compounds were found being higher (cisplatin-resistant colon carcinoma DLD-1) or less effective (lung carcinoma A549 and ovarian cancer A2780) than cisplatin. As supposed for mesoporous silica, these nanomaterials are endocytosed by cells, but also the release of **M9** from **SBA-15pM9** occurs both in extracellular and intracellular matrix. **SBA-15pM9**, analogue to **M9**, is inducing apoptosis via cell death receptor and mitochondrion in A2780 cell line.

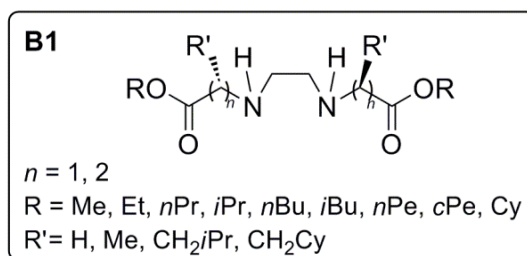
More than drug (**M10**) or material alone (**SBA-15p**), the drug-functionalized material **SBA-15pM10** demonstrated dramatically amplified antitumor activity against melanoma cells and was more than the sum of the cytotoxicities of the drug and the particles. Thus, there is a synergic effect. The first grafted nanomaterial tested *in vivo* on the same tumor model as **Pt1**, synergic C57BL/6 mice infected with B16 melanoma cells, surprisingly totally eliminated tumor from the animals. Thus, pointing advance of using organotin(IV) compounds, precisely using **SBA-15pM10** over platinum-based drugs. It is proved that initially **SBA-15pM10** causes apoptosis of B16 cells. Moreover, on the clones that acquired resistance against apoptosis, **SBA-15pM10** triggered differentiation process. The greatest advantage of this mesoporous silica functionalized with **M10** is the ability to stimulate cell differentiation evading apoptosis in response to treatment. This reversion to normal phenotype is highly compatible with the surrounding tissue and presents the most appropriate and safe way of drug action.

4. SUMMARY

Since discovery of antitumor activity of cisplatin in 1965, only three platinum(II) complexes, cisplatin, carboplatin and oxaliplatin, are used in the cancer treatment worldwide. Undesirably, beneficial effects of platinum drugs are followed by severe toxicity and/or by spontaneous or acquired resistance. Along with intention of overcoming these limits, development of platinum anticancer drugs resulted in broad investigations of a huge number of not only platinum-based, but also other metal-based compounds and, in recent times, different drug carrier systems.

From a bioinorganic chemistry perspective, a prerequisite for a targeted development of new metal-based anticancer drugs is an understanding of structure–activity relationships and of their mode of action. Limitations that will be obvious in investigations of easily accessible metal complexes may be overcome by using existing and innovative carrier systems. Moreover, the bridge from the basic and interdisciplinary research to applications are *in vivo* experiments that may point some promising candidates worth for the forthcoming investigations. Within the framework of this thesis the following results were obtained:

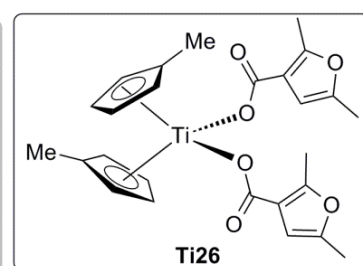
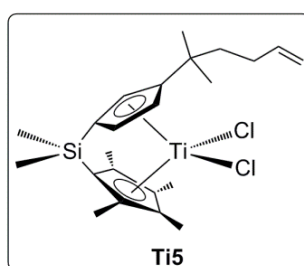
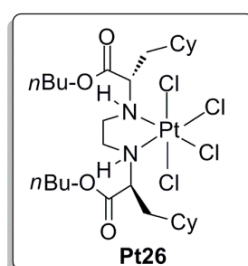
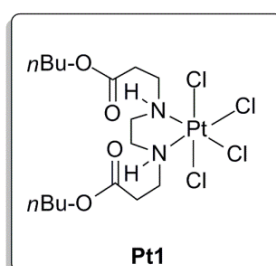
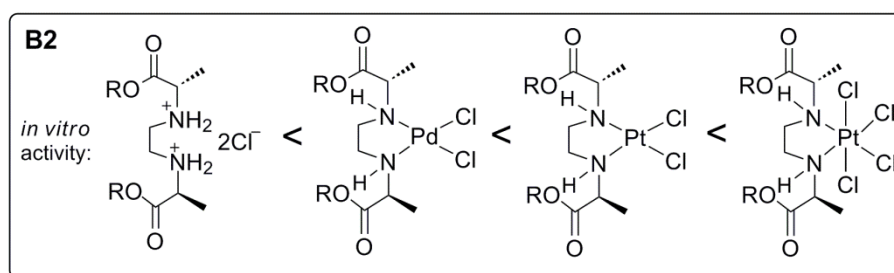
- Numerous platinum(II), platinum(IV), palladium(II), titanium(IV) and tin(IV) compounds were prepared mostly by standard synthetic methods allowing wide variation in the ligand sphere. Characterization of the metallocompounds was performed by different spectroscopic methods (multinuclear NMR, IR). For the several metallocompounds, structures were additionally confirmed by X-ray structural analysis.
- Investigations on cancerostatic properties of platinum(II), platinum(IV) and palladium(II) complexes with R₂edda-type ligands (see box **B1**) showed some structure–activity relationships depending on substituent R, metal center and the oxidation state of platinum. Generally, the *in vitro* activity against tumor cell lines is increasing in the following order: R₂edda-type ligand precursors < palladium(II) complexes < platinum(II) complexes < platinum(IV) complexes as illustrated for the (S,S)-R₂eddip ligands ($n = 1$; R'



4. SUMMARY

= Me) in the box **B2**. Furthermore, in general, the cytotoxicity increases with the ligand lipophilicity which can be tuned, especially, with the substituents in aminocarboxylato backbone R'.

- The active species of $[\text{PtCl}_4(\text{R}_2\text{edda})]$ complexes ($n = 1$, $\text{R}' = \text{H}$) in the cells seems to be corresponding platinum(II) complexes, although a direct binding of platinum(IV) complexes to DNA was observed too. Platinum complexes containing R_2eddp ($n = 2$; $\text{R}' = \text{H}$) or $(S,S)\text{-R}_2\text{eddip}$ ligands are triggering mainly apoptotic pathway (**Pt1**), while those containing $(S,S)\text{-R}_2\text{eddch}$ ($n = 1$; $\text{R}' = \text{CH}_2\text{Cy}$) are inducing necrotic death pathway as **Pt26** of B16 cells, thus indicating that platinum(IV) complexes with R_2edda -type ligands are inducing cell-type specific *in vitro* activity.
- In the *in vivo* melanoma C57BL/6 mouse model, **Pt1** exhibited largely improved antitumor activity and less side effects (without nephrotoxicity signs) compared to cisplatin.
- The investigated titanocene and *ansa*-titanocene compounds proved to have, in most cases, a higher cancerostatic activity than the clinically used titanocene dichloride. The most active compound was found to be *ansa*-titanocene **Ti5** bearing one alkenyl substituted cyclopentadienyl ligand (IC_{50} : $24 \pm 3 \mu\text{M}$ against K562 cells). Furthermore, in general, substitution of chlorido with carboxylato ligands in titanocene complexes improved cytotoxic activity (IC_{50} : $40 \pm 4 \mu\text{M}$ against A2780

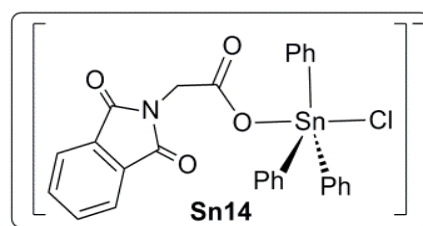


4. SUMMARY

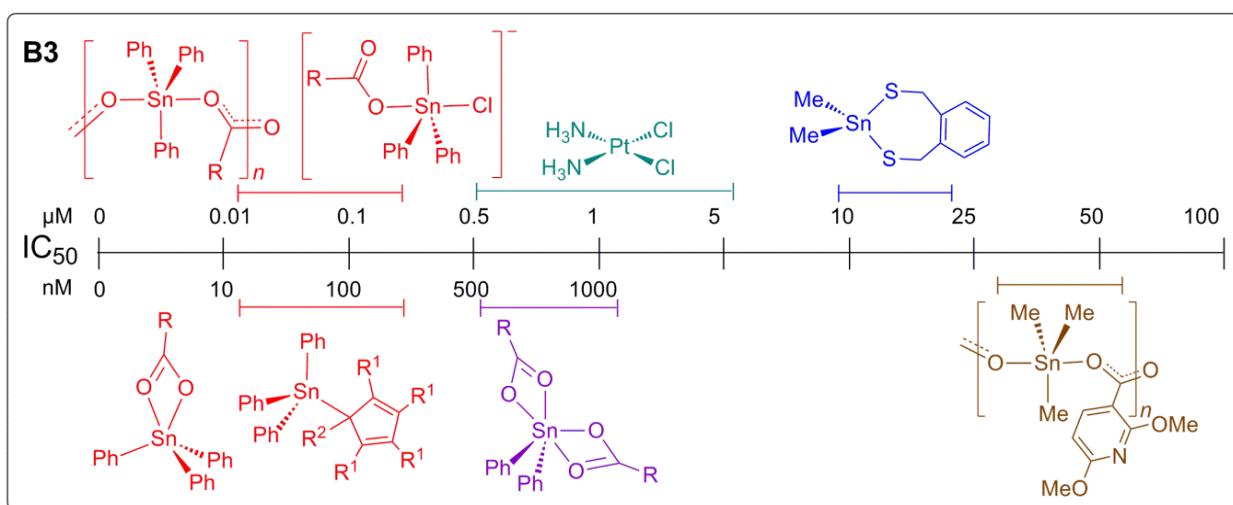
cells, **Ti26**). Although titanium complexes discussed herein are less active than cisplatin, due to a higher tolerance of titanium in biological systems they may be envisaged for cancer treatment.

- Superior activity of triphenyl- over diphenyl-, dimethyl- or trimethyltin(IV) mainly resulted in IC_{50} values in nM range (see box **B3**), while compounds of other metals exhibited activities (IC_{50}) in μ M range only. In addition, diphenyltin(IV) compounds showed greater selectivity between normal and cancer cells than cisplatin.

The anionic stannate compound **Sn14** is causing apoptosis *via* cell death receptor in cisplatin-resistant colon carcinoma DLD-1 cell line, while on the same tumor cell line cisplatin is inducing mitochondrial apoptosis pathway.

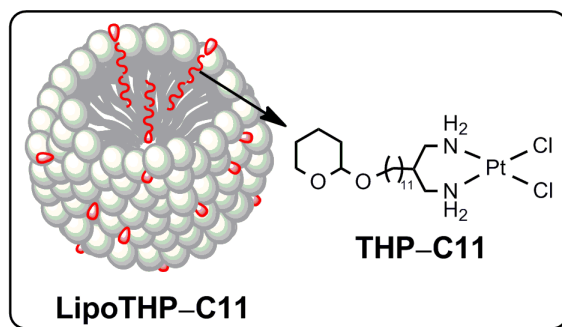


- Water-insoluble platinum(II) compound **THP-C11** was used in preparation of liposomal formulation **LipoTHP-C11** and characterized using light microscopy, dynamic light scattering and asymmetrical flow-field-flow fractionation. Furthermore, titanocene derivatives and organotin(IV) compounds were grafted on mesoporous silica (**MCM-41** and/or **SBA-15**). The functionalized mesoporous nanomaterials were characterized by powder X-ray diffraction analysis, X-ray fluorescence analysis, nitrogen gas sorption, multinuclear MAS NMR spectroscopy, SEM and TEM analyses.



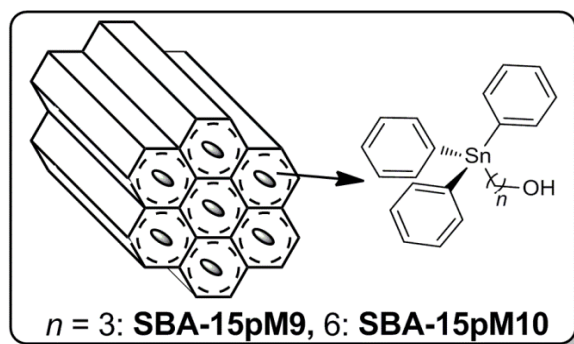
4. SUMMARY

- The water-soluble liposomal formulation **LipoTHP-C11** retained or slightly decreased *in vitro* activity of **THP-C11** dissolved in DMF. The cytotoxicity of **LipoTHP-C11** is only due to the presence of **THP-C11**, since liposomes alone are not cytotoxic. On the contrary, in some cases, toxic effect of the compound was reduced in liposomal formulation by 50%. Thus, liposomes as carrier vehicles have been shown to be a promising strategy for water-insoluble drugs such as **THP-C11**.



- The approach of using mesoporous silica as drug shuttle contributes to the development of a totally new field within antitumor carriers for metal complexes. Mesoporous nanomaterials (**MCM-41** and **SBA-15**) do not possess any cytotoxicity against neither tumor nor normal cells. Moreover, the functionalized nanomaterials showed a titanium-concentration dependent antitumor activity. Nanomaterial **SBA-15** grafted with titanocene derivatives are shown to be superior in cytotoxicity than **MCM-41** analogues.

- Modified **SBA-15 (SBA-15p)** grafted with organotin(IV) compounds (**M9** or **M10**) resulted at least in 100 times higher cytotoxic nanomaterials compared to those containing titanocene derivatives. **SBA-15pM9** is inducing apoptosis via cell death



- receptor and mitochondrion in A2780 cell line. The greatest advantage of **SBA-15p** mesoporous silica functionalized with **M10** is the ability to stimulate cell differentiation of B16 melanoma tumor cells evading apoptosis in response to treatment.
- On the contrary to cisplatin, **SBA-15pM10** is almost completely abolishing tumor progression *in vivo* in melanoma syngeneic C57BL/6 mouse model without visible side effects.

4. SUMMARY

Metallocompounds based on platinum, palladium, titanium and tin are investigated among panels of tumor cell lines derived from a broad spectrum of tumors. Presented results might give some directions for future development by understanding the mode of metal-based drug actions. Reconciling the mechanism of action of these metallocompounds is of essential interest for the design of more effective drugs. Furthermore, considering clinical requirements necessary for novel compounds and an increasing number of platinum-resistant tumors, not only compounds being more active than cisplatin should be taken into account, but also compounds that would have different antitumor mechanisms (such as **Pt1** and **Sn14**) compared to cisplatin.

Considering the biocompatibility of liposomes and mesoporous silica surfaces, this work goes a long way for the design and development of new biocompatible materials that can be presented as an alternative in the treatment of tumors of different origin. Thus liposomal formulation present successful transport concept for water-insoluble metal-based drugs (**THP-C11**). Furthermore, for the first time, mesoporous silicas were used as metal-based antitumor drug carriers. Superiority from the classical metal-based drugs reflect not only in reducing tumor volume without signs of toxicity but, more importantly, they are inducing differentiations of the tumor cells to the normal phenotype (**SBA-15pM10**). Thus, the work opens a new perspective for application of metal-based antitumor compounds by using mesoporous silica as their containers.

5. REFERENCES

- [1] B. Rosenberg, E. Renshaw, L. van Camp, J. Hartwick, J. Drobnik, *J. Bacteriol.* **1967**, *93*, 716–721.
- [2] B. Rosenberg, L. van Camp, T. Krigas, *Nature* **1965**, *205*, 698–699.
- [3] B. Rosenberg, L. van Camp, *Cancer. Res.* **1970**, *30*, 1799–1802.
- [4] T. W. Hambley, *Dalton Trans.* **2007**, 4929–4937.
- [5] L. Kelland, *Nat. Rev. Cancer* **2007**, *7* 573–584.
- [6] F. Arnesano, G. Natile, *Coord. Chem. Rev.* **2009**, *253*, 2070–2081.
- [7] D. Wang, S. J. Lippard, *Nat. Rev. Drug Discov.* **2005**, *4*, 307–320.
- [8] A. E. Egger, C. G. Hartinger, H. Ben, Y. O. Tsybin, B. K. Keppler, P. J. Dyson, *Inorg. Chem.* **2008**, *47*, 10626–10633.
- [9] J. Reedijk, *Platinum Met. Rev.* **2008**, *52*, 2–11.
- [10] A. M. Fichtinger-Schepman, d. V. Van, H. Den, P. H. M. Lohman, J. Reedijk, *Biochemistry* **1985**, *24*, 707–713.
- [11] B. W. Harper, A. M. Krause–Heuer, M. P. Grant, M. Manohar, K. B. Garbutcheon-Singh, J. R. Aldrich-Wright, *Chem.–Eur. J.* **2010**, *16*, 7064–7077.
- [12] G. Natile, M. Coluccia, *Coord. Chem. Rev.* **2001**, *216–217*, 383–410.
- [13] T. Boulikas, M. Vougiouka, *Oncol. Rep.* **2003**, *10*, 1663–1682.
- [14] R. B. Weiss, M. C. Christian, *Drugs* **1993**, *46*, 360–377.
- [15] U. Kalinowska-Lis, J. Ochocki, K. Matlawska-Wasowska, *Coord. Chem. Rev.* **2008**, *252*, 1328–1345.
- [16] J. Reedijk, *Chem. Commun.* **1996**, 801–806.
- [17] N. J. Wheate, S. Walker, G. E. Craig, R. Oun, *Dalton Trans.* **2010**, *39*, 8113–8127.
- [18] B. Drewinko, L. Y. Yang, J. M. Trujillo, *Invest. New Drugs* **1985**, *3*, 335–340.
- [19] T. Uehara, N. Tsuchiya, A. Masuda, M. Torii, M. Nakamura, J. Yamate, T. Maruyama, *J. Appl. Toxicol.* **2008**, *28*, 388–398.
- [20] R. T. Penson, D. S. Dizon, S. A. Cannistra, M. R. Roche, C. N. Krasner, S. T. Berlin, N. S. Horowitz, P. A. DiSilvestro, U. A. Matulonis, H. Lee, M. A. King, S. M. Campos, *J. Clin. Oncol.* **2010**, *28*, 154–159.

5. REFERENCES

- [21] I. Kostova, *Recent Pat. Anticancer Drug Discov.* **2006**, *1*, 1–22.
- [22] M. Coluccia, G. Natile, *Anticancer Agents Med. Chem.* **2007**, *7*, 111–123.
- [23] T. Boulikas, M. Vougiouka, *Oncol. Rep.* **2003**, *10*, 1663–1682.
- [24] A. Bhargava, U. N. Vaishampayan, *Expert Opin. Investig. Drugs* **2009**, *18*, 1787–1797.
- [25] N. Shah, D. S. Dizon, *Future Oncol.* **2009**, *5*, 33–42.
- [26] N. J. Wheate, J. G. Collins, *Coord. Chem. Rev.* **2003**, *241*, 133–145.
- [27] A. Amin, M. A. Buratovich, *Mini-Rev. Med. Chem.* **2009**, *9*, 1489–1503.
- [28] Q. Liu, Y. Qu, R. Van Antwerpen, N. Farrell, *Biochemistry* **2006**, *45*, 4248–4256.
- [29] C. Sessa, G. Capri, L. Gianni, F. Peccatori, G. Grasselli, J. Bauer, M. Zucchetti, L. Viganò, A. Gatti, C. Minoia, P. Liati, S. Van den Bosch, A. Bernareggi, G. Camboni, S. Marsoni, *Ann. Oncol.* **2000**, *11*, 977–983.
- [30] I. Ott, R. Gust, *Arch. Pharm. Pharm. Med. Chem.* **2007**, *340*, 117–126.
- [31] T. Gianferrara, I. Bratsos, E. Alessio, *Dalton Trans.* **2009**, 7588–7598.
- [32] C. G. Hartinger, S. Zorbas-Seifried, M. A. Jakupec, B. Kynast, H. Zorbas, B. K. Keppler, *J. Inorg. Biochem.* **2006**, *100*, 891–904.
- [33] M. M. Hart, C. F. Smith, S. T. Yancey, R. H. Adamson, *J. Natl. Cancer Inst.* **1971**, *47*, 1121–1127.
- [34] K. Strohsfeldt, M. Tacke, *Chem. Soc. Rev.* **2008**, *37*, 1174–1187.
- [35] B. K. Keppler, C. Friesen, H. G. Moritz, H. Vongerichten, E. Vogel, *Struct. Bond.* **1991**, *78*, 97–127.
- [36] P. Köpf-Maier, H. Köpf, in *Bioinorganic Chemistry*, Springer Berlin, Heidelberg, **1988**, pp. 103–185.
- [37] P. Köpf-Maier, *Anticancer Res.* **1999**, *19*, 493–504.
- [38] H. Köpf, P. Köpf-Maier, *Angew. Chem.-Int. Edit.* **1979**, *18*, 477–478.
- [39] E. Meléndez, *Crit. Rev. Oncol. Hematol.* **2002**, *42*, 309–315.
- [40] T. Schilling, K. B. Keppler, M. E. Heim, G. Niebch, H. Dietzfelbinger, J. Rastetter, A. R. Hanauske, *Invest. New Drugs* **1996**, *13*, 327–332.
- [41] G. Lummen, H. Sperling, H. Luboldt, T. Otto, H. Rubben, *Cancer Chemother. Pharmacol.* **1998**, *42*, 415–417.

5. REFERENCES

- [42] N. Kröger, U. R. Kleeberg, K. Mross, L. Edler, D. K. Hossfeld, *Onkologie* **2000**, *23*, 60–62.
- [43] M. Gielen, *Coord. Chem. Rev.* **1996**, *151*, 41–51.
- [44] P. Yang, M. Guo, *Coord. Chem. Rev.* **1999**, *185–186*, 189–211.
- [45] C.-H. Zhou, Y.-Y. Zhang, C.-Y. Yan, K. Wan, L.-L. Gan, Y. Shi, *Anticancer Agents Med. Chem.* **2010**, *10*, 371–395.
- [46] S. K. Hadjikakou, N. Hadjiliadis, *Coord. Chem. Rev.* **2009**, *253*, 235–249.
- [47] N. Gerasimchuk, T. Maher, P. Durham, K. V. Domasevitch, J. Wilking, A. Mokhir, *Inorg. Chem.* **2007**, *46*, 7268–7284.
- [48] D. R. Khan, *J. Cancer Sci. Ther.* **2010**, *2*, 59–62.
- [49] A. Singh, Z. A. Worku, G. Van den Mooter, *Expert Opin. Drug Deliv.* **2011**, *8*, 1361–1378.
- [50] K. H. Bae, H. J. Chung, T. G. Park, *Mol. Cells* **2011**, *31*, 295–302.
- [51] J. A. Barreto, W. O'Malley, M. Kubeil, B. Graham, H. Stephan, L. Spiccia, *Adv. Mater.* **2011**, *23*, H18–H40.
- [52] C. S. S. R. Kumar, F. Mohammad, *Adv. Drug Deliv. Rev.* **2011**, *63*, 789–808.
- [53] Y. J. Liu, B. Zhang, B. Yan, *Int. J. Mol. Sci.* **2011**, *12*, 4395–4413.
- [54] Z. A. Liu, K. Yang, S. T. Lee, *J. Mater. Chem.* **2011**, *21*, 586–598.
- [55] B. L. Peng, N. Dhar, H. L. Liu, K. C. Tam, *Can. J. Chem. Eng.* **2011**, *89*, 1191–1206.
- [56] X. W. Shi, X. X. Li, Y. M. Du, *Acta Polym. Sin.* **2011**, 1–11.
- [57] H. L. Chen, Y. Qin, Q. Y. Zhang, W. Jiang, L. Tang, J. Liu, Q. He, *Eur. J. Pharm. Sci.* **2011**, *44*, 164–173.
- [58] L. R. Guo, L. Fan, Z. Q. Pang, J. F. Ren, Y. L. Ren, J. W. Li, J. Chen, Z. Y. Wen, X. G. Jiang, *J. Control. Release* **2011**, *154*, 93–102.
- [59] Y. Ueno, S. Sonoda, R. Suzuki, M. Yokouchi, Y. Kawasoe, K. Tachibana, K. Maruyama, T. Sakamoto, S. Komiya, *Cancer Biol. Ther.* **2011**, *12*, 270–277.
- [60] Y. Wu, Y. Yang, F. C. Zhang, C. Wu, W. L. Lu, X. G. Mei, *J. Liposome Res.* **2011**, *21*, 221–228.
- [61] Z. Jiao, X. Wang, Z. M. Chen, *Drug Deliv.* **2011**, *18*, 478–484.

5. REFERENCES

- [62] A. M. Harmon, M. H. Lash, S. M. Sparks, K. E. Uhrich, *J. Control. Release* **2011**, *153*, 233–239.
- [63] G. Orive, R. M. Hernández, A. R. Gascón, J. L. Pedraz. Micro and nano drug delivery systems in cancer therapy. *Cancer Ther.* **2005**, *3*, 131–138.
- [64] M. A. Wagle, L. E. Martinville, G. G. M. D'Souza, *Pharm. Res.* **2011**, *28*, 2790–2796.
- [65] S. Yamamoto, Y. Fukui, S. Kaihara, K. Fujimoto, *Langmuir* **2011**, *27*, 9576–9582.
- [66] C. F. Jehn, T. Boulikas, A. Kourvetaris, K. Possinger, D. Luftner, *Anticancer Res.* **2007**, *27*, 471–475.
- [67] T. Boulikas, G. P. Stathopoulos, N. Volakakis, M. Vougiouka, *Anticancer Res.* **2005**, *25*, 3031–3039.
- [68] T. Boulikas, *Expert Opin. Investig. Drugs* **2009**, *18*, 1197–1218.
- [69] G. P. Stathopoulos, T. Boulikas, M. Vougiouka, G. Deliconstantinos, S. Rigatos, E. Darli, V. Viliotou, J. G. Stathopoulos, *Oncol. Rep.* **2005**, *13*, 589–595.
- [70] E. Gaffet, *C. R. Phys.* **2011**, *12*, 648–658.
- [71] S. J. Guo, E. K. Wang, *Nano Today* 2011, *6*, 240–264.
- [72] M. Manzano, M. Colilla, M. Vallet-Regi, *Expert Opin. Drug Deliv.* **2009**, *6*, 1383–1400.
- [73] M. Vallet-Regi, D. Arcos, *Curr. Nanosci.* **2006**, *2*, 179–189.
- [74] M. Vallet-Regi, *C. R. Chim.* **2010**, *13*, 174–185.
- [75] B. Fadeel, A. E. Garcia-Bennett, *Adv. Drug Deliv. Rev.* **2010**, *62*, 362–374.
- [76] M. Colilla, M. Manzano, M. Vallet-Regi, *Int. J. Nanomed.* **2008**, *3*, 403–414.
- [77] I. Izquierdo-Barba, M. Colilla, M. Vallet-Regi, *J. Nanomater.* **2008**, Article ID 106970, 1–14.
- [78] M. Vallet-Regi, F. Balas, D. Arcos, *Angew. Chem.-Int. Edit.* **2007**, *46*, 7548–7558.
- [79] B. Palazzo, M. Iafisco, M. Laforgia, N. Margiotta, G. Natile, C. L. Bianchi, D. Walsh, S. Mann, N. Roveri, *Adv. Funct. Mater.* **2007**, *17*, 2180–2188.
- [80] M. Iafisco, B. Palazzo, M. Marchetti, N. Margiotta, R. Ostuni, G. Natile, M. Morpurgo, V. Gandin, C. Marzano, N. Roveri, *J. Mater. Chem.* **2009**, *19*, 8385–8392.
- [81] I. I. Slowing, B. G. Trewyn, V. S. Y. Lin, *J. Am. Chem. Soc.* **2007**, *129*, 8845–8849.

5. REFERENCES

- [82] T. J. Sabo, G. N. Kaluđerović, S. R. Grgurić-Šipka, F. W. Heinemann, S. R. Trifunović, *Inorg. Chem. Comm.* **2004**, 7, 241–244.
- [83] G. N. Kaluđerović, V. M. Đinović, Z. D. Juranić, T. P. Stanojković, T. J. Sabo, *J. Inorg. Biochem.* **2005**, 99, 488–496.
- [84] G. N. Kaluđerović, Đ. Miljković, M. Momčilović, V. M. Đinović, S. M. Mostarica, T. J. Sabo, V. Trajković, *Int. J. Cancer* **2005**, 116, 479–486.
- [85] S. Mijatović, D. Maksimović-Ivanić, J. Radović, Đ. Miljković, G. N. Kaluđerović, T. J. Sabo, V. Trajković, *Cell. Mol. Life Sci.* **2005**, 62, 1275–1282.
- [86] N. A. Kratochwil, M. Zabel, K. J. Range, P. J. Bednarski, *J. Med. Chem.* **1996**, 39, 2499–2507.
- [87] K. Lemma, T. S. Shi, L. I. Elding, *Inorg. Chem.* **2000**, 39, 1728–1734.
- [88] A. P. Silverman, W. M. Bu, S. M. Cohen, S. J. Lippard, *J. Biol. Chem.* **2002**, 277, 49743–49749.
- [89] W. K. Anderson, D. A. Quagliato, R. D. Haugwitz, V. L. Narayanan, M. K. Wolpertdefilippes, *Cancer Treat. Rep.* **1986**, 70, 997–1002.
- [90] U. Olszewski, F. Ach, E. Ulsperger, G. Baumgartner, R. Zeillinger, P. Bednarski, G. Hamilton, *Met. Based Drugs* 2009, Article ID 348916, 1–12.
- [91] M. D. Hall, T. W. Hambley, *Coord. Chem. Rev.* **2002**, 232, 49–67.
- [92] J. J. Wilson, S. J. Lippard, *Inorg. Chem.* **2011**, 50, 3103–3115.
- [93] O. Nováková, O. Vrána, V. I. Kiseleva, V. Brabec, *Eur. J. Biochem.* **1995**, 228, 616–624.
- [94] H. M. Ushay, T. D. Tullius, S. J. Lippard, *Biochemistry* **1981**, 20, 3744–3748.
- [95] G. B. Onoa, V. Moreno, *Int. J. Pharm.* **2002**, 245, 55–65.
- [96] H. Tsao, L. Chin, L. A. Garraway, D. E. Fisher, *Genes. Dev.* **2012**, 26, 1131–1155.
- [97] M. Pavlaki, K. Debeli, I.-E. Triantaphyllidou, N. Klouras, E. Giannopoulou, A. J. Aletaras, *J. Biol. Inorg. Chem.* **2009**, 14, 947–957.
- [98] A. D. Tinoco, E. V. Eames, A. M. Valentine, *J. Am. Chem. Soc.* **2007**, 130, 2262–2270.
- [99] I. Fichtner, J. Claffey, B. Gleeson, M. Hogan, D. Wallis, H. Weber, M. Tacke, *Lett. Drug Des. Discovery* **2008**, 5, 489–493.

5. REFERENCES

- [100] J. Claffey, M. Hogan, H. Müller-Bunz, C. Pampillón, M. Tacke, *ChemMedChem* **2008**, *3*, 729–731.
- [101] M. Shavit, E.Y. Tshuva, *Eur. J. Inorg. Chem.* **2008**, 1467–1474.
- [102] E. Y. Tshuva, D. Peri, *Coord. Chem. Rev.* **2009**, *253*, 2098–2115.
- [103] S. K. Hadjikakou, N. Hadjiliadis, *Coord. Chem. Rev.* **2009**, *253*, 235–249.
- [104] W. A. Collier, *Z. Hyg. Infektionskr.* **1929**, *110*, 169–174.
- [105] S. Tabassum, C. Pettinari, *J. Organomet. Chem.* **2006**, *691*, 1761–1766.
- [106] F. Cima, L. Ballarin, *Appl. Organomet. Chem.* **1999**, *13*, 697–703.
- [107] C. Pellerito, P. D'Agati, T. Fiore, C. Mansueto, V. Mansueto, G. Stocco, L. Nagy, L. Pellerito, *J. Inorg. Biochem.* **2005**, *99*, 1294–1305.
- [108] D. Hübner, "Zytotoxische *in vitro* Untersuchungen von Organozinn(IV)-Verbindungen", Bachelorarbeit, Martin Luther University Halle–Wittenberg, 2011.
- [109] R. C. Dolman, G. B. Deacon, T. W. Hambley, *J. Inorg. Biochem.* **2002**, *88*, 260–267.
- [110] M. Galanski, B. K. Keppler, *Inorg. Chim. Acta* **2000**, *300–302*, 783–789.
- [111] M. Galanski, B. K. Keppler, *Anticancer Agents Med. Chem.* **2007**, *7*, 55–73.
- [112] A. D. Sezer, A. L. Bas, J. Akbuga, *J. Liposome Res.* **2004**, *14*, 77–86.
- [113] M. V. Landau, S. P. Varkey, M. Herskowitz, O. Regev, S. Pevzner, T. Sen and Z. Luz, *Microporous Mesoporous Mat.* **1999**, *33*, 149–163.
- [114] D. Zhao, Q. Huo, J. Feng, B.F. Chmelka, G.D. Stucky, *J. Am. Chem. Soc.* **1998**, *120*, 6024–6036.
- [115] E. A. J. Bleeker, W. H. de Jong, R. E. Geertsma, M. Groenewold, E. H. W. Heugens, M. Koers-Jacquemijns, D. van de Meent, J. R. Popma, A. G. Rietveld, S. W. P. Wijnhoven, F. R. Cassee, A. G. Oomen, *Regul. Toxicol. Pharm.* **2013**, *65*, 119–125.
- [116] ISO/TS 80004-5:2011 Nanotechnologies - Vocabulary - Part 5: Nano/bio interface. International Organization for Standardization, Geneva, Switzerland. <https://www.iso.org/obp/ui/#iso:std:iso:ts:80004:-5:ed-1:v1:en> (09.09.2013)
- [117] V. P. Torchilin, *AAPS J.* **2007**, *9*, E128–E147.
- [118] A. Dietrich, T. Mueller, R. Paschke, B. Kalinowski, T. Behlendorf, F. Reipsch, A. Fruehauf, H.J. Schmoll, C. Kloft, W. Voigt, *J. Med. Chem.* **2008**, *51*, 5413–5422.
- [119] N. Le Tallec, P. Lacroix, J. D. de Certaines, F. Chagneau, R. Levasseur, E. Le Ru-meur, *J Pharmacol. Toxicol. Methods* **1996**, *35*, 139–143.

5. REFERENCES

- [120] A. J. Di Pasqua, K. K. Sharma, Y.-L. Shi, B. B. Toms, W. Ouellette, J. C. Dabrowiak, T. Asefa, *J. Inorg. Biochem.* **2008**, *102*, 1416–1423.
- [121] W.-K. Oh, S. Kim, M. Choi, C. Kim, Y. S. Jeong, B.-R. Cho, J.-S. Hahn, J. Jang, *ACS Nano* **2010**, *4*, 5301–5313.
- [122] A. Albanese, P. S. Tang, W. C. W. Chan, *Annu. Rev. Biomed. Eng.* **2012**, *14*, 1–16.
- [123] H. Sun, H. Li, R. A. Weir, P. J. Sadler, *Angew. Chem.-Int. Edit.* **1998**, *37*, 1577–1579.
- [124] M. Guo, P. J. Sadler, *J. Chem. Soc., Dalton Trans.* **2000**, 7–10.
- [125] M. Guo, H. Sun, S. Bihari, J. A. Parkinson, R. O. Gould, S. Parsons, P. J. Sadler, *Inorg. Chem.* **2000**, *39*, 206–215.
- [126] M. Guo, H. Sun, H. J. McArdle, L. Gambling, P. J. Sadler, *Biochemistry* **2000**, *39*, 10023–10033.
- [127] P. M. Abeysinghe, M. M. Harding, *Dalton Trans.* **2007**, 3474–3482.
- [128] P. Köpf-Maier, D. Krahl, *Chem.–Biol. Interact.* **1983**, *44*, 317–328.
- [129] P. Köpf-Maier, D. Krahl, *Naturwissenschaften* **1981**, *68*, 273–274.
- [130] P. Köpf-Maier, *J. Struct. Biol.* **1990**, *105*, 35–45.
- [131] C. Bensing, “Mesoporöse Materialien mit Alkyltriphenylzinn(IV)–Verbindungen: Synthese, Charakterisierung und biologische *in vitro* Untersuchungen”, Masterarbeit, Martin Luther University Halle–Wittenberg, 2011.
- [132] E. Obrador, J. Carretero, A. Ortega, I. Medina, V. Rodilla, J. A. Pellicer, J. M. Estrela, *Hepatology* **2002**, *35*, 74–81.
- [133] K. Ogiwara, K. Hata K., *J. Nat. Med.* **2009**, *63*, 323–326.
- [134] A. Kuwajima, M. Sakai, J. Iwashita, T. Abe, *J. Health Sci.* **2009**, *55*, 138–142.
- [135] J. Radović, D. Maksimović-Ivanić, G. Timotijević, S. Popadić, Z. Ramić, V. Trajković, D. Miljković, S. Stošić-Grujičić, S. Mijatović, *Food Chem. Toxicol.* **2012**, *50*, 3181–3189.
- [136] C. D. Gregory, J. D. Pound, *Apoptosis* **2010**, *15*, 1029–1049.

6. CONTRIBUTING REFERENCES RELATED TO HABILITATION THESIS

Corresponding authors are underlined. Appended articles are written in red colour.

Introduction

- [K1] G. N. Kaluđerović, R. Paschke, Anticancer metallotherapeutics in preclinical development. *Curr. Med. Chem.* **2011**, *18*, 4738–4752. (App. 1)
- [K2] S. Gómez-Ruiz, D. Maksimović-Ivanić, S. Mijatović, G. N. Kaluđerović, On the discovery, mechanism and use of cisplatin and metallocenes in anticancer chemotherapy. *Bioinorg. Chem. Appl.* **2012**, Article ID 140284, 1–14. (App. 2)

Pt(II), Pt(IV) complexes

- [K3] G. N. Kaluđerović, H. Schmidt, D. Steinborn, T. J. Sabo, in J. G. Hughes and A. J. Robinson (Ed.): From synthesis to antitumoural activity of platinum(II) and platinum(IV) complexes with bis(carboxyalkylamino)ethane and –propane ligands, Nova Science Publishers, Inc. Hauppauge, NY, Inorganic Biochemistry: Research Progress (2008) pp 305–326.
- [K4] G. N. Kaluđerović, H. Schmidt, S. Schwieger, C. Wagner, R. Paschke, A. Dietrich, T. Mueller, D. Steinborn, Platinum(IV) complexes with edda diester ligands: synthesis, characterization and *in vitro* antitumoral activity. *Inorg. Chim. Acta* **2008**, *361*, 1395–1404.
- [K5] G. N. Kaluđerović, H. Kommera, S. Schwieger, H. Schmidt, A. Paethanom, M. Kunze, R. Paschke, D. Steinborn, Preparation, DFT calculations and antitumoral investigations of some platinum(IV) complexes with O,O'-dialkyl-ethylenediamine-N,N'-di-3-propanoate (R₂eddp) ligands. *Dalton Trans.* **2009**, 10720–10726. (App. 3)
- [K6] B. B. Krajčinović, G. N. Kaluđerović, D. Steinborn, H. Schmidt, C. Wagner, Ž. Žižak, Z. D. Juranić, S. R. Trifunović, T. J. Sabo, Synthesis and *in vitro* antitumoral activity of novel O,O'-di-2-alkyl-(S,S)-ethylenediamine-N,N'-di-2-propanoate ligands and corresponding platinum(II/IV) complexes. *J. Inorg. Biochem.* **2008**, *102*, 892–900.
- [K7] J. M. Lazić, Lj. Vučićević, S. Grgurić-Šipka, K. Janjetović, G. N. Kaluđerović, M. Misirkić, M. Gruden-Pavlović, D. Popadić, R. Paschke, V. Trajković, T. J. Sabo, Synthesis and *in*

6. CONTRIBUTING REFERENCE RELATED TO HABILITATION

- in vitro* anticancer activity of novel octahedral platinum(IV) complexes with cyclohexyl edda-type ligands. *ChemMedChem* **2010**, *5*, 881–889.
- [K8] J. M. Vujić, G. N. Kaluđerović, M. Milovanović, B. B. Zmejkovski, V. Volarević, D. Živić, P. Đurđević, N. Arsenijević, S. R. Trifunović, Stereospecific ligands and their complexes. Part VII. Synthesis, characterization and *in vitro* antitumoral activity of platinum(II) complexes with *O,O'*-dialkyl esters of (*S,S*)-ethylenediamine-*N,N'*-di-2-(4-methyl)pentanoic acid. *Europ. J. Med. Chem.* **2011**, *46*, 4559–4565.
- [K9] J. M. Vujić, G. N. Kaluđerović, B. B. Zmejkovski, M. Milovanović, V. Volarević, N. Arsenijević, T. P. Stanojković, S. R. Trifunović, Stereospecific ligands and their complexes. Part X. Synthesis, characterization and *in vitro* antitumoral activity of platinum(IV) complexes with *O,O'*-dialkyl-(*S,S*)-ethylenediamine-*N,N'*-di-2-(4-methyl)pentanoate ligands. *Inorg. Chim. Acta* **2012**, *390*, 123–128.
- [K10] G. N. Kaluđerović, S. Mijatović, B. B. Zmejkovski, M.Z. Bulatović, S. Gómez-Ruiz, M. Mojić, D. Steinborn, Dj. Miljković, H. Schmidt, S. D. Stošić-Grujičić, T.J. Sabo, D. Maksimović-Ivanić, Platinum(II/IV) complexes containing ethylenediamine-*N,N'*-di-2/3-propionate ester ligands induced caspase-dependent apoptosis in cisplatin resistant colon cancer cells. *Metallomics* **2012**, *4*, 979–987. (App. 4)
- [K11] D. Maksimović-Ivanić, S. Mijatović, I. Mirkov, S. Stošić-Grujičić, D. Miljković, T. J. Sabo, V. Trajković, G. N. Kaluđerović, Melanoma tumor inhibition by tetrachlorido(*O,O'*-dibutylethylenediamine-*N,N'*-di-3-propionate)platinum(IV) complex: *in vitro* and *in vivo* investigations. *Metallomics* **2012**, *4*, 1155–1159. (App. 5)

Pd(II) complexes

- [K12] B. B. Krajčinović, G. N. Kaluđerović, D. Steinborn, C. Wagner, K. Merzweiler, S. R. Trifunović, T. J. Sabo, Palladium(II) complexes with R₂edda derived ligands. Part I. Reaction of *O,O'*-diisopropyl-(*S,S*)-ethylenediamine-*N,N'*-di-2-propanoate ligand with K₂[PdCl₄]. *J. Serb. Chem. Soc.* **2009**, *74*, 389–400.
- [K13] B. B. Zmejkovski, G. N. Kaluđerović, S. Gómez-Ruiz, Ž. Žižak, D. Steinborn, H. Schmidt, R. Paschke, Z. D. Juranić, T. J. Sabo, Palladium(II) complexes with R₂edda derived ligands. Part II. Synthesis, characterization and *in vitro* antitumoral studies of R₂eddip esters and palladium(II) complexes. *Europ. J. Med. Chem.* **2009**, *44*, 3452–3458.
- [K14] B. B. Zmejkovski, G. N. Kaluđerović, S. Gómez-Ruiz, T. J. Sabo, Palladium(II) complexes with R₂edda derived ligands. Part III. *O,O'*-Diisobutyl-(*S,S*)-ethylenediamine-

6. CONTRIBUTING REFERENCE RELATED TO HABILITATION

- N,N'*-di-2-(4-methyl)-pentanoate dihydrochloride and its palladium(II) complex: synthesis and characterization. *J. Serb. Chem. Soc.* **2009**, *74*, 1249–1258.
- [K15] J. M. Vujić, M. Cvijović, G. N. Kaluđerović, M. Milovanović, B. B. Zmejkovski, V. Volarević, N. Arsenijević, S. R. Trifunović, Palladium(II) complexes with R₂edda derived ligands. Part IV. O,O'-dialkyl esters of (S,S)-ethylenediamine-*N,N'*-di-2-(4-methyl)-pentanoic acid dihydrochloride and their palladium(II) complexes: synthesis, characterization and *in vitro* antitumoral activity against chronic lymphocytic leukemia (CLL) cells. *Europ. J. Med. Chem.* **2010**, *45*, 3601–3606.
- [K16] G. P. Vasić, V. V. Glodjović, G. N. Kaluđerović, F. W. Heinemann, S. R. Trifunović, Palladium(II) complexes with R₂edda derived ligands. Part V. Reaction of O,O'-diethyl-(S,S)-ethylenediamine-*N,N'*-di-2-(3-methyl)butanoate with K₂[PdCl₄]. *Trans. Met. Chem.* **2011**, *36*, 331–336.
- [K17] B. B. Zmejkovski, T. J. Sabo, G. N. Kaluđerović, Palladium(II) complexes with R₂edda derived ligands. Part VI. O,O'-Diisopropyl ester of *N,N'*-1,2-ethanediylobis-L-leucine dihydrochloride dihydrate and its palladium(II) complex: synthesis and characterization. *J. Serb. Chem. Soc.* **2013**, *78*, 1171–1176.

Ti(IV) complexes

- [K18] S. Gómez-Ruiz, G. N. Kaluđerović, D. Polo-Cerón, S. Prashar, M. Fajardo, Ž. Žižak, Z. D. Juranić, T. J. Sabo, Study of the cytotoxic activity of alkenyl substituted *ansa*-titanocene complexes. *Inorg. Chem. Comm.* **2007**, *10*, 748–752.
- [K19] S. Gómez-Ruiz, G. N. Kaluđerović, S. Prashar, D. Polo-Cerón, M. Fajardo, Ž. Žižak, T. J. Sabo, Z. D. Juranić, Cytotoxic studies of substituted titanocene and *ansa*-titanocene anticancer drugs. *J. Inorg. Biochem.* **2008**, *102*, 1558–1570. (App. 6)
- [K20] S. Gómez-Ruiz, G. N. Kaluđerović, S. Prashar, Ž. Žižak, I. Besu, Z. D. Juranić, S. Prashar, M. Fajardo, Anticancer drugs based on alkenyl and boryl substituted titanocene complexes. *J. Organomet. Chem.* **2009**, *694*, 1981–1987.
- [K21] S. Gómez-Ruiz, B. Gallego, Ž. Žižak, E. Hey-Hawkins, Z. D. Juranić, G. N. Kaluđerović, Titanium(IV) carboxylate complexes: synthesis, structural characterization and cytotoxic activity. *Polyhedron* **2010**, *29*, 354–360. (App. 7)
- [K22] G. N. Kaluđerović, V. Tayurskaya, R. Paschke, S. Prashar, M. Fajardo, S. Gómez-Ruiz, Synthesis, characterization and biological studies of alkenyl-substituted titanocene(IV) carboxylate complexes. *Appl. Organomet. Chem.* **2010**, *24*, 656–662. (App. 8)

6. CONTRIBUTING REFERENCE RELATED TO HABILITATION

- [K23] [S. Gómez-Ruiz](#), J. Ceballos-Torres, S. Prashar, M. Fajardo, Ž. Žižak, Z. D. Juranić, [G. N. Kaluđerović](#), One ligand different metal complexes: Biological studies of titanium(IV), tin(IV) and gallium(III) derivatives with the 2,6-dimethoxypyridine-3-carboxylato ligand. *J. Organomet. Chem.* **2011**, 696, 3206–3213.
- [K24] J. Ceballos-Torres, [S. Gómez-Ruiz](#), [G. N. Kaluđerović](#), M. Fajardo, R. Paschke, [S. Prashar](#), Naphthyl substituted titanocene dichloride complexes: synthesis, characterization and *in vitro* studies. *J. Organomet. Chem.* **2012**, 700, 188–193.
- [K25] [S. Gómez-Ruiz](#), T. P. Stanojković, [G. N. Kaluđerović](#), Synthesis, characterization and biological studies of tin(IV) and titanium(IV) complexes with the α,α' -dimercapto-*o*-xylene ligand. *Appl. Organomet. Chem.* **2012**, 26, 383–389.
- [K26] J. Ceballos-Torres, M. J. Caballero-Rodriguez, [S. Prashar](#), R. Paschke, D. Steinborn, [G. N. Kaluđerović](#), [S. Gómez-Ruiz](#), Synthesis, characterization and *in vitro* biological studies of titanocene(IV) derivatives containing different carboxylato ligands. *J. Organomet. Chem.* **2012**, 716, 201–207.

Sn(IV) compounds

- [K27] [S. Gómez-Ruiz](#), [G. N. Kaluđerović](#), S. Prashar, E. Hey-Hawkins, A. Erić, Ž. Žižak, Z. D. Juranić, Study of the cytotoxicity of di and triphenyltin(IV) carboxylate complexes. *J. Inorg. Biochem.* **2008**, 102, 2087–2096.
- [K28] [S. Gómez-Ruiz](#), S. Prashar, T. Walther, M. Fajardo, D. Steinborn, R. Paschke, [G. N. Kaluđerović](#), Cyclopentadienyl tin(IV) derivatives; synthesis, characterization and study of their application as anticancer drugs. *Polyhedron* **2010**, 29, 16–23. (App. 9)
- [K29] [G. N. Kaluđerović](#), R. Paschke, S. Prashar, [S. Gómez-Ruiz](#), Synthesis, characterization and biological studies of 1-D polymeric triphenyltin(IV) complexes with carboxylato ligands. *J. Organomet. Chem.* **2010**, 695, 1883–1890. (App. 10)
- [K30] [G. N. Kaluđerović](#), H. Kommera, E. Hey-Hawkins, R. Paschke, [S. Gómez-Ruiz](#), Synthesis and biological applications of ionic triphenyltin(IV) chloride carboxylate complexes with exceptionally high cytotoxicity. *Metallomics* **2010**, 2, 419–428. (App. 11)
- [K31] [S. Gómez-Ruiz](#), Ž. Žižak, [G. N. Kaluđerović](#), A triphenyltin(IV) nicotinate derivative – synthesis and toxicity towards different tumour and normal cell lines. *Lett. Drug Des. Discov.* **2012**, 9, 737–741.

See also K23 and K25.

Drug carriers

- [K32] [G. N. Kaluđerović](#), A. Dietrich, H. Kommera, J. Kuntsche, K. Mäder, T. Mueller, R. Paschke, Liposomes as vehicles for water insoluble platinum-based potential drug: 2-(4-(tetrahydro-2H-pyran-2-yloxy)-undecyl)-propane-1,3-diamminedichloroplatinum(II). *Eur. J. Med. Chem.* **2012**, *54*, 567–572. (App. 12)
- [K33] D. Pérez-Quintanilla, [S. Gómez-Ruiz](#), Ž. Žižak, I. Sierra, S. Prashar, I. Hierro, M. Fajardo, Z. D. Juranić, [G. N. Kaluđerović](#), A new generation of anticancer drugs: Mesoporous materials modified with titanocene complexes. *Chem. – Eur. J.* **2009**, *15*, 5588–5597. (App. 13)
- [K34] [G. N. Kaluđerović](#), D. Pérez-Quintanilla, I. Sierra, S. Prashar, I. Hierro, Ž. Žižak, Z. D. Juranić, M. Fajardo, [S. Gómez-Ruiz](#), Study of the influence of the metal complex on the cytotoxic activity of titanocene-functionalized mesoporous materials. *J. Mater. Chem.* **2010**, *20*, 806–814.
- [K35] [G. N. Kaluđerović](#), [D. Pérez-Quintanilla](#), Ž. Žižak, Z. D. Juranić, [S. Gómez-Ruiz](#), Improvement of cytotoxicity of titanocene-functionalized mesoporous materials by the increase of the titanium content. *Dalton Trans.* **2010**, *39*, 2597–2608. (App. 14)
- [K36] A. García-Peñas, [S. Gómez-Ruiz](#), [D. Pérez-Quintanilla](#), R. Paschke, I. Sierra, S. Prashar, I. Hierro, [G. N. Kaluđerović](#), Study of the cytotoxicity and particle action in human cancer cells of titanocene-functionalized materials with potential application against tumors, *J. Inorg. Biochem.* **2012**, *106*, 100–110.
- [K37] M. Z. Bulatović, C. Bensing, S. Gómez-Ruiz, D. Steinborn, M. Mojić, H. Schmidt, I. Golić, A. Korać, M. Momčilović, D. Pérez-Quintanilla, D. Maksimović-Ivanić, S. Mijatović, [G. N. Kaluđerović](#), Grafted mesoporous silica as promising life-compatible strategy in cancer treatment. in preparation

SUPPLEMENT

Anticancer Metallotherapeutics in Preclinical Development

G.N. Kaluderović*^{1,2} and R. Paschke¹Reproduced from Ref. G.N. Kaluderović, R. Paschke, Curr. Med. Chem. 2011, 18, 4738
Reprinted by permission of Eureka Science Ltd¹Biozentrum, Martin-Luther-Universität Halle-Wittenberg, Weinbergweg 22, D-06120 Halle, Germany; ²Institut für Chemie, Martin-Luther-Universität Halle-Wittenberg, Kurt-Mothes-Straße 2, D-06120 Halle, Germany

Abstract: This article reviews recent studies of platinum and other metal-containing antitumor drugs in preclinical development. A short overview of the development of cisplatin-based drug generations is given. Some pioneering strategies towards unconventional drugs, such as platinum complexes with biomolecules and carrier ligands, organoplatinum and multinuclear platinum complexes developed in recent years are outlined. Furthermore, nonplatinum-based antitumor drugs containing ruthenium(II/III), gallium(III), titanium(IV) or tin(IV) that illustrate the prominent strategies are presented with an emphasis on recent developments. In addition, alternatives for water-insoluble drugs will be discussed. A brief overview of development of nanodrug delivery systems and their potential as alternative cancerostatic carriers are discussed.

Keywords: Anticancer metallotherapeutics, cisplatin, drug delivery system, gallium(III), liposomes, platinum(II), platinum(IV), nanomaterials, organoplatinum(IV), ruthenium(II), ruthenium(III), tin(IV), titanium(IV), transplatinum complexes.

1. FROM CISPLATIN TO THE 3rd GENERATION OF DRUGS AS ANTICANCER AGENTS

Michele Peyrone, a medical doctor from Turin (Italy) who graduated in 1835, first synthesized cisplatin. He abandoned medicine in 1839 for chemistry and spent several years in different laboratories in France, Germany, the Netherlands, Belgium, and Great Britain [1]. In 1845 Peyrone synthesized, in one of Liebig's laboratories (Gießen), a new platinum compound containing two ammine and two chlorido ligands [2]. The compound was like the Reiset's salt [3], [PtCl₂(NH₃)₂], but had different physicochemical properties. At that time, it was not possible to understand the existence of the two different compounds assuming a tetrahedral geometry usual for tetravalent compounds. About 50 years later a square planar geometry was proposed by Alfred Werner for these compounds which can adopt a *cis* (Peyrone's) and a *trans* (Reiset's compound) arrangement (Fig. 1) [4].

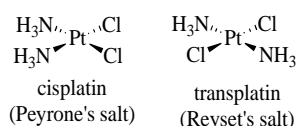


Fig. (1). Peyrone's and Reiset's compounds, *cis*- and *trans*-[PtCl₂(NH₃)₂] isomers.

Professor Barnett Rosenberg accidentally discovered antiproliferative activity of cisplatin. Specifically, in one of his investigations on the influence of the electric field on cell division in bacteria, some Peyrone's salt or "cisplatin", electrochemically generated by the platinum electrodes was produced in the presence of the various components in the cell culture medium [5–7]. Rosenberg proved that cisplatin completely inhibited the development of the solid sarcoma-180 tumor in mice and this serendipitous result was published in 1969 [8,9]. Cisplatin entered into clinical trials in 1971 and was approved by the Food and Drug Administration (FDA) [10,11] for clinical use in 1978, presenting a major landmark in the history of successful anticancer drugs. Cisplatin plays an important role in the treatment of epithelial malignancies and has brought a cure to testicular cancer. It is used as a principal component for the treatment of testicular, ovarian, and bladder cancer. In addition, cisplatin is being used as first-line chemotherapy against cancers of the lung, head and neck, esophagus, stomach, colon, bladder, cervix, and uterus. Furthermore, cisplatin has been used in combination therapy and is

considerably active against ovarian cancer [12]. As a result, cisplatin has become one of the bestselling anticancer drugs in the world [13].

1.1. Basics on the Action of Cisplatin

Subsequent to the route of administration, injection or infusion, cisplatin reaches the blood stream. Blood transports cisplatin throughout the body where a few ligand substitutions occur. The high concentration of chloride ions in the blood (≈100 mM) largely compensates, on a timescale of a few hours, for any exchange of the relatively mobile chlorido ligands. Nevertheless, some hydrolysis products are formed and these are held responsible for such acute toxicities as that causing kidney damage. Cisplatin eventually enters almost all types of cells by passive or even active transport *via* specific receptors (Fig. 2) [13,14]. Additionally, the mechanism by which copper is naturally transported, constitutive triple response 1 (CTR1) receptor mechanism, assists the platinum species to enter the cell [15]. On the other hand, adenosine triphosphate (ATP) plays a role in the process of excretion [14]. Upon entering the cells, cisplatin temporarily binds to one of the membrane components, e.g. phosphatidylserine, as has been proposed on the basis of NMR analysis [16]. In the cell, facilitated by the relatively low chloride concentrations, cisplatin hydrolyses and forms reactive aqua species.

The initial stage of mechanistic research on cisplatin was focused on DNA and its fragments as target molecules. Guanosine (G) in comparison to adenine (A) or other bases, binds more rapidly to platinum [14]. This was explained by a higher pK_a value and by simultaneous hydrogen bonding of the ammine-NH to the O6 of guanosine [14]. About two thirds of all the platinum binds at GG, a much larger proportion of GG adducts than statistically expected [17]. The adducts were characterized as mainly pGpG intrastrand cross-links (65%), followed by pApG intrastrand cross-links (22%), interstrand and/or intrastrand cross-links on pGpXpG sequences (13%) and monofunctional adducts (<1%) (Fig. 3) [18]. The binding process between cisplatin and bases has been studied on the mononucleotide and polynucleotide level by means of NMR spectroscopy and in some cases by crystal structure determination [19–21]. Those investigations also proved that, when cisplatin binds to double-stranded DNA, a clearly kinked chelate structure is formed. In cellular fluid other potential ligands, besides DNA and water, may bind to cisplatin and deactivate it, such as phosphate, carbonate, glutathione and peptides [14].

Cisplatin modulates a number of signalling pathways [13]. It should be emphasized here that activation of signalling pathways by cisplatin is cell-type specific. Cisplatin triggered changes in cell signalling, activity of different transcription factors as well as DNA structure lead to cell cycle arrest or induction of caspase dependent

*Address correspondence to this author at the Institut für Chemie, Martin-Luther-Universität Halle-Wittenberg, Kurt-Mothes-Straße 2, 06120 Halle, Germany; Tel: +49 345 55 25 678; Fax: +49 345 55 27 028; E-mail: goran.kaluderovic@chemie.uni-halle.de

Reproduced from Ref. G.N. Kaluđerović, R. Paschke, Curr. Med. Chem. 2011, 18, 4738
 Reprinted by permission of Eureka Science Ltd

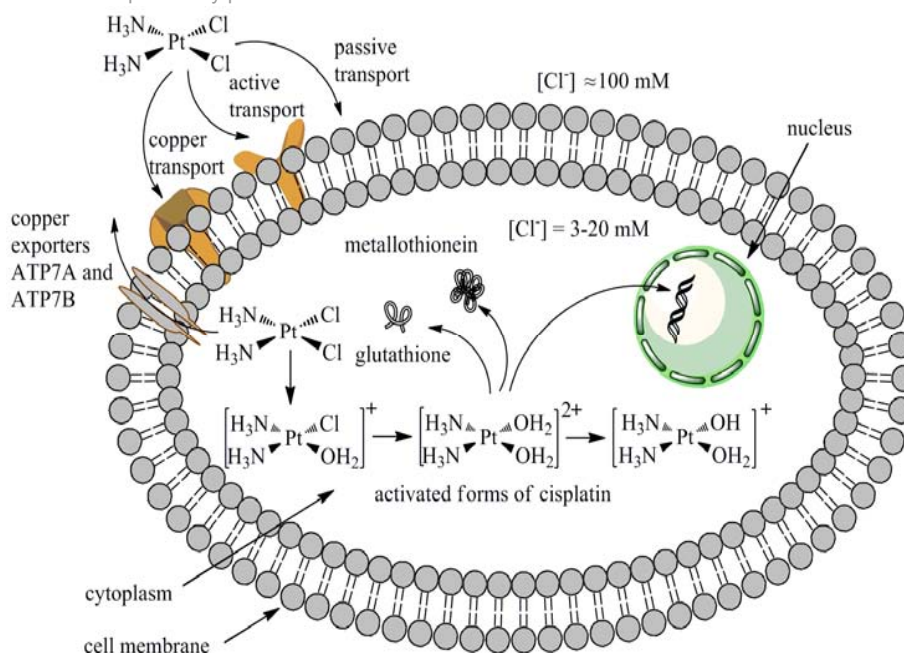


Fig. (2). *In vivo* chemistry of cisplatin.

apoptosis through receptor dependent and/or independent pathways. On some tumor cell lines (e.g. human U251 glioma, rat C6 glioma, mouse L929 fibrosarcoma) cisplatin may trigger activation of adenosine monophosphate-activated protein kinase with subsequent down-regulation of mammalian target of rapamycin-mediated phosphorylation of p70S6 kinase activity, and can induce an autophagic response that protects tumour cells from cisplatin mediated apoptotic death [22].

from side-effects and resistance phenomena [14]. Clinical effectiveness of cisplatin has been limited by significantly unfavourable side-effects, for example dose-dependent ototoxicity, nephrotoxicity, and neurotoxicity. Cisplatin resistance could arise from reduced platinum uptake, increased efflux, intracellular detoxification by glutathione, increased DNA repair, decreased mismatch repair, defective apoptosis, modulation of signalling pathways, or presence of quiescent non-cycling cells [23]. One strategy to overcome cisplatin resistance is to design platinum complexes that specifically deal with some or even all of the above mentioned resistance mechanisms. For these reasons, much attention has been directed towards the design of the new platinum-based complexes. The first stage of variation on cisplatin was derived by substituting chlorido with other anionic ligands (Fig. 4). These studies first produced carboplatin and nedaplatin.

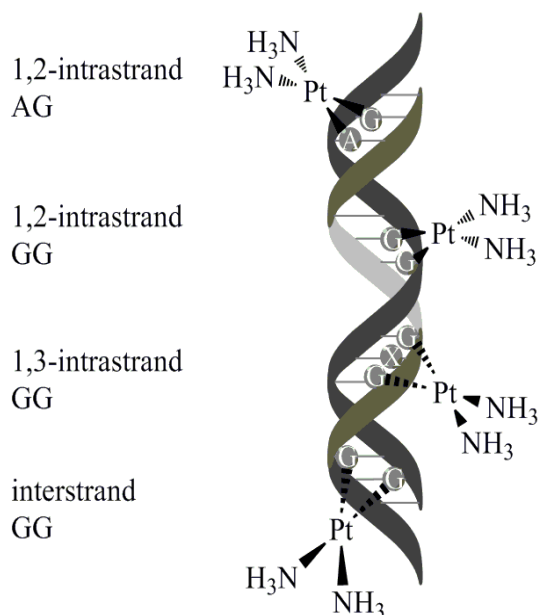


Fig. (3). DNA adduct formation with cisplatin moiety

1.2. Second and Third Generation Drugs

Despite its limitations, cisplatin is one of the most effective and commonly used agents to treat various types of human cancer. The spectrum of cancers that can be treated with cisplatin and other platinum-based agents is narrow and the therapeutic efficacy suffers

from side-effects and resistance phenomena [14]. Clinical effectiveness of cisplatin has been limited by significantly unfavourable side-effects, for example dose-dependent ototoxicity, nephrotoxicity, and neurotoxicity. Cisplatin resistance could arise from reduced platinum uptake, increased efflux, intracellular detoxification by glutathione, increased DNA repair, decreased mismatch repair, defective apoptosis, modulation of signalling pathways, or presence of quiescent non-cycling cells [23]. One strategy to overcome cisplatin resistance is to design platinum complexes that specifically deal with some or even all of the above mentioned resistance mechanisms. For these reasons, much attention has been directed towards the design of the new platinum-based complexes. The first stage of variation on cisplatin was derived by substituting chlorido with other anionic ligands (Fig. 4). These studies first produced carboplatin and nedaplatin.

Carboplatin (Fig. 4) has a cyclobutanedicarboxylato leaving group that facilitates a slower reaction with glutathione and metallothioneins compared to cisplatin. The hydrolysis reaction mechanisms of carboplatin take place through a biphasic mechanism with a ring-opening process followed by the loss of the malonato ligand [24]. Carboplatin obtained FDA approval for clinical use in 1989. Carboplatin has a lower efficiency than cisplatin in germ-cell tumors, head and neck cancers, and bladder and esophageal carcinomas, but both drugs appear to have a comparable effect on ovarian cancer, extensive small-cell lung cancers, and advanced non-small-cell lung cancers [25]. Although carboplatin has the benefits of reduced toxicity compared to cisplatin, it has neither enlarged the spectrum of platinum-sensitive cancers, nor has it proved to be active in cisplatin-resistant cancers.

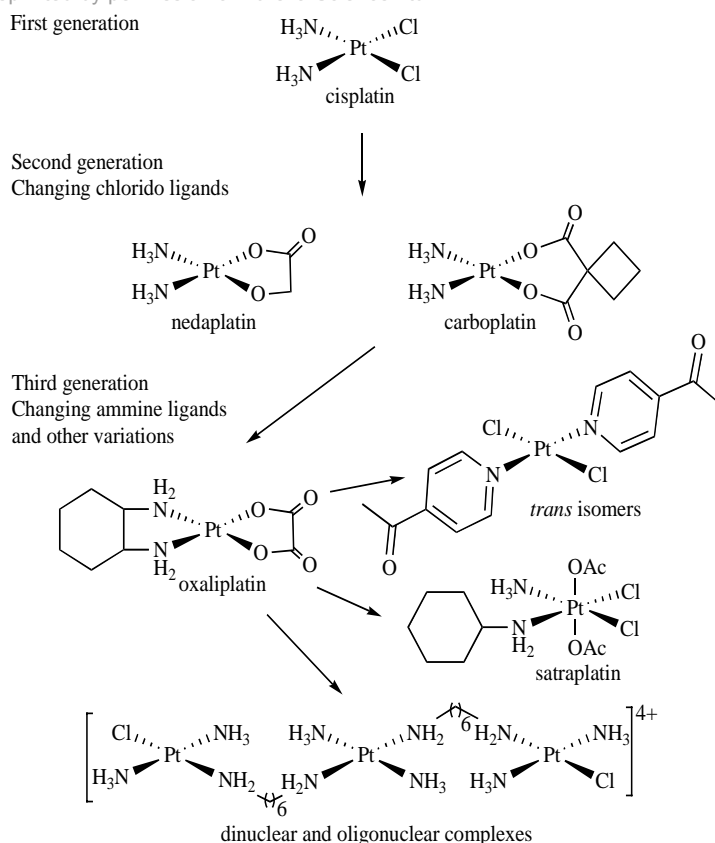


Fig. (4). History of the development of platinum drugs.

The second variation on cisplatin involved substitution of NH_3 ligands by different amine ligands, e.g. oxaliplatin. Furthermore, variation of the oxidation state of platinum from II to IV leads to more kinetically inert compounds like satraplatin.

Oxaliplatin (Fig. 4) with an oxalato leaving group and a diaminocyclohexane (dach) entity belongs to the third generation of platinum drugs. It was approved by FDA for the clinical treatment of colon cancer in 2004, and apparently operates by a different mechanism of action from the classical cisplatin or carboplatin [13]. Oxaliplatin is active against colorectal tumors with an improved therapeutic index compared to cisplatin and carboplatin. The dose-limiting undesirable reaction of oxaliplatin is neurotoxicity. Oxaliplatin has a unique pattern of side-effects, which in addition to neurotoxicity, include hematological toxicity and gastrointestinal tract toxicity.

Satraplatin (Fig. 4), for which clinical trials are in progress, is supposed to be the first orally administrated platinum-based drug against prostate and metastatic breast cancer [12,27]. However, as satraplatin is still a relatively new treatment, it is too early to know all of the possible side-effects (e.g. anaemia, diarrhoea, vomiting, nausea).

Even though transplatin was found to be inactive, a new approach with *trans* geometry of platinum complexes having aromatic or bulky amines is again under investigation [28]. In general, ideas for new compounds arise from mechanistic findings on previous generations of drugs. The second and third generation of platinum-based antitumor drugs have at least one H-donor function available on one of the amine groups. On the other hand, their steric and ligand exchange characteristics are different, especially for the platinum(IV) compounds, as these react very slowly. The role of the NH group has been explained kinetically in terms of its approach to guanosine (G). This H-bond additionally stabilizes G-G chelates coordinated to a platinum moiety. Furthermore, the NH group may exhibit hydrogen bonding to a

DNA backbone phosphate [29,30]. Initially, it was assumed that kinetically inert platinum(IV) compounds have to be reduced to platinum(II) before binding to the DNA. But later studies, however, have shown strong evidence that also unreduced platinum(IV) compounds may react with DNA/DNA fragments [31].

2. UNCONVENTIONAL PLATINUM-BASED DRUGS IN PRECLINICAL DEVELOPMENT

2.1. Transplatinum Complexes

Compared to cisplatin, transplatin showed lower *in vitro* cytotoxicity and lower *in vivo* activity [32]. For these reasons, transplatinum compounds were discharged from investigations for a long time. The first important investigations were published in 1990, when many transplatinum complexes with significant *in vitro* effects on different tumor cells were discovered [33,34]. The most promising results for transplatinum complexes are for those containing heterocyclic, aliphatic, phosphoric or imino ether ligands. Complexes with the general formula *trans*- $[\text{PtCl}_2\text{L}_2]$, where L is pyridine or 4-methylpyridine, showed higher activity than that found for their *cis* counterparts against L1210 leukemia cells [35]. Furthermore, the trinuclear platinum complex (Fig. 4) containing two monofunctional *trans*- $[\text{PtCl}(\text{NH}_3)_2]$ platinum moieties bridged by a platinum tetraamine unit, *trans*- $[\text{Pt}(\text{NH}_3)_2\{\text{NH}_2(\text{CH}_2)_6\text{NH}_2\}_2]$, has entered clinical trials [36,37]. Novel results on the cytotoxicity of transplatinum complexes confirm that there is virtually no structural limitation on potential therapeutically active transplatinum complexes [35,38]. Recently, a study on the *in vitro* activity of transplatinum complexes (Fig. 4), *trans*- $[\text{PtCl}_2(n\text{-ap})_2]$ ($n = 3$ or 4; ap = acetylpyridine), was reported [39]. The complexes showed moderate to potent antiproliferative activity on various cancer cell lines. The transplatinum complex containing 4-acetylpyridine ligands was capable of overcoming cisplatin resistance in the human osteosarcoma cisplatin-resistant cell line U2OScisR.

2.2. Platinum Complexes Containing Amino Acid Derivatives

Platinum(II) and platinum(IV) complexes with amino acids, peptides and their derivatives attracted attention for a long time [40]. Herein we will review some platinum complexes containing amino acid derivatives, such as dipeptides and diaminoacids bridged *via* nitrogen atoms with ethylene or propylene moieties.

Platinum(II) and platinum(IV) complexes containing L-methionine, glycylglycine, glycyl-L-methionine and L-alanyl-L-methionine were tested for antitumor activity against sarcoma 45, guerin carcinoma, sarcoma 180, adenocarcinoma 755, and Krebs 2 ascites carcinoma in mice and rats [41]. Many of the complexes showed cytotoxic activity. The reactive group of peptides to which the platinum was bound, as well as the oxidation state of platinum, affected the activity. Platinum(II) complexes of *S*-(2-aminoethyl)-L-cysteine and *S*-(2-aminoethyl)-D,L-penicillamine were screened against L-1210 lymphoid leukaemia or P388 lymphocytic leukaemia in male or female mice. The platinum(II) complex with *S*-(2-aminoethyl)-D,L-penicillamine showed strong antitumor activity in female mice, doubling their lifespan [42].

Platinum(II) complexes [PtX₂(dipeptide)] (X = Cl, I; dipeptide = L-methionylglycine, L-methionyl-L-leucine) revealed considerable *in vitro* activity in the case of the platinum(II) complex with L-methionylglycine and chloro ligands against liposarcoma, lung carcinoma A549 and melanoma 518A2 human tumor cell lines [43]. A decrease of cytotoxic activity was observed on substitution of glycine by L-leucine, and Cl⁻ with I⁻ ligands. The potential of antitumor drugs of such classes of platinum(II) complexes is dependent on the kind of ligands as well as on tumor cell type. On the other hand, interesting from the metabolic point of view in cancer patients treated with oxaliplatin [44], [Pt(dach)L] complexes (dach = (1*R*,2*R*)-*trans*-diaminocyclohexane; L = L-methionine, *S*-methyl-L-cysteine, L-selenomethionine and *Se*-methylseleno-L-cysteine) have been synthesized and characterized.

Recently reported was the influence on *in vitro* activity on ligand substitution in a model compound K[PtCl₂(L-pro-H)] (L-pro-H = L-prolinato) [45]. Namely, it was found that substitution of one chlorido by a dmso ligand, K[PtCl₂(L-pro-H)] → *SP*-4-4-[PtCl(L-pro-H)(dmso)] greatly decreases cytotoxicity (former: IC₅₀ = 11–30 μM; later: IC₅₀ > 100 μM) against anaplastic thyroid cancer 8505C, head and neck cancer A253, lung cancer A549, and colon cancer DLD-1.

Interestingly, platinum(II) and platinum(IV) complexes containing ethanediybis(glycin), ethanediybis(β-alanin) and propanediybis(glycin) (trivial names: ethylenediamine-*N,N'*-diacetic acid, H₂edda; ethylenediamine-*N,N'*-di-3-propionic acid, H₂eddp; propylenediamine-*N,N'*-diacetic acid, H₂pdda) have been considered as variants of the orally active satraplatin [46,47]. Complexes of the type [PtCl₂(H₂edda-κ²*N,N'*)]-type and [PtCl₂(edda-κ²*N,N'*-κ²*O,O'*)]-type (platinum(II) and platinum(IV), respectively) have shown lower activity than cisplatin or satraplatin [48–50].

Surprisingly, cytotoxic investigations of platinum(II) and platinum(IV) halide complexes containing diesters of eddp showed that the tetrachloroplatinum(IV) complexes were the most efficient complexes against human adenocarcinoma HeLa cells (approx. five times less active than cisplatin) and human myelogenous leukemia K562 cells (comparable with cisplatin) acting through apoptotic cell death [51]. Significant *in vitro* antitumor activity by platinum(IV) complexes with bidentate *n*-dibutyl and *n*-dipentyl esters of eddp, [PtCl₄(*n*-Bu₂eddp)] and [PtCl₄(*n*-Pe₂eddp)], was demonstrated on L929 fibrosarcoma and U251 astrocytoma tumor cells [52,53]. The kinetics of the tumor cell death process induced by these complexes is considerably faster than that induced by the classical platinum(II)-based drug, cisplatin [52]. The best investigated complex (“parent” compound), [PtCl₄(*n*-Bu₂eddp)], of a growing family of R₂edda-type metal complexes [54–64], is now under *in vivo* investigations. The mechanisms of action of [PtCl₄(Et₂edch)]

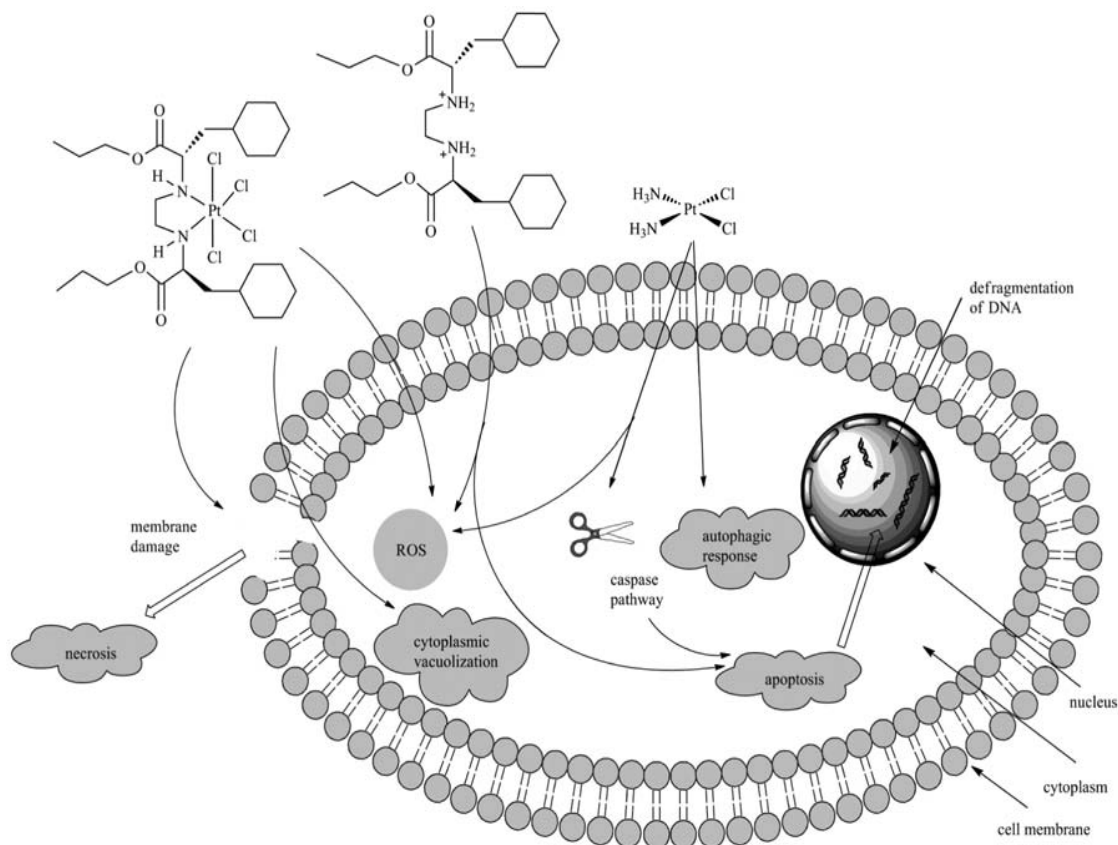


Fig. (5). Mechanism of action of [PtCl₄(Et₂edch)] and [H₄(Et₂edch)]²⁺ on human glioma U251 cell line.

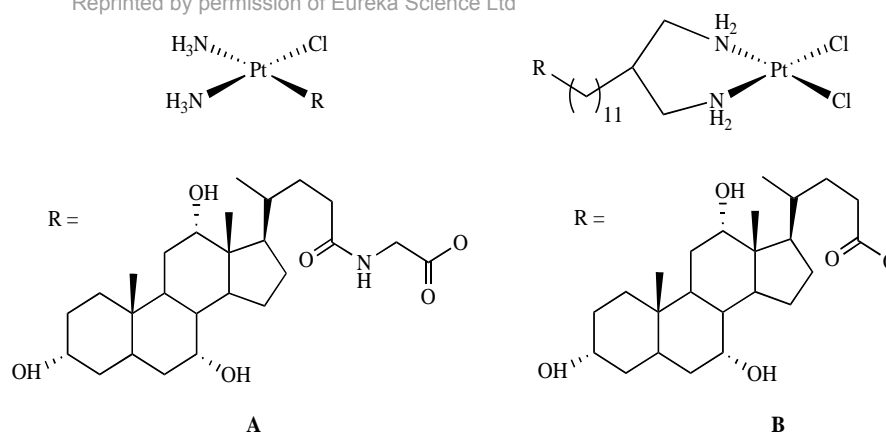


Fig. (6). Platinum(II) complexes with carrier ligands type **A** and **B**.

complex [(*S,S*-ethylenediamine-*N,N'*-di-2-(3-cyclohexyl)propanoic acid, H₂eddch)] and ligand precursor, [H₄(Et₂eddch)]Cl₂, are presented in Fig. (5) [60]. Based on recent work, some structure-activity relationships could be derived: *in vitro* activity decreases from platinum(IV), platinum(II), palladium(II) to ligand precursors. One exception is on CLL cells (chronic lymphocytic leukemia) in which platinum(IV) complexes were found to be less active than platinum(II) and palladium(II) complexes [63,64]¹.

2.3. Platinum Complexes with Carrier Ligands

Compounds consisting of three functional parts: a transport fragment, a spacer and a biologically active 'drug' component have been developed recently (Fig. 6). The role of different types of transporters might modulate the uptake of drugs. Bile acid in the ligand sphere of the platinum compounds (Fig. 6A) was found to be an essential prerequisite for these compounds to target liver tumor cells [65]. It was proved that the Bامت-UD2 is capable of interacting with DNA. Furthermore, the compound is able to inhibit DNA synthesis and consequently to reduce cell proliferation [66].

Recently the synthesis and characterization of platinum(II) compounds with cholic acid are reported [67] (Fig. 6B). The difference between type **A** and **B** complexes (Fig. 6) is in the mode of coordination of the carrier ligands. In type **A** complexes carrier ligands (bile acid) act as leaving groups, while in type **B** complexes carrier ligands (cholic acid) represent nonleaving bidentate diamine ligands. The influence of the length of an alkyl spacer ($n = 4, 6, 8$, or 11) in **B**-type complexes was investigated for *in vitro* cytotoxicity against human head and neck squamous-cell carcinoma, UM-SCC-22B and human cholangio carcinoma, SK-CHA-1 cell lines, in order to optimize the distance between the drug and the transport fragment [68]. The dichlorido complexes were found to be more efficient than their carboplatin analogues, but in both types of complexes the most active compounds contained the longest spacer ($n = 11$) between the cholic acid and platinum moieties. The dichloridoplatinum(II) complex with a long chain linker displayed a significantly higher cytotoxicity than cisplatin or carboplatin and was able to completely circumvent the cisplatin resistance of human testicular 1411HP cancer cells, by inducing apoptosis.

By substituting cholic acid with the tetrahydropyran moiety in type **B** complexes, the compounds are made more accessible [69]. Also here, the influence of the length of an alkyl spacer ($n = 4, 6, 8$, or 11) has been investigated and it was found that the activity increases with alkyl chain length. The cytotoxic effect was retained, as with platinum complexes containing cholic acid, against cisplatin

resistant 1411HP cells. The mechanism of action was studied in more detail and the cytotoxicity was correlated to larger and faster cellular platinum uptake and much faster initiation of apoptotic cell death. The platinum(II) complex with the longest spacer ($n = 11$) overcomes cisplatin resistance and induces programmed cell death with molecular features different from cisplatin, suggesting that both drugs induce apoptosis but through different initial pathways.

2.4. Organoplatinum(IV) Complexes

Reports on anticancer properties of organometallic platinum(IV) complexes are rare similar to those of cisplatin-like derivatives [70,71]. Several promising organoplatinum complexes that came out of our research are presented within this review article.

Dinuclear platinum(IV) metallacrown ethers [PtBr₂Me₂{im(CH₂CH₂O)_xCH₂CH₂im}] [Pt₂Me₂{im(CH₂CH₂O)₂CH₂CH₂im}] (im = imidazol-1-yl; $x = 2, 3$; Fig. 7) and [PtBr₂Me₂{bim(CH₂CH₂O)₂CH₂CH₂bim}] (bim = benzimidazol-1-yl), as well as mononuclear complexes [(PtBr₂Me₂)₂{μ-im(CH₂CH₂O)_xCH₂CH₂im}]₂ ($x = 0, 1$) were tested on the three tumor cell lines: liposarcoma, A549 (non-small-cell lung carcinoma) and 518A2 (melanoma) [72]. These metallacrown ethers possess significant *in vitro* antitumor activity. From the investigations on three chosen tumor cell lines it was found in general that the activity of the [PtBr₂Me₂] moiety is enhanced by coordination to the polyether ligands.

A pair of mononuclear and dinuclear trimethylplatinum(IV) complexes containing similar (iodo, pyrazole/pyrazolato) ligands (Fig. 7) have been tested on nine different tumor cell lines: anaplastic thyroid cancer 8505C, head and neck tumors A253 and FaDu, cervical cancer A431, lung carcinoma A549, ovarian cancer A2780, colon carcinoma DLD-1, HCT-8 and HT-29 [73]. The mononuclear complex exhibited cytotoxic activity about one order of magnitude lower than that of cisplatin (IC₅₀(mononuclear)/IC₅₀(cisplatin) = 7.0–58.4). Contrarily, the dinuclear trimethylplatinum(IV) complex showed activities similar to cisplatin (IC₅₀(dinuclear)/IC₅₀(cisplatin) = 0.4–2.7). Interestingly, the dinuclear complexes are found to be more efficient than cisplatin (IC₅₀(dinuclear)/IC₅₀(cisplatin) = 0.4–0.5) against 8505C and DLD-1 cell lines, even when these are resistant to cisplatin.

Thionucleobases, 2-thiocytosine (SCy) and 1-methyl-2-thiocytosine (1-MeSCy) have been used as ligands in the synthesis of organoplatinum(IV) complexes containing the [PtMe₃(bpy)] moiety, namely [PtMe₃(bpy)(SCy-κS)][BF₄] and [PtMe₃(bpy)(1-MeSCy-κS)][BF₄] complexes, respectively [74]. The complexes have been tested against nine different tumor cell lines 8505C, A253, FaDu, A431, A549, A2780, DLD-1, HCT-8 and HT-29. A

¹Vujić, J.M.; Kaluderović, G.N.; Zmejkovski, B.B.; Milovanović, M.; Volarević, V.; Arsenjević, N.; Trifunović, S.R. unpublished results.

similar antiproliferative activity was observed for these two organoplatinum(IV) complexes, which may indicate that the methyl group in 1-MeSCy in $[\text{PtMe}_3(\text{bpy})(1\text{-MeSCy}-\kappa\text{S})][\text{BF}_4]$ has no obvious influence on the efficacy in all the investigated cell lines except for DLD-1. The compounds have been found to express lower activity than cisplatin.

Furthermore, $[\text{PtMe}_3(\text{bpy})(\text{L}-\kappa\text{S})][\text{BF}_4]$ complexes ($\text{L} = \text{S}^2\text{Ura}$, S^4Ura , $\text{S}^2\text{S}^4\text{Ura}$) with thionucleobases 2-thiouracil (S^2Ura), 4-thiouracil (S^4Ura) and 2,4-dithiouracil ($\text{S}^2\text{S}^4\text{Ura}$; Fig. 7) have been investigated *in vitro* [75]. Cytotoxic studies revealed selective activities which are, in part, comparable to those of cisplatin. In a selected case, cell cycle perturbations and a trypan blue exclusion test indicated the induction of apoptotic cell death.

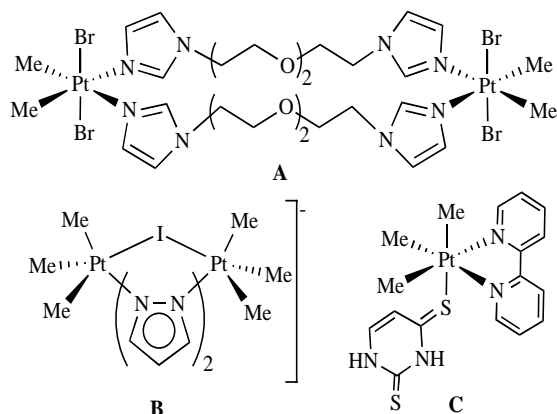


Fig. (7). Highly active organoplatinum(IV) complexes.

Cytotoxic studies of the dinuclear complexes $[(\text{PtMe}_3)_2(\mu\text{-L})_2]$ ($\text{LH} =$ pyridine-2-thione, pytH ; pyrimidine-2-thione, pymtH ; thiazoline-2-thione, tztH) against 8505C, A253, A549, A2780 and DLD-1 revealed moderate to high activities towards the tested cell lines [76]. Furthermore, $[(\text{PtMe}_3)_2(\mu\text{-tzt})_2]$ showed the highest antiproliferative activity which was found to be comparable or even higher, in cisplatin resistant cell lines DLD-1 and 8505C, than that of cisplatin. In contrast to it, the non-coordinated heterocycles $\text{S}^{\text{D}}\text{DH}$ ($\text{D} = \text{N}$ or S) did not show any antitumor activities in concentrations $<125 \mu\text{M}$ against the cell lines tested.

Interestingly, all dinuclear trimethylplatinum(IV) complexes investigated so far, proved to have a moderate to high activity that

was not found for mononuclear complexes $[\text{PtMe}_3\text{I}(\text{bpy})]$ and $[\text{PtMe}_3\text{I}(\text{pzH})_2]$ [73]. Furthermore, ligands/ligand precursors were found to be inactive in direct comparison with the corresponding organoplatinum(IV) complexes [72–76].

3. COMMENCEMENT OF NONPLATINUM COMPLEXES AS ANTITUMORAL AGENTS

The application of platinum complexes as anticancer agents has stimulated examination of other active metal complexes in cancer chemotherapy (Fig. 8) [77,78]. The point towards developing nonplatinum anticancer complexes is to overcome the main limitations of platinum drugs: narrow range of activity, acquired resistance and severe toxicity. Complexes of transition metals other than platinum may demonstrate anticancer activity and toxic side-effects noticeably diverse from that of platinum-based drugs for a number of obvious reasons: they are expected to have different chemical behaviour, hydrolytic rates and mechanism(s) of action (Fig. 9). Several metals have led to biologically active compounds, such as ruthenium, gallium, titanium, tin, etc. (Fig. 8) [77,78].

3.1. Ruthenium(II/III) Complexes

Many ruthenium compounds are soluble in water and active against cancer cells, including cisplatin-resistant cancer cells [79,80]. The interest in cytotoxic ruthenium compounds is mainly directed into two families: octahedral ruthenium(III) and tetrahedral (η^6 -arene)ruthenium(II) complexes coined "piano stool" compounds [81]. From the first family, the most prominent examples are NAMI-A (Fig. 8) and KP1019 which are the first ruthenium agents to enter [82,83], and currently in phase I clinical trials [84,85]. Despite its lack of activity against primary tumors, the drug NAMI-A is a potent antimetastatic agent. KP1019 is in phase I clinical trials for the possible treatment of colon carcinoma and other types of cancer [84,86].

Lately, piano stool compounds with anticancer activity represent an interesting and very broad new class centered on ruthenium arene compounds (Fig. 8). $[\text{Ru}(\eta^6\text{-biphenyl})(\text{en})\text{Cl}]^+$ water-soluble organometallic compound shows good *in vivo* cytotoxicity against primary tumors [87]. A variety of ruthenium arene complexes with different ligands have been tested [88–94]. Ruthenium compounds as antitumor agents represent a growing field. Besides the mentioned compounds, many other ruthenium complexes showed promising *in vitro* antitumor properties.

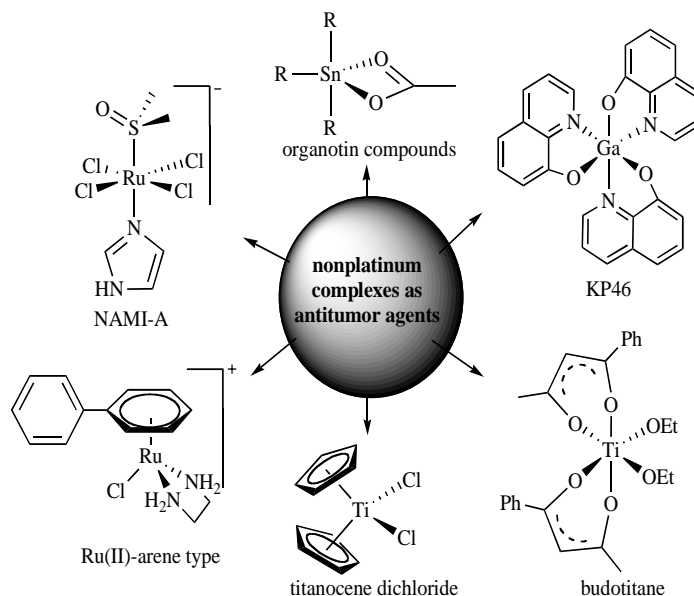


Fig. (8). Some nonplatinum metal-based antitumor agents.

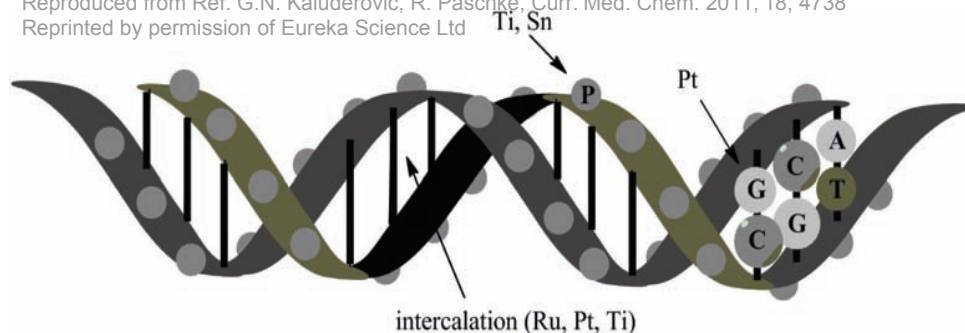


Fig. (9). Interaction of DNA and (non)platinum-based drugs (P – phosphate groups; A, G, C and T nucleobases).

3.2. Gallium(III) Compounds

The antitumor activity of gallium(III) compounds was first observed by Hart *et al.* [95]. The exact mechanism of gallium cytotoxicity is still unknown. It has been assumed that the uptake of gallium into the cell is mediated by transferrin receptors [96]. The mechanism shows a competitive binding to transferrin, which may lead to cellular uptake of high amounts of gallium(III). Furthermore, it is indicated that the enzyme ribonucleotide reductase, inside the cell, might be the biological target of gallium(III) ions [97]. Mechanisms of its action could be mediated by induction of apoptosis through inhibition of proteasome activity, upregulated proapoptotic molecule Bax and activation of effector caspase-3 [98,99]. Gallium(III) chloride and gallium(III) nitrate exhibited antitumoral activity against several tumor cell lines [100–103]. Both salts entered into clinical trials, but were initially discharged from clinical trials shortly. Gallium(III) chloride was abandoned because intestinal absorption was too low to obtain therapeutically active drug doses, while intravenous administration of gallium(III) nitrate was accompanied by nephrotoxicity, optical neuropathy and other severe side effects. Low-dose gallium(III) nitrate is currently under reevaluation in patients with non-Hodgkin's lymphoma [104].

Gallium(III) nitrate undergoes hydrolysis very easily in biological media and forms insoluble gallium(III) oxide blocking the absorption and membrane permeation of the gallium ion. In order to find suitable ligands that stabilize gallium(III) against hydrolysis, and on the other hand to increase cytotoxicity against cancer cells, many gallium(III) complexes with different ligand systems (*O*, *N* and *S* donor atoms) have been synthesized. Gallium(III) complexes as chemotherapeutics deserve a special attention due to the analogy with iron(III), by affecting biochemical pathways similar to those found in iron metabolism in consequence of similar properties of gallium(III) and iron(III) ions [105,106]. The first two promising gallium(III) complexes which are in clinical trials, are gallium(III) maltolate (G4544; Fig. 10A) and (8-quinolinolato)gallium(III) (KP46; Fig. 8) [107–109]. G4544 has been clinically examined for bone metastases and metabolic bone disease but may also prove to be active as an antineoplastic agent [110]. KP46 has been shown to induce apoptosis in a large panel of malignant cell lines.

Gallium(III) complexes with thiosemicarbazones expressed highly cytotoxic potential and were found to be 20-fold more potent than cisplatin against malignant glioblastoma RT2 and T98 cell lines (IC₅₀: 0.81–9.57 μM, RT2 and 3.6–11.30 μM, T98). The recent studies indicate that these compounds might activate apoptotic cell death pathways by mechanisms that are both dependent and independent of p53 [111–114].

Interesting dinuclear and tetranuclear dimethylgallium(III) complexes with carboxylato or thiolato ligands have been investigated against a panel of different tumor cell lines: 8505C anaplastic thyroid cancer, DLD-1 colon carcinoma, A549 lung carcinoma, A2780 ovarian cancer, FaDu, HN, Cal27, Cal33 and

A253 squamous head and neck carcinomas [114–117]. The compounds exhibited much more potent cytotoxicity than gallium(III) nitrate, and similar or lower than cisplatin. Surprisingly, thiolato compounds (Fig. 10B) showed significantly lower toxicity than cisplatin and induce apoptotic cell-death pathways that are cell-type specific.

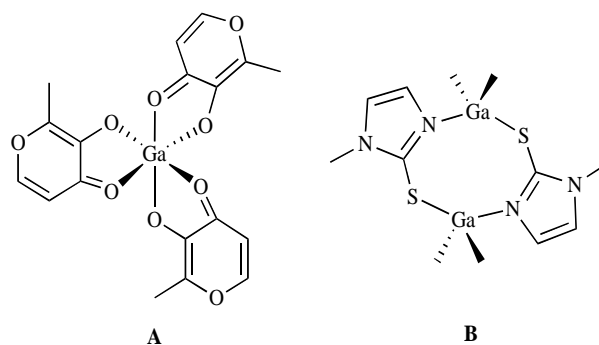


Fig. (10). Active G4544 (A) and dinuclear dimethylgallium(III) complexes (B).

3.3. Titanium(IV) Complexes

Two families of titanium(IV) complexes are used for biological applications. Explicitly, titanocene dichloride and budotitan (Fig. 8) [118–126] and their various close analogues derived from manipulation of Cp or diketonato ligands. Budotitan was the first nonplatinum complex to enter clinical trials for its activity towards colon tumor cells. This compound and several analogues showed high promise in investigations. It was observed that the activity depends on the planarity of the substituents suggesting that the mechanism of its activity involves DNA intercalation. Titanocene dichloride exhibited higher *in vivo* than *in vitro* activity towards cisplatin-resistant cells with different and improved toxicity patterns [127]. This compound entered clinical trials in 1993, and has therefore prompted development of similar compounds (Fig. 11A) [128,129]. While the structural analogy of this agent makes intriguing parallels with cisplatin, in fact the agent is hydrolyzed in water to a variety of species and it is still unclear what the active component is [130]. The biological target of titanocene dichloride was proposed to be DNA [131]. Sadler proposed a mechanism for the delivery of titanium(IV) species to the cell nucleus assisted by transferrin [132–135]. Both, budotitan and titanocene dichloride failed in clinical trials because of low efficacy in terms of activity versus toxicity ratio [136]. The reason is supposed to be a consequence of their rapid hydrolysis to give unidentified aggregates [120,128,137]. At first, the labile ligands (EtO⁻, Cl⁻) hydrolyze within seconds, followed by the hydrolysis of the inert groups (diketonato, Cp) within hours [138,139].

A variety of substituted titanocene and *ansa*-titanocene complexes have been tested against human adenocarcinoma HeLa, human myelogenous leukemia K562, human malignant melanoma Fem-x tumour cell lines and normal immunocompetent cells

Reproduced from Ref. G.N. Kaluđerović, R. Paschke, Curr. Med. Chem. 2011, 18, 4739

Reprinted by permission of Eureka Science Ltd (peripheral blood mononuclear cells PBMC) [140–142]. Manipulating Cp rings with alkyl moieties leads to a slight increase in the cytotoxicity in some studied cells. The highest influence on the activity was observed when a pent-4-enyl fragment is included (Fig. 11B). Other substituents examined on the Cp ring or the silicon *ansa*-bridged titanocene had a negative influence on the activity.

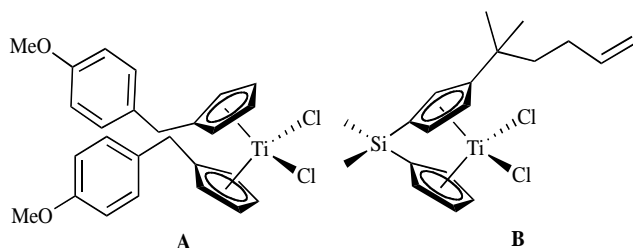


Fig. (11). Titanocene-Y (A) and $[\text{Ti}\{\text{Me}_2\text{Si}(\eta^5\text{-C}_5\text{Me}_4)(\eta^5\text{-C}_5\text{H}_3\{\text{CMe}_2\text{CH}_2\text{CH}_2\text{CH}=\text{CH}_2\})\}\text{Cl}_2]$ (B).

3.4. Tin(IV) Complexes

A large number of organotin-based complexes have been tested *in vitro* and *in vivo*. Firstly, organotin compounds have been analyzed against murine leukemia cell lines and also against different panels of human cancer cell lines. In some studied cytotoxic compounds, the organotin(IV) moiety is bound to a phosphate group of the DNA backbone [143,144]. Organotin(IV) complexes might be designed with attractive properties such as increased water solubility, lower general toxicity than platinum drugs [145–147], better body clearance, fewer side-effects, and no emetogenesis. Most importantly, organotin complexes do not develop the tumor drug tolerance that is well-established for cisplatin and its analogues [148].

Some structure-activity relationship patterns in the area of predicting anticancer activity based on the R and L groups in the $[\text{SnR}_2\text{L}_2]$ moiety of the diorganotin carboxylates and triorganotin $[\text{SnR}_3\text{L}]$ (L = bidentate ligand with O and/or N donor atoms) were recently described [149–156]. Some of the organotin(IV) complexes were found to be even more active *in vitro* than cisplatin [157,158].

It is proved that the moieties $[\text{SnR}_n]^{(4-n)+}$ ($n = 2$ or 3) may bind to membrane proteins or glycoproteins, or to cellular proteins; e.g. hexokinase, ATPase, acetylcholinesterase of human erythrocyte membrane or skeletal muscle membranes [159] or may interact directly with DNA [160].

Uncommon tetraorganotin(IV) derivatives were recently investigated [161]. Cyclopentadienyltin(IV) compounds have been tested against 8505C, A253, A549, A2780 and DLD-1 tumor cell lines. All compounds exhibited higher *in vitro* activity than cisplatin, in nanomolar range from 37 to 351 nM.

Diphenyl and triphenyltin(IV) complexes containing carboxylate ligands [3-methoxyphenylacetic acid (3-MPAH), 4-methoxyphenylacetic acid (4-MPAH), 2,5-dimethyl-3-furoic acid (DMFUH) or 1,4-benzodioxane-6-carboxylic acid] have been studied against HeLa, K562, Fem-x and rested and stimulated normal immunocompetent cells, PBMC [162]. Organotin(IV) complexes showed very high activity, even higher than that of cisplatin. Triphenyltin(IV) compounds were found to be more effective than corresponding diphenyltin(IV) complexes. A triphenyltin(IV) complex with DMFU was found to be the most active against K562 and Fem-x cell lines (30–112 times more effective than cisplatin) and with a relatively high selectivity.

Recently, trigonal-bipyramidal anionic tin(IV) complexes were used for *in vitro* studies [163]. Namely, triphenyltin(IV) chlorides containing *N*-phthaloylglycine (P-Gly), *N*-phthaloyl-L-alanine (P-

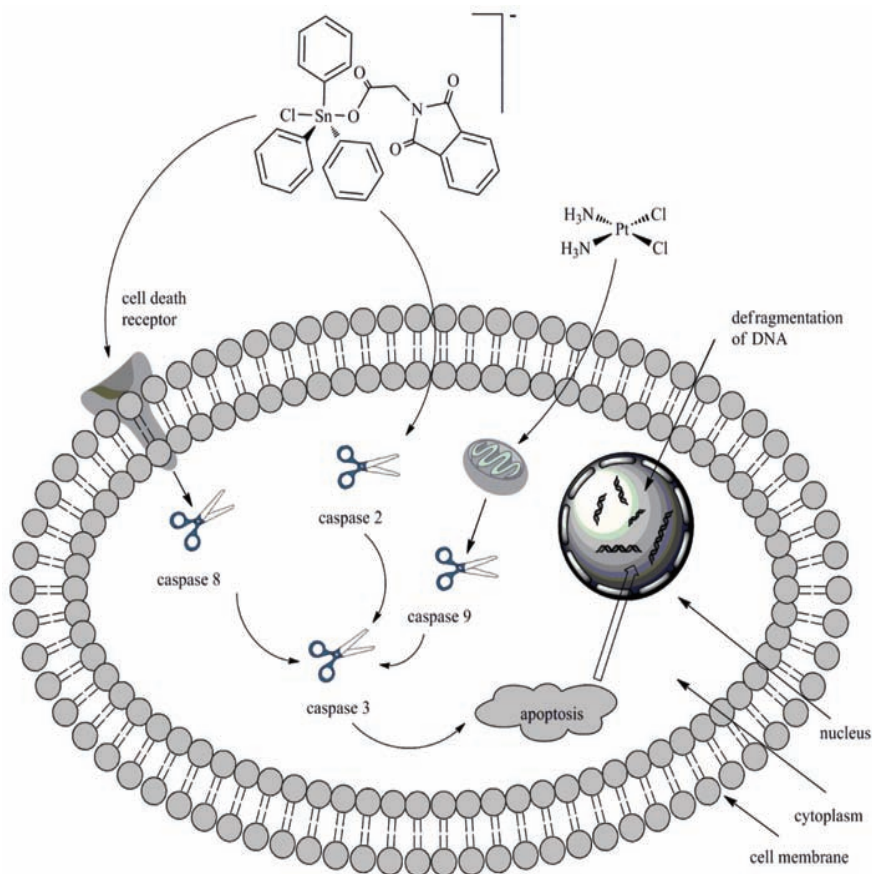


Fig. (12). Mechanism of action of $[\text{SnPh}_3(\text{P-Gly})\text{Cl}]^-$ on human DLD-1 cells.

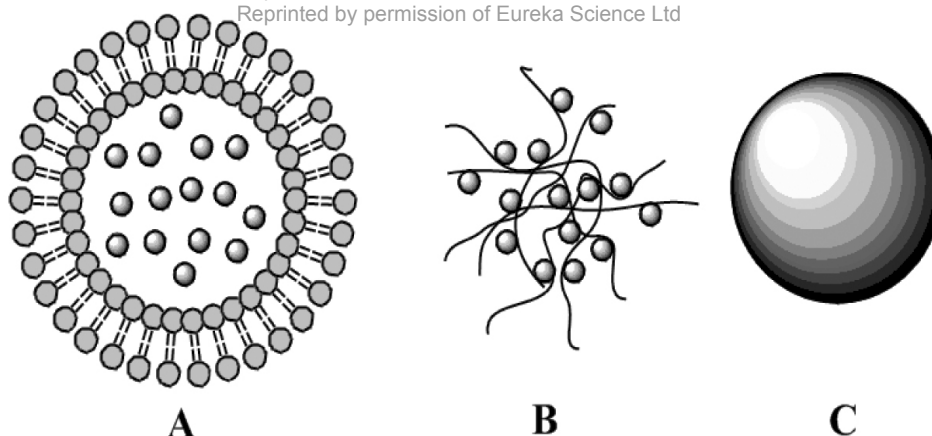


Fig. (13). Pharmaceutical carriers: liposomes (A), polymers (B) and nanomaterials (B).

AlaH), and 1,2,4-benzenetricarboxylic 1,2-anhydride (BTCH) were tested against 8505C, A253, A549, A2780 and DLD-1 tumor cell lines. Compounds expressed high activity against cell lines with lower IC_{50} values than cisplatin. The most active compound was found to be organotin(IV) compound with P-Gly (50 times more active than cisplatin). However, the most promising compound, triethylammonium (*N*-phthaloylglycinato)triphenyltin(IV) chloride, is found to induce apoptosis *via* extrinsic pathways on DLD-1 cell line (Fig. 12).

4. NANODRUG DELIVERY SYSTEM

Traditional therapeutic strategies usually require highly systemic administration due to non-specific biodistribution and rapid metabolism of free drug molecules prior to reaching their targeted sites. The ability to deliver highly efficient therapeutic compounds specifically to diseased sites is crucial for effectively treating all human illnesses [164]. Among many possible applications of nanomaterials in medicine, drug delivery systems within the nanometer-size regime can be developed to alter both pharmacological and therapeutic effects of drug molecules. Furthermore, special interest in the development of drug nanocarriers stems from the existence of some very promising *in vitro* active compounds with relatively poor solubility. The therapeutic application of hydrophobic, poorly water-soluble agents is associated with serious problems since low water-solubility results in poor absorption and low bioavailability [165]. Due to their small size, nanoscale drug delivery systems offer superior advantages, such as altered pharmacokinetic behaviour and improved payload, over conventional large-scale systems [164]. Modifying surfaces of nanomaterials with different molecules or using different building blocks may yield nanomaterials with special functions like targeting, treatment and diagnosis [166–168]. Among drug carriers, many varieties of nanoparticles are available: soluble polymers, microparticles made of insoluble or biodegradable natural/synthetic polymers, microcapsules, cells, cell ghosts, micelles, quantum dots, dendrimers, lipoproteins, liposomes, niosomes, solid lipid particles, and different nanoassemblies (Fig. 13) [164].

4.1. Liposomes as Drug Carriers

For more than twenty years liposomes have been considered promising drug carriers [169,170]. Liposomes are artificial phospholipid vesicles in which an aqueous volume is entirely surrounded by a phospholipid membrane. The size of vesicles may vary in size from 30 to several hundred nanometers. They can be loaded with a variety of water-soluble (into their inner aqueous compartment) and water-insoluble drugs (into the hydrophobic compartment of the phospholipid bilayer) [171]. They have to be

smaller than the vascular cutoff (up to 780 nm) to extravasate and reach solid tumors. Vesicle size also plays a critical role in complement activation. Currently, liposomes are investigated as a vehicle for a variety of therapeutic agents, namely, as carriers for anticancer drugs (doxorubicin, cisplatin, paclitaxel, camptothecin), antibiotics (ciprofloxacin, amikacin, vancomycin), and in biology (antisense oligonucleotides, DNA).

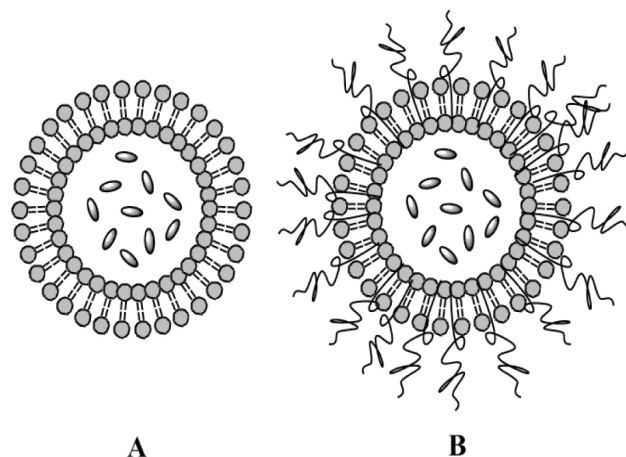


Fig. (14). Schematic presentation of unilamellar non (A) and PEGylated (B) liposomes loaded with cisplatin (○).

Non- and PEGylated liposomal formulations of cisplatin have been investigated (Fig. 14) [172,173]. Non-PEGylated liposomes are taken up by liver macrophages and destroyed with a half-life of 20 min in body fluids. On the other hand, PEGylated liposomes display a half-life of 5 days in body fluids [174]. Phase II clinical studies for Lipoplatin, an improved liposomal PEGylated formulation of cisplatin [175–177] revealed very promising results in the treatment of bladder, pancreatic, prostate, lung, and head and neck tumors. Reduced systemic toxicity and selective accumulation and an extended circulation in the body were observed. The advantage of Lipoplatin over cisplatin results from the ability of Lipoplatin to target primary tumors and metastases [174]. Liposomal oxaliplatin is expected to enter the clinical stage in the near future [178]. Aroplatin, a liposomal formulation of (dach)bis (neodecanoato)platinum(II) (dach = 1,2-diaminocyclohexane), showed positive results from phase II clinical trial in refractory metastatic colorectal cancer.

4.2. Nanostructured Mesoporous Materials as Drug Carriers

Nanotechnology in recent years has encouraged researchers to develop nanostructured materials for biomedical applications [179].

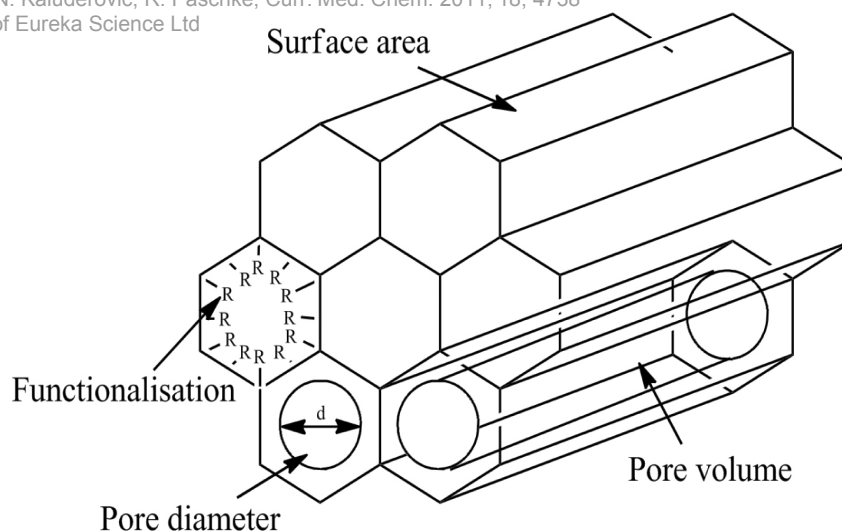


Fig. (15). Schematic representation of MCM-41.

Mesoporous material MCM-41, synthesized in the 1990s as a member of the M41S family of molecular sieves [180], was advised in 2001 as a drug delivery system [181]. These mesoporous materials were synthesized from supramolecular assemblies of surfactants. These surfactants template the inorganic component, commonly silica, during synthesis [182–184]. At the end, surfactant is removed by pyrolysis or dissolution with the appropriated solvent. Silica mesoporous matrices made in this way are potential drug carriers. They are characterized as ordered pore networks, very homogeneous in size, that can allow fine control of the drug load and release kinetics. A large pore volume to host the required amount of drugs, a high surface area implying increased drug adsorption, and a silanol-containing surface that can be functionalized to allow better control over drug loading and release describe the potential of MCM-41 type materials for drug delivery [179] (Fig. 15).

Decrease of the systemic side-effects of a drug could be obtained by local administration [185]. Furthermore, drug delivery systems for local drug release implanted in bone tissue are one of the most promising therapeutic concepts in orthopaedic surgery [179]. Different drugs, such as antibiotics, chemotherapeutic and anti-inflammatory agents, growth factors and others might be loaded in nanomaterials.

The use of mesoporous silicas as drug delivery systems was carried out in 2001 for the first time [186]. Ibuprofen (anti-

inflammatory drug) was confined in a MCM-41 matrix in an effort to design an implantable delivery system [179]. Theoretically, ibuprofen was locally released in bone tissue to reduce the inflammatory response after the implantation of a bioceramic in a bone defect [187].

The first studies regarding incorporation of cisplatin in mesoporous materials (hydroxylapatite) have been conducted very recently in 2007 by Natile and co-workers [188]. The studies were limited to adsorption and release of cisplatin from nanomaterials. Two years later, the first studies on the antiproliferative activity of hydroxylapatite loaded with platinum(II) complexes (Fig. 16A and B) against the HeLa cell line were conducted by the same group. Interestingly, cytotoxicity of platinum(II) complexes released from the hydroxylapatite-adsorbed complexes were found to be more cytotoxic than the unmodified complexes [185].

In parallel, our group investigated the influence of MCM-41 and SBA-15 surfaces grafted with two different titanocene complexes (Fig. 16C and D), $[\text{Ti}(\eta^5\text{-C}_5\text{H}_4\text{Me})_2\text{Cl}_2]$ and $[\text{Ti}\{\text{Me}_2\text{Si}(\eta^5\text{-C}_5\text{Me}_4)(\eta^5\text{-C}_5\text{H}_4)\}\text{Cl}_2]$, on the proliferation of the HeLa, K562, Fem-x and normal immunocompetent PBMC cells [189]. Surfaces MCM-41 and SBA-15 grafted with the $[\text{Ti}\{\text{Me}_2\text{Si}(\eta^5\text{-C}_5\text{Me}_4)(\eta^5\text{-C}_5\text{H}_4)\}\text{Cl}_2]$ complex were found to be the most active but not as active as cisplatin. Furthermore, additional studies suggested that cytotoxicity of the studied materials may be due to action of the released metal complex and is probably not due

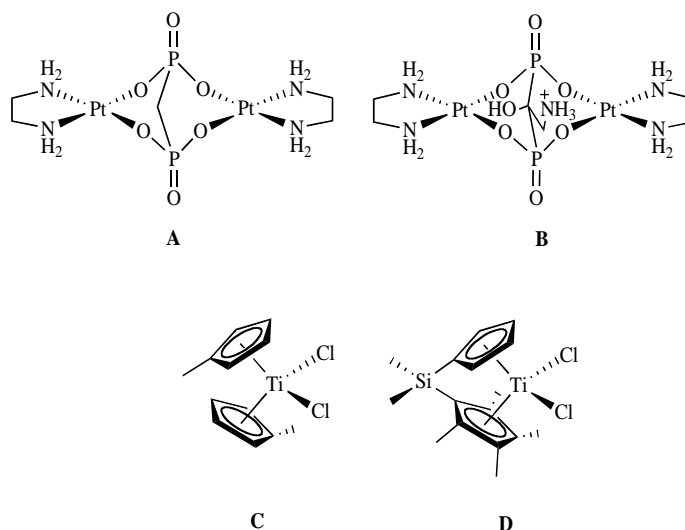


Fig. (16). Hydroxylapatite and MCM-41/SBA-15 nanomaterials loaded with platinum(II) (A, B) and titanium(IV) (C, D) complexes, respectively.

Reprinted by permission of Eureka Science Ltd to the particle action [190]. Namely, the activity of these surfaces strongly depends on the grafted titanocene complex.

CONCLUDING REMARKS

The aim of this review article was to outline some recent research in the field of preclinical investigations of anticancer metalloterapeutics. The article covers literature from the early beginning of the development of platinum-based antitumor drugs including clinically approved ones and those under clinical investigations. Furthermore, novel concepts of metalloterapeutics in *in vitro* investigations using different ligand molecules such as nucleobases, carrier/shuttle molecules and various platinum building blocks (organoplatinum(IV) moieties) are described.

Nonplatinum active compounds, based on ruthenium(II/III), gallium(III), titanium(IV) and tin(IV) are expected to have different mechanisms of action, biodistribution and toxicity from those of platinum drugs suggesting possible activity against tumors that are resistant or have acquired resistance to platinum-based drugs. With some of the nonplatinum complexes reviewed in this article it is shown that they are more selective toward tumor cell lines, exhibited lower toxicity, exhibited a mechanism different than that induced by cisplatin.

The concepts for a nanodrug delivery system using liposomes for water-soluble/insoluble drugs and nanomaterials grafted with platinum(II) and titanium(IV) based drugs, demonstrate the feasibility of these concepts within drug delivery development.

ACKNOWLEDGEMENTS

The authors gratefully acknowledges financial support from the Alexander von Humboldt Foundation (GNK) and BioSolutions Halle GmbH, Germany, and wish to acknowledge with thanks the advice and critical reviews provided by Prof. Dr. Dirk Steinborn and Dr. Harry Schmidt. We would also like to thank to Ms. Heidrun Felgner for language corrections of the manuscript.

REFERENCES

- [1] Doldi, S. Michele Peyrone and his salt. *Chim. Ind.* **1995**, 77(11), 989-994.
- [2] Peyrone, M. Ueber die Einwirkung des Ammoniaks auf Platinchlor. *Liebigs Ann. Chem.* **1844**, 51(1), 1-29.
- [3] Reiset, J. Memoires sur les combinations de deux nouvelles bases alcalines contenant du platine. *C. R. Hebd. Acad. Sci.* **1844**, 18, 1100-1105.
- [4] Werner, A. Beitrag zur Konstitution anorganischer Verbindungen. *Z. Anorg. Chem.* **1893**, 3(1), 267-330.
- [5] Rosenberg, B.; van Camp, L.; Krigast, T. Inhibition of cell division in *Escherichia coli* by electrolysis products from a platinum electrode. *Nature* **1965**, 205, 698-699.
- [6] Rosenberg, B.; van Camp, L.; Grimley, E.B.; Thomson, A.J. The inhibition of growth or cell division in *Escherichia coli* by different ionic species of platinum(IV) complexes. *J. Biol. Chem.* **1967**, 242(6), 1347-1352.
- [7] Rosenberg, B.; Renshaw, E.; van Camp, L.; Hartwick, J.; Drobnik, J. Platinum-induced filamentous growth in *Escherichia coli*. *J. Bacteriol.* **1967**, 93(2), 716-721.
- [8] Rosenberg, B.; van Camp, L. The successful regression of large solid sarcoma 180 tumors by platinum compounds. *Cancer. Res.* **1970**, 30(6), 1799-1802.
- [9] Rosenberg, B.; van Camp, L.; Trosko, J.E.; Mansour, V.H. Platinum compounds: a new class of potent antitumor agents. *Nature* **1969**, 222, 385-386.
- [10] Higby, D.J.; Wallace, H. J.J.; Albert, D.J.; Holland, J.F. Diamminedichloroplatinum: a phase I study showing responses in testicular and other tumors. *Cancer* **1974**, 33(5), 1219-5.
- [11] Hambley, T.W. Developing new metal-based therapeutics: challenges and opportunities. *Dalton Trans.* **2007**, 43, 4929-4937.
- [12] Kelland, L. The resurgence of platinum-based cancer chemotherapy. *Nat. Rev. Cancer* **2007**, 7(8), 573-584.
- [13] Arnesano, F.; Natile, G. Mechanistic insight into the cellular uptake and processing of cisplatin 30 years after its approval by FDA. *Coord. Chem. Rev.* **2009**, 253(15-16), 2070-2081.
- [14] Reedijk, J. Metal-ligand exchange kinetics in platinum and ruthenium complexes. Significance for effectiveness as anticancer drugs. *Platinum Met. Rev.* **2008**, 52(1), 2-11.
- [15] Wang, D.; Lippard, S.J. Cellular processing of platinum anticancer drugs. *Nat. Rev. Drug Discov.* **2005**, 4(4), 307-320.
- [16] Speelmans, G.; Sips, W.H.H.M.; Grisel, R.J.H.; Staffhorst, R.W.H.M.; Fichtinger-Schepman, A.M.; Reedijk, J.; de Kruijff, B. The interaction of the anti-cancer drug cisplatin with phospholipids is specific for negatively charged phospholipids and takes place at low chloride ion concentration. *Biochim. Biophys. Acta, Biomembr.* **1996**, 1283(1), 60-66.
- [17] Fichtinger-Schepman, A. M.; Van, d. V.; Den, H.; Lohman, P. H. M.; Reedijk, J. Adducts of the antitumor drug *cis*-diamminedichloroplatinum(II) with DNA: formation, identification, and quantitation. *Biochemistry* **1985**, 24(3), 707-713.
- [18] Egger, A. E.; Hartinger, C. G.; Ben, H.; Tsybin, Y. O.; Keppler, B. K.; Dyson, P. J. High Resolution Mass Spectrometry for Studying the Interactions of Cisplatin with Oligonucleotides. *Inorg. Chem.* **2008**, 47(22), 10626-10633.
- [19] Marcellis, A. T. M.; Van, K.; Reedijk, J. The interactions of *cis*- and *trans*-diammineplatinum compounds with 5'-guanosine monophosphate and 5'-deoxyguanosine monophosphate. A proton NMR investigation. *J. Inorg. Biochem.* **1980**, 13(3), 213-222.
- [20] den Hartog, J.H.J.; Altona, C.; van Boom, J.H.; Marcellis, A. T. M.; van der Marel, G.A.; Rinkel, L.J.; Wille-Hazeleger, G.; Reedijk, J. *Cis*-Platinum-induced distortions in DNA. Conformational analysis of d(GpCpG) and *cis*-[Pt(NH₃)₂][d(GpCpG)], studied by 500 MHz NMR. *Eur. J. Biochem.* **1983**, 134(3), 485-495.
- [21] Admiraal, G.; van der Veer, J.L.; de Graaff, R.A.G.; den Hartog, J.H.J.; Reedijk, J. Intrastrand bis(guanine) chelation of trinucleoside diphosphate d(CpGpG) to *cis*-platinum: an X-ray single-crystal structure analysis. *J. Am. Chem. Soc.* **1987**, 109(2), 592-594.
- [22] Harhaji-Trajković, L.; Vilimanovich, U.; Kravić-Stevović, T.; Bumbasirević, V.; Trajković, V. AMPK-mediated autophagy inhibits apoptosis in cisplatin-treated tumour cells. *J. Cell. Mol. Med.* **2009**, 13(9B), 3644-3654.
- [23] Rabik, C.A.; Dolan, M.E. Molecular mechanisms of resistance and toxicity associated with platinating agents. *Cancer Treat. Rev.* **2007**, 33(1), 9-23.
- [24] Pavelka, M.; Lucas, M. F.; Russo, N. On the hydrolysis mechanism of the second-generation anticancer drug carboplatin. *Chem. Eur. J.* **2007**, 13(36), 10108-10116.
- [25] Hartmann J.T.; Lipp H-P. Toxicity of platinum compounds. *Expert Opin. Pharmacol.* **2003**, 4, 889-901.
- [26] Uehara, T.; Tsuchiya, N.; Masuda, A.; Torii, M.; Nakamura, M.; Yamate, J.; Maruyama, T. Time course of the change and amelioration of nedaplatin-induced nephrotoxicity in rats. *J. Appl. Toxicol.* **2008**, 28(3), 388-398.
- [27] Choy, H.; Park, C.; Yao, M. Current Status and Future Prospects for Satraplatin, an Oral Platinum Analogue. *Clin. Cancer Res.* **2008**, 14(6), 1633-1638.
- [28] Natile, G.; Coluccia, M. Current status of *trans*-platinum compounds in cancer therapy. *Coord. Chem. Rev.* **2001**, 216-217, 383-410.
- [29] Reedijk, J. The relevance of hydrogen bonding in the mechanism of action of platinum antitumor compounds. *Inorg. Chim. Acta* **1992**, 198-200, 873-881.
- [30] Reedijk, J. Improved understanding in platinum antitumor chemistry. *Chem. Commun.* **1996**, 801-806.
- [31] Nováková, O.; Vrána, O.; Kiseleva, V.I.; Brabec, V. DNA Interactions of Antitumor Platinum(IV) Complexes. *Eur. J. Biochem.* **1995**, 228(3), 616-624.
- [32] Comess, K.M.; Costello, C.E.; Lippard, S.J. Identification and characterization of a novel linkage isomerization in the reaction of *trans*-diamminedichloroplatinum(II) with 5'-d(TCTACGCGTTCT). *Biochemistry* **1990**, 29(8), 2102-2110.
- [33] Farrell, N.; Ha, T.T.B.; Souchard, J.P.; Wimmer, F.L.; Cros, S.; Johnson, N.P. Cytostatic *trans*-platinum(II) complexes. *J. Med. Chem.* **1989**, 32(10), 2240-2241.
- [34] Leng, M.; Locker, D.; Giraud-Panis, M. J.; Schwartz, A.; Intini, F.P.; Natile, G.; Pisano, C.; Bocciarelli, A.; Giordano, D.; Coluccia, M. Replacement of an NH₃ by an Iminoether in Transplatin Makes an Antitumor Drug from an Inactive Compound. *Mol. Pharmacol.* **2000**, 58(6), 1525-1535.
- [35] Kalinowska-Lis, U.; Ochocki, J.; Matlawska-Wasowska, K. *Trans* geometry in platinum antitumor complexes. *Coord. Chem. Rev.* **2008**, 252(12-14), 1328-1345.
- [36] Wheate, N. J.; Collins, J. G. Multi-nuclear platinum complexes as anti-cancer drugs. *Coord. Chem. Rev.* **2003**, 241(1-2), 133-145.
- [37] Servidei, T.; Ferlini, C.; Riccardi, A.; Meco, D.; Scambia, G.; Segni, G.; Manzotti, C.; Riccardi, R. The novel trinuclear platinum complex BBR3464 induces a cellular response different from cisplatin. *Eur. J. Cancer* **1990**, 37(7), 930-938.
- [38] Arandelović, S.; Tešić, Z.L.; Radulović, S.S. *Trans*-Platinum Complexes with Promising Antitumor Properties. *Med. Chem. Rev. Online* **2005**, 2, 415-422.
- [39] Rakić, G.M.; Grgurić-Šipka, S.; Kaluderović, G.N.; Gómez-Ruiz, S.; Bjelogrić, S.K.; Radulović, S.S.; Tešić, Ž.L. Novel *trans*-dichloroplatinum(II) complexes with 3- and 4-acetylpyridine: Synthesis, characterization, DFT calculations and cytotoxicity. *Eur. J. Med. Chem.* **2009**, 44(5), 1921-1925.
- [40] Iakovidis, A.; Hadjiliadis, N. Complex compounds of platinum(II) and platinum(IV) with amino acids, peptides and their derivatives. *Coord. Chem. Rev.* **1994**, 135-136, 17-63.

Appendix 1

- [176] Boulikas, T.; Vougiouka, M. Cisplatin and platinum drugs at the molecular level. *Oncology Rep.* **2003**, *10*(6), 1663-1682.
- [177] Stathopoulos, G.P.; Boulikas, T.; Vougiouka, M.; Deliconstantinos, G.; Rigatos, S.; Darli, E.; Viliotou, V.; Stathopoulos, J.G. Pharmacokinetics and adverse reactions of a new liposomal cisplatin (Lipoplatin): Phase I study. *Oncology Rep.* **2005**, *13*(4), 589-595.
- [178] Galanski, M.; Keppler, B.K. Searching for the Magic Bullet: Anticancer Platinum Drugs Which Can Be Accumulated or Activated in the Tumor Tissue. *Anti-Cancer Agent. Me.* **2007**, *7*(1), 55-73
- [179] Vallet-Regí, M.; Balas, F.; Arcos, D. Mesoporous Materials for Drug Delivery. *Angew. Chem. Int. Ed.* **2007**, *46*(40), 7548-7558.
- [180] Kresge, C.T.; Leonowicz, M.E.; Roth, W.J.; Vartuli, J.C.; Beck, J.S. Ordered mesoporous molecular sieves synthesized by a liquid-crystal template mechanism. *Nature* **1992**, *359*, 710-712.
- [181] Vallet-Regí, M.; Rímila, A.; del Real, R. P.; Pérez-Pariente, J. A New Property of MCM-41: Drug Delivery System. *Chem. Mater.* **2000**, *13*(2), 308-311.
- [182] Zhao, D.; Feng, J.; Huo, Q.; Melosh, N.; Fredrickson, G.H.; Chmelka, B.F.; Stucky, G.D. Triblock Copolymer Syntheses of Mesoporous Silica with Periodic 50 to 300 Angstrom Pores. *Science* **1998**, *279*, 548-552.
- [183] Sakamoto, Y.; Kim, T.W.; Ryoo, R.; Terasaki, O. Three-Dimensional Structure of Large-Pore Mesoporous Cubic *Ia3d* imaged Silica with Complementary Pores and Its Carbon Replica by Electron Crystallography. *Angew. Chem. Int. Ed.* **2004**, *43*(39), 5231-5234.
- [184] Huo, Q.; Margolese, D.I.; Ciesla, U.; Demuth, D.G.; Feng, P.; Gier, T.E.; Sieger, P.; Firouzi, A.; Chmelka, B.F. Organization of Organic Molecules with Inorganic Molecular Species into Nanocomposite Biphase Arrays. *Chem. Mater.* **1994**, *6*(8), 1176-1191.
- [185] Iafisco, M.; Palazzo, B.; Marchetti, M.; Margiotta, N.; Ostuni, R.; Natile, G.; Morpurgo, M.; Gandin, V.; Marzano, C.; Roveri, N. Smart delivery of antitumoral platinum complexes from biomimetic hydroxyapatite nanocrystals. *J. Mater. Chem.* **2009**, *19*(44), 8385-8392.
- [186] Manzano, M.; Vallet-Regí, M. New developments in ordered mesoporous materials for drug delivery. *J. Mater. Chem.* **2010**, *20*(27), 5593-5604.
- [187] Lai, C. Y.; Trewyn, B.G.; Jeftinija, D.M.; Jeftinija, K.; Xu, S.; Jeftinija, S.; Lin, V.S.Y. A Mesoporous Silica Nanosphere-Based Carrier System with Chemically Removable CdS Nanoparticle Caps for Stimuli-Responsive Controlled Release of Neurotransmitters and Drug Molecules. *J. Am. Chem. Soc.* **2003**, *125*(15), 4451-4459.
- [188] Palazzo, B.; Iafisco, M.; Laforgia, M.; Margiotta, N.; Natile, G.; Bianchi, C.; Walsh, D.; Mann, S.; Roveri, N. Biomimetic Hydroxyapatite-Drug Nanocrystals as Potential Bone Substitutes with Antitumor Drug Delivery Properties. *Adv. Funct. Mater.* **2007**, *17*(13), 2180-2188.
- [189] Perez-Quintanilla, D.; Gómez-Ruiz, S.; Žižak, Ž.; Sierra, I.; Prashar, S.; del, H. I.; Fajardo, M.; Juranić, Z.D.; Kaluderović, G.N. A new generation of anticancer drugs: mesoporous materials modified with titanocene complexes. *Chem. Eur. J.* **2009**, *15*(22), 5588-5597.
- [190] Kaluderović, G.N.; Perez-Quintanilla, D.; Sierra, I.; Prashar, S.; Hierro, I.; Žižak, Ž.; Juranić, Z.D.; Fajardo, M.; Gómez-Ruiz, S. Study of the influence of the metal complex on the cytotoxic activity of titanocene-functionalized mesoporous materials. *J. Mater. Chem.* **2010**, *20*(4), 806-814.

Received: May 18, 2011

Revised: July 24, 2011

Accepted: July 28, 2011

Review Article

On the Discovery, Biological Effects, and Use of Cisplatin and Metallocenes in Anticancer Chemotherapy

Santiago Gómez-Ruiz,¹ Danijela Maksimović-Ivanić,²
Sanja Mijatović,² and Goran N. Kaluđerović³

¹Departamento de Química Inorgánica y Analítica, E.S.C.E.T., Universidad Rey Juan Carlos, 28933 Móstoles, Spain

²Institute for Biological Research "Sinisa Stankovic", University of Belgrade, Boulevard of Despot Stefan 142, 11060 Belgrade, Serbia

³Institut für Chemie, Martin-Luther-Universität Halle-Wittenberg, Kurt-Mothes-Straße 2, 06120 Halle, Germany

Correspondence should be addressed to Goran N. Kaluđerović, goran.kaluderovic@chemie.uni-halle.de

Received 11 March 2012; Accepted 19 May 2012

Academic Editor: Zhe-Sheng Chen

Copyright © 2012 Santiago Gómez-Ruiz et al. This is an open access article distributed under the Creative Commons Attribution License, which permits unrestricted use, distribution, and reproduction in any medium, provided the original work is properly cited.

The purpose of this paper is to summarize mode of action of cisplatin on the tumor cells, a brief outlook on the metallocene compounds as antitumor drugs as well as the future tendencies for the use of the latter in anticancer chemotherapy. Molecular mechanisms of cisplatin interaction with DNA, DNA repair mechanisms, and cellular proteins are discussed. Molecular background of the sensitivity and resistance to cisplatin, as well as its influence on the efficacy of the antitumor immune response was evaluated. Furthermore, herein are summarized some metallocenes (titanocene, vanadocene, molybdocene, ferrocene, and zirconocene) with high antitumor activity.

1. Cisplatin

Since 1845, when Italian doctor Peyrone synthesized cisplatin (Figure 1), through Rosenberg's discovery of cisplatin antiproliferative potential [1], and subsequent approval for clinical usage in 1978, this drug is considered as most promising anticancer therapeutic [2, 3]. Cisplatin is highly effective against testicular, ovarian, head and neck, bladder, cervical, oesophageal as well as small cell lung cancer [4].

For more than 150 years, first exaltation about this "drug of the 20th century" was replaced with discouraging data about its toxicity and ineffectiveness got from clinical practice. It was found that cisplatin induced serious side effects such as nephrotoxicity, neurotoxicity, ototoxicity, nausea, and vomiting [5]. General toxicity and low biological availability restricted its therapeutically application. In addition, it is known that some tumors such as colorectal and nonsmall lung cancers are initially resistant to cisplatin while other like ovarian and small cell lung cancers easily acquired resistance to drug [6]. Numerous examples from *in vitro* studies confirmed that exposure to cisplatin often resulted in development of apoptotic resistant phenotype

[7–9]. Following this, development of cisplatin resistant cell lines is found useful for testing the efficacy of future cisplatin modified drugs and on the other hand for evaluation of mechanisms involved in development of resistance. For better understanding of unresponsiveness to cisplatin, it is necessary to define the exact molecular targets of drug action from the moment of entering tumor cell. It is proposed the intact cisplatin which avoided bounding to plasma proteins enter the cell by diffusion or active transport via specific receptors (Figure 2) [10, 11]. Cisplatin is able to use copper-transporting proteins to reach intracellular compartments [12–14]. In addition, regarding to its chemical reactivity, cisplatin can influence cell physiology even through interaction with cell membrane molecules such as different receptors.

1.1. Cisplatin and DNA. Although it is known that DNA is a major target for cisplatin, only 5–10% intracellular concentration of cisplatin is found in DNA fraction while 75–85% binds to nucleophilic sites of intracellular constituents like thiol containing peptides, proteins, replication enzymes, and RNA [6, 15–17]. This preferential binding to non-DNA targets offers the explanation for cisplatin resistance but

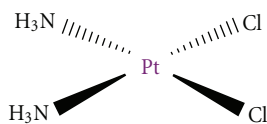


FIGURE 1: Cisplatin.

also its high toxicity. Prerequisite of efficient formation of cisplatin DNA adducts is hydration of cisplatin enabled by low chloride ions content inside the cells [18]. N7 of guanine and in less extent adenine nucleotide are targeted by platinum [19]. Binding of cisplatin to DNA is irreversible and structurally different adducts are formed. The adducts are classified as intrastrand crosslinking of two nucleobases of single DNA strand, interstrand crosslinking of two different strands of one DNA molecule, chelate formation through *N*- and *O*-atoms of one guanine, and DNA-protein crosslinks [20, 21]. Cisplatin forms about 65% pGpG-intrastrand crosslinks, 25% pApG-intrastrand crosslinks, 13% interstrand or intrastrand crosslinks on pGpXpG sequences, and less than 1% of monofunctional adducts (Figure 3) [22]. Crucial role of 1,2-intrastrand crosslinks in antitumor potential of the cisplatin is supported by two facts. First, high mobility group proteins (HMG) specifically recognize this type of cisplatin-DNA interaction and second, these adducts are less efficiently removed by repair enzymes [17]. In addition, important mediators of cisplatin toxicity are ternary DNA-platinum-protein crosslinks (DPCL) whose frequency is dependent from the cell type as well as the type of the treatment. DPCLs inhibited DNA polymerization or their own removal by nucleotide excision repair system more potently than other DNA adducts [17]. In fact, cisplatin DNA adducts can be repaired by nucleotide excision repair proteins (NER), mismatch repair (MMR), and DNA-dependent protein kinases protein [17].

1.2. DNA Repair Mechanism. Nucleotide excision repair proteins are ATP-dependent multiprotein complex able to efficiently repair both inter as well as intrastrand DNA-cisplatin adducts. Successful repair of 1,2-d(GpG) and 1,3-d(GpNpG) intrastrand crosslinks has been found in different human and rodent NER systems [23, 24]. This repair mechanism is able to correct the lesions promoted by chemotherapeutic drugs, UV radiation as well as oxidative stress [17]. Efficacy of NER proteins varying in different type of tumors and is responsible for acquirement of cisplatin resistance. Low level of mentioned proteins is found in testis tumor defining their high sensitivity to cisplatin treatment. Oppositely, ovarian, bladder, prostate, gastric, and cervical cancers are resistant to cisplatin based therapy due to overexpression of several NER genes [25, 26].

Mismatch repair (MMR) proteins are the post replication repair system for correction of mispaired and unpaired bases in DNA caused by DNA Pt adducts. MMR recognized the DNA adducts formed by ligation of cisplatin but not oxaliplatin [27–30]. Defective MMR is behind the resistance of ovarian cancer to cisplatin and responsible for the mutagenicity of cisplatin [31].

DNA dependent protein kinase is a part of eukaryotic DNA double strand repair pathway. This protein is involved in maintaining of genomic stability as well as in repair of double strand breaks induced by radiation [31]. In ovarian cancer presence of cisplatin DNA adducts inhibited translocation of DNA-PK subunit Ku resulting in inhibition of this repair protein [32].

Special attention is focused on recognition of cisplatin-modified DNA by HMG proteins (HMG). It is hypothesized that HMG proteins protected adducts from recognition and reparation [17, 31]. Moreover, it was postulated that these proteins modulate cell cycle events and triggered cell death as a consequence of DNA damage. One of the members from this group marked as HMGB1 is involved in MMR, increased the p53 DNA-binding activity and further stimulated binding of different sequence specific transcription factors [33]. Few studies revealed that cisplatin sensitivity was in correlation with HMGB level, while other studies eliminated its significance in response to cisplatin treatment. Contradictory data about the relevance of HMG proteins in efficacy of cisplatin therapy indicated that this relation is defined by cell specificity.

1.3. Cytotoxicity of Cisplatin. Other non-HMG nuclear proteins are also involved in cytotoxicity of cisplatin. Presence of cisplatin DNA adducts is able to significantly change or even disable the primary function of nuclear proteins essential for transcription of mammalian genes (TATA binding protein, histon-linker protein H1 or 3-methyladenine DNA glycosylase mammalian repair protein) [34–36].

Although cytotoxicity of cisplatin is usually attributed to its reactivity against DNA and subsequent lesions, the fact that more than 80% of internalized drug did not reach DNA indicated the involvement of numerous non-DNA cellular targets in mediation of cisplatin anticancer action [6]. As a consequence of exposure to cisplatin, different signaling pathways are affected. There is no general concept applicable to all types of tumor. It is evident that response to cisplatin is defined by cell specificity. Numerous data revealed changes in activity of most important signaling pathways involved in cell proliferation, differentiation and cell death such as PI3K/Akt, MAPK as well as signaling pathways involved in realization of death signals dependent or independent of death receptors [33]. It is very important to note that alteration in signal transduction upon the cisplatin treatment could be the consequence of both, DNA damage or interaction with exact protein or protein which is relevant for appropriate molecular response. Some of the interactions between protein and cisplatin are already described. Therefore, it was found that cisplatin directly interacts with telomerase, an enzyme that repairs the ends of eukaryotic chromosomes [31, 37]. In parallel, cisplatin-induced damage of telomeres which are not transcribed and therefore hidden from NER. Other important protein targeted by cisplatin is small, tightly folded molecule known as ubiquitin (Ub) [38]. Ub is implicated in selective degradation of short-lived cellular proteins [39]. It has been hypothesized that direct interaction of cisplatin with this protein presented a strong signal for cell death [40]. Two binding sites were identified as target

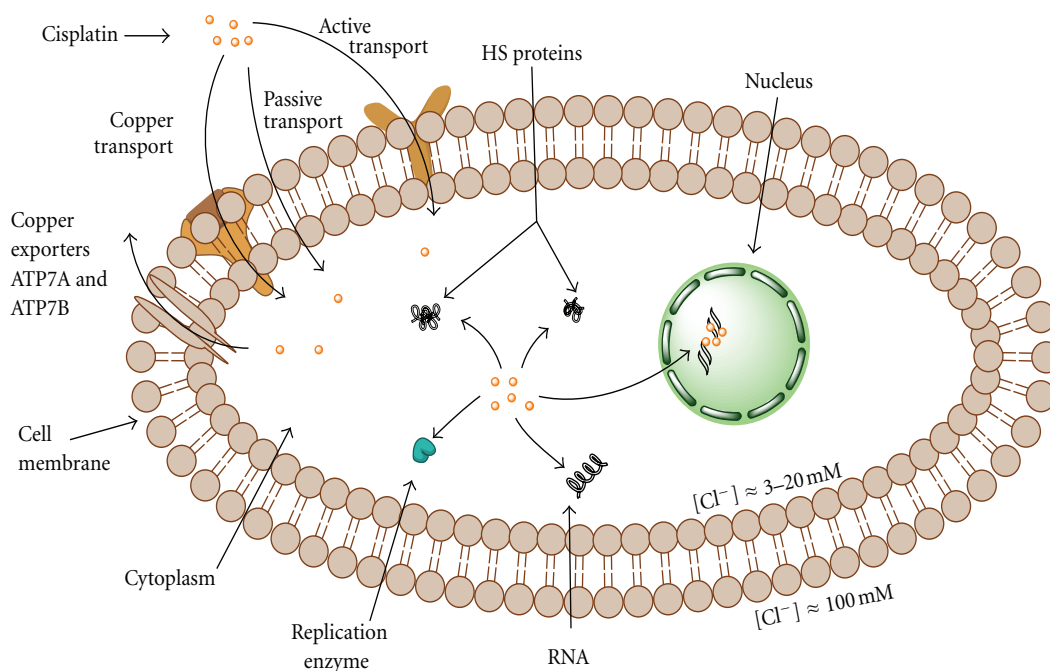


FIGURE 2: Cisplatin and the cell: transport/export and targets.

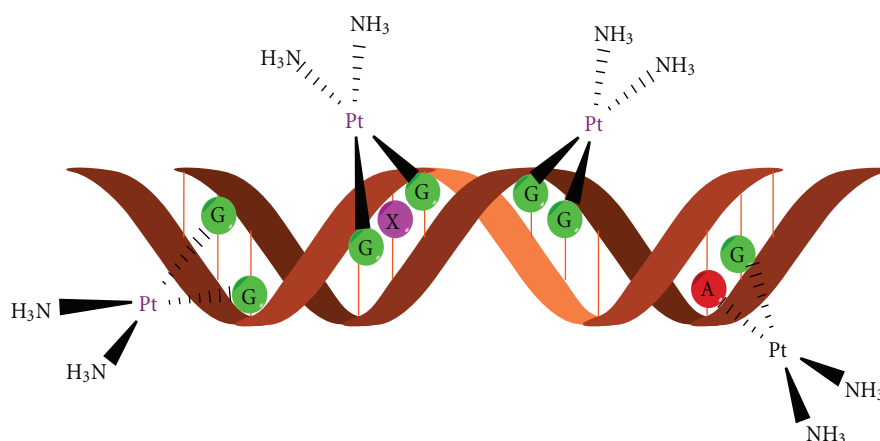


FIGURE 3: DNA adduct formation with cisplatin moiety.

for cisplatin ligation: *N*-terminal methionine (Met1) and histidine at position 68, while the drug makes at least four types of adducts with protein [38]. This resulted in disturbed proteasomal activity and further cell destruction. Having in mind that proteasomal inactivation by specific inhibitors showed promising results in cancer treatment, this aspect of cisplatin reactivity can be leading cytotoxic effect even to be more powerful than DNA damage [41]. One of the crucial molecules involved in propagation of apoptotic signal through depolarization of mitochondrial potential—cytochrome *c* is also targeted by cisplatin on Met65 [42]. Further, on the list of protein or peptide targets for cisplatin are glutathione and metallothioneins, superoxide dismutase, lysozyme as well as extracellular protein such as albumin, transferrin, and hemoglobin [43]. Some of mentioned interactions served as drug intracellular pool while their biological relevance is still under investigation.

1.4. Activation of Signaling Pathways Induced with Cisplatin. DNA damage induced by cisplatin represent strong stimulus for activation of different signaling pathways. It was found that AKT, c-Abl, p53, MAPK/JNK/ERK/p38 and related pathways respond to presence of DNA lesions [31, 33]. AKT molecule as most important Ser/Thr protein kinase in cell survival protects cells from damage induced by different stimuli as well as cisplatin [44]. Cisplatin downregulated XIAP protein level and promoted AKT cleavage resulting in apoptosis in chemosensitive but not in resistant ovarian cancer cells [45, 46]. Recently published data about synergistic effect of XIAP, c-FLIP, or NFκB inhibition with cisplatin are mainly mediated by AKT pathway [47].

Protein marked as the most important in signaling of the DNA damage is c-Abl which belongs to SRC family of non-receptor tyrosine kinases [31, 33]. This molecule acts as transmitter of DNA damage triggered by cisplatin from nucleus

to cytoplasm [48]. Moreover, sensitivity to cisplatin induced apoptosis is directly related with c-Abl content and could be blocked by c-Abl overexpression [33]. Key role of c-Abl in propagation of cisplatin signals is confirmed in experiments with ABL deficient cells [49]. It was found that cisplatin failed to activate p38 and JNK in the absence of c-Abl. Homology of this kinases with HMGB indicated the possibility that c-Abl recognized and interact with cisplatin DNA lesions like HMGB1 protein [31].

1.5. The Role of the Functional p53 Protein. Evaluation of a 60 cell line conducted by the National Cancer Institute revealed that functional p53 protein is very important for successful response to cisplatin treatment [33]. This tumor suppressor is crucial for many cellular processes and determined the balance between cell cycle arrest as a chance for repair and induction of apoptotic cell death [33]. However, despite extensive NCI study, there are controversial data about correlation between cisplatin sensitivity and p53. For example, it was found that functional p53 was associated with amplified cisplatin sensitivity in SaOS-2 osteosarcoma cells in high serum growth conditions while the opposite relation was observed upon starvation [33]. This phenomenon could be connected to autophagic process triggered in serum deficient conditions, which in turn downregulate cisplatin promoted apoptosis [50]. In some other studies, the response to cisplatin was not influenced by p53. It is indicative that antitumor potential of cisplatin and its interaction with p53 is a question of multiple factors such as tumor cell type, specific signaling involved in cancerogenesis, as well as other genetic alterations. In addition, protein involved or influenced by p53 pathway such as Aurora kinase A, cyclin G, BRCA1 as well as proapoptotic or antiapoptotic mediators are also able to control cisplatin toxicity [33].

1.6. Relation between Cisplatin and Mitogen-Activated Protein (MAP) Kinases. Finally, signaling pathways mediated by mitogen-activated kinases are strongly influenced by cisplatin. These enzymes are highly important in definition of cellular response to applied treatment because they are the major regulators of cell proliferation, differentiation, and cell death. ERK (extracellular signal-related kinase) preferentially responds to growth factor and cytokines but also determines cell reaction to different stress conditions, particularly, oxidative [33]. Cisplatin treatment mainly activated ERK in a dose- and time-dependent manner [33, 51, 52]. However, like as previously described, changes in ERK activity upon the exposure to cisplatin varying from type to type of the malignant cell and is defined by their intrinsic features. Following this, in some circumstances ERK activation antagonized cisplatin toxicity. In cells with significant upregulation of ERK activity in response to cisplatin treatment, exposure to specific MEK1 inhibitor PD98052 abrogated its toxicity. Also, development of the resistance to the cisplatin in HeLa cells is connected with reduced ERK response to the treatment [52]. Moreover, combined treatment with some of the naturally occurring compounds such as aloemodin-neutralized cisplatin toxicity through inhibition of

ERK, indicated possible negative outcome of combining of conventional and phytotherapy [53, 54].

Regardless of numerous evidences about its critical role in cisplatin-mediated cell death, ERK is not the only molecule from MAP family which responded to cisplatin. Several studies revealed JNK (c-Jun N-terminal kinase) activation upon the cisplatin addition [55, 56]. However, similarly to other molecules previously mentioned this signal is not the unidirectional and could be responsible for realization but also protection from death triggered by the cisplatin [57, 58]. Finally, there are numerous evidences about highly important role of third member of MAP kinases, p38, in response to cisplatin [59, 60]. Lack of p38 MAPK leads to appearance of resistant phenotype in human cells [55, 60]. Early and short p38 activation is principally described in cells unresponsive to cisplatin while long-term activation was found in sensitive clones. Moreover, in the light of the fact that this kinase has a role in modifying the chromatin environment of target genes, its involvement in cisplatin-induced phosphorylation of histon 3 was determined [61].

1.7. On the Mode of Cell Death Induced by Cisplatin. The net effect of intracellular interaction of cisplatin with DNA and non-DNA targets is the cell cycle arrest and subsequent death in sensitive clones. There are two type of death signals resulting from cellular intoxication by this drug (Figure 4). Fundamentally, the drug concentration presents the critical point for cell decision to undergo apoptotic or necrotic cell death [62]. Primary cultures of proximal tubular cells isolated from mouse died by necrosis if they were exposed to high doses of cisplatin just for a few hours while apoptotic cell death is often triggered by long-term exposure to significantly lower concentrations [63]. However, the presence of necrosis in parallel with apoptosis in tumor-cell population indicated that type of cell death is not just the question of dose but also is defined by cell intrinsic characteristics and energetic status of each cell at the moment of the treatment. In fact, it was considered that intracellular ATP level dictate cell decision to die by necrotic or apoptotic cell death [64, 65]. One of the signals which are provoked with DNA damage is PARP-1 activation and subsequent ATP depletion caused by PARP-1 mediated cleavage of NAD⁺. This event is a trigger for necrotic cell death. However, activated caspases cleaved the PARP-1, preventing necrotic signal and favor the execution of apoptotic process. On the other hand, the inhibition of caspases by intracellular inhibitors IAP together with continual PARP activity and ATP depletion resulted in necrosis [31]. As numerous biological phenomena, this one is not unidirectional. It was found that failure in PARP cleavage may also serve to apoptosis [66]. This paradox was ascribed to changes in pyridine nucleotide pool as well as in pool of ATP/ADP responsible for regulation of mitochondrial potential [67]. Atypical apoptosis was observed in L1210 leukemia cell line exposed to cisplatin. Different death profiles in cisplatin treated cells confirmed plasticity of signals involved in cell destruction and focus the attention to the molecules responsible for resistance to death as possible targets for the therapy. Having in mind that

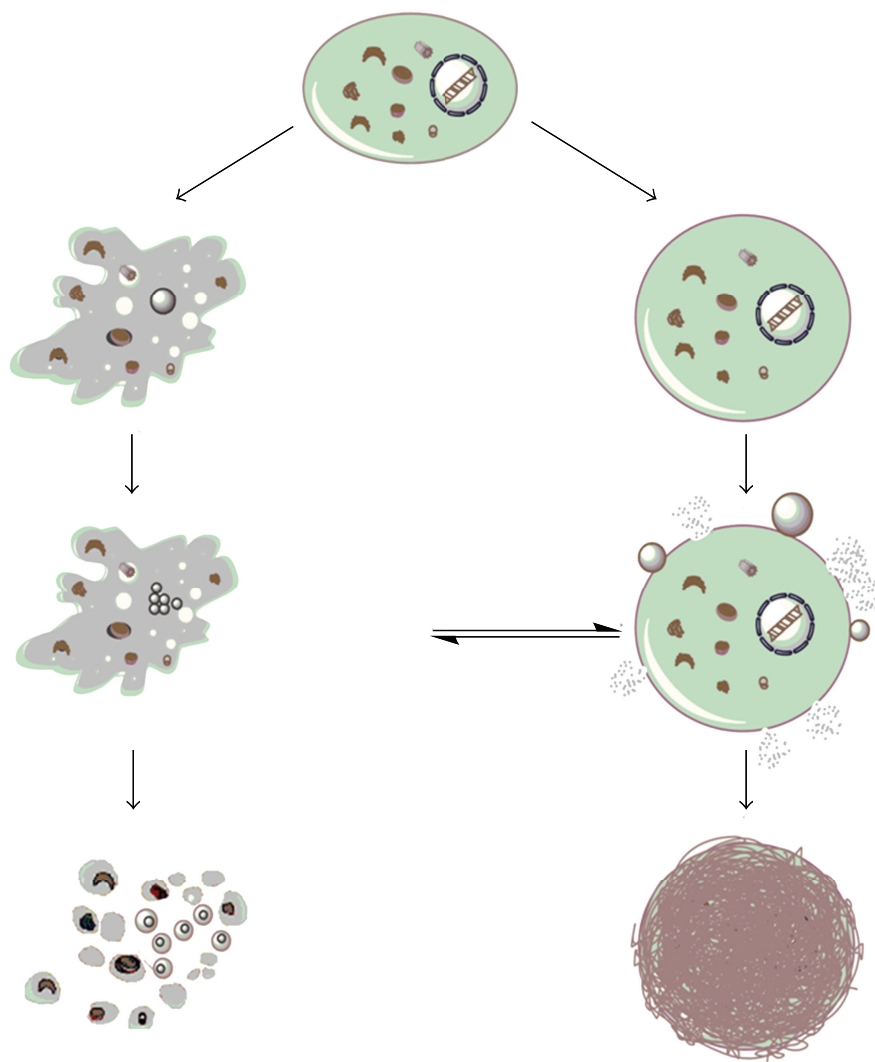


FIGURE 4: Mode of cell death induced by cisplatin: apoptosis (left) and necrosis (right).

cisplatin is toxic agent against whom the cell can activate autophagy as protective process; the specific inhibition of autophagy by certain type of molecules could amplify the effectiveness of cisplatin [50].

1.8. Cisplatin in Immune Sensitization. One of the rarely mentioned but very important aspects of antitumor activity of cisplatin is based on the experimental data about its potential to amplified the sensitivity of malignant cells to one or the most potent and selective antitumor immune response mediated by TNF-related apoptosis inducing ligand TRAIL [68, 69]. This molecule is produced by almost all immune cells involved in nonspecific as well as adoptive immune response. Unfortunately, in the moment when tumor is diagnosed, its sensitivity to natural immunity is debatable. In most of the situations, malignant cells became resistant to TRAIL-mediated cytotoxicity [70]. Moreover, it was confirmed that cisplatin promoted their sensitivity to TRAIL. Nature of its immune sensitizing potential is at least partly due to upregulation of expression of TRAIL receptors—DR4 and DR5 on the cellular membrane glioma,

colon and prostate cell lines as well as downregulation of cellular form of caspase 8 inhibitor FLIP [68, 69]. In addition, presence of cysteine rich domen in the structure of TRAIL specific death receptors indicated possibility that cisplatin directly interact with them.

1.9. Resistance to Cisplatin and How to Surmount It. Resistance to cisplatin could be established at multiple levels, from cellular uptake of the drug through interaction with protein and DNA and finally activation of signals which lead the cell to death. Disturbed drug uptake, drug scavenging by cellular proteins, upregulation of prosurvival signals together with upregulated expression of antiapoptotic molecules such as Bcl-2 and BclXL, overexpressed natural inhibitors of caspases like FLIP and XIAP, diminished MAP signaling pathway or deficiency in proteins involved in signal transferring from damaged DNA to cytoplasm, enhanced activity of repair mechanisms and efficient redox system are features mainly responsible for unsuccessful treatment with cisplatin [33]. Well defined molecular background of the resistance to cisplatin point out the way on how to surmount it. It was

already known that some of combined treatments of cisplatin with other chemotherapeutics such as 5-fluorouracil improved therapeutic response rates in patients with head and neck cancer [71, 72]. Furthermore, inhibition of NER DNA repair system, cotreatment with histone deacetylase inhibitors (HDAC) such as trichostatin A (TSA) or suberoylanilide hydroxamic (SAHA) [73], small molecules inhibitors of FLIP and XIAP as well as topoisomerase inhibitors strongly synergized with cisplatin, elevating its therapeutic potential.

2. Metallocenes in Anticancer Chemotherapy

Most of the metallo drugs used currently in chemotherapy treatment are based on platinum (cisplatin analogues), although as side effects are the weakest point in the use of cisplatin-based drugs in chemotherapy are the high number of side effects, many efforts are focused on the search of novel metal complexes with similar antineoplastic activity and less side effects as an alternative for platinum complexes. Transition-metal complexes have shown very useful properties in cancer treatment, and the most important work in chemotherapy with transition metals has been carried out with Group 4, 5, 6, 8, and 11 metal complexes.

From all the studied metal complexes, a wide variety of studies have been carried out for metallocenes which have become an alternative to platinum-based drugs.

According to the IUPAC classification metallocene contains a transition metal and two cyclopentadienyl ligands coordinated in a sandwich structure. These compounds have caused a great interest in chemistry due to their versatility which comes from their interesting physical properties, electronic structure, bonding, and their chemical and spectroscopical properties [74]. Academic and industrial research on metallocene chemistry has led to the utilization of these derivatives in many different applications such as olefin polymerization catalysis, asymmetric catalysis or organic syntheses, preparation of magnetic materials, use as nonlinear optics or molecular recognizers, flame retardants or in medicine [74].

Within medicine, metallocene complexes are being normally used as biosensors or as antitumor agents. Regarding their anticancer applicability, titanocene, vanadocene, molybdocene, and ferrocene have been traditionally used with very good results, however, recently also zirconocene derivatives have pointed towards a future potential applicability due to the increase of their cytotoxicity. All the other metallocene derivatives have been either not tested or have demonstrated no remarkable applicability in the fight against cancer.

In this part of the paper, we will briefly discuss separately the properties of metallocene derivatives of titanium, zirconium, vanadium, molybdenum, and iron.

2.1. Titanocene Derivatives. Titanocene derivatives are together with ferrocene complexes the most studied metallocenes in the fight against cancer. The pioneering work of Köpf and Köpf-Maier in the early 1980's showed the antiproliferative properties of titanocene dichloride, $[\text{TiCp}_2\text{Cl}_2]$

($\text{Cp} = \eta^5\text{-C}_5\text{H}_5$, Figure 5(a)). This compound was studied in phase I clinical trials in 1993 [75–77] using water soluble formulations developed by Medac GmbH (Germany) [78].

Phase I clinical trials pointed towards a dose-limiting side effect associated to nephrotoxicity which together with hypoglycemia, nausea, reversible metallic taste immediately after administration, and pain during infusion, seemed to be the weakest part of the administration of titanocene dichloride in humans. On the other hand, the absence of any effect on proliferative activity of the bone marrow, one of the most common dose-limiting side-effect of nonmetallic drugs, was an interesting result that increased the potential applicability of this compound in humans.

Although phase I clinical trials were not as satisfactory as expected, some phase II clinical trials with patients with breast metastatic carcinoma [79] and advanced renal cell carcinoma [80] have been carried out observing a low activity which discouraged further studies.

However, after the recent work of many groups such as Tacke, Meléndez, McGowan, Baird, and Valentine the interest in this field has been renewed [81–85]. In this context a wide variety of titanocene derivatives with amino acids [86, 87], benzyl-substituted titanocene or *ansa*-titanocene derivatives [81], amide functionalized titanocenylys [88, 89], titanocene derivatives with alkylammonium substituents on the cyclopentadienyl rings [90–92], steroid-functionalized titanocenes [93], and alkenyl-substituted titanocene or *ansa*-titanocene derivatives (Figure 5) [94–96], have been reported with very interesting cytotoxic properties which enhance their applicability in humans. In particular, $[\text{Ti}\{\eta^5\text{-C}_5\text{H}_4(\text{CH}_2\text{C}_6\text{H}_4\text{OCH}_3)\}_2\text{Cl}_2]$ (titanocene Y, Figure 5(b)) and its family, reported by Tacke and coworkers, have demonstrated to have extremely interesting anticancer properties which need to be highlighted.

In general, the cytotoxic activity of titanocene complexes has been correlated to their structure, however, there are still several questions regarding the anticancer mechanism of titanocene(IV) complexes. According to the reported studies in the topic, it seems clear titanium ions reach cells assisted by the major iron transport protein “transferrin” [97–100], and the nucleus in an active transport facilitated probably by ATP. In a final step, binding of titanium ion to DNA leads to cell death (Figure 6) [101, 102]. However, recent experiments have shown interactions of a ligand-bound Ti(IV) complex to other proteins or enzymes [103–105], indicating alternatives in cell death mechanisms, which is currently leading to intensive studies by several research groups.

2.2. Zirconocene Derivatives. An alternative to titanium complexes may be zirconium(IV) derivatives which are in a very early stage of preclinical experiments. Already in the 1980's Köpf and Köpf-Maier showed the potential of zirconocene derivatives as anticancer agents and very recently, two different studies on zirconocene anticancer chemistry have been reported [106, 107]. These studies by Allen et al. [106] and Wallis et al. [107] have described the cytotoxic activity of different functionalized zirconocene complexes, observing an irregular behavior in the anticancer tests, from which only the complexes $[\text{Zr}\{\eta^5\text{-C}_5\text{H}_4(\text{CH}_2)_2\text{N}(\text{CH}_2)_5\}_2\text{Cl}_2 \cdot 2\text{HCl}]$

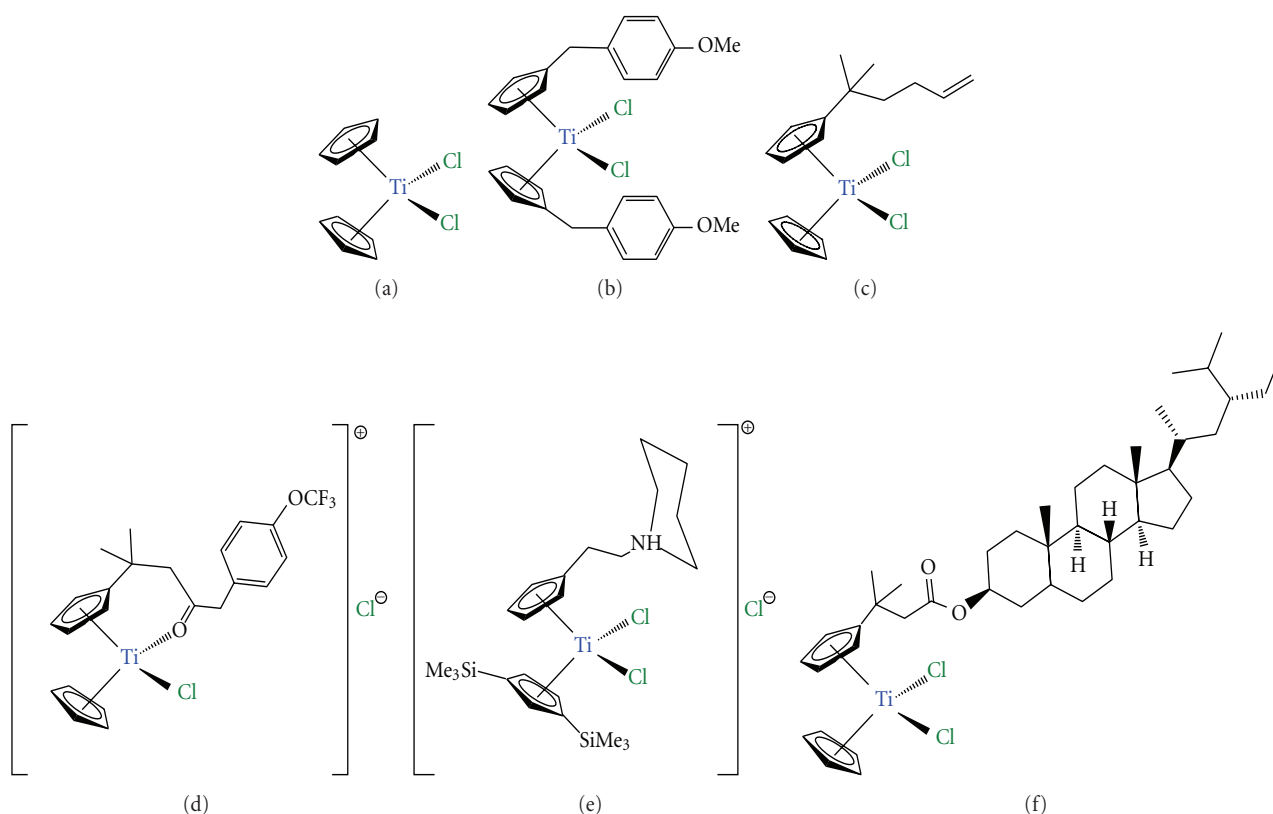


FIGURE 5: Titanocene derivatives used in preclinical and clinical trials: (a) titanocene dichloride; (b) titanocene-Y; (c) alkenyl-substituted titanocene derivative; (d) titanocenyl complex; (e) titanocene derivative with alkylammonium substituents; (f) steroid-functionalized titanocene derivative.

(Figure 7(a)) and $[\text{Zr}\{\eta^5\text{-C}_5\text{H}_4(\text{CH}_2\text{C}_6\text{H}_4\text{OCH}_3)\}_2\text{Cl}_2]$ (zirconocene Y, Figure 7(b)) have shown promising activity that needs to be improved in order to apply them in anticancer chemotherapy.

In parallel, our research group reported the synthesis, structural characterization, catalytic behavior in the polymerization of ethylene and copolymerization of ethylene and 1-octene and the cytotoxic activity on different human cancer cell lines of a novel alkenyl substituted silicon-bridged *ansa*-zirconocene complex (Figure 7(c)) which proved to be the most active zirconocene complex on human A2780 ovarian cancer cells, reported to date [108].

There is still hard work to do in this field to find a suitable zirconocene complex with increased cytotoxic activity and good applicability in humans.

2.3. Vanadocene Derivatives. Vanadocene dichloride, $[\text{VCp}_2\text{Cl}_2]$ ($\text{Cp} = \eta^5\text{-C}_5\text{H}_5$), was extensively studied in preclinical testing against both animal and human cancer cell lines, observing a higher *in vitro* activity of vanadocene(IV) dichloride on direct comparison with titanocene(IV) dichloride [109–111].

These results encouraged further preclinical studies which were restarted around eight years ago [112–114], and have been recently extended [115–118] with the study of the cytotoxic properties of vanadocene Y (Figure 8(a)) and similar derivatives. In addition, a comprehensive study of

the cytotoxic activity of methyl- and methoxy-substituted vanadocene(IV) dichloride toward T-lymphocytic leukemia cells MOLT-4 has also been recently reported [119]. In most cases, vanadocene derivatives are more active than their corresponding titanocene analogues, however, the paramagnetic nature of the vanadium center, which precludes the use of classical NMR tools, makes the characterization of these compounds and their biologically active species more difficult. The need of the use of X-ray crystallography and other methods such as electron-spin resonance (ESR) spectroscopy slows down their analysis and the advances in this topic.

2.4. Molybdocene Derivatives. After the work of Köpf and Köpf-Maier there were some evidences of the potential properties as anticancer agents of molybdocene dichloride derivatives. In recent years, the extensive work carried out by many different research groups confirmed the anticancer properties of molybdocene [120–124]. But not only the cytotoxic properties of these compounds have been reported, the hydrolysis chemistry of $[\text{MoCp}_2\text{Cl}_2]$ has been intensively studied [125–127]. In the case of molybdocene derivatives the stability of the Cp ligands at physiological pH has led to the study of many different biological experiments with results which show new insights on the mechanism of antitumor action of $[\text{MoCp}_2\text{Cl}_2]$ and some analogous carboxylate derivatives (Figure 8(b)) [117, 128–130].

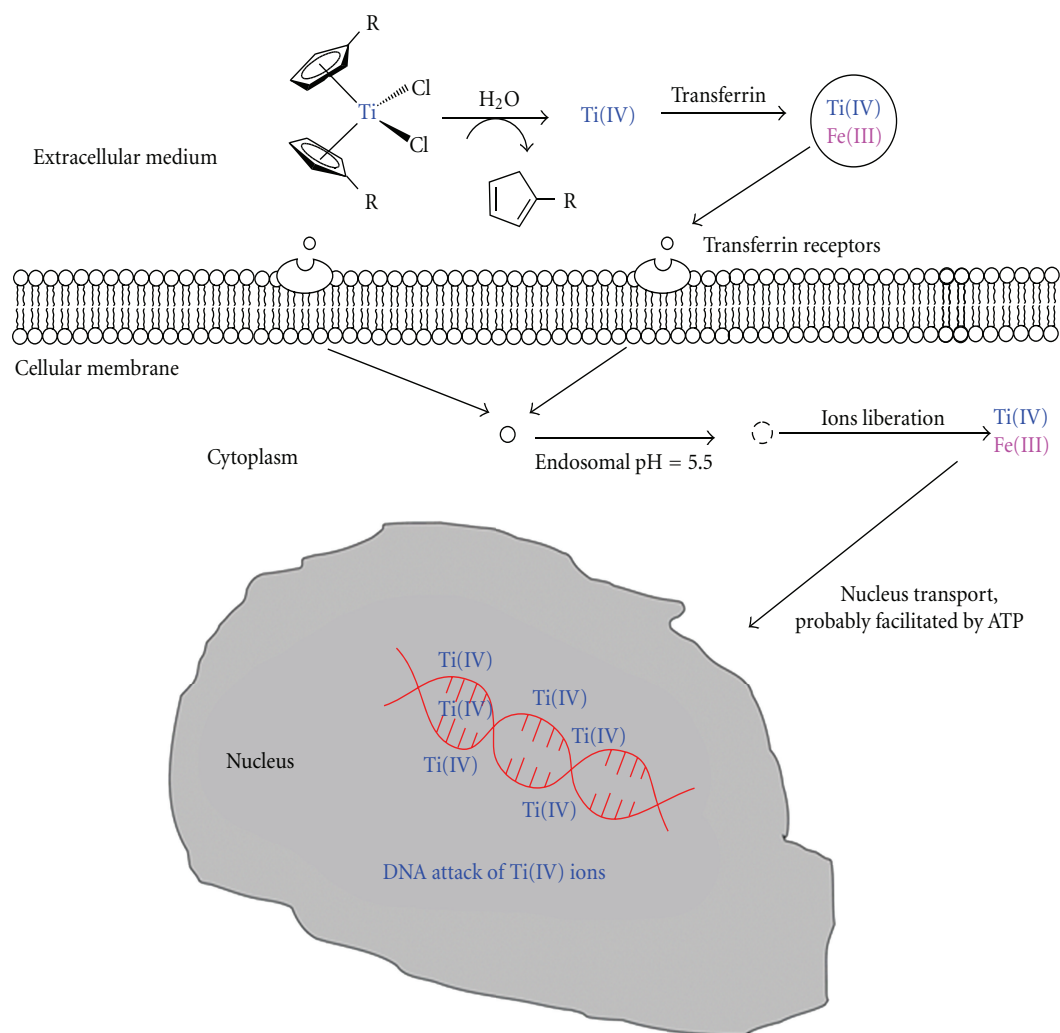


FIGURE 6: Proposed mechanism of action of titanocene derivatives (adapted from Abeysinghe and Harding, Dalton Trans. 32 (2007) 3474).

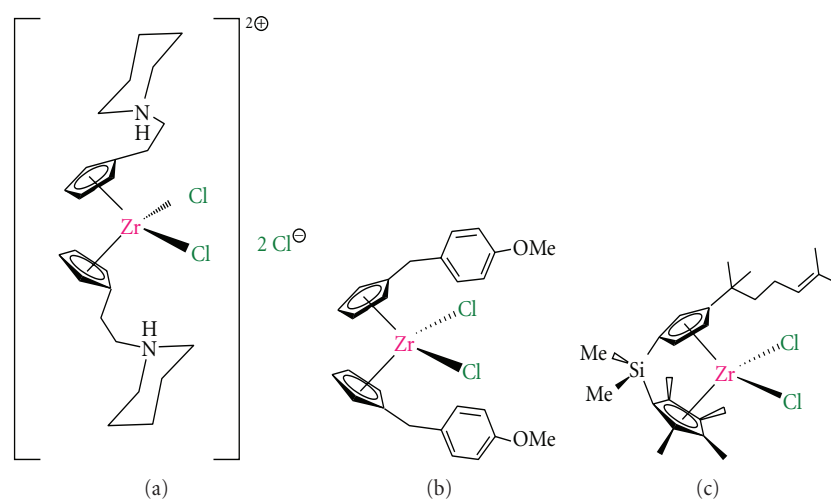


FIGURE 7: Zirconocene derivatives with anticancer activity: (a) zirconocene derivative with alkyllammonium substituents; (b) zirconocene-Y; (c) alkenyl-substituted *ansa*-zirconocene complex.

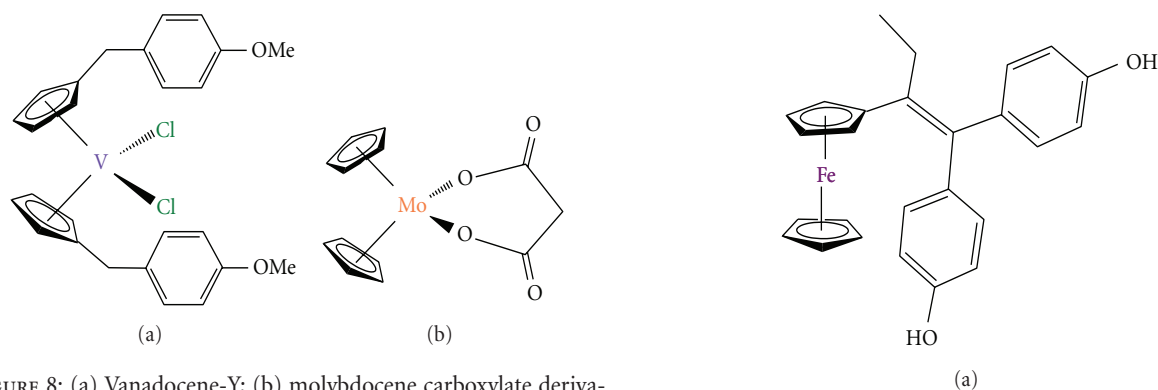


FIGURE 8: (a) Vanadocene-Y; (b) molybdocene carboxylate derivative.

2.5. Ferrocene Derivatives. The discovery of the cytotoxic properties of ferricinium salts on Ehrlich ascite tumors by Köpf and Köpf-Maier [131, 132] were an early breakthrough for the subsequent development of novel preparations of this class of anticancer agents.

There are different groups working in this field, however, to date, the most interesting work in the field of anticancer applications of ferrocene derivatives is being carried out by Jaouen and coworkers.

This group has published several reports on the synthesis of novel functionalized ferrocene derivatives “hydroxyferrocifens” which consist of the linking of the active metabolite of tamoxifen and ferrocene moieties (Figure 9(a)) [133, 134]. This novel class of compounds are able to combine the antioestrogenic properties of tamoxifen with the cytotoxic effects of ferrocene [135–137]. From all these complexes, the outstanding cytotoxicity of a ferrocene complex with a [3] ferrocenophane moiety conjugated to the phenol group (Figure 9(b)) is important to be remarked [138].

In addition, ferrocene-functionalized complexes with steroids or nonsteroidal antiandrogens have also been reported to be very effective to target prostate cancer cells [139].

But not only the design and synthesis of novel ferrocene derivatives with different ligands and cytotoxic properties have been studied, several investigations on the cell death induced mechanism of these anticancer drugs have been reported. Thus, two different action mechanisms have been proposed for ferrocene derivatives, production of electrophilic species, and/or production of ROS species [140].

2.6. Future Tendencies in the Use of Metallocenes in Anticancer Chemotherapy. Almost all metallocene derivatives which have been studied either in preclinical or clinical trials are extremely hydrophobic to be intravenously administered, thus limiting their bioavailability for clinical applications.

Novel formulations of metallocene derivatives in macromolecular systems such as cucurbit(n)urils [140] or cyclodextrins [141] leading to a presumably higher applicability in humans.

In addition, using a different approach, but with the same goal of circumventing the solubility problems of metallocenes in biological media, several metallocene-functionalized MCM-41 or SBA-15 starting from different

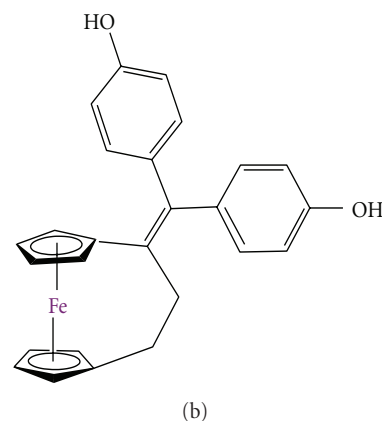


FIGURE 9: Ferrocene derivatives used in preclinical trials: (a) hydroxyferrocifens; (b) ferrocene complex with a [3] ferrocenophane moiety.

titanocene dichloride derivatives with anticancer activity have been reported and may be a good starting point for the development of novel metallocene-based drugs for the treatment of bone tumors [142–145].

3. Conclusions

One of the most potent antitumoral drugs cisplatin deserves special attention as exceptional of few with healing effect. Important role in the action of cisplatin is interaction with nuclear DNA and unfeasibility of the cell response to repair DNA strain containing covalently bonded diammine-platinum(II) moiety (nucleotide excision repair mechanism). Beside DNA, cisplatin might interact with other biomolecules (thioprotenes, RNA) and in that way could be deactivated or even may possibly tune different signaling pathways involved in mediation of cell death, which is cell type specific. Namely, cisplatin has intense effects on signaling pathways facilitated by MAPs (e.g., ERK, JNK, p38). In recent years information on the cellular processing of cisplatin has essentially arisen. Knowledge collected from studies about biological effects of cisplatin and development of cisplatin resistant phenotype afford important clues for the design of more efficient and less toxic platinum and nonplatinum metal based drugs in cancer therapy. It is to be expected that nonplatinum metal compounds may

demonstrate anticancer activity and toxic side effects noticeably different from that of platinum based drugs. Thus titanocene, vanadocene, molybdocene, ferrocene, and zirconocene revealed encouraging results in *in vitro* studies. These compounds might enter by different transport mechanism through cell membrane and distinctly interact with biomolecules than cisplatin. Notwithstanding the extensive applications of cisplatin in the new investigations will provide us with powerful facts for finding a novel efficient and nontoxic metallotherapeutics in anticancer treatment.

Acknowledgments

The authors would like to acknowledge financial support from Alexander von Humboldt Foundation (GNK, SGR), from the Ministerio de Educación y Ciencia, Spain (Grant no. CTQ2011-24346), and from the Ministry of Science and Technological Development of the Republic of Serbia (Grant no. 173013 DMI, SI).

References

- [1] F. Arnesano and G. Natile, "Mechanistic insight into the cellular uptake and processing of cisplatin 30 years after its approval by FDA," *Coordination Chemistry Reviews*, vol. 253, no. 15-16, pp. 2070-2081, 2009.
- [2] D. J. Higby, H. J. Wallace, D. J. Albert, and J. F. Holland, "Diaminodichloroplatinum: a phase I study showing responses in testicular and other tumors," *Cancer*, vol. 33, no. 5, pp. 1219-1225, 1974.
- [3] T. W. Hambley, "Developing new metal-based therapeutics: challenges and opportunities," *Dalton Transactions*, vol. 21, no. 43, pp. 4929-4937, 2007.
- [4] E. R. Jamieson and S. J. Lippard, "Structure, recognition, and processing of cisplatin-DNA adducts," *Chemical Reviews*, vol. 99, no. 9, pp. 2467-2498, 1999.
- [5] G. Giaccone, "Clinical perspectives on platinum resistance," *Drugs*, vol. 59, no. 4, pp. 9-17, 2000, discussion 37-38.
- [6] M. A. Fuertes, C. Alonso, and J. M. Pérez, "Biochemical modulation of cisplatin mechanisms of action: enhancement of antitumor activity and circumvention of drug resistance," *Chemical Reviews*, vol. 103, no. 3, pp. 645-662, 2003.
- [7] B. Köberle, J. R. W. Masters, J. A. Hartley, and R. D. Wood, "Defective repair of cisplatin-induced DNA damage caused by reduced XPA protein in testicular germ cell tumours," *Current Biology*, vol. 9, no. 5, pp. 273-276, 1999.
- [8] E. L. Mamenta, E. E. Poma, W. K. Kaufmann, D. A. Delmastro, H. L. Grady, and S. G. Chaney, "Enhanced replicative bypass of platinum-DNA adducts in cisplatin-resistant human ovarian carcinoma cell lines," *Cancer Research*, vol. 54, no. 13, pp. 3500-3505, 1994.
- [9] A. G. Eliopoulos, D. J. Kerr, J. Herod et al., "The control of apoptosis and drug resistance in ovarian cancer: influence of p53 and Bcl-2," *Oncogene*, vol. 11, no. 7, pp. 1217-1228, 1995.
- [10] A. I. Ivanov, J. Christodoulou, J. A. Parkinson et al., "Cisplatin binding sites on human albumin," *The Journal of Biological Chemistry*, vol. 273, no. 24, pp. 14721-14730, 1998.
- [11] R. C. DeConti, B. R. Toftness, R. C. Lange, and W. A. Creasey, "Clinical and pharmacological studies with cis diamminedichloroplatinum(II)," *Cancer Research*, vol. 33, no. 6, pp. 1310-1315, 1973.
- [12] D. P. Gately and S. B. Howell, "Cellular accumulation of the anticancer agent cisplatin: a review," *British Journal of Cancer*, vol. 67, no. 6, pp. 1171-1176, 1993.
- [13] S. Ishida, J. Lee, D. J. Thiele, and I. Herskowitz, "Uptake of the anticancer drug cisplatin mediated by the copper transporter Ctr1 in yeast and mammals," *Proceedings of the National Academy of Sciences of the United States of America*, vol. 99, no. 22, pp. 14298-14302, 2002.
- [14] R. A. Alderden, M. D. Hall, and T. W. Hambley, "The discovery and development of cisplatin," *Journal of Chemical Education*, vol. 83, no. 5, pp. 728-734, 2006.
- [15] A. R. Timerbaev, C. G. Hartinger, S. S. Aleksenko, and B. K. Keppler, "Interactions of antitumor metallodrugs with serum proteins: advances in characterization using modern analytical methodology," *Chemical Reviews*, vol. 106, no. 6, pp. 2224-2248, 2006.
- [16] E. Volckova, F. Evanics, W. W. Yang, and R. N. Bose, "Unwinding of DNA polymerases by the antitumor drug, cis-diamminedichloroplatinum(II)," *Chemical Communications*, vol. 9, no. 10, pp. 1128-1129, 2003.
- [17] S. Ahmad, "Platinum-DNA interactions and subsequent cellular processes controlling sensitivity to anticancer platinum complexes," *Chemistry and Biodiversity*, vol. 7, no. 3, pp. 543-566, 2010.
- [18] R. J. Knox, F. Friedlos, D. A. Lydall, and J. J. Roberts, "Mechanism of cytotoxicity of anticancer platinum drugs: evidence that cis-diamminedichloroplatinum(II) and cis-diammine-(1,1-cyclobutanedicarboxylato)platinum(II) differ only in the kinetics of their interaction with DNA," *Cancer Research*, vol. 46, no. 4, pp. 1972-1979, 1986.
- [19] L. L. Munchausen and R. O. Rahn, "Physical studies on the binding of cis dichlorodiamine platinum(II) to DNA and homopolynucleotides," *Biochimica et Biophysica Acta*, vol. 414, no. 3, pp. 242-255, 1975.
- [20] A. Eastman, "Characterization of the adducts produced in DNA by cis-diamminedichloroplatinum(II) and cis-dichloro(ethylenediamine)platinum(II)," *Biochemistry*, vol. 22, no. 16, pp. 3927-3933, 1983.
- [21] A. C. M. Plooy, A. M. J. Fichtinger-Schepman, and H. H. Schutte, "The quantitative detection of various Pt-DNA-adducts in Chinese hamster ovary cells treated with cisplatin: application of immunochemical techniques," *Carcinogenesis*, vol. 6, no. 4, pp. 561-566, 1985.
- [22] A. E. Egger, C. G. Hartinger, H. B. Hamidane, Y. O. Tsybin, B. K. Keppler, and P. J. Dyson, "High resolution mass spectrometry for studying the interactions of cisplatin with oligonucleotides," *Inorganic Chemistry*, vol. 47, no. 22, pp. 10626-10633, 2008.
- [23] D. B. Zamble, D. Mu, J. T. Reardon, A. Sancar, and S. J. Lippard, "Repair of cisplatin-DNA adducts by the mammalian excision nuclease," *Biochemistry*, vol. 35, no. 31, pp. 10004-10013, 1996.
- [24] J. T. Reardon, A. Vaisman, S. G. Chaney, and A. Sancar, "Efficient nucleotide excision repair of cisplatin, oxaliplatin, and bis-acetoammine-dichloro-cyclohexylamine-platinum(IV) (JM216) platinum intrastrand DNA diadducts," *Cancer Research*, vol. 59, no. 16, pp. 3968-3971, 1999.
- [25] S. W. Johnson, R. P. Perez, A. K. Godwin et al., "Role of platinum-DNA adduct formation and removal in cisplatin resistance in human ovarian cancer cell lines," *Biochemical Pharmacology*, vol. 47, no. 4, pp. 689-697, 1994.
- [26] K. V. Ferry, T. C. Hamilton, and S. W. Johnson, "Increased nucleotide excision repair in cisplatin-resistant ovarian

- cancer cells: role of ERCC1-XPF," *Biochemical Pharmacology*, vol. 60, no. 9, pp. 1305–1313, 2000.
- [27] D. Fink, H. Zheng, S. Nebel et al., "In vitro and in vivo resistance to cisplatin in cells that have lost DNA mismatch repair," *Cancer Research*, vol. 57, no. 10, pp. 1841–1845, 1997.
- [28] E. D. Scheeff, J. M. Briggs, and S. B. Howell, "Molecular modeling of the intrastrand guanine-guanine DNA adducts produced by cisplatin and oxaliplatin," *Molecular Pharmacology*, vol. 56, no. 3, pp. 633–643, 1999.
- [29] A. Vaisman, M. Varchenko, A. Umar et al., "The role of hMLH1, hMSH3, and hMSH6 defects in cisplatin and oxaliplatin resistance: correlation with replicative bypass of platinum-DNA adducts," *Cancer Research*, vol. 58, no. 16, pp. 3579–3585, 1998.
- [30] S. G. Chaney, S. L. Campbell, E. Bassett, and Y. Wu, "Recognition and processing of cisplatin- and oxaliplatin-DNA adducts," *Critical Reviews in Oncology/Hematology*, vol. 53, no. 1, pp. 3–11, 2005.
- [31] V. Cepeda, M. A. Fuertes, J. Castilla, C. Alonso, C. Quevedo, and J. M. Pérez, "Biochemical mechanisms of cisplatin cytotoxicity," *Anti-Cancer Agents in Medicinal Chemistry*, vol. 7, no. 1, pp. 3–18, 2007.
- [32] K. M. Henkels and J. J. Turchi, "Induction of apoptosis in cisplatin-sensitive and -resistant human ovarian cancer cell lines," *Cancer Research*, vol. 57, no. 20, pp. 4488–4492, 1997.
- [33] D. Wang and S. J. Lippard, "Cellular processing of platinum anticancer drugs," *Nature Reviews Drug Discovery*, vol. 4, no. 4, pp. 307–320, 2005.
- [34] Z. S. Juo, T. K. Chiu, P. M. Leiberman, I. Baikalov, A. J. Berk, and R. E. Dickerson, "How proteins recognize the TATA box," *Journal of Molecular Biology*, vol. 261, no. 2, pp. 239–254, 1996.
- [35] J. Yaneva, S. H. Leuba, K. Van Holde, and J. Zlatanova, "The major chromatin protein histone H1 binds preferentially to cis-platinum-damaged DNA," *Proceedings of the National Academy of Sciences of the United States of America*, vol. 94, no. 25, pp. 13448–13451, 1997.
- [36] M. Kartalou, L. D. Samson, and J. M. Essigmann, "Cisplatin adducts inhibit 1,N⁶-ethenoadenine repair by interacting with the human 3-methyladenine DNA glycosylase," *Biochemistry*, vol. 39, no. 27, pp. 8032–8038, 2000.
- [37] C. Söti, A. Rác, and P. Csérmely, "A nucleotide-dependent molecular switch controls ATP binding at the C-terminal domain of Hsp90. N-terminal nucleotide binding unmasks a C-terminal binding pocket," *The Journal of Biological Chemistry*, vol. 277, no. 9, pp. 7066–7075, 2002.
- [38] T. Peleg-Shulman and D. Gibson, "Cisplatin-protein adducts are efficiently removed by glutathione but not by 5'-guanosine monophosphate," *Journal of the American Chemical Society*, vol. 123, no. 13, pp. 3171–3172, 2001.
- [39] H. Daino, I. Matsumura, K. Takada et al., "Induction of apoptosis by extracellular ubiquitin in human hematopoietic cells: possible involvement of STAT3 degradation by proteasome pathway in interleukin 6-dependent hematopoietic cells," *Blood*, vol. 95, no. 8, pp. 2577–2585, 2000.
- [40] P. A. Nguewa, M. A. Fuertes, V. Cepeda et al., "Pentamidine is an antiparasitic and apoptotic drug that selectively modifies ubiquitin," *Chemistry and Biodiversity*, vol. 2, no. 10, pp. 1387–1400, 2005.
- [41] D. Maksimovic-Ivanic, S. Mijatovic, D. Miljkovic et al., "The antitumor properties of a nontoxic, nitric oxide-modified version of saquinavir are independent of Akt," *Molecular Cancer Therapeutics*, vol. 8, no. 5, pp. 1169–1178, 2009.
- [42] A. Casini, C. Gabbiani, G. Mastrobuoni et al., "Insights into the molecular mechanisms of protein platination from a case study: the reaction of anticancer platinum(II) iminoethers with horse heart cytochrome C," *Biochemistry*, vol. 46, no. 43, pp. 12220–12230, 2007.
- [43] F. Arnesano and G. Natile, "'Platinum on the road': interactions of antitumoral cisplatin with proteins," *Pure and Applied Chemistry*, vol. 80, no. 12, pp. 2715–2725, 2008.
- [44] S. R. Datta, A. Brunet, and M. E. Greenberg, "Cellular survival: a play in three acts," *Genes and Development*, vol. 13, no. 22, pp. 2905–2927, 1999.
- [45] M. Fraser, B. M. Leung, X. Yan, H. C. Dan, J. Q. Cheng, and B. K. Tsang, "p53 is a determinant of X-linked inhibitor of apoptosis protein/Akt-mediated chemoresistance in human ovarian cancer cells," *Cancer Research*, vol. 63, no. 21, pp. 7081–7088, 2003.
- [46] H. C. Dan, M. Sun, S. Kaneko et al., "Akt phosphorylation and stabilization of X-linked inhibitor of apoptosis protein (XIAP)," *The Journal of Biological Chemistry*, vol. 279, no. 7, pp. 5405–5412, 2004.
- [47] J. G. Viniegra, J. H. Losa, V. J. Sánchez-Arévalo et al., "Modulation of PI3K/Akt pathway by E1a mediates sensitivity to cisplatin," *Oncogene*, vol. 21, no. 46, pp. 7131–7136, 2002.
- [48] Y. Shaul, "c-Abl: activation and nuclear targets," *Cell Death and Differentiation*, vol. 7, no. 1, pp. 10–16, 2000.
- [49] J. Gong, A. Costanzo, H. Q. Yang et al., "The tyrosine kinase c-Abl regulates p73 in apoptotic response to cisplatin-induced DNA damage," *Nature*, vol. 399, no. 6738, pp. 806–809, 1999.
- [50] L. Harhaji-Trajkovic, U. Vilimanovich, T. Kravic-Stevovic, V. Bumbasirevic, and V. Trajkovic, "AMPK-mediated autophagy inhibits apoptosis in cisplatin-treated tumour cells," *Journal of Cellular and Molecular Medicine*, vol. 13, no. 9, pp. 3644–3654, 2009.
- [51] X. Wang, J. L. Martindale, and N. J. Holbrook, "Requirement for ERK activation in cisplatin-induced apoptosis," *The Journal of Biological Chemistry*, vol. 275, no. 50, pp. 39435–39443, 2000.
- [52] W. Cui, E. M. Yazlovitskaya, M. S. Mayo et al., "Cisplatin-induced response of c-jun N-terminal kinase 1 and extracellular signal-regulated protein kinases 1 and 2 in a series of cisplatin-resistant ovarian carcinoma cell lines," *Molecular Carcinogenesis*, vol. 29, pp. 219–228, 2000.
- [53] S. Mijatovic, D. Maksimovic-Ivanic, J. Radovic et al., "Aloe emodin decreases the ERK-dependent anticancer activity of cisplatin," *Cellular and Molecular Life Sciences*, vol. 62, no. 11, pp. 1275–1282, 2005.
- [54] S. Mijatovic, D. Maksimovic-Ivanic, J. Radovic et al., "Antiglioma action of aloe emodin: the role of ERK inhibition," *Cellular and Molecular Life Sciences*, vol. 62, no. 5, pp. 589–598, 2005.
- [55] A. Mansouri, L. D. Ridgway, A. L. Korapati et al., "Sustained activation of JNK/p38 MAPK pathways in response to cisplatin leads to Fas ligand induction and cell death in ovarian carcinoma cells," *The Journal of Biological Chemistry*, vol. 278, no. 21, pp. 19245–19256, 2003.
- [56] I. Sánchez-Perez, J. R. Murguía, and R. Perona, "Cisplatin induces a persistent activation of JNK that is related to cell death," *Oncogene*, vol. 16, no. 4, pp. 533–540, 1998.
- [57] J. Hayakawa, M. Ohmichi, H. Kurachi et al., "Inhibition of extracellular signal-regulated protein kinase or c-Jun N-terminal protein kinase cascade, differentially activated by

- cisplatin, sensitizes human ovarian cancer cell line," *The Journal of Biological Chemistry*, vol. 274, no. 44, pp. 31648–31654, 1999.
- [58] R. J. Davis, "Signal transduction by the JNK group of MAP kinases," *Cell*, vol. 103, no. 2, pp. 239–252, 2000.
- [59] P. Pandey, J. Raingeaud, M. Kaneki et al., "Activation of p38 mitogen-activated protein kinase by c-Abl-dependent and -independent mechanisms," *The Journal of Biological Chemistry*, vol. 271, no. 39, pp. 23775–23779, 1996.
- [60] J. Hernández Losa, C. Parada Cobo, J. Guinea Viniegra, V. J. Sánchez-Arevalo Lobo, S. Ramón y Cajal, and R. Sánchez-Prieto, "Role of the p38 MAPK pathway in cisplatin-based therapy," *Oncogene*, vol. 22, no. 26, pp. 3998–4006, 2003.
- [61] D. Wang and S. J. Lippard, "Cisplatin-induced post-translational modification of histones H3 and H4," *The Journal of Biological Chemistry*, vol. 279, no. 20, pp. 20622–20625, 2004.
- [62] V. M. Gonzalez, M. A. Fuertes, C. Alonso, and J. M. Perez, "Is cisplatin-induced cell death always produced by apoptosis?" *Molecular Pharmacology*, vol. 59, no. 4, pp. 657–663, 2001.
- [63] W. Lieberthal, V. Triaca, and J. Levine, "Mechanisms of death induced by cisplatin in proximal tubular epithelial cells: apoptosis vs. necrosis," *American Journal of Physiology*, vol. 270, no. 4, pp. F700–F708, 1996.
- [64] Y. Eguchi, S. Shimizu, and Y. Tsujimoto, "Intracellular ATP levels determine cell death fate by apoptosis or necrosis," *Cancer Research*, vol. 57, no. 10, pp. 1835–1840, 1997.
- [65] R. Zhou, M. G. Vander Heiden, and C. M. Rudin, "Genotoxic exposure is associated with alterations in glucose uptake and metabolism," *Cancer Research*, vol. 62, no. 12, pp. 3515–3520, 2002.
- [66] Z. Herceg and Z. Q. Wang, "Failure of poly(ADP-ribose) polymerase cleavage by caspases leads to induction of necrosis and enhanced apoptosis," *Molecular and Cellular Biology*, vol. 19, no. 7, pp. 5124–5133, 1999.
- [67] T. Hirsch, P. Marchetti, S. A. Susin et al., "The apoptosis-necrosis paradox. Apoptogenic proteases activated after mitochondrial permeability transition determine the mode of cell death," *Oncogene*, vol. 15, no. 13, pp. 1573–1581, 1997.
- [68] L. Ding, C. Yuan, F. Wei et al., "Cisplatin restores TRAIL apoptotic pathway in glioblastoma-derived stem cells through up-regulation of DR5 and down-regulation of c-FLIP," *Cancer Investigation*, vol. 29, pp. 511–520, 2011.
- [69] O. Vondálová Blanárová, I. Jelínková, A. Szöör et al., "Cisplatin and a potent platinum(IV) complex-mediated enhancement of TRAIL-induced cancer cells killing is associated with modulation of upstream events in the extrinsic apoptotic pathway," *Carcinogenesis*, vol. 32, no. 1, pp. 42–51, 2011.
- [70] D. Maksimovic-Ivanic, S. Stosic-Grujicic, F. Nicoletti, and S. Mijatovic, "Resistance to TRAIL and how to surmount it," *Immunology Research*, vol. 52, no. 1-2, pp. 157–168, 2012.
- [71] M. P. Decatris, S. Sundar, and K. J. O'Byrne, "Platinum-based chemotherapy in metastatic breast cancer: current status," *Cancer Treatment Reviews*, vol. 30, no. 1, pp. 53–81, 2004.
- [72] M. D. Shelley, K. Burgon, and M. D. Mason, "Treatment of testicular germ-cell cancer: a cochrane evidence-based systematic review," *Cancer Treatment Reviews*, vol. 28, no. 5, pp. 237–253, 2002.
- [73] M. S. Kim, M. Blake, J. H. Baek, G. Kohlhagen, Y. Pommier, and F. Carrier, "Inhibition of histone deacetylase increases cytotoxicity to anticancer drugs targeting DNA," *Cancer Research*, vol. 63, no. 21, pp. 7291–7300, 2003.
- [74] N. J. Long, *Metalloenes*, Blackwell Science, Oxford, UK, 1998.
- [75] A. Korfel, M. E. Scheulen, H. J. Schmoll et al., "Phase I clinical and pharmacokinetic study of titanocene dichloride in adults with advanced solid tumors," *Clinical Cancer Research*, vol. 4, no. 11, pp. 2701–2708, 1998.
- [76] C. V. Christodoulou, D. R. Ferry, D. W. Fyfe et al., "Phase I trial of weekly scheduling and pharmacokinetics of titanocene dichloride in patients with advanced cancer," *Journal of Clinical Oncology*, vol. 16, no. 8, pp. 2761–2769, 1998.
- [77] K. Mross, P. Robben-Bathe, L. Edler et al., "Phase I clinical trial of a day-1, -3, -5 every 3 weeks schedule with titanocene dichloride (MKT 5) in patients with advanced cancer: a study of the phase I study group of the association for medical oncology (AIO) of the German Cancer Society," *Onkologie*, vol. 23, no. 6, pp. 576–579, 2000.
- [78] B. W. Müller, R. Müller, S. Lucks, and W. Mohr, "Medac Gesellschaft für Klinische Spezialpräparate GmbH," US Patent 5, 296, 237, 1994.
- [79] N. Kröger, U. R. Kleeberg, K. Mross, L. Edler, G. Saß, and D. K. Hossfeld, "Phase II clinical trial of titanocene dichloride in patients with metastatic breast cancer," *Onkologie*, vol. 23, no. 1, pp. 60–62, 2000.
- [80] G. Lümmer, H. Sperling, H. Luboldt, T. Otto, and H. Rübber, "Phase II trial of titanocene dichloride in advanced renal-cell carcinoma," *Cancer Chemotherapy and Pharmacology*, vol. 42, no. 5, pp. 415–417, 1998.
- [81] E. Meléndez, "Titanium complexes in cancer treatment," *Critical Reviews in Oncology/Hematology*, vol. 42, no. 3, pp. 309–315, 2002.
- [82] F. Caruso and M. Rossi, "Antitumor titanium compounds and related metallocenes," in *Metal Ions in Biological System*, A. Sigel and H. Sigel, Eds., vol. 42 of *Metal Complexes in Tumor Diagnostics and as Anticancer Agents*, Marcel Dekker, New York, NY, USA, 2004.
- [83] J. C. Dabrowiak, *Metals in Medicine*, John Wiley & Sons, West Sussex, UK, 2009.
- [84] U. Olszewski and G. Hamilton, "Mechanisms of cytotoxicity of anticancer titanocenes," *Anti-Cancer Agents in Medicinal Chemistry*, vol. 10, no. 4, pp. 302–311, 2010.
- [85] K. Strohsfeldt and M. Tacke, "Bioorganometallic fulvene-derived titanocene anti-cancer drugs," *Chemical Society Reviews*, vol. 37, no. 6, pp. 1174–1187, 2008.
- [86] R. Hernández, J. Lamboy, L. M. Gao, J. Matta, F. R. Román, and E. Meléndez, "Structure-activity studies of Ti(IV) complexes: aqueous stability and cytotoxic properties in colon cancer HT-29 cells," *Journal of Biological Inorganic Chemistry*, vol. 13, no. 5, pp. 685–692, 2008.
- [87] R. Hernández, J. Méndez, J. Lamboy, M. Torres, F. R. Román, and E. Meléndez, "Titanium(IV) complexes: cytotoxicity and cellular uptake of titanium(IV) complexes on caco-2 cell line," *Toxicology in Vitro*, vol. 24, no. 1, pp. 178–183, 2010.
- [88] L. M. Gao, J. Matta, A. L. Rheingold, and E. Meléndez, "Synthesis, structure and biological activity of amide-functionalized titanocenes: improving their cytotoxic properties," *Journal of Organometallic Chemistry*, vol. 694, no. 26, pp. 4134–4139, 2009.
- [89] A. Gansäuer, I. Winkler, D. Worgull et al., "Carbonyl-substituted titanocenes: a novel class of cytostatic compounds with high antitumor and antileukemic activity," *Chemistry*, vol. 14, no. 14, pp. 4160–4163, 2008.
- [90] O. R. Allen, L. Croll, A. L. Gott, R. J. Knox, and P. C. McGowan, "Functionalized cyclopentadienyl titanium organometallic compounds as new antitumor drugs," *Organometallics*, vol. 23, no. 2, pp. 288–292, 2004.

- [91] O. R. Allen, A. L. Gott, J. A. Hartley, J. M. Hartley, R. J. Knox, and P. C. McGowan, "Functionalised cyclopentadienyl titanium compounds as potential anticancer drugs," *Dalton Transactions*, no. 43, pp. 5082–5090, 2007.
- [92] G. D. Potter, M. C. Baird, and S. P. C. Cole, "A new series of titanocene dichloride derivatives bearing chiral alkylammonium groups; Assessment of their cytotoxic properties," *Inorganica Chimica Acta*, vol. 364, no. 1, pp. 16–22, 2010.
- [93] L. M. Gao, J. L. Vera, J. Matta, and E. Meléndez, "Synthesis and cytotoxicity studies of steroid-functionalized titanocenes as potential anticancer drugs: sex steroids as potential vectors for titanocenes," *Journal of Biological Inorganic Chemistry*, vol. 15, no. 6, pp. 851–859, 2010.
- [94] S. Gómez-Ruiz, G. N. Kaluderović, S. Prashar et al., "Cytotoxic studies of substituted titanocene and ansa-titanocene anticancer drugs," *Journal of Inorganic Biochemistry*, vol. 102, no. 8, pp. 1558–1570, 2008.
- [95] S. Gómez-Ruiz, G. N. Kaluderović, Ž. Žižak et al., "Anticancer drugs based on alkenyl and boryl substituted titanocene complexes," *Journal of Organometallic Chemistry*, vol. 694, no. 13, pp. 1981–1987, 2009.
- [96] G. N. Kaluderović, V. Tayurskaya, R. Paschke, S. Prashar, M. Fajardo, and S. Gómez-Ruiz, "Synthesis, characterization and biological studies of alkenyl-substituted titanocene(IV) carboxylate complexes," *Applied Organometallic Chemistry*, vol. 24, no. 9, pp. 656–662, 2010.
- [97] H. Sun, H. Li, R. A. Weir, and P. J. Sadler, "You have full text access to this content the first specific Ti^{IV} -protein complex: potential relevance to anticancer activity of titanocenes," *Angewandte Chemie International Edition*, vol. 37, no. 11, pp. 1577–1579, 1998.
- [98] M. Guo and P. J. Sadler, "Competitive binding of the anticancer drug titanocene dichloride to N,N' -ethylenebis(o-hydroxyphenylglycine) and adenosine triphosphate: a model for Ti^{IV} uptake and release by transferrin," *Journal of the Chemical Society, Dalton Transactions*, vol. 1, pp. 7–9, 2000.
- [99] M. Guo, H. Sun, S. Bihari et al., "Stereoselective formation of seven-coordinate titanium(IV) monomer and dimer complexes of ethylenebis(o-hydroxyphenyl)glycine," *Inorganic Chemistry*, vol. 39, no. 2, pp. 206–215, 2000.
- [100] M. Guo, H. Sun, H. J. McArdle, L. Gambling, and P. J. Sadler, " $Ti(IV)$ uptake and release by human serum transferrin and recognition of $Ti(IV)$ -transferrin by cancer cells: understanding the mechanism of action of the anticancer drug titanocene dichloride," *Biochemistry*, vol. 39, no. 33, pp. 10023–10033, 2000.
- [101] P. Köpf-Maier and D. Krahl, "Tumor inhibition by metallo-genes: ultrastructural localization of titanium and vanadium in treated tumor cells by electron energy loss spectroscopy," *Chemico-Biological Interactions*, vol. 44, no. 3, pp. 317–328, 1983.
- [102] P. Köpf-Maier, "Intracellular localization of titanium within xenografted sensitive human tumors after treatment with the antitumor agent titanocene dichloride," *Journal of Structural Biology*, vol. 105, no. 1–3, pp. 35–45, 1990.
- [103] A. D. Tinoco, C. D. Incarvito, and A. M. Valentine, "Calorimetric, spectroscopic, and model studies provide insight into the transport of $Ti(IV)$ by human serum transferrin," *Journal of the American Chemical Society*, vol. 129, no. 11, pp. 3444–3454, 2007.
- [104] A. D. Tinoco, E. V. Eames, and A. M. Valentine, "Reconsideration of serum $Ti(IV)$ transport: albumin and transferrin trafficking of $Ti(IV)$ and its complexes," *Journal of the American Chemical Society*, vol. 130, no. 7, pp. 2262–2270, 2008.
- [105] M. Pavlaki, K. Debeli, I. E. Triantaphyllidou, N. Klouras, E. Giannopoulou, and A. J. Aletras, "A proposed mechanism for the inhibitory effect of the anticancer agent titanocene dichloride on tumour gelatinases and other proteolytic enzymes," *Journal of Biological Inorganic Chemistry*, vol. 14, no. 6, pp. 947–957, 2009.
- [106] O. R. Allen, R. J. Knox, and P. C. McGowan, "Functionalised cyclopentadienyl zirconium compounds as potential anticancer drugs," *Dalton Transactions*, no. 39, pp. 5293–5295, 2008.
- [107] D. Wallis, J. Claffey, B. Gleeson, M. Hogan, H. Müller-Bunz, and M. Tacke, "Novel zirconocene anticancer drugs?" *Journal of Organometallic Chemistry*, vol. 694, no. 6, pp. 828–833, 2009.
- [108] S. Gómez-Ruiz, G. N. Kaluderović, D. Polo-Cerón et al., "A novel alkenyl-substituted ansa-zirconocene complex with dual application as olefin polymerization catalyst and anticancer drug," *Journal of Organometallic Chemistry*, vol. 694, no. 18, pp. 3032–3038, 2009.
- [109] P. Köpf-Maier, "Antitumor bis(cyclopentadienyl) metal complexes," in *Metal Complexes in Cancer Chemotherapy*, B. K. Keppler, Ed., pp. 259–296, VCH Verlagsgesellschaft, Weinheim, Germany, 1993.
- [110] C. S. Navara, A. Benyumov, A. Vassilev, R. K. Narla, P. Ghosh, and F. M. Uckun, "Vanadocenes as potent anti-proliferative agents disrupting mitotic spindle formation in cancer cells," *Anti-Cancer Drugs*, vol. 12, no. 4, pp. 369–376, 2001.
- [111] P. Ghosh, O. J. D'Cruz, R. K. Narla, and F. M. Uckun, "Apoptosis-inducing vanadocene compounds against human testicular cancer," *Clinical Cancer Research*, vol. 6, no. 4, pp. 1536–1545, 2000.
- [112] H. Paláčková, J. Vinklárěk, J. Holubová, I. Císařová, and M. Erben, "The interaction of antitumor active vanadocene dichloride with sulfur-containing amino acids," *Journal of Organometallic Chemistry*, vol. 692, no. 17, pp. 3758–3764, 2007.
- [113] J. Vinklárěk, J. Honzíček, and J. Holubová, "Interaction of the antitumor agent vanadocene dichloride with phosphate buffered saline," *Inorganica Chimica Acta*, vol. 357, no. 12, pp. 3765–3769, 2004.
- [114] J. Vinklárěk, H. Paláčková, J. Honzíček, J. Holubová, M. Holčápek, and I. Císařová, "Investigation of vanadocene(IV) α -amino acid complexes: synthesis, structure, and behavior in physiological solutions, human plasma, and blood," *Inorganic Chemistry*, vol. 45, no. 5, pp. 2156–2162, 2006.
- [115] B. Gleeson, J. Claffey, A. Deally et al., "Synthesis and cytotoxicity studies of fluorinated derivatives of vanadocene Y," *European Journal of Inorganic Chemistry*, no. 19, pp. 2804–2810, 2009.
- [116] B. Gleeson, J. Claffey, M. Hogan, H. Müller-Bunz, D. Wallis, and M. Tacke, "Novel benzyl-substituted vanadocene anticancer drugs," *Journal of Organometallic Chemistry*, vol. 694, no. 9–10, pp. 1369–1374, 2009.
- [117] B. Gleeson, J. Claffey, A. Deally et al., "Novel benzyl-substituted molybdocene anticancer drugs," *Inorganica Chimica Acta*, vol. 363, no. 8, pp. 1831–1836, 2010.
- [118] B. Gleeson, M. Hogan, H. Müller-Bunz, and M. Tacke, "Synthesis and preliminary cytotoxicity studies of indole-substituted vanadocenes," *Transition Metal Chemistry*, vol. 35, no. 8, pp. 973–983, 2010.
- [119] J. Honzíček, I. Klepalová, J. Vinklárěk et al., "Synthesis, characterization and cytotoxic effect of ring-substituted and ansa-bridged vanadocene complexes," *Inorganica Chimica Acta*, vol. 373, no. 1, pp. 1–7, 2011.

- [120] J. B. Waern and M. M. Harding, "Bioorganometallic chemistry of molybdocene dichloride," *Journal of Organometallic Chemistry*, vol. 689, no. 25, pp. 4655–4668, 2004.
- [121] J. B. Waern, C. T. Dillon, and M. M. Harding, "Organometallic anticancer agents: cellular uptake and cytotoxicity studies on thiol derivatives of the antitumor agent molybdocene dichloride," *Journal of Medicinal Chemistry*, vol. 48, no. 6, pp. 2093–2099, 2005.
- [122] J. B. Waern, H. H. Harris, B. Lai, Z. Cai, M. M. Harding, and C. T. Dillon, "Intracellular mapping of the distribution of metals derived from the antitumor metallocenes," *Journal of Biological Inorganic Chemistry*, vol. 10, no. 5, pp. 443–452, 2005.
- [123] J. B. Waern, P. Turner, and M. M. Harding, "Synthesis and hydrolysis of thiol derivatives of molybdocene dichloride incorporating electron-withdrawing substituents," *Organometallics*, vol. 25, no. 14, pp. 3417–3421, 2006.
- [124] K. S. Campbell, A. J. Foster, C. T. Dillon, and M. M. Harding, "Genotoxicity and transmission electron microscopy studies of molybdocene dichloride," *Journal of Inorganic Biochemistry*, vol. 100, no. 7, pp. 1194–1198, 2006.
- [125] J. H. Toney and T. J. Marks, "Hydrolysis chemistry of the metallocene dichlorides $M(\eta^5\text{-C}_5\text{H}_5)_2\text{Cl}_2$, $M = \text{Ti, V, Zr}$. Aqueous kinetics, equilibria, and mechanistic implications for a new class of antitumor agents," *Journal of the American Chemical Society*, vol. 107, no. 4, pp. 947–953, 1985.
- [126] C. Balzarek, T. J. R. Weakley, L. Y. Kuo, and D. R. Tyler, "Investigation of the monomer-dimer equilibria of molybdocenes in water," *Organometallics*, vol. 19, no. 15, pp. 2927–2931, 2000.
- [127] L. Y. Kuo, M. G. Kanatzidis, M. Sabat, A. L. Tipton, and T. J. Marks, "Metallocene antitumor agents. Solution and solid-state molybdocene coordination chemistry of DNA constituents," *Journal of the American Chemical Society*, vol. 113, no. 24, pp. 9027–9045, 1991.
- [128] P. M. Abeyasinghe and M. M. Harding, "Antitumour bis(cyclopentadienyl) metal complexes: titanocene and molybdocene dichloride and derivatives," *Dalton Transactions*, no. 32, pp. 3474–3482, 2007.
- [129] M. M. Harding and G. Mokdsi, "Antitumour metallocenes: structure-activity studies and interactions with biomolecules," *Current Medicinal Chemistry*, vol. 7, no. 12, pp. 1289–1303, 2000.
- [130] K. S. Campbell, C. T. Dillon, S. V. Smith, and M. M. Harding, "Radiotracer studies of the antitumor metallocene molybdocene dichloride with biomolecules," *Polyhedron*, vol. 26, no. 2, pp. 456–459, 2007.
- [131] P. Köpf-Maier, H. Köpf, and E. W. Neuse, "Ferrocenium salts—the first antineoplastic iron compounds," *Angewandte Chemie—International Edition in English*, vol. 23, no. 6, pp. 456–457, 1984.
- [132] P. Köpf-Maier, H. Köpf, and E. W. Neuse, "Ferricenium complexes: a new type of water-soluble antitumor agent," *Journal of Cancer Research and Clinical Oncology*, vol. 108, no. 3, pp. 336–340, 1984.
- [133] S. Top, J. Tang, A. Vessières, D. Carrez, C. Provot, and G. Jaouen, "Ferrocenyl hydroxytamoxifen: a prototype for a new range of oestradiol receptor site-directed cytotoxics," *Chemical Communications*, vol. 8, pp. 955–956, 1996.
- [134] S. Top, B. Dauer, J. Vaissermann, and G. Jaouen, "Facile route to ferrocifen, 1-[4-(2-dimethylaminoethoxy)]-1-(phenyl-2-ferrocenyl-but-1-ene), first organometallic analogue of tamoxifen, by the McMurry reaction," *Journal of Organometallic Chemistry*, vol. 541, no. 1-2, pp. 355–361, 1997.
- [135] S. Top, A. Vessières, C. Cabestaing et al., "Studies on organometallic selective estrogen receptor modulators. (SERMs) Dual activity in the hydroxy-ferrocifen series," *Journal of Organometallic Chemistry*, vol. 637–639, no. 1, pp. 500–506, 2001.
- [136] S. Top, A. Vessières, G. Leclercq et al., "Synthesis, biochemical properties and molecular modelling studies of organometallic Specific Estrogen Receptor Modulators (SERMs), the ferrocifens and hydroxyferrocifens: evidence for an antiproliferative effect of hydroxyferrocifens on both hormone-dependent and hormone-independent breast cancer cell lines," *Chemistry*, vol. 9, no. 21, pp. 5223–5236, 2003.
- [137] G. Jaouen, S. Top, A. Vessières, G. Leclercq, and M. J. McGlinchey, "The first organometallic selective estrogen receptor modulators (SERMs) and their relevance to breast cancer," *Current Medicinal Chemistry*, vol. 11, no. 18, pp. 2505–2517, 2004.
- [138] D. Plazuk, A. Vessières, E. A. Hillard et al., "A [3]ferrocenophane polyphenol showing a remarkable antiproliferative activity on breast and prostate cancer cell lines," *Journal of Medicinal Chemistry*, vol. 52, no. 15, pp. 4964–4967, 2009.
- [139] E. A. Hillard, A. Vessières, and G. Jaouen, "Ferrocene functionalized endocrine modulators as anticancer agents," *Topics in Organometallic Chemistry*, vol. 32, pp. 81–117, 2010.
- [140] D. P. Buck, P. M. Abeyasinghe, C. Cullinane, A. I. Day, J. G. Collins, and M. M. Harding, "Inclusion complexes of the antitumour metallocenes Cp_2MCl_2 ($M = \text{Mo, Ti}$) with cucurbit[n]urils," *Dalton Transactions*, no. 17, pp. 2328–2334, 2008.
- [141] C. C. L. Pereira, C. V. Diogo, A. Burgeiro et al., "Complex formation between heptakis(2,6-di-O-methyl)- β -cyclodextrin and cyclopentadienyl molybdenum(II) dicarbonyl complexes: structural studies and cytotoxicity evaluations," *Organometallics*, vol. 27, no. 19, pp. 4948–4956, 2008.
- [142] D. Pérez-Quintanilla, S. Gomez-Ruiz, Ž. Žižak et al., "A new generation of anticancer drugs: mesoporous materials modified with titanocene complexes," *Chemistry*, vol. 15, no. 22, pp. 5588–5597, 2009.
- [143] G. N. Kaluđerović, D. Pérez-Quintanilla, I. Sierra et al., "Study of the influence of the metal complex on the cytotoxic activity of titanocene-functionalized mesoporous materials," *Journal of Materials Chemistry*, vol. 20, no. 4, pp. 806–814, 2010.
- [144] G. N. Kaluđerović, D. Pérez-Quintanilla, Ž. Žižak, Z. D. Juranić, and S. Gómez-Ruiz, "Improvement of cytotoxicity of titanocene-functionalized mesoporous materials by the increase of the titanium content," *Dalton Transactions*, vol. 39, no. 10, pp. 2597–2608, 2010.
- [145] A. García-Peñas, S. Gómez-Ruiz, D. Pérez-Quintanilla et al., "Study of the cytotoxicity and particle action in human cancer cells of titanocene-functionalized materials," *Journal of Inorganic Biochemistry*, vol. 106, no. 2, pp. 100–110, 2012.

Synthesis, characterization, *in vitro* antitumoral investigations and interaction with plasmid pBR322 DNA of R₂eddp-platinum(IV) complexes (R = Et, *n*-Pr)

Goran N. Kaluđerović,^{*†a,b} Harish Kommera,^b Sebastian Schwieger,^a Anchan Paethanom,^a Michael Kunze,^c Harry Schmidt,^a Reinhard Paschke^b and Dirk Steinborn^a

Received 15th June 2009, Accepted 12th August 2009

First published as an Advance Article on the web 27th August 2009

DOI: 10.1039/b911597h

The studies on synthetic, spectroscopic and biological properties of platinum(IV) complexes, [PtCl₄(R₂eddp)] (R = Et, **1**; *n*-Pr, **2**), containing κ²N,N' bidentate ligands, esters of ethylenediamine-*N,N'*-di-3-propionic acid (HOOCCH₂CH₂NHCH₂CH₂NHCH₂CH₂COOH, H₂eddp), are reported. Complexes have been characterized by infrared, ¹H and ¹³C NMR spectroscopy and elemental analysis and it was concluded that the coordination of the ligands occurs *via* nitrogen donor atoms of the ester ligands (R₂eddp). Cytotoxicity studies were performed for ligand precursors and corresponding platinum(IV) complexes. Although the *n*-Pr₂eddp·2HCl itself showed no activity (IC₅₀ values > 125 μM) in selected cell lines, the activity of complex **2**, *via* apoptotic mode of cell death, has increased significantly for a broad range of cancer cell lines tested *in vitro* (IC₅₀ = 8.6–49 μM). As it was found that complexes **1** and **2** are able to interact with pBR322 plasmid DNA, platinum(IV) complexes of this type may act as drugs and pro-drugs.

Introduction

The platinum(II) anticancer drug cisplatin has been widely used effectively in treating a wide variety of solid tumours, especially testicular cancer.¹ However, the toxic side effects of cisplatin therapy particularly peripheral neuropathy, nephrotoxicity and ototoxicity present a major disadvantage for cisplatin application.² Many efforts have been made towards designing new platinum compounds with improved pharmacological properties. Because platinum(IV) complexes are more kinetically inert than platinum(II) complexes, there is a growing interest in platinum(IV) compounds. This property lends itself favourably to the possible oral administration of platinum(IV) drugs and to reduced toxicity during platinum-based chemotherapy.³

Recently, some platinum(IV) complexes containing R₂eddp (esters of ethylenediamine-*N,N'*-di-3-propionic acid) and halide ligands have been tested against human adenocarcinoma HeLa cells and human myelogenous leukemia K562 cells and showed that the most efficient complexes were the tetrachloroplatinum(IV) complexes acting through apoptotic cell death.⁴ In addition, significant *in vitro* antitumoral activity by two platinum(IV) complexes [PtCl₄(*n*-Bu₂eddp)] and [PtCl₄(*n*-Pe₂eddp)] was demonstrated on L929 fibrosarcoma and U251 astrocytoma tumour cells.⁵ Results

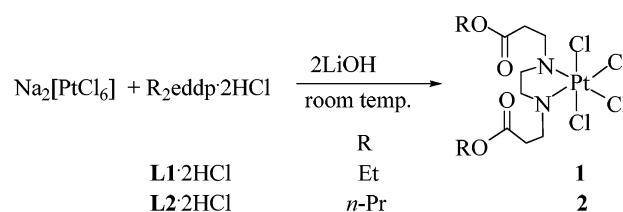
have shown that these platinum(IV) complexes displayed cytotoxic effects more rapidly than cisplatin.

In the present work two analogues of these high active platinum(IV) complexes with shorter chain in ester function, [PtCl₄(R₂eddp)] (R = Et and *n*-Pr), have been synthesized. Furthermore cytotoxicity, mode of cell death, kinetics, platinum uptake and interaction of the complexes **1** and **2** with pBR322 plasmid DNA were studied.

Results and discussion

Synthesis and characterization

The platinum(IV) complexes, **1** and **2**, were synthesized in the reaction of Na₂[PtCl₆], R₂eddp·2HCl and LiOH in water, molar ratio 1 : 1 : 2 (Scheme 1).



Scheme 1

Elemental analyses confirmed the molecular formulae. In the IR spectra, strong bands for the ν(COO) vibrations at around 1742 cm⁻¹ confirmed the presence of the ester group (**L1**·2HCl and **L2**·2HCl at 1730 cm⁻¹).^{4,6} Asymmetric CH₂ stretching vibrations from the ester group were found between 2951 and 2979 cm⁻¹ (**L1**·2HCl and **L2**·2HCl between 2940 and 2980 cm⁻¹) while those bending deformations were found at 1340 cm⁻¹ (**L1**·2HCl and **L2**·2HCl: 1330 cm⁻¹) for **1** and **2**, respectively.

^aInstitut für Chemie, Martin-Luther-Universität Halle-Wittenberg, Kurt-Mothes-Straße 2, D-06120, Halle, Germany. E-mail: goran.kaluderovic@chemie.uni-halle.de; Fax: +49 345 552 7028; Tel: +49 345 552 5639

^bBiozentrum, Martin-Luther-Universität Halle-Wittenberg, Weinbergweg 22, D-06120, Halle, Germany

^cAbteilung Chemie (FB3) im Institut für Integrierte Naturwissenschaften, Universität Koblenz-Landau, Universitätsstraße 1, 56070 Koblenz, Germany

[†]Corresponding author permanent address: Department of Chemistry, Institute of Chemistry, Technology and Metallurgy, University of Belgrade, Studentski trg 14, 11000 Belgrade, Serbia; E-mail: goran@chem.bg.ac.rs

Recently it has been shown that NMR spectroscopy can be used advantageously for the characterization of the $[\text{PtCl}_4(\text{R}_2\text{edda-type})]$ complexes.^{4,7,8} Two nitrogen atoms from $\text{R}_2\text{edda-type}$ ligands, as shown by NMR, are coordinated to platinum(IV) center, while ester moieties remain intact. Furthermore, $\kappa^2\text{N,N}'$ coordination mode is supported by X-ray structural analysis for several complexes, in which no interactions between ester oxygen atoms and platinum(IV) were observed.^{7,8} Also here, for complexes **1** and **2** NMR spectroscopic measurements gave proof of their constitution. Hydrogen and carbon atoms from the R groups of both complexes show shifts similar to those observed for their corresponding free ligands in NMR spectra.⁶ All signals are found on expected chemical shifts, as known for analogous compounds.^{4,7,8} The coordination of the N atoms gives rise to the formation of chiral N centers, thus in principle one enantiomeric pair and its diastereoisomer can be formed [*anti*: (*R,R*), (*S,S*) with C_2 symmetry and *syn*: (*R,S*) \equiv (*S,R*) with C_s symmetry] (Fig. 1). Only one set of signals was found indicating the formation of either the enantiomeric pair (*R,R*) and (*S,S*), identical in achiral surrounding in NMR, or its diastereoisomer (*R,S*).

The redox potentials of the electrochemical studies (*vs.* $\text{Ag}|\text{AgCl}$) are -705 mV for **1** and -846 mV for **2**. Reduction occurs more readily in the platinum(IV) complex with the R_2eddp ligand with the shorter alkyl substituent (**1**: Et). It is important to note that the reduction is irreversible, and consequently the reported E_p values are cathodic forward half-wave potentials, and are kinetic, not thermodynamic values.

Quantum chemical calculations

To deal with the question of structural feasibility DFT calculations were conducted for the diastereoisomers (*anti* and *syn*) arising

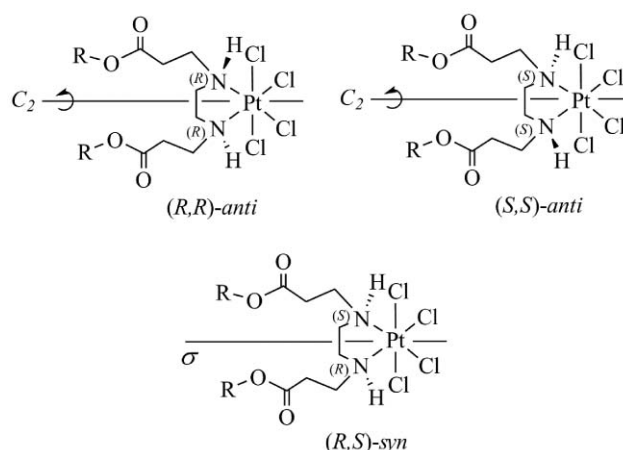


Fig. 1 Possible isomers of $[\text{PtCl}_4(\text{R}_2\text{eddp})]$.

from coordination of R_2eddp to platinum(IV). Each isomer has been calculated in three conformations, namely, with one or two $\text{N-H}\cdots\text{O}$ bonds and without $\text{N-H}\cdots\text{O}$ bonds (abbreviated *anti-nH* and *syn-nH*; $n = 0, 1$ and 2). Optimized structures are presented in Fig. 2.

As can be seen from Fig. 2, the results obtained from DFT calculations in gas phase show that the most stable conformers are with two $\text{N-H}\cdots\text{O}$ bonds in case of *anti* and *syn* isomers by 3.9 – 8.8 kcal mol⁻¹ relative to other conformers. Comparing the energies between *anti-nH* and *syn-nH* ($n = 0, 1$ and 2) with the same number of H bonds it can be concluded that the very small differences (-0.4 up to 0.6 kcal mol⁻¹) are within the error of DFT calculations. For all compounds of the class $[\text{PtCl}_4(\text{R}_2\text{eddp})]$ ($\text{R} = \text{Me}, \text{Et}, n\text{-Pr}, n\text{-Bu}$

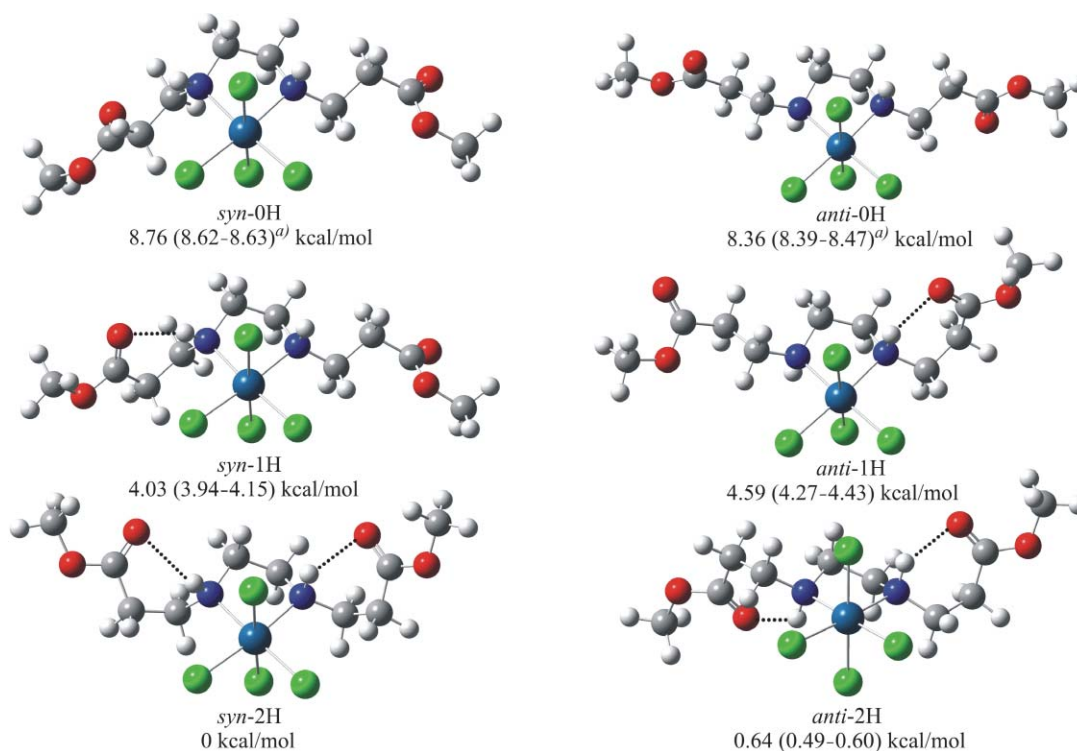


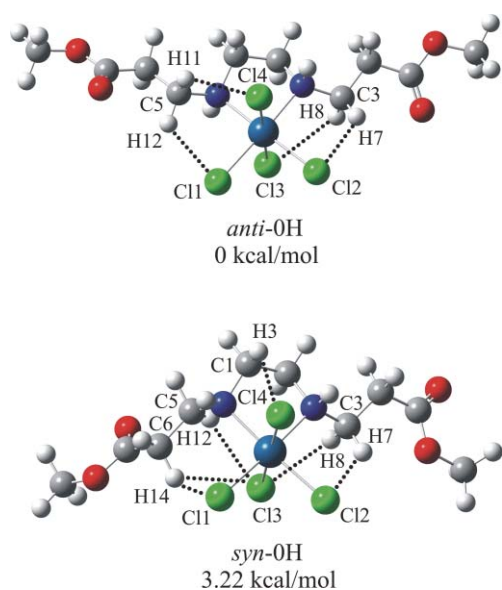
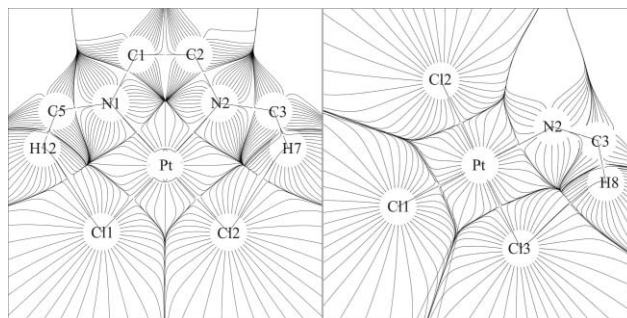
Fig. 2 Equilibrium structures of *syn* and *anti* isomers of $[\text{PtCl}_4(\text{R}_2\text{eddp})]$ ($\text{R} = \text{Me}$) complexes. Energies are relative to the most stable isomer (*syn*-2H). In parentheses the requisite values for $\text{R} = \text{Et}, n\text{-Pr}, n\text{-Bu}$ and $n\text{-Pe}$ are given.

Table 1 C–H⋯Cl interactions (distances in Å, angles in °) in *anti*-0H- and *syn*-0H-[PtCl₄(Me₂eddp)] complexes

		C⋯Cl	C–H	H⋯Cl	C–H⋯Cl
<i>anti</i> -0H	C5–H11⋯Cl4	3.415	1.091	2.772	117.4
	C5–H12⋯Cl1	3.306	1.089	2.602	121.6
	C3–H7⋯Cl2	3.309	1.089	2.597	122.3
	C3–H8⋯Cl3	3.395	1.090	2.750	117.6
<i>syn</i> -0H	C1–H3⋯Cl4	3.306	1.085	2.724	112.9
	C3–H7⋯Cl2	3.358	1.087	2.609	125.3
	C3–H8⋯Cl3	3.307	1.091	2.717	113.5
	C5–H12⋯Cl3	3.230	1.089	2.709	108.8
	C6–H14⋯Cl3	3.483	1.093	2.820	118.9
	C6–H14⋯Cl1	3.380	1.093	2.713	118.9

and *n*-Pe) *syn*-2H is more stable than *anti*-2H by 0.5–0.6 kcal mol⁻¹, thus also within the error of DFT calculations. Furthermore, calculation for platinum(IV) complexes bearing Me₂eddp ester, as the most simple compound, have been performed with the PCM method including solvent effects. Because corresponding platinum(IV) complexes were obtained from aqueous solution, dielectric constant of water was used in calculations. In contrast to gas phase, calculations including solvent effects show that the most stable isomer is *anti*-0H (by 3.2 kcal mol⁻¹ in comparison to *syn*-0H). These results are in full agreement with the experimental findings that only one isomer is formed (NMR) and which proved to be the *anti*-0H isomer (X-ray) in the case of [PtCl₂(R₂edda)] (H₂edda = ethylenediamine-*N,N'*-diacetic acid; R = Me, Et).⁸

The topological analysis of the electronic charge density $\rho(r)$, representing the structure in water phase and those having most stable conformers both in the *anti*-0H and *syn*-0H isomers of [PtCl₄(Me₂eddp)], using the quantum theory of atoms in molecules (QTAIM)⁹ revealed stabilization of the structure with C–H⋯Cl interactions (Fig. 3). For both isomers two representative figures with trajectories of $\rho(r)$ of the molecules including bond paths and bond critical points are shown (Fig. 4) and C–H⋯Cl interactions are summarized in Table 1.

**Fig. 3** The most stable *anti*- and *syn*-[PtCl₄(Me₂eddp)] isomers optimized including solvent effect.**Fig. 4** Gradient paths of the electron density $\rho(r)$ in the calculated structures *anti*-0H- (left, plane C5C3H12H7) and *syn*-0H-[PtCl₄(Me₂eddp)] (right, plane PtCl2Cl3H8) in water phase.

In vitro antitumoral studies

The *in vitro* cytotoxic activity of L1·2HCl, L2·2HCl, **1** and **2** was studied on ten different tumour cell lines, A2780 (ovarian), A431 (cervix), 518A2 (melanoma), A549 (lung), FaDu (head and neck), HT-29, HCT-8, DLD-1, 8505C, SW480 (colon) by the SRB colorimetric assay method. The IC₅₀ values of each compound on these cell lines are given in Table 2. An increase in cytotoxic potential can be observed from **1** to **2**.

Treatment with L1·2HCl and L2·2HCl did not show any toxicity in the dose range used (1–125 μM), whereas **1** and **2** showed much better activity in all cell lines in comparison with their parent ligand precursors (L1·2HCl and L2·2HCl). The activity of platinum(IV) complexes was observed to be highest in A2780 and A431 cell lines. Complex **2** expresses high activity against ovarian, melanoma and lung cell lines A2780, 518A2 and A549, respectively. In comparison to cisplatin complexes **1** and **2** are less active on all investigated cell lines. Mediated antiproliferative activity of **1** and **2** has been shown against head and neck and colon tumour cell lines. As it was observed for similar compounds with the ester arms, each shorter by one CH₂ group in the aminocarboxylato substituent, (R = Me, Et, *n*-Pr),⁸ it was found that the activity of the complexes depends upon the number of carbon atoms on the ester chain, from which it could be inferred that the longer the chain the greater the activity. Comparing results between these two types of compounds, [PtCl₄(R₂edda)] and [PtCl₄(R₂eddp)] (R = Me, Et, *n*-Pr), on the same cell lines can be concluded that tetrachloroplatinum(IV) complexes bearing R₂eddp ester ligands possesses greater activity (*i.e.* IC₅₀ [μM] of [PtCl₄(R₂edda)] against A549 *ca.* 60–86, 518A2 *ca.* 60–74, for DLD-1 IC₅₀ not reached). Because platinum(IV) complexes **1** and

Table 2 IC₅₀ values [μM] of L1·2HCl and L2·2HCl, corresponding platinum(IV) complexes, **1** and **2**, and cisplatin

Compound	L1·2HCl, L2·2HCl	1	2	Cisplatin
A2780	>125	13.78 ± 0.37	8.60 ± 0.23	0.5
A431		32.30 ± 0.21	19.62 ± 0.48	0.6
518A2		43.95 ± 2.57	17.99 ± 2.38	1.5
A549		35.06 ± 0.27	20.81 ± 0.47	1.5
FaDu		48.20 ± 0.47	31.24 ± 0.45	1.2
HT-29		38.23 ± 0.90	32.80 ± 0.35	0.6
HCT-8		36.24 ± 0.31	31.78 ± 0.55	1.5
SW480		35.48 ± 2.54	26.24 ± 4.61	3.2
8505C		48.04 ± 4.76	25.23 ± 1.73	5
DLD-1		89.26 ± 1.17	49.03 ± 4.02	5

Appendix 3

Reproduced from Ref. G.N. Kaluđerović, H. Kommera, S. Schwieger, A. Paethanom, M. Kunze, H. Schmidt, R. Paschke, D. Steinborn, Dalton Trans. 2009, 10720 with permission from The Royal Society of Chemistry.

2 were found to be most cytotoxic towards ovarian A2780 and cervical A431 cancer cell lines, in comparison to other investigated from this study, these cell lines were chosen for further studies.

To investigate if differences in platinum accumulation in A431 and A2780 cells contribute to the diverse cellular response of **1** and **2**, the intracellular platinum uptake of 10 μM concentrations was determined. Treatment of A2780 cells with **1** and **2** for 24 h resulted in similar platinum uptake (**1**: 189 ± 14 ; **2**: 198 ± 14 ppm) and the same was observed for A431 cell line (**1**: 71 ± 12 ; **2**: 76 ± 7 ppm), from which it can be inferred that the greater accumulation of the compound the better the activity. *In vitro* antitumoral activity for these two cell lines can be correlated to the platinum uptake of the investigated complexes.

To test whether **1** and **2** induced cell death was mediated by apoptosis, floating cells from A2780 and A431 after 24 h treatment with the IC_{50} concentrations were collected and analysed by the DNA laddering technique. In both cell models with both compounds occurrence of typical DNA ladders was observed. Furthermore, programmed cell death was confirmed by trypan blue exclusion test, in which floating cells showed the ability to exclude the blue dye indicating that **1** and **2** causes cell death by the induction of apoptosis (Fig. 5).

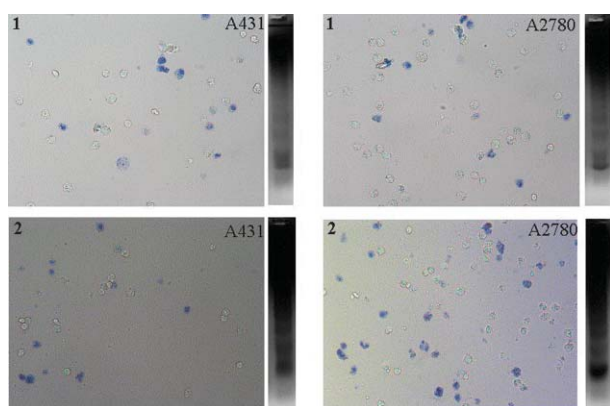


Fig. 5 Dye exclusion test and DNA laddering.

The comparative analysis was performed on A2780 and A431 cell lines with equitoxic concentrations of cisplatin, **1** and **2** (see Table 2) at different times (Fig. 6). It was observed that the complexes **1**, **2** and cisplatin showed similar activity until 8 h treatment on the cervical cancer cell line (A431) and cisplatin showed

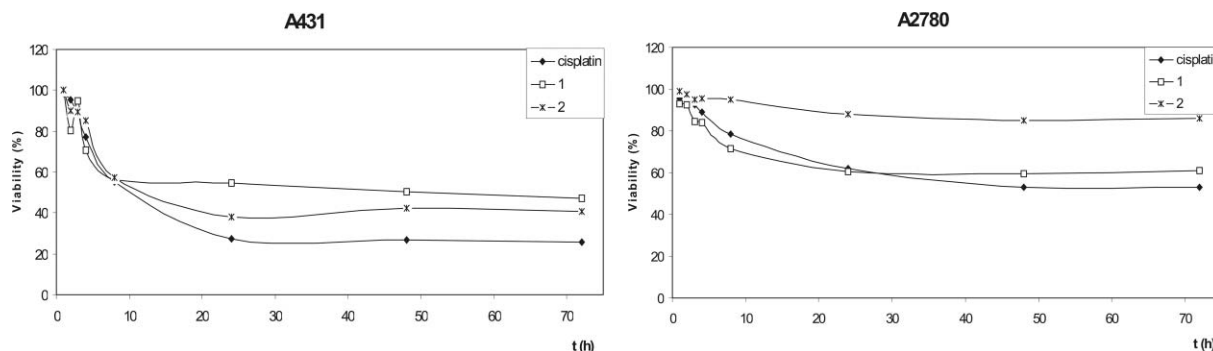


Fig. 6 Kinetics of tumour cell growth inhibition of A431 or A2780 cells treated with equitoxic concentrations of **1**, **2** and cisplatin for various time periods.

the most pronounced activity after that period. Interestingly in ovarian cancer cell line complex **1** was marginally more active in the first 24 h of treatment than cisplatin. Furthermore, the complex **1** is acting faster than **2** on A2780 cell line and the opposite was found in the case of A431 cell line. In both cell lines it was observed that the activity of all compounds was much higher in the final 24 h period of treatment during the assay (from 72–96 h).

Platinum(IV) complexes as drugs and pro-drugs

The ability of binding metals from complexes to DNA is generally monitored by agarose gel electrophoresis and the pBR322 plasmid DNA is usually involved.¹⁰ The degree to which the synthesized complexes could produce changes in the electrophoretic mobility of the open circular form (I) and the supercoiled form (II) of pBR322 plasmid could function as DNA-cleavage agents. Fig. 7 shows the electrophoregram of the action of complex **2**. Lane 0 was used as blank. Two clear bands were observed for the control in which the metal complex was absent, see lane 1. The amount of form II of pBR322 DNA gradually increases from $r_i = 0.01$ to $r_i = 0.75$ (lanes 2–6). At high r_i (1.00), interaction of complex **2** with DNA seems to be so extensive that both the supercoiled and the open circular forms of pBR322 disappear (lanes 7). This indicates that platinum(IV) complexes may act as drugs. The results show that both complexes can interact with the pBR322 plasmid DNA without addition of external agents.

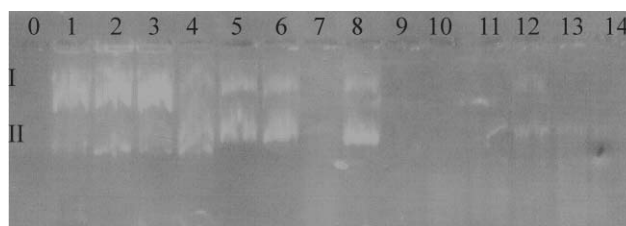


Fig. 7 Agarose gel (1.5%) electrophoresis showing the DNA cleavage induced in the open (I) and supercoiled forms (II) of pBR322 after incubation for 24 h with various concentrations of complex **2** in the absence (lanes 2–7) and presence of 1.8 mM of ascorbate (lanes 9–14). Lane 0, blank; lane 1, control unmodified pBR322 DNA; lane 8, control unmodified pBR322 DNA incubated with 1.8 mM of ascorbate; lanes 2–7 and 9–14, pBR322 incubated with increasing molar ratios of **2** per nucleotide, r_i of 0.01, 0.10, 0.25, 0.50, 0.75 and 1.00, respectively.

It is known that platinum(IV) complexes may be activated *in vivo* by reduction to corresponding platinum(II) species.¹¹ Since the primary reducing agent of transition metal complexes within the cell seems to be mainly ascorbate¹¹ (vitamin C, physiological concentration ~ 1.8 mM) the presence of this biomolecule in interaction between plasmid pBR322 DNA and complexes **1** and **2** was investigated. The electrophoretic mobility pattern of native pBR322 DNA incubated with 1.8 mM ascorbate is shown in Fig. 7, see lane 8. The same system in the presence of **2** at increasing r_i values (0.01–1.00; lane 9–14) was also investigated. It may be seen that at r_i from 0.01 DNA is not detected at all (lanes 9–14). Complex **1** shows the similar behaviour. Indicating that those results are presumably the consequence of the reaction of DNA with activated platinum(II) species, formed upon reduction of platinum(IV) by ascorbate. Altogether these data support the hypothesis that platinum(IV) complexes may act as pro-drugs, which are transformed *in vivo* into reactive platinum(II) species.

Conclusions

Synthesis and characterization of two platinum(IV) complexes, **1** and **2**, were described here. The IR, ¹H, and ¹³C NMR spectroscopic data support chelation of these ligands *via* two nitrogen donor atoms (κ^2N,N' coordination). The ligand precursors (**L1**·2HCl, **L2**·2HCl) did not show toxicity in the dose range used ($IC_{50} > 125 \mu\text{M}$), and complexes **1** and **2** showed moderate anticancer activity compared to cisplatin. Remarkable inhibition properties for platinum(IV) complex **2**, [PtCl₄(Pr₂eddp)] were observed, *via* apoptotic mode of cell death, up to twenty times higher activity than the parental ligand dihydrochloride. *In vitro* antitumoral activity for A2780 and A431 cell lines can be correlated to the platinum uptake of the investigated complexes. Interaction studies between **2** and pBR322 DNA clearly showed that both, the platinum(IV) complex and the corresponding reduced species may act as drugs.

Experimental

Material and methods

The elemental analyses (C, H, N) were carried out on a CHNS-93 (LECO) elemental analyzer. Infrared spectra were recorded in KBr pellets on a Mattson Galaxy 5000 FT-IR spectrometer, covering the region 4000–300 cm⁻¹. The ¹H and ¹³C NMR spectra were recorded on a Varian Unity 400 NMR spectrometer in acetone-*d*₆ ([PtCl₄(R₂eddp)]·H₂O) at 27 °C. Diethyl (Et₂eddp·2HCl; **L1**·2HCl) and dipropyl-ethylenediamine-*N,N'*-di-3-propanoate dihydrochloride (Pr₂eddp·2HCl; **L2**·2HCl) were synthesized by the procedures reported in the literature.⁶

General procedure for the preparation of [PtCl₄(R₂eddp)] complexes **1** and **2**

Na₂[PtCl₆] (0.100 g, 0.22 mmol) was dissolved in 10 mL water and the appropriate ligand (**L1**·2HCl: 0.071 g; **L2**·2HCl: 0.077 g, each 0.22 mmol) was added. The mixture was stirred for 5 h and during this period 3.92 mL LiOH ($c = 0.107 \text{ mM}$, 0.44 mmol) were introduced. The complexes were yellow precipitates which were filtered off, washed with water (2 × 5 mL) and dried on air.

1. Yield: 94 mg, 75%. Anal. calcd for [PtCl₄(Et₂eddp)], C₁₂H₂₄Cl₄N₂O₄Pt: C 24.13, H 4.05, N 4.69. Found: C 23.87, H 4.29, N 4.55%. ¹H NMR: δ 1.23 (t, 6 H, CH₃), 2.94 and 3.01 (m, 4 H, NHCH₂CH₂NH), 3.16 (m, 4 H, NHCH₂CH₂CO₂), 3.37 (m, 4 H, NHCH₂CH₂CO₂), 4.14 (qu, 4 H, CO₂CH₂). ¹³C NMR: δ 14.6 (CH₃), 31.3 (NHCH₂CH₂NH), 49.5 (NHCH₂CH₂CO₂), 55.1 (NHCH₂CH₂CO₂), 61.7 (CO₂CH₂), 170.1 (CO₂). IR: ν 3193 (s), 3141 (s), 2979 (m), 2951 (m), 1741 (vs), 1618 (w), 1471 (w), 1429 (w), 1373 (m), 1340 (m), 1278 (w), 1228 (s), 1186 (m), 1078 (m), 1047 (w), 1010 (w), 970 (w), 899 (w), 858 (w), 729 (w), 582 (w), 345 (s) cm⁻¹.

2. Yield: 103 mg, 76%. Anal. calcd for [PtCl₄(*n*-Pr₂eddp)], C₁₄H₂₈Cl₄N₂O₄Pt: C 26.89, H 4.51, N 4.48. Found: C 27.01, H 4.72, N 4.49%. ¹H NMR: δ 0.91 (t, 6 H, CH₃), 1.64 (se, 4 H, CH₂CH₃), 2.95 and 3.02 (m, 4 H, NHCH₂CH₂NH), 3.19 (m, 4 H, NHCH₂CH₂CO), 3.39 (m, 4 H, NHCH₂CH₂CO), 4.04 (m, 4 H, CO₂CH₂). ¹³C NMR: δ 10.6 (CH₃), 22.6 (CH₂CH₃), 31.3 (NHCH₂CH₂NH), 49.4 (NHCH₂CH₂CO₂), 55.0 (NHCH₂CH₂CO₂), 67.1 (CO₂CH₂), 172.2 (CO₂). IR: ν 3191 (s), 3141 (s), 2952 (m), 2879 (m), 1743 (vs), 1654 (w), 1454 (w), 1417 (w), 1398 (m), 1361 (m), 1340 (m), 1279 (w), 1226 (s), 1184 (m), 1080 (m), 1047 (w), 981 (w), 968 (w), 852 (w), 730 (w), 669 (w), 582 (w), 513 (w), 341 (s) cm⁻¹.

Electrochemistry

An Autolab Typ III potentiostat/galvanostat instrument was used to carry out cyclic voltammetry at a scan rate of 50 mV s⁻¹ using a Pt disk working electrode (d 2.0 mm), a Pt wire (0.8 × 6.0 mm) counter electrode and a silver|silver chloride double junction reference electrode (filled with acetonitrile/0.1 M [Bu₄N]BF₄ electrolyte). The reference electrode was calibrated against [FeCp₂] dissolved in acetonitrile/0.1 M [Bu₄N]BF₄ electrolyte. The desired complex was dissolved in acetonitrile/0.1 M [Bu₄N]BF₄ solution and prior to measurement was purged free of oxygen by passing a stream of argon through the solution (for 5 min).

Theoretical calculations

All DFT calculations were performed by employing the Gaussian 03 program package¹³ using the MPW1PW91 functional.¹² The 6-31+G** basis set was used for all atoms, with the exception of a Stuttgart basis set for the Pt atom.¹⁴ This included the use of an effective core potential with consideration of relativistic effects relevant to platinum. The appropriateness of the chosen functional and basis set for platinum complexes has been stated elsewhere.¹⁵ All systems have been optimized without symmetry restrictions. The resulting geometries were characterized as equilibrium structures by the analysis of the force constants of normal vibrations. Furthermore, full geometry optimization with Polarizable Continuum Model (PCM) as implemented in Gaussian 03 was used for the prediction of solvent influence (water).^{12,16} The QTAIM analysis as well as the visualization were performed using the program package AIMPAC as provided by Bader *et al.*¹⁷ Supplementary data associated with quantum chemical calculations can be obtained from the authors upon request.

In vitro studies

The compounds **L1**·2HCl, **L2**·2HCl, **1** and **2** were dissolved in *N,N*-dimethyl formamide (DMF, Sigma Aldrich) to a concentration of 20 mM and diluted by nutrient medium to various working concentrations. Nutrient medium was RPMI-1640 (PAA Laboratories) supplemented with 10% fetal bovine serum (Biochrom AG) and penicillin/streptomycin (PAA Laboratories).

Cell lines and culture conditions. The cell lines 518A2, 8505C, A2780, A431, HCT-8, HT-29, DLD-1, SW480, FaDu, A549 were included in this study. All these cell lines were kindly provided by Dr Thomas Mueller, Department of Hematology/Oncology, Martin Luther University of Halle-Wittenberg, Halle (Saale), Germany. Cultures were maintained as monolayers in RPMI 1640 (PAA Laboratories, Pasching, Germany) supplemented with 10% heat inactivated fetal bovine serum (Biochrom AG, Berlin, Germany) and penicillin/streptomycin (PAA Laboratories) at 37 °C in a humidified atmosphere with 5% CO₂.

Cytotoxicity assay. The cytotoxic activities of the platinum compounds were evaluated using the sulforhodamine-B (SRB) (Sigma Aldrich) microculture colorimetric assay.¹⁸ In short, exponentially growing cells were seeded into 96 well plates on day 0 at the appropriate cell densities to prevent confluence of the cells during the period of experiment. After 24 h, the cells were treated with serial dilutions of the platinum compounds (0–125 μM) for 96 h. The final concentration of DMF solvent never exceeded 0.5%, which was non-toxic to the cells. The percentages of surviving cells relative to untreated controls were determined 96 h after the beginning of drug exposure. After 96 h treatment, the supernatant medium from the 96 well plates was thrown away and the cells were fixed with 10% TCA. For a thorough fixation plates are now allowed to stand at 4 °C. After fixation the cells are washed in a strip washer. The washing is done four times with water using alternate dispensing and aspiration procedures. The plates are then dyed with 100 μL of 0.4% SRB for about 45 min. After dyeing the plates are again washed to remove the dye with 1% acetic acid and allowed to air dry overnight. 100 μL of 10 mM Tris base solution was added to each well of the plate and absorbance was measured at 570 nm using a 96 well plate reader (Tecan Spectra, Crailsheim, Germany). The IC₅₀ and IC₉₀ values, defined as the concentrations of the compound at which 50% and 90% cell inhibition is observed, was estimated from the semi-logarithmic dose-response curves.

Platinum drug accumulation in cells. The platinum uptake studies were performed with A2780 and A431 cell lines. The cells were seeded in 25 cm² flasks and allowed to grow for 24 h. After 24 h the exponentially growing cells were treated with 10 μM concentrations of each of **1** and **2** for 24 h. The cells were then washed with PBS, trypsinated and then dried. Prior to measurement, the cells were lyophilized and then submitted to a temperature ramp ranging from 100 to 2550 °C, atomized, and analyzed at $\lambda = 265.9$ nm. The platinum concentrations were measured by flame-less atomic absorption spectroscopy using an AAS-5 EA including the semiautomatic solid sampling dispensing system SSA 51 (Analytic Jena AG, Germany). Cellular platinum levels were expressed as parts per million (ppm) platinum.

Apoptosis tests—Trypan blue exclusion test. Apoptotic cell death was analysed by trypan blue dye (Sigma Aldrich, Germany) on A431 and A2780 cell lines. The cell culture flasks with 70 to 80% confluence were treated with IC₉₀ doses of **1** and **2** for 24 h. The supernatant medium with floating cells was collected after treatment and centrifuged to collect the dead and apoptotic cells. The cell pellet was re-suspended in serum free media. Equal amounts of cell suspension and trypan blue were mixed and this was analysed under a microscope. The cells, which were viable, excluded the dye and were colourless and the ones whose cell membrane was destroyed were turning into blue. If the proportion of colourless cells were more compared to the ones that were coloured then the death can be characterised as apoptotic.

DNA fragmentation assay. Determination of apoptotic cell death was performed by DNA gel electrophoresis. Briefly, A431 and A2780 were treated with respective IC₉₀ doses of **1** and **2** for 24 h. Floating cells induced by drug exposure were collected, washed with PBS and lysed with lysis buffer (100 mM Tris-HCl Ph 8.0; 20 mM EDTA; 0.8% SDS; all from Sigma Aldrich). Then, cells were treated with RNase A at 37 °C for 2 h and proteinase K at 50 °C (both from Roche Diagnostics chemical company, Mannheim, Germany). DNA laddering was observed by running the samples on 2% agarose gel followed by ethidium bromide (Sigma Aldrich) staining.

Kinetic studies. Activity of the platinum compounds **1** and **2** along with cisplatin on A431 and A2780 was analysed by treating them for 1, 2, 3, 4, 8, 24, 48 and 72 h at a equitoxic concentrations of each compound, respectively. The cytotoxic activity was performed exactly in accordance with the SRB microculture colorimetric assay except that after each scheduled time point the cells were washed with phosphate buffered saline (PBS) and further grown in drug free media for the remaining time to complete 96 h. After working up the 96 well plates according to the published SRB assay protocol, absorbance was measured at 570 nm in a 96 well plate reader. The cell viability was estimated at different times of treatment using a semi-logarithmic plot.

Interaction of platinum(IV) complexes with plasmid pBR322 DNA. Plasmid pBR322 DNA (4363 base pairs in length, Sigma) was incubated for 24 h at several variable r_i (input molar ratio of platinum(IV) to nucleotide) ranging r_i from 0.01 to 1.00. Electrophoretic analysis used ascorbic acid (Sigma) dissolved in 10 mM NaClO₄, pH 6.5 as 1 mg mL⁻¹ stock solution. 20 mM stock solutions of complexes **1** and **2** as prepared in *in vitro* studies were used for the different working concentrations dissolved in 10 mM NaClO₄, pH 6.5. Fractions of the plasmid pBR322 DNA (25 μg mL⁻¹) were incubated with the platinum(IV) complexes at 37 °C in 10 mM NaClO₄, pH 6.5 at r_i of 0.01, 0.10, 0.25, 0.50, 0.75 and 1.00 in the absence or presence of 1.8 mM of ascorbic acid. Equal volumes (50 μL) of platinum(IV) complexes and DNA solution were subjected to 1.5% agarose gel electrophoresis for 16 h at 25 V in TAE buffer (40 mM Tris-acetate, 2 mM edta, pH 8.0) as previously reported.¹⁹

Acknowledgements

G. N. K. gratefully acknowledges support from the Alexander von Humboldt Foundation.

Appendix 3

Reproduced from Ref. G.N. Kaluđerović, H. Kommera, S. Schwieger, A. Paethanom, M. Kunze, H. Schmidt, R. Paschke, D. Steinborn, Dalton Trans. 2009, 10720 with permission from The Royal Society of Chemistry.

References

- 1 L. Kelland, *Nat. Rev. Cancer*, 2007, **7**, 573–584.
- 2 See for example: (a) M. A. Jakupec, M. Galanski and B. K. Keppler, *Reviews of Physiology Biochemistry and Pharmacology*, 2003, **146**, 1–53; (b) D. Wang and S. J. Lippard, *Nat. Rev. Drug Discovery*, 2005, **4**, 307–320.
- 3 (a) M. Galanski, V. B. Arion, M. A. Jakupec and B. K. Keppler, *Curr. Pharm. Des.*, 2003, **9**, 2078–2089; (b) M. D. Hall and T. W. Hambley, *Coord. Chem. Rev.*, 2002, **232**, 49–67.
- 4 G. N. Kaluđerović, V. M. Đinović, Z. D. Juranić, T. P. Stanojković and T. J. Sabo, *J. Inorg. Biochem.*, 2005, **99**, 488–496.
- 5 (a) G. N. Kaluđerović, D. Miljković, M. Momilović, V. M. Đinović, M. Mostarica-Stojković, T. J. Sabo and V. Trajković, *Int. J. Cancer*, 2005, **116**, 479–486; (b) S. Mijatović, D. Maksimović-Ivanić, J. Radovica, D. Miljković, G. N. Kaluđerović, T. J. Sabo and V. Trajković, *Cell. Mol. Life Sci.*, 2005, **62**, 1275–1282.
- 6 G. N. Kaluđerović and T. J. Sabo, *Polyhedron*, 2002, **21**, 2277–2282.
- 7 B. B. Krajinović, G. N. Kaluđerović, D. Steinborn, H. Schmidt, Ch. Wagner, Ž. Žizak, Z. D. Juranić, S. R. Trifunović and T. J. Sabo, *J. Inorg. Biochem.*, 2008, **102**, 892.
- 8 G. N. Kaluđerović, H. Schmidt, S. Schwieger, Ch. Wagner, R. Paschke, A. Dietrich, T. Müller and D. Steinborn, *Inorg. Chim. Acta*, 2008, **361**, 1395.
- 9 R. F. W. Bader, in *Atoms in Molecules: A Quantum Theory*, Clarendon Press, Oxford, UK, 1990.
- 10 (a) G. B. Onoa and V. Moreno, *Int. J. Pharm.*, 2002, **245**, 55–65; (b) H. M. Ushay, T. D. Tullius and S. J. Lippard, *Biochemistry*, 1981, **20**, 3744–3748.
- 11 (a) H. Choy, C. Park and M. Yao, *Clin. Cancer Res.*, 2008, **14**, 1633–1638.
- 12 M. J. Frisch, G. W. Trucks, H. B. Schlegel, G. E. Scuseria, M. A. Robb, J. R. Cheeseman, J. A. Montgomery Jr., T. Vreven, K. N. Kudin, J. C. Burant, J. M. Millam, S. S. Iyengar, J. Tomasi, V. Barone, B. Mennucci, M. Cossi, G. Scalmani, N. Rega, G. A. Petersson, H. Nakatsuji, M. Hada, M. Ehara, K. Toyota, R. Fukuda, J. Hasegawa, M. Ishida, T. Nakajima, Y. Honda, O. Kitao, H. Nakai, M. Klene, X. Li, J. E. Knox, H. P. Hratchian, J. B. Cross, V. Bakken, C. Adamo, J. Jaramillo, R. Gomperts, R. E. Stratmann, O. Yazyev, A. J. Austin, R. Cammi, C. Pomelli, J. W. Ochterski, P. Y. Ayala, K. Morokuma, G. A. Voth, P. Salvador, J. J. Dannenberg, V. G. Zakrzewski, S. Dapprich, A. D. Daniels, M. C. Strain, O. Farkas, D. K. Malick, A. D. Rabuck, K. Raghavachari, J. B. Foresman, J. V. Ortiz, Q. Cui, A. G. Baboul, S. Clifford, J. Cioslowski, B. B. Stefanov, G. Liu, A. Liashenko, P. Piskorz, I. Komaromi, R. L. Martin, D. J. Fox, T. Keith, M. A. Al-Laham, C. Y. Peng, A. Nanayakkara, M. Challacombe, P. M. W. Gill, B. Johnson, W. Chen, M. W. Wong, C. Gonzalez, *GAUSSIAN 03, Revision C.02*, Gaussian, J. A. Pople, Inc., Wallingford, CT, 2004.
- 13 C. Adamo and V. Barone, *J. Chem. Phys.*, 1998, **108**, 664–675.
- 14 (a) A. Bergner, M. Dolg, W. Kuechle, H. Stoll and H. Preuss, *Mol. Phys.*, 1993, **80**, 1431–1441; (b) M. Kaupp, P. v. R. Schleyer, H. Stoll and H. Preuss, *J. Chem. Phys.*, 1991, **94**, 1360–1366; (c) M. Dolg, H. Stoll, H. Preuss and R. M. Pitzer, *J. Phys. Chem.*, 1993, **97**, 5852–5859.
- 15 (a) R. Wysokiński and D. Michalska, *J. Comput. Chem.*, 2001, **22**, 901–912; (b) S. Schwieger, C. Wagner, C. Bruhn, H. Schmidt and D. Steinborn, *Z. Anorg. Allg. Chem.*, 2005, **631**, 2696–2704.
- 16 M. Cossi, G. Scalmani, N. Rega and V. Barone, *J. Chem. Phys.*, 2002, **117**, 43–54.
- 17 See: <http://www.chemistry.mcmaster.ca/aimpac/>. 2000. The program was slightly changed in order to allow the appropriate number of basis functions.
- 18 P. Skehan, R. Storeng, D. Scudiero, A. Monks, J. McMahon, D. Vistica, J. T. Warren, H. Bokesch, S. Kenney and M. R. Boyd, *Journal of the National Cancer Institute*, 1990, **82**, 1107–1112.
- 19 S. R. Grgurić-Šipka, R. A. Vilaplana, J. M. Pérez, M. A. Fuertes, C. Alonso, Y. Alvarez, T. J. Sabo and F. González-Vilchez, *J. Inorg. Biochem.*, 2003, **97**, 215–220.

Reproduced from Ref. G.N. Kaluđerović, S.A. Mijatović, B.B. Zmejkovski, M.Z. Bulatović, S. Gómez-Ruiz, M.K. Mojić, D. Steinborn, D. M. Miljković, H. Schmidt, S.D. Stošić-Grujičić, T.J. Sabo, D.D. Maksimović-Ivanić, *Metallomics* 2012, 4, 979 with permission from The Royal Society of Chemistry.

Cite this: *Metallomics*, 2012, 4, 979–987

www.rsc.org/metallomics

PAPER

Platinum(II/IV) complexes containing ethylenediamine-*N,N'*-di-2/3-propionate ester ligands induced caspase-dependent apoptosis in cisplatin-resistant colon cancer cells†

Goran N. Kaluđerović,^{*a} Sanja A. Mijatović,^b Bojana B. Zmejkovski,^{ac}
Mirna Z. Bulatović,^b Santiago Gómez-Ruiz,^d Marija K. Mojić,^b Dirk Steinborn,^a
Djordje M. Miljković,^b Harry Schmidt,^a Stanislava D. Stošić-Grujičić,^b
Tibor J. Sabo^e and Danijela D. Maksimović-Ivanić^{*b}

Received 21st March 2012, Accepted 2nd July 2012

DOI: 10.1039/c2mt20058a

Several new R₂eddp (R = *i*-Pr, *i*-Bu; eddp = ethylenediamine-*N,N'*-di-3-propionate) esters and corresponding platinum(II) and platinum(IV) complexes of the general formula [PtCl_n(R₂edda-type)] (*n* = 2, 4) were synthesized and characterized by spectroscopic methods (IR, ¹H and ¹³C NMR) and elemental analysis. The crystal structure of platinum(IV) complex [PtCl₄{(*c*-Pe)₂eddp}] (**3a**) was resolved and is given herein. Ligand precursors, platinum(II), and platinum(IV) complexes were tested against eight tumor cell lines (CT26CL25, HTC116, SW620, PC3, LNCaP, U251, A375, and B16). Selectivity in the action of those compounds between tumor and two normal primary cells (fibroblasts and keratinocytes) are discussed. A structure–activity relationship of these compounds is discussed. Furthermore, cell cycle distribution, induction of necrosis, apoptosis, autophagy, anoikis, caspase activation, ROS, and RNS are presented on the cisplatin-resistant colon carcinoma HCT116 cell line.

Introduction

The discovery of cisplatin led scientists to synthesize many platinum-based drugs that could potentially be less toxic to healthy tissue and overcome the resistance of some tumors to this drug.^{1–3} Besides cisplatin, carboplatin and oxaliplatin are in worldwide clinical use.⁴ The success of metallodrugs is closely linked with the proper choice of ligands, as they play a crucial role in modifying reactivity and lipophilicity, in stabilizing specific oxidation states, and in imparting substitution inertness.⁵

Platinum(II) and platinum(IV) complexes containing ethylenediamine-*N,N'*-diacetic acid (H₂edda) and derivatives (e.g. ethylenediamine-*N,N'*-di-3-propionic acid, H₂eddp; propylenediamine-*N,N'*-diacetic acid, H₂pdda) have been considered to be variants of cisplatin and orally active satraplatin, respectively.^{6–8} Complexes of platinum(II) and platinum(IV) containing edda-type ligands coordinated in κ²*N,N'* and κ²*N,N'*, κ²*O,O'* mode, respectively, expressed lower cytotoxic activity than cisplatin or satraplatin.^{6–11} On the other hand, complexes containing diesters of eddp were found to be very active.¹²

The most efficient complexes were shown to be tetrachloroplatinum(IV) complexes with *n*-Bu and *n*-Pe esters, [PtCl₄{(*n*-Bu)₂eddp}] and [PtCl₄{(*n*-Pe)₂eddp}] (Fig. 1C). Their efficacy was confirmed against human adenocarcinoma HeLa cells (approx. five times less active than cisplatin) and human myelogenous leukemia K562 cells (comparable with cisplatin). Proposed mechanism of action was induction of apoptotic cell death.¹³ Noteworthy *in vitro* activity caused by these two platinum(IV) complexes was demonstrated on L929 fibrosarcoma and U251 astrocytoma tumor cells.^{14,15} The compounds are found to induce considerably faster tumor cell death process than cisplatin.¹⁴ The growing family of such compounds, obtained by structural variations of the aminocarboxylato arms and alkyl groups of the ester moiety (normal and branched chains), yielded a variety of R₂edda-type platinum complexes (Fig. 1A–D).^{11,16–22} Furthermore, a more

^a Institut für Chemie, Martin-Luther-Universität Halle-Wittenberg, Kurt-Mothes-Straße 2, 06120 Halle, Germany.
E-mail: goran.kaluderovic@chemie.uni-halle.de;
Tel: +49 345 5525678

^b Institute for Biological Research “Sinisa Stankovic”, University of Belgrade, Bulevar despota Stefana 142, 11060 Belgrade, Serbia. E-mail: nelamax@yahoo.com;
Tel: +381 11 207 8390

^c Department of Chemistry, Institute of Chemistry, Technology and Metallurgy, University of Belgrade, Studentski Trg 12-16, 11000 Belgrade, Serbia

^d Departamento de Química Inorgánica y Analítica, E.S.C.E.T., Universidad Rey Juan Carlos, 28933 Móstoles, Madrid, Spain

^e Faculty of Chemistry, University of Belgrade, Studentski trg 12-16, 11000 Belgrade, Serbia

† Electronic supplementary information (ESI) available. CCDC 855121. For ESI and crystallographic data in CIF or other electronic format See DOI: 10.1039/c2mt20058a

Appendix 4

Reproduced from Ref. G.N. Kaluđerović, S.A. Mijatović, B.B. Zmejkovski, M.Z. Bulatović, S. Gómez-Ruiz, M.K. Mojić, D. Steinborn, D. M. Mijlković, H. Schmidt, S.D. Stošić-Grujičić, T.J. Sabo, D.D. Maksimović-Ivanić, *Metallomics* 2012, 4, 979 with permission from The Royal Society of Chemistry.

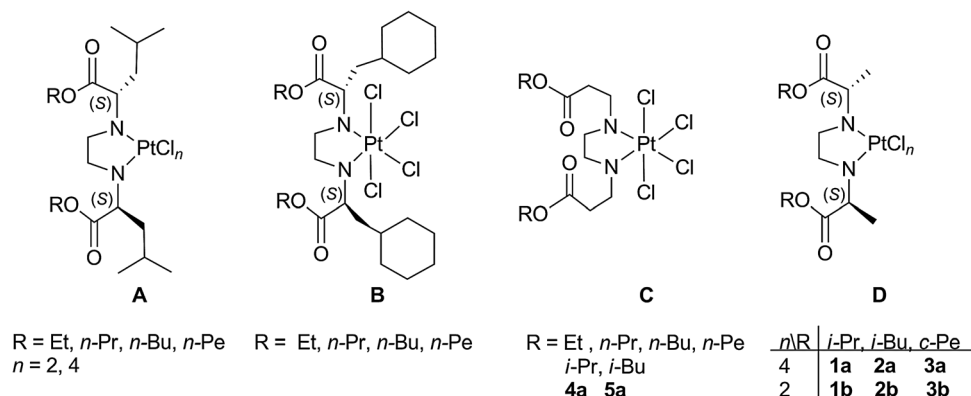


Fig. 1 Some platinum(II) and platinum(IV) complexes containing R₂edda-type ligands. Numbered compounds are used in this study.

selective effect toward malignant in comparison to normal cells was obtained, but the drugs were less active than cisplatin, *e.g.* [PtCl₄{(*i*-Pr)₂eddip}] (Fig. 1D).¹⁸ [PtCl₂{(*n*-Pr)₂edd}] [H₂edd] = (*S,S*)-ethylenediamine-*N,N'*-di-2-(4-methyl)pentanoic acid] complex (Fig. 1A) expressed remarkably higher activity than cisplatin (*ca.* 48 times) against primary chronic lymphocytic leukemia cells induced by apoptotic mode of cell death.¹⁹

Herein, as continuation of our work, the synthesis and characterization of several new R₂edda-type ligand precursors ([H₂(*i*-Pr)₂eddp]Cl₂ and [H₂(*i*-Bu)₂eddp]Cl₂, **L4**·2HCl and **L5**·2HCl, respectively), platinum(II), and platinum(IV) complexes are reported (Fig. 1A: see **4a**, **5a**; Fig. 1B: see **3a** and **3b**).

Additionally, *in vitro* investigations against different tumor cell lines and primary normal cells and their mechanism of action against cisplatin-resistant HCT116 cell line were studied.

Experimental

Synthesis of the ligand precursors, L1·2HCl–L5·2HCl, and platinum(IV) and platinum(II) complexes, 1a–5a and 1b–3b

[H₄edda-type]Cl₂ esters, **L1**·2HCl–**L3**·2HCl, and the corresponding platinum(II) and platinum(IV) complexes, **1a–2b**, were prepared by methods described in the literature.^{18,20} Novel compounds **L4**·2HCl, **L5**·2HCl and platinum(II) and platinum(IV) complexes (**3b** and **3a–5a**, respectively) were synthesized by the procedures given in ESI.†

Reagents and cells

Fetal calf serum (FCS), RPMI-1640, phosphate-buffered saline (PBS), dimethyl sulfoxide (DMSO), 3-(4,5-dimethylthiazol-2-yl)-2,5-diphenyltetrazolium bromide (MTT), collagenase IV from *Clostridium histolyticum*, DNase, dihydrorhodamine 123 (DHR) and propidium iodide (PI) were obtained from Sigma (St. Louis, MO). Annexin V-FITC (AnnV) and ethidium bromide (EtBr) were from Biotium (Hayward, CA). Acridine orange (AO) was provided by Labo-Moderna (Paris, France). The U251 glioblastoma cell line was a kind gift from Dr Pedro Tranque (Universidad de Castilla-La Mancha, Albacete, Spain). The B16 murine melanoma was a kind gift from Dr Sinisa Radulovic (Institute for Oncology and Radiology of Serbia, Belgrade, Serbia). Human melanoma A375, colon cancer HCT116 and SW620, prostate PC3 and LNCap and mouse colon CT26CL25 were kind gifts from Prof. Ferdinando Nicoletti

(Department of Biomedical Sciences, University of Catania, Italy). Cells are routinely maintained in HEPES-buffered RPMI-1640 medium supplemented with 10% FCS, 2 mM L-glutamine, 0.01% sodium pyruvate, 5 × 10⁻⁵ M 2-mercaptoethanol, and antibiotics (culture medium) at 37 °C in a humidified atmosphere with 5% CO₂ (doubling time for the used cell lines varying from 48–72 h). After standard trypsinization, cells were seeded at 1 × 10⁴ per well in 96-well plates for viability determination and 2.5 × 10⁵ per well in 6-well plates for flow cytometry.

Preparation of keratinocytes

Epidermal cell suspensions were prepared from mouse ear skin. Ears were split into two pieces and left to float on 0.5% trypsin–PBS solution for 1 h at 37 °C. Epidermis was removed, cut into small pieces, and transferred to a conus tube. Cells were rapidly resuspended to obtain single cell suspension and filtered through nylon meshes. Cells were finally resuspended into RPMI supplemented with 15% FCS.

Preparation of adult lung fibroblasts

Lung fibroblasts were prepared from mouse lungs. In brief, lungs were aseptically removed, rinsed in PBS, and cut into small pieces. Tissue was incubated in collagenase IV from *Clostridium histolyticum* (0.7 mg ml⁻¹) + DNase (30 mg ml⁻¹) with slow stirring for 1 h at 37 °C. Cells were washed three times and resuspended in RPMI supplemented with 15% FCS. After 24 h, non-adherent cells were removed and medium was replaced. After the cells had reached 80–90% of confluence they were split and used for experiments.

Determination of cell viability by MTT and crystal violet assay

The number of adherent viable cells was evaluated with crystal violet assay, while mitochondrial dehydrogenase activity, as an indicator of cell viability, was used for non-adherent cells and determined by mitochondria-dependent reduction of 3-(4,5-dimethylthiazol-2-yl)-2,5-diphenyltetrazolium bromide (MTT) to colored formazan.

Cells (1 × 10⁴ per well) were treated with the wide range of doses of the drugs for 24 h and viability was estimated. Both tests were performed as previously described.²³ The results are presented as percentage of the control (untreated cells) that was arbitrarily set to 100%.

Appendix 4

Reproduced from Ref. G.N. Kaluđerović, S.A. Mijatović, B.B. Zmejkovski, M.Z. Bulatović, S. Gómez-Ruiz, M.K. Mojić, D. Steinborn, D. M. Miljković, H. Schmidt, S.D. Stošić-Grujičić, T.J. Sabo, D.D. Maksimović-Ivanić, *Metallomics* 2012, 4, 979 with permission from The Royal Society of Chemistry.

Lactate dehydrogenase release assay

For determination of LDH release, cells were cultivated in phenol red free medium for 6, 12, 18, and 24 h in the presence of different doses of tested compounds and assay was performed as described previously.¹⁵

Cell cycle analysis

Cells (2.5×10^5 per well) were treated with IC_{50} doses of each compound for 24 h, then trypsinized and fixed in 70% ethanol at 4 °C for 30 min. After washing in PBS, cells were incubated with PI ($20 \mu\text{g ml}^{-1}$) and RNase (0.1 mg ml^{-1}) for 30 min at 37 °C in dark. Red fluorescence was analysed with a FACS Calibur flow cytometer (BD, Heidelberg, Germany). The distribution of cells in different cell cycle phases was determined with Cell Quest Pro software (BD).

AnnexinV-FITC/EtBr staining

Cells (2.5×10^5 per well) were treated with IC_{50} doses of each compound for 5 h, then trypsinized and stained with AnnexinV-FITC/EtBr according to manufacturer's instructions (Biotium, Hayward, CA). Cells were analysed with a FACS Calibur flow cytometer (BD, Heidelberg, Germany) and Cell Quest Pro software (BD).

Caspase detection

Cells (2.5×10^5 per well) were treated with IC_{50} doses of each compound for 24 h, then trypsinized and stained with apostat (R&D Systems, Minneapolis, MN, USA) in phenol red free RPMI supplemented with 15% FCS for 15 min at 37 °C. After washing, cells were analysed with the FACS Calibur flow cytometer (BD, Heidelberg, Germany) using Cell Quest Pro software (BD).

Acridine orange and dihydrorhodamine-123 (DHR) staining

Cells (2.5×10^5 per well) were treated with IC_{50} doses of each compound for 24 h, then trypsinized and stained with acridine orange for detection of autophagy or DHR for measurement of reactive oxygen species (ROS) release, exactly as described previously.²⁴

PI staining of cells

Cells (1×10^4 per well) were treated with IC_{50} doses of each compound for 24 h, then PI staining was performed as indicated previously.²⁴

Statistical analysis

The results are presented as mean \pm SD of triplicate observations from one representative of at least three experiments with similar results, unless indicated otherwise. The significance of the differences between various treatments was assessed by ANOVA followed by the Student–Newman–Keuls test. $p < 0.05$ was considered to be significant.

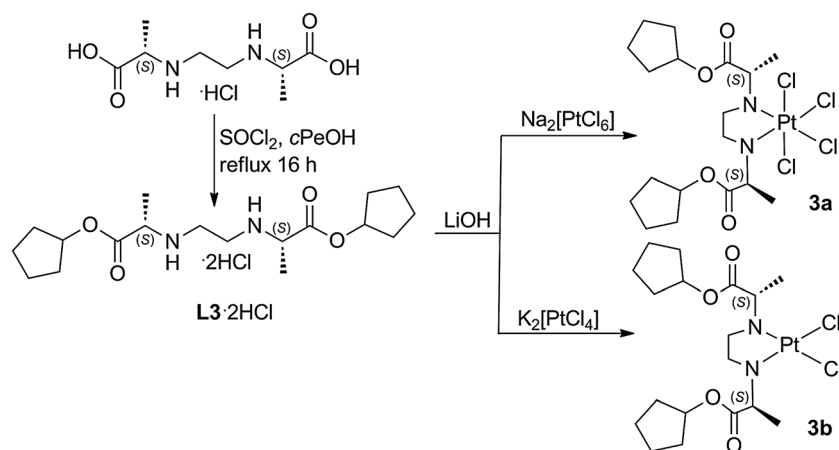
Results and discussion

Chemistry

Synthesis and characterization. Esters **L1-2HCl**–**L3-2HCl** and platinum(II/IV) complexes **1a**–**2b** were prepared as described previously.^{18,20} New compounds of this type, ligand precursors, and platinum(II/IV) complexes were prepared as presented for **L3-2HCl**, **3a**, and **3b** in Scheme 1.

IR spectra of **3a**–**5a** showed specific absorption bands: $\nu(\text{C}=\text{O})$ between 1734 – 1740 cm^{-1} , $\nu(\text{C}-\text{O})$ from 1212 – 1223 cm^{-1} and $\nu(\text{CH}_3)$ at 2940 – 2965 cm^{-1} (**L3-2HCl**–**L5-2HCl**: $\nu(\text{C}=\text{O})$ 1739 – 1744 cm^{-1} ; $\nu(\text{C}-\text{O})$ 1224 – 1233 cm^{-1} and $\nu(\text{CH}_3)$ 2940 – 2970 cm^{-1}). Indication of nitrogen coordination can be proved by the presence of bands for secondary amino groups (3113 – 3125 cm^{-1}), while in the spectra of ligand precursors **L3-2HCl**–**L5-2HCl** the band for a secondary ammonium group was observed, $\nu(\text{R}_2\text{NH}_2^+)$ from 3415 – 3449 cm^{-1} , respectively.

The coordination of $R_2\text{edda}$ -type ligands to platinum(II/IV) gives rise to the formation of chiral N centers. Thus in principle, the following isomers can be formed (R,R), (S,S) (enantiomeric pair in case of achiral $R_2\text{edda}$ -type ligands) and (R,S) \equiv (S,R). In the ^1H and ^{13}C NMR spectra of complex **3a** only one set of signals was observed indicating formation of one diastereoisomer (see section Molecular structure of **3a**). Similar observations were made for complexes **1a** and **2a** previously, where R,R,S,S -configuration for N,N,C,C atoms were assigned (single crystal X-ray diffraction, as well as NMR).¹⁸ Platinum(II) complex, **3b**, in NMR spectra showed two sets of signals (isomer ratio $A/B = 3/2$).



Scheme 1 Synthesis of ligand precursor, platinum(II) and platinum(IV) complexes: **L3-2HCl**, **3a**, and **3b** as an example.

Appendix 4

Reproduced from Ref. G.N. Kaluđerović, S.A. Mijatović, B.B. Zmejtkovski, M.Z. Bulatović, S. Gómez-Ruiz, M.K. Mojić, D. Steinborn, D. M. Miljković, H. Schmidt, S.D. Stošić-Grujičić, T.J. Sabo, D.D. Maksimović-Ivanić, *Metallomics* 2012, 4, 979 with permission from The Royal Society of Chemistry.

DFT calculations for the corresponding palladium(II) complex, $[\text{PdCl}_2\{(c\text{-Pe})_2\text{eddip}]\}$, indicate formation of (*R,R*) and (*R,S*) diastereoisomers²⁰ which might be also formed in the case of complex **3b**. For complexes **4a** and **5a**, only one set of signals in ¹H and ¹³C NMR spectra was observed.

In ¹H NMR spectra, coordination-induced shifts (up to 0.9 ppm) for the signals of CH₂ protons (ethylenediamine bridge) gave a clear indication of nitrogen coordination. For compounds **3a** and **3b**, signals of cyclopentyl protons were found between 1.1 and 1.9 ppm. Methylene protons from complexes **4a** and **5a** from the α -alaninato moiety were found at around 2.8 ppm, and methyl protons from the isopropyl/isobutyl group in cases of **L4**·2HCl/**L5**·2HCl and **4a/5a** were found at 1.2 and 0.9 ppm, respectively. Ester carbon atom resonances were found for COO at around 170 ppm for all compounds verifying that the oxygen atom is not coordinated as expected. For the complexes **3a–5a**, NMR spectroscopic measurements confirmed their constitution. The stability of all complexes in DMSO solutions was also studied. ¹H NMR spectra of all complexes were recorded in deuterated DMSO freshly prepared showing no evidence of decomposition or evolution to other products after 7 days, thus suggesting stability of platinum(II) and platinum(IV) complexes in DMSO.

Molecular structure of 3a. Single crystals suitable for X-ray diffraction analysis were obtained as discrete molecules without any unusual intermolecular contacts (Fig. 2). The molecular

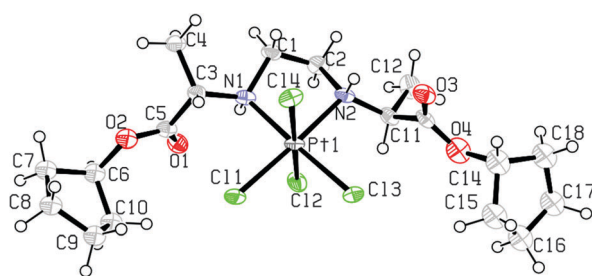


Fig. 2 ORTEP²⁹ diagram of **3a** with thermal ellipsoids at 30% probability.

structure of **3a** shows that the platinum atom has a distorted octahedral geometry with four chlorine atoms located in both axial and two equatorial positions. The other two equatorial positions of the octahedron are occupied by the nitrogen atoms N1 and N2 of the ester ligand. Bond lengths and angles were found to be in the expected range of other platinum complexes^{16,18,25–28} (see ESI†, Table S2). The chelating N1,N2 ester ligand gives rise to the formation of a five-membered ring, exhibiting an envelope conformation on C1 (*ca.* 67 pm of the mean plane formed by Pt1, N1, C2, and N2). The configuration of chiral centers N1, N2, C3, and C11 in this structure was assigned as *R, R, S, and S*, respectively, according to the solved configuration and the very low value of the Flack parameter.

Biological studies

Cytotoxicity of ligand precursors and their corresponding platinum complexes. To test the antitumor potential of ligand precursors (**L1**·2HCl–**L5**·2HCl), platinum(IV) (**1a–5a**), and platinum(II) (**1b–3b**) complexes different cell lines were exposed to the wide range of doses of each compound. Cell viability was estimated by the crystal violet test after 24 h of incubation (see ESI†, Fig. S1). While compounds **L1**·2HCl, **1b**, **L4**·2HCl, and **L5**·2HCl did not disturb viability of all tested cells, compound **L2**·2HCl was efficient only on human colon SW620, human prostate PC3, and human glioblastoma U251 cells. It is interesting that mentioned cell lines possess a defect in tumor suppressor p53.^{30–32} On the other hand, platinum(IV) (**1a–5a**), two platinum(II) (**2b**, **3b**) complexes, and ligand precursor (**L3**·2HCl) strongly downregulated viability of all examined cancer cells.

Ligand precursors are found to exhibit low to no activity in investigated conditions (Table 1). The activity of the ligand precursors against investigated cell lines is increasing in the following order: **L1**·2HCl \approx **L4**·2HCl \approx **L5**·2HCl \leq **L2**·2HCl \leq **L3**·2HCl. An improvement in cytotoxicity has been observed by coordination of ligands to the dichloro-platinum(II) moiety. It was observed that the cytotoxicity is more induced by the platinum(II) compounds having more lipophilic ester part (isopropyl \rightarrow isobutyl \rightarrow cyclopentyl), namely from **1b**, **2b** to **3b**.

Table 1 IC₅₀^a [μM] values of ligand precursors and corresponding platinum(II) and platinum(IV) complexes after 24 h of action against selected tumor cell lines

Compound	Cell line							
	CT26CL25	HCT116	SW620	PC3	LNCAp	U251	A375	B16
L1 ·2HCl	>200	>200	>200	>200	>200	>200	>200	>200
1a	136.6 \pm 24.4	120.1 \pm 4.4	78.7 \pm 11.2	>200	99.2 \pm 10.5	96.5 \pm 9.8	200 \pm 13	138.5 \pm 6.1
1b	>200	>200	191.8 \pm 7.6	>200	>200	>200	>200	>200
L2 ·2HCl	>200	>200	198.2 \pm 2.6	189.1 \pm 15.4	>200	185.6 \pm 17.9	>200	>200
2a	75.9 \pm 7.8	67.5 \pm 4	55.3 \pm 13	77 \pm 16	60.9 \pm 5	39.6 \pm 3.7	100 \pm 14	72.5 \pm 2.7
2b	172 \pm 12	103.5 \pm 6.9	68.2 \pm 10	111.5 \pm 4.1	105 \pm 14	135 \pm 22	185 \pm 6.3	101 \pm 5
L3 ·2HCl	>200	170.4 \pm 13.2	143.6 \pm 26.2	135.3 \pm 19.7	150 \pm 27	136.7 \pm 11	>200	200 \pm 5
3a	41.4 \pm 9	39.2 \pm 3.7	43.9 \pm 9	55.8 \pm 6.4	39 \pm 2	48 \pm 6	47.3 \pm 4.7	77.7 \pm 10
3b	76.3 \pm 10.7	68.1 \pm 2.6	55.1 \pm 9	54.4 \pm 9.7	50.3 \pm 2	87.2 \pm 10	91 \pm 12	66 \pm 6.5
L4 ·2HCl	>200	>200	>200	>200	>200	>200	>200	>200
4a	105 \pm 13.6	102.4 \pm 15	71.5 \pm 14	>200	87 \pm 4	98.4 \pm 12.1	195.3 \pm 14	93 \pm 6
L5 ·2HCl	>200	>200	>200	>200	>200	>200	>200	>200
5a	35 \pm 6	38.6 \pm 5.5	38.9 \pm 4.5	35.2 \pm 4.4	30.4 \pm 7.6	38.7 \pm 7.3	67 \pm 8	30.8 \pm 4.3
Cisplatin	120.0	>120	120.0	12.5	12.8	20.0	45.0	94.3

^a IC₅₀ values were calculated as mean \pm SD from three independent experiments.

Appendix 4

Reproduced from Ref. G.N. Kaluđerović, S.A. Mijatović, B.B. Zmejovski, M.Z. Bulatović, S. Gómez-Ruiz, M.K. Mojić, D. Steinborn, D. M. Miljković, H. Schmidt, S.D. Stošić-Grujičić, T.J. Sabo, D.D. Maksimović-Ivanić, *Metallomics* 2012, 4, 979 with permission from The Royal Society of Chemistry.

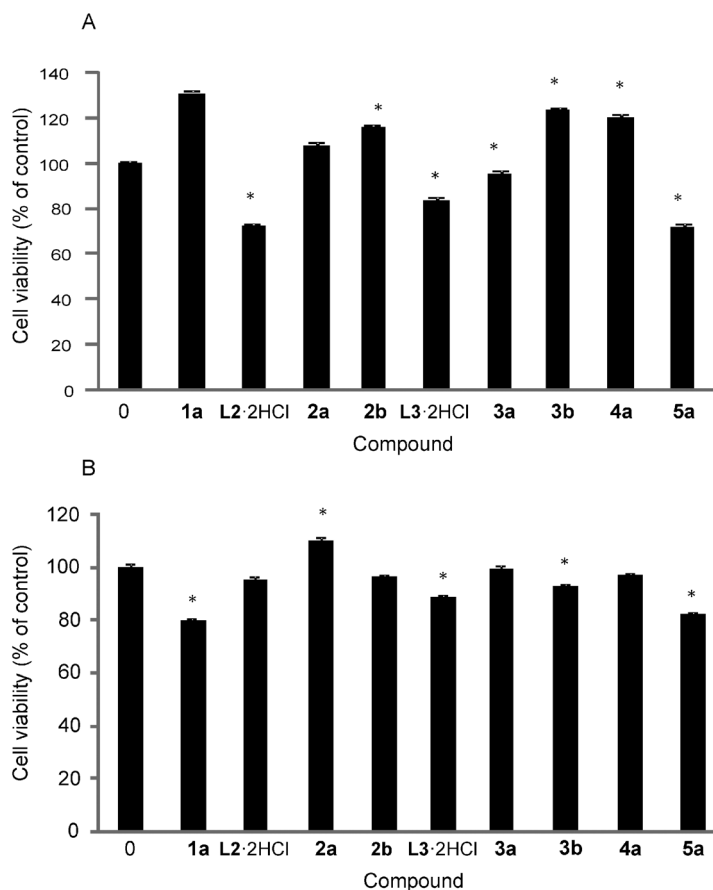


Fig. 3 The effect of ligand precursors and their derivatives on viability of normal cells. (A) Keratinocytes (8×10^4 cells per well) and (B) fibroblasts (3×10^4 per well) were treated with an IC_{50} dose of each compound specific for HCT116 cells for 24 h, after which cell viability was determined by MTT and CV assays, respectively. The data are presented as mean \pm SD from representative of three independent experiments, * $p < 0.05$ refers to untreated cultures.

Furthermore, when platinum(II) is exchanged with a platinum(IV) ion, higher cytotoxic activity is achieved. The IC_{50} value of platinum(IV) complexes **1b–3b** is up to 3 times lower than that of the corresponding platinum(II) complexes **1a–3a**.

Comparison of the structure–activity relationship of platinum(II) **1b–3b** and platinum(IV) complexes **1a–3a** relieved the same trend of cytotoxicity (IC_{50} : **1a** > **2a** > **3a**) with exception of cell lines that possess defect in tumor suppressor p53 (SW620, PC3, and U251) as well as B16 cell line. Changing of alaninato to the β -alaninato moiety in platinum(IV) complexes **1a** \rightarrow **4a** did not significantly improve antitumoral activity. On the other hand, the same change in the structure for **2a** \rightarrow **5a** led to higher cytotoxic agent, excluding U251 cell line on which comparable cytotoxicity was found.

Cisplatin as a clinical drug was used for comparison. Generally, cisplatin induced higher efficiency against selected tumor cell lines than ligand precursors, **L1·2HCl–L5·2HCl**. In direct comparison with platinum(II) complexes, cisplatin has been found to be less active than **2b** against HCT116 and SW620 cell lines and **3b** against CT26CL25, HCT116, SW620, and B16 cell lines. Platinum(IV) complexes **2a–5a** exhibited higher activity than cisplatin on CT26CL25, HCT116, SW620, and B16 cell lines. Complex **1a** showed higher effectiveness than cisplatin only on the SW620 cell line.

From the investigated platinum(IV) complexes, similar or slightly different activity depending on the cell line are observed for complexes having an isobutyl or a cyclopentyl ester moiety (**2a**, **3a** and **5a**). On the other hand, platinum(IV) complexes with isopropyl moiety (**1a** and **4a**) showed lower activity. It is interesting to observe that the ligands with more hydrophobic alkyl side chain are apparently improving activity of complexes. This structure–activity relationship is in accordance with previous studies.^{13,18} The *in vitro* activity is increasing in the following order $L\cdot 2HCl \leq [PtCl_2L] < [PtCl_4L]$.

Cisplatin-resistant subclone of human colon cancer cell line HCT116 was chosen as representative for further investigation and compounds **L3·2HCl**, **1a–5a**, **2b**, and **3b** that showed efficacy in all tested tumor cells included in following experiments.

Selectivity studies. To compare the toxicity of compounds on non-transformed and malignant cells, primary fibroblasts and keratinocytes were exposed to IC_{50} doses observed on HCT116 cells and viability was detected after 24 h. As seen in Fig. 3, viability of primary cells was minimally disturbed indicating that novel compounds are significantly less toxic to normal than transformed cells.

Apoptosis is the dominant mode of drug action. To evaluate the reason for decreased viability, cells were treated with IC_{50}

Appendix 4

Reproduced from Ref. G.N. Kaluđerović, S.A. Mijatović, B.B. Zmejovski, M.Z. Bulatović, S. Gómez-Ruiz, M.K. Mojić, D. Steinborn, D. M. Miljković, H. Schmidt, S.D. Stošić-Grujičić, T.J. Sabo, D.D. Maksimović-Ivanić, *Metallomics* 2012, 4, 979 with permission from The Royal Society of Chemistry.

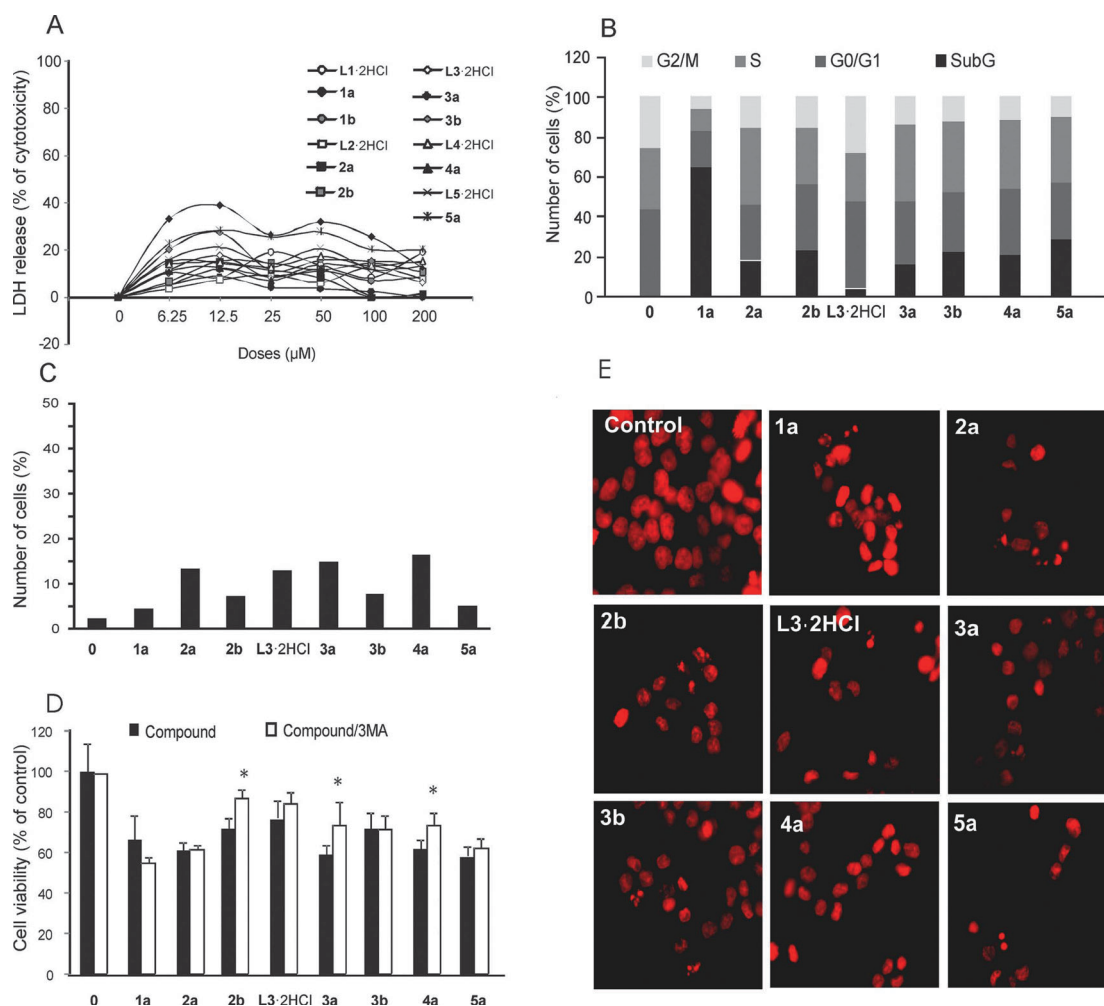


Fig. 4 The effect of ligand precursors and their derivatives on malignant cell death. (A) HCT116 cells (1×10^4 per well) were treated with a range of concentrations of each tested compound and after 24 h of incubation LDH release was assessed. The data are presented as means from representative of three independent experiments while SD did not exceed 10%. Cells (2×10^5 per well) were exposed to IC_{50} doses of each compound for 24 h and (B) cell cycle distribution or (C) presence of autophagic vesicles in AO stained cells were evaluated. (D) Cells (1×10^4 per well) were treated with chosen IC_{50} doses alone as well as in combination with 3-MA (1 mM) and CV assay were performed after 24 h. (E) Cells exposed to the drugs for 24 h were stained by PI and visualized by a fluorescent microscope.

doses of L3-2HCl, 1a–5a, 2b, and 3b and release of LDH into culture supernatant was measured at different time points (6, 12, 18, and 24 h). Release of LDH was only detected in supernatants of cells treated for 24 h with compounds 2b, 3b, and 3a–5a indicating that necrosis is not the primary mode of action of these derivatives (Fig. 4A). On the other hand, cell cycle analysis revealed massive subG accumulation upon 24 h of treatment with all tested compounds except in cells exposed to compound L3-2HCl (Fig. 4B).

Cells were further evaluated for the presence of autophagy. After the 24 h-treatment increased, percentage of autophagosomes was detected in the cytoplasm of cells treated with the ligand precursor L3-2HCl, all platinum(IV), 1a–5a, and platinum(II) complexes, 2b and 3b (Fig. 4C). Concomitant treatment with compounds 2b, 3a, or 4a and 3-MA (inhibitor of autophagy) partly restored cell viability confirming that autophagic cell death contributes to decrease of cell viability (Fig. 4D). Concordantly to elevated subG compartment, staining with PI showed the presence of typical apoptotic cells

with shrinkage of nucleus and apoptotic bodies upon the treatment with all tested drugs (Fig. 4E).

To determine the presence of apoptotic cell death, Annexin-PI double staining was performed. Early signs of apoptosis manifested through inverted phosphatidylserine were observed even 5 h after drugs addition (Fig. 5A). Although it is known that HCT116 cells under treatment with some agents underlie to anoikis, form of apoptotic cell death triggered by detachment from the extracellular matrix, we counted the floating cells during 15 h of incubation with compounds.^{33,34} The number of floating cells did not significantly increase during this time period (not shown) while estimation of cell viability by the crystal violet test revealed the absence of marked changes in a number of adherent cells exposed to the drugs in comparison to control (Fig. 5B). These results indicated that compounds induced apoptosis in adherent cells eliminating the relevance of anoikis as possible mode of drug action. In parallel, the high rate of caspase activation was detected after 24 h in all samples except in cells exposed to ligand precursor

Appendix 4

Reproduced from Ref. G.N. Kaluđerović, S.A. Mijatović, B.B. Zmejovski, M.Z. Bulatović, S. Gómez-Ruiz, M.K. Mojić, D. Steinborn, D. M. Miljković, H. Schmidt, S.D. Stošić-Grujičić, T.J. Sabo, D.D. Maksimović-Ivanić, *Metallomics* 2012, 4, 979 with permission from The Royal Society of Chemistry.

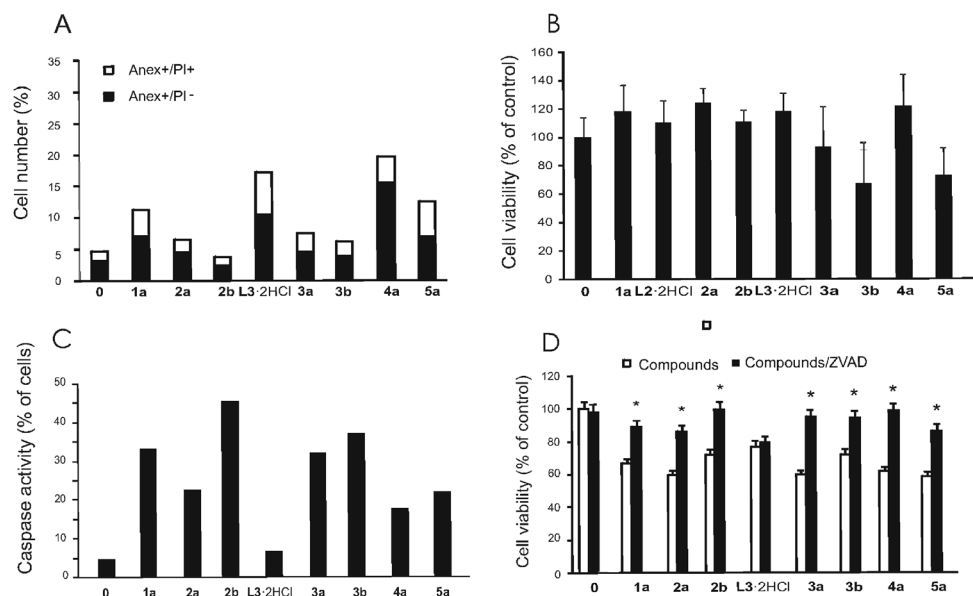


Fig. 5 Induction of caspase-dependent apoptosis by ligand precursors and their derivatives. (A) Cells (2×10^5 per well) were exposed to IC_{50} doses, and Annexin–PI double staining was performed after 5 h. (B) Cells (1×10^4 per well) were treated with IC_{50} doses, and after 24 h of incubation CV was performed. (C) Cells (2×10^5 per well) were exposed to IC_{50} doses, and after 24 h caspase activity was assessed. (D) Cells (1×10^4 per well) were treated with IC_{50} doses alone as well as in combination with ZVAD (20 μ M) and CV was done after 24 h. Results (A, C) from one of three representative flow cytometric analyses were presented. Data (B, D) are presented as mean \pm SD from representative of three independent experiments. * $p < 0.05$ refers to untreated cultures.

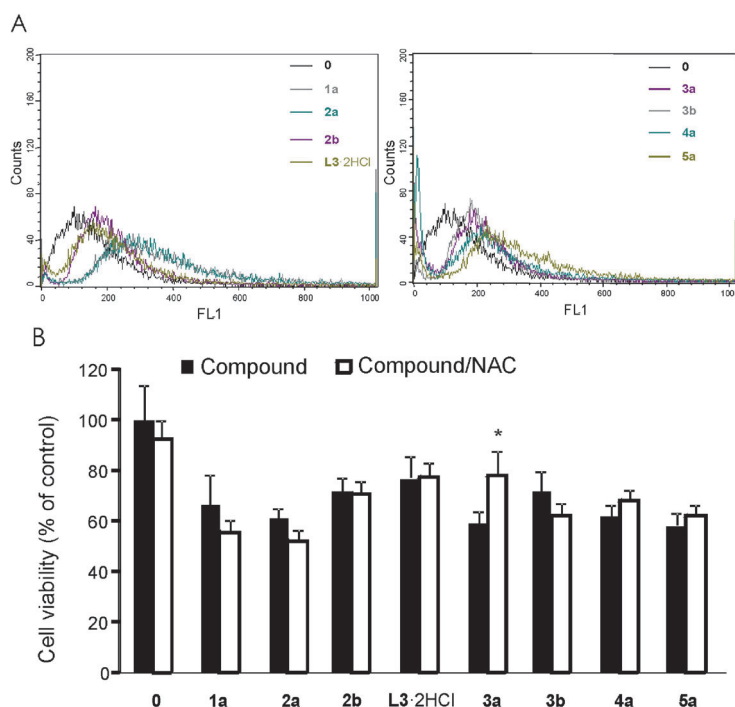


Fig. 6 ROS and RNS are irrelevant for drugs triggered toxicity. (A) Cells (2×10^5 per well) stained with DHR were exposed to IC_{50} doses for 24 h and flow cytometric analysis was performed. (B) Cells (1×10^4 per well) were treated with IC_{50} doses of each compound alone or in combination with NAC (2.5 μ M) and cell viability was estimated by CV assay after 24 h.

L3-2HCl, where low caspase activity was in concordance with insignificant DNA fragmentation (Fig. 5C).

Co-treatment with pan-caspase inhibitor ZVAD resulted in significant recovery of cell viability in cultures exposed to all compounds except L3-2HCl confirming the key role of caspases

in apoptosis triggered by these drugs (Fig. 5D). Together, results suggested that compounds induced caspase-dependent apoptosis. The similar mechanism behind the action of numerous cytotoxic drugs is already described in preclinical and clinical practice such as metal-based or anthracyclin type drugs, satraplatin or

doxorubicine, respectively.^{35–38} The most important fact is that novel cisplatin-modified compounds evaluated in this study are able to overcome the intrinsic resistance of HCT116 cells to cisplatin. Unresponsiveness to cisplatin or other chemotherapeutic drugs is often related to general resistance to induction of apoptosis by external stimuli or immune system mediated death signals.³⁹ In this light, the ability of novel drugs to finalize apoptotic process despite a strong intracellular blockade, together with less toxicity against primary tissues, represent their great advantage.

Oxidative stress triggered by the drugs is not crucial for their toxicities. To elucidate the role of oxidative stress, cells were treated with IC₅₀ doses (each compound) and production of reactive oxygen and nitrogen species was determined after 24 h. Treatment with all tested compounds promoted significant release of these highly reactive molecules (Fig. 6A). However, parallel treatment with antioxidant *N*-acetylcysteine significantly restored the viability of cells only in culture exposed to compound **3a** (Fig. 6B).

In summary, despite of intensive oxidative stress, ROS and RNS are not major mediators of drug toxicity. Cytotoxicity of numerous chemotherapeutics is mediated by hyperproduction of ROS and RNS.⁴⁰ Under these circumstances, antioxidant supplementation even through food consumption can greatly modify drug efficacy.^{41,42} Having in mind this, the feature of synthesized compounds being independent from reactive molecule generation and therefore being less influenced by antioxidants is their benefit.

Conclusions

Ligand precursors (**L4**·2HCl and **L5**·2HCl), platinum(IV) (**3a–5a**), and platinum(II) (**3b**) complexes were synthesized and characterized by traditional methods. In addition, the crystal structure of **3a** was resolved by X-ray structural analysis and configuration of chiral centers N1, N2, C3, and C11 was assigned in this structure as *R*, *R*, *S*, and *S*, respectively. Synthesized compounds and some others which were described earlier were tested against eight tumor cell lines (CT26CL25, HTC116, SW620, PC3, LNCaP, U251, A375, and B16) and two normal primary cells (fibroblasts and keratinocytes). From the ligand precursors, only **L3**·2HCl exhibited significant antitumoral activity, while platinum(II) complexes were found more active. The highest activity was observed when cell lines were treated with platinum(IV) complexes. Some structure–activity relationships could be derived: *in vitro* activity decreases from platinum(IV), platinum(II) to ligand precursors. On the representative cisplatin-resistant HCT116 cell line, human colon cancer compounds **L3**·2HCl, **1a–5a**, **2b**, and **3b** were studied with regard to the mechanism of action. Compounds **L3**·2HCl, **1a–5a**, **2b**, and **3b** were found to be not toxic to normal primary cells (fibroblasts and keratinocytes). Platinum(IV) and platinum(II) complexes (**1a–5a**, **2b**, and **3b**) induced caspase-dependent apoptosis followed by autophagic cell death upon treatment with **2b**, **3a** or **4a**. Furthermore, ROS and RNS are not major mediators of drug toxicity.

Acknowledgements

GNK acknowledges financial support from the Alexander von Humboldt Foundation. The authors are grateful to the

Ministry of Science and Technological Development of the Republic of Serbia for financial support (Grant Nos. 172035 and 173013). We would also like to thank Mrs Heidrun Felgner for language corrections of the manuscript.

References

- C. A. Rabik and M. E. Dolan, *Cancer Treat. Rev.*, 2007, **33**, 9–23.
- J. T. Hartmann and H.-P. Lipp, *Expert Opin. Pharmacother.*, 2003, **4**, 889–901.
- A. Dietrich, T. Mueller, R. Paschke, B. Kalinowski, T. Behlendorf, F. Reipsch, A. Fruehauf, H. J. Schmoll, C. Kloft and W. Voigt, *J. Med. Chem.*, 2008, **51**, 5413–5422.
- L. Kelland, *Nat. Rev. Cancer*, 2007, **7**, 573–584.
- F. Arnesano and G. Natile, *Coord. Chem. Rev.*, 2009, **253**, 2070–2081.
- J. N. Jolley, A. I. Yanovsky, L. R. Kelland and K. B. Nolan, *J. Inorg. Biochem.*, 2001, **83**, 91–100.
- M. S. Davies, P. N. Wong, A. R. Battle, G. Haddad, M. J. McKeage and T. W. Hambley, *J. Inorg. Biochem.*, 2002, **91**, 205–211.
- G. N. Kaluđerović, H. Schmidt, D. Steinborn and T. J. Sabo, in *Inorganic Biochemistry: Research Progress*, ed. J. G. Hughes and A. J. Robinson, Nova Science Publishers, Hauppauge, NY, 2008, pp. 305–326.
- T. J. Sabo, G. N. Kaluđerović, D. Poleti, L. Karanović, A. Boccarelli, F. Cannito and G. Natile, *J. Inorg. Biochem.*, 2004, **98**, 1378–1384.
- G. N. Kaluđerović, V. M. Đinović, Z. D. Juranić, T. P. Stanojković and T. J. Sabo, *J. Coord. Chem.*, 2006, **59**, 815–819.
- J. M. Lazić, L. Vucicević, S. Grgurić-Šipka, K. Janjetović, G. N. Kaluđerović, M. Misirkic, M. Gruden-Pavlović, D. Popadić, R. Paschke, V. Trajković and T. J. Sabo, *ChemMedChem*, 2010, **5**, 881–889.
- G. N. Kaluđerović and R. Paschke, *Curr. Med. Chem.*, 2011, **18**, 4738–4752.
- G. N. Kaluđerović, V. M. Đinović, Z. D. Juranić, T. P. Stanojković and T. J. Sabo, *J. Inorg. Biochem.*, 2005, **99**, 488–496.
- G. N. Kaluđerović, D. Miljković, M. Momčilović, V. M. Đinović, M. Mostarica-Stojković, T. J. Sabo and V. Trajković, *Int. J. Cancer*, 2005, **116**, 479–486.
- S. Mijatović, D. Maksimović-Ivanić, J. Radović, D. Miljković, G. N. Kaluđerović, T. J. Sabo and V. Trajković, *Cell. Mol. Life Sci.*, 2005, **62**, 1275–1282.
- G. N. Kaluđerović, H. Schmidt, S. Schwieger, Ch. Wagner, R. Paschke, A. Dietrich, T. Mueller and D. Steinborn, *Inorg. Chim. Acta*, 2008, **361**, 1395–1404.
- G. N. Kaluđerović, H. Kommera, S. Schwieger, A. Paethanom, M. Kunze, H. Schmidt, R. Paschke and D. Steinborn, *Dalton Trans.*, 2009, 10720–10726.
- B. B. Krajčinović, G. N. Kaluđerović, D. Steinborn, H. Schmidt, Ch. Wagner, Ž. Žizak, Z. D. Juranić, S. R. Trifunović and T. J. Sabo, *J. Inorg. Biochem.*, 2008, **102**, 892–900.
- J. M. Vujić, G. N. Kaluđerović, M. Milovanović, B. B. Zmejkovski, V. Volarević, D. Zivic, P. N. Djurdjević, T. J. Sabo and S. R. Trifunović, *Eur. J. Med. Chem.*, 2011, **46**, 4559–4565.
- B. B. Zmejkovski, G. N. Kaluđerović, S. Gómez-Ruiz, Ž. Žizak, D. Steinborn, H. Schmidt, R. Paschke, Z. D. Juranić and T. J. Sabo, *Eur. J. Med. Chem.*, 2009, **44**, 3452–3458.
- J. M. Vujić, G. N. Kaluđerović, B. B. Zmejkovski, M. Milovanović, V. Volarević, N. Arsenijević, T. P. Stanojković and S. R. Trifunović, *Inorg. Chim. Acta*, 2012, **390**, 123–128.
- L. E. Mihajlović, A. Savić, J. Poljarević, I. Vučković, M. Mojić, M. Bulatović, D. Maksimović-Ivanić, S. Mijatović, G. N. Kaluđerović, S. Stošić-Grujičić, D. Miljković, S. Grgurić-Šipka and T. J. Sabo, *J. Inorg. Biochem.*, 2012, **109**, 40–48.
- D. Mijatović, D. Maksimović-Ivanić, J. Radović, D. Popadić, M. Momčilović, L. Harhaji, D. Miljković and V. Trajković, *Cell. Mol. Life Sci.*, 2004, **61**, 1805–1815.
- D. Maksimović-Ivanić, S. Mijatović, L. Harhaji, D. Miljković, D. Dabideen, K. Fan Cheng, K. Mangano, G. Malaponte, Y. Al-Abed, M. Libra, G. Garotta and F. Nicoletti, *Mol. Cancer Ther.*, 2008, **7**, 510–520.
- C. Tessier and F. D. Rochon, *Inorg. Chim. Acta*, 1999, **295**, 25–38.

Appendix 4

Reproduced from Ref. G.N. Kaluđerović, S.A. Mijatović, B.B. Zmejkovski, M.Z. Bulatović, S. Gómez-Ruiz, M.K. Mojić, D. Steinborn, D. M. Miljković, H. Schmidt, S.D. Stošić-Grujičić, T.J. Sabo, D.D. Maksimović-Ivanić, *Metallomics* 2012, 4, 979 with permission from The Royal Society of Chemistry.

- 26 G. M. Rakić, S. Grgurić-Šipka, G. N. Kaluđerović, S. Gómez-Ruiz, S. K. Bjelogrić, S. S. Radulović and Ž. Lj. Tešić, *Eur. J. Med. Chem.*, 2009, **44**, 1921–1925.
- 27 G. N. Kaluđerović, H. Schmidt, Ch. Wagner and D. Steinborn, *Acta Crystallogr., Sect. E: Struct. Rep.*, 2007, **63**, m1985.
- 28 M. Z. Stanković, G. P. Radić, V. V. Glođović, I. D. Radojević, O. D. Stefanović, Lj. R. Čomić, O. R. Klisurić, V. M. Djinović and S. R. Trifunović, *Polyhedron*, 2011, **30**, 2203–2209.
- 29 L. J. Farrugia, *J. Appl. Cryst.*, 1997, **30**, 565, ORTEP, 3, for windows, .
- 30 S. Luan, L. Sun and F. Huang, *Arch. Med. Res.*, 2010, **41**, 67–74.
- 31 V. Souza, Y. B. Dong, H. S. Zhou, W. Zacharias and K. M. McMasters, *J. Transl. Med.*, 2005, **3**, 44.
- 32 S. L. Scott, J. D. Earle and P. H. Gumerlock, *Cancer Res.*, 2003, **63**, 7190–7196.
- 33 K. V. Balan, C. Demetzos, J. Prince, K. Dimas, M. Cladaras, Z. Han, J. H. Wyche and P. Pantazis, *In Vivo*, 2005, **19**, 93–102.
- 34 R. Supino, A. I. Scovassi, A. C. Croce, L. Dal Bo, E. Favini, A. Corbelli, C. Farina, P. Misiano and F. Zunino, *Ann. N. Y. Acad. Sci.*, 2009, **1171**, 606–616.
- 35 M. Kalimutho, A. Minutolo, S. Grelli, G. Federici and S. Bernardini, *Acta Pharmacol. Sin.*, 2011, **32**, 1387–1396.
- 36 M. Kalimutho, A. Minutolo, S. Grelli, A. Formosa, G. Sancesario, A. Valentini, G. Federici and S. Bernardini, *Cancer Chemother. Pharmacol.*, 2011, **67**, 1299–1312.
- 37 C. Friesen, S. Fulda and K. M. Debatin, *Leukemia*, 1999, **13**, 1854–1858.
- 38 A. M. Havelka, M. Berndtsson, M. H. Olofsson, M. C. Shoshan and S. Linder, *Mini-Rev. Med. Chem.*, 2007, **7**, 1035–1039.
- 39 D. Maksimovic-Ivanic, S. Stosic-Grujicic, F. Nicoletti and S. Mijatovic, *Immunol. Res.*, 2012, **52**, 157–168.
- 40 A. J. Montero and J. Jassem, *Drugs*, 2011, **71**, 1385–1396.
- 41 C. D. Scripture and W. D. Figg, *Nat. Rev. Cancer*, 2006, **6**, 546–558.
- 42 R. Henriksson, K. O. Rogo and K. Grankvist, *Med. Oncol. Tumor Pharmacother.*, 1991, **8**, 79–86.

Reproduced from Ref. D. Maksimović-Ivanić, S. Mijatović, I. Mirkov, S. Stošić-Grujičić, D. Miljković, T.J. Sabo, V. Trajković, G.N. Kaluđerović, *Metallomics* 2012, 4, 1155 with permission from The Royal Society of Chemistry.

Cite this: *Metallomics*, 2012, 4, 1155–1159

www.rsc.org/metallomics

COMMUNICATION

Melanoma tumor inhibition by tetrachlorido(*O,O'*-dibutyl-ethylenediamine-*N,N'*-di-3-propionate)platinum(IV) complex: *in vitro* and *in vivo* investigations

Danijela Maksimović-Ivanić,^a Sanja Mijatović,^a Ivana Mirkov,^a Stanislava Stošić-Grujičić,^a Djordje Miljković,^a Tibor J. Sabo,^b Vladimir Trajković^c and Goran N. Kaluđerović^{*d}

Received 25th July 2012, Accepted 24th August 2012

DOI: 10.1039/c2mt20150j

Tetrachlorido(*O,O'*-dibutyl-ethylenediamine-*N,N'*-di-3-propionate)-platinum(IV) complex, [PtCl₄(*n*-Bu₂eddp)], was previously found to be effective against fibrosarcoma and glioma cell lines. Here we presented that [PtCl₄(*n*-Bu₂eddp)] strongly reduced the growth of B16 melanoma cells *in vitro*. Inhibition of cell viability was accompanied with induction of both necrotic and apoptotic cell death. In addition, [PtCl₄(*n*-Bu₂eddp)] concealed the expansion of tumors induced in syngeneic C57Bl/6 mice without visible signs of nephrotoxicity.

Introduction

Cisplatin, discovered by Rosenberg *et al.* (Fig. 1),¹ as a “drug of the 20th century” stimulated many scientists to search for development of new antitumoral drugs.^{2–6} Successful application of cisplatin has been found against head and neck, testicular, cervical, bladder, ovarian and small cell lung cancer.^{7,8} Besides therapeutic action it possesses unfavorable severe impacts on different organs inducing neurotoxicity, nephrotoxicity, ototoxicity, vomiting and nausea,⁹ restricting its therapeutic application.¹⁰ Furthermore, some tumors are developing resistance to cisplatin after a certain period of treatment.^{11,12} The first stage of development ended with second generation of platinum-based

antitumoral drugs, carboplatin and nedaplatin, in which chlorido ligands are substituted with anions of cyclobutanedicarboxylic or hydroxyacetic acids, respectively.¹³ Nevertheless, both complexes showed side effects. One of the possible variations changing the oxidation state of platinum (from +2 to +4) produced satraplatin (Fig. 1) which is now under clinical investigations. Platinum(IV) complexes are more kinetically inert than platinum(II) complexes, thus enabling possible oral administration of platinum(IV) drugs, to reduce toxicity during platinum-based chemotherapy and to decrease the amount of the drug lost or deactivated through side reactions before reaching the target site.¹⁴

In this context our research group focused on the synthesis of platinum(IV) complexes having *N,N'*-disubstituted ethylenediamine derivatives with esters of different carboxylic acids.^{15–20} Moreover, the *in vitro* structure–activity relationship along with mechanistic studies has been investigated. From all tested [PtCl₄(R₂edda-type)] compounds till now the most prominent place in the light of *in vitro* exploration deserves the “parent compound”, at first synthesized and tested against several tumor cell lines, [PtCl₄(*n*-Bu₂eddp)], tetrachlorido(*O,O'*-dibutyl-ethylenediamine-*N,N'*-di-3-propionate)platinum(IV) complex (Fig. 1).

As a continuation in this field we present here *in vitro* cytotoxic activity of [PtCl₄(*n*-Bu₂eddp)] against the melanoma B16 murine cell line. Furthermore, herein is reported the first *in vivo* study of the same complex as a representative of the [PtCl₄(R₂edda)]-type complexes on the corresponding syngeneic C57BL/6 mice model animals.

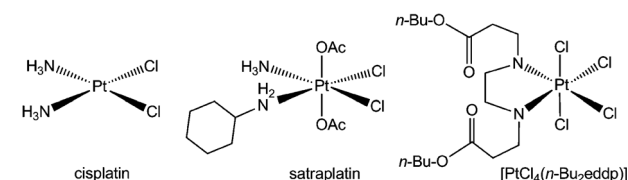


Fig. 1 Cisplatin, satraplatin and [PtCl₄(*n*-Bu₂eddp)] complexes.

^a Institute for Biological Research “Sinisa Stankovic”, University of Belgrade, Bulevar despota Stefana 142, 11060 Belgrade, Serbia

^b Faculty of Chemistry, University of Belgrade, Studentskitrg 12-16, 11 000 Belgrade, Serbia

^c Institute of Microbiology and Immunology, School of Medicine, University of Belgrade, Dr Subotica 1, 11000 Belgrade, Serbia

^d Institut für Chemie, Martin-Luther-Universität Halle-Wittenberg, Kurt-Mothes-Str. 2, 06120 Halle, Germany.

E-mail: goran.kaluderovic@chemie.uni-halle.de;
Fax: +49 345 5527028; Tel: +49 345 5525678

Materials and methods

Synthesis of [PtCl₄(*n*-Bu₂eddp)]

The platinum(IV) complex, [PtCl₄(*n*-Bu₂eddp)], was synthesized as described in the literature²¹ and structure was confirmed with ¹H and ¹³C NMR spectroscopy.

In vitro studies

Drug solution preparation. A stock solution of the studied platinum complexes, cisplatin and [PtCl₄(*n*-Bu₂eddp)], was made in dimethyl sulfoxide (DMSO) at a concentration of 10 mM,

filtered through a Millipore filter, 0.22 μm , before use, and diluted by nutrient medium to various working concentrations. DMSO was used due to solubility problems. Nutrient medium was HEPES-buffered RPMI-1640 medium supplemented with 10% FCS, 2 mM L-glutamine, 0.01% sodium pyruvate, 5×10^{-5} M 2-mercaptoethanol, and antibiotics (culture medium).

Reagents and cells

Fetal calf serum (FCS), RPMI-1640, phosphate-buffered saline (PBS), dimethyl sulfoxide (DMSO), 3-(4,5-dimethylthiazol-2-yl)-2,5-diphenyltetrazolium bromide (MTT), propidium iodide (PI) were obtained from Sigma (St. Louis, MO). Annexin V-FITC (AnnV) was from Biotium (Hayward, CA). The B16 murine melanoma was kindly provided by Dr Sinisa Radulovic (Institute for Oncology and Radiology of Serbia, Belgrade, Serbia).

Cells are routinely maintained in HEPES-buffered RPMI-1640 medium supplemented with 10% FCS, 2 mM L-glutamine, 0.01% sodium pyruvate, and antibiotics (culture medium) at 37 °C in a humidified atmosphere with 5% CO₂. After standard trypsinization, cells were seeded at 1×10^4 per well in 96-well plates for viability determination and 2.5×10^5 per well in 6-well plates for flow cytometry.

Determination of cell viability by MTT and crystal violet assay

The viability of cells was evaluated with crystal violet (CV) and 3-(4,5-dimethylthiazol-2-yl)-2,5-diphenyltetrazolium bromide (MTT) tests. Cells (1×10^4 per well) were treated with the wide range of doses of the drugs for 24 h and viability was measured as described.¹⁹

Lactate dehydrogenase release assay

For determination of LDH release cells were cultivated in phenol red free medium for indicated time in the presence of different doses of tested compounds and assay was performed as described previously.¹⁶

Cell cycle analysis

Cells (2.5×10^5 per well) were treated with 40 μM of each compound for 24 h, then trypsinized and fixed in 70% ethanol at 4 °C for 30 min. After washing in PBS, cells were incubated with PI (20 $\mu\text{g mL}^{-1}$) and RNase (0.1 mg mL^{-1}) for 30 min at 37 °C in the dark. Red fluorescence was analyzed using a FACS Calibur flow cytometer (BD, Heidelberg, Germany). The distribution of cells in different cell cycle phases was determined with Cell Quest Pro software (BD).

PI staining of cells

Cells (2×10^4 per well) were treated with 40 μM of each compound for 24 h, and then PI staining was performed as indicated previously.²²

In vivo studies

Primary tumors were induced by s.c. injection of 2×10^5 B16 melanoma cells in the dorsal right lumbosacral region of syngeneic C57BL/6 mice. The mice were randomized into the vehicle-treated group, cisplatin and [PtCl₄(*n*-Bu₂eddp)] group. Tumor growth was observed daily, and the treatment with tested compounds started

from day 11 after inoculation. The drugs were applied i.p. three times a week at a dose of 2 mg kg^{-1} cisplatin or corresponding dose of [PtCl₄(*n*-Bu₂eddp)] 4 mg kg^{-1} . The animals were sacrificed on day 24 and the tumor volume was determined by three-dimensional measurements. Tumor volume was calculated using the following formula: $[0.52 \times a \times b^2]$, where *a* is the longest and *b* is the shortest diameter.²² The research work involving experimental animals (mouse C57Bl) were conducted in accordance with national and institutional guidelines for the protection and animal welfare. All experimental protocols were approved by Ethical Commission of the Institute for Biological Research “Siniša Stanković”, University of Belgrade (No: 2-41/11).

Protein/creatinine ratio

Creatinine concentration was determined by Jaffe's reaction²³ while Bradford's method was used for detection of protein concentration.²⁴

Statistical analysis

The results are presented as mean \pm SD of triplicate observations from one representative of at least three experiments with similar results. The significance of the differences between various treatments was assessed by ANOVA followed by the Student Newman-Keuls test or Mann-Whitney U test for evaluating drugs efficacy *in vivo*. *P* < 0.05 was considered to be significant.

Results and discussion

Study of the cytotoxic activity of [PtCl₄(*n*-Bu₂eddp)] against B16 cells

Cells were exposed to a wide range of [PtCl₄(*n*-Bu₂eddp)] or cisplatin doses and after 24 h cell viability was estimated by MTT and CV tests. Results presented in Fig. 2A clearly indicate that novel compounds decreased the number of viable cells in culture more potently than original drug. Decreased viability was associated with enhanced release of lactate dehydrogenase in culture supernatants upon the treatment with [PtCl₄(*n*-Bu₂eddp)] but not with cisplatin, implying involvement of necrotic cell death in novel drug action (Fig. 2A, right panel).

Having in mind that observed necrosis could be a primary mode of drug action but also a secondary event due to induction of apoptosis in cell cultures, cells were treated with 40 μM of each compound and cell viability as well as LDH release were determined in indicated time points. It is obvious that reduction of mitochondrial respiration in cultures exposed to [PtCl₄(*n*-Bu₂eddp)] preceded the decrease of cell viability (Fig. 2B). In parallel with this, early detection of LDH in culture supernatants (after 3 h) indicated that one of the leading events in novel drug anti-cancer action is disturbance of cell membrane permeability.

In addition, Annex/PI double staining of cells treated with [PtCl₄(*n*-Bu₂eddp)] or cisplatin revealed the presence of early as well as late apoptosis after 18 h of incubation (Fig. 3A). The effect was more pronounced in cultures treated with [PtCl₄(*n*-Bu₂eddp)].

Concordantly, intensive, time dependent fragmentation of DNA, marked as an elevated percentage of hypodiploid cells in the subG compartment, was evident upon the treatment with [PtCl₄(*n*-Bu₂eddp)] (Fig. 3B). Pertinent to this, the presence of apoptotic cells was further confirmed by PI staining of

Appendix 5

Reproduced from Ref. D. Maksimović-Ivanić, S. Mijatović, I. Mirkov, S. Stošić-Grujičić, D. Miljković, T.J. Sabo, V. Trajković, G.N. Kaluđerović, *Metallomics* 2012, 4, 1155 with permission from The Royal Society of Chemistry.

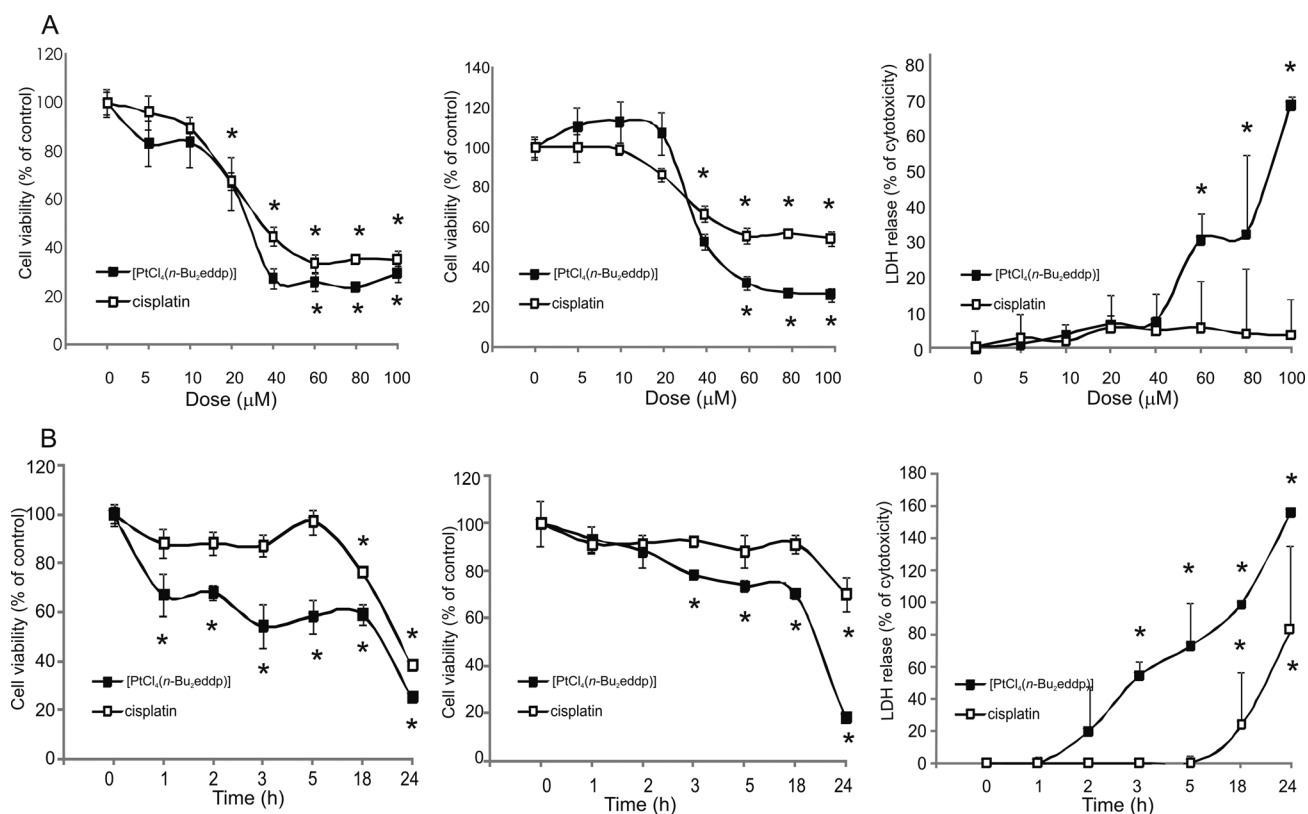


Fig. 2 The effect of [PtCl₄(n-Bu₂eddp)] on B16 cell viability. Cells (1×10^4 per well) were treated with a range of concentrations of tested compounds for 24 h, and cell viability was determined by MTT (left panel) and CV (middle panel), and LDH release was measured in the supernatants of the same cultures (right panel). Alternatively cells were treated with 40 μM of the compounds and viability and LDH release were determined in indicated time points (B). The data are presented as mean from representative of three independent experiments, **p* < 0.05 refers to untreated cultures.

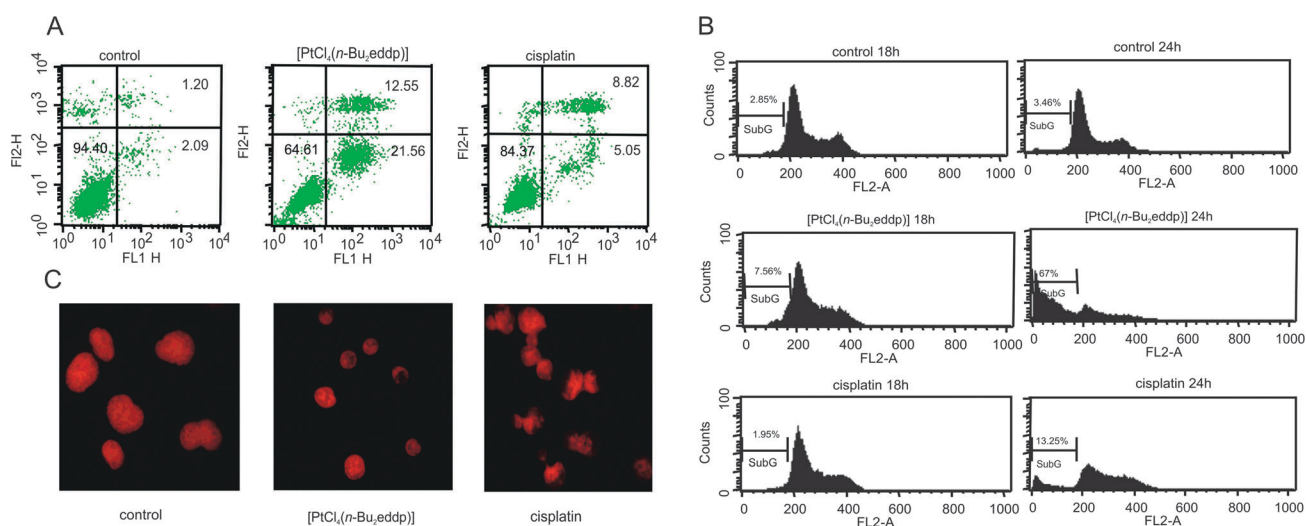


Fig. 3 The effect of [PtCl₄(n-Bu₂eddp)] on B16 cell death. Cells were treated with 40 μM of the compounds and Annexin/PI double staining after 18 h (A), cell cycle distribution after 18 and 24 h (B) and PI staining after 24 h (C) were performed.

chamber slides (Fig. 3C). Morphological changes typical for cells that underwent the process of apoptosis were obvious in cultures exposed to both compounds.

In vivo studies

To evaluate the novel drug efficacy *in vivo*, tumors were induced in syngeneic strain of C57BL/6 mice and the treatment

started when tumors were palpable. After 24 days from induction of the disease, animals were sacrificed and tumor volumes were calculated. As seen in Fig. 4 animals receiving [PtCl₄(n-Bu₂eddp)] displayed significantly lower tumor volume in comparison to control. On the other hand, 3 animals treated with cisplatin died before the execution while animals which survived the treatment showed higher tumor volume in comparison

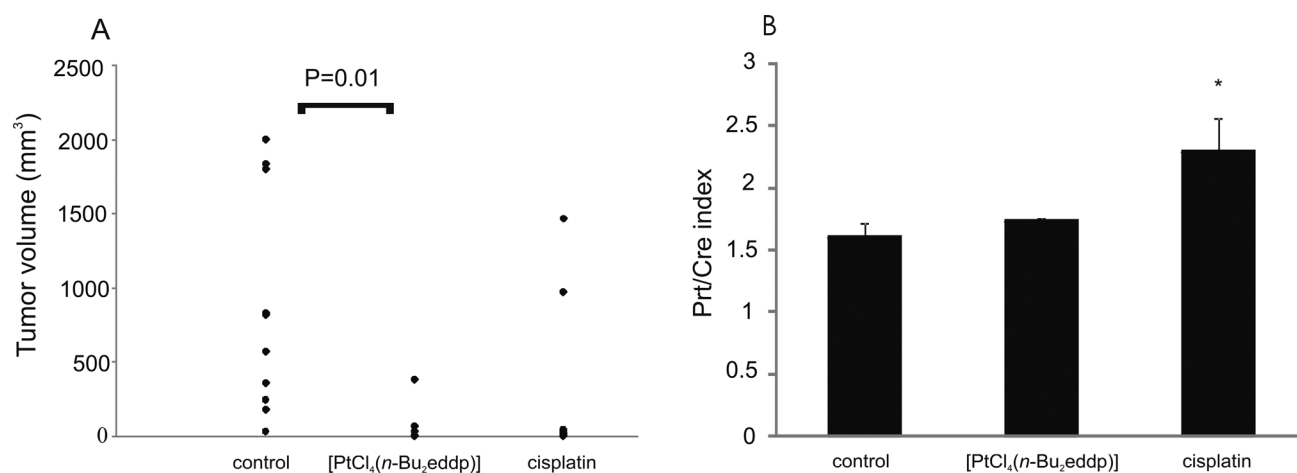


Fig. 4 The effect of [PtCl₄(n-Bu₂eddp)] on B16 cell growth in C57BL/6 mice. Tumors were induced by s.c. implantation of 2×10^5 B16 melanoma cells, and either cisplatin or [PtCl₄(n-Bu₂eddp)] was injected i.p. every second day starting on day 11 following tumor implantation ($n = 10$ animals in control, $n = 6$ animals in cisplatin and $n = 8$ in [PtCl₄(n-Bu₂eddp)] treated groups). Tumors were harvested, and tumor volumes calculated 24 d after tumor implantation (A). Protein/creatinine concentrations were measured in urine of animals on day 24 (B).

to those treated with [PtCl₄(n-Bu₂eddp)]. In urine of animals exposed to cisplatin an elevated protein/creatinine ratio was detected, indicating disturbance in glomerular filtration. Animals treated with [PtCl₄(n-Bu₂eddp)] have a similar Prt/Cre index as nontreated control as well as healthy animals suggesting that they have preserved kidney function.

One of the most serious adverse effects of cisplatin treatment is nephrotoxicity. Studies on rodents specify that cisplatin undergoes metabolic activation in the kidney to a more potent toxin through biochemical transformation in contact with a proximal tubule cell membrane and high affinity to copper transporter Ctr1 remarkably expressed on the basolateral membrane of these cells.²⁵ As a consequence of this, concentrations within the kidney exceed those in blood suggesting an active accumulation of drug in renal parenchymal cells. The fact that novel compound did not disturb renal function under the same therapeutic regiment *in vivo* indicated different biochemical features and even affinity to membrane transporters precisely overexpressed in this tissue resulting in less intracellular destruction at the level of glomerular filtration. Overcoming nephrotoxicity, which is one of the most serious limitations of cisplatin application,^{9,10,26–28} together with enhanced antitumor potential of novel compound present the hopeful baseline for future investigation of this substance class in cancer treatment.

Conclusions

Herein it is shown that [PtCl₄(n-Bu₂eddp)] exhibits dose- and time-dependent cytotoxic effects with significantly faster activity than cisplatin against B16 melanoma cells *in vitro* with induction of both necrotic and apoptotic cell death. *In vivo*, results clearly illustrate that [PtCl₄(n-Bu₂eddp)] is more effective than cisplatin at reducing tumour cell growth in syngeneic strain of C57BL/6 mice at their respective dose (4 mg kg^{-1} and 2 mg kg^{-1}), when compared to drug untreated animals. Furthermore, significant difference was observed in kidney damage, the investigated platinum(IV) complex did not show any sign of nephrotoxicity making a promising candidate for the further studies which may provide improved treatment options.

Acknowledgements

We gratefully acknowledge financial support from the Ministry of Education and Science of Serbia (Grant no. 173013 and 172035).

Notes and references

- B. Rosenberg, L. Van Camp, J. E. Trosko and V. H. Mansour, *Nature*, 1969, **222**, 385–386.
- F. Arnesano and G. Natile, *Coord. Chem. Rev.*, 2009, **253**, 2070–2081.
- T. W. Hambley, *Dalton Trans.*, 2007, 4929–4937.
- M. E. Kelly, A. Dietrich, S. Gómez-Ruiz, B. Kalinowski, G. N. Kaluđerović, T. Mueller, R. Paschke, J. Schmidt, D. Steinborn, C. Wagner and H. Schmidt, *Organometallics*, 2008, **27**, 4917–4927.
- I. Ott and R. Gust, *Arch. Pharm. (Weinheim, Ger.)*, 2007, **340**, 117–126.
- S. Komeda and A. Casini, *Curr. Top. Med. Chem.*, 2012, **12**, 219–235.
- C. Monneret, *Ann. Pharm. Fr.*, 2011, **69**, 286–295.
- S. Gómez-Ruiz, D. Maksimović-Ivanić, S. Mijatović and G. N. Kaluđerović, *Bioinorg. Chem. Appl.*, 2012, 140284.
- G. Giaccone, *Drugs*, 2000, **59**, 9–17, 37, 38.
- N. Lameire, V. Kruse and S. Rottey, *Acta Clin. Belg.*, 2011, **66**, 337–345.
- M. A. Fuertes, C. Alonso and J. M. Pérez, *Chem. Rev.*, 2003, **103**, 645–662.
- A. G. Eliopoulos, D. J. Kerr, J. Herod, L. Hodgkins, S. Krajewski, J. C. Reed and L. S. Young, *Oncogene*, 1995, **1**, 1217–1228.
- G. N. Kaluđerović and R. Paschke, *Curr. Med. Chem.*, 2011, **18**, 4738–4752.
- L. Kelland, *Nat. Rev. Cancer*, 2007, **7**, 573–584.
- G. N. Kaluđerović, H. Schmidt, D. Steinborn and T. J. Sabo, in *Inorganic Biochemistry: Research Progress*, ed. J. G. Huges and A. J. Robinson, Nova Science Publishers Inc, Hauppauge NY, 2008, pp. 305–326.
- S. Mijatović, D. Maksimović-Ivanić, J. Radović, D. Miljković, G. N. Kaluđerović, T. J. Sabo and V. Trajković, *Cell. Mol. Life Sci.*, 2005, **62**, 1275–1282.
- G. N. Kaluđerović, V. M. Đinović, Z. D. Juranić, T. P. Stanojković and T. J. Sabo, *J. Inorg. Biochem.*, 2005, **99**, 488–496.
- G. N. Kaluđerović, D. Miljković, M. Momčilović, V. M. Đinović, M. M. Stojković, T. J. Sabo and V. Trajković, *Int. J. Cancer*, 2005, **116**, 479–486.
- L. E. Mihajlović, A. Savić, J. Poljarević, I. Vučković, M. Mojić, M. Bulatović, D. Maksimović-Ivanić, S. Mijatović, G. N. Kaluđerović,

Appendix 5

Reproduced from Ref. D. Maksimović-Ivanić, S. Mijatović, I. Mirkov, S. Stošić-Grujičić, D. Miljković, T.J. Sabo, V. Trajković, G.N. Kaluđerović, *Metallomics* 2012, 4, 1155 with permission from The Royal Society of Chemistry.

- S. Stošić-Grujičić, D. Miljković, S. Grgurić-Šipka and T. J. Sabo, *J. Inorg. Biochem.*, 2012, **109**, 40–48.
- 20 G. N. Kaluđerović, S. Mijatović, B. B. Zmekovski, M. Z. Bulatović, S. Gómez-Ruiz, M. Mojić, D. Steinborn, D. Miljković, H. Schmidt, S. D. Stošić-Grujičić, T. J. Sabo and D. Maksimović-Ivanić, *Metallomics*, 2012, **4**, 979–987.
- 21 T. J. Sabo, G. N. Kaluđerović, S. R. Grgurić-Šipka, F. W. Heinemann and S. R. Trifunović, *Inorg. Chem. Commun.*, 2004, **7**, 241–244.
- 22 D. Maksimovic-Ivanic, S. Mijatovic, L. Harhaji, D. Miljkovic, D. Dabideen, K. Fan Cheng, K. Mangano, G. Malaponte, Y. Al-Abed, M. Libra, G. Garotta and F. Nicoletti, *Mol. Cancer Ther.*, 2008, **7**, 510–520.
- 23 K. Spencer, *Ann. Clin. Biochem.*, 1986, **23**, 1–25.
- 24 M. M. Bradford, *Anal. Biochem.*, 1976, **72**, 248–254.
- 25 R. P. Miller, R. K. Tadagavadi, G. Ramesh and W. B. Reeves, *Toxins*, 2010, **2**, 2490–2518.
- 26 X. Yao, K. Panichpisal, N. Kurtzman and K. Nugent, *Am. J. Med. Sci.*, 2007, **334**, 115–124.
- 27 I. Arany and R. L. Safirstein, *Semin. Nephrol.*, 2003, **23**, 460–464.
- 28 N. Pabla and Z. Dong, *Oncotarget*, 2012, **3**, 107–111.



Cytotoxic studies of substituted titanocene and *ansa*-titanocene anticancer drugs

Santiago Gómez-Ruiz^{a,*}, Goran N. Kaluđerović^{b,*}, Sanjiv Prashar^a, Dorian Polo-Cerón^a, Mariano Fajardo^a, Željko Žižak^c, Tibor J. Sabo^d, Zorica D. Juranić^c

^aDepartamento de Química Inorgánica y Analítica, E.S.C.E.T., Universidad Rey Juan Carlos, 28933 Móstoles, Madrid, Spain

^bDepartment of Chemistry, Institute of Chemistry, Technology and Metallurgy, Studentski trg 14, 11000 Belgrade, Serbia

^cInstitute of Oncology and Radiology of Serbia, 11000 Belgrade, Serbia

^dFaculty of Chemistry, University of Belgrade, P.O. Box 158, 11001 Belgrade, Serbia

Received 14 December 2007; received in revised form 23 January 2008; accepted 4 February 2008

Available online 12 February 2008

Abstract

A variety of substituted titanocene and *ansa*-titanocene complexes have been synthesized and characterized using traditional methods. The cytotoxic activity of the different titanocene complexes was tested against tumour cell lines human adenocarcinoma HeLa, human myelogenous leukemia K562, human malignant melanoma Fem-x and normal immunocompetent cells, peripheral blood mononuclear cells PBMC. Alkenyl substitution, either on the cyclopentadienyl ring or on the silicon-atom *ansa*-bridge of the titanocene compounds [Ti{Me₂Si(η⁵-C₅Me₄)(η⁵-C₅H₃{CMe₂CH₂CH₂CH=CH₂)})Cl₂] (**8**), [Ti{Me(CH₂=CH)Si(η⁵-C₅Me₄)(η⁵-C₅H₄)Cl₂] (**9**) and [Ti(η⁵-C₅H₄{CMe₂CH₂CH₂CH=CH₂)₂Cl₂] (**12**) showed higher cytotoxic activities (IC₅₀ values from 24 ± 3 to 151 ± 10 μM) relative to complexes bearing an additional alkenyl-substituted silyl substituent on the silicon bridge [Ti{Me{(CH₂=CH)Me₂SiCH₂CH₂}Si(η⁵-C₅Me₄)(η⁵-C₅H₄)Cl₂] (**10**) and [Ti{Me{(CH₂=CH)₃SiCH₂CH₂}Si(η⁵-C₅Me₄)(η⁵-C₅H₄)Cl₂] (**11**) which causes a dramatic decrease of the cytotoxicity (IC₅₀ values from 155 ± 9 to >200 μM). In addition, the synthesis of the analogous niobocene complex [Nb(η⁵-C₅H₄{CMe₂CH₂CH₂CH=CH₂)₂Cl₂] (**13**), is described. Structural studies based on DFT calculations of the most active complexes **8**, **9** and **12** and the X-ray crystal structure of **13** are reported.

© 2008 Elsevier Inc. All rights reserved.

Keywords: Anticancer drugs; Titanocene; Adenocarcinoma HeLa; Human myelogenous leukemia K562; Human malignant melanoma Fem-x

1. Introduction

Bioorganometallic chemistry has emerged in the last decade as an important new field of medicinal chemistry [1]. While ferroquine type complexes [2,3] have received some attention regarding their anti-malarial properties, there has been slow progress in cytotoxic studies with organometallic compounds compared to studies with organic compounds and inorganic platinum species [4–10]. From

the pioneering work of Köpf and Köpf–Maier, who discovered the potential of organometallic compounds such as metallocene dihalides as a new class of compounds with potential anticancer properties 30 years ago [11–20], phase I clinical trials carried out for titanocene dichloride in 1993 [21–25] followed and has consequently triggered development of similar compounds [26,27]. Nephrotoxicity was always identified as the dose-limiting side effect using titanocene-based antitumor agents; however, the absence of any effect on proliferative activity of the bone marrow cells, the most usual dose-limiting side-effect of organic drugs, was a very promising result that suggested the potential of titanocene dichlorides as additives in combination therapy. Unfortunately, clinical trials in patients with

* Corresponding authors. Fax: +34 914888143 (S. Gómez-Ruiz), +38 111636061 (G.N. Kaluđerović).

E-mail addresses: santiago.gomez@urjc.es (S. Gómez-Ruiz), goran@chem.bg.ac.yu (G.N. Kaluđerović).

metastatic renal-cell carcinoma [28] or metastatic breast cancer [29] did not have a successful outcome. Alternatively, many biological experiments have demonstrated that titanium derived from administered titanocene dichloride accumulates in the nucleic acid rich regions of tumour cells [30–32] and exhibits pronounced inhibition of nucleic acid synthesis [14,30–32], suggesting that DNA is the biological target of titanocene compounds. Studies reported by Sadler and coworkers [33–36], have provided a plausible mechanisms for the delivery of Ti(IV) species to the cell nucleus assisted by the major iron transport protein, “transferrin”.

On the other hand, the current efforts in the chemistry of titanocenes are focused on the design of new compounds with different substituents which may increase their cytotoxicity [37–41]. Synthesis starting from titanium dichloride and fulvenes [42–45] led to substituted *ansa*-titanocenes with a carbon–carbon bridge [46–49]. Using similar synthetic paths, many different substituted complexes were prepared and tested as anticancer drugs [50–64]. Most of the analyzed titanocene complexes have polar substituents on the cyclopentadienyl ring such as alkoxo, amino, or electron withdrawing groups which have demonstrated, in some cases, very high activity in antitumoral tests. However, Köpf and coworkers discarded alkyl, alkenyl or aryl substituted *ansa*-titanocene complexes based on preliminary test results reported which showed a lack of cytotoxicity [65]. Thus, these complexes have not been extensively screened for their antiproliferative activity. This low cytotoxicity was assumed to be associated to the absence of polar groups in their structure, which would increase the Lewis acidity of the titanium atoms and hence enhance interaction with Lewis base sites in DNA. However, we have recently communicated, in our preliminary results, a moderate cytotoxicity of alkenyl-substituted silicon-bridge *ansa*-titanocene compounds against tumour cell lines human adenocarcinoma HeLa, human myelogenous leukemia K562 and human malignant melanoma Fem-x [66]. These investigations have been extended to other new alkyl, aryl and alkenyl substituted complexes, in order to understand the possible relationship between cytotoxic activity and the substituents on either the cyclopentadienyl ring or the silicon atom-*ansa*-bridge. The present results show an increase of the cytotoxicity for titanocene and *ansa*-titanocene complexes that have alkenyl substituents on the cyclopentadienyl rings.

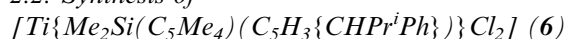
2. Experimental

2.1. General manipulations

All reactions were performed using standard Schlenk tube techniques in an atmosphere of dry nitrogen. Solvents were distilled from the appropriate drying agents and degassed before use. $C_5H_2Me_4$, $Li(C_5H_4Bu^t)$, $[TiCl_4(THF)_2]$, $[NbCl_4(THF)_2]$, $SiMe_2Cl_2$, $HSiMeCl_2$, $Si(CH=CH_2)MeCl_2$, $Si(CH=CH_2)_2Me_2$, $Si(CH=CH_2)_4$,

$GeMe_2Cl_2$, $LiBu^n$ (1.6 M in hexane), $LiMe$ (1.6 M in Et_2O), $LiPh$ (2.0 M in Bu^t_2O), and $CH_3COCH_2CH_2CH=CH_2$ were purchased from Aldrich. All the commercial reagents were used directly. $Na(C_5H_5)$ and $Na(C_5H_4Me)$ were prepared according to literature procedures [67]. 6-(Methyl),6-(4-buten-1-yl)fulvene, 6-(Bu^t)fulvene and 6-(Pr^i)fulvene were prepared using the methodology described by Little and co-workers [68]. The titanocene complexes $[Ti\{Me_2Si(\eta^5-C_5Me_4)(\eta^5-C_5H_4)\}Cl_2]$ (1) [69], $[Ti\{Me_2Ge(\eta^5-C_5Me_4)(\eta^5-C_5H_4)\}Cl_2]$ (2) [70], $[Ti\{Me(H)Si(\eta^5-C_5Me_4)_2\}Cl_2]$ (3) [71], $[Ti\{Me_2-Si(\eta^5-C_5Me_4)(\eta^5-C_5H_3Me)\}Cl_2]$ (4) $[Ti\{Me_2-Si(\eta^5-C_5Me_4)(\eta^5-C_5H_3Bu^t)\}Cl_2]$ (5) [72], $[Ti\{Me_2Si(\eta^5-C_5Me_4)(\eta^5-C_5H_3\{CMe_2CH_2CH_2CH=CH_2\})\}Cl_2]$ (8) [73], and $[Ti\{Me(CH_2=CH)Si(\eta^5-C_5Me_4)(\eta^5-C_5H_4)\}Cl_2]$ (9) [74] were prepared by the reaction of the corresponding di-lithium salts and $[TiCl_4(THF)_2]$ according to synthetic methods described by us. The complexes $[Ti\{Me\{(\text{CH}_2=CH)Me_2SiCH_2CH_2\}Si(\eta^5-C_5Me_4)(\eta^5-C_5H_4)\}Cl_2]$ (10) and $[Ti\{Me\{(\text{CH}_2=CH)_3SiCH_2CH_2\}Si(\eta^5-C_5Me_4)(\eta^5-C_5H_4)\}Cl_2]$ (11) were synthesized via the hydrosilylation reaction of $[Ti\{Me(H)Si(\eta^5-C_5Me_4)(\eta^5-C_5H_4)\}Cl_2]$ and $Si(CH=CH_2)_2Me_2$ or $Si(CH=CH_2)_4$, respectively, as we have previously reported [71]. IR spectra were recorded on a Thermo Nicolet Avatar 330 FT-IR spectrophotometer. 1H and $^{13}C\{^1H\}$ NMR spectra were recorded on a Varian Mercury FT-400 spectrometer. Microanalyses were carried out with a Perkin-Elmer 2400 or LECO CHNS-932 microanalyzer. Mass spectroscopic analyses were performed on a Hewlett–Packard 5988A (*m/z* 50–1000) instrument.

2.2. Synthesis of



$Li_2\{Me_2Si(C_5Me_4)(C_5H_3\{CHPr^iPh\})\}$ [75] (1.00 g, 2.57 mmol) was added dropwise over 15 min to a solution of $[TiCl_4(THF)_2]$ (0.86 g, 2.57 mmol) in THF (50 mL) at 0 °C. The reaction mixture was allowed to warm to room temperature before stirring under reflux for 18 h. Solvent was then removed *in vacuo* and toluene (120 mL) was added to the resulting solid. The mixture was filtered and the filtrate concentrated (20 mL) and cooled to –30 °C to give crystals of the title complex. Yield: 0.74 g, 59%. Isolated isomer: 1H NMR (400 MHz, $CDCl_3$, 25 °C): δ 0.89, 0.91 (s, 3H, $SiMe_2$), 0.83, 0.96 (d, 3H, $CHMe_2$), 2.49 (m, 1H, $CHMe_2$), 1.85, 1.91, 2.11, 2.21 (s, 3H, C_5Me_4), 4.41 (d, 1H, $CHPr^iPh$), 5.46, 5.54, 6.56 (m, 1H, C_5H_3), 7.15 (2H), 7.24 (2H), 7.28 (1H) (m, *Ph*). $^{13}C\{^1H\}$ NMR (100 MHz, $CDCl_3$, 25 °C): δ –0.5, –0.1 ($SiMe_2$), 13.6, 13.7, 21.9, 22.0 (C_5Me_4), 16.4, 18.5, 31.7 (Pr^i), 52.5 (CpC), 96.7, 102.5 ($C^1 - Cp$), 115.8, 116.5, 130.2, 131.6 (C_5H_3), 137.9, 142.6, 143.3, 148.8 (C_5Me_4), 126.0, 127.4, 130.5, 140.9 (*Ph*). EI-MS (*m/e* (relative intensity)): 492 (6) $[M^+]$, 457 (12) $[M^+ - Cl]$, 449 (31) $[M^+ - Pr^i]$, 420 (100) $[M^+ - 2 \times Cl]$, 377 (12) $[M^+ - 2 \times Cl - Pr^i]$. $C_{26}H_{34}Cl_2SiTi$ (493.4): calc. C, 63.29; H, 6.95; found C, 63.00; H, 6.92%.

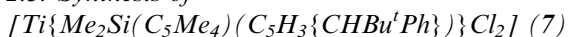
Appendix 6

Reproduced from Ref. S. Gómez-Ruiz, G.N. Kaluderović, S. Prashar, D. Polo-Cerón, M. Fajardo, Ž. Žižak, T.J. Sabo, Z.D. Juranić, J. Inorg. Biochem. 2008, 102, 1558 with permission from Elsevier.

1560

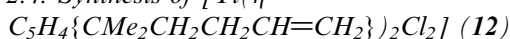
S. Gómez-Ruiz et al. / Journal of Inorganic Biochemistry 102 (2008) 1558–1570

2.3. Synthesis of



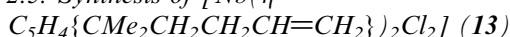
The synthesis of **7** was carried out in an identical manner to **6**. $[TiCl_4(THF)_2]$ (0.81 g, 2.44 mmol) and $Li_2\{Me_2Si(C_5Me_4)(C_5H_3\{CHBu^tPh\})\}$ [75] (1.00 g, 2.44 mmol). Yield: 0.83 g, 68%. Isolated isomer: 1H NMR (400 MHz, $CDCl_3$, 25 °C): δ 0.82, 0.99 (s, 3 H, $SiMe_2$), 1.11 (s, 9H, Bu^t), 1.93, 2.01, 2.08, 2.17 (s, 3H, C_5Me_4), 4.41 (s, 1H, $CHBu^tPh$), 4.89, 5.71, 7.12 (m, 1H, C_5H_3), 7.19 (2H), 7.26 (2H), 7.29 (1H) (m, Ph). $^{13}C\{^1H\}$ NMR (100 MHz, $CDCl_3$, 25 °C): δ -0.6, -0.2 ($SiMe_2$), 13.4, 13.7, 16.0, 16.4 (C_5Me_4), 29.5, 35.0 (Bu^t), 57.2 (CpC), 96.7, 102.4 (C^1-Cp), 118.0, 118.4, 125.7, 127.1 (C_5H_3), 131.6, 132.3, 143.6, 149.8 (C_5Me_4), 125.9, 130.1, 136.7, 141.8 (Ph). EI-MS (*m/e* (relative intensity)): 506 (5) [M^+], 449 (59) [M^+-Bu^t], 414 (16) [M^+-Bu^t-Cl], 211 (32) [$M^+-Cl-C_5H_3(CHBu^tPh)$]. $C_{27}H_{36}Cl_2SiTi$ (507.4): calc. C, 63.91; H, 7.15; found C, 63.49; H, 7.01%.

2.4. Synthesis of $[Ti(\eta^5-$



The synthesis of **12** was carried out in an identical manner to **6**. $[TiCl_4(THF)_2]$ (1.98 g, 5.95 mmol) and $Li\{C_5H_4(CMe_2\{CH_2CH_2CH=CH_2\})\}$ [73] (2.00 g, 11.89 mmol) Yield 1.23 g, 47%. IR (ZnSe): $\nu = 3109$ (ν_{CH}), 1641 ($\nu_{CH=CH_2}$) cm^{-1} . 1H NMR (400 MHz, $CDCl_3$, 25 °C): δ 1.39 (s, 12 H, CMe_2), 1.56, 1.76 (m, 8H, CH_2CH_2), 4.89 (*cis*), 4.94 (*trans*) (dd, $^3J_{cis} = 10.2$ Hz, $^3J_{trans} = 17.2$ Hz, 4H, $CH_2-CH=CH_2$), 5.70 (m, 2H, $CH_2-CH=CH_2$), 6.55, 6.72 (m, 8H, C_5H_4). $^{13}C\{^1H\}$ NMR (100 MHz, $CDCl_3$, 25 °C): δ 27.2, 29.1 (CH_2CH_2), 37.7 (CMe_2), 46.5 (CpC), 117.9, 121.0, 147.6 (C_5H_4), 114.6 ($CH_2-CH=CH_2$), 138.8 ($CH_2-CH=CH_2$). EI-MS: *m/z* (%) = 441 (3) [M^+], 279 (100) [$M^+-C_5H_4(CMe_2(CH_2CH_2CH=CH_2))$], 181 (22) [$M^+-C_5H_4(CMe_2(CH_2CH_2CH=CH_2))-CH_2CH_2CH=CH_2$]. $C_{24}H_{34}Cl_2Ti$ (441.3): calcd. C 65.32, H 7.77; found C 65.80, H 7.55.

2.5. Synthesis of $[Nb(\eta^5-$



The synthesis of **13** was carried out in an identical manner to **6**. $[NbCl_4(THF)_2]$ (2.25 g, 5.95 mmol) and $Li\{C_5H_4(CMe_2\{CH_2CH_2CH=CH_2\})\}$ [73] (2.00 g, 11.89 mmol) Yield 1.99 g, 69%. IR (ZnSe): $\nu = 3103$ (ν_{CH}), 1629 ($\nu_{CH=CH_2}$) cm^{-1} . EI-MS: *m/z* (%) = 486 (12) [M^+], 449 (24) [M^+-H-Cl], 415 (31) [$M^+-H-2\times Cl$], 323 (100) [$M^+-C_5H_4(CMe_2(CH_2CH_2CH=CH_2))$]. $C_{24}H_{34}Cl_2Nb$ (486.3): calcd. C 59.27, H 7.05; found C 59.11, H 7.03.

2.6. Data collection and structural refinement of **13**

The data of **13** were collected with a CCD Oxford Xcalibur S ($\lambda(MoK\alpha) = 0.71073$ Å) using ω and φ scans mode.

Semi-empirical from equivalents absorption corrections were carried out with SCALE3 ABSPACK [76]. All the structures were solved by direct methods [77]. Structure refinement was carried out with SHELXL-97 [78]. All non-hydrogen atoms were refined anisotropically, and hydrogen atoms were located by difference maps and refined isotropically. Table 1 lists crystallographic details.

2.7. Computational details

All DFT calculations were performed by employing the Gaussian 03 program package [79] using the B3LYP functional [80–83]. The 6-31 G^{**} basis set was used for all atoms [84–87]. The appropriateness of the chosen functional and basis set for titanium complexes have been stated elsewhere [57,59,88]. All systems have been optimized without symmetry restrictions. The resulting geometries were characterized as equilibrium structures by the analysis of the force constants of normal vibrations (see Supplementary material).

2.8. In vitro studies

2.8.1. Preparation of solutions of drugs

Stock solutions of investigated titanium complexes were made in dimethyl sulfoxide (DMSO) at a concentration of 10 mM, filtered through Millipore filter, 0.22 μ m, before use, and diluted by nutrient medium to various working concentrations. DMSO was used due to solubility problems. Nutrient medium was RPMI 1640 medium, without phenol red, supplemented with L-glutamine

Table 1
Crystallographic data for **13**

	13
Formula	$C_{24}H_{34}Cl_2Nb$
Fw	486.32
<i>T</i> (K)	130(2)
Crystal system	Monoclinic
Space group	<i>I2/a</i>
<i>a</i> (pm)	1380.46(5)
<i>b</i> (pm)	663.90(2)
<i>c</i> (pm)	2608.01(11)
β (deg)	102.587(4)
<i>V</i> (nm ³)	2.33276(15)
<i>Z</i>	4
<i>D_c</i> (Mg m ⁻³)	1.385
μ (mm ⁻¹)	0.752
<i>F</i> (000)	1012
Crystal dimensions (mm)	0.4 × 0.05 × 0.02
θ range (deg)	3.02–28.28
<i>hkl</i> ranges	−18 ≤ <i>h</i> ≤ 18, −8 ≤ <i>k</i> ≤ 8, −32 ≤ <i>l</i> ≤ 34
Data/parameters	2903/125
Goodness-of-fit on <i>F</i> ²	0.969
Final <i>R</i> indices [<i>I</i> > 2σ(<i>I</i>)]	0.0396
<i>R</i> indices (all data)	0.0713
Largest diff. peak and hole (e Å ⁻³)	0.718/−0.573

Appendix 6

Reproduced from Ref. S. Gómez-Ruiz, G.N. Kaluđerović, S. Prashar, D. Polo-Cerón, M. Fajardo, Ž. Žižak, T.J. Sabo, Z.D. Juranić, J. Inorg. Biochem. 2008, 102, 1558 with permission from Elsevier.

S. Gómez-Ruiz et al. / Journal of Inorganic Biochemistry 102 (2008) 1558–1570

1561

(3 mM), streptomycin (100 µg/mL), and penicillin (100 IU/mL), 10% fetal bovine serum (FBS) and 25 mM Hepes, and was adjusted to pH 7.2 by bicarbonate solution. MTT, 3-(4,5-dimethylthiazol-2-yl)-2,5-diphenyl tetrazolium bromide was dissolved (5 mg/mL) in phosphate buffer saline pH 7.2, and filtered through Millipore filter, 0.22 µm, before use. All reagents were purchased from Sigma Chemicals.

2.8.2. Cell culture

Human cervix adenocarcinoma HeLa and malignant melanoma Fem-x cells were cultured as monolayers in the nutrient medium, while human myelogenous leukemia K562 cells were maintained as suspension culture. The cells were grown at 37 °C in 5% CO₂ and humidified air atmosphere. Peripheral blood mononuclear cells (PBMC) were separated from whole heparinized blood from a healthy

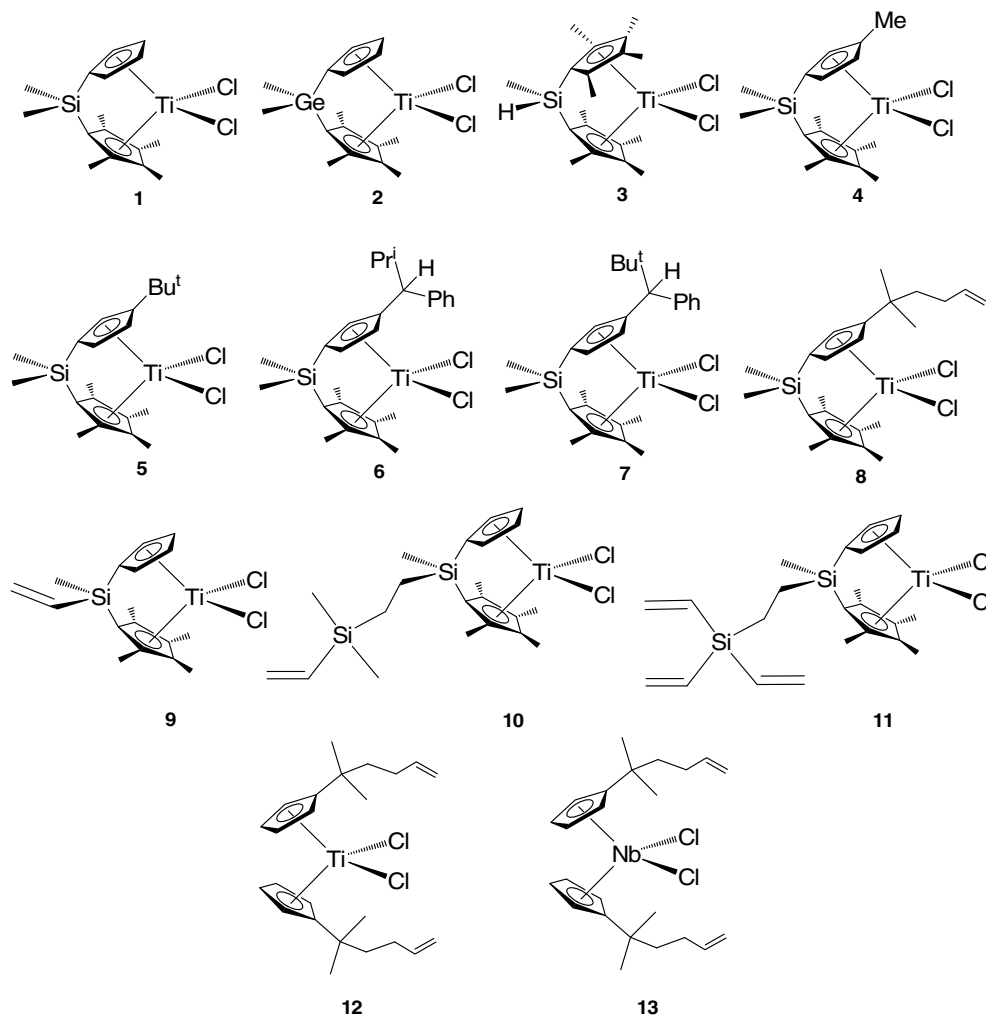
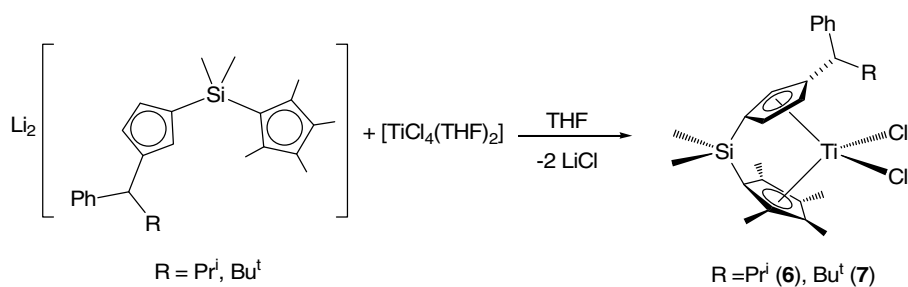


Fig. 1. Metallocene complexes used in the cytotoxicity analysis.



Scheme 1.

Appendix 6

Reproduced from Ref. S. Gómez-Ruiz, G.N. Kaluđerović, S. Prashar, D. Polo-Cerón, M. Fajardo, Ž. Žižak, T.J. Sabo, Z.D. Juranić, J. Inorg. Biochem. 2008, 102, 1558 with permission from Elsevier.

1562

S. Gómez-Ruiz et al. / Journal of Inorganic Biochemistry 102 (2008) 1558–1570

volunteer by Lymphoprep (Nycomed, Oslo, Norway) gradient centrifugation. Interface cells, washed three times with Haemacel (aqueous solution supplemented with 145 mM Na⁺, 5.1 mM K⁺, 6.2 mM Ca²⁺, 145 mM Cl⁻ and 35 g/L gelatine polymers, pH 7.4) were counted and resuspended in nutrient medium.

2.8.3. Cell sensitivity analysis

HeLa and Fem-x cells were seeded (2000 cells per well) into 96-well microtiter plates and 20 h later, after the cell adherence, five different concentrations of investigated compounds were added to the wells. Final concentrations were in the range from 25 to 300 μM for PBMC and 12.5 to 200 μM for all other cell lines. Only nutrient medium was added to the cells in the control wells. Investigated compounds were added to a suspension of leukemia K562 cells (3000 cells per well) 2 h after cell seeding, in the same final concentrations applied to HeLa and Fem-x cells. All experiments were done in triplicate. Nutrient medium with corresponding concentrations of compounds, but void of cells was used as blank. PBMC were seeded (150,000 cells per well) into nutrient medium or in nutrient medium enriched with (5 μg/mL) phytohaemagglutinin (PHA – Welcome Diagnostics, England) in 96-well microtiter plates and 2 h later, investigated compounds were added to the wells, in triplicates, to five final concentrations, except to the control wells where a nutrient medium only was added to the cells. Nutrient medium with corresponding concentrations of compounds, but void of cells was used as blank.

2.8.4. Determination of target cell survival

Cell survival was determined by MTT test according to the method of Mosmann [89] and modified by Ohno and Abe [90], 72 h after the drug addition. Briefly, 20 μL of MTT solution (5 mg/mL in phosphate buffered saline) was added to each well. Samples were incubated for further 4 h at 37 °C in humidified atmosphere with 5% CO₂. Then, 100 μL of 10% SDS was added to the wells. Absorbance was measured at 570 nm the next day. To achieve cell survival (%), absorbance at 570 nm of a sample with cells grown in the presence of various concentrations of agent was divided with absorbance of control sample (the absorbance of cells grown only in nutrient medium), having sub-

tracted from absorbance of a corresponding sample with target cells the absorbance of the blank.

3. Results and discussion

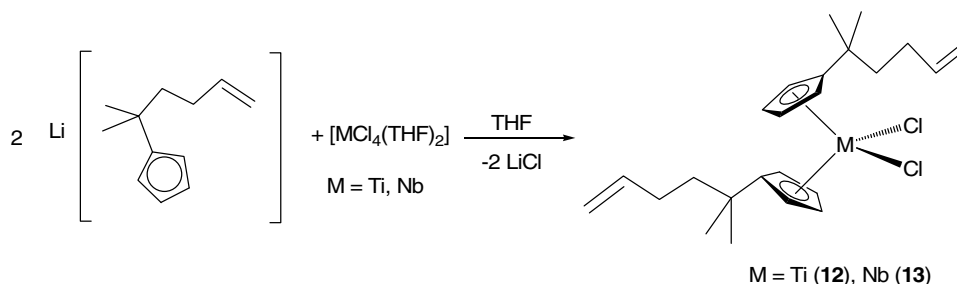
3.1. Synthesis and characterization

The *ansa*-titanocene complexes [Ti{Me₂Si(η⁵-C₅Me₄)(η⁵-C₅H₄)Cl₂}] (**1**) [69], [Ti{Me₂Ge(η⁵-C₅Me₄)(η⁵-C₅H₄)Cl₂}] (**2**) [70], [Ti{Me(H)Si(η⁵-C₅Me₄)₂Cl₂}] (**3**) [71], [Ti{Me₂Si(η⁵-C₅Me₄)(η⁵-C₅H₃Me)}Cl₂}] (**4**) [72], [Ti{Me₂Si(η⁵-C₅Me₄)(η⁵-C₅H₃Bu')}Cl₂}] (**5**) [72], [Ti{Me₂-Si(η⁵-C₅Me₄)(η⁵-C₅H₃{CMe₂CH₂CH₂CH=CH₂)}Cl₂}] (**8**) [73], [Ti{Me(CH₂=CH)Si(η⁵-C₅Me₄)(η⁵-C₅H₄)Cl₂}] (**9**) [74], [Ti{Me{(CH₂=CH)Me₂SiCH₂CH₂}Si(η⁵-C₅Me₄)(η⁵-C₅H₄)Cl₂}] (**10**) [71] and [Ti{Me{(CH₂=CH)₃SiCH₂CH₂-Si(η⁵-C₅Me₄)(η⁵-C₅H₄)Cl₂}] (**11**) [71] (Fig. 1) were prepared according to the different synthetic methods described by our research group.

[Ti{Me₂Si(η⁵-C₅Me₄)(η⁵-C₅H₃{CHPr^{*r*}Ph)}Cl₂}] (**6**) and [Ti{Me₂Si(η⁵-C₅Me₄)(η⁵-C₅H₃{CHBu^{*r*}Ph)}Cl₂}] (**7**) were prepared by the reaction of the corresponding *ansa*-dilithium salts Li₂{Me₂Si(C₅Me₄)(C₅H₃{CHPr^{*r*}Ph)}} [75] and Li₂{Me₂Si(C₅Me₄)(C₅H₃{CHBu^{*r*}Ph)}} [75] respectively with [TiCl₄(THF)₂] (1:1) in THF under reflux overnight (Scheme 1).

[Ti(η⁵-C₅H₄{CMe₂CH₂CH₂CH=CH₂})₂Cl₂] (**12**) and [Nb(η⁵-C₅H₄{CMe₂CH₂CH₂CH=CH₂})₂Cl₂] (**13**) were synthesized *via* the reaction of Li(C₅H₄{CMe₂CH₂CH₂CH=CH₂}) [73] and [TiCl₄(THF)₂] or [NbCl₄(THF)₂] (2:1) in THF, respectively (Scheme 2). The NMR, mass and IR spectra showed that all the complexes were isolated as crystalline solids of high purity.

The planar chirality about the monosubstituted cyclopentadienyl ring in **6** and **7** combined with the presence of a chiral centre in the bulky substituent gives rise to the possibility of the formation of two diastereoisomers. NMR spectroscopy confirmed the presence of the two diastereoisomers in the isolated products. The separation of one of the isomers from the mixture was achieved by fractional recrystallization. The ¹H NMR spectra for **6** and **7** gave three multiplets for the protons of the monosubstituted C₅ ring (between ca. 5.1 and 7.0 ppm), four singlets for the methyl groups of the tetramethyl-substituted C₅ ring (between 1.7 and 2.3 ppm), and two singlets



Scheme 2.

Appendix 6

Reproduced from Ref. S. Gómez-Ruiz, G.N. Kaluđerović, S. Prashar, D. Polo-Cerón, M. Fajardo, Ž. Žižak, T.J. Sabo, Z.D. Juranić, J. Inorg. Biochem. 2008, 102, 1558 with permission from Elsevier.

S. Gómez-Ruiz et al. / Journal of Inorganic Biochemistry 102 (2008) 1558–1570

1563

corresponding to the methyl groups of the SiMe_2 bridging unit (between 0.8 and 1.0 ppm). Additional signals were observed for the alkyl substituent, thus, **6** has two doublets at ca. 0.9 ppm and a multiplet at 2.49 ppm for the two diastereotopic methyl groups and proton of the *isopropyl* fragment, respectively. The proton bonded to the chiral carbon atom gave a doublet signal at 4.41 ppm. Three multiplets (between 7.1 and 7.3 ppm) were also recorded for the phenyl moiety of **6**. On the other hand, **7** shows the *tert*butyl signal as a singlet at 1.11 ppm, the proton bonded to the chiral carbon atom gave a singlet signal at 4.41 ppm and three multiplets (between 7.1 and 7.3 ppm) were assigned to the phenyl moiety.

The ^1H NMR spectrum for the non-*ansa* complex **12** showed a singlet at 1.39 ppm (assigned to the two methyl groups) and two multiplets at 6.55 and 6.72 ppm for the cyclopentadienyl protons. In addition the signals assigned to the butenyl fragment were observed as two multiplets at 1.56 and 1.76 ppm (corresponding to the CH_2 alkylic protons), a multiplet at 5.70 ppm (for the proton of the C- γ) and two multiplets at 4.89 and 4.94 ppm (corresponding to the terminal olefinic protons). **6**, **7** and **12** were also characterized by $^{13}\text{C}\{^1\text{H}\}$ NMR spectroscopy, MS and elemental analysis (see Sections 2.2–2.4).

The successful synthesis of paramagnetic niobocene complex **13** was confirmed by elemental analysis, mass spectrometry (see Section 2.5) and also by single crystal X-ray crystal diffraction studies (see Section 3.3).

3.2. Cytotoxic studies

Titanocene complexes from this study **1–4** and **8–12** have been used in order to understand the possible relationship between the different substituents, either on the cyclopentadienyl ring or on the silicon-atom *ansa*-bridge, and the cytotoxic activity. Unfortunately, the cytotoxicity of titanocene **5–7** and niobocene **13** complexes could not be studied due to their lack of solubility.

The *in vitro* cytotoxicities of complexes **1–4** and **8–12** against human adenocarcinoma HeLa (Fig. 2), human myelogenous leukemia K562, human malignant melanoma Fem-x and on normal immunocompetent cells, i.e., on human peripheral blood mononuclear cells were determined by MTT-based assays.

The investigated titanocene anti-tumour agents showed a dose-dependent antiproliferative effect toward all cell lines and on human PBMC and stimulated PBMC (Fig. 3). Estimations based on the IC_{50} values show that

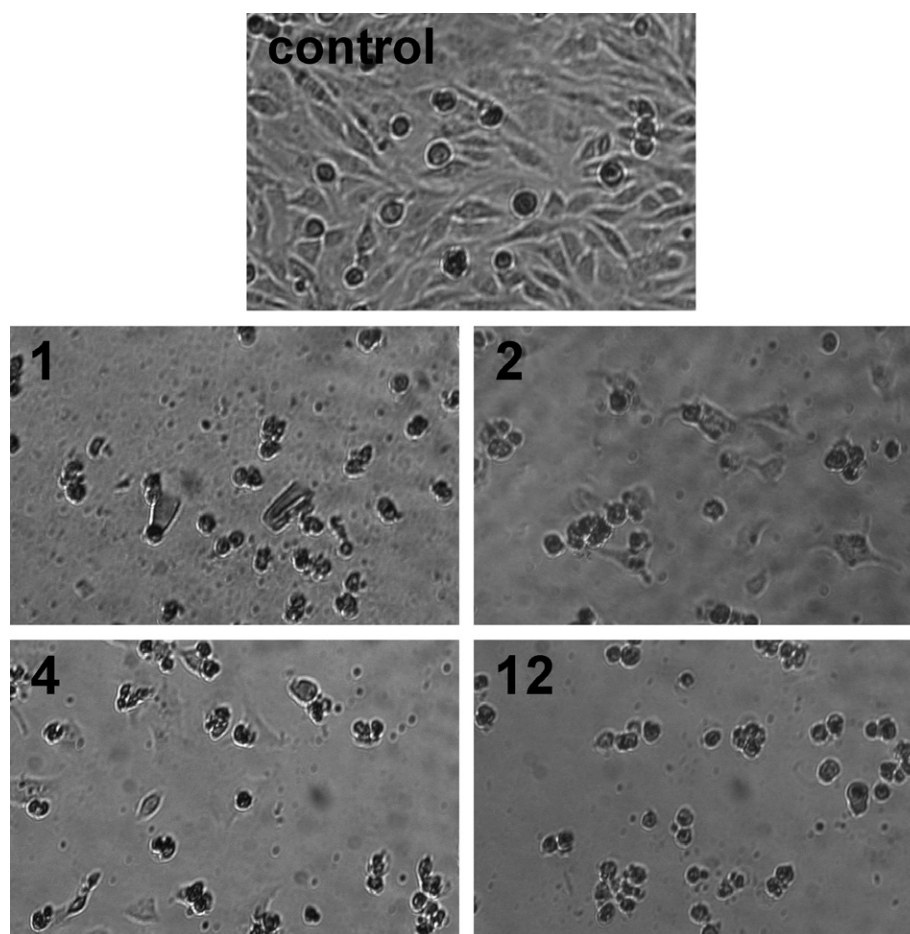


Fig. 2. Photographed under an inverted microscope. Untreated HeLa cells (control) and cells treated for 72 h with 200 μM of **1**, **2**, **4** and **12**.

Appendix 6

Reproduced from Ref. S. Gómez-Ruiz, G.N. Kaluđerović, S. Prashar, D. Polo-Cerón, M. Fajardo, Ž. Žižak, T.J. Sabo, Z.D. Juranić, J. Inorg. Biochem. 2008, 102, 1558 with permission from Elsevier.

1564

S. Gómez-Ruiz et al. / Journal of Inorganic Biochemistry 102 (2008) 1558–1570

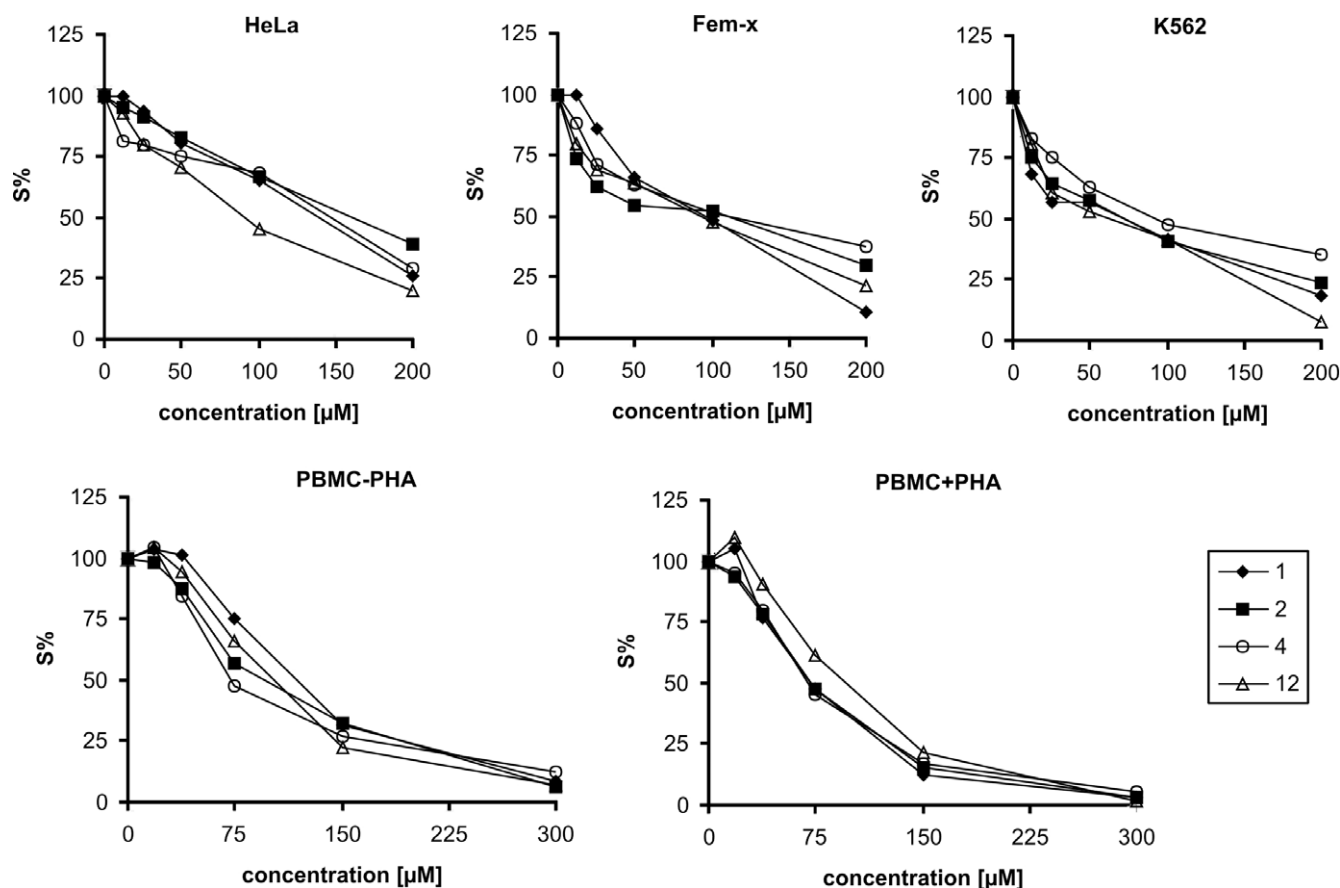


Fig. 3. Representative graphs show survival of HeLa, K562, Fem-x, PBMC and PBMC + PHA (PBMC stimulated with PHA) cells grown for 72 h in the presence of increasing concentrations of some investigated titanium complexes (1, 2, 4 and 12).

almost all complexes (except **11**) are more active against K562 (IC_{50} values from 24 ± 3 to $155 \pm 9 \mu\text{M}$) than against HeLa and Fem-x cells, and that complex **4** is most active against stimulated PBMC (IC_{50} $82 \pm 12 \mu\text{M}$) compared to activity on other cell lines used in this study (Table 2).

Table 2

IC_{50} (μM) for the 72 h of action of investigated compounds and cisplatin [91] on HeLa, K562, Fem-x cells, on PBMC and PBMC stimulated with PHA determined by MTT test

Complex	$IC_{50} \pm SD$				
	HeLa	K562	Fem-x	PBMC	PBMC + PHA
1	135 ± 6	66 ± 6	96 ± 4	112 ± 7	77 ± 6
2	154 ± 4	73 ± 1	106 ± 5	101 ± 6	83 ± 11
3	109 ± 9	59 ± 8	116 ± 9	72 ± 2	87 ± 2
4	117 ± 3	88 ± 4	101 ± 9	83 ± 10	82 ± 12
8	84 ± 9	24 ± 3	89 ± 9	55 ± 8	70 ± 6
9	79 ± 7	64 ± 9	134 ± 18	140 ± 1	151 ± 10
10	189 ± 13	155 ± 9	>200	>200	195 ± 5
11	>200	>200	nd ^a	nd	nd
12	86 ± 3	66 ± 4	99 ± 6	96 ± 3	101 ± 5
Cisplatin	4.4 ± 0.3	5.7 ± 0.3	4.7 ± 0.3	33.6	26 ± 6

The values for complex **3**, **8**, **9** and **10** were previously communicated by us [66].

^a nd – not determined.

The silicon- (**1**) and germanium-bridged (**2**) analogues have similar level of antiproliferative activity on each tumour cell line. In addition, it could be noticed that while **1** has higher activity than **2** on HeLa, K652 and Fem-x cells, **1** and **2** presented almost the same activity on normal immunocompetent cells PBMC, although the differences in the IC_{50} values for these two compounds were in the limits of experimental errors. It seems that the bridge-atom has no remarkable influence on the cytotoxic behaviour.

Complex **4**, (with a methyl group in one of the cyclopentadienyl rings) shows almost the same activity on tumour cell lines as **1**, with the only difference found for PBMC on which **4** is more active (IC_{50} $83 \pm 10 \mu\text{M}$ for **4** and $112 \pm 7 \mu\text{M}$ for **1**). The influence of the methyl group is only perceptible on this cell line.

The titanium complex with the most pronounced *in vitro* antitumoral activity against K562 (IC_{50} $24 \pm 3 \mu\text{M}$), PBMC rested (IC_{50} $55 \pm 8 \mu\text{M}$) and stimulated PBMC (IC_{50} $70 \pm 6 \mu\text{M}$) is compound **8**, which bears an alkenyl-substituent on one of the cyclopentadienyl rings. The presence of the alkenyl substituent leads to an increase of activity on most cell lines (Table 2). On direct comparison with the value for cisplatin ($5.0 \mu\text{M}$) [91], the IC_{50} value for this titanocene shows an approximate five-fold increase on the K562 cell line.

Appendix 6

Reproduced from Ref. S. Gómez-Ruiz, G.N. Kaluđerović, S. Prashar, D. Polo-Cerón, M. Fajardo, Ž. Žižak, T.J. Sabo, Z.D. Juranić, J. Inorg. Biochem. 2008, 102, 1558 with permission from Elsevier.

S. Gómez-Ruiz et al. / Journal of Inorganic Biochemistry 102 (2008) 1558–1570

1565

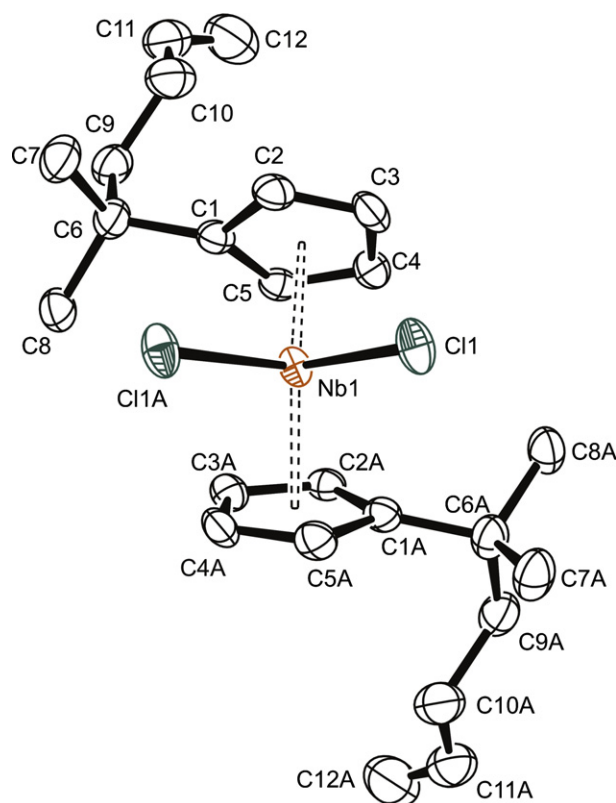


Fig. 4. Molecular structure and atom-labelling scheme for **13** with thermal ellipsoids at 50% probability (hydrogen atoms are omitted for clarity).

Alternatively, substitution of a methyl for a vinyl group on silicon atom of **1** (complex **9**) changed the order of activity in all investigated cell lines, as has been previously discussed for complex **8** (the most active against K562). However, on direct comparison with **8**, complex **9** shows here *ca.* 2.7 times lower antitumoral activity against K562 (IC_{50} values $24 \pm 3 \mu\text{M}$ and $64 \pm 9 \mu\text{M}$ for **8** and **9**, respectively).

The presence of a tetramethylcyclopentadienyl ring instead of unsubstituted cyclopentadienyl ligand and

hydrogen instead of the methyl group bonded to silicon on going from complex **1** to **3** has a similar effect on the antiproliferative activity on the tumour cell lines as substituting the methyl with an alkenyl group on going from complex **1** to **9**.

Almost no antiproliferative effect under physiological conditions was found for complex **10** ($IC_{50} > 155 \mu\text{M}$). It seems that the bulky alkenyl-group bonded to the silicon bridge atom deactivates dramatically the *in vitro* activity of **1**. This fact seems to be plausible due to the more pronounced decreased activity ($IC_{50} > 200 \mu\text{M}$) found for **11**, which has a slightly bulkier alkenyl-group on the silicon bridge atom. It may also be that the presence of a second sterical hindered silyl group on the *ansa*-bridge substituent, results in a decrease of cytotoxicity of the corresponding titanocene complexes **10** and **11**.

Table 3
Selected bond lengths (pm) and angles ($^{\circ}$) for **13**

13	
Nb(1)–Cent(1) ^a	209.2
av Nb(1)–C(C(1)–C(5)) ^b	240.9(3)
Nb(1)–C(1)	243.0(3)
Nb(1)–C(2)	238.1(3)
Nb(1)–C(3)	239.2(3)
Nb(1)–C(4)	242.5(3)
Nb(1)–C(5)	241.7(3)
C(9)–C(10)	151.9(4)
C(10)–C(11)	149.4(5)
C(11)–C(12)	128.0(5)
Nb(1)–Cl(1)	246.37(7)
Cent(1)–Nb(1)–Cent(1A)	132.2
Cl(1)–Nb(1)–Cent(1)	106.0
Cl(1)–Nb(1)–Cl(1A)	85.38(3)
C(9)–C(10)–C(11)	111.8(3)
C(10)–C(11)–C(12)	126.4(4)

^a Cent(1) is the centroid of C(1)–C(5).

^b Refers to the average bond distance between Nb(1) and the carbon atoms of the C5 ring of the cyclopentadienyl moiety.

Table 4
Selected structural data of some niobocene complexes

Complex	Nb–Cp (pm) ^a	Nb–Cl (pm)	Cp–Nb–Cp ($^{\circ}$)	Cl–Nb–X ($^{\circ}$) ^b	Ref.
$[\text{Nb}(\eta^5\text{-C}_5\text{H}_4\{\text{CMe}_2\text{CH}_2\text{CH}_2\text{CH}=\text{CH}_2\})_2\text{Cl}_2]$ (13)	209.2	246.37(7)	132.2	85.38(3)	This work
$[\text{Nb}(\eta^5\text{-C}_5\text{H}_4\text{SiMe}_3)\{\eta^5\text{-C}_5\text{H}_4(\text{B}(\text{Cl})(\text{C}_6\text{F}_5)_2)\}\text{Cl}_2]$	211.5	233.67(9) 236.15(11)	130.0	97.90(4)	[95]
$[\text{Nb}(\eta^5\text{-C}_5\text{H}_4\text{Bu}^t)_2\text{Cl}_2]$	209.4 210.3	247.7(2) 248.3(2)	131.0	84.15(6)	[96]
$[\text{Nb}(\eta^5\text{-C}_5\text{H}_4\text{SiMe}_3)_2\text{Cl}_2]^c$	210(2) 207(3) 207(3)	247.5(8) 247.5(9) 246.7(7)	132.5(9) 129.9(9)	83.8(3) 86.0(3)	[97,98]
$[\text{Nb}(\eta^5\text{-C}_5\text{H}_4\text{SiMe}_3)_2(=\text{NPh})\text{Cl}]$	205(3) 217.6 218.3	245.0(10) 245.27(10)	124.9	100.37(6)	[99]
$[\text{Nb}(\eta^5\text{-C}_5\text{H}_4\text{SiMe}_3)_2(=\text{NC}_6\text{H}_4\text{OMe-4})\text{Cl}]$	218.8(1) 218.9(1)	245.7(3)	125.23(2)	100.82(10)	[100]

^a Cp refers to the $\text{C}_5\text{H}_4\text{R}$ moiety.

^b X refers to Cl or N in each case.

^c Two independent molecules in the asymmetric unit.

Appendix 6

Reproduced from Ref. S. Gómez-Ruiz, G.N. Kaluđerović, S. Prashar, D. Polo-Cerón, M. Fajardo, Ž. Žižak, T.J. Sabo, Z.D. Juranić, J. Inorg. Biochem. 2008, 102, 1558 with permission from Elsevier.

1566

S. Gómez-Ruiz et al. / Journal of Inorganic Biochemistry 102 (2008) 1558–1570

The non-ansa complex **12**, which has an alkenyl substituent on each cyclopentadienyl ligand, showed worse antiproliferative activity against K562 and Fem-x cells than **8** (ca. 2.8 times less active than **8** on K562, and 1.1 times less active than **8** on Fem-x). **12** also shows increased activity, relative to **1**, of ca. 1.6 times on HeLa (IC₅₀ values 135 ± 6 μM and 86 ± 3 μM for **1** and **12**, respectively). The activity of **1** relative to **12** decrease on resting PBMC cells and the reverse order is found for stimulated PBMC cells.

In general, the increase of the antitumoral activity of the alkenyl-substituted titanocene complexes may be due to a cooperative effect of those substituents, which may increase the delivery of the Ti(IV) unit to the cell.

Table 5
Selected bond lengths (pm) and angles (°) for **8**, **9** and **12**

	8	9	12
Ti(1)–Cent(1)	214.6	211.5	213.0
Ti(1)–Cent(2)	214.2	214.2	213.1
av Ti(1)–C(C(1)–C(5)) ^a	246.1	243.6	244.7
av Ti(1)–C(C(1A)–C(5A)) ^a			244.8
av Ti(1)–C(C(6)–C(10)) ^a	246.3	246.2	
Ti(1)–C(1)	236.4	241.5	255.9
Ti(1)–C(1A)			258.8
Ti(1)–C(2)	247.3	239.6	250.7
Ti(1)–C(2A)			248.0
Ti(1)–C(3)	262.4	248.0	242.5
Ti(1)–C(3A)			236.1
Ti(1)–C(4)	251.2	248.6	233.2
Ti(1)–C(4A)			233.7
Ti(1)–C(5)	233.4	240.3	241.2
Ti(1)–C(5A)			247.3
Ti(1)–C(6)	237.9	237.7	
Ti(1)–C(7)	248.3	241.9	
Ti(1)–C(8)	255.5	256.1	
Ti(1)–C(9)	252.5	255.2	
Ti(1)–C(10)	237.2	240.1	
Ti(1)–Cl(1)	233.6	234.2	235.5
Ti(1)–Cl(1A)			234.2
Ti(1)–Cl(2)	235.0	234.3	
C(11)–C(12)			133.4
C(11A)–C(12A)			133.4
C(16)–C(17)		134.0	
C(22)–C(23)	133.3		
Cent(1)–Ti(1)–Cent(2)	131.05	130.32	132.05
Cl(1)–Ti(1)–Cent(1)	105.52	105.88	106.39
Cl(1)–Ti(1)–Cent(2)	104.88	106.21	104.62
Cl(2)–Ti(1)–Cent(1)	106.54	106.11	
Cl(2)–Ti(1)–Cent(2)	107.06	106.34	
Cl(1A)–Ti(1)–Cent(1)			105.84
Cl(1A)–Ti(1)–Cent(2)			106.34
Cl(1)–Ti(1)–Cl(2)	96.49	97.16	
Cl(1)–Ti(1)–Cl(1A)			95.85
Si(1)–C(16)–C(17)		124.18	
C(10)–C(11)–C(12)			127.39
C(10A)–C(11A)–C(12A)			127.29
C(21)–C(22)–C(23)	125.30		

Cent(1) and Cent(2) are the centroids of C(1)–C(5) and C(6)–C(10) or C(1A)–C(5A), respectively.

^a Refers to the average bond distance between Ti(1) and the carbon atoms of the C₅ ring of the corresponding cyclopentadienyl moiety.

3.3. Structural studies

Our efforts to crystallize some of the titanocene complexes were unsuccessful. In order to circumvent this problem, we considered the possibility of synthesising analogous biologically active complexes, to compare their structures. As it has been previously reported by Köpf and coworkers, niobocene complexes showed, as titanocene compounds, cytotoxic activity on tumour cell lines [92–94]. Thus, we synthesised the niobocene complex [Nb(η⁵-C₅H₄{CMe₂CH₂CH₂CH=CH₂})₂Cl₂] (**13**), to compare its cytotoxic activity with those found for titanocene complexes. Unfortunately due to the lack of solubility of this complex **13**, we were unable to study its activity, however, we were able to obtain suitable crystals for the X-ray diffraction analysis.

13 crystallizes in the centrosymmetric monoclinic *I2/a* space group with four molecules in the unit cell, with only half of the molecule being located in the asymmetric unit and the other half being generated by symmetry operations. The niobium atom lies on a symmetry centre. The molecular structure of **13** (Fig. 4) reveals that the niobium atom has a distorted tetrahedral geometry with both C₅ rings bound to the metal in an η⁵ mode. The centroids of the cyclopentadienyl rings form an angle with the niobium atom of 132.2°, typical for niobocene dichloride complexes [95–100]. The distance Nb–Cl (246.37(7) pm) and angle Cl–Nb–Cl ca. (85.38(3)°) are in the expected range [95–100].

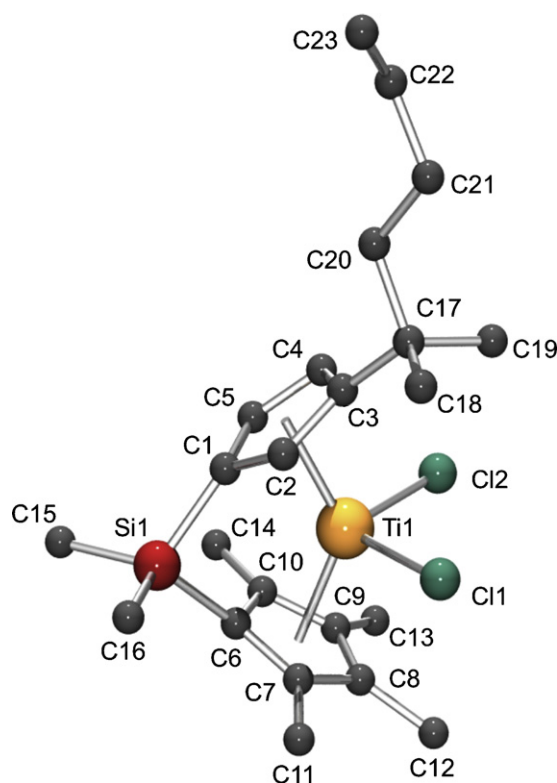


Fig. 5. DFT-calculated structure of **8** (hydrogen atoms are omitted for clarity).

Appendix 6

Reproduced from Ref. S. Gómez-Ruiz, G.N. Kaluđerović, S. Prashar, D. Polo-Cerón, M. Fajardo, Ž. Žižak, T.J. Sabo, Z.D. Juranić, J. Inorg. Biochem. 2008, 102, 1558 with permission from Elsevier.

S. Gómez-Ruiz et al. / Journal of Inorganic Biochemistry 102 (2008) 1558–1570

1567

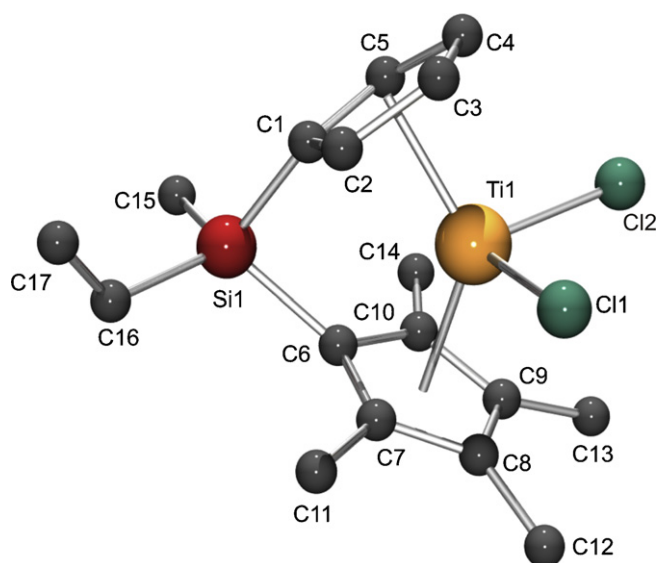


Fig. 6. DFT-calculated structure of **9** (hydrogen atoms are omitted for clarity).

The butenyl moiety bond distances are C(9)–C(10) 151.9(4); C(10)–C(11) 149.4(5); C(11)–C(12) 128.0(5) pm. The distance C(11)–C(12) is typical for terminal C–C double bonds [73,74,101–103] and the angle C(10)–C(11)–C(12), 126.4(4)°, confirms the sp^2 hybridization of C(12). Selected bond lengths and angles for **13** are summarized in Table 3. Selected structural data of **13** with similar niobocene complexes can be compared using Table 4.

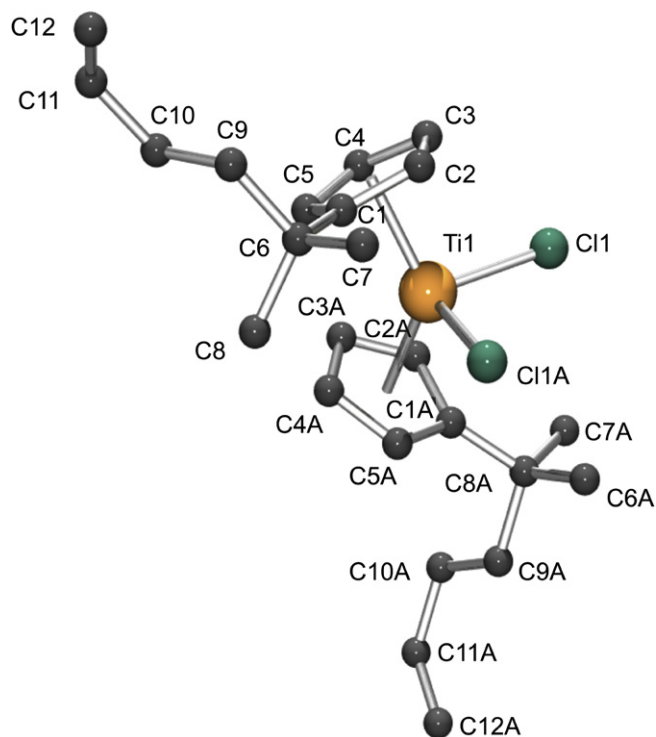


Fig. 7. DFT-calculated structure of **12** (hydrogen atoms are omitted for clarity).

In addition, density functional theory (DFT) calculations were carried out for the most active titanocenes **8**, **9** and **12** at the B3LYP level [80–83] using the 6-31 G** basis set [84–87]. Selected bond lengths and angles of the optimized structure of the titanocenes are listed in Table 5. The calculated structures of **8**, **9** and **12** are presented in Figs. 5–7, respectively.

The bond lengths between titanium and the cyclopentadienyl carbons differ for the different C_5 rings from 233.2 to 262.4 pm. The longest Ti–C lengths are found for the substituted carbon atoms of the cyclopentadienyl ring (especially for C(3) in **8** and **9** and for C(1) and C(1A) in **12**). Nevertheless, the calculated distances Ti–Cent are all close to 213 pm.

The Cent–Ti–Cent angles of about 131° for the *ansa*-titanocene **8** and **9** differ by only ca. 1° for that found for **12**. The Cl(1)–Ti(1)–Cl(2) angle for the calculated titanocene of ca. 96° are all similar, and comparable with those recorded for the X-ray crystal structures of related *ansa*-titanocene complexes [104–109].

The C–C distances for the double bonds of the alkenyl chains reveal comparable distances (133.3–134.0 pm) and are in very good agreement with others reported in X-ray crystal structures of metallocene complexes with alkenyl groups [73,74].

4. Conclusions and outlook

We have synthesized a family of titanocene and *ansa*-titanocene complexes which have been tested as antitumoral agents in different tumour cell lines, in order to understand the possible relationship between the different substituents and the cytotoxic activity. Investigated titanocene anti-tumour agents showed a dose-dependent antiproliferative effect toward all cell lines and on human PBMC and stimulated PBMC. It has been observed that there is no remarkable difference in the cytotoxicity using germanium instead of silicon as the bridging atom. The presence of alkyl groups on the cyclopentadienyl rings leads to a slight increase in the cytotoxicity in some studied cells. However, this increase becomes much higher when an alkenyl fragment is included, in particular as a substituent of the cyclopentadienyl moiety. These facts are reflected in the highest activity being observed for **8**. Other substituents examined in this study on the cyclopentadienyl ring or the silicon *ansa*-bridged titanocene had a negative influence on the activity. **8** and **12** present similar activities, and sometimes even higher, than some of the previously analyzed titanocene complexes which have polar substituents such as alkoxy-, or amino-groups on the cyclopentadienyl ring. The increased antitumoural activity of alkenyl-substituted titanocene complexes may be due to a better delivery of the Ti(IV) unit to the cell by “transferrin”, which may be favoured by the alkenyl groups attached to the Cp-rings.

Future work, already in progress, will now focus on the improvement of the cytotoxic nature of **8** and **12**, by the manipulation of the alkenyl groups and introduction of

other amine- or alkoxy-groups. These structural variations may have a positive effect in terms of increasing stability in aqueous biological medium and in terms of cytotoxicity. Further studies on other cells will also be carried out.

5. Abbreviations

Cent	centroid
Cp η^5	cyclopentadienyl
DFT	density functional theory
EI-MS	electronic impact mass spectrometry
FBS	fetal bovine serum
MTT	tetrazolium salt (3-(4,5-dimethylthiazol-2-yl)-2,5-diphenyl tetrazolium bromide)
PBMC	peripheral blood mononuclear cells
PHA	phytohaemagglutinin
SDS	sodium dodecylsulfate
THF	tetrahydrofuran

Acknowledgments

We gratefully acknowledge financial support from the Ministerio de Educación y Ciencia, Spain (Grant no. CTQ2005-07918-C02-02/BQU), the Comunidad de Madrid (S-0505/PPQ-0328) and the Universidad Rey Juan Carlos (graduate fellowship for D.P.-C.). We would also like to thank to the Ministry of Science and Environmental Protection of the Republic of Serbia (Grant Nos. 142010 and 145006). We thank Prof. Dr. Dirk Steinborn, Mairead E. Kelly (Martin-Luther Universität, Halle-Wittenberg, Germany) and Prof. Dr. Evamarie Hey-Hawkins (Universität Leipzig, Germany) for helpful discussions.

Appendix A. Supplementary data

Crystallographic data for the structural analysis of **13** have been deposited with the Cambridge Crystallographic Data Centre, CCDC-670564. Copies of this information may be obtained free of charge from The Director, CCDC, 12 Union Road, Cambridge CB2 1EZ, UK (Fax: +44 1223 336033; E-mail: deposit@ccdc.cam.ac.uk or <http://www.ccdc.cam.ac.uk>). DFT data of the calculated structures are also included in the supplementary material. Supplementary data associated with this article can be found, in the online version, at [doi:10.1016/j.jinorgbio.2008.02.001](https://doi.org/10.1016/j.jinorgbio.2008.02.001).

References

- [1] R.H. Fish, G. Jaouen, *Organometallics* 22 (2003) 2166–2177.
- [2] C. Biot, G. Glorian, L.A. Maciejewski, J.S. Brocard, O. Domarle, G. Blampain, P. Millet, A.J. Georges, H. Abessolo, D. Dive, J. Lebib, *J. Med. Chem.* 40 (1997) 3715–3718.
- [3] L. Delhaes, C. Biot, L. Berry, P. Delcourt, A.M. Lucien, D. Camus, S. Brocard Jacques, D. Dive, *Chem. Biochem.* 3 (2002) 418–423.
- [4] B. Rosenberg, L. Van Camp, J.E. Trosko, V.H. Mansour, *Nature* (London) 222 (1969) 385–386.
- [5] N.J. Wheate, J.G. Collins, *Coord. Chem. Rev.* 241 (2003) 133–145.
- [6] J.M. Pérez, C. Alonso, M.A. Fuertes, *Chem. Rev.* 103 (2003) 645–662.
- [7] P.M. Takahara, C.A. Frederick, S.J. Lippard, *J. Am. Chem. Soc.* 118 (1996) 12309–12321.
- [8] G.N. Kaluđerović, Dj. Miljković, M. Momčilović, V.M. Đinović, M. Mostarica Stojković, T.J. Sabo, V. Trajković, *Int. J. Cancer* 116 (2005) 479–486.
- [9] S. Mijatović, D. Maksimović-Ivanić, J. Radović, D. Miljković, G.N. Kaluđerović, T.J. Sabo, V. Trajković, *Cell. Mol. Life Sci.* 62 (2005) 1275–1282.
- [10] T.J. Sabo, G.N. Kaluđerović, D. Poleti, Lj. Karanović, A. Boccarcelli, F. Cannito, G. Natile, *J. Inorg. Biochem.* 98 (2004) 1378–1384.
- [11] P. Köpf-Maier, H. Köpf, *Angew. Chem. Int. Ed. Engl.* 18 (1979) 477–478.
- [12] P. Köpf-Maier, H. Köpf, *Z. Naturforsch. B: Anorg. Chem. Org. Chem.* 34 (1979) 805–807.
- [13] P. Köpf-Maier, M. Leitner, R. Voigtländer, H. Köpf, *Z. Naturforsch. Teil. C* 34 (1979) 1174–1176.
- [14] P. Köpf-Maier, B. Hesse, R. Voigtländer, H. Köpf, *J. Cancer Res. Clin. Oncol.* 97 (1980) 31–39.
- [15] P. Köpf-Maier, B. Hesse, H. Köpf, *J. Cancer Res. Clin. Oncol.* 96 (1980) 43–51.
- [16] P. Köpf-Maier, M. Leitner, H. Köpf, *J. Inorg. Nucl. Chem.* 42 (1980) 1789–1791.
- [17] P. Köpf-Maier, H. Köpf, *Naturwissenschaften* 67 (1980) 415–416.
- [18] P. Köpf-Maier, W. Wagner, H. Köpf, *Naturwissenschaften* 68 (1981) 272–273.
- [19] P. Köpf-Maier, S. Grabowski, H. Köpf, *Eur. J. Med. Chem.* 19 (1984) 347–352.
- [20] P. Köpf-Maier, S. Grabowski, J. Liegener, H. Köpf, *Inorg. Chim. Acta* 108 (1985) 99–103.
- [21] W.E. Berdel, H.J. Schmoll, M.E. Scheulen, A. Korfel, M.F. Knoche, A. Harstrick, F. Bach, J. Baumgart, G. Saß, *Onkologie* 16 (1993) R172.
- [22] W.E. Berdel, H.J. Schmoll, M.E. Scheulen, A. Korfel, M.F. Knoche, A. Harstrick, F. Bach, J. Baumgart, G. Saß, *J. Cancer Res. Clin. Oncol.* 120 (1994) R172.
- [23] A. Korfel, M.E. Scheulen, H.J. Schmoll, O. Gründel, A. Harstrick, M. Knoche, L.M. Fels, M. Skorzec, F. Bach, J. Baumgart, G. Saß, S. Seeber, E. Thiel, W.E. Berdel, *Clin. Cancer Res.* 4 (1998) 2701–2708.
- [24] C.V. Christodoulou, D.R. Ferry, D.W. Fyfe, A. Young, J. Doran, T.M.T. Sheehan, A. Eliopoulos, K. Hale, J. Baumgart, G. Saß, D.J. Kerr, *J. Clin. Oncol.* 16 (1998) 2761–2769.
- [25] T. Schilling, K.B. Keppler, M.E. Heim, G. Niebch, H. Dietzfelbinger, J. Rastetter, A.-R. Hanauske, *Invest. New Drugs* 13 (1996) 327–332.
- [26] M.M. Harding, G. Mokdsi, *Curr. Med. Chem.* 7 (2000) 1289–1303.
- [27] P.M. Abeyasinghe, M.M. Harding, *Dalton Trans.* (2007) 3474–3482.
- [28] G. Lummen, H. Sperling, H. Luboldt, T. Otto, H. Rubben, *Cancer Chemother. Pharmacol.* 42 (1998) 415–417.
- [29] N. Kröger, U.R. Kleeberg, K.B. Mross, L. Edler, G. Saß, D.K. Hossfeld, *Onkologie* 23 (2000) 60–62.
- [30] P. Köpf-Maier, D. Krahl, *Chem.-Biol. Interact.* 44 (1983) 317–328.
- [31] P. Köpf-Maier, D. Krahl, *Naturwissenschaften* 68 (1981) 273–274.
- [32] P. Köpf-Maier, *J. Struct. Biol.* 105 (1990) 35–45.
- [33] H. Sun, H. Li, R.A. Weir, P.J. Sadler, *Angew. Chem. Int. Ed.* 37 (1998) 1577–1579.
- [34] M. Guo, P.J. Sadler, *J. Chem. Soc. Dalton Trans.* (2000) 7–9.
- [35] M. Guo, H. Sun, S. Bihari, J.A. Parkinson, R.O. Gould, S. Parsons, P.J. Sadler, *Inorg. Chem.* 39 (2000) 206–215.
- [36] M. Guo, H. Sun, H.J. McArdle, L. Gambling, P.J. Sadler, *Biochemistry* 39 (2000) 10023–10033.
- [37] G. Mokdsi, M.M. Harding, *Metal-Based Drug* 5 (1998) 207–215.

Appendix 6

Reproduced from Ref. S. Gómez-Ruiz, G.N. Kaluđerović, S. Prashar, D. Polo-Cerón, M. Fajardo, Ž. Žižak, T.J. Sabo, Z.D. Juranić, J. Inorg. Biochem. 2008, 102, 1558 with permission from Elsevier.

S. Gómez-Ruiz et al. / *Journal of Inorganic Biochemistry* 102 (2008) 1558–1570

1569

- [38] O.R. Allen, L. Croll, A.L. Gott, R.J. Knox, P.C. McGowan, *Organometallics* 23 (2004) 288–292.
- [39] J.R. Boyles, M.C. Baird, B.G. Campling, N. Jain, *J. Inorg. Biochem.* 84 (2001) 159–162.
- [40] P.W. Causey, M.C. Baird, *Organometallics* 23 (2004) 4486–4494.
- [41] R. Meyer, S. Brink, C.E.J. van Rensburg, G.K. Joone, H. Görls, S. Lotz, *J. Organometall. Chem.* 690 (2005) 117–125.
- [42] J.J. Eisch, S. Xian, F.A. Owuor, *Organometallics* 17 (1998) 5219–5221.
- [43] J.J. Eisch, F.A. Owuor, S. Xian, *Organometallics* 18 (1999) 1583–1585.
- [44] K.M. Kane, P.J. Shapiro, A. Vij, R. Cubbon, A.L. Rheingold, *Organometallics* 16 (1997) 4567–4571.
- [45] S. Fox, J.P. Dunne, M. Tacke, J.F. Gallagher, *Inorg. Chim. Acta* 357 (2004) 225–234.
- [46] R. Teuber, G. Linti, M. Tacke, *J. Organometall. Chem.* 545–546 (1997) 105–110.
- [47] F. Hartl, L. Cuffe, J.P. Dunne, S. Fox, T. Mahabiersing, M. Tacke, *J. Mol. Struct. Theochem.* 559 (2001) 331–339.
- [48] M. Tacke, J.P. Dunne, S. Fox, G. Linti, R. Teuber, *J. Mol. Struct.* 570 (2001) 197–202.
- [49] S. Fox, J.P. Dunne, D. Dronskowski, D. Schmitz, M. Tacke, *Eur. J. Inorg. Chem.* (2002) 3039–3046.
- [50] M. Tacke, L.T. Allen, L.P. Cuffe, W.M. Gallagher, Y. Lou, O. Mendoza, H. Müller-Bunz, F.J.K. Rehmman, N. Sweeney, *J. Organometall. Chem.* 689 (2004) 2242–2249.
- [51] F.J.K. Rehmman, L.P. Cuffe, O. Mendoza, D.K. Rai, N. Sweeney, K. Strohfeltdt, W.M. Gallagher, M. Tacke, *Appl. Organometall. Chem.* 19 (2005) 293–300.
- [52] M. Tacke, L.P. Cuffe, W.M. Gallagher, Y. Lou, O. Mendoza, H. Müller-Bunz, F.J.K. Rehmman, N. Sweeney, *J. Inorg. Biochem.* 98 (2004) 1987–1994.
- [53] F.J.K. Rehmman, A.J. Rous, O. Mendoza, C. Pampillon, K. Strohfeltdt, N. Sweeney, W.M. Gallagher, M. Tacke, *Polyhedron* 24 (2005) 1250–1255.
- [54] N. Sweeney, O. Mendoza, H. Müller-Bunz, C. Pampillon, F.-J.K. Rehmman, K. Strohfeltdt, M. Tacke, *J. Organometall. Chem.* 690 (2005) 4537–4544.
- [55] G. Kelter, N. Sweeney, K. Strohfeltdt, H.-H. Fiebig, M. Tacke, *Anti-Cancer Drug* 16 (2005) 1091–1098.
- [56] N. Sweeney, W.M. Gallagher, H. Müller-Bunz, C. Pampillon, K. Strohfeltdt, M. Tacke, *J. Inorg. Biochem.* 100 (2006) 1479–1486.
- [57] M. Hogan, J. Claffey, C. Pampillon, R.W.G. Watson, M. Tacke, *Organometallics* 26 (2007) 2501–2506.
- [58] O.R. Allen, A. L. Gott, J.A. Hartley, J.M. Hartley, R.J. Knox, P.C. McGowan, *Dalton* (2007) 5082–5090.
- [59] C. Pampillon, N.J. Sweeney, K. Strohfeltdt, M. Tacke, *J. Organometall. Chem.* 692 (2007) 2153–2159.
- [60] C. Pampillon, J. Claffey, M. Hogan, K. Strohfeltdt, M. Tacke, *Trans. Metal Chem.* 32 (2007) 434–441.
- [61] T. Hickey, J. Claffey, E. Fitzpatrick, M. Hogan, C. Pampillon, M. Tacke, *Invest. New Drugs* 25 (2007) 425–433.
- [62] C. Pampillon, J. Claffey, M. Hogan, M. Tacke, *Z. Anorg. Allgem. Chem.* 633 (2007) 1695–1700.
- [63] P.W. Causey, M.C. Baird, S.P.C. Cole, *Organometallics* 23 (2004) 4486–4494.
- [64] G.D. Potter, M.C. Baird, M. Chan, S.P.C. Cole, *Inorg. Chem. Commun.* 9 (2006) 1114–1116.
- [65] P. Köpf-Maier, H. Köpf, *Chem. Rev.* (1987) 1137–1152.
- [66] S. Gómez-Ruiz, G.N. Kaluđerović, D. Polo-Cerón, S. Prashar, M. Fajardo, Ž. Žižak, Z.D. Juranić, T.J. Sabo, *Inorg. Chem. Commun.* 10 (2007) 748–752.
- [67] T.K. Panda, M.T. Gamer, P.W. Roesky, *Organometallics* 22 (2003) 877–890.
- [68] K.J. Stone, R.D. Little, *J. Org. Chem.* 49 (1984) 1849–1853.
- [69] A. Antiñolo, I. López-Solera, I. Orive, A. Otero, S. Prashar, A.M. Rodríguez, E. Villaseñor, *Organometallics* 20 (2001) 71–78.
- [70] C. Alonso-Moreno, A. Antiñolo, I. López-Solera, A. Otero, S. Prashar, A.M. Rodríguez, E. Villaseñor, *J. Organometall. Chem.* 656 (2002) 129–138.
- [71] A. Antiñolo, M. Fajardo, S. Gómez-Ruiz, I. López-Solera, A. Otero, S. Prashar, *Organometallics* 23 (2004) 4062–4069.
- [72] A. Antiñolo, I. López-Solera, A. Otero, S. Prashar, A.M. Rodríguez, E. Villaseñor, *Organometallics* 21 (2002) 2460–2467.
- [73] S. Gómez-Ruiz, D. Polo-Cerón, S. Prashar, M. Fajardo, A. Antiñolo, A. Otero, *Eur. J. Inorg. Chem.* (2007) 4445–4455.
- [74] A. Antiñolo, M. Fajardo, S. Gómez-Ruiz, I. López-Solera, A. Otero, S. Prashar, A.M. Rodríguez, *J. Organometall. Chem.* 683 (2003) 11–22.
- [75] S. Gómez-Ruiz, S. Prashar, L.F. Sánchez-Barba, D. Polo-Cerón, M. Fajardo, A. Antiñolo, A. Otero, M.A. Maestro, C.J. Pastor, *J. Mol. Catal. A: Chem.* 264 (2007) 260–269.
- [76] SCALE3 ABSPACK: Empirical Absorption Correction, CrysAlis – Software Package, Oxford Diffraction Ltd., 2006.
- [77] G.M. Sheldrick, SHELXS-97, Program for Crystal Structure Solution, Göttingen, 1997.
- [78] G.M. Sheldrick, SHELXL-97, Program for the Refinement of Crystal Structures, Göttingen, 1997.
- [79] M.J. Frisch, G.W. Trucks, H.B. Schlegel, G.E. Scuseria, M.A. Robb, J.R. Cheeseman, J.A. Montgomery Jr., T. Vreven, K.N. Kudin, J.C. Burant, J.M. Millam, S.S. Iyengar, J. Tomasi, V. Barone, B. Mennucci, M. Cossi, G. Scalmani, N. Rega, G.A. Petersson, H. Nakatsuji, M. Hada, M. Ehara, K. Toyota, R. Fukuda, J. Hasegawa, M. Ishida, T. Nakajima, Y. Honda, O. Kitao, H. Nakai, M. Klene, X. Li, J.E. Knox, H.P. Hratchian, J.B. Cross, V. Bakken, C. Adamo, J. Jaramillo, R. Gomperts, R.E. Stratmann, O. Yazyev, A.J. Austin, R. Cammi, C. Pomelli, J.W. Ochterski, P.Y. Ayala, K. Morokuma, G.A. Voth, P. Salvador, J.J. Dannenberg, V.G. Zakrzewski, S. Dapprich, A.D. Daniels, M.C. Strain, O. Farkas, D.K. Malick, A.D. Rabuck, K. Raghavachari, J. B. Foresman, J.V. Ortiz, Q. Cui, A.G. Baboul, S. Clifford, J. Cioslowski, B.B. Stefanov, G. Liu, A. Liashenko, P. Piskorz, I. Komaromi, R.L. Martin, D.J. Fox, T. Keith, M.A. Al-Laham, C.Y. Peng, A. Nanayakkara, M. Challacombe, P.M.W. Gill, B. Johnson, W. Chen, M.W. Wong, C. Gonzalez, J.A. Pople, *Gaussian 03, Revision C.02*, Gaussian Inc., Wallingford, CT, 2004.
- [80] A.D. Becke, *J. Chem. Phys.* 98 (1993) 5648–5652.
- [81] C. Lee, W. Yang, R.G. Parr, *Phys. Rev. B* 37 (1988) 785–789.
- [82] S.H. Vosko, L. Wilk, M. Nusair, *Can. J. Phys.* 58 (1980) 1200–1211.
- [83] P.J. Stephens, F.J. Devlin, C.F. Chabalowski, M.J. Frisch, *J. Phys. Chem.* 98 (1994) 11623–11627.
- [84] W.J. Hehre, R. Ditchfield, J.A. Pople, *J. Chem. Phys.* 56 (1972) 2257–2261.
- [85] J.D. Dill, J.A. Pople, *J. Chem. Phys.* 62 (1975) 2921–2923.
- [86] M.M. Francl, W.J. Pietro, W.J. Hehre, J.S. Binkley, M.S. Gordon, D.J. DeFrees, J.A. Pople, *J. Chem. Phys.* 77 (1982) 3654–3665.
- [87] V. Rassolov, J.A. Pople, M.A. Ratner, T.L. Windus, *J. Chem. Phys.* 109 (1998) 1223–1229.
- [88] C. Pampillon, J. Claffey, M. Hogan, M. Tacke, *BioMetals*, 2007. <<http://dx.doi.org/10.1007/s10534-007-9108-5>>.
- [89] T. Mosmann, *J. Immunol. Meth.* 65 (1983) 55–63.
- [90] M. Ohno, T. Abe, *J. Immunol. Meth.* 145 (1991) 199–203.
- [91] G.N. Kaluđerović, V.M. Đinović, Z.D. Juranić, T.P. Stanojković, T.J. Sabo, *J. Inorg. Biochem.* 99 (2005) 488–498.
- [92] P. Köpf-Maier, H. Köpf, *Chem. Rev.* 87 (1987) 1137–1152.
- [93] P. Köpf-Maier, T. Klapoetke, *J. Cancer Res. Clin. Oncol.* 118 (1992) 216–221.
- [94] P. Köpf-Maier, H. Köpf, *Metal Comp. Cancer Ther.* (1994) 109–146.
- [95] S.J. Lancaster, D.L. Hughes, *Dalton Trans.* (2003) 1779–1789.
- [96] A. McCamley, T.J. Miller, W. Clegg, *Acta Cryst. Section C* 50 (1994) 33–36.
- [97] A. Antiñolo, J.M. de Ilarduya, A. Otero, P. Royo, A.M.M. Lanfredi, A. Tiripicchio, *J. Chem. Soc. Dalton Trans.* (1988) 2685–2693.

Appendix 6

Reproduced from Ref. S. Gómez-Ruiz, G.N. Kaluderović, S. Prashar, D. Polo-Cerón, M. Fajardo, Ž. Žižak, T.J. Sabo, Z.D. Juranić, J. Inorg. Biochem. 2008, 102, 1558 with permission from Elsevier.

1570

S. Gómez-Ruiz et al. / Journal of Inorganic Biochemistry 102 (2008) 1558–1570

- [98] A.M.M. Lanfredi, A. Tiripicchio, M. Kapon, G.M. Reisner, J. Chem. Soc. Dalton Trans. (1990) 375.
- [99] A. Antiñolo, P. Espinosa, M. Fajardo, P. Gómez-Sal, C. López-Mardomingo, A. Martín-Alonso, A. Otero, J. Chem. Soc. Dalton Trans. (1995) 1007–1013.
- [100] A. Antiñolo, M. Fajardo, C. Huertas, A. Otero, S. Prashar, A.M. Rodríguez, J. Organometall. Chem. 585 (1999) 154–161.
- [101] J.C. Sierra, D. Hüerländer, M. Hill, G. Kehr, G. Erker, R. Fröhlich, Chem. Eur. J. 9 (2003) 3618–3622.
- [102] J. Paradies, G. Kehr, R. Fröhlich, G. Erker, Proc. Natl. Acad. Sci. USA 103 (2006) 15333–15337.
- [103] S. Gómez-Ruiz, S. Prashar, M. Fajardo, A. Antiñolo, A. Otero, M.A. Maestro, V. Volkis, M.S. Eisen, C.J. Pastor, Polyhedron 24 (2005) 1298–1313.
- [104] P. Beagley, P. Davies, H. Adams, C. White, Can. J. Chem. (2001) 731–741.
- [105] S.T. Chacon, E.B. Coughlin, L.M. Henling, J.E. Bercaw, J. Organometall. Chem. 497 (1995) 171–180.
- [106] H. Lang, S. Blau, B. Nuber, L. Zsolnai, Organometallics 14 (1995) 3216–3223.
- [107] S.-J. Kim, Y.-J. Lee, E. Kang, S.H. Kim, J. Ko, B. Lee, M. Cheong, I.-H. Suh, S.O. Kang, Organometallics 22 (2003) 3958–3966.
- [108] B. Douzief, R. Choukroun, C. Lorber, B. Donnadiou, J. Organometall. Chem. 649 (2002) 15–20.
- [109] G. Tian, B. Wang, X. Dai, S. Xu, X. Zhou, J. Sun, J. Organometall. Chem. 634 (2001) 145–152.



Contents lists available at ScienceDirect

Polyhedron

journal homepage: www.elsevier.com/locate/poly



Titanium(IV) carboxylate complexes: Synthesis, structural characterization and cytotoxic activity

Santiago Gómez-Ruiz^{a,b,*}, Beatriz Gallego^b, Željko Žižak^c, Evamarie Hey-Hawkins^b, Zorica D. Juranić^c, Goran N. Kaluđerović^{d,e,*}

^a Departamento de Química Inorgánica y Analítica, E.S.C.E.T., Universidad Rey Juan Carlos, 28933 Móstoles, Madrid, Spain

^b Institut für Anorganische Chemie der Universität Leipzig, Johannisallee 29, D-04103 Leipzig, Germany

^c Institute of Oncology and Radiology of Serbia, 11000 Belgrade, Serbia

^d Institut für Chemie, Martin-Luther-Universität Halle-Wittenberg, Kurt-Mothes-Straße 2, D-06120 Halle, Germany

^e Department of Chemistry, Institute of Chemistry, Technology and Metallurgy, University of Belgrade, Studentski trg 14, 11000 Belgrade, Serbia

ARTICLE INFO

Article history:

Available online 6 June 2009

Keywords:

Anticancer drugs
Titanocene complexes
Cytotoxic activity
Carboxylato ligands

ABSTRACT

Four titanium(IV) carboxylate complexes [Ti(η^5 -C₅H₅)₂(O₂CCH₂SMes)₂] (**1**), [Ti(η^5 -C₅H₄Me)₂(O₂CCH₂SMes)₂] (**2**), [Ti(η^5 -C₅H₅)(η^5 -C₅H₄SiMe₃)(O₂CCH₂SMes)₂] (**3**) and [Ti(η^5 -C₅Me₅)(O₂CCH₂SMes)₃] (**4**; Mes = 2,4,6-Me₃C₆H₂) have been synthesised by the reaction of the corresponding titanium derivatives [Ti(η^5 -C₅H₅)₂Cl₂], [Ti(η^5 -C₅H₄Me)₂Cl₂], [Ti(η^5 -C₅H₅)(η^5 -C₅H₄SiMe₃)Cl₂] and [Ti(η^5 -C₅Me₅)Cl₃] and two (for **1–3**) or three (for **4**) equivalents of mesitylthioacetic acid. Complexes **1–4** have been characterized by spectroscopic methods and the molecular structure of the complexes **1, 2** and **4** have been determined by X-ray diffraction studies. The cytotoxic activity of **1–4** was tested against tumor cell lines human adenocarcinoma HeLa, human myelogenous leukemia K562, human malignant melanoma Fem-x, and normal immunocompetent cells, that is peripheral blood mononuclear cells PBMC and compared with those of the reference complexes [Ti(η^5 -C₅H₅)₂Cl₂] (**R1**), [Ti(η^5 -C₅H₄Me)₂Cl₂] (**R2**), [Ti(η^5 -C₅H₅)(η^5 -C₅H₄SiMe₃)Cl₂] (**R3**) and cisplatin. In all cases, the cytotoxic activity of the carboxylate derivatives was higher than that of their corresponding dichloride analogues, indicating a positive effect of the carboxylato ligand on the final anticancer activity. Complexes **1–4** are more active against K562 (IC₅₀ values from 72.2 to 87.9 μ M) than against HeLa (IC₅₀ values from 107.2 to 142.2 μ M) and Fem-x cells (IC₅₀ values from 90.2 to 191.4 μ M).

© 2009 Elsevier Ltd. All rights reserved.

1. Introduction

Since the pioneering work of Köpf and Köpf-Maier [1–3] and the phase I clinical trials carried out for titanocene dichloride in 1993 [4–8], metallocene and non-metallocene titanium(IV) complexes have been studied intensively due to their anticancer properties [9–15], even though clinical trials in patients did not have a successful outcome [16,17].

Mechanistic studies have indicated that one of the possible pathways is that titanium may reach the cells assisted by the major iron transport protein “transferrin” [18–21], binding to DNA which may be the biological target of these complexes [22–24]. In

* Corresponding authors. Addresses: Departamento de Química Inorgánica y Analítica, E.S.C.E.T., Universidad Rey Juan Carlos, Móstoles (Madrid), Spain (S. Gómez-Ruiz); Institut für Chemie, Martin-Luther-Universität Halle-Wittenberg, Kurt-Mothes-Straße 2, D-06120 Halle, Germany (G.N. Kaluđerović). Fax: +34 914888143 (S. Gómez-Ruiz), tel.: +49 345 5525678; fax: +49 345 5527028 (G.N. Kaluđerović).

E-mail addresses: santiago.gomez@urjc.es (S. Gómez-Ruiz), goran.kaluderovic@chemie.uni-halle.de, goran@chem.bg.ac.rs (G.N. Kaluđerović).

addition, there are other interesting studies that report potential binding of a ligand-bound titanium(IV) complex to proteins [25,26].

Thus, one of the most active fields in titanium(IV) anticancer chemistry is focused in the design of new compounds with different substituents which may increase their cytotoxicity in comparison with that of titanocene dichloride [9–15,27–29]. It has been observed that titanocene complexes which present polar substituents or electron withdrawing groups in their structure, present higher *in vitro* anticancer activity [11]. In addition, we have recently reported an increase of the cytotoxicity in titanocene and *ansa*-titanocene complexes that have pendant alkenyl substituents on the cyclopentadienyl rings [27–29].

However, almost all the studied titanium(IV) complexes are dichloride derivatives and the number of studies on the anticancer activity of titanium(IV) alkoxy or carboxylate derivatives is still relatively small [10,30–37].

In view of our good results on the synthesis, characterization and evaluation of the cytotoxic activity of metal carboxylate complexes [38–40], here we present the synthesis, characterization

and study of the influence of the substituents on the cyclopentadienyl ring and the carboxylato ligand in the stability and cytotoxicity of four new titanium(IV) carboxylate complexes.

2. Experimental

2.1. General manipulations

All reactions were performed using standard Schlenk tube techniques in an atmosphere of dry nitrogen. Solvents were distilled from the appropriate drying agents and degassed before use. Na(C₅H₅) and Na(C₅H₄Me) were prepared according to literature procedures [41]. Li(C₅H₄SiMe₃) [42], [Ti(η⁵-C₅H₅)Cl₃] [43] and [Ti(η⁵-C₅Me₅)Cl₃] [44] were prepared as previously reported. [Ti(η⁵-C₅H₅)₂Cl₂] (**R1**) and [Ti(η⁵-C₅H₄Me)₂Cl₂] (**R2**) were synthesised by the reaction of two equivalents of Na(C₅H₅) or Na(C₅H₄Me) with [TiCl₄(THF)₂], respectively. [Ti(η⁵-C₅H₅)(η⁵-C₅H₄SiMe₃)Cl₂] (**R3**) was prepared by the reaction of [Ti(η⁵-C₅H₅)Cl₃] and Li(C₅H₄SiMe₃). Mesitylthioacetic acid was prepared with slight modification of the literature procedure [45]. IR spectra (KBr pellets prepared in a nitrogen-filled glove box) were recorded on a Perkin–Elmer System 2000 FT-IR spectrometer in the range 350–4000 cm⁻¹. ¹H and ¹³C{¹H} NMR spectra were recorded on a Varian Mercury FT-400 spectrometer or on a Bruker AVANCE-400 and referenced to the residual deuterated solvent. Microanalyses were carried out with a Perkin–Elmer 2400 or LECO CHNS-932 microanalyzer. FAB MS spectra were recorded on a MASPEC II spectrometer with 3-nitrobenzylalcohol as matrix.

2.2. Preparation of [Ti(η⁵-C₅H₅)₂(O₂CCH₂SMes)₂] (**1**)

A solution of mesitylthioacetic acid [42] (0.84 g, 4.02 mmol) in toluene (50 mL) was added dropwise over 15 min to a solution of [Ti(η⁵-C₅H₅)₂Cl₂] (0.50 g, 2.01 mmol) in toluene (50 mL) at room temperature. The reaction mixture was stirred for 20 min, subsequently NEt₃ (0.58 mL, 4.02 mmol) was added dropwise. The reaction was then stirred at 80 °C overnight. The mixture was decanted and filtered and the filtrate concentrated (10 mL) and cooled to –30 °C to give crystals of the title complex which were isolated by filtration. Yield: 0.51 g, 43%. FT-IR (KBr): 1635 (s) (ν_a COO⁻), 1334 (s) (ν_s COO⁻); ¹H NMR (400 MHz, CDCl₃, 25 °C): δ 2.23 (s, 6H, *p*-Me of mesityl), 2.55 (s, 12H, *o*-Me of mesityl), 3.38 (s, 4H, CH₂), 6.33 (s, 10H, C₅H₅), 6.92 (s, 4H, *m*-H of mesityl); ¹³C{¹H} NMR (100.6 MHz, CDCl₃, 25 °C): δ 21.4 (*p*-Me of mesityl), 22.0 (*o*-Me of mesityl), 41.6 (CH₂), 118.5 (C₅H₅), 129.1 (C-4 of mesityl), 129.3 (C-3 and C-5 of mesityl), 138.4 (C-2 and C-6 of mesityl), 142.9 (C-1 of mesityl), 186.4 (COO); FAB MS: *m/z* (%) 596 (1) [M⁺], 531 (5) [M⁺-C₅H₅], 403 (8) [M⁺-COCH₂SMes], 387 (100) [M⁺-OOCCH₂SMes]. Anal. Calc. for C₃₂H₃₆O₄S₂Ti: C, 64.42; H, 6.08. Found: C, 64.00; H, 6.01%.

2.3. Preparation of [Ti(η⁵-C₅H₄Me)₂(O₂CCH₂SMes)₂] (**2**)

The synthesis of **2** was carried out in an identical manner to **1** starting from mesitylthioacetic acid [42] (0.84 g, 4.02 mmol), [Ti(η⁵-C₅H₄Me)₂Cl₂] (0.56 g, 2.01 mmol) and NEt₃ (0.58 mL, 4.02 mmol). Yield: 0.36 g, 55%. FT-IR (KBr): 1648 (s) (ν_a COO⁻), 1332 (s) (ν_s COO⁻); ¹H NMR (400 MHz, CDCl₃, 25 °C): δ 1.96 (s, 6H, Me of Cp), 2.17 (s, 6H, *p*-Me of mesityl), 2.47 (s, 12H, *o*-Me of mesityl), 3.34 (s, 4H, CH₂), 6.05, 6.28 (m, 4H each, C₅H₄Me), 6.84 (s, 4H, *m*-H of mesityl); ¹³C{¹H} NMR (100.6 MHz, CDCl₃, 25 °C): δ 15.7 (Me of Cp), 20.9 (*p*-Me of mesityl), 21.9 (*o*-Me of mesityl), 39.9 (CH₂), 113.4, 115.7, 121.7 (Cp), 129.0 (C-4 of mesi-

tyl), 129.3 (C-3 and C-5 of mesityl), 138.3 (C-2 and C-6 of mesityl), 143.0 (C-1 of mesityl), 186.2 (COO); FAB MS: *m/z* (%) 625 (1) [M⁺], 545 (13) [M⁺-C₅H₄Me], 415 (100) [M⁺-OOCCH₂SMes]. Anal. Calc. for C₃₄H₄₀O₄S₂Ti: C, 65.37; H, 6.45. Found: C, 64.88; H, 6.31%.

2.4. Preparation of [Ti(η⁵-C₅H₅)(η⁵-C₅H₄SiMe₃)(O₂CCH₂SMes)₂] (**3**)

The synthesis of **3** was carried out in an identical manner to **1** starting from mesitylthioacetic acid [42] (0.84 g, 4.02 mmol), [Ti(η⁵-C₅H₅)(η⁵-C₅H₄SiMe₃)Cl₂] (0.64 g, 2.01 mmol) and NEt₃ (0.58 mL, 4.02 mmol). Yield: 0.94 g, 69%. FT-IR (KBr): 1645 (s) (ν_a COO⁻), 1335 (s) (ν_s COO⁻); ¹H NMR (400 MHz, CDCl₃, 25 °C): δ 0.12 (s, 9H, SiMe₃), 2.16 (s, 6H, *p*-Me of mesityl), 2.47 (s, 12H, *o*-Me of mesityl), 3.34 (s, 4H, CH₂), 6.24 (s, 5H, C₅H₅), 6.51, 6.55 (m, 2H each, C₅H₄SiMe₃), 6.84 (s, 4H, *m*-H of mesityl); ¹³C{¹H} NMR (100.6 MHz, CDCl₃, 25 °C): δ 5.2 (SiMe₃), 21.0 (*p*-Me of mesityl), 21.8 (*o*-Me of mesityl), 38.8 (CH₂), 102.9, 113.7, 114.3 (C₅H₄SiMe₃), 118.3 (C₅H₅), 128.9 (C-4 of mesityl), 129.2 (C-3 and C-5 of mesityl), 138.6 (C-2 and C-6 of mesityl), 142.9 (C-1 of mesityl), 186.0 (COO); FAB MS: *m/z* (%) 669 (1) [M⁺], 603 (5) [M⁺-C₅H₅], 531 (6) [M⁺-C₅H₄SiMe₃], 459 (100) [M⁺-OOCCH₂SMes]. Anal. Calc. for C₃₅H₄₄O₄S₂Ti: C, 62.85; H, 6.63. Found: C, 62.69; H, 6.59%.

2.5. Preparation of [Ti(η⁵-C₅Me₅)(O₂CCH₂SMes)₃] (**4**)

A solution of mesitylthioacetic acid [42] (0.63 g, 3.00 mmol) in toluene (70 mL) was added dropwise over 15 min to a solution of [Ti(η⁵-C₅Me₅)₃Cl] (0.29 g, 1.00 mmol) in toluene (30 mL) at room temperature. The reaction mixture was stirred for 20 min, subsequently NEt₃ (0.43 mL, 3.00 mmol) was added dropwise. The reaction was then stirred at room temperature overnight. The mixture was decanted and filtered and the filtrate evaporated to dryness. The resulting yellow oily solid was dissolved in diethyl ether (30 mL), filtered, concentrated to 10 mL and cooled to –30 °C to give crystals of the title complex which were isolated by filtration. Yield: 0.61 g, 76%. FT-IR (KBr): 1556 (s) 1531 (s) (ν_a COO⁻), 1451 (vs) (ν_s COO⁻); ¹H NMR (400 MHz, CDCl₃, 25 °C): δ 1.92 (s, 15H, C₅Me₅), 2.13 (s, 9H, *p*-Me of mesityl), 2.51 (s, 18H, *o*-Me of mesityl), 3.30 (s, 6H, CH₂), 6.90 (s, 6H, *m*-H of mesityl); ¹³C{¹H} NMR (100.6 MHz, CDCl₃, 25 °C): δ 11.3 (C₅Me₅), 20.9 (*p*-Me of mesityl), 21.9 (*o*-Me of mesityl), 38.6 (CH₂), 129.1 (C-4 of mesityl), 132.6 (C-3 and C-5 of mesityl), 135.7 (C₅Me₅), 138.3 (C-2 and C-6 of mesityl), 143.0 (C-1 of mesityl), 186.5 (COO); FAB MS: *m/z* (%) 811 (1) [M⁺], 601 (100) [M⁺-OOCCH₂SMes], 544 (35) [M⁺-OOCCH₂SMes - 4 × Me]. Anal. Calc. for C₄₃H₅₄O₆S₃Ti: C, 63.69; H, 6.71. Found: C, 63.45; H, 6.56%.

2.6. Data collection and structural refinement of **1**, **2** and **4**

The data of **1**, **2** and **4** were collected with a CCD Oxford Xcalibur S (λ(Mo Kα) = 0.71073 Å) using ω and φ scans mode. Semi-empirical from equivalents absorption corrections were carried out with SCALE3 ABSPACK [46]. All the structures were solved by direct methods [47]. Structure refinement was carried out with SHELXL-97 [48]. All non-hydrogen atoms were refined anisotropically, and hydrogen atoms were calculated with the riding model and refined isotropically. Table 1 lists crystallographic details.

2.7. In vitro studies

2.7.1. Preparation of complex solutions

Stock solutions of the studied titanium complexes were made in dimethyl sulfoxide (DMSO) at a concentration of 20 mM, filtered through Millipore filter, 0.22 μm, before use, and diluted by nutrient medium to various working concentrations. DMSO was used

Appendix 7

Reproduced from Ref. S. Gómez-Ruiz, B. Gallego, Ž. Žižak, E. Hey-Hawkins, Z.D. Juranić, G.N. Kaluđerović, *Polyhedron* 2010, 29, 354 with permission from Elsevier.

356

S. Gómez-Ruiz et al. / *Polyhedron* 29 (2010) 354–360

Table 1
Crystallographic data for **1**, **2** and **4**.

	1	2	4
Formula	C ₃₂ H ₃₆ O ₄ S ₂ Ti	C ₃₄ H ₄₀ O ₄ S ₂ Ti	C ₄₃ H ₅₄ O ₆ S ₃ Ti
Fw	596.63	624.68	810.94
T (K)	130(2)	130(2)	130(2)
Crystal system	monoclinic	monoclinic	monoclinic
Space group	P2(1)/c	P2(1)/c	P2(1)
a (Å)	13.833(5)	1.3197(5)	8.20190(10)
b (Å)	7.979(5)	7.934(5)	17.8397(3)
c (Å)	26.555(5)	28.594(5)	14.2823(2)
α (°)	90	90	90
β (°)	97.499(5)	95.286(5)	95.758(2)
γ (°)	90	90	90
V (nm ³)	2.91(1)	2.98(1)	2.07923(5)
Z	4	4	2
Dc (Mg m ⁻³)	1.364	1.392	1.295
μ (mm ⁻¹)	0.474	0.466	0.402
F(0 0 0)	1256	1320	860
Crystal dimension (mm)	0.4 × 0.3 × 0.2	0.35 × 0.03 × 0.02	0.3 × 0.1 × 0.04
θ range (°)	2.67–28.28	2.67–25.35	2.70–26.02
hkl ranges	–18 ≤ h ≤ 18 –10 ≤ k ≤ 10 –35 ≤ l ≤ 35	–15 ≤ h ≤ 15 –9 ≤ k ≤ 9 –34 ≤ l ≤ 34	–10 ≤ h ≤ 10 –22 ≤ k ≤ 21 –17 ≤ l ≤ 17
Data/parameters/ restraints	7207/358/0	5453/378/0	8177/492/1
Goodness-of-fit on F ²	0.823	0.833	0.821
Final R indices [I > 2σ(I)]	R ₁ = 0.0322, wR ₂ = 0.0564	R ₁ = 0.0486, wR ₂ = 0.0657	R ₁ = 0.0353, wR ₂ = 0.0542
R indices (all data)	R ₁ = 0.0801, wR ₂ = 0.0615	R ₁ = 0.1313, wR ₂ = 0.0788	R ₁ = 0.0566, wR ₂ = 0.0570
Largest difference in peak and hole (e Å ⁻³)	0.233 and –0.327	0.448 and –0.396	0.366 and –0.265
Absolute structure parameter			–0.010(17)

due to solubility problems. Nutrient medium was RPMI 1640 medium, without phenol red, supplemented with L-glutamine (3 mM), streptomycin (100 μg/mL), penicillin (100 IU/mL), 10% fetal bovine serum (FBS) and 25 mM Hepes, and was adjusted to pH 7.2 by bicarbonate solution. MTT (3-(4,5-dimethylthiazol-2-yl)-2,5-diphenyl tetrazolium bromide) was dissolved (5 mg/mL) in phosphate buffer saline pH 7.2, and filtered through Millipore filter, 0.22 μm, before use. All reagents were purchased from Sigma Chemicals.

2.7.2. Cell culture

Human cervix adenocarcinoma HeLa and malignant melanoma Fem-x cells were cultured as monolayers in the nutrient medium, while human myelogenous leukemia K562 cells were maintained as suspension culture. The cells were grown at 37 °C in 5% CO₂ and humidified air atmosphere. Peripheral blood mononuclear cells (PBMC) were separated from whole heparinized blood from healthy volunteers by Lymphoprep (Nycomed, Oslo, Norway) gra-

dient centrifugation. Interface cells, washed three times with Haemacel (aqueous solution supplemented with 145 mM Na⁺, 5.1 mM K⁺, 6.2 mM Ca²⁺, 145 mM Cl⁻ and 35 g/L gelatine polymers, pH 7.4) were counted and resuspended in nutrient medium.

2.7.3. Cell sensitivity analysis

HeLa and Fem-x (2000 cells per well) were seeded into 96-well microtitre plates and 20 h later, after the cell adherence, five different concentrations of the studied compounds were added to the wells. Final concentrations were in the range from 12.5 to 200 μM. The studied compounds were added to a suspension of leukemia K562 cells (3000 cells per well) 2 h after cell seeding, in the same final concentrations applied to HeLa and Fem-x cells. All experiments were carried out in triple triplicate. PBMC were seeded (150000 cells per well) in nutrient medium enriched with (5 μg/mL) phytohaemagglutinin (PHA – Welcome Diagnostics, England) in 96-well microtitre plates and 2 h later, the studied compounds were added to the wells, in triplicate, to five final concentrations. Only nutrient medium was added to the cells in the control wells. Nutrient medium with corresponding concentrations of compounds, but void of cells was used as blank.

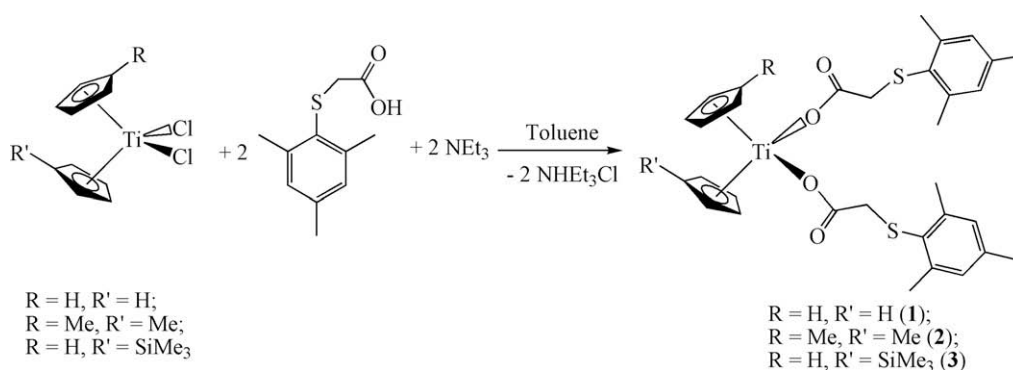
2.7.4. Determination of target cell survival

Cell survival was determined by MTT test according to the method of Mosmann [49] and modified by Ohno and Abe [50], 72 h after complex addition. Immediately afterwards, 20 μL of MTT solution (5 mg/mL in phosphate buffered saline) was added to each well. Samples were incubated for a further 4 h at 37 °C in a humidified atmosphere with 5% CO₂. Then, 100 μL of 10% SDS was added to the wells. Absorbance was measured at 570 nm the next day. To achieve cell survival percentages, absorbance at 570 nm of a sample with cells grown in the presence of various concentrations of agent was divided with absorbance of control sample (the absorbance of cells grown only in nutrient medium), having subtracted from absorbance of a corresponding sample with target cells the absorbance of the blank.

3. Results and discussion

3.1. Synthesis and characterization of the titanium(IV) complexes **1–4**

Titanium(IV) carboxylate complexes [Ti(η⁵-C₅H₅)₂(O₂CCH₂SMes)₂] (**1**), [Ti(η⁵-C₅H₄Me)(O₂CCH₂SMes)₂] (**2**) and [Ti(η⁵-C₅H₅)(η⁵-C₅H₄SiMe₃)(O₂CCH₂SMes)₂] (**3**) were synthesised by the reaction of the corresponding titanium derivatives [Ti(η⁵-C₅H₅)₂Cl₂], [Ti(η⁵-C₅H₄Me)₂Cl₂] and [Ti(η⁵-C₅H₅)(η⁵-C₅H₄SiMe₃)Cl₂], respectively, and two equivalents of mesitylthioacetic acid in toluene at 80 °C (Scheme 1). Analogously, [Ti(η⁵-C₅Me₅)(O₂CCH₂SMes)₃] (**4**) was prepared by the reaction of one equivalent of [Ti(η⁵-C₅Me₅)Cl₃] and three equivalents of mesitylthioacetic acid in



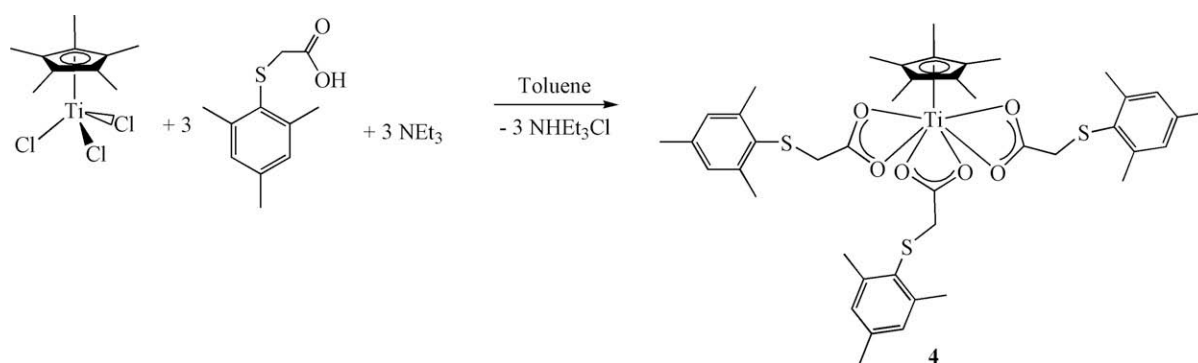
Scheme 1. Synthesis of **1–3**.

Appendix 7

Reproduced from Ref. S. Gómez-Ruiz, B. Gallego, Ž. Žižak, E. Hey-Hawkins, Z.D. Juranić, G.N. Kaluđerović, *Polyhedron* 2010, 29, 354 with permission from Elsevier.

S. Gómez-Ruiz et al. / *Polyhedron* 29 (2010) 354–360

357



Scheme 2. Synthesis of **4**.

toluene at room temperature (Scheme 2). Complexes **1–4** were isolated as orange (**1–3**) or yellow (**4**) crystalline solids of high purity.

In the ^1H NMR spectra of **1–4**, the resonances of the carboxylate ligand were observed as four signals at different chemical shifts. Two singlets at ca. 2.2 and 2.5 corresponding to the protons of the methyl groups of the mesityl moiety, one slightly broad singlet at ca. 3.3 assigned to the methylene protons and one singlet at 6.9 ppm for the aromatic protons. In addition to these signals, the protons of the cyclopentadienyl ligands show the expected different patterns for the four different complexes.

The $^{13}\text{C}\{^1\text{H}\}$ NMR spectra of **1–4** show eight signals corresponding to the carboxylate ligand. A signal at ca. 40 ppm corresponding to the carbon atom of the methylene group and six signals, two between ca. 20 and 23 ppm and four between 128 and 144 ppm, corresponding to the carbon atoms of the mesityl moiety, finally the signal assigned to the carbon atom of the COO moiety is observed at ca. 186 ppm. In addition, the $^{13}\text{C}\{^1\text{H}\}$ NMR spectra of **1–4** show the expected signals for the Cp ligands.

The IR spectra of the complexes **1–3** show strong bands in two different regions between 1648–1635 and 1335–1332 cm^{-1} , which correspond to the asymmetric and symmetric vibrations, respectively, of the COO moiety. The differences, in all cases of more than 200 cm^{-1} , between the asymmetric and symmetric vibrations, indicate monodentate coordination of the carboxylate ligand [51]. This phenomenon was also confirmed by single crystal X-ray diffraction studies (see Section 3.2). In contrast, IR spectrum of complex **4** show two strong bands at 1556 and 1451 assigned to the asymmetric and symmetric vibrations of the COO moiety, in this case the difference of less than 200 cm^{-1} , indicate bidentate coordination of the carboxylate ligand [51].

Complexes **1–4** were also characterized by FAB MS. The mass spectra showed the molecular ion peaks. Fragments indicative of the loss of different number of carboxylate or cyclopentadienyl ligands were also observed (see Section 2).

3.2. Structural studies

Molecular structure of complexes **1**, **2** and **4** have been determined by X-ray diffraction studies. Selected bond lengths and angles of **1**, **2** and **4** are given in Table 2.

Molecular structure of **1** (Fig. 1) and **2** (Fig. 2) confirm the bent metallocene conformation of these complexes. Titanium atoms are in a distorted tetrahedral environment and present two O-monodentate carboxylate groups [Ti–O 1.956(1) and 1.943(1) Å for **1** and 1.907(2) and 1.904(2) Å for **2**]. These distances are in agreement with the monodentate coordination indicated by the large difference of about 300 cm^{-1} between the asymmetric and symmetric vibration of the COO moiety in the IR spectra (see Section 3.1).

These structural parameters are similar to those reported for other titanocene carboxylate complexes with monodentate coordination [52–57].

Table 2

Selected bond lengths (Å) and angles ($^\circ$) for **1**, **2** and **4**.

	1	2	4
Ti(1)–Cent(1)	2.042	2.035	2.063
Ti(1)–Cent(2)	2.053	2.025	
Ti(1)–O(1)	1.956(1)	1.907(2)	2.173(2)
Ti(1)–O(2)	3.556	3.637	2.143(2)
Ti(1)–O(3)	1.943(1)	1.904(2)	2.161(2)
Ti(1)–O(4)	3.480	3.722	2.099(2)
Ti(1)–O(5)			2.178(2)
Ti(1)–O(6)			2.145(2)
O(1)–C(11)	1.287(2)		126.6(3)
O(2)–C(11)	1.219(2)		125.9(3)
O(1)–C(13)		1.271(4)	
O(2)–C(13)		1.200(4)	
O(3)–C(22)	1.299(2)		125.9(3)
O(4)–C(22)	1.211(2)		126.4(3)
O(3)–C(24)		1.283(4)	
O(4)–C(24)		1.190(4)	
O(5)–C(33)			125.9(3)
O(6)–C(33)			126.1(3)
Cent(1)–Ti(1)–Cent(2)	131.1	133.0	
Cent(1)–Ti(1)–O(1)	106.6	104.3	101.9
Cent(1)–Ti(1)–O(2)	92.2	104.3	106.8
Cent(1)–Ti(1)–O(3)	108.5	107.6	167.0
Cent(1)–Ti(1)–O(4)	91.9	84.2	106.6
Cent(1)–Ti(1)–O(5)			102.7
Cent(1)–Ti(1)–O(6)			105.3
Cent(2)–Ti(1)–O(1)	107.8	106.7	
Cent(2)–Ti(1)–O(2)	97.4	86.5	
Cent(2)–Ti(1)–O(3)	104.7	105.3	
Cent(2)–Ti(1)–O(4)	94.8	115.5	
O(1)–Ti(1)–O(2)	33.9	30.2	60.28(6)
O(1)–Ti(1)–O(3)	90.74(5)	92.7(1)	75.99(6)
O(1)–Ti(1)–O(4)	126.3	111.0	73.46(6)
O(1)–Ti(1)–O(5)			143.53(6)
O(1)–Ti(1)–O(6)			132.71(6)
O(2)–Ti(1)–O(3)	124.6	120.2	82.71(6)
O(2)–Ti(1)–O(4)	159.8	141.1	129.45(7)
O(2)–Ti(1)–O(5)			131.19(7)
O(2)–Ti(1)–O(6)			75.10(6)
O(3)–Ti(1)–O(4)	35.8	26.5	61.35(6)
O(3)–Ti(1)–O(5)			75.20(6)
O(3)–Ti(1)–O(6)			84.07(6)
O(4)–Ti(1)–O(5)			75.04(6)
O(4)–Ti(1)–O(6)			129.12(6)
O(5)–Ti(1)–O(6)			59.92(6)
O(1)–C(11)–O(2)	124.7(2)		118.3(2)
O(1)–C(13)–O(2)		126.6(3)	
O(3)–C(22)–O(4)	124.2(3)		118.9(2)
O(3)–C(24)–O(4)		124.6(4)	
O(5)–C(33)–O(6)			117.9(2)

Appendix 7

Reproduced from Ref. S. Gómez-Ruiz, B. Gallego, Ž. Žižak, E. Hey-Hawkins, Z.D. Juranić, G.N. Kaluđerović, *Polyhedron* 2010, 29, 354 with permission from Elsevier.

358

S. Gómez-Ruiz et al. / *Polyhedron* 29 (2010) 354–360

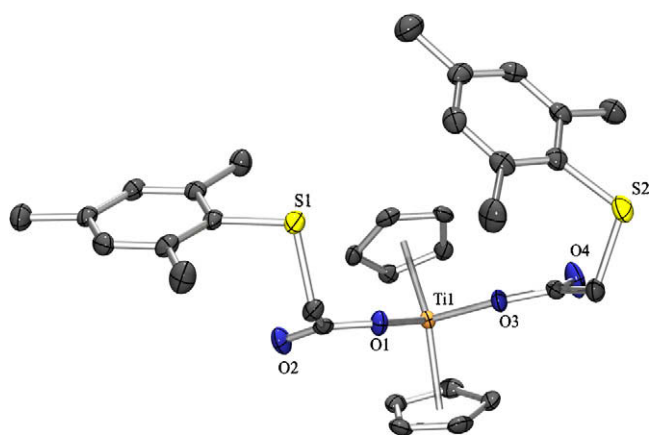


Fig. 1. Molecular structure and atom-labelling scheme for **1** with thermal ellipsoids at 50% probability (hydrogen atoms are omitted for clarity).

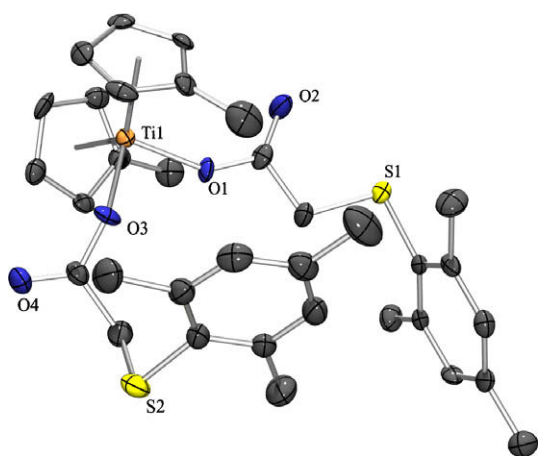


Fig. 2. Molecular structure and atom-labelling scheme for **2** with thermal ellipsoids at 50% probability (hydrogen atoms are omitted for clarity).

The distortion from regular geometry is evident from the Cent–Ti–Cent angles of 131.1° for **1** and 133.0° for **2**, and the O(1)–Ti–O(3) angle of $90.74(5)^\circ$ for **1** and $92.7(1)^\circ$ for **2**. The distances between titanium atoms and the two non bound carboxylate oxygens, O(2) and O(4), are longer than 3.5 \AA , indicating no interaction.

Monodentate coordination of the carboxylato ligand is also confirmed by the significant differences in C–O bond lengths depending whether the oxygen is coordinated to titanium (between $1.271(4)$ and $1.299(2) \text{ \AA}$) or not (between $1.190(4)$ and $1.219(2) \text{ \AA}$).

Both carboxylate groups are bound to titanium atoms in slightly different manner, one carboxylato ligand has a slightly longer Ti–O bond and a smaller Ti–O–C angle. This may imply the presence of a differing extent of Ti–O π -interaction supporting the primary σ -bonding for the two carboxylato ligands [55]. The average Ti–C and C–C bond lengths of the cyclopentadienyl groups in **1** and **2** are in a good agreement with the values from structure determinations of other titanocene derivatives [56–58].

Interestingly, the X-ray structure of the complex **4** (Fig. 3) shows the bidentate coordination of the three carboxylato ligands. The Ti–O bond lengths are all similar between $2.099(2)$ and $2.178(2) \text{ \AA}$. In addition the distances C–O of the carboxylato ligands are also very close with values of ca. 1.26 \AA , indicating some multiple bond character.

The geometry around titanium is a distorted pentagonal bipyramid and the metal attains the 18-electron configuration.

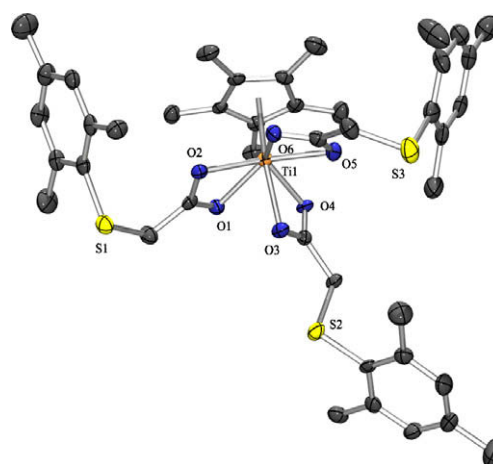


Fig. 3. Molecular structure and atom-labelling scheme for **4** with thermal ellipsoids at 50% probability (hydrogen atoms are omitted for clarity).

The pentagon formed by O(1)–O(2)–O(4)–O(5) and O(6) is a bit distorted and not regular as a consequence of the different distances and angles O–Ti–O. The axial positions of this pentagonal bipyramidal geometry are occupied by the centroid of the cyclopentadienyl ring and O(3) with an Cent(1)–Ti–O(3) angle of 168.0° .

3.3. Cytotoxic studies

Titanocene complexes from this study **1–4** have been used in order to understand the possible relationship between the different substituents, the auxiliary ligands (carboxylato or chloride) and the cytotoxic activity.

The *in vitro* cytotoxicities of complexes **1–4** against human adenocarcinoma HeLa, human malignant melanoma Fem-x, human myelogenous leukemia K562 and on normal immunocompetent cells (human peripheral blood mononuclear cells, PBMC) were determined by MTT-based assays (Table 3).

The investigated titanocene anti-tumor agents showed a dose-dependent antiproliferative effect toward all cell lines and on human PBMC and stimulated PBMC. Estimations based on the IC_{50} values show that complexes **1–4** are more active against K562 (IC_{50} values from 72.2 to $87.9 \mu\text{M}$) than against HeLa (IC_{50} values from 107.2 to $142.2 \mu\text{M}$) and Fem-x cells (IC_{50} values from 90.2 to $191.4 \mu\text{M}$).

From all the studied complexes, **3** and **4** present the highest cytotoxic activity. The results corresponding to complex **4** were totally unexpected, because monocyclopentadienyl titanium(IV) complexes have been usually discarded as potential anticancer drugs due to possible hydrolysis problems. Thus, with the observed cytotoxic activities for complex **4**, new ways in the anticancer

Table 3

IC_{50} (μM) for the 72 h of action of the studied compounds and cisplatin on HeLa, Fem-x, K562 cells, on PBMC and PBMC stimulated with PHA determined by MTT test.

Compound	$IC_{50} \pm \text{SD}$				
	HeLa	Fem-x	K562	PBMC-PHA	PBMC + PHA
1	142.2 ± 5.8	164.9 ± 9.4	86.8 ± 0.3	146.2 ± 3.8	148.0 ± 1.3
2	139.4 ± 12.7	191.4 ± 5.5	78.2 ± 0.7	162.0 ± 3.7	156.1 ± 7.4
3	107.2 ± 6.9	90.2 ± 6.8	87.9 ± 3.6	104.6 ± 5.3	116.8 ± 11.7
4	117.4 ± 8.1	123.0 ± 5.2	72.2 ± 1.7	132.9 ± 0.6	127.3 ± 1.4
R1	>200	177.7 ± 4.9	>200	>200	199.8 ± 9.9
R2	>200	198.6 ± 4.3	173.3 ± 6.0	>200	180.9 ± 4.3
R3	>200	>200	>200	>200	>200
Cisplatin	4.4 ± 0.3	5.7 ± 0.3	4.7 ± 0.3	33.6	26 ± 6

chemistry of monocyclopentadienyl titanium(IV) complexes can be made out.

In order to determine the selectivity in the *in vitro* cytotoxicity of **1–4**, some additional experiments were conducted on normal and stimulated PBMC cells. Generally, complexes **1–4** showed marginal or no selectivity on HeLa or Fem-x cell lines, however, slight selectivity is observed on K562 cells, especially with complex **2**.

Titanocene complexes **1–4** are in all cases more active than the reference complexes **R1**, **R2** and **R3**, indicating that the substitution of the chlorides by carboxylato ligands has a positive effect on the anticancer activity of the studied complexes. Carboxylate complexes **1–4** are about ca. 1.5–3 times more active than the chloride derivatives **R1**, **R2** and **R3**. In view of the difference of the cytotoxic activity, it seems that the carboxylate derivatives (or their corresponding hydrolysis product) present either higher affinity to the binding to transferrin or albumin [25,26], or higher stability to the decomposition in the biological medium, which leads to a more effective action against the tumor cell.

The cytotoxic activities of complexes **1–4** are not as high as the activity reported by Tacke and coworkers in their oxali-titanocene derivatives [35,36], however, they are comparable to those described for other titanium(IV) carboxylate complexes [10,37].

On direct comparison with cisplatin, the cytotoxic activity of complexes **1–4** is significantly lower, however, a higher tolerance of relatively high titanium amounts in biological systems may be possible, in comparison with the high number of side-effects associated to very low concentrations of platinum. This may make these results very promising for further experiments which will be focused on the modification of the nature and number of carboxylato and cyclopentadienyl ligands, in order to find titanocene complexes with higher cytotoxic activities.

4. Conclusions

Four different titanium(IV) carboxylate complexes have been synthesised and structurally characterized. The cytotoxic activity of **1–4** was tested against tumor cell lines human adenocarcinoma HeLa, human myelogenous leukemia K562, human malignant melanoma Fem-x, and normal immunocompetent cells peripheral blood mononuclear cells PBMC, observing that from all the studied complexes, **3** and **4** present the highest cytotoxic activity. An increment on the cytotoxic activity was observed through the substitution of the chloride by carboxylate ligands. In addition, the totally unexpected good results in the cytotoxic activity of monocyclopentadienyl titanium(IV) complex **4**, opens up the possibility on further investigations on this kind of complexes.

Supplementary data

CCDC 729913, 729914 and 729915 contain the supplementary crystallographic data for **1**, **2** and **4**. These data can be obtained free of charge via <http://www.ccdc.cam.ac.uk/conts/retrieving.html>, or from the Cambridge Crystallographic Data Centre, 12 Union Road, Cambridge CB2 1EZ, UK; fax: (+44) 1223-336-033; or e-mail: deposit@ccdc.cam.ac.uk.

Acknowledgements

We gratefully acknowledge financial support from the Universidad Rey Juan Carlos (postdoctoral fellowship for S.G-R) and Junta de Comunidades de Castilla-La Mancha (postdoctoral fellowship for B.G.) We would also like to thank financial support

from the Ministerio de Educación y Ciencia, Spain (Grant No. CTQ2008-05892/BQU) and Ministry of Science and Technological Development of the Republic of Serbia (Grant Nos. 142010 and 145006).

References

- [1] P. Köpf-Maier, H. Köpf, *Angew. Chem., Int. Ed. Engl.* 18 (1979) 477.
- [2] P. Köpf-Maier, H. Köpf, *Chem. Rev.* 87 (1987) 1137.
- [3] P. Köpf-Maier, *Eur. J. Clin. Pharm.* 47 (1994) 1.
- [4] W.E. Berdel, H.J. Schmoll, M.E. Scheulen, A. Korfel, M.F. Knoche, A. Harstrick, F. Bach, J. Baumgart, G. Sass, *Onkologie* 16 (1993) R172.
- [5] W.E. Berdel, H.J. Schmoll, M.E. Scheulen, A. Korfel, M.F. Knoche, A. Harstrick, F. Bach, J. Baumgart, G. Sass, *J. Cancer Res. Clin. Oncol.* 120 (1994) 172.
- [6] A. Korfel, M.E. Scheulen, H.J. Schmoll, O. Gründel, A. Harstrick, M. Knoche, L.M. Fels, M. Skorzec, F. Bach, J. Baumgart, G. Sass, S. Seeber, E. Thiel, W.E. Berdel, *Clin. Cancer Res.* 4 (1998) 2701.
- [7] C.V. Christodoulou, D.R. Ferry, D.W. Fyfe, A. Young, J. Doran, T.M.T. Sheehan, A. Eliopoulos, K. Hale, J. Baumgart, G. Sab, D.J. Kerr, *J. Clin. Oncol.* 16 (1998) 2761.
- [8] T. Schilling, B.K. Keppler, M.E. Heim, G. Niebch, H. Dietzfelbinger, J. Rastetter, A.-R. Hanauske, *Invest. New Drugs* 13 (1996) 327.
- [9] P.M. Aboysinghe, M.M. Harding, *Dalton Trans.* (2007) 3474–3482.
- [10] E.Y. Tshuva, D. Peri, *Coord. Chem. Rev.* (2009), doi:10.1016/j.ccr.2008.11.015.
- [11] K. Strohfeldt, M. Tacke, *Chem. Soc. Rev.* 37 (2008) 1174.
- [12] C.G. Hartinger, P.J. Dyson, *Chem. Soc. Rev.* 38 (2009) 391.
- [13] F. Caruso, M. Rossi, *Met. Ions Biol. Syst.* 42 (2004) 353.
- [14] M. Harding, G. Mokdsi, *Curr. Med. Chem.* 7 (2000) 1289.
- [15] J.H. Bannon, I. Fichtner, A. O'Neill, C. Pampillon, N.J. Sweeney, K. Strohfeldt, R.W. Watson, M. Tacke, M.M. Mc Gee, *Brit. J. Cancer* 97 (2007) 1234.
- [16] G. Lummen, H. Sperling, H. Luboldt, T. Otto, H. Rubben, *Cancer Chemother. Pharmacol.* 42 (1998) 415.
- [17] N. Kröger, U.R. Kleeborg, K.B. Mross, L. Edler, G. Sass, D.K. Hossfeld, *Onkologie* 23 (2000) 60.
- [18] H. Sun, H. Li, R.A. Weir, P.J. Sadler, *Angew. Chem., Int. Ed.* 37 (1998) 1577.
- [19] M. Guo, P.J. Sadler, *J. Chem. Soc., Dalton Trans.* (2000) 7–9.
- [20] M. Guo, H. Sun, S. Bihari, J.A. Parkinson, R.O. Gould, S. Parsons, P.J. Sadler, *Inorg. Chem.* 39 (2000) 206.
- [21] M. Guo, H. Sun, H.J. McArdle, L. Gambling, P.J. Sadler, *Biochemistry* 39 (2000) 10023.
- [22] P. Köpf-Maier, D. Krahl, *Chem.-Biol. Interact.* 44 (1983) 317.
- [23] P. Köpf-Maier, D. Krahl, *Naturwissenschaften* 68 (1981) 273.
- [24] P. Köpf-Maier, *J. Struct. Biol.* 105 (1990) 35.
- [25] A.D. Tinoco, C.D. Incarvito, A.M. Valentine, *J. Am. Chem. Soc.* 129 (2007) 3444.
- [26] A.D. Tinoco, E.V. Eames, A.M. Valentine, *J. Am. Chem. Soc.* 130 (2007) 2262.
- [27] S. Gómez-Ruiz, G.N. Kaluderović, D. Polo-Cerón, S. Prashar, M. Fajardo, Ž. Žižak, Z.D. Juranić, T.J. Sabo, *Inorg. Chem. Commun.* 10 (2007) 748.
- [28] S. Gómez-Ruiz, G.N. Kaluderović, S. Prashar, D. Polo-Cerón, M. Fajardo, Ž. Žižak, T.J. Sabo, Z.D. Juranić, *J. Inorg. Biochem.* 102 (2008) 1558.
- [29] S. Gómez-Ruiz, G.N. Kaluderović, Ž. Žižak, I. Besu, Z.D. Juranić, S. Prashar, M. Fajardo, *J. Organomet. Chem.* 694 (2009) 1981.
- [30] Y. Perez, V. Lopez, L. Rivera-Rivera, A. Cardona, E. Melendez, *J. Biol. Inorg. Chem.* 10 (2005) 94.
- [31] D. Peri, S. Meker, M. Shavit, E.Y. Tshuva, *Chem. Eur. J.* 15 (2009) 2403.
- [32] T. Schilling, B.K. Keppler, M.E. Heim, G. Niebch, H. Dietzfelbinger, J. Rastetter, A.-R. Hanauske, *Invest. New Drugs* 13 (1995) 327.
- [33] F. Caruso, M. Rossi, J. Tanski, R. Sartori, R. Sariego, S. Moya, S. Diez, E. Navarrete, A. Cingolani, F. Marchetti, C. Pettinari, *J. Med. Chem.* 43 (2000) 3665.
- [34] F. Caruso, C. Pettinari, F. Marchetti, P. Natanti, C. Phillips, J. Tanski, M. Rossi, *Inorg. Chem.* 46 (2007) 7553.
- [35] J. Claffey, M. Hogan, H. Müller-Bunz, C. Pampillón, M. Tacke, *Chem. Med. Chem.* 3 (2008) 729.
- [36] I. Fichtner, J. Claffey, B. Gleeson, M. Hogan, D. Wallis, H. Weber, M. Tacke, *Lett. Drug Des. Discovery* 5 (2008) 489.
- [37] M. Shavit, E.Y. Tshuva, *Eur. J. Inorg. Chem.* (2008) 1467–1474.
- [38] S. Gómez-Ruiz, G.N. Kaluderović, S. Prashar, E. Hey-Hawkins, A. Erić, Ž. Žižak, Z.D. Juranić, *J. Inorg. Biochem.* 102 (2008) 2087.
- [39] S. Gómez-Ruiz, B. Gallego, M.R. Kaluderović, H. Kommera, E. Hey-Hawkins, R. Paschke, G.N. Kaluderović, *J. Organomet. Chem.* 694 (2009) 2191.
- [40] M.R. Kaluderović, S. Gómez-Ruiz, B. Gallego, E. Hey-Hawkins, R. Paschke, G.N. Kaluderović, *Eur. J. Med. Chem.*, submitted for publication.
- [41] T.K. Panda, M.T. Gamer, P.W. Roesky, *Organometallics* 22 (2003) 877.
- [42] W.J. Evans, T.J. Boyle, J.W. Ziller, *Organometallics* 11 (1992) 3903.
- [43] A.M. Cardoso, R.J.H. Clark, S. Moorhouse, *J. Chem. Soc., Dalton Trans.* (1980) 1156–1160.
- [44] G. Hidalgo-Llinás, M. Mena, F. Palacios, P. Royo, R. Serrano, *J. Organomet. Chem.* 340 (1988) 37.
- [45] Q.F. Soper, C.W. Whitehead, O.K. Behrens, J.J. Corse, R.G. Jones, *J. Am. Chem. Soc.* 70 (1948) 2849.
- [46] SCALE3 ABSPACK: Empirical Absorption Correction, CRYSLIS – Software Package, Oxford Diffraction Ltd., 2006.
- [47] G.M. Sheldrick, *SHELXS-97*, Program for Crystal Structure Solution, Göttingen, 1997.
- [48] G.M. Sheldrick, *SHELXL-97*, Program for the Refinement of Crystal Structures, Göttingen, 1997.

Appendix 7

Reproduced from Ref. S. Gómez-Ruiz, B. Gallego, Ž. Žižak, E. Hey-Hawkins, Z.D. Juranić, G.N. Kaluđerović, *Polyhedron* 2010, 29, 354 with permission from Elsevier.

360

S. Gómez-Ruiz et al. / Polyhedron 29 (2010) 354–360

- [49] T. Mosmann, *J. Immunol. Methods* 65 (1983) 55.
- [50] M. Ohno, T. Abe, *J. Immunol. Methods* 145 (1991) 199.
- [51] G.B. Deacon, R.J. Philips, *Coord. Chem. Rev.* 33 (1980) 227.
- [52] L.F. Cannizzo, R.H. Grubbs, *J. Org. Chem.* 50 (1985) 2316.
- [53] K. Doppert, H.-P. Klein, U. Thewalt, *J. Organomet. Chem.* 303 (1986) 205.
- [54] C.R. Lucas, E.J. Gabe, F.L. Lee, *Can. J. Chem.* 66 (1988) 429.
- [55] D.A. Edwards, M.F. Mahon, T.J. Paget, *Polyhedron* 19 (2000) 757.
- [56] T. Krüger, C. Wagner, T. Lis, R. Kluge, W. Mörke, D. Steinborn, *Inorg. Chim. Acta* 359 (2006) 2489.
- [57] R. Bina, M. Pavlista, Z. Cernosek, I. Cisarova, I. Pavlik, *Appl. Organomet. Chem.* 19 (2005) 701.
- [58] S. Gómez-Ruiz, A. Garcés, S. Prashar, M. Fajardo, A. Antiñolo, A. Otero, *Inorg. Chim. Acta* 362 (2009) 1042.

Synthesis, characterization and biological studies of alkenyl-substituted titanocene(IV) carboxylate complexes

Goran N. Kaluđerović^{a,b*}, Valentina Tayurskaya^c, Reinhard Paschke^a, Sanjiv Prashar^d, Mariano Fajardo^d and Santiago Gómez-Ruiz^{d*}



The carboxylate compounds $[\text{Ti}(\eta^5\text{-C}_5\text{H}_5)(\eta^5\text{-C}_5\text{H}_4\{\text{CMe}_2(\text{CH}_2\text{CH}_2\text{CH}=\text{CH}_2)\})(\text{O}_2\text{CCH}_2\text{SXyl})_2]$ (2; Xyl = 3,5-Me₂C₆H₃) and $[\text{Ti}(\eta^5\text{-C}_5\text{H}_5)(\eta^5\text{-C}_5\text{H}_4\{\text{CMe}_2(\text{CH}_2\text{CH}_2\text{CH}=\text{CH}_2)\})(\text{O}_2\text{CCH}_2\text{SMes})_2]$ (3; Mes 1 = 2,4,6-Me₃C₆H₂) were synthesized by the reaction of $[\text{Ti}(\eta^5\text{-C}_5\text{H}_5)(\eta^5\text{-C}_5\text{H}_4\{\text{CMe}_2(\text{CH}_2\text{CH}_2\text{CH}=\text{CH}_2)\})\text{Cl}_2]$ (1) with 2 equivalents of xylylthioacetic acid or mesitylthioacetic acid, respectively. Compounds 2 and 3 were characterized by spectroscopic methods. The cytotoxic activity of 1–3 was tested against human tumor cell lines from four different histogenic origins – 8505C (anaplastic thyroid cancer), DLD-1 (colon cancer) and the cisplatin sensitive A253 (head and neck cancer) and A549 (lung carcinoma) – and compared with those of the reference complex $[\text{Ti}(\eta^5\text{-C}_5\text{H}_5)_2\text{Cl}_2]$ (R1) and cisplatin. Surprisingly, the cytotoxic activities of the carboxylate derivatives were lower than those of their corresponding dichloride analogue (1). However, complexes 1–3 were more active than titanocene dichloride against all the studied cells with the exception of complex 2 against A253 and A549 cell lines. DNA-interaction tests were also carried out. Solutions of all the studied complexes were treated with different concentrations of fish sperm DNA, observing modifications of the UV spectra with intrinsic binding constants of 2.99×10^5 , 2.45×10^5 , and $2.35 \times 10^5 \text{ M}^{-1}$ for 1–3. Structural studies based on density functional theory calculations of 2 and 3 were also carried out. Copyright © 2010 John Wiley & Sons, Ltd.

Supporting information may be found in the online version of this article.

Keywords: anticancer agents; titanocene complexes; cytotoxic activity; carboxylato ligands; cyclopentadienyl ligands; DNA-binding properties

Introduction

About 30 years ago, Köpf and Köpf-Maier observed interesting anticancer properties of titanocene dichloride and other analogous compounds.^[1–3] Their studies led to subsequent phase I clinical trials carried out for titanocene dichloride in 1993.^[4–8] All these studies enhanced the exploration of the cytotoxic properties of metallocene and non-metallocene titanium(IV) complexes,^[9–15] even though clinical trials in patients did not have a successful outcome.^[16,17]

Thus, the study of the anticancer mechanism of these complexes has also been an active research field which has led to the proposal that titanium may reach cells assisted by the major iron transport protein 'transferrin',^[18–21] binding to DNA and leading to the cell death.^[22–24] In addition, recent experiments have reported potential interaction of a ligand-bound Ti(IV) complex to other proteins,^[25–27] which may be implicated in the cell death.

However, this is not the only active field in titanium(IV) anticancer chemistry; the search and design of new compounds with different substituents with positive influence in the cytotoxicity in comparison with that of titanocene dichloride is one of the most active fields in this topic.^[9–15,28–30] Many of the studied titanium(IV) complexes are dichloride derivatives and the study of the cytotoxic properties of alkoxy or carboxylate derivatives is still relatively small.^[8,10,31–37]

In this context, in addition to the reported increase of the cytotoxicity in titanocene and *ansa*-titanocene complexes

that have pendant alkenyl substituents on the cyclopentadienyl rings,^[28–30] our research group has recently reported a study of the positive influence of carboxylato ligands in the stability and cytotoxicity of several titanium(IV) carboxylate complexes.^[38]

As a continuation of our work on metal carboxylate complexes,^[39–41] we present here the synthesis, characterization and study of the cytotoxicity of novel alkenyl-substituted titanocene(IV) carboxylate complexes with cytotoxic activity against cancer cells.

* Correspondence to: Santiago Gómez-Ruiz, Departamento de Química Inorgánica y Analítica, ESCET, Universidad Rey Juan Carlos, 28933 Móstoles, Madrid, Spain. E-mail: santiago.gomez@urjc.es

Goran N. Kaluđerović, Biozentrum, Martin-Luther-Universität Halle-Wittenberg, Weinbergweg 22, 06120 Halle, Germany. E-mail: goran.kaluderovic@chemie.uni_halle.de

a Biozentrum, Martin-Luther-Universität Halle-Wittenberg, Weinbergweg 22, 06120 Halle, Germany

b Department of Chemistry, Institute of Chemistry, Technology and Metallurgy, University of Belgrade, Studentski trg 14, 11000 Belgrade, Serbia

c BioSolutions Halle GmbH; Weinbergweg 22, 06120 Halle, Germany

d Departamento de Química Inorgánica y Analítica, ESCET, Universidad Rey Juan Carlos, 28933 Móstoles, Madrid, Spain

Experimental

General Manipulations

All reactions were performed using standard Schlenk tube techniques in an atmosphere of dry nitrogen. Solvents were distilled from the appropriate drying agents and degassed before use. $[\text{Ti}(\eta^5\text{-C}_5\text{H}_5)_2\text{Cl}_2]$ was prepared as previously reported. $[\text{Ti}(\eta^5\text{-C}_5\text{H}_5)(\eta^5\text{-C}_5\text{H}_4\{\text{CMe}_2(\text{CH}_2\text{CH}_2\text{CH}=\text{CH}_2)\})\text{Cl}_2]$ (**1**) was synthesized as described previously by us.^[43] $[\text{Ti}(\eta^5\text{-C}_5\text{H}_5)_2\text{Cl}_2]$ was purchased from Aldrich. Mesitylthioacetic acid and xylylthioacetic acid were prepared with slight modification of the literature procedure.^[44] IR spectra (KBr pellets prepared in a nitrogen-filled glove box) were recorded on a Perkin-Elmer System 2000 FTIR spectrometer in the range 350–4000 cm^{-1} . ^1H and $^{13}\text{C}\{^1\text{H}\}$ NMR spectra were recorded on a Varian Mercury FT-400 spectrometer or on a Bruker Avance-400 and referenced to the residual deuterated solvent. UV–vis measurements were performed at room temperature with a Analytik Jena Specord 200 spectrophotometer between 190 and 900 nm. Microanalyses were carried out with a Perkin-Elmer 2400 or LECO CHNS-932 microanalyzer.

Preparation of $[\text{Ti}(\eta^5\text{-C}_5\text{H}_5)(\eta^5\text{-C}_5\text{H}_4\{\text{CMe}_2(\text{CH}_2\text{CH}_2\text{CH}=\text{CH}_2)\})\text{(O}_2\text{CCH}_2\text{SXYl)}_2]$ (**2**)

A solution of xylylthioacetic acid (0.51 g, 2.60 mmol) in toluene (50 ml) was added dropwise to a solution of $[\text{Ti}(\eta^5\text{-C}_5\text{H}_5)(\eta^5\text{-C}_5\text{H}_4\{\text{CMe}_2(\text{CH}_2\text{CH}_2\text{CH}=\text{CH}_2)\})\text{Cl}_2]$ (**1**) (0.45 g, 1.30 mmol) in toluene (50 ml) at room temperature. The reaction mixture was stirred for 20 min and NEt_3 (0.38 mL, 2.60 mmol) was then added dropwise. The reaction was then stirred at 80 °C overnight. The mixture was filtered and the filtrate concentrated (10 ml) and cooled to –30 °C. Microcrystals of the title complex were isolated by filtration. Yield: 0.43 g, 49%. FT-IR (KBr): 1724 (m) ($\nu_{\text{CH}=\text{CH}_2}$), 1645 (f) ($\nu_{\text{a}} \text{COO}^-$), 1410 (f) ($\nu_{\text{s}} \text{COO}^-$) cm^{-1} . ^1H NMR (400 MHz, CDCl_3 , 25 °C): δ 1.19 (s, 6 H, CMe_2), 1.44, 1.68 (m, 2 H each, CH_2CH_2), 2.29 (s, 12 H, *m*-Me of xylyl), 3.68 (s, 4 H, *S*- CH_2), 4.88, 4.92 (*cis* and *trans*, 1 H each, $\text{CH}_2\text{-CH}=\text{CH}_2$), 5.66 (m, 1 H, $\text{CH}_2\text{-CH}=\text{CH}_2$), 6.33 (s, 5 H, C_5H_5), 6.37, 6.46 (m, 2 H each, C_5H_4), 6.81 (m, 4 H, *o*-protons of xylyl) 7.04 (m, 2 H, *p*-protons of xylyl), ppm. $^{13}\text{C}\{^1\text{H}\}$ NMR (100.6 MHz, CDCl_3 , 25 °C): δ 21.3 (*m*-Me of xylyl), 26.6, 28.7 (CH_2CH_2), 36.3 (CMe_2), 38.4 (*S*- CH_2), 45.1 (CpC), 112.8 ($\text{CH}_2\text{-CH}=\text{CH}_2$), 114.4, 118.6, 120.0 (C_5H_4), 118.0 (C_5H_5), 126.1 (*C*-3 and *C*-5 of xylyl), 127.9 (*C*-4 of xylyl), 136.1 (*C*-1 of xylyl), 138.5 (*C*-2 and *C*-6 of xylyl), 148.8 ($\text{CH}_2\text{-CH}=\text{CH}_2$), 174.4 (COO) ppm. Elemental analysis: $\text{C}_{37}\text{H}_{44}\text{O}_4\text{S}_2\text{Ti}$: (664.74) calculated: C 66.85, H 6.67; found: C 66.59, H 6.45%

Preparation of $[\text{Ti}(\eta^5\text{-C}_5\text{H}_5)(\eta^5\text{-C}_5\text{H}_4\{\text{CMe}_2(\text{CH}_2\text{CH}_2\text{CH}=\text{CH}_2)\})\text{(O}_2\text{CCH}_2\text{SMes)}_2]$ (**3**)

The synthesis of **3** was carried out in an identical manner to **2** starting from mesitylthioacetic acid (0.55 g, 2.60 mmol), $[\text{Ti}(\eta^5\text{-C}_5\text{H}_5)(\eta^5\text{-C}_5\text{H}_4\{\text{CMe}_2(\text{CH}_2\text{CH}_2\text{CH}=\text{CH}_2)\})\text{Cl}_2]$ (**1**) (0.45 g, 1.30 mmol) and NEt_3 (0.38 mL, 2.60 mmol). Yield: 0.72 g, 80%. FT-IR (KBr): 1721 (m) ($\nu_{\text{CH}=\text{CH}_2}$), 1641 (f) ($\nu_{\text{a}} \text{COO}^-$), 1412 (f) ($\nu_{\text{s}} \text{COO}^-$); ^1H NMR (400 MHz, CDCl_3 , 25 °C): δ 1.16 (s, 6 H, CMe_2), 1.41, 1.66 (m, 2 H each, CH_2CH_2), 2.25 (s, 12 H, *o*-Me of Mes), 2.56 (s, 6 H, *p*-Me of Mes), 3.35 (s, 4 H, *S*- CH_2), 4.86, 4.91 (*cis* and *trans*, 1 H each, $\text{CH}_2\text{-CH}=\text{CH}_2$), 5.63 (m, 1 H, $\text{CH}_2\text{-CH}=\text{CH}_2$), 6.31 (s, 5 H, C_5H_5), 6.31, 6.44 (m, 2 H each, C_5H_4), 6.93 (s, 4 H, *m*-protons of Mes) ppm. $^{13}\text{C}\{^1\text{H}\}$ NMR (100.6 MHz, CDCl_3 , 25 °C): δ 21.2 (*p*-Me of Mes), 22.1 (*o*-Me of Mes), 26.8, 29.0 (CH_2CH_2), 36.5 (CMe_2), 40.1 ($\text{CH}_2\text{-S}$),

45.4 (CpC), 112.1 ($\text{CH}_2\text{-CH}=\text{CH}_2$), 114.6, 118.7, 120.9 (C_5H_4), 118.3 (C_5H_5), 128.4 (*C*-4 of Mes), 129.3 (*C*-3 and *C*-5 of Mes), 138.6 (*C*-2 and *C*-6 of Mes), 143.2 (*C*-1 of Mes), 148.7 ($\text{CH}_2\text{-CH}=\text{CH}_2$), 175.1 (COO) ppm. Elemental analysis: $\text{C}_{39}\text{H}_{48}\text{O}_4\text{S}_2\text{Ti}$: (692.79); calculated: C 67.61, H 6.98; found: C 67.33, H 6.81%.

Computational Details

All density functional theory (DFT) calculations were performed by employing the Gaussian 03 program package^[45] using the B3LYP functional.^[46–50] The 6-31G** basis set was used for all atoms.^[51–53] The appropriateness of the chosen functional and basis set for titanium complexes has been stated elsewhere.^[54] All systems were optimized without symmetry restrictions. The resulting geometries were characterized as equilibrium structures by the analysis of the force constants of normal vibrations (see the Supporting Information).

In Vitro Studies

Preparation of drug solutions

Stock solutions of the investigated compounds (**1–3**) were prepared in dimethyl sulfoxide (DMSO, Sigma Aldrich) at a concentration of 20 mM, filtered through Millipore filter, 0.22 μm , before use, and diluted by nutrient medium to various working concentrations. Nutrient medium was RPMI-1640 (PAA Laboratories) supplemented with 10% fetal bovine serum (Biochrom AG) and penicillin/streptomycin (PAA Laboratories).

Cell lines and culture conditions

The cell lines 8505C, A253, A549 and DLD-1, included in this study, were kindly provided by Dr Thomas Mueller, Department of Hematology/Oncology, Martin Luther University of Halle-Wittenberg, Halle (Saale), Germany. Cultures were maintained as monolayer in RPMI 1640 (PAA Laboratories, Pasching, Germany) supplemented with 10% heat-inactivated fetal bovine serum (Biochrom AG, Berlin, Germany) and penicillin–streptomycin (PAA Laboratories) at 37 °C in a humidified atmosphere of 5% (v/v) CO_2 .

Cytotoxicity assay

The cytotoxic activities of the compounds were evaluated using the sulforhodamine-B (SRB, Sigma Aldrich) microculture colorimetric assay.^[55] In short, exponentially growing cells were seeded into 96-well plates on day 0 at the appropriate cell densities to prevent confluence of the cells during the period of experiment. After 24 h, the cells were treated with serial dilutions of the studied compounds for 96 h. Final concentrations achieved in treated wells were 0, 12.5, 25.0, 37.5, 50.0, 75.0, 100.0, 150.0, 200.0 and 300.0 μM for **1–3**. Each concentration was tested in triplicate on each cell line. The final concentration of DMSO solvent never exceeded 0.5%, which was non-toxic to the cells. The percentages of surviving cells relative to untreated controls were determined 96 h after the beginning of drug exposure. After 96 h treatment, the supernatant medium from the 96 well plates was eliminated and the cells were fixed with 10% TCA. For a thorough fixation, plates were then allowed to stand at 4 °C. After fixation, the cells were washed in a strip washer. The washing was carried out four times with water using alternate dispensing and aspiration procedures. The plates were then dyed with 100 μL of 0.4% SRB for about 45 min. After dying, the plates were again washed to remove the

dye with 1% acetic acid and allowed to air dry overnight. 100 μL of 10 mM Tris base solutions were added to each well of the plate and absorbance was measured at 570 nm using a 96 well plate reader (Tecan Spectra, Crailsheim, Germany). The IC_{50} value, defined as the concentrations of the compound at which 50% cell inhibition was observed, was estimated from the dose-response curves.

DNA Binding Experiments Monitored by UV–vis Spectroscopy

Fish sperm DNA (FS-DNA) was kindly provided by Departamento de Ciencias de la Salud from Universidad Rey Juan Carlos (Spain). The spectroscopic titration of FS-DNA was carried out in the buffer (50 mM NaCl–5 mM Tris–HCl, pH 7.1) at room temperature. A solution of FS-DNA in the buffer gave a ratio of UV absorbance 1.8–1.9:1 at 260 and 280 nm, indicating that the DNA was sufficiently free of protein.^[56] Milli-Q water was used to prepare the solutions. The DNA concentration per nucleotide was determined adopting absorption spectroscopy using the known molar extinction coefficient value of $6600 \text{ M}^{-1} \text{ cm}^{-1}$ at 260 nm.^[57] Absorption titrations were performed by using a fixed titanium(IV) complex concentration to which increments of the DNA stock solution were added. Complex–DNA adducts solutions were incubated at 37 °C for 30 min before the absorption spectra were recorded.

Results and Discussion

Synthesis and Characterization of the Titanocene(IV) Complexes 1–3

Titanocene(IV) carboxylate complexes $[\text{Ti}(\eta^5\text{-C}_5\text{H}_5)(\eta^5\text{-C}_5\text{H}_4\{\text{CMe}_2(\text{CH}_2\text{CH}_2\text{CH}=\text{CH}_2)\})_2(\text{O}_2\text{CCH}_2\text{SXY})_2]$ (**2**) and $[\text{Ti}(\eta^5\text{-C}_5\text{H}_5)(\eta^5\text{-C}_5\text{H}_4\{\text{CMe}_2(\text{CH}_2\text{CH}_2\text{CH}=\text{CH}_2)\})_2(\text{O}_2\text{CCH}_2\text{SMes})_2]$ (**3**) were synthesized by the reaction of $[\text{Ti}(\eta^5\text{-C}_5\text{H}_5)(\eta^5\text{-C}_5\text{H}_4\{\text{CMe}_2(\text{CH}_2\text{CH}_2\text{CH}=\text{CH}_2)\})_2\text{Cl}_2]$ (**1**) with two equivalents of xylylthioacetic acid or mesitylthioacetic acid in toluene at 80 °C (Scheme 1). Complexes **2** and **3** were isolated as orange microcrystalline solids.

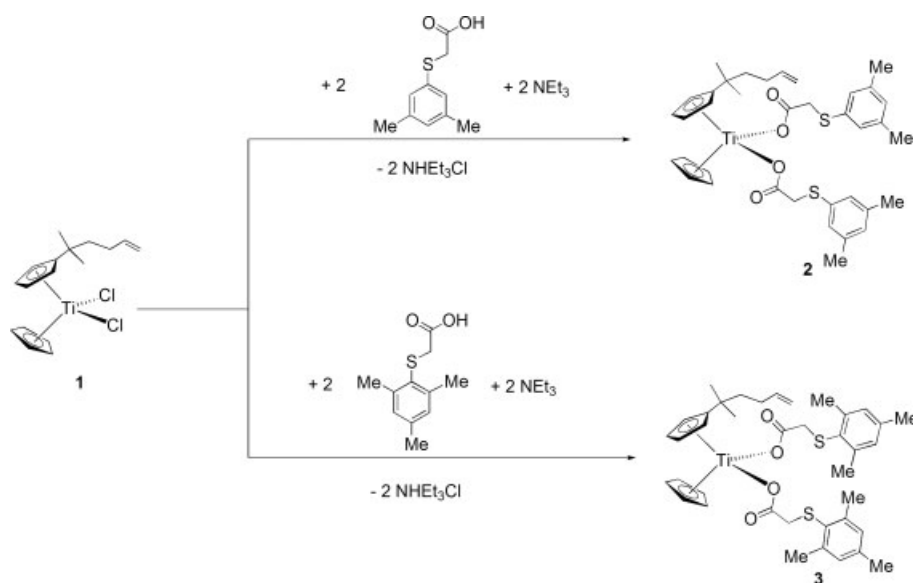
In the ^1H NMR spectrum of **2** the carboxylato ligands gave three signals at different chemical shifts: a singlet at 2.29 corresponding

to the protons of the methyl groups of the xylyl moiety; a singlet at 3.68 assigned to the methylene protons; and one broad singlet at 6.81 ppm for the aromatic protons of the phenyl ring. In the ^1H NMR spectrum of **3**, the resonances of the carboxylato ligands were two singlets at 2.25 and 2.56 ppm corresponding to the protons of the two different methyl groups of the mesityl moiety (*o*-methyl and *p*-methyl): one singlet at 3.35 corresponding to the methylene protons and one singlet at 6.93 ppm for the *m*-aromatic protons. In addition to these signals, the protons of the cyclopentadienyl ligands showed similar spectral patterns to that observed for **1**, that is one singlet for the unsubstituted cyclopentadienyl ring protons at *ca* 6.3 ppm, two multiplets between 6.3 and 6.5 ppm for the substituted cyclopentadienyl ring protons, a singlet at *ca* 1.2 ppm corresponding to the two methyl groups of the substituent and four sets of signals for the alkenyl fragment (two corresponding to the CH_2 allylic protons consisting of two multiplets between 1.4 and 1.7 ppm, one multiplet at *ca* 5.7 ppm for the proton of the C- γ and two multiplets at *ca* 4.8 and 4.9 ppm corresponding to the terminal olefinic protons).

The $^{13}\text{C}\{^1\text{H}\}$ NMR spectra of **2** and **3** showed the expected signals for both carboxylato and cyclopentadienyl ligands. The IR spectra of the complexes **2** and **3** showed strong bands in two different regions at *ca* 1645 and 1410 cm^{-1} , which corresponded to the asymmetric and symmetric vibrations, respectively, of the COO moiety. The differences, in all cases more than 200 cm^{-1} , between the asymmetric and symmetric vibrations, indicate monodentate coordination of the carboxylato ligand.^[58] This phenomenon was also confirmed by DFT calculations.

Structural Studies

We were unable to obtain crystals of **2** and **3** suitable for characterization by X-ray diffraction studies. In order to circumvent this problem, DFT calculations were carried out in the gas phase for **2** and **3** at the B3LYP level^[45] using the 6-31G** basis set.^[46] Geometry optimization without any symmetry restriction led to the calculated equilibrium structures **2** and **3** which are shown in Figs 1 and 2, respectively. For a detailed table with selected bond lengths and angles of the optimized structure



Scheme 1. Synthesis of titanocene complexes **2** and **3**.

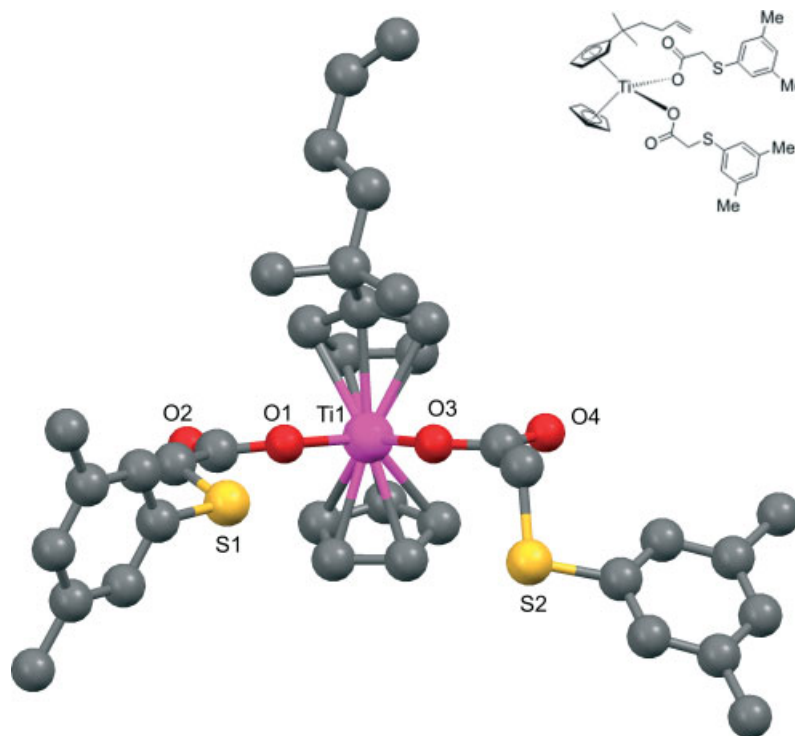


Figure 1. DFT-calculated structure of **2** (hydrogen atoms are omitted for clarity).

of the titanocene compounds see the Supporting Information. The calculated structures of **2** and **3** are presented in Figs 1 and 2, respectively, and show the bent metallocene conformation of both compounds observing that the cyclopentadienyl rings coordinate the metal atom in an η^5 -manner.

The average Ti–C and C–C bond lengths of the cyclopentadienyl groups in **2** and **3** are in a good agreement with the values from structure determinations of other titanocene derivatives.^[30,59]

Titanium atoms are in a distorted tetrahedral environment and present two O-monodentate carboxylate groups [Ti–O 1.941 and 1.935 Å for **2** and 1.938 and 1.934 Å for **3**]. These distances are in agreement with the monodentate coordination indicated by the large difference of more than 200 cm^{-1} between the asymmetric and symmetric vibration of the COO moiety in the IR spectra (see above) and similar to the crystallographic structural data reported for other titanocene carboxylate complexes with monodentate coordination.^[60–64]

The distances between titanium atoms and the two non bound carboxylate oxygens, O(2) and O(4), are longer than 3.4 Å, indicating no interaction. There are also significant differences in C–O bond lengths which indicate monodentate coordination of the carboxylate ligand (*ca* 1.31 Å for coordinated O and *ca* 1.22 Å for non coordinated O).

Cytotoxic Studies

Previous studies carried out by our research group showed the positive influence of the incorporation of an alkenyl substituent on the cyclopentadienyl ligand,^[28,29,30,65] as well as enhancement of the cytotoxicity of titanocene(IV) carboxylate complexes in comparison with their corresponding chloride derivatives.^[38] Titanocene complexes from this study **1–3** were used in order to evaluate a possible cooperative effect of both ligands on the final cytotoxic activity of the final complexes.

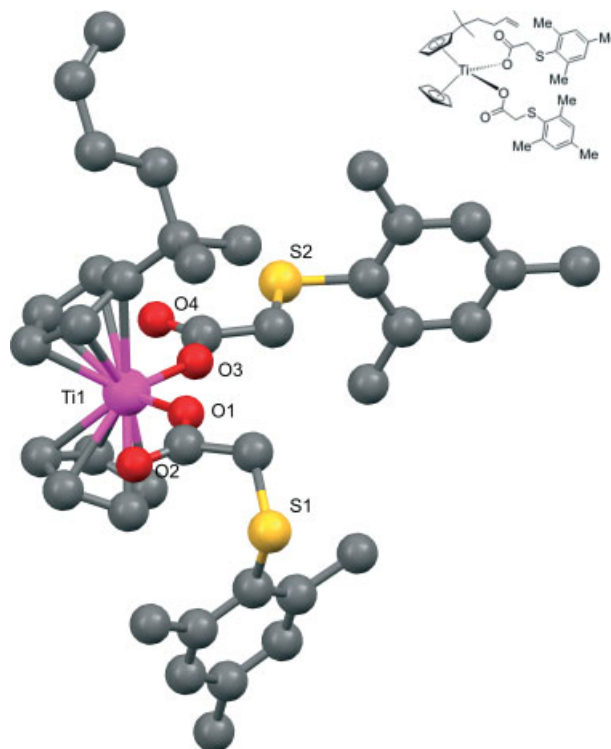
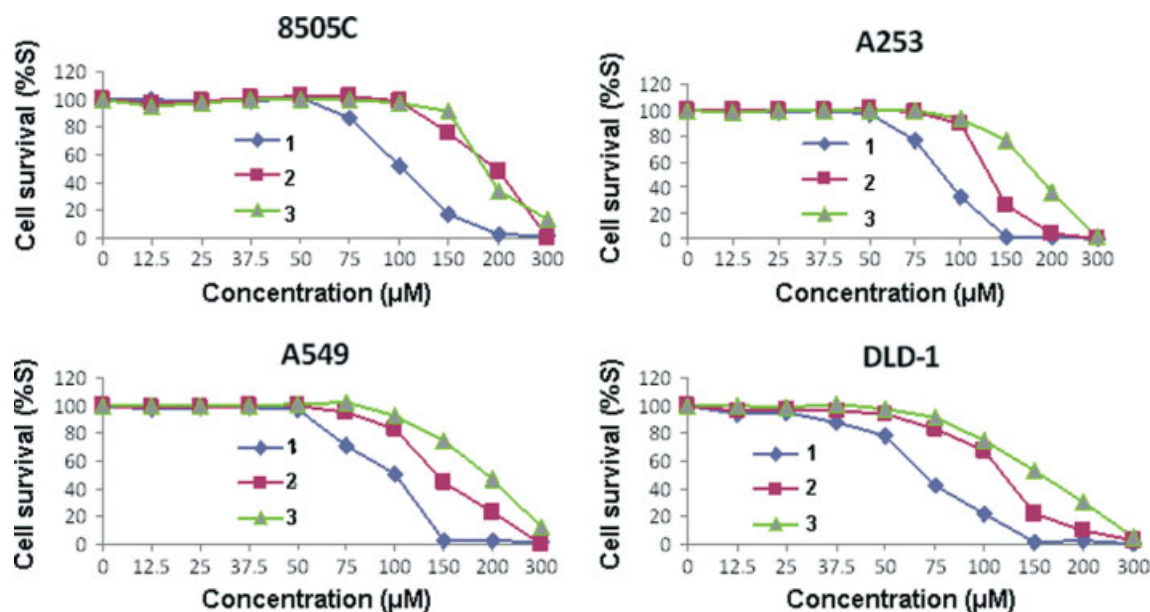


Figure 2. DFT-calculated structure of **3** (hydrogen atoms are omitted for clarity).

Thus, the *in vitro* cytotoxicities of titanocene compounds **1–3** against human tumor cell lines 8505C anaplastic thyroid cancer, A253 head and neck tumor, A549 lung carcinoma and DLD-1 colon carcinoma were determined using the SRB microculture

Table 1. IC₅₀ (μM) for the 96 h of action of **1–3**, titanocene dichloride and cisplatin on 8505C anaplastic thyroid cancer, A253 head and neck tumor, A549 lung carcinoma and DLD-1 colon carcinoma determined by sulforhodamine-B microculture colorimetric assay

Complex	IC ₅₀ ± SD [μM]			
	8505C	A253	A549	DLD-1
1	103.3 ± 2.4	89.6 ± 0.5	96.0 ± 2.9	70.6 ± 1.7
2	182.3 ± 2.5	182.6 ± 2.0	192.5 ± 1.1	151.2 ± 4.2
3	190.8 ± 2.2	131.2 ± 0.5	144.6 ± 2.9	115.7 ± 2.9
[Ti(η ⁵ -C ₅ H ₅) ₂ Cl ₂]	>200	188.71 ± 6.36	167.62 ± 3.31	>200
Cisplatin	5.0 ± 0.2	0.81 ± 0.02	1.51 ± 0.02	5.1 ± 0.1

**Figure 3.** Representative graphs show survival of 8505C, A253, A549 and DLD-1 cells grown for 96 h in the presence of increasing concentrations of **1–3**. Standard deviations (all less than 10%) are omitted for clarity.

colorimetric assay.^[55] In addition, cytotoxicity of cisplatin and titanocene dichloride were included for comparison (Table 1).

The studied titanocene anti-tumor agents showed a dose-dependent antiproliferative effect toward all the studied cancer cell lines (Fig. 3). Estimations based on the IC₅₀ values showed that complexes **2** and **3** are more active than titanocene dichloride, with the exception of complex **2** against A253 and A549 cell lines. However, they are less active against all the studied cells than their corresponding dichloride derivative **1**, indicating that there is no summative effect of the alkenyl-substituted cyclopentadienyl and carboxylato ligands on the cytotoxicity. However, as the cytotoxicity of **1** is relatively high, the principal positive influence on the cytotoxic activity may be due to the alkenyl-substituted cyclopentadienyl ligand rather than the carboxylato ligand.

The cytotoxic activities of **2** and **3** (from 151.2 ± 4.2 to 192.5 ± 1.1 μM in **2** and from 115.7 ± 2.9 to 190.8 ± 2.2 μM in **3**) were very similar; however, a higher activity was observed for **3** compared with **2** in all the studied cells except against 8505C, in which **2** was slightly more active. In addition, the cytotoxic activities of complexes **2** and **3** were not as high as the activity reported by Tacke and coworkers in their oxalitanocene derivatives,^[35,36] however, they were comparable to those described for other titanium(IV) carboxylate complexes.^[38] All the titanocene derivatives **1–3** showed higher cytotoxic activity

against DLD-1 cells (IC₅₀ values up to 70.6 ± 1.7 μM) compared with all the other studied cells, in which IC₅₀ values from 96.0 ± 2.9 to 192.5 ± 1.1 μM were observed.

On direct comparison with cisplatin, the cytotoxic activity of complexes **1–3** was significantly lower; however, a higher tolerance of relatively high titanium amounts in biological systems may be possible, in comparison with the high number of side-effects associated with very low concentrations of platinum.

DNA-interaction Studies

Although recent experiments have reported potential interaction of a ligand-bound Ti(IV) complex to other proteins which may be implicated in cell death,^[25–27] it has been generally accepted that DNA is the biological target in the anticancer action of titanocene derivatives.^[9,22–24]

Thus, the binding behavior of the studied titanocene(IV) complexes to DNA helix was followed through absorption spectral titrations, because absorption spectroscopy is one of the most useful techniques to study the binding of any drug to DNA.^[66–69] The absorption spectra of the complexes in the absence and in the presence of FS-DNA (fish sperm DNA) were recorded. With increasing concentrations of FS-DNA, the absorption bands of the complexes were affected, resulting in the tendency towards hyperchromism and a very slight blue shift. The titanocene

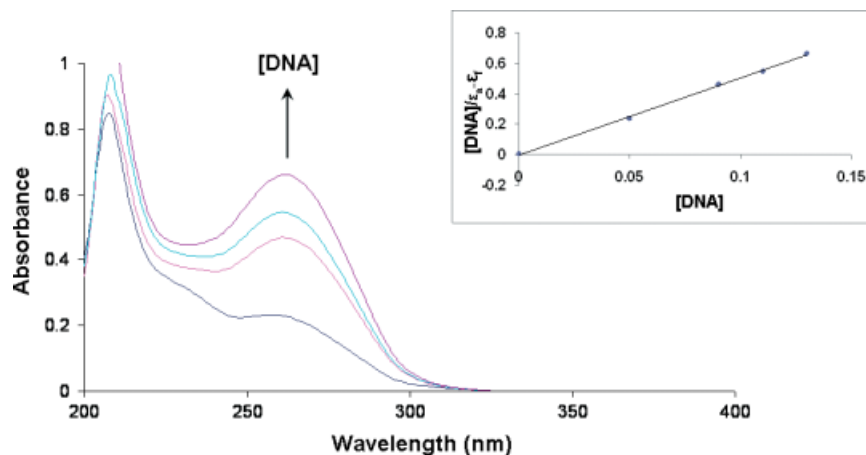


Figure 4. Absorption spectra of **3** in the presence of increasing amounts of DNA. The arrow indicates that absorbance changes upon increasing DNA concentrations. Inset: plot of

$$\frac{[\text{DNA}]}{\varepsilon_a - \varepsilon_f} = \frac{[\text{DNA}]}{\varepsilon_0 - \varepsilon_f} + \frac{1}{K_b(\varepsilon_0 - \varepsilon_f)}$$

experimental data points; solid line, linear fitting of the data.

complexes **1–3** may bind to the DNA in different modes on the basis of their structure and charge and type of ligands. Since DNA possesses several hydrogen bonding sites in the minor and major grooves, the titanocene complexes (**1–3**) may be protonated and there could be hydrogen bonding between the complexes and the base pairs in DNA.^[70–73] In addition, classical electrostatic interactions may be responsible for the hyperchromism and a very slight blue shift observed in the study. In order to compare the binding strengths of the complexes, the intrinsic binding constant, K_b , was determined using the following equation:^[74]

$$\frac{[\text{DNA}]}{\varepsilon_a - \varepsilon_f} = \frac{[\text{DNA}]}{\varepsilon_0 - \varepsilon_f} + \frac{1}{K_b(\varepsilon_0 - \varepsilon_f)}$$

where [DNA] is the concentration of DNA in base pairs, ε_a , ε_f and ε_0 correspond to $A_{\text{obs}}/[\text{Complex}]$, the extinction coefficient of the free titanium complexes and the extinction coefficient of the complexes in the fully bound form, respectively, and K_b is the intrinsic binding constant. The ratio of slope to intercept in the plot of $[\text{DNA}]/(\varepsilon_a - \varepsilon_f)$ vs [DNA] gives the value of K_b (inset Fig. 4). As an example, Fig. 4 shows the absorption spectra of complex **3** in the presence of increasing amounts of DNA

Thus, the intrinsic binding constants of 2.99×10^5 , 2.45×10^5 and $2.35 \times 10^5 \text{ M}^{-1}$ for **1–3**, respectively, were successfully calculated, observing that complex **1**, which is the most cytotoxic compound, gives a K_b slightly higher than those of **2** and **3**, indicating a slightly higher affinity from DNA, which may be implicated in the higher cytotoxic activity shown by **1**.

Conclusions

New alkenyl-substituted titanocene(IV) complexes were synthesized and characterized. The cytotoxic activity of these compounds was tested against human tumor cell lines observing that the dichloride derivative (**1**) shows the highest cytotoxic activity. A decrease in the cytotoxic activity was observed on the substitution of the chlorido by carboxylato ligands. However, complexes **1–3** were more cytotoxic against the studied cells than titanocene

dichloride, with the exception of **2** on A253 and A549 cell lines. In addition, DNA interaction tests were carried out, observing classical electrostatic interactions of all the complexes with DNA with intrinsic binding constants of 2.99×10^5 , 2.45×10^5 and $2.35 \times 10^5 \text{ M}^{-1}$ for **1–3**, respectively.

Supporting Information

DFT data, fully labelled figures and selected bond lengths and angles of the calculated structures are included in the Supporting Information, which can be found in the online version of this article.

Acknowledgments

We gratefully acknowledge financial support from the Ministerio de Educación y Ciencia, Spain (grant no. CTQ2008-05892/BQU) and the Ministerium für Wirtschaft und Arbeit des Landes Sachsen-Anhalt, Deutschland (grant no. 6003368706). We would also like to thank Sara Bravo for her help in the preparation of the titanocene derivatives and BioSolutions Halle GmbH (Germany) for the cell culture facilities.

References

- [1] P. Köpf-Maier, H. Köpf, *Angew. Chem., Int. Ed. Engl.* **1979**, 18, 477.
- [2] P. Köpf-Maier, H. Köpf, *Chem. Rev.* **1987**, 87, 1137.
- [3] P. Köpf-Maier, *Eur. J. Clin. Pharm.* **1994**, 47, 1.
- [4] W. E. Berdel, H. J. Schmoll, M. E. Scheulen, A. Korfel, M. F. Knoche, A. Harstrick, F. Bach, J. Baumgart, G. Sass, *Onkologie* **1993**, 16, R172.
- [5] W. E. Berdel, H. J. Schmoll, M. E. Scheulen, A. Korfel, M. F. Knoche, A. Harstrick, F. Bach, J. Baumgart, G. Sass, *J. Cancer Res. Clin. Oncol.* **1994**, 120, 172.
- [6] A. Korfel, M. E. Scheulen, H. J. Schmoll, O. Gründel, A. Harstrick, M. Knoche, L. M. Fels, M. Skorzec, F. Bach, J. Baumgart, G. Sass, S. Seeber, E. Thiel, W. E. Berdel, *Clin. Cancer Res.* **1998**, 4, 2701.
- [7] C. V. Christodoulou, D. R. Ferry, D. W. Fyfe, A. Young, J. Doran, T. M. T. Sheehan, A. Eliopoulos, K. Hale, J. Baumgart, G. Sab, D. J. Kerr, *J. Clin. Oncol.* **1998**, 16, 2761.

- [8] T. Schilling, B. K. Keppler, M. E. Heim, G. Niebch, H. Dietzfelbinger, J. Rastetter, A.-R. Hanauke, *Invest. New Drugs* **1995**, *13*, 327.
- [9] P. M. Abeyasinghe, M. M. Harding, *Dalton Trans.* **2007**, 3474.
- [10] E. Y. Tshuva, D. Peri, *Coord. Chem. Rev.* **2009**, *253*, 2098.
- [11] K. Strohfeltd, M. Tacke, *Chem. Soc. Rev.* **2008**, *37*, 1174.
- [12] C. G. Hartinger, P. J. Dyson, *Chem. Soc. Rev.* **2009**, *38*, 391.
- [13] F. Caruso, M. Rossi, *Met. Ions Biol. Syst.* **2004**, *42*, 353.
- [14] M. Harding, G. Mokdsi, *Curr. Med. Chem.* **2000**, *7*, 1289.
- [15] J. H. Bannon, I. Fichtner, A. O'Neill, C. Pampillon, N. J. Sweeney, K. Strohfeltd, R. W. Watson, M. Tacke, M. M. McGee, *Br. J. Cancer* **2007**, *97*, 1234.
- [16] G. Lummen, H. Sperling, H. Luboldt, T. Otto, H. Rubben, *Cancer Chemother. Pharmacol.* **1998**, *42*, 415.
- [17] N. Kröger, U. R. Kleeberg, K. B. Mross, L. Edler, G. Sass, D. K. Hossfeld, *Onkology* **2000**, *23*, 60.
- [18] H. Sun, H. Li, R. A. Weir, P. J. Sadler, *Angew. Chem., Int. Ed.* **1998**, *37*, 1577.
- [19] M. Guo, P. J. Sadler, *J. Chem. Soc., Dalton Trans.* **2000**, 7.
- [20] M. Guo, H. Sun, S. Bihari, J. A. Parkinson, R. O. Gould, S. Parsons, P. J. Sadler, *Inorg. Chem.* **2000**, *39*, 206.
- [21] M. Guo, H. Sun, H. J. McArdle, L. Gambling, P. J. Sadler, *Biochemistry* **2000**, *39*, 10023.
- [22] P. Köpf-Maier, D. Krah, *Chem.-Biol. Interact.* **1983**, *44*, 317.
- [23] P. Köpf-Maier, D. Krah, *Naturwissenschaften* **1981**, *68*, 273.
- [24] P. Köpf-Maier, *J. Struct. Biol.* **1990**, *105*, 35.
- [25] A. D. Tinoco, C. D. Incarvito, A. M. Valentine, *J. Am. Chem. Soc.* **2007**, *129*, 3444.
- [26] A. D. Tinoco, E. V. Eames, A. M. Valentine, *J. Am. Chem. Soc.* **2007**, *130*, 2262–2270.
- [27] M. Pavlaki, K. Debeli, I.-E. Triantaphyllidou, N. Klouras, E. Giannopoulou, A. J. Aletras, *J. Biol. Inorg. Chem.* **2009**, *14*, 947.
- [28] S. Gómez-Ruiz, G. N. Kaluđerović, D. Polo-Cerón, S. Prashar, M. Fajardo, Ž. Žižak, Z. D. Juranić, T. J. Sabo, *Inorg. Chem. Commun.* **2007**, *10*, 748.
- [29] S. Gómez-Ruiz, G. N. Kaluđerović, S. Prashar, D. Polo-Cerón, M. Fajardo, Ž. Žižak, T. J. Sabo, Z. D. Juranić, *J. Inorg. Biochem.* **2008**, *102*, 1558.
- [30] S. Gómez-Ruiz, G. N. Kaluđerović, Ž. Žižak, I. Besu, Z. D. Juranić, S. Prashar, M. Fajardo, *J. Organomet. Chem.* **2009**, *694*, 1981.
- [31] Y. Perez, V. Lopez, L. Rivera-Rivera, A. Cardona, E. Melendez, *J. Biol. Inorg. Chem.* **2005**, *10*, 94.
- [32] D. Peri, S. Meker, M. Shavit, E. Y. Tshuva, *Chem. Eur. J.* **2009**, *15*, 2403.
- [33] F. Caruso, M. Rossi, J. Tanski, R. Sartori, R. Sario, S. Moya, S. Diez, E. Navarrete, A. Cingolani, F. Marchetti, C. Pettinari, *J. Med. Chem.* **2000**, *43*, 3665.
- [34] F. Caruso, C. Pettinari, F. Marchetti, P. Natanti, C. Phillips, J. Tanski, M. Rossi, *Inorg. Chem.* **2007**, *46*, 7553.
- [35] J. Claffey, M. Hogan, H. Müller-Bunz, C. Pampillon, M. Tacke, *Chem. Med. Chem.* **2008**, *3*, 729.
- [36] I. Fichtner, J. Claffey, B. Gleeson, M. Hogan, D. Wallis, H. Weber, M. Tacke, *Lett. Drug Des. Disc.* **2008**, *5*, 489.
- [37] M. Shavit, E. Y. Tshuva, *Eur. J. Inorg. Chem.* **2008**, 1467.
- [38] S. Gómez-Ruiz, B. Gallego, Ž. Žižak, E. Hey-Hawkins, Z. D. Juranić, G. N. Kaluđerović, *Polyhedron* **2010**, *29*, 354.
- [39] S. Gómez-Ruiz, G. N. Kaluđerović, S. Prashar, E. Hey-Hawkins, A. Erić, Ž. Žižak, Z. D. Juranić, *J. Inorg. Biochem.* **2008**, *102*, 2087.
- [40] S. Gómez-Ruiz, B. Gallego, M. R. Kaluđerović, H. Kommera, E. Hey-Hawkins, R. Paschke, G. N. Kaluđerović, *J. Organomet. Chem.* **2009**, *694*, 2191.
- [41] M. R. Kaluđerović, S. Gómez-Ruiz, B. Gallego, E. Hey-Hawkins, R. Paschke, G. N. Kaluđerović, *Eur. J. Med. Chem.* **2010**, *45*, 519.
- [42] A. M. Cardoso, R. J. H. Clark, S. Moorhouse, *J. Chem. Soc., Dalton Trans.* **1980**, 1156.
- [43] S. Gómez-Ruiz, D. Polo-Cerón, S. Prashar, M. Fajardo, A. Antiñolo, A. Otero, *Eur. J. Inorg. Chem.* **2007**, 4445–4455.
- [44] Q. F. Soper, C. W. Whitehead, O. K. Behrens, J. J. Corse, R. G. Jones, *J. Am. Chem. Soc.* **1948**, *70*, 2849.
- [45] M. J. Frisch, G. W. Trucks, H. B. Schlegel, G. E. Scuseria, M. A. Robb, J. R. Cheeseman, J. A. Montgomery, Jr., T. Vreven, K. N. Kudin, J. C. Burant, J. M. Millam, S. S. Iyengar, J. Tomasi, V. Barone, B. Mennucci, M. Cossi, G. Scalmani, N. Rega, G. A. Petersson, H. Nakatsuji, M. Hada, M. Ehara, K. Toyota, R. Fukuda, J. Hasegawa, M. Ishida, T. Nakajima, Y. Honda, O. Kitao, H. Nakai, M. Klene, X. Li, J. E. Knox, H. P. Hratchian, J. B. Cross, V. Bakken, C. Adamo, J. Jaramillo, R. Gomperts, R. E. Stratmann, O. Yazyev, A. J. Austin, R. Cammi, C. Pomelli, J. W. Ochterski, P. Y. Ayala, K. Morokuma, G. A. Voth, P. Salvador, J. J. Dannenberg, V. G. Zakrzewski, S. Dapprich, A. D. Daniels, M. C. Strain, O. Farkas, D. K. Malick, A. D. Rabuck, K. Raghavachari, J. B. Foresman, J. V. Ortiz, Q. Cui, A. G. Baboul, S. Clifford, J. Cioslowski, B. B. Stefanov, G. Liu, A. Liashenko, P. Piskorz, I. Komaromi, R. L. Martin, D. J. Fox, T. Keith, M. A. Al-Laham, C. Y. Peng, A. Nanayakkara, M. Challacombe, P. M. W. Gill, B. Johnson, W. Chen, M. W. Wong, C. Gonzalez, J. A. Pople, *Gaussian 03, Revision C.02*, Gaussian Inc., Wallingford, CT, **2004**.
- [46] A. D. Becke, *J. Chem. Phys.* **1993**, *98*, 5648.
- [47] C. Lee, W. Yang, R. G. Parr, *Phys. Rev. B* **1988**, *37*, 785.
- [48] S. H. Vosko, L. Wilk, M. Nusair, *Can. J. Phys.* **1980**, *58*, 1200.
- [49] P. J. Stephens, F. J. Devlin, C. F. Chabalowski, M. J. Frisch, *J. Phys. Chem.* **1994**, *98*, 11623.
- [50] W. J. Hehre, R. Ditchfield, J. A. Pople, *J. Chem. Phys.* **1972**, *56*, 2257.
- [51] J. D. Dill, J. A. Pople, *J. Chem. Phys.* **1975**, *62*, 2921.
- [52] M. M. Francl, W. J. Pietro, W. J. Hehre, J. S. Binkley, M. S. Gordon, D. J. DeFrees, J. A. Pople, *J. Chem. Phys.* **1982**, *77*, 3654.
- [53] V. Rassolov, J. A. Pople, M. A. Ratner, T. L. Windus, *J. Chem. Phys.* **1998**, *109*, 1223.
- [54] C. Pampillon, J. Claffey, M. Hogan, M. Tacke, *BioMetals* **2008**, *21*, 197.
- [55] P. Skehan, R. Storeng, D. Scudiero, A. Monks, J. McMahon, D. Vistica, J. T. Warren, H. Bokesch, S. Kenney, M. R. Boyd, *J. Natl. Cancer Inst.* **1990**, *82*, 1107.
- [56] J. A. Marmur, *J. Mol. Biol.* **1961**, *3*, 208.
- [57] M. F. Reichmann, S. A. Rice, C. A. Thomas, P. Doty, *J. Am. Chem. Soc.* **1954**, *76*, 3047.
- [58] G. B. Deacon, R. J. Philips, *Coord. Chem. Rev.* **1980**, *33*, 227.
- [59] S. Gómez-Ruiz, A. Garcés, S. Prashar, M. Fajardo, A. Antiñolo, A. Otero, *Inorg. Chim. Acta* **2009**, *362*, 1042.
- [60] L. F. Cannizzo, R. H. Grubbs, *J. Org. Chem.* **1985**, *50*, 2316.
- [61] K. Doppert, H.-P. Klein, U. Thewalt, *J. Organomet. Chem.* **1986**, *303*, 205.
- [62] D. A. Edwards, M. F. Mahon, T. J. Paget, *Polyhedron* **2000**, *19*, 757.
- [63] T. Krüger, C. Wagner, T. Lis, R. Kluge, W. Mörke, D. Steinborn, *Inorg. Chim. Acta* **2006**, *359*, 2489.
- [64] R. Bina, M. Pavlista, Z. Cernosek, I. Cisarova, I. Pavlik, *Appl. Organomet. Chem.* **2005**, *19*, 701.
- [65] S. Gómez-Ruiz, G. N. Kaluđerović, D. Polo-Cerón, V. Tayurskaya, S. Prashar, M. Fajardo, R. Paschke, *J. Organomet. Chem.* **2009**, *694*, 3032.
- [66] T. M. Kelly, A. B. Tossi, D. J. McConnell, T. C. Streckas, *Nucleic Acids Res.* **1985**, *13*, 6017.
- [67] J. K. Barton, A. T. Danishefsky, J. M. Goldberg, *J. Am. Chem. Soc.* **1984**, *106*, 2172.
- [68] S. A. Tyscoe, R. J. Morgan, A. D. Baker, T. C. Streckas, *J. Phys. Chem.* **1993**, *97*, 1707.
- [69] R. F. Pasternack, E. J. Gibbs, J. J. Villafranca, *Biochemistry* **1983**, *22*, 2406.
- [70] J. Liu, T. Zhang, T. Lu, L. Qu, H. Zhou, Q. Zhang, L. Ji, *J. Inorg. Biochem.* **2002**, *91*, 269.
- [71] C. Liu, J. Y. Zhou, Q. X. Li, L. J. Wang, Z. R. Liao, H. B. Xu, *J. Inorg. Biochem.* **1999**, *75*, 233.
- [72] S. Zhang, Y. Zhu, C. Tu, H. Wei, Z. Yang, L. Lin, J. Ding, J. Zhang, Z. Guo, *J. Inorg. Biochem.* **2004**, *98*, 2099.
- [73] M. T. Carter, M. Rodriguez, A. J. Bard, *J. Am. Chem. Soc.* **1989**, *111*, 8901.
- [74] A. M. Pyle, J. P. Rehmann, R. Meshoyrer, C. V. Kumar, N. J. Turro, J. K. Barton, *J. Am. Chem. Soc.* **1989**, *111*, 3051.



Contents lists available at ScienceDirect

Polyhedron

journal homepage: www.elsevier.com/locate/poly



Cyclopentadienyltin(IV) derivatives: synthesis, characterization and study of their cytotoxic activities

Santiago Gómez-Ruiz^{a,*}, Sanjiv Prashar^a, Till Walther^b, Mariano Fajardo^a, Dirk Steinborn^b, Reinhard Paschke^c, Goran N. Kaluđerović^{b,c,d,*}

^a Departamento de Química Inorgánica y Analítica, E.S.C.E.T., Universidad Rey Juan Carlos, 28933 Móstoles, Madrid, Spain

^b Institut für Chemie, Martin-Luther-Universität Halle-Wittenberg, Kurt-Mothes-Straße 2, D-06120 Halle, Germany

^c Biozentrum, Martin-Luther-Universität Halle-Wittenberg, Weinbergweg 22, 06120 Halle, Germany

^d Department of Chemistry, Institute of Chemistry, Technology and Metallurgy, University of Belgrade, Studentski trg 14, 11000 Belgrade, Serbia

ARTICLE INFO

Article history:

Available online 2 June 2009

Keywords:

Anticancer drugs

Tin

Cytotoxicity

Cyclopentadienyl ligands

Cisplatin

ABSTRACT

The organotin compounds, $[\text{SnPh}_3(\text{C}_5\text{H}_4\text{R})]$ ($\text{R} = \text{Bu}^t$ (**1**), $\text{CMe}_2(\text{CH}_2\text{CH}_2\text{CH}=\text{CH}_2)$ (**2**) and $[\text{SnPh}_3(\text{C}_5\text{Me}_4\text{R})]$ ($\text{R} = \text{H}$ (**3**), SiMe_3 (**4**)), were prepared by the reaction of SnPh_3Cl with the lithium derivative of the corresponding cyclopentadiene. **1–4** have been characterized by multinuclear NMR spectroscopy (^1H , $^{13}\text{C}\{^1\text{H}\}$ and $^{119}\text{Sn}\{^1\text{H}\}$). In addition, the molecular structures of **1**, **2** and **4** were determined by single-crystal X-ray diffraction studies. The cytotoxic activity of the organotin(IV) complexes (**1–4**) was tested against human tumour cell lines 8505C anaplastic thyroid cancer, A253 head and neck tumour, A549 lung carcinoma, A2780 ovarian cancer, DLD-1 colon carcinoma. Compounds **1–4** present higher activities than cisplatin in all the studied cells. The highest sensitivity of the synthesized tin(IV) complexes was observed against A2780 ovarian cancer and DLD-1 colon carcinoma. Complex **3** presents the highest cytotoxic activity of all the studied complexes in all the cancer cells, with IC_{50} values from 0.037 to 0.085 μM , however, its trimethylsilyl-substituted analogue (**4**), showed the lowest activity against all the studied cells with IC_{50} values from 0.163 to 0.351 μM . Complexes **1** and **2** presented very similar activities on all the cancer cells (IC_{50} values from 0.044 to 0.119 μM).

© 2009 Elsevier Ltd. All rights reserved.

1. Introduction

Research on the synthesis and applications of metal-based drugs are currently considered as one of the most expanding areas in biomedical and inorganic chemistry [1–3]. Recent studies have shown very promising *in vitro* antitumour properties of organotin compounds against a wide panel of tumour cell lines of human origin [4–10]. In some cases, organotin(IV) derivatives have also shown acceptable antiproliferative *in vivo* activity as new chemotherapy agents [11–16]. From all the studied tin(IV) derivatives, di and triorganotin(IV) carboxylate [17–23], thiolate [24–30] and dithiocarbamate [31] complexes have been studied extensively, while cyclopentadienyltin(IV) derivatives have only recently been studied very briefly [32].

In this context, and taking into account that the modification of the cyclopentadienyl ligands has a notable effect on the antiproliferative effect of metallocene complexes in anticancer tests [33–39], we decided to study the cytotoxic activity of cyclopentadienyltin(IV)

derivatives, in order to observe the influence of the substituents attached to the cyclopentadienyl ring on the final anticancer activity of the organotin(IV) complexes. Thus, as a continuation of our work in the synthesis of cyclopentadienyltin(IV) derivatives [40], we report the synthesis, structural characterization and evaluation of the cytotoxic activity on human cancer cells of four triphenyltin(IV) complexes with different cyclopentadienyl ligands (Fig. 1). One of the studied complexes is $[\text{SnPh}_3\{\text{C}_5\text{H}_4\text{CMe}_2(\text{CH}_2\text{CH}_2\text{CH}=\text{CH}_2)\}]$, which contains the alkenyl-substituted cyclopentadienyl ligand $\text{C}_5\text{H}_4\text{CMe}_2(\text{CH}_2\text{CH}_2\text{CH}=\text{CH}_2)$ that has proven to induce an increase in the cytotoxic activity of titanocene complexes [36–38], however, in this study with cyclopentadienyltin(IV) derivatives, this positive effect of the alkenyl substituent is not observed and, in contrast to the results obtained for titanocene complexes [36–38], the compound $[\text{SnPh}_3(\text{C}_5\text{Me}_4\text{H})]$ containing a tetramethylcyclopentadienyl moiety is the most active of the studied compounds.

2. Experimental

2.1. General manipulations

All reactions were performed using standard Schlenk tube techniques in an atmosphere of dry nitrogen. Solvents were distilled

* Corresponding authors. Tel.: +34 914888527; fax: +34 914888143 (S. Gómez-Ruiz), fax: +38 111636061 (G.N. Kaluđerović).

E-mail addresses: santiago.gomez@urjc.es (S. Gómez-Ruiz), goran.kaluderovic@chemie.uni-halle.de, goran@chem.bg.ac.rs (G.N. Kaluđerović).

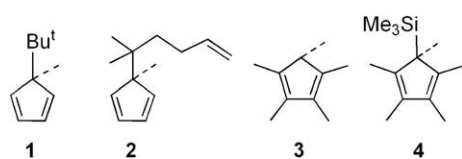


Fig. 1. Cyclopentadienyl derivatives used in this study.

from the appropriate drying agents and degassed before use. SnPh₃Cl and Li(C₅H₄Bu^t) were purchased from Aldrich and used without further purification. Li(C₅H₄CMe₂(CH₂CH₂CH=CH₂)) [41], Li(C₅Me₄H) [42] and Li(C₅Me₄SiMe₃) [43] were prepared as previously reported. ¹H, ¹³C{¹H} and ¹¹⁹Sn{¹H} NMR spectra were recorded on a Varian Mercury FT-400 spectrometer and referenced to the residual deuterated solvent or to SnMe₄ in the case of ¹¹⁹Sn{¹H} NMR. Microanalyses were carried out with a Perkin–Elmer 2400 microanalyzer. IR spectra (KBr pellets were prepared in a nitrogen-filled glove box) were recorded on a Nicolet Avatar 380 FTIR spectrometer in the range 350–4000 cm⁻¹. FAB-MS spectra were recorded on a MASPEC II spectrometer with 3-nitrobenzylalcohol as matrix.

2.2. Synthesis of [SnPh₃(C₅H₄Bu^t)] (1)

Li(C₅H₄Bu^t) (0.75 g, 5.85 mmol) was added to a solution of SnPh₃Cl (2.25 g, 5.85 mmol) in THF (50 ml) at -78 °C. The reaction mixture was allowed to reach room temperature and stirred for 16 h. Solvent was removed by applying reduced pressure and hexane (40 ml) added. The suspension was filtered and the filtrate concentrated (5 ml). Cooling to -30 °C yielded the title compound as a yellow crystalline solid. Yield: 2.34 g, 85%. FT-IR (KBr): 3139 (m), 3065 (s), 2972 (s), 2912 (s), 2845 (s), 2723 (w), 1946 (m), 1887 (m), 1813 (m), 1615 (w), 1476 (s), 1432 (s), 1372 (m), 1301 (m), 1263 (w), 1190 (w), 1074 (s), 1022 (s), 997 (m), 975 (m), 890 (s), 850 (m), 829 (m), 805 (m), 725 (s), 697 (s), 669 (s), 658 (s), 643 (m), 447 (s); ¹H NMR (400 MHz, CDCl₃, 25 °C): δ 1.03 (s, 9H, Bu^t), 5.65 (m, 2H, ³J(¹H–Sn) = 61.2 Hz, C₅H₄), 6.57 (m, 2H, C₅H₄) 7.42 (br m, 9H, *m*- and *p*-protons in SnPh₃), 7.56 (br m, 6H, ³J(¹H–Sn) = 50.2 Hz, *o*-protons in SnPh₃); ¹³C{¹H} NMR (100.6 MHz, CDCl₃, 25 °C): δ 30.8 (Me of Bu^t, ³J(¹³C–Sn) = 9.2 Hz), 32.2 (C-*ipso* of Bu^t, ²J(¹³C–Sn) not observed), 90.7 (C-1 of Cp, ¹J(¹³C–Sn) not observed) 125.0, 154.5 (C-2 and C-3 of Cp), 128.7 (C-3 and C-5 of SnPh₃, ³J(¹³C–Sn) = 52.3 Hz), 129.5 (C-4 of SnPh₃, ⁴J(¹³C–Sn) = 9.2 Hz), 137.2 (C-2 and C-6 of SnPh₃, ²J(¹³C–Sn) = 38.4 Hz), 138.4 (C-1 of SnPh₃, ¹J(¹³C–Sn) not observed); ¹¹⁹Sn{¹H} NMR (149.2 MHz, CDCl₃, 25 °C): δ -101.7; MS FAB (*m/e* (relative intensity)): 472 (1) [M⁺+H], 395 (10) [M⁺-Ph], 351 (100) [M⁺-C₅H₄Bu^t], 241 (13) [M⁺-3 × Ph]. *Anal. Calc.* for C₂₇H₂₈Sn: C, 68.82; H, 5.99. Found: C, 68.77; H, 5.81%.

2.3. Synthesis of [SnPh₃(C₅H₄CMe₂(CH₂CH₂CH=CH₂))] (2)

The preparation of **2** was carried out in an identical manner to **1**. Li(C₅H₄CMe₂(CH₂CH₂CH=CH₂)) (0.75 g, 4.46 mmol) and SnPh₃Cl (1.72 g, 4.46 mmol). Yield: 1.64 g, 72%. FT-IR (KBr): 3138 (m), 3065 (s), 3049 (s), 3018 (s), 2922 (s), 1946 (m), 1887 (m), 1871 (m), 1813 (m), 1756 (w), 1640 (s), 1579 (s), 1480 (s), 1430 (s), 1377 (m), 1300 (s), 1260 (m), 1190 (m), 1156 (m), 1075 (s), 1022 (m), 997 (m), 977 (m), 906 (m), 806 (s), 725 (s), 698 (m), 675 (m), 658 (m), 644 (w), 567 (m), 525 (m), 447 (s); ¹H NMR (400 MHz, CDCl₃, 25 °C): δ 1.00 (s, 6H, CMe₂), 1.45, 1.78 (m, 2H each, CH₂CH₂), 4.89 (*cis*), 4.95 (*trans*) (dd, 1H each, ³J(¹H–¹H)_{*cis*} = 11.7 Hz, ³J(¹H–¹H)_{*trans*} = 16.9 Hz, CH₂-CH=CH₂), 5.64 (m, 2H, ³J(¹H–Sn) = 53.1 Hz, C₅H₄), 5.73 (m, 1H, CH₂-CH=CH₂), 6.55 (m, 2H, C₅H₄) 7.42 (br m, 9H, *m*- and *p*-protons in SnPh₃),

7.56 (br m, 6H, ³J(¹H–Sn) = 45.0 Hz, *o*-protons in SnPh₃); ¹³C{¹H} NMR (100.6 MHz, CDCl₃, 25 °C): δ 28.4, 29.4 (CH₂CH₂), 35.2 (CMe₂), 42.5 (CpC), 113.7 (CH₂-CH=CH₂), 90.7 (C-1 of Cp, ¹J(¹³C–Sn) not observed), 125.7, 153.0 (C-2 and C-3 of Cp), 128.8 (C-3 and C-5 of SnPh₃, ³J(¹³C–Sn) = 52.5 Hz), 129.5 (C-4 of SnPh₃, ⁴J(¹³C–Sn) = 12.1 Hz), 137.2 (C-2 and C-6 of SnPh₃, ²J(¹³C–Sn) = 38.3 Hz), 138.4 (C-1 of SnPh₃, ¹J(¹³C–Sn) not observed), 140.1 (CH₂-CH=CH₂); ¹¹⁹Sn{¹H} NMR (149.2 MHz, CDCl₃, 25 °C): δ -101.2; MS FAB (*m/e* (relative intensity)): 511 (2) [M⁺], 433 (7) [M⁺-H-Ph], 380 (6) [M⁺-Ph-CH₂CH₂CH=CH₂], 351 (100) [M⁺-C₅H₄(CMe₂(CH₂CH₂CH=CH₂))]. *Anal. Calc.* for C₃₀H₃₂Sn: C, 70.47; H, 6.31. Found: C, 70.10; H, 6.20%.

2.4. Synthesis of [SnPh₃(C₅Me₄H)] (3)

The preparation of **3** was carried out in an identical manner to **1**. Li(C₅Me₄H) (0.75 g, 5.85 mmol) and SnPh₃Cl (2.25 g, 5.85 mmol). Yield: 1.82 g, 67%. FT-IR (KBr): 3135 (m), 3063 (s), 3016 (s), 2960 (s), 2910 (s), 2854 (s), 2730 (w), 1952 (m), 1877 (m), 1817 (m), 1773 (w), 1619 (m), 1578 (m), 1480 (s), 1428 (s), 1384 (m), 1332 (m), 1258 (w), 1225 (w), 1109 (s), 1040 (m), 1022 (m), 997 (m), 908 (m), 727 (m), 670 (m), 658 (m), 555 (m), 453 (s); ¹H NMR (400 MHz, CDCl₃, 25 °C): δ 1.75 (s, 6H, ⁴J(¹H–Sn) = 19.2 Hz, C₅Me₄), 1.82 (s, 6H, C₅Me₄), 4.09 (s, 1H, ¹J(¹H–Sn) = 100.1 Hz, C₅Me₄H), 7.39 (br m, 9H, *m*- and *p*-protons in SnPh₃), 7.50 (br m, 6H, ³J(¹H–Sn) = 51.5 Hz, *o*-protons in SnPh₃); ¹³C{¹H} NMR (100.6 MHz, CDCl₃, 25 °C): δ 11.8 (C₅Me₄, ³J(¹³C–Sn) = 9.0 Hz), 14.0 (C₅Me₄), 57.7 (C-1 of Cp, ¹J(¹³C–Sn) not observed), 128.3 (C-3 and C-5 of SnPh₃, ³J(¹³C–Sn) = 50.4 Hz), 128.9 (C-4 of SnPh₃, ⁴J(¹³C–Sn) = 11.6 Hz), 130.3, 134.2 (C-2 and C-3 of Cp), 137.0 (C-2 and C-6 of SnPh₃, ²J(¹³C–Sn) = 38.7 Hz), 138.7 (C-1 of SnPh₃, ¹J(¹³C–Sn) not observed); ¹¹⁹Sn{¹H} NMR (149.2 MHz, CDCl₃, 25 °C): δ -113.8; MS FAB (*m/e* (relative intensity)): 472 (6) [M⁺+H], 395 (9) [M⁺-Ph], 351 (100) [M⁺-C₅Me₄H], 241 (22) [M⁺-3 × Ph]. *Anal. Calc.* for C₂₇H₂₈Sn: C, 68.82; H, 5.99. Found: C, 68.69; H, 5.90%.

2.5. Synthesis of [SnPh₃(C₅Me₄SiMe₃)] (4)

The preparation of **4** was carried out in an identical manner to **1**. Li(C₅Me₄SiMe₃) (0.75 g, 3.74 mmol) and SnPh₃Cl (1.44 g, 3.74 mmol). Yield: 1.56 g, 77%. FT-IR (KBr): 3133 (m), 3065 (s), 3020 (s), 2960 (s), 2920 (s), 2870 (s), 2725 (w), 1949 (m), 1877 (m), 1814 (m), 1772 (w), 1623 (m), 1603 (s), 1578 (m), 1481 (s), 1429 (s), 1376 (m), 1302 (s), 1247 (m), 1205 (m), 1155 (m), 1109 (w), 1073 (m), 1022 (m), 997 (m), 960 (s), 891 (w), 836 (m), 727 (s), 698 (s), 656 (m), 628 (m), 556 (m), 452 (s); ¹H NMR (400 MHz, CDCl₃, 25 °C): δ -0.04 (s, 9H, SiMe₃), 1.86 (s, 6H, ⁴J(¹H–Sn) = 17.4 Hz, C₅Me₄), 1.90 (s, 6H, C₅Me₄), 7.37 (br m, 9H, *m*- and *p*-protons in SnPh₃), 7.51 (br m, 6H, ³J(¹H–Sn) = 49.5 Hz, *o*-protons in SnPh₃); ¹³C{¹H} NMR (100.6 MHz, CDCl₃, 25 °C): δ -0.2 (SiMe₃), 11.4 (C₅Me₄, ³J(¹³C–Sn) not observed), 15.6 (C₅Me₄), 61.2 (C-1 of Cp, ¹J(¹³C–Sn) not observed), 128.1 (C-3 and C-5 of SnPh₃, ¹J(¹³C–Sn) = 48.9 Hz), 128.7 (C-4 of SnPh₃, ⁴J(¹³C–Sn) = 10.6 Hz), 129.0, 136.2 (C-2 and C-3 of Cp), 137.4 (C-2 and C-6 of SnPh₃, ²J(¹³C–Sn) = 35.8 Hz), 139.9 (C-1 of SnPh₃, ¹J(¹³C–Sn) not observed); ¹¹⁹Sn{¹H} NMR (149.2 MHz, CDCl₃, 25 °C): δ -135.2; MS FAB (*m/e* (relative intensity)): 544 (5) [M⁺], 467 (8) [M⁺-Ph], 351 (100) [M⁺-C₅Me₄SiMe₃], 313 (9) [M⁺-3 × Ph]. *Anal. Calc.* for C₃₀H₃₆SiSn: C, 66.31; H, 6.68. Found: C, 65.97; H, 6.52%.

2.6. Data collection and structural refinement of **1**, **2** and **4**

The data of **1**, **2** and **4** were collected with a CCD Oxford Xcalibur S (λ (Mo K α) = 0.71073 Å) using ω and ϕ scans mode. Semi-empir-

Appendix 9

Reproduced from Ref. S. Gómez-Ruiz, S. Prashar, T. Walther, M. Fajardo, D. Steinborn, R. Paschke, G.N. Kaluđerović, *Polyhedron* 2010, 29, 16 with permission from Elsevier.

18

S. Gómez-Ruiz et al./Polyhedron 29 (2010) 16–23

ical from equivalents absorption corrections were carried out with SCALE3 ABSPACK [44]. All the structures were solved by direct methods [45]. Structure refinement was carried out with SHELXL-97 [46]. All non-hydrogen atoms were refined anisotropically, and hydrogen atoms were calculated with the riding model and refined isotropically. Crystallographic details are listed in Table 1.

2.7. In vitro studies

2.7.1. Preparation of drug solutions

Stock solutions of the studied tin compounds were prepared in dimethyl sulfoxide (**1** and **2**; DMSO, Sigma Aldrich) and dimethyl formamide (**3** and **4**; DMF, Sigma Aldrich) at a concentration of 20 mM, filtered through Millipore filter, 0.22 μm, before use, and diluted by nutrient medium to various working concentrations. Nutrient medium was RPMI-1640 (PAA Laboratories) supplemented with 10% fetal bovine serum (Biochrom AG) and penicillin/streptomycin (PAA Laboratories).

2.7.2. Cell lines and culture conditions

The cell lines 8505C, A253, A549, A2780 and DLD-1 that were included in this study, were kindly provided by Dr. Thomas Mueller, Department of Hematology/Oncology, Martin Luther University of Halle-Wittenberg, Halle (Saale), Germany. Cultures were maintained as monolayer in RPMI 1640 (PAA Laboratories, Pasching, Germany) supplemented with 10% heat inactivated fetal bovine serum (Biochrom AG, Berlin, Germany) and penicillin/streptomycin (PAA Laboratories) at 37 °C in a humidified atmosphere of 5% (*v/v*) CO₂.

2.7.3. Cytotoxicity assay

The cytotoxic activities of the tin complexes were evaluated using the sulforhodamine-B (SRB, Sigma Aldrich) microculture colorimetric assay [47]. In short, exponentially growing cells were seeded into 96-well plates on day zero at the appropriate cell densities to prevent confluence of the cells during the period of the experiment. After 24 h, the cells were treated with serial dilutions of the studied compounds for 96 h. Final concentrations

achieved in treated wells were 0.01, 0.03, 0.1, 0.3, 1, 3, 10, 30 and 100 μmol/l. Each concentration was tested in triple quadruplicate on each cell line. The final concentrations (<0.1%) of DMSO and DMF, were non-toxic to the cells. The percentages of surviving cells relative to untreated controls were determined 96 h after the beginning of drug exposure. After 96 h treatment, the supernatant medium from the 96-well plates was thrown away and the cells were fixed with 10% TCA. For a thorough fixation, plates were now allowed to stand at 4 °C. After fixation the cells were washed in a strip washer. The washing was carried out four times with water using alternate dispensing and aspiration procedures. The plates were then dyed with 100 μl of 0.4% SRB for about 45 min. After dyeing the plates were again washed to remove the dye with 1% acetic acid and allowed to air dry overnight. 100 μl of 10 mM Tris base solutions was added to each well of the plate and absorbance was measured at 570 nm using a 96-well plate reader (Tecan Spectra, Crailsheim, Germany). The IC₅₀ values, defined as the concentrations of the compound at which 50% cell inhibition was observed, was estimated from the dose-response curves.

3. Results and discussion

3.1. Synthesis and characterization of the cyclopentadienyltin(IV) complexes **1–4**

The preparation of tin complexes was achieved via the reaction of one equivalent of the lithium cyclopentadienyl derivative with SnPh₃Cl (Schemes 1 and 2).

Complexes **1–4** have been characterized by ¹H, ¹³C{¹H} and ¹¹⁹Sn{¹H} NMR spectroscopy, mass spectrometry and elemental analysis (see Sections 2.2–2.5). NMR spectral data for **1–4** indicated that, in solution, only one of the possible double bond positional isomers was present. This phenomenon differs from the observation of multiple isomers in analogous silicon and germanium bridged cyclopentadiene ligands [48–52].

In the ¹H NMR spectra of **1–4**, two different multiplets, at ca. 7.2 corresponding to the *m*- and *p*-protons and at 7.5 ppm assigned to

Table 1
Crystallographic data for **1**, **2** and **4**.

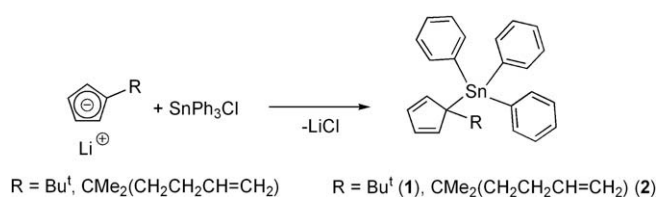
	1	2	4
Formula	C ₂₇ H ₂₈ Sn	C ₃₀ H ₃₂ Sn	C ₃₀ H ₃₆ SiSn
Fw	471.18	511.25	543.37
T (K)	130(2)	130(2)	130(2)
Crystal system	triclinic	triclinic	triclinic
Space group	Pī	Pī	Pī
a (Å)	11.0569(7)	9.394(1)	8.4654(5)
b (Å)	13.7460(8)	11.682(1)	9.8404(8)
c (Å)	16.5966(9)	12.396(2)	17.866(1)
α (°)	80.945(5)	71.007(9)	93.486(6)
β (°)	88.554(5)	86.457(9)	101.221(6)
γ (°)	66.918(6)	78.040(8)	111.870(7)
V (nm ³)	2.2898(3)	1.2584(3)	1.3402(2)
Z	4	2	2
D _c (Mg m ⁻³)	1.367	1.349	1.346
μ (mm ⁻¹)	1.125	1.029	1.013
F(0 0 0)	960	524	560
Crystal dimension (mm)	0.3 × 0.15 × 0.04	0.3 × 0.1 × 0.1	0.4 × 0.2 × 0.04
θ Range (°)	2.75–25.68	2.61–26.37	2.65–30.51
hkl Ranges	–12 ≤ h ≤ 12 –16 ≤ k ≤ 16 –20 ≤ l ≤ 17	–11 ≤ h ≤ 11 –14 ≤ k ≤ 14 –15 ≤ l ≤ 15	–12 ≤ h ≤ 11 –14 ≤ k ≤ 13 –25 ≤ l ≤ 17
Data/parameters/restraints	8645/511/0	5152/282/0	8165/296/0
Goodness-of-fit (GOF) on F ²	0.940	0.916	0.885
Final R indices [I > 2σ(I)]	R ₁ = 0.0530, wR ₂ = 0.1045	R ₁ = 0.0344, wR ₂ = 0.0562	R ₁ = 0.0324, wR ₂ = 0.0544
R indices (all data)	R ₁ = 0.1130, wR ₂ = 0.1114	R ₁ = 0.0538, wR ₂ = 0.0588	R ₁ = 0.0456, wR ₂ = 0.0558
Largest difference in peak and hole (e Å ⁻³)	1.545 and –0.542	1.196 and –0.583	0.885 and –0.353

Appendix 9

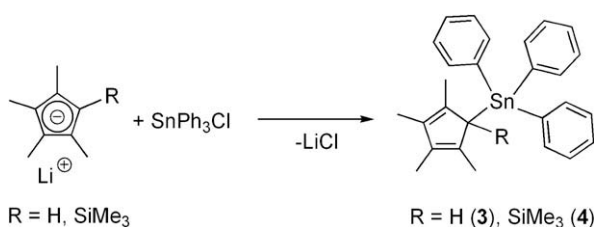
Reproduced from Ref. S. Gómez-Ruiz, S. Prashar, T. Walther, M. Fajardo, D. Steinborn, R. Paschke, G.N. Kaluđerović, *Polyhedron* 2010, 29, 16 with permission from Elsevier.

S. Gómez-Ruiz et al. / *Polyhedron* 29 (2010) 16–23

19



Scheme 1. Synthesis of complexes **1** and **2**.



Scheme 2. Synthesis of complexes **3** and **4**.

the *o*-protons of SnPh₃ moiety respectively, were observed. In addition, satellite signals of the *o*-protons, due to coupling with the ¹¹⁷Sn and ¹¹⁹Sn isotopes at a three bond distance were observed, however, we were unable to resolve the independent satellite signals corresponding to the two tin nuclei. Therefore, the observed coupling constant for these protons of approximately 50 Hz is an approximate value that can be applied to either nucleus.

In the ¹H NMR spectra of **1** and **2**, two multiplets, at ca. 5.6 and 6.6 ppm, were assigned to the four C₅ ring protons. This indicates that the symmetry of the molecule is such that the alkyl substituent is located in the C-1 position of the cyclopentadienyl ring. For the equivalent cyclopentadienyl ring protons, C-2 and C-5, at three bond distance to the tin atom, tin satellite signals were observed with values of ³J(¹H–Sn) of ca. 30 Hz.

For **1**, a singlet signal at 1.03 ppm was observed in the ¹H NMR spectrum and assigned to the protons of the *tert*-butyl group. For **2** a singlet due to the two methyl groups substituting the carbon atom adjacent to the cyclopentadienyl ring was observed at 1.00 ppm. The alkenyl fragment exhibited five sets of signals, two corresponding to the methylene protons (two multiplets at ca. 1.5 and 1.8 ppm), one for the proton of the C-γ (a multiplet at ca. 5.6 ppm) and two for the terminal olefinic protons (multiplets at 4.89 and 4.95 ppm).

The ¹H NMR spectra of **3** and **4** are very similar. Both spectra show two singlets for the methyl substituents of the cyclopentadienyl rings between 1.7 and 1.9 ppm, one of which corresponds to the protons of the methyl groups in the C-2 and C-5 of the ring and shows satellites with ⁴J(¹H–Sn) of ca. 18 Hz, and the other to the protons of the C-3 and C-4 methyl groups in the cyclopentadienyl ligand. In the ¹H NMR spectrum of **3** a signal, at 4.09 ppm, with tin satellites (²J(¹H–Sn) 100.1 Hz) was recorded for the proton in the C-1 position, while in the ¹H NMR spectrum of **4** a singlet was observed at –0.04 ppm and assigned to the trimethylsilyl protons.

In the ¹³C{¹H} NMR spectra of **1–4**, four signals at ca. 128, 129, 137 and 139 ppm were observed for the C-3/C-5, C-4, C-1 and C-2/C-6 carbon atoms of the phenyl groups. Tin–carbon coupling constants for these signals gave values of approximately ²J(¹³C–Sn) 35 Hz, ³J(¹³C–Sn) 50 Hz, and ⁴J(¹³C–Sn) 10 Hz.

In addition to the signals assigned to the phenyl groups, three signals were recorded for the cyclopentadienyl carbon atoms. The C-1 atom gave a signal at ca. 100 ppm for **1** and **2** and 60 ppm for **3** and **4**. In all cases, the coupling constant at one bond distance, between the ¹³C and ¹¹⁷Sn and ¹¹⁹Sn nuclei was not observed due

to the low intensity of these signals, even when recording the spectra at very long relaxation times. Two signals assigned to the remaining carbon atoms of the cyclopentadienyl ring, were observed at ca. 125 and 154 ppm for **1** and **2**, and at ca. 130 and 135 ppm for **3** and **4**.

The expected signals corresponding to the different substituents of the cyclopentadienyl moiety were observed in the ¹³C{¹H} NMR spectra of **1–4** (see Sections 2.2–2.5). One signal was observed in the ¹¹⁹Sn{¹H} NMR spectra of **1–4** between –100 and –135 ppm.

The ¹¹⁹Sn{¹H} NMR characterization of all complexes was repeated with the solutions being prepared in an air atmosphere. Spectra were recorded in DMSO/CDCl₃ or DMF/CDCl₃ at 2, 4, 12, 24 and 48 h and no evidence of decomposition or evolution to other tin-containing products was observed.

Complexes **1–4** were also characterized by FAB-MS. The mass spectra showed the molecular ion peaks. Fragments indicative of the loss of different numbers of substituents were also observed (see Sections 2.2–2.5).

3.2. Structural studies

The molecular structures of **1**, **2** and **4** were established by single-crystal X-ray diffraction studies. The molecular structures and atomic numbering schemes are shown in Figs. 2–4, respectively. Selected bond lengths and angles for **1**, **2** and **4** are given in Table 2.

For **1**, two almost identical crystallographic independent molecules were located in the asymmetric unit, of which only one will be discussed.

The molecular structures of **1**, **2** and **4** are of a similar nature, all of them crystallize in the triclinic space group *P* $\bar{1}$ with four (**1**) or two (**2** and **4**) molecules located in the unit cell. In the molecular structures of **1**, **2** and **4** the geometry around the tin atom is clearly tetrahedral. The cyclopentadienyl units are essentially planar with the C-1 atom located only 0.108 Å for **1**, 0.077 Å for **2** and 0.011 Å for **4**, out of the plane defined by the other four carbon atoms (C(2) to C(5)). Three long bond lengths of about 1.47 Å and two short bond distances of ca. 1.35 Å are observed between the carbon atoms of the C₅ ring.

The hybridization of the C-1 atom of the cyclopentadienyl moiety is sp³ and the σ-bond lengths with the tin atom of about 2.19 Å are slightly longer than those recorded for the tin-phenyl carbon distances (ca. 2.13 Å). The tin–C-1–ring plane angles (110.90° for **1**, 111.70° for **2** and 115.86° for **4**) rule out an

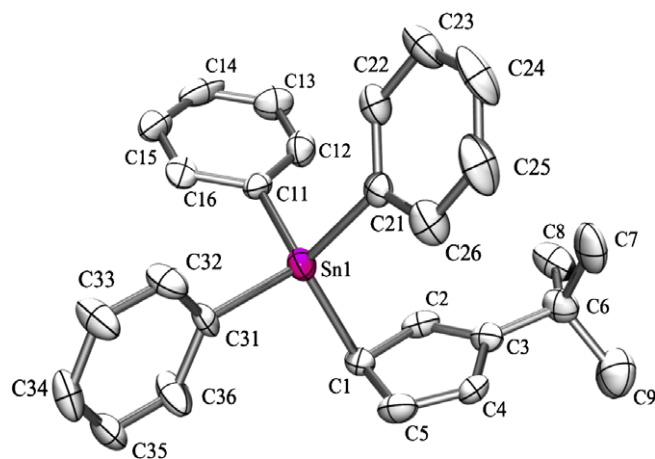


Fig. 2. Molecular structure and atom-labelling scheme for one of the two symmetry independent molecules of **1** with thermal ellipsoids at 50% probability (hydrogen atoms are omitted for clarity).

Appendix 9

Reproduced from Ref. S. Gómez-Ruiz, S. Prashar, T. Walther, M. Fajardo, D. Steinborn, R. Paschke, G.N. Kaluđerović, *Polyhedron* 2010, 29, 16 with permission from Elsevier.

20

S. Gómez-Ruiz et al. / *Polyhedron* 29 (2010) 16–23

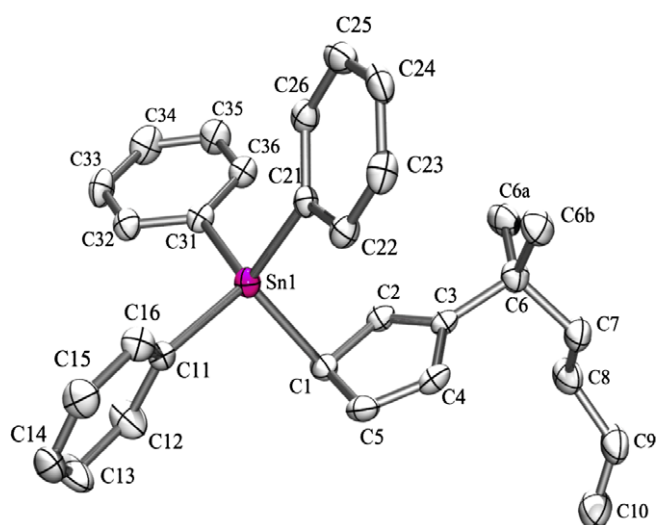


Fig. 3. Molecular structure and atom-labelling scheme for **2** with thermal ellipsoids at 50% probability (hydrogen atoms are omitted for clarity).

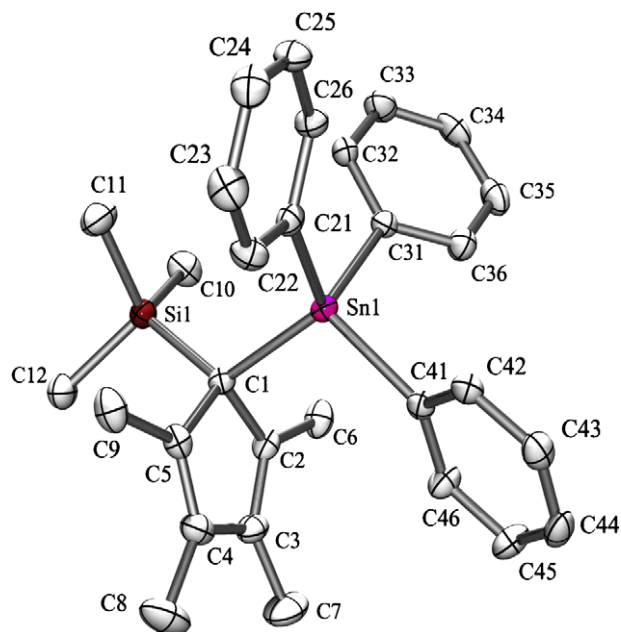


Fig. 4. Molecular structure and atom-labelling scheme for **4** with thermal ellipsoids at 50% probability (hydrogen atoms are omitted for clarity).

π - η^1 type interaction of the metal with the aromatic ring as has been previously observed in beryllium and zinc metallocene complexes [53–59].

In contrast to the observed spectroscopic data of the complexes **1** and **2** in solution, in which the obtained signals showed that the substituent at the cyclopentadienyl ligand was located in the C-1 position, due the rapid sigmatropic migration in solution of the tin atom around the cyclopentadienyl ring [60], in solid state, this substituent is located in the C-3 position, probably in order to minimize steric impediments as has been previously observed for other cyclopentadienyltin(IV) derivatives [60]. Thus, complex **1** presents the Bu^t substituent at the C-3 position and shows typical C–C bond lengths and angles. The alkenyl substituent of **2**, is also located at the C-3 atom of the C₅ ring. The distance C(9)–C(10) is typical for terminal C–C double bonds [41,61–63] and the angle C(8)–C(9)–C(10), 126.2(3)° confirms the sp² hybridization of C(9).

Table 2
Selected bond lengths (Å) and angles (°) for **1**, **2** and **4**.

	1 ^a	2	4
Sn(1)–C(1)	2.183(7)/2.193(6)	2.197(3)	2.189(2)
Sn(1)–C(11)	2.127(7)/2.132(7)	2.137(3)	
Sn(1)–C(21)	2.147(7)/2.126(8)	2.128(3)	2.147(2)
Sn(1)–C(31)	2.135(7)/2.135(7)	2.140(3)	2.143(2)
Sn(1)–C(41)			2.149(2)
Si(1)–C(1)			1.907(2)
C(1)–C(2)	1.454(9)/1.476(9)	1.466(4)	1.501(3)
C(1)–C(5)	1.459(9)/1.440(9)	1.470(4)	1.495(3)
C(2)–C(3)	1.363(9)/1.344(9)	1.346(4)	1.354(3)
C(3)–C(4)	1.435(9)/1.452(9)	1.442(4)	1.444(3)
C(4)–C(5)	1.352(9)/1.36(1)	1.344(4)	1.354(3)
C(3)–C(6)	1.49(2)/1.50(1)	1.522(4)	
C(6)–C(7)	1.54(1)/1.50(2)	1.541(4)	
C(7)–C(8)		1.530(4)	
C(8)–C(9)		1.496(5)	
C(9)–C(10)		1.296(5)	
C(1)–Sn(1)–C(11)	109.4(3)/105.9(3)	105.7(1)	
C(1)–Sn(1)–C(21)	113.2(3)/111.2(3)	112.2(2)	117.34(7)
C(1)–Sn(1)–C(31)	106.8(3)/111.1(3)	105.9(2)	110.10(7)
C(1)–Sn(1)–C(41)			109.79(7)
C(11)–Sn(1)–C(21)	105.9(3)/109.8(3)	111.2(1)	
C(11)–Sn(1)–C(31)	108.4(3)/112.4(3)	111.1(2)	
C(21)–Sn(1)–C(31)	113.0(3)/106.5(3)	110.5(1)	105.76(8)
C(21)–Sn(1)–C(41)			105.97(7)
C(31)–Sn(1)–C(41)			107.37(7)
C(1)–C(2)–C(3)	109.9(6)/110.1(6)	109.7(3)	109.3(2)
C(1)–C(5)–C(4)	109.0(7)/109.5(7)	108.0(3)	109.2(2)
C(2)–C(3)–C(4)	107.5(6)/107.3(7)	107.7(3)	109.1(2)
C(3)–C(4)–C(5)	109.3(6)/109.0(7)	110.3(3)	109.6(2)
C(5)–C(1)–C(2)	103.7(6)/103.8(6)	104.2(2)	102.8(2)
C(7)–C(8)–C(9)		113.3(3)	
C(8)–C(9)–C(10)		126.2(3)	

^a Values of the two symmetry independent molecules are given.

Selected structural data of **1**, **2** and **4** can be compared with similar cyclopentadienyltin(IV) compounds using Table 3.

3.3. Cytotoxic studies

The *in vitro* cytotoxicities of complexes **1–4** and cisplatin against human tumour cell lines 8505C anaplastic thyroid cancer, A253 head and neck tumour, A549 lung carcinoma, A2780 ovarian cancer and DLD-1 colon carcinoma were determined by using the sulforhodamine-B microculture colorimetric assay [47]. This study has been carried out in order to understand the relationship between the different tin(IV) compounds and the cytotoxic activity. The IC₅₀ values of the studied compounds and cisplatin are summarized in Table 4.

Triphenyltin(IV) complexes (**1–4**) showed a dose-dependent antiproliferative effect toward all cancer cell lines (Fig. 5), presenting, in all cases, lower IC₅₀ values than those of cisplatin. These results indicate their high activity against the tumoural cell lines evaluated.

In contrast to the results obtained for titanocene complexes with similar cyclopentadienyl ligands [36–38], **3** (which contains the tetramethylcyclopentadienyl moiety) is the most active compound with cytotoxic activities from 17 (against A253) to 104 times (against DLD-1) better than that of cisplatin, and IC₅₀ values between ca. 0.037 and 0.085 μM. Complexes **1** and **2**, which contain alkyl and alkenyl-substituted cyclopentadienyl ligands, present comparable cytotoxic activities on all the studied cells, showing IC₅₀ values from 0.044 to 0.119 μM. However, their activities are, in all cases, lower than those observed for **3**, indicating the absence of the positive effect on the cytotoxic activity provided by alkenyl-substituted cyclopentadienyl ligands [36–38], in tin(IV) complexes.

Appendix 9

Reproduced from Ref. S. Gómez-Ruiz, S. Prashar, T. Walther, M. Fajardo, D. Steinborn, R. Paschke, G.N. Kaluđerović, Polyhedron 2010, 29, 16 with permission from Elsevier.

S. Gómez-Ruiz et al. / Polyhedron 29 (2010) 16–23

21

Table 3
Selected structural data of cyclopentadienyln(IV) compounds.

Compound	Sn–C _(cp) ¹ (Å)	C–C _(cp) (Å)	C=C _(cp) (Å)	Si–C _(cp) ¹ (Å)	Reference
[SnPh ₃ (C ₅ H ₄ Bu ^t)] (1) ^a	2.183(7) 2.193(6)	1.435(9) 1.440(9) 1.452(9) 1.454(9) 1.459(9) 1.476(9)	1.363(9) 1.344(9) 1.352(9) 1.36(1)		This work
[SnPh ₃ (C ₅ H ₄ CMe ₂ (CH ₂ CH ₂ CH=CH ₂))] (2)	2.197(3)	1.442(4) 1.466(4) 1.470(4)	1.344(4) 1.346(4)		This work
[SnPh ₃ (C ₅ Me ₄ SiMe ₃)] (3)	2.189(2)	1.444(3) 1.495(3) 1.501(3)	1.354(3) 1.354(3)	1.907(2)	This work
[SnMe ₂ (C ₅ Me ₄ H) ₂] ^a	2.195(4) 2.205(4) 2.206(4) 2.202(4)	1.457(6) 1.459(5) 1.475(6) 1.480(5) 1.480(6) 1.497(5)	1.353(6) 1.353(6) 1.356(5) 1.359(5)		[40]
[SnMe ₂ (C ₅ Me ₄ SiMe ₃) ₂]	2.190(2)	1.456(3) 1.502(3) 1.505(3)	1.350(3) 1.358(3)	1.905(2)	[40]

^a Values for the two independent molecules found in the asymmetric unit are given.

Table 4
IC₅₀ (μM) for the 96 h of action of the studied compounds and cisplatin on 8505C anaplastic thyroid cancer, A253 head and neck tumour, A549 lung carcinoma, A2780 ovarian cancer and DLD-1 colon carcinoma determined by sulforhodamine-B microculture colorimetric assay.

Compound	IC ₅₀ ±SD				
	8505C	A253	A549	A2780	DLD-1
1	0.103 ± 0.015	0.077 ± 0.012	0.079 ± 0.002	0.042 ± 0.004	0.044 ± 0.007
2	0.110 ± 0.011	0.118 ± 0.028	0.108 ± 0.018	0.061 ± 0.002	0.119 ± 0.004
3	0.085 ± 0.007	0.045 ± 0.004	0.038 ± 0.003	0.037 ± 0.007	0.048 ± 0.002
4	0.343 ± 0.046	0.351 ± 0.045	0.384 ± 0.021	0.163 ± 0.002	0.309 ± 0.003
Cisplatin	5	0.8	1.5	0.55	5

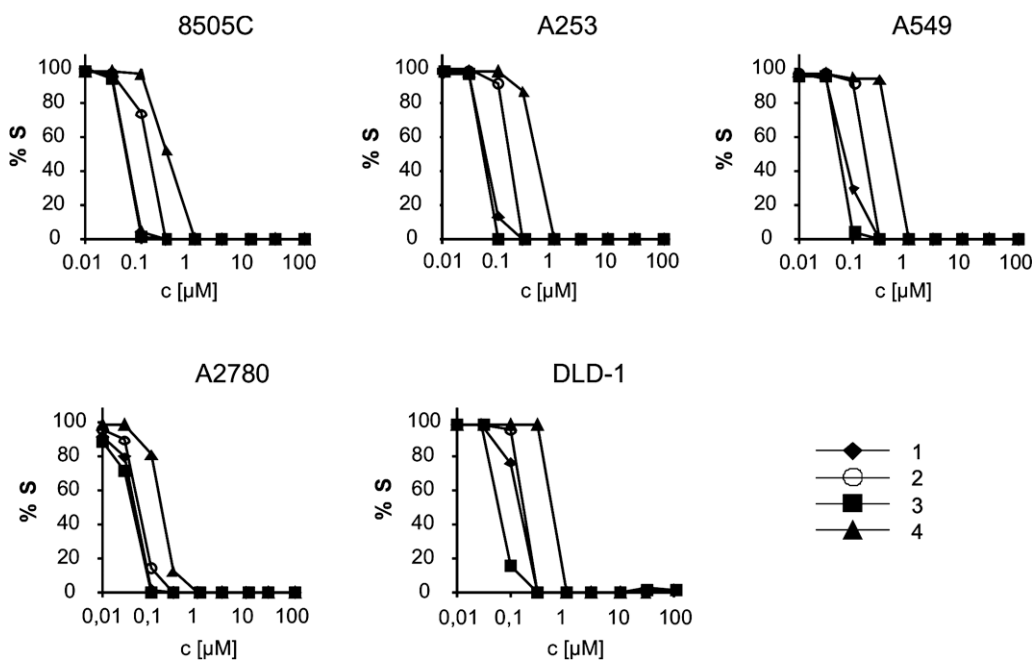


Fig. 5. Representative graphs showing survival of 8505C, A253, A549, A2780 and DLD-1 cells grown for 96 h in the presence of increasing concentrations of the studied compounds (1–4). Standard deviations are omitted for clarity.

Interestingly, the trimethylsilyl-substituted complex **4** showed lower *in vitro* antitumoural activity in comparison to other studied

derivatives, with IC₅₀ values from ca. 0.163 to 0.351 μM. Again, the enhancement of the antiproliferative activity of SiMe₃ groups

reported by McGowan and coworkers using trimethylsilyl-substituted titanocene complexes [64], is not observed for tin(IV) complexes. In addition, complexes 1–4 present substantially higher cytotoxic activity on cancer cell lines (up to 5000 times) than other reported cyclopentadienyltin(IV) derivatives [32].

With these data, one can conclude a ligand-dependent activity of the studied complexes on the different cells. Complexes bearing monosubstituted cyclopentadienyl ligands present different cytotoxic activities with respect to their tetra- and pentasubstituted analogues. In addition, one can conclude a different behaviour in the influence of the substituents of the cyclopentadienyl ligands on the final cytotoxic activity of titanocene and organotin(IV) complexes, indicating a substantial difference in the anticancer mechanism of these two class of metal-based drugs.

In addition, the cytotoxic activities of the previously reported titanocene complexes bearing similar ligands presented IC₅₀ values from 24 to 175 μM [36–38] which are much lower than those found in the cyclopentadienyltin(IV) derivatives with IC₅₀ values from 0.037 to 0.384 μM.

4. Conclusions

A variety of cyclopentadienyltin(IV) compounds have been synthesized and structurally characterized. Metal derivatives, were tested *in vitro* against human tumour cell lines 8505C anaplastic thyroid cancer, A253 head and neck tumour, A549 lung carcinoma, A2780 ovarian cancer and DLD-1 colon carcinoma. The studied tin(IV) compounds presented very high activity against the evaluated tumoural cell lines, up to ca. 100 times higher than that of cisplatin and up to ca. 5000 times higher than those reported for similar cyclopentadienyltin(IV) derivatives [32].

3 (which contains the tetramethylcyclopentadienyl ligand) is the most active compound against all the studied cancer cells, presenting IC₅₀ values between 0.037 and 0.085 μM.

Following on from these results, intensive studies on the mechanism of action of cyclopentadienyltin(IV) derivatives against the different studied cancer cells are currently being carried out.

Supplementary data

CCDC 729606, 729607 and 729608 contain the supplementary crystallographic data for 1, 2 and 4, respectively. These data can be obtained free of charge via <http://www.ccdc.cam.ac.uk/conts/retrieving.html>, or from the Cambridge Crystallographic Data Centre, 12 Union Road, Cambridge CB2 1EZ, UK; fax: (+44) 1223-336-033; or e-mail: deposit@ccdc.cam.ac.uk.

Acknowledgements

We gratefully acknowledge financial support from the Ministerio de Educación y Ciencia, Spain (Grant no. CTQ2008-05892/BQU) and Ministerium für Wirtschaft und Arbeit des Landes Sachsen-Anhalt, Deutschland (Grant No. 6003368706). We would also like to thank Ioana Grosu (Universität Leipzig) for her help in the preparation of samples for mass spectrometry.

References

- [1] Medicinal inorganic chemistry, Chem. Rev. (Special Thematic Issue) 99 (1999).
- [2] J.L. Sessler, S.R. Doctrow, J. McMurry, S.J. Lippard (Eds.), Medicinal Inorganic Chemistry, American Chemical Society Symposium Series 903, American Chemical Society, Washington DC, 2005.
- [3] M. Gielen, E.R.T. Tiekink, *Metallotherapeutic Drugs and Metal-Based Diagnostic Agents: The Use of Metals in Medicine*, Wiley, Chichester, 2005.
- [4] M. Gielen (Ed.), *Tin-Based Anti-Tumor Drugs*, Springer-Verlag, Berlin, 1990.
- [5] M. Gielen, *Coord. Chem. Rev.* 151 (1996) 41.
- [6] P. Yang, M. Guo, *Coord. Chem. Rev.* 185–186 (1999) 189.

- [7] M. Gielen, M. Biesemans, D. De Vos, R. Willem, J. Inorg. Biochem. 79 (2000) 139.
- [8] M. Gielen, *Appl. Organomet. Chem.* 16 (2002) 481.
- [9] S.K. Hadjikakou, N. Hadjiliadis, *Coord. Chem. Rev.* 253 (2009) 235.
- [10] M. Gielen, A.G. Davies, K. Pannell, E. Tiekink, *Tin Chemistry: Fundamentals, Frontiers, and Applications*, John Wiley and Sons, Wiltshire, 2008.
- [11] L. Nagy, A. Szorcik, K. Kovacs, *Pharm. Hungarica* 70 (2000) 53.
- [12] M. Nath, S. Pokharia, R. Yadav, *Coord. Chem. Rev.* 215 (2001) 99.
- [13] M. Gielen, in: *NATO ASI Ser. 2*, vol. 26, 1997, p. 445.
- [14] D. De Vos, R. Willem, M. Gielen, K.E. Van Wingerden, K. Nooter, *Met.-Based Drugs* 5 (1998) 179.
- [15] C. Pettinari, *Main Group Met. Chem.* 22 (1999) 661.
- [16] S.P. Fricker (Ed.), *Metal Compounds in Cancer Therapy*, Chapman & Hall, London, UK, 1994, pp. 147–179.
- [17] A.K. Saxena, F. Huber, *Coord. Chem. Rev.* 95 (1989) 109.
- [18] J. Susperregui, M. Bayle, G. Lain, C. Giroud, T. Baltz, G. Deleris, *Eur. J. Med. Chem.* 34 (1999) 617.
- [19] L. Pellerito, L. Nagy, *Coord. Chem. Rev.* 224 (2002) 111.
- [20] T.S. Basu Baul, W. Rynjah, E. Rivarola, A. Lycka, M. Holcapek, R. Jirasko, D. de Vos, R.J. Butcher, A. Linden, *J. Organomet. Chem.* 691 (2006) 4850.
- [21] L. Tian, Y. Sun, H. Li, X. Zheng, Y. Cheng, X. Liu, B. Qian, *J. Inorg. Biochem.* 99 (2005) 1646.
- [22] G. Han, P. Yang, *J. Inorg. Biochem.* 91 (2002) 230.
- [23] S. Gómez-Ruiz, G.N. Kaluderović, S. Prashar, E. Hey-Hawkins, A. Erić, Ž. Žižak, Z.D. Juranić, *J. Inorg. Biochem.* 102 (2008) 2087.
- [24] M.N. Xanthopoulou, S.K. Hadjikakou, N. Hadjiliadis, M. Schurmann, K. Jurkschat, A. Michaelides, S. Skoulika, T. Bakas, J.J. Binolis, S. Karkabounas, K. Charalabopoulos, *J. Inorg. Biochem.* 96 (2003) 425.
- [25] M.N. Xanthopoulou, S.K. Hadjikakou, N. Hadjiliadis, E.R. Milaeva, J.A. Gracheva, V.-Y. Tyurin, N. Kourkoumelis, K.C. Christoforidis, A.K. Metsios, S. Karkabounas, K. Charalabopoulos, *Eur. J. Med. Chem.* 43 (2008) 327.
- [26] M.N. Xanthopoulou, S.K. Hadjikakou, N. Hadjiliadis, M. Kubicki, S. Skoulika, T. Bakas, M. Baril, I.S. Butler, *Inorg. Chem.* 46 (2007) 1187.
- [27] M.N. Xanthopoulou, S.K. Hadjikakou, N. Hadjiliadis, N. Kourkoumelis, E.R. Milaeva, J.A. Gracheva, V.-Y. Tyurin, I.I. Verginadis, S. Karkabounas, M. Baril, I.S. Butler, *Rus. Chem. Bull.* 56 (2007) 767.
- [28] C. Ma, Q. Jiang, R. Zhang, *Appl. Organomet. Chem.* 17 (2003) 623.
- [29] C. Ma, J. Zhang, *Appl. Organomet. Chem.* 17 (2003) 788.
- [30] F. Barbieri, F. Sparatore, R. Bonavia, C. Bruzzo, G. Schettini, A. Alama, *J. Neuro-Oncol.* 60 (2002) 109.
- [31] E.R.T. Tiekink, *Appl. Organometal. Chem.* 22 (2008) 533.
- [32] B. Gleeson, J. Claffey, D. Ertler, M. Hogan, H. Müller-Bunz, F. Paradisi, D. Wallis, M. Tacke, *Polyhedron* 27 (2008) 3619.
- [33] P.M. Abeyasinghe, M.M. Harding, *Dalton Trans.* (2007) 3474.
- [34] K. Strohfeldt, M. Tacke, *Chem. Soc. Rev.* 37 (2008) 1174.
- [35] C.G. Hartinger, P.J. Dyson, *Chem. Soc. Rev.* 38 (2009) 391.
- [36] S. Gómez-Ruiz, G.N. Kaluderović, D. Polo-Cerón, S. Prashar, M. Fajardo, Ž. Žižak, Z.D. Juranić, T.J. Sabo, *Inorg. Chem. Commun.* 10 (2007) 748.
- [37] S. Gómez-Ruiz, G.N. Kaluderović, S. Prashar, D. Polo-Cerón, M. Fajardo, Ž. Žižak, T.J. Sabo, Z.D. Juranić, *J. Inorg. Biochem.* 102 (2008) 1558.
- [38] S. Gómez-Ruiz, G.N. Kaluderović, Ž. Žižak, I. Besu, Z.D. Juranić, S. Prashar, M. Fajardo, *J. Organomet. Chem.* 694 (2009) 1981.
- [39] D. Pérez-Quintanilla, S. Gómez-Ruiz, Ž. Žižak, I. Sierra, S. Prashar, I. del Hierro, M. Fajardo, Z.D. Juranić, G.N. Kaluderović, *Chem. Eur. J.* 15 (2009) 5588.
- [40] S. Gómez-Ruiz, S. Prashar, M. Fajardo, A. Antiñolo, A. Otero, *J. Organomet. Chem.* 692 (2007) 3057.
- [41] S. Gómez-Ruiz, D. Polo-Cerón, S. Prashar, M. Fajardo, A. Antiñolo, A. Otero, *Eur. J. Inorg. Chem.* (2007) 4445.
- [42] A. Antiñolo, I. López-Solera, I. Orive, A. Otero, S. Prashar, A.M. Rodríguez, E. Villaseñor, *Organometallics* 20 (2001) 71.
- [43] C.E. Zachmanoglou, A. Doctar, B.M. Bridgewater, G. Parkin, C.G. Brandow, J.E. Bercaw, C.N. Jardine, M. Lyall, J.C. Green, *J. Am. Chem. Soc.* 124 (2002) 9525.
- [44] SCALE3 ABSPACK: Empirical Absorption Correction, CrysAlis – Software package, Oxford Diffraction Ltd., 2006.
- [45] G.M. Sheldrick, *SHELXS-97*, Program for Crystal Structure Solution, Göttingen, 1997.
- [46] G.M. Sheldrick, *SHELXL-97*, Program for the Refinement of Crystal Structures, Göttingen, 1997.
- [47] P. Skehan, R. Storeng, D. Scudiero, A. Monks, J. McMahon, D. Vistica, J.T. Warren, H. Bokesch, S. Kenney, M.R. Boyd, *J. Natl. Cancer Inst.* 82 (1990) 1107.
- [48] H. Schumann, L. Esser, J. Loebel, A. Dietrich, *Organometallics* 10 (1991) 2585.
- [49] H. Wiesenfeldt, A. Reinmuth, E. Barsties, K. Evertz, H.-H. Brintzinger, *J. Organomet. Chem.* 369 (1989) 359.
- [50] P. Jutzi, R. Dickbreder, *Chem. Ber.* 119 (1986) 1750.
- [51] C. Alonso-Moreno, A. Antiñolo, I. López-Solera, A. Otero, S. Prashar, A.M. Rodríguez, E. Villaseñor, *J. Organomet. Chem.* 656 (2002) 129.
- [52] S. Xu, X. Dai, B. Wang, X. Zhou, *J. Organomet. Chem.* 645 (2002) 262.
- [53] R. Fernández, E. Carmona, *Eur. J. Inorg. Chem.* (2005) 3197.
- [54] D. del Río, A. Galindo, I. Resa, E. Carmona, *Angew. Chem. Int. Ed.* 44 (2005) 1244.
- [55] I. Resa, E. Carmona, E. Gutiérrez-Puebla, A. Monge, *Science* 305 (2004) 1136.
- [56] M. Conejo, R. Fernández, D. del Río, E. Carmona, A. Monge, C. Ruiz, A.M. Márquez, J.F. Sanz, *Chem. Eur. J.* (2003) 4452.
- [57] R. Fernández, I. Resa, D. del Río, E. Carmona, E. Gutiérrez-Puebla, A. Monge, *Organometallics* 22 (2003) 381.

Appendix 9

Reproduced from Ref. S. Gómez-Ruiz, S. Prashar, T. Walther, M. Fajardo, D. Steinborn, R. Paschke, G.N. Kaluđerović, *Polyhedron* 2010, 29, 16 with permission from Elsevier.

S. Gómez-Ruiz et al./Polyhedron 29 (2010) 16–23

23

- [58] M.M. Conejo, R. Fernández, D. del Río, E. Carmona, A. Monge, C. Ruiz, *Chem. Commun.* (2002) 2916.
- [59] M.M. Conejo, R. Fernández, E. Gutiérrez-Puebla, A. Monge, C. Ruiz, E. Carmona, *Angew. Chem. Int. Ed.* 39 (2000) 1949.
- [60] P. Jutzi, *Chem. Rev.* 86 (1986) 983.
- [61] A. Antiñolo, M. Fajardo, S. Gómez-Ruiz, I. López-Solera, A. Otero, S. Prashar, A.M. Rodríguez, *J. Organomet. Chem.* 683 (2003) 11.
- [62] A. Antiñolo, M. Fajardo, S. Gómez-Ruiz, I. López-Solera, A. Otero, S. Prashar, *Organometallics* 23 (2004) 4062.
- [63] S. Gómez-Ruiz, S. Prashar, M. Fajardo, A. Antiñolo, A. Otero, M.A. Maestro, V. Volkis, M.S. Eisen, C.J. Pastor, *Polyhedron* 24 (2005) 1298.
- [64] O.R. Allen, A. L. Gott, J.A. Hartley, J.M. Hartley, R.J. Knox, P.C. McGowan, *Dalton Trans.* (2007) 5082.



Contents lists available at ScienceDirect

Journal of Organometallic Chemistry

journal homepage: www.elsevier.com/locate/jorganchem

Synthesis, characterization and biological studies of 1-D polymeric triphenyltin(IV) carboxylates

Goran N. Kaluderović^{a,b,**}, Reinhard Paschke^a, Sanjiv Prashar^c, Santiago Gómez-Ruiz^{c,*}^a Biozentrum, Martin-Luther-Universität Halle-Wittenberg, Weinbergweg 22, 06120 Halle, Germany^b Institut für Chemie Martin-Luther-Universität Halle-Wittenberg, Kurt-Mothes-Straße 2, 06120 Halle, Germany^c Departamento de Química Inorgánica y Analítica, E.S.C.E.T., Universidad Rey Juan Carlos, 28933 Móstoles, Madrid, Spain

ARTICLE INFO

Article history:

Available online 29 April 2010

Keywords:

Anticancer agents

Tin

Cytotoxic activity

Carboxylato ligands

DNA-binding properties

ABSTRACT

The triphenyltin(IV) carboxylate compounds $[\{\text{SnPh}_3(\text{O}_2\text{CCH}_2\text{SXyl})\}_\infty]$ (**1**) (Xyl = 3,5-Me₂C₆H₃) and $[\{\text{SnPh}_3(\text{O}_2\text{CCH}_2\text{SMes})\}_\infty]$ (**2**) (Mes = 2,4,6-Me₃C₆H₂) have been synthesized by the reaction of SnPh₃Cl with one equivalent of xylylthioacetic acid or mesitylthioacetic acid, respectively. **1** and **2** have been characterized by spectroscopic methods. The cytotoxic activity of **1** and **2** was tested against human tumour cell lines from four different histogenic origin: 8505C (anaplastic thyroid cancer), DLD-1 (colon cancer) and the cisplatin sensitive A253 (head and neck cancer) and A549 (lung carcinoma) and compared with those of the reference complex cisplatin. Interestingly, the cytotoxic activities of the carboxylate derivatives were higher than those of cisplatin against all the studied cells. DNA-interaction tests have been also carried out. Solutions of all the studied complexes have been treated with different concentrations of fish sperm DNA (FS-DNA), observing modifications of the UV spectra with intrinsic binding constants of 1.68×10^5 and 1.02×10^5 , M⁻¹ for **1** and **2**, respectively. In addition, the molecular structure of **2** has been determined by single crystal X-ray diffraction studies, observing that **2** consists of a 1-D coordination polymer in which the tin atoms present a five-coordinated geometry by coordination of two different oxygen atoms of two crystallographically dependent carboxylato ligands.

© 2010 Elsevier B.V. All rights reserved.

1. Introduction

Research on medicinal applications of metal complexes is an area of current interest and one of the most studied facets in biomedical and inorganic chemistry [1–3]. In this context, the potential therapeutic properties of tin compounds were observed as early as 1929 [4], however, the antiproliferative properties of these complexes were not studied in detail until 1980 [5]. More recently, different studies with very interesting results on the *in vitro* antitumour properties of organotin compounds against a wide panel of tumour cell lines of human origin have been reported [6–12]. Thus, tin(IV) derivatives such as cyclopentadienyltin(IV) derivatives have only recently been studied very briefly [13,14], while other tin(IV) complexes such as those with carboxylato [15–22], thiolato [23–29] and dithiocarbamate [30] ligands have been extensively studied, observing that tin(IV) carboxylate complexes present usually the highest cytotoxic activity [11]. Modification of the carboxylato ligands or the alkyl or aryl substituents at tin(IV) has a notable effect on the antiproliferative

effect of di- or tri-alkyl or aryltin(IV) carboxylate complexes in anticancer tests [11,21]. Usually, triorganotin(IV) compounds display a higher biological activity than their di- and mono-organotin(IV) counterparts, which has been related to their ability to bind to proteins [31–33]. Thus, as a continuation of our work on the cytotoxic properties of metal carboxylate complexes [21,34–37], we decided to synthesize novel triphenyltin(IV) carboxylate complexes with the xylylthioacetato or mesitylthioacetato ligands, which seem to have a positive influence on the cytotoxicity of gallium [36] and titanium [34] complexes.

In this report we present the synthesis, characterization and study of the cytotoxicity of the triphenyltin(IV) carboxylate compounds $[\{\text{SnPh}_3(\text{O}_2\text{CCH}_2\text{SXyl})\}_\infty]$ (**1**) (Xyl = 3,5-Me₂C₆H₃) and $[\{\text{SnPh}_3(\text{O}_2\text{CCH}_2\text{SMes})\}_\infty]$ (**2**) (Mes = 2,4,6-Me₃C₆H₂). In addition, the molecular structure of **2** which consists of a 1-D coordination polymer is described.

2. Experimental

2.1. General manipulations

All reactions were performed using standard Schlenk tube techniques in an atmosphere of dry nitrogen. Solvents and NEt₃

* Corresponding author. Tel.: +34 914888527; fax: +34 914888143.

** Corresponding author. Tel.: +49 345 5525678; fax: +49 345 5527028.

E-mail addresses: goran.kaluderovic@chemie.uni-halle.de, goran@chem.bg.ac.rs (G.N. Kaluderović), santiago.gomez@urjc.es (S. Gómez-Ruiz).

were distilled from the appropriate drying agents and degassed before use. SnPh_3Cl and NEt_3 were purchased from Aldrich. Mesitylthioacetic acid and xylylthioacetic acid were prepared with slight modification of the literature procedure [38]. IR spectra (KBr pellets prepared in a nitrogen-filled glove box) were recorded on a Perkin–Elmer System 2000 or on a Nicolet Avatar FT-IR spectrometer in the range 350–4000 cm^{-1} . ^1H , $^{13}\text{C}\{^1\text{H}\}$ and ^{119}Sn NMR spectra were recorded on a Varian Mercury FT-400 spectrometer or on a Bruker AVANCE-400 and referenced to the residual deuterated solvent. UV–vis measurements were performed at room temperature with an Analytik Jena Specord 200 spectrophotometer between 190 and 900 nm. Microanalyses were carried out with a Perkin–Elmer 2400 or LECO CHNS-932 microanalyzer.

2.2. Preparation of $[\{\text{SnPh}_3(\text{O}_2\text{CCH}_2\text{SXyl})\}_\infty] (\mathbf{1})$

A solution of xylylthioacetic acid (0.26 g, 1.30 mmol) in toluene (50 mL) was added dropwise to a solution of SnPh_3Cl (0.50 g, 1.30 mmol) in toluene (50 mL) at room temperature. The reaction mixture was stirred for 20 min and NEt_3 (0.19 mL, 1.30 mmol) was then added dropwise. The reaction was then stirred at room temperature overnight. The mixture was filtered and the filtrate concentrated (10 mL) and cooled to -30°C . Microcrystals of the title complex were isolated by filtration. Yield (calculated for the monomeric unit): 0.44 g, 62%. FT-IR (KBr): 1552 (s) ($\nu_a \text{COO}^-$), 1426 (s) ($\nu_s \text{COO}^-$), 694 (s) ($\nu \text{Sn-C}$), 452 (m) ($\nu \text{Sn-O}$); ^1H NMR (400 MHz, CDCl_3 , 25°C): δ 2.19 (s, 6H, *m*-Me of xylyl), 3.72 (s, 4H, CH_2), 6.75 (s, 2H, *o*-protons of xylyl), 6.95 (s, 1H, *p*-proton of xylyl), 7.46 (br m, 9H, *m*- and *p*- protons of SnPh_3), 7.70 (br m, 6H, *o*-protons of SnPh_3 , $^3J(^1\text{H-Sn}) = \text{ca. } 50.2 \text{ Hz}$); $^{13}\text{C}\{^1\text{H}\}$ RMN (100.6 MHz, CDCl_3 , 25°C): δ 21.1 (*m*-Me of xylyl), 37.1 (CH_2), 128.9 (C-3 and C-5 of SnPh_3 , $^3J(^{13}\text{C-}^{117}\text{Sn}) = 62.1 \text{ Hz}$ and $^3J(^{13}\text{C-}^{119}\text{Sn}) = 64.7 \text{ Hz}$), 130.2 (C-4 of SnPh_3 , $^4J(^{13}\text{C-}^{117,119}\text{Sn}) = 13.1 \text{ Hz}$), 136.7 (C-2 and C-6 of SnPh_3 , $^2J(^{13}\text{C}\{^1\text{H}\}-^{117,119}\text{Sn}) = 48.7 \text{ Hz}$), 137.4 (C-1 of SnPh_3 , $^1J(^{13}\text{C-}^{117,119}\text{Sn}) = 634.4 \text{ Hz}$ and $^1J(^{13}\text{C-}^{119}\text{Sn}) = 662.8 \text{ Hz}$), 126.7 (C-2 and C-6 of xylyl), 128.0 (C-4 of xylyl), 135.6 (C-3 and C-5 of xylyl), 138.0 (C-1 of xylyl), 175.5 (COO) ppm. $^{119}\text{Sn}\{^1\text{H}\}$ NMR (149.2 MHz, CDCl_3 , 25°C): δ -101.9 ppm. FAB-MS (*m/e* (relative intensity)): 546 (1) [M^+], 367 (5) [$\text{M}^+ - \text{OCCH}_2\text{SMes}$]. Elemental analysis, monomeric unit: $\text{C}_{28}\text{H}_{26}\text{O}_2\text{SSn}$ (545.28) calculated: C 61.67, H 4.81, found: C 61.29, H 4.70%.

2.3. Preparation of $[\{\text{SnPh}_3(\text{O}_2\text{CCH}_2\text{SMes})\}_\infty] (\mathbf{2})$

The synthesis of **2** was carried out in an identical manner to **1** starting from mesitylthioacetic acid (0.27 g, 1.30 mmol), SnPh_3Cl (0.50 g, 1.30 mmol) and NEt_3 (0.19 mL, 1.30 mmol). Yield: 0.51 g, 70%. FT-IR (KBr): 1547 (s) ($\nu_a \text{COO}^-$), 1392 (s) ($\nu_s \text{COO}^-$), 695 (s) ($\nu \text{Sn-C}$), 451 (m) ($\nu \text{Sn-O}$); ^1H RMN (400 MHz, CDCl_3 , 25°C): δ 2.24 (s, 3H, *p*-Me of mesityl), 2.39 (s, 6H, *o*-Me of mesityl), 3.47 (s, 2H, CH_2), 6.82 (s, 2H, *m*-H of mesityl) 7.46 (br s, 9H, *m*- and *p*- protons of SnPh_3), 7.77 (br m, 6H, *o*-protons of SnPh_3 , $^3J(^1\text{H-Sn}) = \text{ca. } 51.0 \text{ Hz}$); $^{13}\text{C}\{^1\text{H}\}$ RMN (100.6 MHz, CDCl_3 , 25°C): δ 21.0 (*p*-Me of mesityl), 21.7 (*o*-Me of mesityl), 37.1 (CH_2), 128.8 (C-3 and C-5 of SnPh_3 , $^3J(^{13}\text{C-}^{117}\text{Sn}) = 61.7 \text{ Hz}$ and $^3J(^{13}\text{C-}^{119}\text{Sn}) = 64.3 \text{ Hz}$), 130.2 (C-4 of SnPh_3 , $^4J(^{13}\text{C-}^{117,119}\text{Sn}) = 13.4 \text{ Hz}$), 136.8 (C-2 and C-6 of SnPh_3 , $^2J(^{13}\text{C}\{^1\text{H}\}-^{117,119}\text{Sn}) = 48.3 \text{ Hz}$), 137.8 (C-1 of SnPh_3 , $^1J(^{13}\text{C-}^{117}\text{Sn}) = 614.7 \text{ Hz}$ and $^1J(^{13}\text{C-}^{119}\text{Sn}) = 640.4 \text{ Hz}$), 125.3 (C-4 of mesityl), 129.0 (C3-C5 of mesityl), 138.2 (C2-C6 of mesityl), 143.0 (C-1 of mesityl), 176.1 (COO) ppm. $^{119}\text{Sn}\{^1\text{H}\}$ NMR (149.2 MHz, CDCl_3 , 25°C): δ -102.7 ppm. FAB-MS (*m/e* (relative intensity)): 483 (5) [$\text{M}^+ - \text{Ph}$], 351 (10) [$\text{M}^+ - \text{OOCCH}_2\text{SMes}$], 195 (21) [$\text{M}^+ - \text{SnPh}_3\text{O}$]. Elemental analysis, monomeric unit: $\text{C}_{29}\text{H}_{28}\text{O}_2\text{SSn}$ (559.31) calculated: C 62.28, H 5.05, found: C 62.11, H 5.09%.

2.4. Data collection and structural refinement of **2**

The data of **2** were collected with a CCD Oxford Xcalibur S ($\lambda(\text{MoK}\alpha) = 0.71073 \text{ \AA}$) using ω and ϕ scans mode. Semi-empirical from equivalents absorption corrections were carried out with SCALE3 ABSPACK [39]. All the structures were solved by direct methods [40]. Structure refinement was carried out with SHELXL-97 [41]. All non-hydrogen atoms were refined anisotropically, and hydrogen atoms were calculated with the riding model and refined isotropically. Crystallographic details are listed in Table 1.

2.5. In vitro studies

2.5.1. Preparation of drug solutions

Stock solutions of studied tin(IV) compounds (**1–2**) were prepared, for solubility reasons, in dimethyl sulfoxide (DMSO, Sigma Aldrich) at a concentration of 20 mM, filtered through Millipore filter (0.22 μm) before use, and diluted by nutrient medium to various working concentrations. Nutrient medium was RPMI-1640 (PAA Laboratories) supplemented with 10% fetal bovine serum (Biochrom AG) and 1% penicillin/streptomycin (PAA Laboratories).

2.5.2. Cell lines and culture conditions

The cell lines 8505C, A253, A549 and DLD-1, included in this study, were kindly provided by Dr. Thomas Mueller, Department of Hematology/Oncology, Martin Luther University of Halle-Wittenberg, Halle (Saale), Germany. Cultures were maintained as monolayer in RPMI-1640 (PAA Laboratories, Pasching, Germany) supplemented with 10% heat inactivated fetal bovine serum (Biochrom AG, Berlin, Germany) and penicillin/streptomycin (PAA Laboratories) at 37°C in a humidified atmosphere of 5% (v/v) CO_2 .

2.5.3. Cytotoxicity assay

The cytotoxic activities of the compounds were evaluated using the sulforhodamine-B (SRB, Sigma Aldrich) microculture

Table 1
Crystal data and structure refinement for **2**.

Formula	$\text{C}_{29}\text{H}_{28}\text{O}_2\text{SSn}$
Fw	559.26
T (K)	130(2)
Cryst syst	Monoclinic
Space group	C2/c
<i>a</i> (pm)	2649.25(6)
<i>b</i> (pm)	992.66(2)
<i>c</i> (pm)	1945.19(4)
α (deg)	90
β (deg)	104.670(2)
γ (deg)	90
<i>V</i> (nm^3)	4.94871(18)
<i>Z</i>	8
<i>D_c</i> (Mg m^{-3})	1.501
μ (mm^{-1})	1.141
<i>F</i> (000)	2272
Cryst dimens (mm)	$0.4 \times 0.3 \times 0.1$
θ range (deg)	$2.94\text{--}28.28$
<i>hkl</i> ranges	$-35 \leq h \leq 35$, $-13 \leq k \leq 13$, $-25 \leq l \leq 25$
Data/parameters	6140/301
Goodness-of-fit on F^2	0.984
Final <i>R</i> indices [$I > 2\sigma(I)$]	$R_1 = 0.0210$, $wR_2 = 0.0477$
<i>R</i> indices (all data)	$R_1 = 0.0311$, $wR_2 = 0.0490$
Largest diff. peak and hole ($\text{e}\cdot\text{\AA}^{-3}$)	0.719 and -0.318

$$R_1 = \sum ||F_o| - |F_c|| / \sum |F_o|; \quad wR_2 = \left[\frac{\sum [w(F_o^2 - F_c^2)^2]}{\sum [w(F_o^2)^2]} \right]^{0.5}$$

colorimetric assay [42]. In short, exponentially growing cells were seeded into 96-well plates on day 0 at the appropriate cell densities to prevent confluence of the cells during the period of experiment. After 24 h, the cells were treated with serial dilutions of the studied compounds for 96 h. Final concentrations achieved in treated wells were 0.01, 0.03, 0.1, 0.3, 1.0, 3.0, 10.0, 30.0, 100.0 μM for **1** and **2**. Each concentration was tested in triplicates on each cell line. The final concentration of DMSO solvent never exceeded 0.5%, which was non-toxic to the cells. The percentages of surviving cells relative to untreated controls were determined 96 h after the beginning of drug exposure. After 96 h treatment, the supernatant medium from the 96 well plates was eliminated and the cells were fixed with 10% TCA. For a thorough fixation, plates were then allowed to stand at 4 °C. After fixation, the cells were washed in a strip washer. The washing was carried out four times with water using alternate dispensing and aspiration procedures. The plates were then dyed with 100 μL of 0.4% SRB for about 45 min. After dyeing, the plates were again washed to remove the dye with 1% acetic acid and allowed to air dry overnight. 100 μL of 10 mM Tris base solutions were added to each well of the plate and absorbance was measured at 570 nm using a 96 well plate reader (Tecan Spectra, Crailsheim, Germany). The IC_{50} value, defined as the concentrations of the compound at which 50% cell inhibition was observed, was estimated from the dose-response curves.

2.6. DNA binding experiments monitored by UV–visible spectroscopy

Fish sperm DNA (FS-DNA) was kindly provided by the Departamento de Ciencias de la Salud of the Universidad Rey Juan Carlos (Spain). The spectroscopic titration of FS-DNA was carried out in the buffer (50 mM NaCl–5 mM Tris–HCl, pH 7.1) at room temperature. A solution of FS-DNA in the buffer gave a ratio of UV absorbance 1.8–1.9:1 at 260 and 280 nm, indicating that the DNA was sufficiently free of protein [43]. Milli-Q water was used to prepare

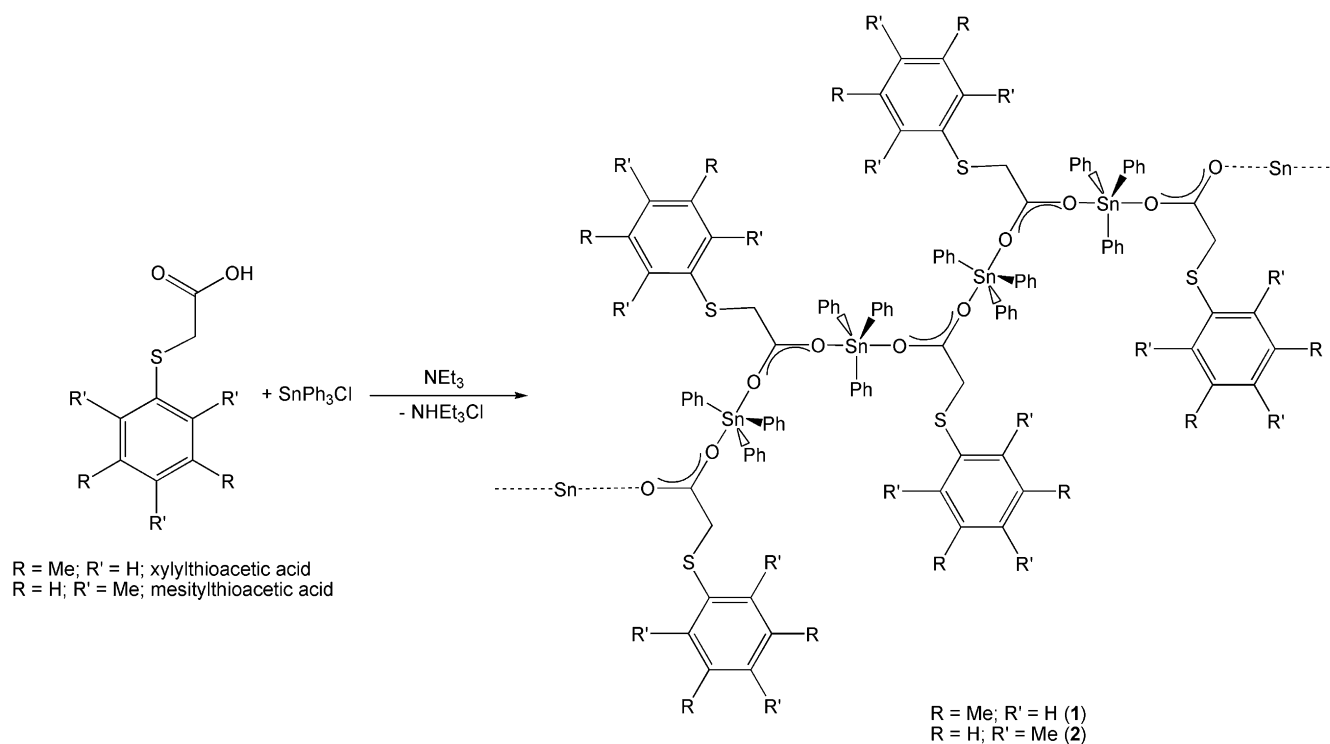
the solutions. The DNA concentration per nucleotide was determined adopting absorption spectroscopy using the known molar extinction coefficient value of $6600 \text{ M}^{-1} \text{ cm}^{-1}$ at 260 nm [44]. Absorption titrations were performed by using a fixed tin(IV) complex concentration to which increments of the DNA stock solution were added. Complex–DNA adducts solutions were incubated at 37 °C for 30 min before the absorption spectra were recorded.

3. Results and discussion

3.1. Synthesis and characterization of the triphenyltin(IV) complexes **1** and **2**

Triphenyltin(IV) carboxylate complexes $[\{\text{SnPh}_3(\text{O}_2\text{CCH}_2\text{SXyl})\}_\infty]$ (**1**) (Xyl = 3,5-Me₂C₆H₃) and $[\{\text{SnPh}_3(\text{O}_2\text{CCH}_2\text{SMes})\}_\infty]$ (**2**) (Mes = 2,4,6-Me₃C₆H₂) were synthesized by the reaction of SnPh₃Cl with one equivalent of xylylthioacetic acid or mesitylthioacetic acid in toluene at room temperature in the presence of stoichiometric amounts of NEt₃ (Scheme 1). Complexes **1** and **2** were isolated as colourless microcrystalline solids of high purity.

In the ¹H NMR spectrum of **1** the xylylthioacetato ligand gave a singlet at 2.19 ppm corresponding to the protons of the methyl groups of the xylyl moiety, a singlet at 3.72 ppm assigned to the methylene protons and a singlet at 6.75 ppm due to the aromatic protons of the phenyl ring. On the other hand, in the ¹H NMR spectrum of **2**, the mesitylthioacetato ligand gave two singlets at 2.24 and 2.39 ppm corresponding to the protons of the two different methyl groups of the mesityl moiety (*o*-methyl and *p*-methyl), one singlet at 3.47 corresponding to the methylene protons and one singlet at 6.82 ppm for the *m*-aromatic protons. In addition to these signals, two different multiplets, at ca. 7.5 ppm corresponding to the *m*- and *p*- protons and at 7.7 ppm assigned to the *o*-protons of SnPh₃ moiety, respectively, were observed. Satellite signals of the *o*-protons, due to coupling with the ¹¹⁷Sn and



Scheme 1. Synthesis of triphenyltin(IV) complexes **1** and **2**.

Appendix 10

Reproduced from Ref. G.N. Kaluđerović, R. Paschke, S. Prashar, S. Gómez-Ruiz, J. Organomet. Chem. 2010, 695, 1883 with permission from Elsevier.

1886

G.N. Kaluđerović et al. / Journal of Organometallic Chemistry 695 (2010) 1883–1890

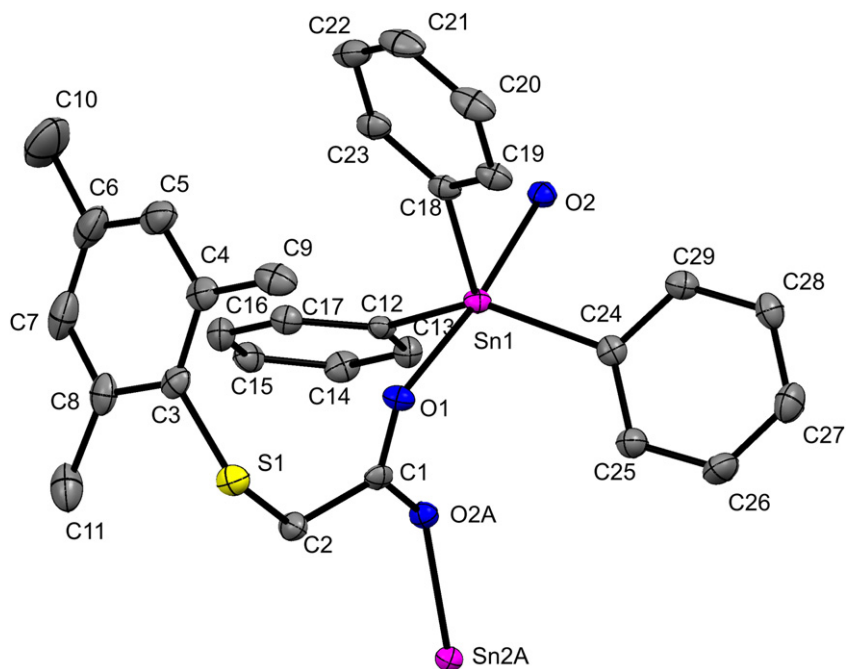


Fig. 1. Molecular structure and atom-labelling scheme for the monomeric unit of **2** with thermal ellipsoids at 50% probability (hydrogen atoms have been omitted for clarity).

^{119}Sn isotopes at a three bond distance were also observed, however, we were unable to resolve the independent satellite signals corresponding to the two tin nuclei. Therefore, the observed coupling constant for these protons of approximately 50 Hz is an approximate value that can be applied to either nucleus.

In the $^{13}\text{C}\{^1\text{H}\}$ NMR spectra of **1–2**, four signals at ca. 129, 130, 137 and 138 ppm were observed for the C-3/C-5, C-4, C-2/C-6 and C-1 carbon atoms of the phenyl groups. Tin-carbon coupling constants for these signals gave values of approximately $^1J(^{13}\text{C}-\text{Sn})$ 610–660 Hz, $^2J(^{13}\text{C}-\text{Sn})$ 48 Hz, $^3J(^{13}\text{C}-\text{Sn})$ 65 Hz, and $^4J(^{13}\text{C}-\text{Sn})$ 13 Hz. The $^1J(^{13}\text{C}-\text{Sn})$ 610–660 Hz coupling constants show that the C–Sn–C angles in solution may be similar to those found in the solid state (see Section 3.2).

In addition to the signals assigned to the phenyl groups the carboxylato ligands showed the expected signals.

The IR spectra of the complexes **1** and **2** show strong bands in two different regions at ca. 1550 and 1400 cm^{-1} , which correspond to the asymmetric and symmetric vibrations, respectively, of the COO moiety. The differences between the asymmetric and

symmetric vibrations of about 150 cm^{-1} indicate bridging bidentate coordination of the carboxylato ligand [45]. This phenomenon was also confirmed by X-ray diffraction studies (see Section 3.2).

3.2. Structural studies

2 crystallizes in the monoclinic space group $C2/c$ with eight molecules of the monomeric unit located in the unit cell. The asymmetric unit of **2** (Fig. 1) consists of a carboxylato ligand coordinated to a SnPh_3 unit by a single oxygen, which aggregates via further Sn–O interactions to form a zig-zag 1-D coordination polymer (Fig. 2). Generally, triorganotin(IV) carboxylates with bulky R groups attached to the Sn atom favour tetrahedral monomeric structures, while sterically less demanding R groups favour bridged polymeric structures [46]. However, the molecular structure of **2** reveals that the central tin atom is penta-coordinated in slightly distorted trigonal bipyramidal geometry with the phenyl groups in equatorial positions and two oxygen atoms of two different carboxylato ligands in axial positions. This geometry is

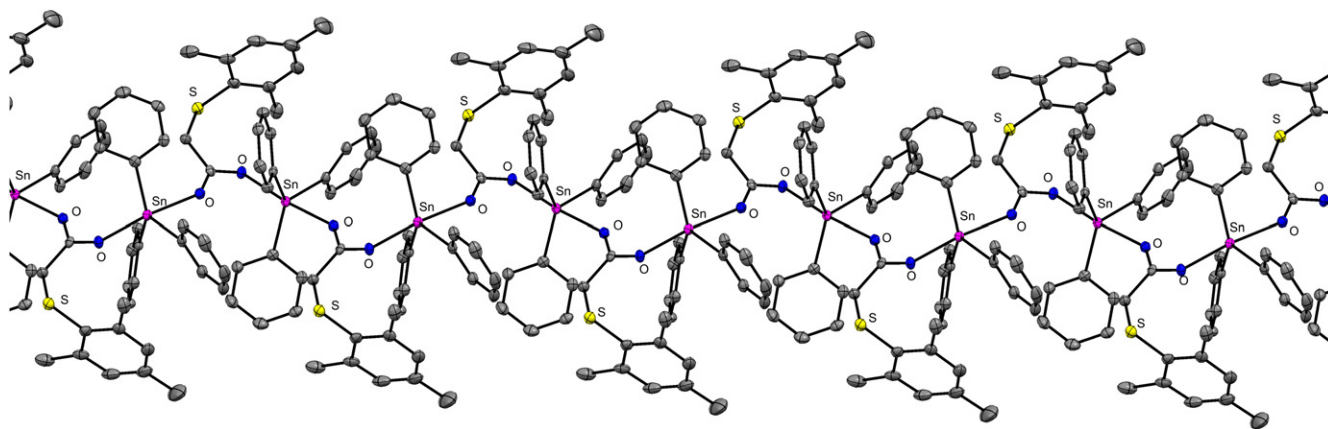


Fig. 2. 1-D zig-zag chain structure of **2**, propagation via $\text{O} \rightarrow \text{Sn}$ coordination.

Appendix 10

Reproduced from Ref. G.N. Kaluđerović, R. Paschke, S. Prashar, S. Gómez-Ruiz, J. Organomet. Chem. 2010, 695, 1883 with permission from Elsevier.

G.N. Kaluđerović et al. / Journal of Organometallic Chemistry 695 (2010) 1883–1890

1887

Table 2
Selected Bond Lengths (pm) and Angles (°) for **2**.

2	
Sn(1)–C(24)	211.9(2)
Sn(1)–C(18)	212.3(2)
Sn(1)–C(12)	212.3(2)
Sn(1)–O(1)	219.9(2)
Sn(1)–O(2)	233.7(1)
O(1)–C(1)	126.7(2)
O(2A)–C(1)	125.2(2)
C(24)–Sn(1)–C(18)	108.80(7)
C(24)–Sn(1)–C(12)	134.67(6)
C(18)–Sn(1)–C(12)	115.95(7)
C(24)–Sn(1)–O(1)	96.96(6)
C(18)–Sn(1)–O(1)	91.71(5)
C(12)–Sn(1)–O(1)	88.77(5)
C(24)–Sn(1)–O(2)	90.32(5)
C(18)–Sn(1)–O(2)	88.05(5)
C(12)–Sn(1)–O(2)	84.51(5)
O(1)–Sn(1)–O(2)	172.39(4)

Symmetry transformations used to generate equivalent atoms: A = $-x+1/2, y+1/2, -z+3/2$.

indicated by the sum of the angles C(24)–Sn(1)–C(18) 108.80(7)°, C(24)–Sn(1)–C(12) 134.67(6)°, C(18)–Sn(1)–C(12) 115.95(7)° which is 359.42° and shows that Sn(1), C(12), C(18) and C(24) are coplanar. In addition, the angles C(24)–Sn(1)–O(1) 96.96(6)°, C(18)–Sn(1)–O(1) 91.71(5)°, C(12)–Sn(1)–O(1) 88.77(5)°, C(24)–Sn(1)–O(2A) 90.32(5)°, C(18)–Sn(1)–O(2) 88.05(5)°, C(12)–Sn(1)–O(2) 84.51(5)° (close to 90°) and O(1)–Sn(1)–O(2) 172.39(4)° (close to 180°) show that O(1) and O(2) are located in axial positions.

The Sn–O bond lengths Sn(1)–O(1) 219.9(2) Sn(1)–O(2) 233.7(1) pm, and the Sn–C bond lengths, Sn(1)–C(24) 211.9(2), Sn(1)–C(18) 212.3(2), Sn(1)–C(12) 212.3(2) pm are similar to those found in other similar triorganotin(IV) carboxylate complexes [47–51]. With these distances one can envisage that the carboxylato ligand chelates to two symmetry related Sn atoms giving rise to different Sn–O bond distances. The inequality in the Sn–O bonds is reflected in the associated C–O bond distances (C(1)–O(2A) 125.2(2) and C(1)–O(1) 126.7(2) pm), the longer C–O bond (C(1)–O(1) 126.7(2) pm) is involved with the shorter Sn–O interaction (Sn(1)–O(1) 219.9(2) pm).

These structural parameters are in agreement with the difference of ca. 150 cm⁻¹ between the asymmetric and symmetric vibration of the COO moiety in the IR spectra (see Section 3.1) which indicates bridging behaviour [45,52].

Selected bond lengths and angles for **2** are given in Table 2.

According to the different IR and NMR data, the solid-state structure of **1** should present a similar structure; however, we were unable to obtain crystals suitable for their analysis by X-ray diffraction studies.

Additionally, it seems that the polymeric chain is not retained in solution of donor solvents such as DMSO, which coordinate to the metal centre leading to a mononuclear species, as observed in NMR spectroscopy.

Table 3

IC₅₀ (μM) for the 96 h of action of **1**, **2**, [Ti(η⁵-C₅H₅)(η⁵-C₅H₄(CMe₂(CH₂CH₂CH=CH₂))(O₂CCH₂SXyl)₂], [Ti(η⁵-C₅H₅)(η⁵-C₅H₄(CMe₂(CH₂CH₂CH=CH₂))(O₂CCH₂SMes)₂] [37], [(Me₂Ga(μ-O₂CCH₂SMes))₂] [36] and cisplatin on 8505C anaplastic thyroid cancer, A253 head and neck tumor, A549 lung carcinoma and DLD-1 colon carcinoma determined by sulforhodamine-B microculture colorimetric assay.

Complex	IC ₅₀ ± SD [μM]			
	8505C	A253	A549	DLD-1
1	0.132 ± 0.010	0.081 ± 0.003	0.094 ± 0.013	0.060 ± 0.001
2	0.172 ± 0.003	0.100 ± 0.014	0.129 ± 0.014	0.178 ± 0.002
[Ti(η ⁵ -C ₅ H ₅)(η ⁵ -C ₅ H ₄ (CMe ₂ (CH ₂ CH ₂ CH=CH ₂))(O ₂ CCH ₂ SXyl) ₂]	182.3 ± 2.5	182.6 ± 2.0	192.5 ± 1.1	151.2 ± 4.2
[Ti(η ⁵ -C ₅ H ₅)(η ⁵ -C ₅ H ₄ (CMe ₂ (CH ₂ CH ₂ CH=CH ₂))(O ₂ CCH ₂ SMes) ₂]	190.8 ± 2.2	131.2 ± 0.5	144.6 ± 2.9	115.7 ± 2.9
[(Me ₂ Ga(μ-O ₂ CCH ₂ SMes)) ₂]	20.5 ± 2.3	7.7 ± 0.3	26.9 ± 7.0	12.4 ± 0.1
cisplatin	5.0 ± 0.2	0.81 ± 0.02	1.51 ± 0.02	5.1 ± 0.1

3.3. Cytotoxic studies

The *in vitro* cytotoxicities of organotin(IV) compounds **1** and **2** against human tumour cell lines 8505C anaplastic thyroid cancer, A253 head and neck tumour, A549 lung carcinoma and DLD-1 colon carcinoma were determined by using the SRB microculture colorimetric assay [42]. In addition, cytotoxicities of cisplatin and related titanocene(IV) [37] and organogallium(III) [36] compounds with the same carboxylato ligands have been included for comparison (Table 3).

The studied organotin antitumour agents showed a dose-dependent antiproliferative effect toward all the studied cancer cell lines (Fig. 3). Estimates based on the IC₅₀ values show that the studied tin complexes are more active than cisplatin and all the titanocene(IV) and organogallium(III) derivatives against all the studied human cancer cell lines.

Taking into account the standard deviation, there is not a substantial higher activity of any of the tin complex over the other, with the exception of the DLD-1 cells where the IC₅₀ value for **1** is 0.060 ± 0.001 μM while for **2** is much higher, 0.178 ± 0.002 μM, indicating a preference of complex **1** on DLD-1 cells.

On direct comparison with cisplatin, the cytotoxic activity of complexes **1** and **2** is from 8 to 85 times higher. Again, the highest activity ratio cytotoxicity of organotin complex/cisplatin activity was observed for **1** in the DLD-1 cell. Also the fact that greater tolerances of high tin concentrations in biological systems may be possible (in direct contrast to the large number of side-effects associated to very low concentrations of platinum), makes these tin compounds ideal candidates for further studies.

In addition, **1** and **2** present activities up to 285 and 2520 times higher than their gallium(III) and titanocene(IV) analogues, respectively.

3.4. DNA-interaction studies

The R₃Sn⁺ moieties have been observed to directly affect DNA [53] as well as binding to membrane proteins or glycoproteins, or to cellular proteins; e.g. to ATPase, hexokinase, acetylcholinesterase of human erythrocyte membrane or to skeletal muscle membranes [54]. In addition, a wide number of reports have been published concerning the possible mechanisms for the interaction of alkyl or aryltin moieties with the membrane or constituents within the cell [55–58], although the exact mechanism is still unclear. However, it is generally agreed that the R₃Sn⁺ fragments may bind to the phosphate groups in DNA [59–61], changing the intracellular metabolism of the phospholipids of the endoplasmic reticulum [62,63].

Thus, the binding behaviour of the studied organotin(IV) compounds to DNA helix has been followed through absorption spectral titrations, because absorption spectroscopy is one of the most useful techniques to study the binding of any drug to DNA [64–67]. The absorption spectra of the complexes in the absence

Appendix 10

Reproduced from Ref. G.N. Kaluđerović, R. Paschke, S. Prashar, S. Gómez-Ruiz, J. Organomet. Chem. 2010, 695, 1883 with permission from Elsevier.

1888

G.N. Kaluđerović et al. / Journal of Organometallic Chemistry 695 (2010) 1883–1890

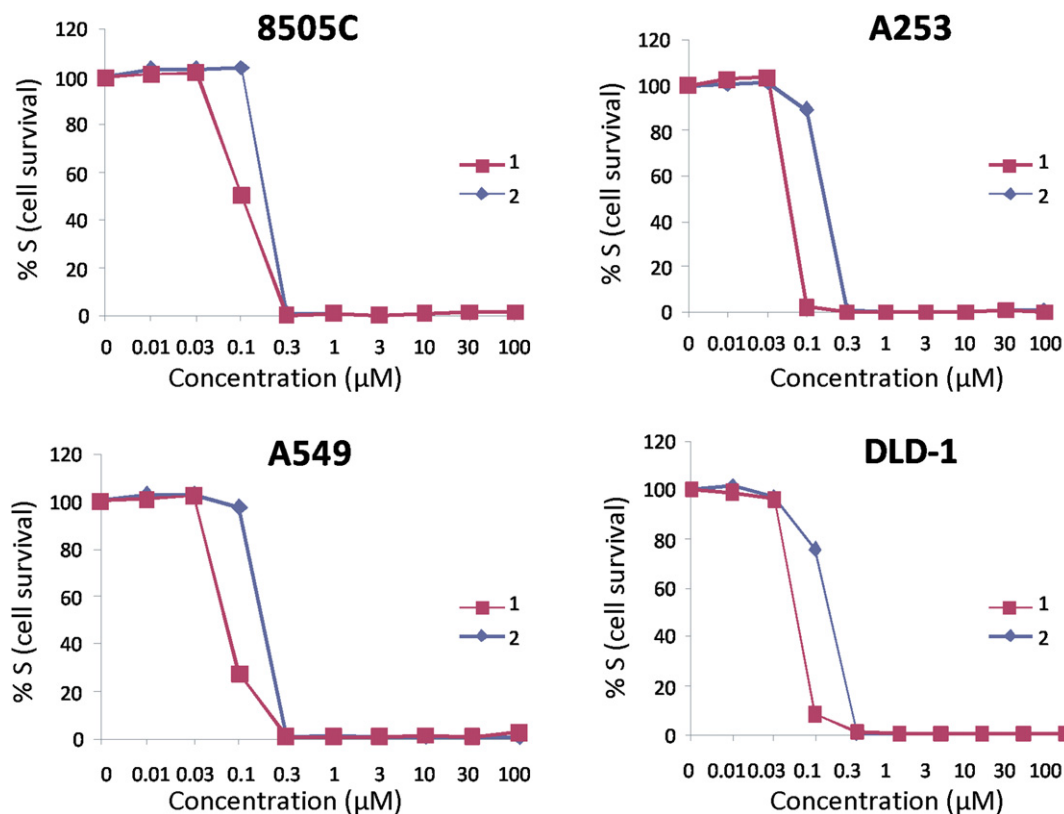


Fig. 3. Representative graphs show survival of 8505C, A253, A549 and DLD-1 cells grown for 96 h in the presence of increasing concentrations of **1** and **2**. Standard deviations (all less than 10%) are omitted for clarity.

and in the presence of FS-DNA (fish sperm DNA) have been recorded. With increasing concentrations of FS-DNA, the absorption bands of the complexes were affected, resulting in the tendency of hyperchromism and a very slight blue shift. The organotin(IV) compounds **1** and **2** may bind to the DNA in different modes on the basis of their structure and charge. The organotin(IV) compounds (**1** and **2**) may be charged (R_3Sn^+) and there could be classical

electrostatic interactions which may be responsible for the spectral changes observed in the study. However, other electrostatic effects such as hydrogen bonding between the complexes and the base pairs in DNA may also be present [68–71].

In order to compare the binding strengths of the complexes, the intrinsic binding constant, K_b , was determined using the following equation [72]:

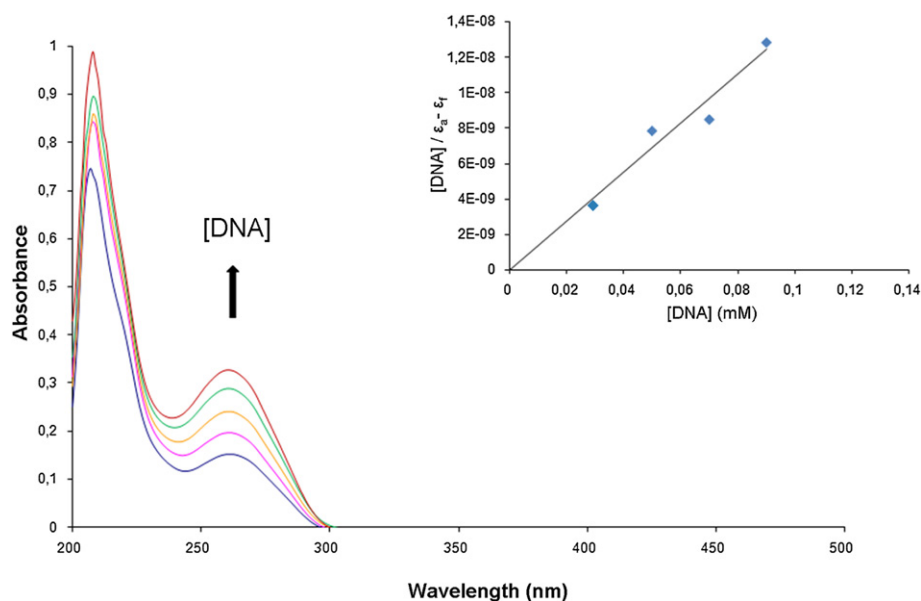


Fig. 4. Absorption spectra of **1** in the presence of increasing amounts of DNA. Arrow indicates that absorbance changes upon increasing DNA concentrations. Inset: plot of $[DNA] / \epsilon_a - \epsilon_f = [DNA] / \epsilon_0 - \epsilon_f + 1 / K_b (\epsilon_0 - \epsilon_f)$, experimental data points; solid line, linear fitting of the data.

$$\frac{[\text{DNA}]}{\epsilon_a - \epsilon_f} = \frac{[\text{DNA}]}{\epsilon_0 - \epsilon_f} + \frac{1}{K_b(\epsilon_0 - \epsilon_f)}$$

where [DNA] is the concentration of DNA in base pairs, ϵ_a , ϵ_f and ϵ_0 correspond to $A_{\text{obs}}/[\text{Complex}]$, the extinction coefficient of the free tin complexes and the extinction coefficient of the complexes in the fully bound form, respectively, and K_b is the intrinsic binding constant. The ratio of slope to intercept in the plot of $[\text{DNA}]/(\epsilon_a - \epsilon_f)$ versus [DNA] gives the value of K_b (inset Fig. 4).

As an example, Fig. 4 shows the absorption spectra of complex **1** in the presence of increasing amounts of DNA.

Thus, the intrinsic binding constants of 1.68×10^5 and 1.02×10^5 , M^{-1} for **1** and **2**, respectively, have been successfully calculated, observing that complex **1**, which is the most cytotoxic compound, gives a K_b slightly higher than that of **2**, indicating a slightly higher affinity from DNA, which may be implicated in the higher cytotoxic activity shown by **1**.

4. Conclusions

Two new triphenyltin(IV) carboxylate complexes have been synthesized and characterized. The molecular structure of **2** consists of a carboxylato ligand coordinated to a SnPh_3 unit by a single oxygen, which aggregates via further Sn–O interactions to form a zig-zag 1-D coordination polymer, which is surprising because generally, triorganotin(IV) carboxylates with bulky R groups attached to the Sn atom favour tetrahedral monomeric structures. The cytotoxic activity of these compounds has been tested against human tumour cell lines observing that both tin(IV) compounds present higher cytotoxic activity than cisplatin and titanocene(IV) and organogallium(III) compounds with the same ligands. From the studied cell lines compound **1** presents the highest cytotoxicity (IC_{50} of 0.060 ± 0.001 μM) against DLD-1 cell line. In addition, DNA-interaction tests have been carried out, observing classical electrostatic interactions of all the complexes with DNA with intrinsic binding constants of 1.68×10^5 and 1.02×10^5 , M^{-1} for **1** and **2**, respectively.

Acknowledgements

We gratefully acknowledge financial support from the Ministerio de Educación y Ciencia, Spain (Grant no. CTQ2008-05892/BQU) and from the Ministerio für Wirtschaft und Arbeit des Landes Sachsen-Anhalt, Deutschland (Grant No. 6003368706). We would also like to thank Sara Bravo for her help in the preparation of the organotin(IV) derivatives and BioSolutions Halle GmbH (Germany) for the cell culture facilities.

Appendix. Supplementary material

Crystallographic data for the structural analysis of **2** have been deposited with the Cambridge Crystallographic Data Centre, CCDC-772114 (**2**). Copies of this information may be obtained free of charge from The Director, CCDC, 12 Union Road, Cambridge CB2 1EZ, UK (Fax: +44 1223 336033; E-mail: deposit@ccdc.cam.ac.uk or <http://www.ccdc.cam.ac.uk>).

Supplementary data associated with this article can be found, in the online version, at doi:10.1016/j.jorganchem.2010.04.029.

References

- [1] Medicinal inorganic chemistry Special Thematic Issue. Chem. Rev. 99 (1999).
- [2] J.L. Sessler, S.R. Doctrow, J. McMurry, S.J. Lippard (Eds.), Medicinal Inorganic Chemistry; American Chemical Society Symposium Series 903, American Chemical Society, Washington DC, 2005.

- [3] M. Gielen, E.R.T. Tiekink, Metallotherapeutic Drugs and Metal-Based Diagnostic Agents: The Use of Metals in Medicine. Wiley, Chichester, 2005.
- [4] W.A. Collier, Z. Hyg. Infektionskr 110 (1929) 169.
- [5] A.J. Crowe, P.J. Smith, G. Atassi, Chem.-Bid. Interact. 32 (1980) 171–178.
- [6] M. Gielen (Ed.), Tin-Based Anti-Tumor Drugs, Springer-Verlag, Berlin, 1990, pp. 139–145.
- [7] M. Gielen, Coord. Chem. Rev. 151 (1996) 41–51.
- [8] P. Yang, M. Guo, Coord. Chem. Rev. 185–186 (1999) 189–211.
- [9] M. Gielen, M. Biesemans, D. De Vos, R. Willem, J. Inorg. Biochem. 79 (2000).
- [10] M. Gielen, Appl. Organomet. Chem. 16 (2002) 481–494.
- [11] S.K. Hadjilakou, N. Hadjiliadis, Coord. Chem. Rev. 253 (2009) 235–249.
- [12] M. Gielen, A.G. Davies, K. Pannell, E. Tiekink, Tin Chemistry: Fundamentals, Frontiers, and Applications. John Wiley and Sons, Wiltshire, 2008.
- [13] B. Gleeson, J. Claffey, D. Ertler, M. Hogan, H. Müller-Bunz, F. Paradisi, D. Wallis, M. Tacke, Polyhedron 27 (2008) 3619–3624.
- [14] S. Gómez-Ruiz, S. Prashar, T. Walthar, M. Fajardo, D. Steinborn, R. Paschke, G. N. Kaluderović, Polyhedron 29 (2010) 16–23.
- [15] A.K. Saxena, F. Huber, Coord. Chem. Rev. 95 (1989) 109–123.
- [16] J. Susperregui, M. Bayle, G. Lain, C. Giroud, T. Baltz, G. Deleris, Eur. J. Med. Chem. 34 (1999) 617–623.
- [17] L. Pellerito, L. Nagy, Coord. Chem. Rev. 224 (2002) 111–150.
- [18] T.S. Basu Baul, W. Rynjah, E. Rivarola, A. Lycka, M. Holcapek, R. Jirasko, D. de Vos, R.J. Butcher, A. Linden, J. Organomet. Chem. 691 (2006) 4850–4862.
- [19] L. Tian, Y. Sun, H. Li, X. Zheng, Y. Cheng, X. Liu, B. Qian, J. Inorg. Biochem. 99 (2005) 1646–1652.
- [20] G. Han, P. Yang, J. Inorg. Biochem. 91 (2002) 230–236.
- [21] S. Gómez-Ruiz, G.N. Kaluderović, S. Prashar, E. Hey-Hawkins, A. Erić, Ž. Žizak, Z.D. Juranić, J. Inorg. Biochem. 102 (2008) 2087–2096.
- [22] D. Tzimopoulos, I. Sanidas, A.-C. Varvogli, A. Czapik, M. Gdaniec, E. Nikolakaki, P.D. Akriovs, J. Inorg. Biochem. 104 (2010) 423–430.
- [23] M.N. Xanthopoulou, S.K. Hadjilakou, N. Hadjiliadis, M. Schurmann, K. Jurkschat, A. Michaelides, S. Skoulika, T. Bakas, J.J. Binolis, S. Karkabounas, K. Charalabopoulos, J. Inorg. Biochem. 96 (2003) 425–434.
- [24] M.N. Xanthopoulou, S.K. Hadjilakou, N. Hadjiliadis, E.R. Milaeva, J.A. Gracheva, V.-Y. Tyurin, N. Kourkoumelis, K.C. Christoforidis, A.K. Metsios, S. Karkabounas, K. Charalabopoulos, Eur. J. Med. Chem. 43 (2008) 327–335.
- [25] M.N. Xanthopoulou, S.K. Hadjilakou, N. Hadjiliadis, M. Kubicki, S. Skoulika, T. Bakas, M. Baril, I.S. Butler, Inorg. Chem. 46 (2007) 1187–1195.
- [26] M.N. Xanthopoulou, S.K. Hadjilakou, N. Hadjiliadis, N. Kourkoumelis, E. R. Milaeva, J.A. Gracheva, V.-Y. Tyurin, I.I. Verginadis, S. Karkabounas, M. Baril, I.S. Butler, Russ. Chem. Bull. 56 (2007) 767–773.
- [27] C. Ma, Q. Jiang, R. Zhang, Appl. Organomet. Chem. 17 (2003) 623–630.
- [28] C. Ma, J. Zhang, Appl. Organomet. Chem. 17 (2003) 788–794.
- [29] F. Barbieri, F. Sparatore, R. Bonavia, C. Bruzzo, G. Schettini, A. Alama, J. Neuro-Oncol. 60 (2002) 109–116.
- [30] E.R.T. Tiekink, Appl. Organomet. Chem. 22 (2008) 533–550.
- [31] A.G. Davies, P.J. Smith, Adv. Inorg. Chem. Radiochem. 23 (1980) 1–77.
- [32] W.N. Aldridge, in: J.J. Zuckerman (Ed.), Organotin Compounds. New Chemistry and Applications, Adv. Chem. Ser., vol. 168, Am. Chem. Soc., Washington, 1976, p. 157.
- [33] B.M. Elliot, W.N. Aldridge, J.M. Bridges, Biochem. J. 177 (1979) 461–470.
- [34] S. Gómez-Ruiz, B. Gallego, Ž. Žizak, E. Hey-Hawkins, Z.D. Juranić, G. N. Kaluderović, Polyhedron 29 (2010) 354–360.
- [35] S. Gómez-Ruiz, B. Gallego, M.R. Kaluderović, H. Kommera, E. Hey-Hawkins, R. Paschke, G.N. Kaluderović, J. Organomet. Chem. 694 (2009) 2191–2197.
- [36] M.R. Kaluderović, S. Gómez-Ruiz, B. Gallego, E. Hey-Hawkins, R. Paschke, G. N. Kaluderović, Eur. J. Med. Chem. 45 (2010) 519–525.
- [37] G.N. Kaluderović, V. Tayurskaya, R. Paschke, S. Prashar, M. Fajardo, S. Gómez-Ruiz, Appl. Organomet. Chem., article, in press, doi:10.1002/aoc.1670.
- [38] Q.F. Soper, C.W. Whitehead, O.K. Behrens, J.J. Corse, R.G. Jones, J. Am. Chem. Soc. 70 (1948) 2849–2855.
- [39] SCALE3 ABSPACK, Empirical absorption correction, CrysAlis – Software package. Oxford Diffraction Ltd, 2006.
- [40] G.M. Sheldrick, SHELXS-97, Program for Crystal Structure Solution, 1997, Göttingen.
- [41] G.M. Sheldrick, SHELXL-97, Program for the Refinement of Crystal Structures, 1997, Göttingen.
- [42] P. Skehan, R. Storeng, D. Scudiero, A. Monks, J. McMahon, D. Vistica, J. T. Warren, H. Bokesch, S. Kenney, M.R. Boyd, J. Natl. Cancer Inst. 82 (1990) 1107–1112.
- [43] J.A. Marmur, J. Mol. Biol. 3 (1961) 208–218.
- [44] M.F. Reichmann, S.A. Rice, C.A. Thomas, P. Doty, J. Am. Chem. Soc. 76 (1954) 3047–3053.
- [45] G.B. Deacon, R.J. Philips, Coord. Chem. Rev. 33 (1980) 227–251.
- [46] E.R.T. Tiekink, Appl. Organomet. Chem. 5 (1991) 1–23.
- [47] N. Muhammad, Z. Rehman, S. Ali, A. Meetsma, F. Shaheen, Inorg. Chim. Acta 362 (2009) 2842–2848.
- [48] R.R. Holmes, R.O. Day, V. Chandrasekhar, J.F. Vollano, J.M. Holmes, Inorg. Chem. 25 (1986) 2490–2494.
- [49] S.W. Ng, V.G. Kumar Das, A. Syed, J. Organomet. Chem. 364 (1989) 353–362.
- [50] D.R. Smyth, E.R.T. Tiekink, Z. Kristall, New Cryst. Struct. 215 (2000) 81–82.
- [51] C. Ma, J. Sun, L. Qiu, J. Cui, J. Inorg. Organomet. Polym. Mater 15 (2005) 341–347.
- [52] G. Eng, X. Song, A. Zapata, A.C. de Dios, L. Casabiana, R.D. Pike, J. Organomet. Chem. 692 (2007) 1398–1404.

Appendix 10

Reproduced from Ref. G.N. Kaluđerović, R. Paschke, S. Prashar, S. Gómez-Ruiz, J. Organomet. Chem. 2010, 695, 1883 with permission from Elsevier.

1890

G.N. Kaluđerović et al. / Journal of Organometallic Chemistry 695 (2010) 1883–1890

- [53] M.L. Falcioni, M. Pellei, R. Gabbianelli, *Mutat. Res.* 653 (2008) 57–62 and references therein.
- [54] L. Pellerito, L. Nagy, *Coord. Chem. Rev.* 224 (2002) 111–150 and references therein.
- [55] C. Syng-Ai, T.S. Basu Baul, A. Chatterijee, *J. Environ. Pathol. Toxicol. Oncol.* 20 (2001) 333–342.
- [56] F. Barbieri, M. Viale, F. Sparatore, G. Schettini, A. Favre, C. Bruzzo, F. Novelli, A. Alema, *Anticancer Drug* 13 (2002) 599–604.
- [57] H. Seibert, S. Moerchel, M. Guelden, *Cell. Biol. Toxicol.* 20 (2004) 273–283.
- [58] N. Hoti, J. Ma, S. Tabassum, Y. Wang, M. Wu, *J. Biochem.* 134 (2003) 521–528.
- [59] Q. Li, N. Jin, P. Yang, J. Wan, W. Wu, J. Wan, *Synt. React. Inorg. Met.-Org. Chem.* 27 (1997) 811–823.
- [60] Q. Li, P. Yang, H. Wang, M. Guo, *J. Inorg. Biochem.* 64 (1996) 181–195.
- [61] J.S. Casas, E.E. Castellano, M.D. Couce, J. Ellena, A. Sanchez, J.L. Sanchez, J. Sordo, C. Taboada, *Inorg. Chem.* 43 (2004) 1957–1963.
- [62] Y. Arakawa, *Biomed. Res. Trace Elem.* 4 (1993) 129–130.
- [63] Y. Arakawa, *Biomed. Res. Trace Elem.* 11 (2000) 259–286.
- [64] T.M. Kelly, A.B. Tossi, D.J. McConnell, T.C. Streckas, *Nucleic Acids Res.* 13 (1985) 6017–6034.
- [65] J.K. Barton, A.T. Danishefsky, J.M. Goldberg, *J. Am. Chem. Soc.* 106 (1984) 2172–2176.
- [66] S.A. Tysoe, R.J. Morgan, A.D. Baker, T.C. Streckas, *J. Phys. Chem.* 97 (1993) 1707–1711.
- [67] R.F. Pasternack, E.J. Gibbs, J.J. Villafranca, *Biochemistry* 22 (1983) 2406–2414.
- [68] J. Liu, T. Zhang, T. Lu, L. Qu, H. Zhou, Q. Zhang, L. Ji, *J. Inorg. Biochem.* 91 (2002) 269–276.
- [69] C.L. Liu, J.Y. Zhou, Q.X. Li, L.J. Wang, Z.R. Liao, H.B. Xu, *J. Inorg. Biochem.* 75 (1999) 233–240.
- [70] S. Zhang, Y. Zhu, C. Tu, H. Wei, Z. Yang, L. Lin, J. Ding, J. Zhang, Z. Guo, *J. Inorg. Biochem.* 98 (2004) 2099–2116.
- [71] M.T. Carter, M. Rodriguez, A.J. Bard, *J. Am. Chem. Soc.* 111 (1989) 8901–8911.
- [72] A.M. Pyle, J.P. Rehmann, R. Meshoyrer, C.V. Kumar, N.J. Turro, J.K. Barton, *J. Am. Chem. Soc.* 111 (1989) 3051–3058.

Synthesis and biological applications of ionic triphenyltin(IV) chloride carboxylate complexes with exceptionally high cytotoxicity†

Goran N. Kaluđerović,^{*ab} Harish Kommera,^b Evamarie Hey-Hawkins,^c Reinhard Paschke^b and Santiago Gómez-Ruiz^{*cd}

Received 15th February 2010, Accepted 4th May 2010

First published as an Advance Article on the web 20th May 2010

DOI: 10.1039/c0mt00007h

The reaction of *N*-phthaloylglycine (*P*-GlyH), *N*-phthaloyl-L-alanine (*P*-AlaH), and 1,2,4-benzenetricarboxylic 1,2-anhydride (BTCH) with triethylamine led to the formation of the corresponding ammonium salts [NH₄Et₃][*P*-Gly] (**1**), [NH₄Et₃][*P*-Ala] (**2**) and [NH₄Et₃][BTC] (**3**) in very high yields. The subsequent reaction of **1–3** with triphenyltin(IV) chloride (1 : 1) yielded the compounds [NH₄Et₃][SnPh₃Cl(*P*-Gly)] (**4**), [NH₄Et₃][SnPh₃Cl(*P*-Ala)] (**5**), and [NH₄Et₃][SnPh₃Cl(BTC)] (**6**), respectively. The molecular structure of **4** was determined by X-ray diffraction studies. The cytotoxic activity of the ammonium salts (**1–3**) and the triphenyltin(IV) chloride derivatives (**4–6**) were tested against human tumor cell lines from five different histogenic origins: 8505C (anaplastic thyroid cancer), A253 (head and neck cancer), A549 (lung carcinoma), A2780 (ovarian cancer) and DLD-1 (colon cancer). Triphenyltin(IV) chloride derivatives (**4–6**) show very high activity against these cell lines while the ammonium salts of the corresponding carboxylic acids (**1–3**) are totally inactive. The most active compound is **4** which is 50 times more active than cisplatin. Compound **4** is found to induce apoptosis *via* extrinsic pathways on DLD-1 cell lines, probably by accumulation of caspases 2, 3 and 8. Furthermore, compound **4** seems to cause disturbances in G1 and G2/M phases in cell cycle of DLD-1 cell line.

1. Introduction

The fight against cancer is one of the primary targets concerning medicinal chemistry, in which bioorganometallic chemistry has become an interesting and fruitful research field.¹ The initial efforts in the evaluation of platinum-based anticancer drugs, have been shifted to non-platinum metal-based agents.^{2–14} Many different metals, for example Ti, Ga, Ge, Pd, Au, Co, Ru and Sn have been already used for these purposes and have helped in the minimization of the side effects associated with the use of platinum compounds as anticancer drugs.^{2–11} In this context, many organotin(IV) complexes have shown interesting *in vivo* anticancer activity as new chemotherapy agents.^{15–20} However, the possible application of the synthesized organotin derivatives was very limited by their poor water solubility.⁷ Thus, solubility seems to be the one of the main problems for the use of tin(IV) in anticancer drugs, however, with a rational design and functionalization of the corresponding complexes, some new

tin(IV) complexes with higher water solubility have been reported.^{21–23} Additional interest, due to solubility reasons, have been paid to the synthesis and evaluation of the cytotoxicity of organotin(IV) compounds containing carboxylate ligands.^{24–31} In addition, coordination of carboxylates to organotin moieties offers the possibility of studying the variations of the coordination mode from monodentate or chelate (symmetric or asymmetric) to bridging which may give rise to oligomeric or polymeric structures.³² The moieties R_nSn⁽⁴⁻ⁿ⁾⁺ (*n* = 2 or 3) may bind to membrane proteins or glycoproteins, or to cellular proteins; *e.g.* to hexokinase, ATPase, acetylcholinesterase of human erythrocyte membrane or to skeletal muscle membranes²⁶ or may interact directly with DNA.³³

Following our research on the synthesis, characterization and cytotoxic properties of metal-based anticancer drugs,^{34–43} and using carboxylate ligands which have shown interesting biological properties when bound to metals,^{31,38,39} here we present the synthesis, characterization and the study of the cytotoxicity of three different ionic triphenyltin(IV) chloride complexes containing carboxylate ligands which present, according to their ionic nature, higher solubility in polar solvents. These compounds represent the first examples of triethylammonium salts of triphenyltin(IV) carboxylates which have shown an extremely high cytotoxic activity.

The carboxylic acids used in this study (Fig. 1) have been previously used in the synthesis of different neutral triorganotin(IV) carboxylates,^{44–52} however, the synthesis and characterization of more convenient ionic tin(IV) complexes containing these ligands have not yet been reported and their

^a Biozentrum, Martin-Luther-Universität Halle-Wittenberg, Weinbergweg 22, 06120 Halle, Germany.

E-mail: goran.kaluderovic@chemie.uni-halle.de;
Fax: +49-345 5527028

^b Institut für Chemie, Martin-Luther-Universität Halle-Wittenberg, Kurt-Mothes-Straße 2, D-06120 Halle, Germany

^c Institut für Anorganische Chemie der Universität Leipzig, Johannisallee 29, D-04103 Leipzig, Germany.

E-mail: santiago.gomez@urjc.es; Fax: +34-914888143

^d Departamento de Química Inorgánica y Analítica, E.S.C.E.T., Universidad Rey Juan Carlos, 28933 Móstoles, Madrid, Spain

† CCDC reference number 759465. For crystallographic data in CIF or other electronic format see DOI: 10.1039/c0mt00007h

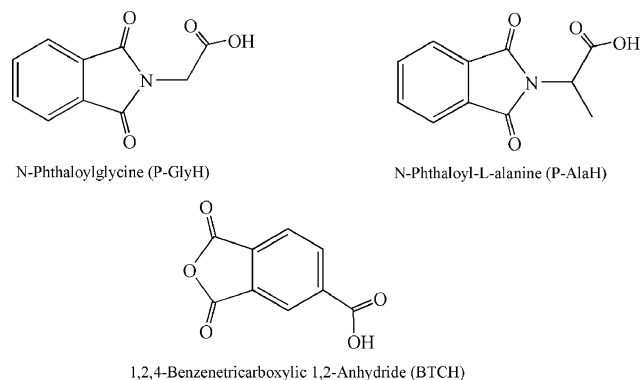


Fig. 1 Carboxylic acids used in the study.

cytotoxicity has not been studied. Thus, as numerous reports show that there is not a single or a well-defined number of pathways for the interaction of tin compounds with the membrane or constituents within the cell^{53–56} and many other studies indicate the possible mechanisms of action of tin compounds, the study of the biological properties and anticancer mechanisms of this new group of anionic organotin carboxylates, which may give rise to intermolecular interactions with an effect on the overall and the local tin environment and in the final cytotoxicity, is very useful for gaining novel insights on the cellular action of organotin complexes.

2. Experimental

2.1 General manipulations

All experiments were performed under an atmosphere of dry nitrogen using standard Schlenk techniques. Solvents and triethylamine were distilled from the appropriate drying agents and degassed before use. NMR spectra were recorded on a Bruker AVANCE DRX 400 spectrometer. ¹H NMR (400.13 MHz): internal standard solvent, external standard TMS; ¹³C{¹H} NMR (100.6 MHz): internal standard solvent, external standard TMS; ¹¹⁹Sn{¹H} NMR (149.2 MHz): internal standard solvent, external standard tetramethyltin. The splitting of proton resonances in the reported ¹H NMR spectra are defined as *s* = singlet, *d* = doublet, *t* = triplet, *q* = quadruplet, *br* = broad and *m* = multiplet. IR spectra: KBr pellets were prepared in a nitrogen-filled glove box and the spectra were recorded on a Perkin-Elmer System 2000 FTIR spectrometer in the range 350–4000 cm⁻¹. ESI MS were recorded with a FT-ICR MS Bruker-Daltonics (APEX II, 7 Tesla, MASPEC II), and solutions of *ca.* 1 mg mL⁻¹ of the compounds in a mixture of dry CHCl₃–CH₃CN (1 : 1) were injected. All solvents were purified by distillation, dried, saturated with nitrogen and stored over potassium mirror. *N*-phthaloylglycine (*P*-GlyH), *N*-phthaloyl-L-alanine (*P*-AlaH), and 1,2,4-benzenetricarboxylic 1,2-anhydride (BTCH) and triphenyltin(IV) chloride were purchased from Alfa Aesar or Acros Organics. All the commercial reagents were used directly, without further purification.

2.2 Synthesis of [NHEt₃][*P*-Gly] (1)

A solution of NEt₃ (1.76 mL, 12.19 mmol) in THF (20 mL) was added dropwise over 15 min to a solution of *P*-GlyH

(2.50 g, 12.19 mmol) in THF (130 mL) at room temperature. The reaction mixture was stirred under reflux overnight. The solvent was then evaporated under reduced pressure and the resulting white solid was washed twice with hexane (40 mL) to give a white solid characterized as **1**. Yield: 3.32 g, 89%. FT-IR (KBr): 3491 (*s*) (*v* NH), 1720 (*s*) (*v* CO) 1616 (*s*) (*v_a* COO⁻), 1383 (*s*) (*v_s* COO⁻); ¹H NMR (400 MHz, CDCl₃, 25 °C): δ 1.25 (*t*, 9H, ³*J*(¹H-¹H) = 7.6 Hz, CH₃ of Et), 3.01 (*q*, 6H, ³*J*(¹H-¹H) = 7.6 Hz, CH₂ of Et), 4.28 (*s*, 2H, CH₂ of *P*-Gly), 7.67 (*m*, 2H, aromatic H in *P*-Gly), 7.83 (*m*, 2H, aromatic H in *P*-Gly), 14.31 (*br*, 1H, NHEt₃); ¹³C{¹H} NMR (100.6 MHz, CDCl₃, 25 °C): δ 8.5 (CH₃ of Et), 41.3 (CH₂ of *P*-Gly), 44.9 (CH₂ of Et), 123.1, 133.5 (aromatic CH of *P*-Gly) 132.7 (aromatic *ipso*-C of *P*-Gly), 168.3 (CO of *P*-Gly), 172.3 (COO); ESI-MS (negative)(*m/z*): 203.8 [M⁺-NHEt₃], 159.9 [M⁺-NHEt₃-COO]; ESI-MS (positive)(*m/z*): 102.1 [M⁺-(*P*-Gly) + H]; elemental analysis for C₁₆H₂₂N₂O₄ (306.4): calc. C, 62.73; H, 7.24; N, 9.14, found C, 62.40; H, 7.19; N 9.09%.

2.3 Synthesis of [NHEt₃][*P*-Ala] (2)

The synthesis of **2** was carried out in an identical manner to **1**. NEt₃ (1.65 mL, 11.46 mmol) and *P*-AlaH (2.50 g, 11.46 mmol). Yield: 3.41 g, 93%. FT-IR (KBr): 3460 (*s*) (*v* NH), 1710 (*s*) (*v* CO) 1650 (*s*) (*v_a* COO⁻), 1390 (*s*) (*v_s* COO⁻); ¹H NMR (400 MHz, CDCl₃, 25 °C): δ 1.25 (*t*, 9H, ³*J*(¹H-¹H) = 7.2 Hz, CH₃ of Et), 1.56 (*d*, 3H, ³*J*(¹H-¹H) = 7.6 Hz, CH₃ of *P*-Ala), 3.08 (*q*, 6H, ³*J*(¹H-¹H) = 7.6 Hz, CH₂ of Et), 4.73 (*q*, 1H, ³*J*(¹H-¹H) = 7.2 Hz, CH of *P*-Ala), 7.67 (*m*, 2H, aromatic H in *P*-Ala), 7.79 (*m*, 2H, aromatic H in *P*-Ala), 11.88 (*br*, 1H, NHEt₃); ¹³C{¹H} NMR (100.6 MHz, CDCl₃, 25 °C): δ 8.9 (CH₃ of Et), 16.3 (CH₂ of *P*-Ala) 41.9 (CH of *P*-Ala), 44.8 (CH₂ of Et), 123.7, 133.2 (aromatic CH of *P*-Ala) 132.9 (aromatic *ipso*-C of *P*-Ala), 168.9 (CO of *P*-Ala), 172.5 (COO); ESI-MS (negative)(*m/z*): 217.9 [M⁺-NHEt₃], 174.2 [M⁺-NHEt₃-COO]; ESI-MS (positive)(*m/z*): 102.1 [M⁺-(*P*-Ala) + H]; elemental analysis for C₁₇H₂₄N₂O₄ (320.4): calc. C, 63.73; H, 7.55; N, 8.74, found C, 63.55; H, 7.39; N 8.79%.

2.4 Synthesis of [NHEt₃][BTC] (3)

The synthesis of **3** was carried out in an identical manner to **1**. NEt₃ (1.88 mL, 13.01 mmol) and BTCH (2.50 g, 13.01 mmol). Yield: 3.09 g, 81%. FT-IR (KBr): 3435 (*s*) (*v* NH), 1778, 1715 (*s*) (*v* CO) 1615 (*s*) (*v_a* COO⁻), 1351 (*s*) (*v_s* COO⁻); ¹H NMR (400 MHz, CDCl₃, 25 °C): δ 1.39 (*t*, 9H, ³*J*(¹H-¹H) = 7.2 Hz, CH₃ of Et), 3.23 (*q*, 6H, ³*J*(¹H-¹H) = 7.2 Hz, CH₂ of Et), 7.99 (*d*, 1H, ³*J*(¹H-¹H) = 8.0 Hz, aromatic H in BTC), 8.58 (*d*, 1H, ³*J*(¹H-¹H) = 8.0 Hz, aromatic H in BTC), 8.64 (*s*, 1H, aromatic H in BTC), 13.33 (*br*, 1H, NHEt₃); ¹³C{¹H} NMR (100.6 MHz, CDCl₃, 25 °C): δ 8.6 (CH₃ of Et), 45.6 (CH₂ of Et), 125.1, 126.8, 137.2 (aromatic CH of BTC), 145.5 (aromatic C-COO of BTC), 162.8, 162.9 (C-CO of BTC), 169.3 (COO of BTC), 170.7, 170.8 (C=O of anhydride of BTC); ESI-MS (negative)(*m/z*): 190.8 [M⁺-NHEt₃], 164.9 [M⁺-NHEt₃-O], 146.9 [M⁺-NHEt₃-COO]; ESI-MS (positive)(*m/z*): 102.1 [M⁺-BTC + H]; elemental analysis for C₁₅H₁₉NO₅ (293.3): calc. C, 61.42; H, 6.53; N, 4.78, found C, 61.21; H, 6.44; N 4.79%.

2.5 Synthesis of [NH₃Et₃][SnPh₃Cl(*P*-Gly)] (4)

A solution of [NH₃Et₃][*P*-Gly] (**1**) (0.79 g, 2.59 mmol) in THF (20 mL) was added dropwise over 15 min to a solution of SnPh₃Cl (1.00 g, 2.59 mmol) in THF (80 mL) at room temperature. The reaction mixture was stirred under reflux overnight. The solvent was then evaporated under reduced pressure and the resulting white solid was washed twice with hexane (40 mL) to give a white solid characterized as **4**. The product is totally soluble in EtOH, DMSO, CHCl₃, CH₂Cl₂, CH₃CN and in mixtures EtOH–H₂O and is partially soluble in toluene. Crystallization in toluene afforded crystals suitable for X-ray diffraction analysis. Yield: 1.32 g, 74%. FT-IR (KBr): 3436 (s) (ν NH), 1718 (s) (ν CO) 1623 (s) (ν_a COO⁻), 1370 (s) (ν_s COO⁻), 457 (m) (ν Sn–O); ¹H NMR (400 MHz, CDCl₃, 25 °C): δ 1.05 (t, 9H, ³J(¹H–¹H) = 7.2 Hz, CH₃ of Et), 2.70 (q, 6H, ³J(¹H–¹H) = 7.6 Hz, CH₂ of Et), 4.15 (s, 2H, CH₂ of *P*-Gly), 7.35 (br m, 9H, *m*- and *p*-protons in SnPh₃), 7.66 (m, 2H, aromatic H in *P*-Gly), 7.73 (br m, 6H, *o*-protons in SnPh₃, ³J(¹H–Sn) = ca. 60 Hz); 7.80 (m, 2H, aromatic H in *P*-Gly), 11.62 (br, 1H, NH₃Et₃); ¹³C{¹H} NMR (100.6 MHz, CDCl₃, 25 °C): δ 8.4 (CH₃ of Et), 40.9 (CH₂ of *P*-Gly), 45.4 (CH₂ of Et), 123.2, 133.8 (aromatic CH of *P*-Gly), 128.6 (C-3 and C-5 of SnPh₃, ³J(¹³C–Sn) = 67.2 Hz), 129.4 C-4 of SnPh₃, ⁴J(¹³C–Sn) = 46.5 Hz), 132.4 (aromatic *ipso*-C of *P*-Gly), 136.4 (C-2 and C-6 of SnPh₃, ²J(¹³C–Sn) = 48.7 Hz), 140.4 (C-1 of SnPh₃, ¹J(¹³C–Sn) not observed), 167.9 (CO of *P*-Gly), 171.9 (COO); ¹¹⁹Sn{¹H} NMR (149.2 MHz, CDCl₃, 25 °C): δ –144.5; ESI-MS (negative)(*m/z*): 590.02 [M⁺-NH₃Et₃]; elemental analysis for C₃₄H₃₇ClN₂O₄Sn (691.8): calc. C, 59.03; H, 5.39; N, 4.05, found C, 58.59; H, 5.29; N 4.09%.

2.6 Synthesis of [NH₃Et₃][SnPh₃Cl(*P*-Ala)] (5)

The synthesis of **5** was carried out in an identical manner to **4**. [NH₃Et₃][*P*-Ala] (**2**) (0.83 g, 2.59 mmol) and SnPh₃Cl (1.00 g, 2.59 mmol). Yield: 1.42 g, 78%. FT-IR (KBr): 3447 (s) (ν NH), 1713 (s) (ν CO) 1618 (s) (ν_a COO⁻), 1389 (s) (ν_s COO⁻), 455 (m) (ν Sn–O); ¹H NMR (400 MHz, CDCl₃, 25 °C): δ 1.22 (t, 9H, ³J(¹H–¹H) = 7.2 Hz, CH₃ of Et), 1.71 (d, 3H, ³J(¹H–¹H) = 7.2 Hz, CH₃ of *P*-Ala), 2.93 (q, 6H, ³J(¹H–¹H) = 7.6 Hz, CH₂ of Et), 4.99 (q, 1H, ³J(¹H–¹H) = 7.6 Hz, CH of *P*-Ala), 7.44 (br m, 9H, *m*- and *p*- protons in SnPh₃), 7.68 (m, 2H, aromatic H in *P*-Ala), 7.70 (br m, 6H, *o*- protons in SnPh₃, ³J(¹H–Sn) = ca. 52 Hz); 7.83 (m, 2H, aromatic H in *P*-Ala), 11.70 (br, 1H, NH₃Et₃); ¹³C{¹H} NMR (100.6 MHz, CDCl₃, 25 °C): δ 8.5 (CH₃ of Et), 16.0 (CH₃ of *P*-Ala) 45.6 (CH of *P*-Ala), 48.2 (CH₂ of Et), 123.3, 133.9 (aromatic CH of *P*-Ala), 129.0 (C-3 and C-5 of SnPh₃, ³J(¹³C–Sn) = 65.1 Hz), 130.2 (C-4 of SnPh₃, ⁴J(¹³C–Sn) = 13.6 Hz), 132.1 (aromatic *ipso*-C of *P*-Gly), 136.3 (C-2 and C-6 of SnPh₃, ²J(¹³C–Sn) = 48.7 Hz), 139.8 (C-1 of SnPh₃, ¹J(¹³C–Sn) not observed), 167.5 (CO of *P*-Ala), 178.1 (COO); ¹¹⁹Sn{¹H} NMR (149.2 MHz, CDCl₃, 25 °C): δ –94.0; ESI-MS (negative)(*m/z*): 604.03 [M⁺-NH₃Et₃]; elemental analysis for C₃₅H₃₉ClN₂O₄Sn (705.9): calc. C, 59.56; H, 5.57; N, 3.97, found C, 59.49; H, 5.48; N 3.98%.

2.7 Synthesis of [NH₃Et₃][SnPh₃Cl(*BTC*)] (6)

The synthesis of **6** was carried out in an identical manner to **4**. [NH₃Et₃][*BTC*] (**3**) (0.76 g, 2.59 mmol) and SnPh₃Cl (1.00 g,

2.59 mmol). Yield: 1.16 g, 66%. FT-IR (KBr): 3433 (s) (ν NH), 1780, 1719 (s) (ν CO) 1616 (s) (ν_a COO⁻), 1362 (s) (ν_s COO⁻), 454 (m) (ν Sn–O); ¹H NMR (400 MHz, CDCl₃, 25 °C): δ 1.33 (t, 9H, ³J(¹H–¹H) = 7.2 Hz, CH₃ of Et), 3.07 (q, 6H, ³J(¹H–¹H) = 7.2 Hz, CH₂ of Et), 7.46 (br m, 9H, *m*- and *p*- protons in SnPh₃), 7.75 (br m, 6H, *o*- protons in SnPh₃, ³J(¹H–Sn) = 61.1 Hz), 7.98 (d, 1H, ³J(¹H–¹H) = 7.9 Hz, aromatic H in *BTC*), 8.56 (d, 1H, ³J(¹H–¹H) = 7.9 Hz, aromatic H in *BTC*), 8.65 (s, 1H, aromatic H in *BTC*), 12.67 (br, 1H, NH₃Et₃); ¹³C{¹H} NMR (100.6 MHz, CDCl₃, 25 °C): δ 8.6 (CH₃ of Et), 45.9 (CH₂ of Et), 125.3, 127.1, 137.5 (aromatic CH of *BTC*), 128.9 (C-3 and C-5 of SnPh₃, ³J(¹³C–Sn) = 63.8 Hz), 130.1 (C-4 of SnPh₃, ⁴J(¹³C–Sn) = 13.6 Hz), 136.4 (C-2 and C-6 of SnPh₃, ²J(¹³C–Sn) = 48.8 Hz), 138.9 (C-1 of SnPh₃, ¹J(¹³C–Sn) not observed), 142.6 (aromatic C-COO of *BTC*), 162.5, 162.6 (C-CO of *BTC*), 168.7 (COO of *BTC*), 170.6, 170.8 (C=O of anhydride of *BTC*); ¹¹⁹Sn{¹H} NMR (149.2 MHz, CDCl₃, 25 °C): δ –95.0; ESI-MS (negative)(*m/z*): 576.99 [M⁺-NH₃Et₃]; elemental analysis for C₃₃H₃₄ClN₂O₅Sn (705.9): calc. C, 58.39; H, 5.05; N, 2.06, found C, 58.10; H, 4.97; N 2.19%.

2.8 Data Collection and Structural Refinement of 4

The data of **4** were collected with a CCD Oxford Xcalibur S (λ(Mo-Kα) = 0.71073 Å) using ω and φ scans mode. Semi-empirical from equivalents absorption corrections were carried out with SCALE3 ABSPACK.⁵⁷ The structure was solved by Patterson methods.⁵⁸ Structure refinement was carried out with SHELXL-97.⁵⁹ All non-hydrogen atoms were refined anisotropically, H atom bonded to nitrogen was localized and refined freely and the other hydrogen atoms were placed in calculated positions and refined with calculated isotropic displacement parameters. Table 1 lists crystallographic details. Crystallographic data for the structural

Table 1 Crystallographic data for **4**

Formula	C ₃₄ H ₃₇ ClN ₂ O ₄ Sn
Fw	691.80
T/K	130(2)
Cryst syst	Monoclinic
Space group	P2 ₁ /n
<i>a</i> /pm	990.82(5)
<i>b</i> /pm	3066.76(9)
<i>c</i> /pm	1121.89(4)
α (°)	90
β (°)	107.661(5)
γ (°)	90
<i>V</i> (nm ³)	3.2483(2)
<i>Z</i>	4
<i>D</i> _c (Mg m ⁻³)	1.415
μ/mm ⁻¹	0.908
<i>F</i> (000)	1416
Cryst dimens/mm	0.3 × 0.2 × 0.2
θ range (°)	2.66 to 28.28
<i>hkl</i> ranges	–13 ≤ <i>h</i> ≤ 13, –37 ≤ <i>k</i> ≤ 40, –14 ≤ <i>l</i> ≤ 14
Data/parameters	8049/350
goodness-of-fit on <i>F</i> ²	1.055
Final <i>R</i> indices [<i>I</i> > 2σ(<i>I</i>)]	<i>R</i> ₁ = 0.0558, <i>wR</i> ₂ = 0.1264
<i>R</i> indices (all data)	<i>R</i> ₁ = 0.0837, <i>wR</i> ₂ = 0.1352
largest diff. peak and hole/e Å ⁻³	1.769 and –1.353

analysis **4** have been deposited with the Cambridge Crystallographic Data Centre, CCDC-759465 (**4**).[†]

2.9. *In vitro* studies

2.9.1. Preparation of drug solutions. Stock solutions of investigated compounds (**1–6**) were prepared in dimethyl sulfoxide (DMSO, Sigma Aldrich) at a concentration of 20 mM, filtered through Millipore filter, 0.22 μm , before use, and diluted by nutrient medium to various working concentrations. Nutrient medium was RPMI-1640 (PAA Laboratories) supplemented with 10% fetal bovine serum (Biocrom AG) and penicillin/streptomycin (PAA Laboratories).

2.9.2. Cell lines and culture conditions. The cell lines 8505C, A253, A549, A2780 and DLD-1, included in this study, were kindly provided by Dr Thomas Mueller, Department of Hematology/Oncology, Martin Luther University of Halle-Wittenberg, Halle (Saale), Germany. Cultures were maintained as monolayer in RPMI 1640 (PAA Laboratories, Pasching, Germany) supplemented with 10% heat inactivated fetal bovine serum (Biocrom AG, Berlin, Germany) and penicillin/streptomycin (PAA Laboratories) at 37 °C in a humidified atmosphere of 5% (v/v) CO_2 .

2.9.3. Cytotoxicity assay. The cytotoxic activities of the compounds were evaluated using the sulforhodamine-B (SRB, Sigma Aldrich) microculture colorimetric assay.⁶⁰ In short, exponentially growing cells were seeded into 96-well plates on day 0 at the appropriate cell densities to prevent confluence of the cells during the period of experiment. After 24 h, the cells were treated with serial dilutions of the studied compounds for 96 h. Final concentrations achieved in treated wells were 0–100 μM for **1–3** and 0.008, 0.02, 0.04, 0.08, 0.12, 0.16, 0.2, 0.3 and 0.4 μM for tin(IV) complexes (**4–6**). Each concentration was tested in triplicate on each cell line. The final concentration of DMSO solvent never exceeded 0.5%, which was non-toxic to the cells. The percentages of surviving cells relative to untreated controls were determined 96 h after the beginning of drug exposure. After 96 h treatment, the supernatant medium from the 96 well plates was thrown away and the cells were fixed with 10% TCA. For a thorough fixation, plates were then allowed to stand at 4 °C. After fixation, the cells were washed in a strip washer. The washing was carried out four times with water using alternate dispensing and aspiration procedures. The plates were then dyed with 100 μL of 0.4% SRB for about 45 min. After dyeing, the plates were again washed to remove the dye with 1% acetic acid and allowed to air dry overnight. 100 μL of 10 mM Tris base solutions were added to each well of the plate and absorbance was measured at 570 nm using a 96 well plate reader (Tecan Spectra, Crailsheim, Germany). The IC_{50} value, defined as the concentrations of the compound at which 50% cell inhibition was observed, was estimated from the dose-response curves.

2.9.4 Apoptosis tests

2.9.4.1 Trypan blue exclusion test. Apoptotic cell death was analyzed by trypan blue dye (Sigma Aldrich, Germany) on DLD-1 cell line. The cell culture flasks with 70% to 80% confluence were treated with IC_{90} dose of **4** for 24 h. The

supernatant medium with floating cells was collected after treatment and centrifuged to collect the dead and apoptotic cells. The cell pellet was resuspended in serum free media. Equal amounts of cell suspension and trypan blue were mixed and this was analyzed under a microscope. The cells which were viable excluded the dye and were colorless while those whose cell membrane was destroyed were blue. If the proportion of colorless cells is higher than the colored cells, then the death can be characterized as apoptotic.

2.9.4.2 DNA fragmentation assay. Determination of apoptotic cell death was performed by DNA gel electrophoresis. Briefly, DLD-1 cells were treated with the respective IC_{90} dose of **4** for 24 h. Floating cells induced by drug exposure were collected, washed with PBS and lysed with lysis buffer (100 mM Tris-HCl pH 8.0; 20 mM EDTA; 0.8% SDS; all from Sigma Aldrich). Then they were treated with RNase A at 37 °C for 2 h and proteinase K at 50 °C (both from Roche Diagnostics chemical company, Mannheim, Germany). DNA laddering was observed by running the samples on 2% agarose gel followed by ethidium bromide (Sigma Aldrich) staining.

2.9.5 Caspase 2, 3, 8 and 9 enzyme activity assay. Activity of caspases 2, 3, 8 and 9 was measured using the caspase substrate cleavage assay. After exposure to equitoxic IC_{50} concentration of **4**, DLD-1 cells were sampled 2 and 6 h for cleavage of caspases. To summarize, adherent cells were washed with cold PBS, collected with a cell scraper, and suspended in cell lyses buffer (50 mM Hepes pH 7.4, 1% Triton X100, all from Sigma-Aldrich). After incubation for 10 min on ice and centrifugation, protein concentrations of the supernatants were measured according to the method of Bradford (Bio-Rad Laboratories). Samples (50 μg protein extract respectively) were incubated on a microplate at 37 °C overnight in reaction buffer (50 mM Hepes pH 7.4, 0.1% CHAPS, 5 mM EGTA, 5% glycerol) containing 10 mM DTT (all from Sigma-Aldrich) and a specific substrate of caspases (2, Ac-VDVAD-pNA; 3, Ac-DEVD-pNA; 8, Ac-IETD-pNA; 9, Ac-LEHD-pNA, Axxora, Loerrach, Germany). Extinction of released *p*-nitroaniline was measured at 405 nm (Tecan Spectra, Crailsheim, Germany) and activity of caspases 2, 3, 8 and 9 was evaluated by OD ratio of treated/untreated samples.⁶¹

2.9.6 Cell cycle analysis. Cell cycle was assessed by flow cytometry using a fluorescence-activated cell sorter (FACS). For this assay, 1×10^6 DLD-1 cells, were seeded in 25 cm^2 cell culture flasks, with 10 mL of medium. After 24 h of incubation, **4** was added at IC_{90} concentration. Following 24 h of incubation, cells were harvested by mild trypsinization, collected by centrifugation, washed with PBS and both adherent and floating cells were resuspended in 100 μL of PBS and fixed with 2 mL of 70% ethanol at 4 °C for at least 1 h. The fixed samples were then centrifuged, the cell pellet was washed with 2 mL of staining buffer (PBS + 2% FCS + 0.01% NaN_3) and again centrifuged. The cell pellet was resuspended in 100 μL of RNase A (1 mg mL^{-1}) and incubated for 30 min at 37 °C. At the end of incubation the samples were treated with propidium iodide (20 $\mu\text{g}/1 \text{ mL}$

of staining buffer) and allowed to stand in the dark at least for 30 min before analysis. The fluorescence intensity was determined by a FacsCalibur (Becton Dickinson, Heidelberg, Germany). Each analysis was done using *ca.* 1×10^4 events.

3. Results and discussion

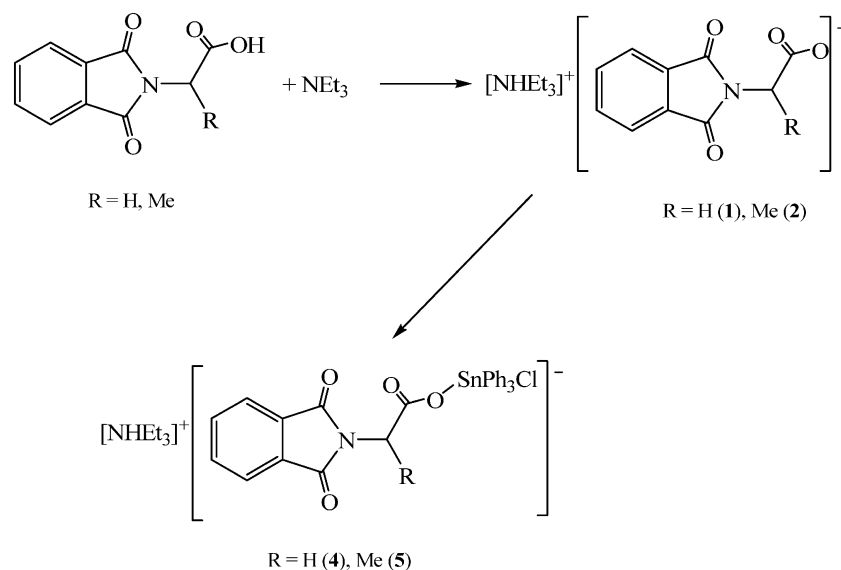
3.1 Synthesis and spectroscopic studies

The ammonium salts $[\text{NHET}_3][P\text{-Gly}]$ (**1**), $[\text{NHET}_3][P\text{-Ala}]$ (**2**) (Scheme 1) and $[\text{NHET}_3][\text{BTC}]$ (**3**) (Scheme 2) were prepared, in very high yields, by the reaction of *N*-phthaloylglycine (*P*-GlyH), *N*-phthaloyl-L-alanine (*P*-AlaH), or 1,2,4-benzenetricarboxylic 1,2-anhydride (BTCH) with triethylamine respectively. The NMR, mass and IR spectra showed that all the complexes, isolated as crystalline solids, were of high purity. In the ^1H NMR spectra of **1–3**, a set of three signals consisting in a triplet at *ca.* 1.3 ppm, a quadruplet at *ca.* 3.2 and a broad signal between 11 and 13 ppm corresponding to protons of the triethylammonium cation were observed. For each compound, signals corresponding to the different carboxylate anions were recorded. For **1** one singlet at 4.28 ppm corresponding to the $-\text{CH}_2-$ protons and two multiplets at 7.67 and 7.83 ppm assigned to the aromatic protons of the *N*-phthaloyl group were observed. In the case of **2**, two multiplets (at 7.67 and 7.79 ppm) were also recorded for the phthaloyl group and a doublet at 1.56 and a quadruplet at 3.08 ppm were assigned for the $\text{CH}-\text{CH}_3$ moiety of the *N*-phthaloyl-L-alanine. In the ^1H NMR spectrum of compound **3**, two doublets and one singlet between 7.9 and 8.7 ppm were assigned to the aromatic protons of the carboxylate, in addition to the signals corresponding to the cation. The $^{13}\text{C}\{^1\text{H}\}$ NMR spectra of **1–3** showed the expected signals. The IR spectra of the ionic ligands present strong bands in two different regions between 1650–1610 and 1390–1350 cm^{-1} , which correspond to the asymmetric and symmetric vibrations, respectively, of the COO moiety. The difference between the asymmetric and symmetric vibrations of more than 200 cm^{-1} in

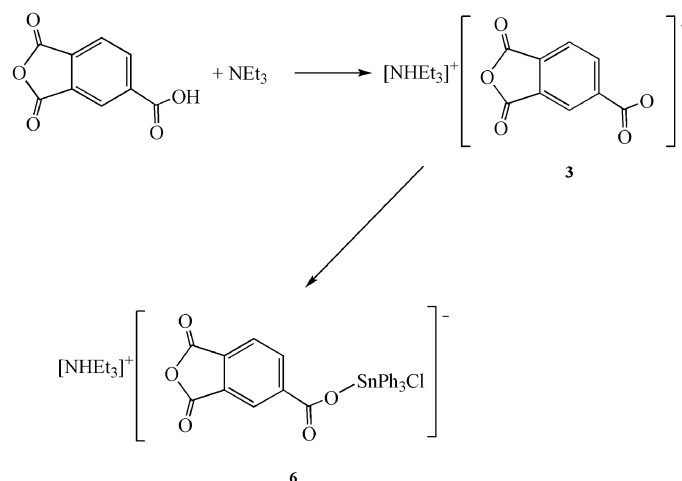
all cases, indicates monodentate coordination of the carboxylate ligand,⁶² in addition to these signals, a typical band at *ca.* 3450 cm^{-1} assigned to the N–H vibration was observed in all the spectra.⁶³ The ESI-MS spectra of **1–3** recorded in negative mode showed the peaks of the anionic part of these molecules, while recorded in positive mode, presented a peak corresponding to the triethylammonium cation.

The subsequent reaction of **1–3** with triphenyltin chloride (1 : 1) yielded the compounds $[\text{NHET}_3][\text{SnPh}_3\text{Cl}(P\text{-Gly})]$ (**4**), $[\text{NHET}_3][\text{SnPh}_3\text{Cl}(P\text{-Ala})]$ (**5**) (Scheme 1) and $[\text{NHET}_3][\text{SnPh}_3\text{Cl}(\text{BTC})]$ (**6**) (Scheme 2), respectively.

The organotin(IV) complexes **4–6** were characterized by multinuclear NMR spectroscopy, mass spectrometry, IR spectroscopy and elemental analysis. In the ^1H NMR spectra of all the compounds a set of two signals at *ca.* 7.3 and 7.7 ppm corresponding to the protons of the phenyl groups of the SnPh_3Cl moiety, was observed in addition to the signals corresponding to the carboxylate ligands, which presented similar spectral patterns to those observed in the ^1H NMR spectra of **1–3**. $^{13}\text{C}\{^1\text{H}\}$ NMR spectra for **4–6** showed the expected signals for the phenyl groups, as well as the signals corresponding to the different carboxylate ligands. A typical signal at low field (*ca.* 170 ppm) was observed in all the spectra and assigned to the carbon atom of the carboxylate group. Analogously to the IR spectra of the starting carboxylate **1–3**, the spectra of **4–6** present strong bands between 1630–1610 and 1390–1360 cm^{-1} , which correspond to the asymmetric and symmetric vibrations, respectively, of the COO moiety. Again, the difference between the asymmetric and symmetric vibrations of more than 200 cm^{-1} in all cases, indicates monodentate coordination of the carboxylate ligand,⁶² as was also confirmed, in the case of complex **4**, by single crystal X-ray diffraction studies (see section 3.2). In addition, medium absorptions corresponding to the Sn–O stretching mode of vibration appeared at *ca.* 455 cm^{-1} . **4–6** were also characterized by ESI-MS observing, in all cases in the negative mode; the peaks corresponding to the anionic parts of **4–6** (see sections 2.2–2.7).



Scheme 1



Scheme 2

Stability of the synthesized complexes in d_6 -DMSO and d_6 -DMSO/ D_2O solutions has been followed by NMR spectroscopy. After several hours in dry d_6 -DMSO, the NMR spectra of the studied compounds suffered apparent no changes, indicating their relatively high stability. The analysis of the spectra of **4–6** in d_6 -DMSO/ D_2O show a very slow decomposition process which over 72 h leads to the formation of a mixture of tin-containing products which included $Ph_3SnOSnPh_3$, $SnPh_3OH$, $SnPh_3L$ ($L = P\text{-Gly}, P\text{-Ala}, BTC$) and the free carboxylic acids, between other unidentified compounds.

3.2 Structural studies

Complex **4** (Fig. 2) crystallizes in the centrosymmetric monoclinic space group $P2_1/n$ with four molecules in the unit cell.

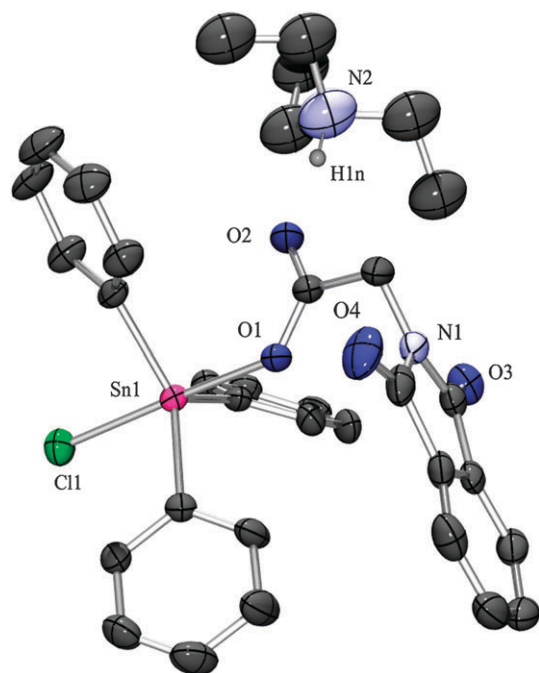


Fig. 2 Molecular structure and atom-labeling scheme for **4** with thermal ellipsoids at 50% probability (hydrogen atoms, except at nitrogen, are omitted for clarity).

The molecular structure of **4** reveals that the central tin atom is pentacoordinated; presenting a almost ideal trigonal bipyramidal geometry with the $Cl(1)\text{-Sn}(1)\text{-O}(1)$ angle of $177.23(8)^\circ$ and $O(1)\text{-Sn}(1)\text{-C}_{\text{phenyl}}$ and $Cl(1)\text{-Sn}(1)\text{-C}_{\text{phenyl}}$ close to 90° . The $Sn\text{-O}$ bond lengths $Sn(1)\text{-O}(1)$ 223.1(3) and $Sn(1)\text{-O}(2)$ 333.8(3) pm are quite different indicating monodentate coordination to tin of the carboxylate ligand. Weak interionic interactions ($O(2)\cdots H(2N)$ *ca.* 168 pm) between the hydrogen atom of the ammonium cation and the non-coordinated oxygen of the anion were observed. The bond length $N(2)\text{-H}(1N)$ yielded reasonable distances of *ca.* 98 pm. The most interesting structural parameter of this complex is the bond length $Sn(1)\text{-Cl}(1)$ of 256.5(2) pm which is in agreement with other $Sn\text{-Cl}$ bonds in zwitterionic complexes and about *ca.* 10 pm longer than the expected for a triaryltin(IV) chloride derivative,^{64–68} indicating some repulsive effect of the carboxylate ligand on the $Sn\text{-Cl}$ bond which elongates the distance between the two atoms. Selected bond lengths and angles for **4** are summarized in Table 2.

3.3 In vitro studies

3.3.1 Cytotoxic studies. The *in vitro* cytotoxicities of triethylammonium carboxylates **1–3** as well as corresponding

Table 2 Selected Bond Lengths (pm) and Angles ($^\circ$) for **4**

	4
$Sn(1)\text{-O}(1)$	223.1(3)
$Sn(1)\text{-O}(2)$	333.8(3)
$Sn(1)\text{-Cl}(1)$	256.5(2)
$C(19)\text{-O}(1)$	125.8(5)
$C(19)\text{-O}(2)$	123.4(6)
$C(22)\text{-O}(3)$	119.5(5)
$C(23)\text{-O}(4)$	120.4(6)
$N(2)\text{-H}(1N)$	98(2)
$O(2)\cdots H(2N)$	168(2)
$Cl(1)\text{-Sn}(1)\text{-O}(1)$	177.23(8)
$Cl(1)\text{-Sn}(1)\text{-O}(2)$	141.45(9)
$Cl(1)\text{-Sn}(1)\text{-C}(1)$	91.0(2)
$Cl(1)\text{-Sn}(1)\text{-C}(7)$	92.7(1)
$Cl(1)\text{-Sn}(1)\text{-C}(13)$	91.2(2)
$O(1)\text{-C}(19)\text{-O}(2)$	125.3(5)

triphenyltin(IV) complexes **4–6** against human tumor cell lines 8505C anaplastic thyroid cancer, A253 head and neck tumor, A549 lung carcinoma, A2780 ovarian cancer and DLD-1 colon carcinoma were determined by using the SRB micro-culture colorimetric assay.⁶⁰ In addition, cytotoxicity of cisplatin have been included for comparison.

Triethylammonium salts of carboxylic acids were inactive against the investigated panel of tumor cell lines ($IC_{50} > 100 \mu M$). In this way is also proved that neither hypothetical activity of the free triethylammonium cation nor the uncoordinated carboxylato ligand have influence on the activity of the studied triphenyltin(IV) complexes. The IC_{50} values of the studied compounds and cisplatin are summarized in Table 3. The triphenyltin(IV) compounds showed a dose-dependent anti-proliferative effect toward all the studied cancer cell lines (Fig. 3). Triphenyltin(IV) compounds present lower IC_{50} values than those of cisplatin. The difference in activity of compounds **4–6** and cisplatin presents a maximum of up to 50 times, in cisplatin resistant cell line DLD-1. A similar efficiency was found against anaplastic thyroid cancer cisplatin resistant cell line 8505C, where triphenyltin(IV) compounds are almost up to 40 times more active than cisplatin. These values become lower in cisplatin sensitive A2780, A253 and A549 cell lines where triphenyltin(IV) compounds are only between 3.2 and 14.8 times more cytotoxic than cisplatin.

Triphenyltin(IV) complexes **4** and **5** bearing very similar moieties showed notable differences in the cytotoxic activity. From those results one can envisage that small structural changes, (replacement of H with Me group (**4** to give **5**)) led

to a significant decrease of the final cytotoxic activity. On the other hand, triphenyltin(IV) compound substitution of the phthaloyl aminoacids by 1,2,4-benzenetricarboxylic-1,2-anhydride (**6**) led to further decreases in the cytotoxicity, except in A2780 cell line, when compared with **4** and **5**. Thus, one can think that the incorporation of biocompatible phthaloyl aminoacids as carboxylato ligands may have a positive influence in the final cytotoxicity of the tin(IV) complexes when compared with other different carboxylato ligands.

3.3.2 Apoptosis studies

3.3.2.1 Dye exclusion test and DNA laddering. Apoptosis and cell mediated cytotoxicity are characterized by a fragmentation of the genomic DNA. These DNA fragments have a length of about 180 base pairs or multiples of this number (360, 540, 720, ...), this is, the characteristic DNA-length of a nucleosome (DNA-histone-complex). Endonucleases cleave selectively DNA at sites located between nucleosomal units (linker DNA). In agarose gel electrophoresis of these, DNA fragments are resolved to a distinctive ladder pattern. To test whether complex **4** induced cell death mediated by apoptosis, floating cells from DLD-1 colon carcinoma cell line after 24 h treatment with the IC_{90} concentration were collected and analyzed by DNA laddering technique. In DLD-1 cell line with triphenyltin(IV) compound **4**, typical DNA laddering was observed (Fig. 4). Furthermore, DLD-1 cells were exposed to IC_{90} dose of complex **4**, the ability to exclude trypan blue and detached cells were investigated. The treatment with IC_{90} dose

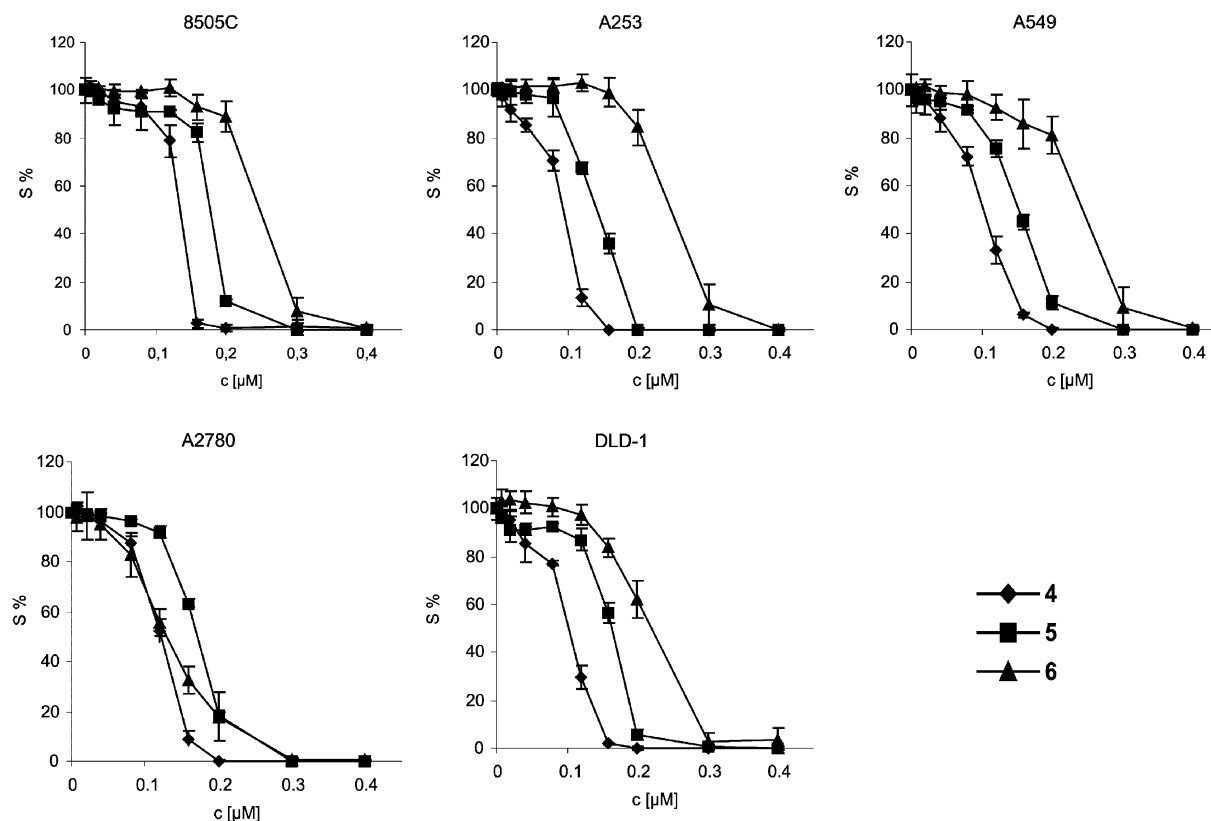


Fig. 3 Representative graphs show survival of 8505C, A253, A549, A2780 and DLD-1 cells grown for 96 h in the presence of increasing concentrations of triphenyltin(IV) complexes **4–6**.

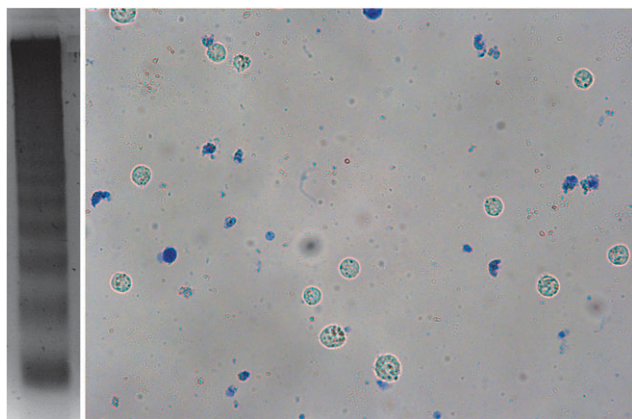
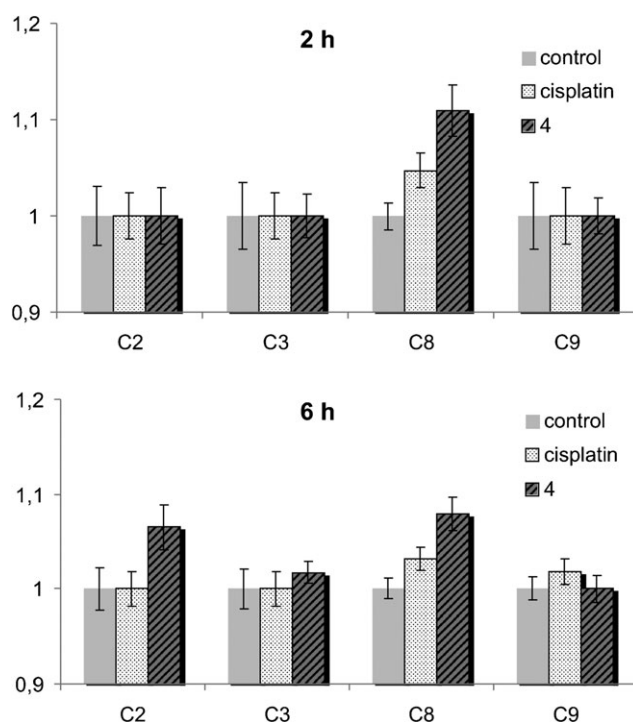
Table 3 IC₅₀ [μM] for the 96 h of action of investigated compounds and cisplatin on 8505C, A253, A549, A2780 and DLD-1 cells determined by SRB test

Compound	IC ₅₀ /μM				
	8505C	A253	A549	A2780	DLD-1
1–3	> 100	> 100	> 100	> 100	> 100
4	0.129 ± 0.004	0.093 ± 0.003	0.102 ± 0.004	0.121 ± 0.002	0.103 ± 0.004
5	0.179 ± 0.003	0.139 ± 0.005	0.152 ± 0.003	0.170 ± 0.002	0.165 ± 0.003
6	0.241 ± 0.058	0.238 ± 0.002	0.236 ± 0.011	0.130 ± 0.003	0.210 ± 0.006
cisplatin	5.02 ± 0.23	0.81 ± 0.02	1.51 ± 0.02	0.55 ± 0.03	5.14 ± 0.12

of **4** resulted in apoptotic cell death, in which floating cells showed the ability to exclude the blue dye (Fig. 4).

3.3.2.2 Effect of 4 on the caspase 2, 3, 8 and 9 activities. In order to gain insights into the induced apoptosis mechanism by the most active triphenyltin(IV) complex **4**, we analyzed whether caspases were involved as downstream effectors in the induced cell death. The upstream caspases 2, 8 and 9, and the downstream caspase 3 were used for the present study. DLD-1 colon carcinoma cell line was chosen for investigation of the activity of caspases 2, 3, 8 and 9. When treated with compound **4** for 2 h, only caspase 8 was found to be upregulated. Similarly to that, when cisplatin was used for the same time period also activation of only caspase 8 was observed (Fig. 5). The cells treated for 6 h with **4** show activation of caspase 2 and 8 (apoptosis activator) as well as caspase 3 (apoptosis executioner). On the other hand, treatment for 6 h with cisplatin showed activation of caspase 8 and 9 (apoptosis activators). As shown here, complex **4** is activating apoptosis faster than cisplatin within 6 h of action on DLD-1 cell line. Furthermore, complex **4** and cisplatin seem to express a different apoptosis pathway on DLD-1 cell line. In the case of cisplatin, apoptosis is triggered by both internal (intrinsic or mitochondrial pathway, caspase 9 dependent pathway) and external signals (extrinsic or death receptor pathway), while for triphenyltin(IV) complex **4** apoptosis is induced *via* extrinsic receptor pathway on DLD-1 cell line.

3.3.2.3 Cell cycle perturbations. Cell cycle perturbations were analyzed on colon carcinoma DLD-1 cell line. The cells were treated with IC₉₀ concentration of **4** for 24 h (Fig. 6). When compared to control, compound **4** caused almost no

**Fig. 4** Dye exclusion test (right) and DNA laddering (left) for DLD-1 cell line treated 24 h with **4**.**Fig. 5** Activity of caspases 2 (C2), 3 (C3), 8 (C8) and 9 (C9) on DLD-1 colon cancer cell line treated for 2 and 6 h with **4** and cisplatin.

changes S phases, however, a decrease at around 46 and 40% in the number of cells in G1 and G2/M phases, respectively, with an increase in the number of apoptotic cells (SubG1-peak), was observed. Those results indicate that apoptosis caused by **4** on colon carcinoma DLD-1 cell line may be due to disturbances caused in both G1 and G2/M phases in the cell cycle.

4. Conclusions and outlook

Novel triethylammonium salts of triphenyltin(IV) chloride carboxylate complexes have been synthesized and structurally characterized. The complexes were tested for *in vitro* antiproliferative activity against five cell lines of different histogenic origin. The triphenyltin(IV) complexes exhibited much higher cytotoxicity than cisplatin, up to 50 times (**4**). Although it seems that the active species of these mixtures beside complexes **4–6** may be SnPh₃⁺ cations, based on the stability studies carried out for these compounds in aqueous solutions. In addition, a positive influence in the final cytotoxicity of the tin(IV) complexes has been observed with the incorporation of

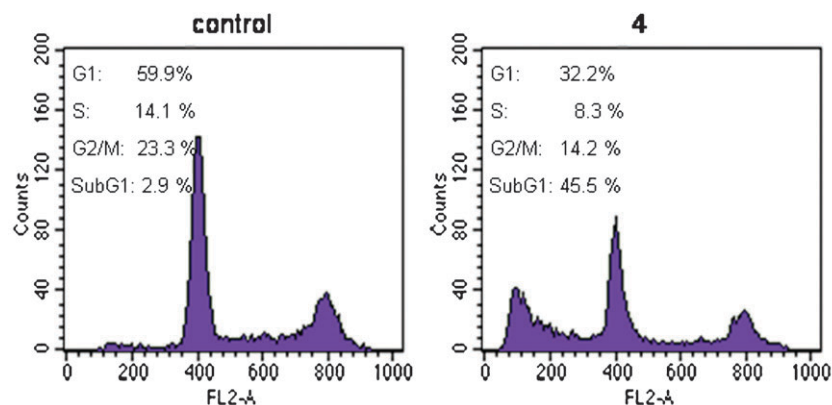


Fig. 6 Cell cycle analysis of DLD-1 cells untreated (control) and treated with the IC₉₀ concentration of **4** for 24 h.

biocompatible phthaloyl aminoacids as ligands when compared with other different carboxylato ligands.

Complex **4** seems to induce apoptosis *via* extrinsic or death receptor pathway. The presented data clearly demonstrate a cell-cycle dependence of triphenyltin(IV) compound **4** which induced cell death in DLD-1 cell line. Following compound **4** exposure, cells undergo G1 and G2/M arrest and apoptosis is finally induced in these phases of the cell cycle. Thus, while the phases affected by the tin compounds are G1 (when organelles are being synthesized resulting in a great amount of protein synthesis and a high metabolic rate in the cell) and G2/M (when the protein kinase plays a quite important role), the action mechanism of these compounds seem to be related either to the interaction of SnPh₃⁺ moieties with protein kinases and DNA, as previously reported for other neutral triphenyltin(IV) carboxylates,^{26,33} or to the possible binding to the phosphate groups in DNA,^{69–71} changing the intracellular metabolism of the phospholipids of the endoplasmic reticulum.^{72,73} However, further studies, already in progress in our laboratories, will try to clarify this fact.

Therefore, complex **4** seems to be a very promising candidate for further *in vivo* tests which will be carried in the near future.

Acknowledgements

We gratefully acknowledge financial support from the Ministerio de Educación y Ciencia, Spain (Grant no. CTQ2008-05892/BQU) the Universidad Rey Juan Carlos and Comunidad de Madrid (postdoctoral fellowship for S.G-R). We would also like to thank Ministerium für Wirtschaft und Arbeit des Landes Sachsen-Anhalt, Deutschland (Grant No. 6003368706) and BioSolutions Halle for cell culture facilities.

References

- R. H. Fish and G. Jaouen, *Organometallics*, 2003, **22**, 2166–2177.
- M. Nikolini, *Platinum and Other Coordination Compounds in Cancer Chemotherapy*, ed. Martinus-Nijhoff Publishing, Boston, MA, 1988.
- I. Ott and R. Gust, *Arch. Pharm.*, 2007, **340**, 117–126.
- M. A. Jakupec, M. Galanski, V. B. Arion, C. G. Hartinger and B. K. Keppler, *Dalton Trans.*, 2008, 183–194.
- M. Gielen, *Coord. Chem. Rev.*, 1996, **151**, 41–51.
- P. Yang and M. Guo, *Coord. Chem. Rev.*, 1999, **185–186**, 189–211.
- S. K. Hadjikakou and N. Hadjilias, *Coord. Chem. Rev.*, 2009, **253**, 235–249.
- K. Strohfeldt and M. Tacke, *Chem. Soc. Rev.*, 2008, **37**, 1174–1187.
- P. M. Abeysinghe and M. M. Harding, *Dalton Trans.*, 2007, 3474–3482.
- R. Gust, D. Posselt and K. Sommer, *J. Med. Chem.*, 2004, **47**, 5837–5846.
- C. G. Hartinger and P. J. Dyson, *Chem. Soc. Rev.*, 2009, **38**, 391–401.
- P. C. A. Bruijninx and P. J. Sadler, *Adv. Inorg. Chem.*, 2009, **61**, 1–62.
- P. C. A. Bruijninx and P. J. Sadler, *Curr. Opin. Chem. Biol.*, 2008, **12**, 197–206.
- Y. K. Yan, M. Melchart, A. Habtemariam and P. J. Sadler, *Chem. Commun.*, 2005, 4764–4776.
- L. Nagy, A. Szorcsik and K. Kovacs, *Pharm. Hungarica*, 2000, **70**, 53–71.
- M. Nath, S. Pokharia and R. Yadav, *Coord. Chem. Rev.*, 2001, **215**, 99–149.
- M. Gielen, *Tin-Based Antitumor Drugs; NATO ASI Ser., Ser. 2*, 1997, **26**, 445–455.
- D. De Vos, R. Willem, M. Gielen, K. E. Van Wingerden and K. Nooter, *Met.-Based Drugs*, 1998, **5**, 179–188.
- C. Pettinari, *Main Group Met. Chem.*, 1999, **22**, 661–692.
- S. P. Fricker, in *Metal Compounds in Cancer Therapy*, ed. Chapman & Hall, London, UK, 1994, pp. 147–179.
- M. Gielen, *Main Group Met. Chem.*, 1994, **17**, 1–8.
- M. G. Mirisola, A. Pellerito, T. Fiore, G. C. Stocco, A. Celli and I. Di Liegro, *Appl. Organomet. Chem.*, 1997, **11**, 499–511.
- M. Kemmer, M. Gielen, M. Biesemans, D. de Vos and R. Willem, *Met.-Based Drugs*, 1998, **5**, 189–196.
- A. K. Saxena and F. Huber, *Coord. Chem. Rev.*, 1989, **95**, 109–123.
- J. Susperregui, M. Bayle, G. Lain, C. Giroud, T. Baltz and G. Deleris, *Eur. J. Med. Chem.*, 1999, **34**, 617–623.
- L. Pellerito and L. Nagy, *Coord. Chem. Rev.*, 2002, **224**, 111–150 and references therein.
- M. Gielen and E. R. T. Tiekink, *Metallotherapeutic Drugs and Metal-Based Diagnostic Agents: The Use of Metals in Medicine*, ed. John Wiley & Sons, Ltd., 2005, p. 421.
- T. S. Basu Baul, W. Rynjah, E. Rivaola, A. Lycka, M. Holcapek, R. Jirasko, D. de Vos, R. J. Butcher and A. Linden, *J. Organomet. Chem.*, 2006, **691**, 4850–4862.
- L. Tian, Y. Sun, H. Li, X. Zheng, Y. Cheng, X. Liu and B. Qian, *J. Inorg. Biochem.*, 2005, **99**, 1646–1652.
- G. Han and P. Yang, *J. Inorg. Biochem.*, 2002, **91**, 230–236.
- S. Gómez-Ruiz, G. N. Kaluđerović, S. Prashar, E. Hey-Hawkins, A. Erić, Ž. Žižak and Z. D. Juranić, *J. Inorg. Biochem.*, 2008, **102**, 2087–2096.
- E. R. T. Tiekink, *Trends Organomet. Chem.*, 1994, **1**, 71–116.
- M. L. Falcioni, M. Pelli and R. Gabbianelli, *Mutat. Res., Genet. Toxicol. Environ. Mutagen.*, 2008, **653**, 57–62 and references therein.
- S. Gómez-Ruiz, G. N. Kaluđerović, D. Polo-Cerón, S. Prashar, M. Fajardo, Ž. Žižak, Z. D. Juranić and T. J. Sabo, *Inorg. Chem. Commun.*, 2007, **10**, 748–752.

- 35 S. Gómez-Ruiz, G. N. Kaluđerović, S. Prashar, D. Polo-Cerón, M. Fajardo, Ž. Žižak, T. J. Sabo and Z. D. Juranić, *J. Inorg. Biochem.*, 2008, **102**, 1558–1570.
- 36 M. E. Kelly, A. Dietrich, S. Gómez-Ruiz, B. Kalinowski, G. N. Kaluđerović, T. Müller, R. Paschke, J. Schmidt, D. Steinborn, C. Wagner and H. Schmidt, *Organometallics*, 2008, **27**, 4917–4927.
- 37 D. Pérez-Quintanilla, S. Gómez-Ruiz, Ž. Žižak, I. Sierra, S. Prashar, I. del Hierro, M. Fajardo, Z. D. Juranić and G. N. Kaluđerović, *Chem.–Eur. J.*, 2009, **15**, 5588–5597.
- 38 S. Gómez-Ruiz, B. Gallego, M. R. Kaluđerović, H. Kommera, E. Hey-Hawkins, R. Paschke and G. N. Kaluđerović, *J. Organomet. Chem.*, 2009, **694**, 2191–2197.
- 39 S. Gómez-Ruiz, B. Gallego, Ž. Žižak, E. Hey-Hawkins, Z. D. Juranić and G. N. Kaluđerović, *Polyhedron*, 2010, **29**, 354–360.
- 40 S. Gómez-Ruiz, S. Prashar, T. Walther, M. Fajardo, D. Steinborn, R. Paschke and G. N. Kaluđerović, *Polyhedron*, 2010, **29**, 16–23.
- 41 M. R. Kaluđerović, S. Gómez-Ruiz, B. Gallego, E. Hey-Hawkins, R. Paschke and G. N. Kaluđerović, *Eur. J. Med. Chem.*, 2010, **45**, 519–525.
- 42 G. N. Kaluđerović, D. Pérez-Quintanilla, I. Sierra, S. Prashar, I. del Hierro, Ž. Žižak, Z. D. Juranić, M. Fajardo and S. Gómez-Ruiz, *J. Mater. Chem.*, 2010, **20**, 806–814.
- 43 G. N. Kaluđerović, D. Pérez-Quintanilla, Ž. Žižak, Z. D. Juranić and S. Gómez-Ruiz, *Dalton Trans.*, 2010, **39**, 2597.
- 44 M. Ashfaq, *J. Organomet. Chem.*, 2006, **691**, 1803–1808.
- 45 S. Verma, A. Joshi, R. B. Gaur and R. R. Sharma, *Main Group Met. Chem.*, 2005, **28**, 185–192.
- 46 M. K. Lo and S. W. Ng, *Main Group Met. Chem.*, 2000, **23**, 733–734.
- 47 S. W. Ng and V. G. Kumar Das, *Acta Crystallogr., Sect. C: Cryst. Struct. Commun.*, 1997, **53**, 546–548.
- 48 S. W. Ng, A. J. Kuthubutheen, V. G. Kumar Das, A. Linden and E. R. T. Tiekink, *Appl. Organomet. Chem.*, 1994, **8**, 37–42.
- 49 N. W. Ahmad, S. A. Mohd, S. Balabaskaran and V. G. K. Das, *Appl. Organomet. Chem.*, 1993, **7**, 583–591.
- 50 V. I. Shcherbakov, E. F. Ivanov, S. Y. Khorshev, M. S. Feldman, E. B. Kopytov and T. N. Konkina, *Synth. React. Inorg., Met.-Org., Nano-Met. Chem.*, 1991, **21**, 1549–1567.
- 51 S. W. Ng, C. Wei, V. G. K. Das, R. J. Wang and T. C. W. Mak, *J. Crystallogr. Spectrosc. Res.*, 1991, **21**, 375–377.
- 52 V. I. Shcherbakov, I. P. Malysheva, O. N. Druzhkova and T. N. Chulkova, *J. Organomet. Chem.*, 1991, **407**, 181–189.
- 53 C. Syng-Ai, T. S. Basu Baul and A. Chatterjee, *J. Environ. Pathol. Toxicol. Oncol.*, 2001, **20**, 333–342.
- 54 F. Barbieri, M. Viale, F. Sparatore, G. Schettini, A. Favre, C. Bruzzo, F. Novelli and A. Alema, *Anti-Cancer Drugs*, 2002, **13**, 599–604.
- 55 H. Seibert, S. Moerchel and M. Guelden, *Cell Biol. Toxicol.*, 2004, **20**, 273–283.
- 56 N. Hoti, J. Ma, S. Tabassum, Y. Wang and M. Wu, *J. Biochem.*, 2003, **134**, 521–528.
- 57 SCALE3 ABSPACK: Empirical absorption correction, *CrysAlis—Software package*, Oxford Diffraction Ltd., 2006.
- 58 G. M. Sheldrick, *SHELXS-97, Program for Crystal Structure Solution*, Göttingen, 1997.
- 59 G. M. Sheldrick, *SHELXL-97, Program for the Refinement of Crystal Structures*, Göttingen, 1997.
- 60 P. Skehan, R. Storeng, D. Scudiero, A. Monks, J. McMahon, D. Vistica, J. T. Warren, H. Bokesch, S. Kenney and M. R. Boyd, *J. Natl. Cancer Inst.*, 1990, **82**, 1107–1112.
- 61 A. Dietrich, T. Mueller, R. Paschke, B. Kalinowski, T. Behlendorf, F. Reipsch, A. Fruehauf, H. J. Schmoll, C. Kloft and W. Voigt, *J. Med. Chem.*, 2008, **51**, 5413–5422.
- 62 G. B. Deacon and R. J. Philips, *Coord. Chem. Rev.*, 1980, **33**, 227–250.
- 63 O. Knop, T. S. Cameron, M. A. James and M. Falk, *Can. J. Chem.*, 1981, **59**, 2550–2555.
- 64 M. C. Carcelli, C. Ferrari, C. Pelizzi, G. Pelizzi and G. Predieri, *J. Chem. Soc., Dalton Trans.*, 1992, 2127–2128.
- 65 M. Suzuki, I. H. Son and R. Noyori, *Organometallics*, 1990, **9**, 3043–3053.
- 66 D. Dakternieks, T. S. Basu Baul, S. Duta and E. R. T. Tiekink, *Organometallics*, 1998, **17**, 3058–3062.
- 67 J. P. Charland, F. L. Lee, E. J. Gabe, L. E. Khoo and F. E. Smith, *Inorg. Chim. Acta*, 1987, **130**, 55–60.
- 68 E. J. Gabe, F. L. Lee, L. E. Khoo and F. E. Smith, *Inorg. Chim. Acta*, 1985, **105**, 103–106.
- 69 Q. Li, N. Jin, P. Yang, J. Wan, W. Wu and J. Wan, *Synth. React. Inorg., Met.-Org., Nano-Met. Chem.*, 1997, **27**, 811–823.
- 70 Q. Li, P. Yang, H. Wang and M. Guo, *J. Inorg. Biochem.*, 1996, **64**, 181–195.
- 71 J. S. Casas, E. E. Castellano, M. D. Couce, J. Ellena, A. Sanchez, J. L. Sanchez, J. Sordo and C. Taboada, *Inorg. Chem.*, 2004, **43**, 1957–1963.
- 72 Y. Arakawa, *Biomed. Res. Trace Elem.*, 1993, **4**, 129–130.
- 73 Y. Arakawa, *Biomed. Res. Trace Elem.*, 2000, **11**, 259–286.



Original article

Liposomes as vehicles for water insoluble platinum-based potential drug: 2-(4-(Tetrahydro-2H-pyran-2-yloxy)-undecyl)-propane-1,3-diamminedichloroplatinum(II)

Goran N. Kaluderović^{a,b,*}, Andrea Dietrich^c, Harish Kommera^a, Judith Kuntsche^d, Karsten Mäder^d, Thomas Mueller^c, Reinhard Paschke^a

^a Biozentrum, Martin-Luther-Universität Halle-Wittenberg, Weinbergweg 22, D-06120 Halle, Germany

^b Institut für Chemie, Martin-Luther-Universität Halle-Wittenberg, Kurt-Mothes-Straße 2, D-06120 Halle, Germany

^c Department of Internal Medicine IV, Oncology/Hematology, Research Laboratory, Martin-Luther-Universität Halle-Wittenberg, Ernst-Grube-Straße 40, D-06120 Halle, Germany

^d Institute of Pharmacy, Martin-Luther-Universität Halle-Wittenberg, Wolfgang-Langenbeck Str. 4, D-06120 Halle, Germany

ARTICLE INFO

Article history:

Received 11 October 2011

Received in revised form

23 April 2012

Accepted 4 June 2012

Available online 13 June 2012

Keywords:

Cisplatin

Platinum(II) complexes

Liposomes

Antitumoral activity

Selectivity

ABSTRACT

Formulation of liposome delivery system loaded with water insoluble 2-(4-(tetrahydro-2H-pyran-2-yloxy)-undecyl)-propane-1,3-diamminedichloroplatinum(II), LipoTHP-C11 was carried out. The particle size distributions were determined by dynamic light scattering and asymmetrical flow field-flow fractionation indicating size of around 120 nm. Stability study showed that LipoTHP-C11 was stable at 4 °C for more than two months. To test suitability of chosen formulation, LipoTHP-C11 was investigated against several tumor cell lines: H12.1, 1411HP, 518A2, A549, HT-29, MCF-7 and SW1736. Furthermore, toxicity against normal fibroblasts was examined. LipoTHP-C11 may be used as an attractive candidate for further assessment *in vivo* as antitumor agent.

© 2012 Elsevier Masson SAS. All rights reserved.

1. Introduction

In last few decades development of platinum based drugs gave some promising candidates for the treatment of different cancer types [1–6]. The well known drugs cisplatin and several other (e.g. carboplatin and oxaliplatin) are the few of thousands platinum compounds that are in clinical use [7–10]. The criteria for selecting promising candidates to be evaluated in clinical trials are favorable physicochemical properties such as solubility and stability and possible therapeutic advantages in comparison to cisplatin, derived from preclinical studies (high efficacy, favorable spectrum of activity, high therapeutic index and low toxicity). The solubility problem could be overcome by structural modification of the platinum complex or including platinum complex in some carrier system [11–17]. In contrast to structural modification, the inclusion of platinum based drugs in lipid based micelles, liposomes and

hydrocolloids have received, until now, far less attention [18,19]. Although, investigations regarding incorporation poorly water soluble platinum compounds into water compartment of liposomes are known in literature (cisplatin, oxaliplatin; Fig. 1) [20–22], but for water insoluble platinum based drugs up to our knowledge there are no reports. It is well known that structural modification may lead to the deactivation of antitumoral activity of compounds [23,24]. Such deactivation was observed also in the case of 2-(4-(tetrahydro-2H-pyran-2-yloxy)-undecyl)-propane-1,3-diamminedichloroplatinum(II) complex (THP-C11) – potent antitumor compound able to overcome cisplatin resistance in several tumor cell lines [25]. Namely, compounds with a shorter spacer between THP and cisplatin fragment (eg. THP-C4) are less active.

Herein, formulation of a novel liposome delivery system, loaded with water insoluble THP-C11 compound is reported (Fig. 1). The main reason using liposomes was to get an aqueous stable formulation of the drug, thus solubilization of THP-C11 in water. It is shown on one sample of platinum complexes with excellent antitumoral properties idea how to overcome insolubility problem. The principle can be adapted and equally well used with other insoluble metal complexes exhibiting antitumoral activity.

* Corresponding author. Biozentrum, Martin-Luther-Universität Halle-Wittenberg, Weinbergweg 22, D-06120 Halle, Germany. Tel.: +49 345 5525678, +381 11 3336735; fax: +49 345 5527028, +381 11 636061.

E-mail addresses: goran.kaluderovic@chemie.uni-halle.de, goran@chem.bg.ac.rs (G.N. Kaluderović).

Appendix 12

Reproduced from Ref. G.N. Kaluđerović, A. Dietrich, H. Kommera, J. Kuntsche, K. Mäder, T. Muller, R. Paschke, *Europ. J. Med. Chem.* 2012, 54, 567 with permission from Elsevier Masson SAS.

568

G.N. Kaluđerović et al. / *European Journal of Medicinal Chemistry* 54 (2012) 567–572

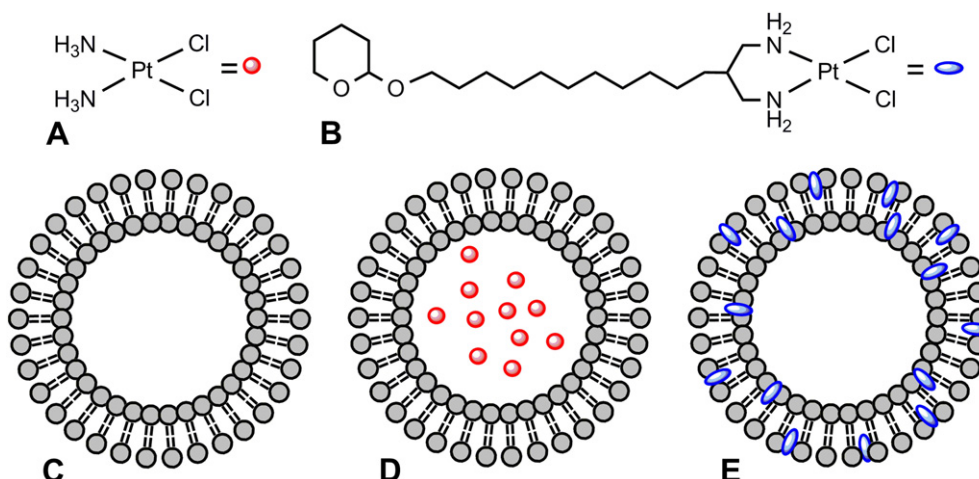


Fig. 1. Cisplatin (A), THP–C11 (B), empty (C) and loaded liposomes (lipoplatin, D; LipoTHP–C11, E).

2. Results and discussion

2.1. Formulation and characterization of the liposomes

The synthesis of THP–C11 was performed as described in literature [25]. Liposomes were composed of purified soybean lecithin S75 and active liposomes (LipoTHP–C11), in which THP–C11 was incorporated into the liposomal structures, and empty liposomes were formulated. The liposomes were formulated by the lipid film method followed by hydration [27]. Following hydration, the liposomes were successfully extruded through a polycarbonate membrane with a pore size of 400 and 100 nm. Both formulations were macroscopically homogeneous after extrusion. Formulations have been checked in a light microscope and relieved no presence of larger particles neither drug precipitate. The concentration THP–C11 in LipoTHP–C11 formulation was determined to be 4.75 mM (95% of the drug included in liposomes). As lipophilic compound, the drug should be situated in the liposome bilayer and not in the (aqueous) core.

Mean particle size was estimated by dynamic light scattering and the data of the stepwise extrusion through 400 and 100 nm membranes are shown in Table 1. After extrusion of LipoTHP–C11 through 100 nm a comparable size to unloaded liposomes was observed, but with a larger PDI which indicates broader size distribution in drug-loaded formulations. Comparison between three batches indicates a good agreement for formulations extruded through 100 nm.

To get more information about size distribution samples were measured on asymmetrical flow field-flow fractionation (AF4)

system coupled with a MALLS instrument (Table 1). Size/size distribution have been determined by the light scattering data. In size distributions, fractions of vesicles with larger size are clearly visible in both batches of drug-loaded liposomes.

In order to provide stable liposomal formulations in which liposomes are distributed uniformly and their structure is preserved, a storage stability study was performed. LipoTHP–C11 and empty liposomes were kept for 2 months at 4 °C. During storage, the size distribution and the mean diameter of the liposomes by dynamic light scattering were determined. Results presented in Fig. 2 demonstrate preservation of the original size distribution of LipoTHP–C11 (100 nm) and empty liposomes. The mean diameter of LipoTHP–C11 (100 nm) was 123 nm (immediately after extrusion). After 2 months of storage, the mean diameter changed to 117 nm for LipoTHP–C11 (100 nm) but the distribution remained almost unchanged. On the other hand storage over 2 months of the LipoTHP–C11 (400 nm) showed that the percentage of smaller liposomes increased in number (Fig. 2). In addition, with light microscopy no presence of drug precipitate over 2 months period was observed. Results of PCS and AF4/MALLS cannot be directly compared (e.g. different measurement principles, data analysis etc.). Worth to note that even by using different instruments (PCS) rather large differences in size can be obtained [26,27].

2.2. Cytotoxicity testings of LipoTHP–C11

Because of very promising *in vitro* antitumoral results of THP–C11, against testicular germ cell tumors (TGCT), as a next step and before *in vivo* activity in a nude mouse model, liposomal

Table 1
PCS and A4F size results of three batches of liposomes.

Code ^a	Batch	PCS ^b		A4F ^c			
		Z-average (nm)	PDI	D10 (nm)	D50 (nm)	Mean (nm)	D90 (nm)
Liposome (100)	a	118 ± 1	0.09 ± 0.03	77.3 ± 1.1	97.5 ± 0.8	111.7 ± 1.5	123.8 ± 0.7
	b	116 ± 5	0.11 ± 0.02	81.2 ± 0.4	110.8 ± 0.3	145.0 ± 1.3	143.4 ± 0.3
	c	119 ± 3	0.10 ± 0.02	nd			
LipoTHP–C11 (400)	a	163 ± 1	0.27 ± 0.01				
	b	197 ± 2	0.33 ± 0.05				
	c	187 ± 3	0.35 ± 0.06				
LipoTHP–C11 (100)	a	123 ± 2	0.23 ± 0.01	67.3 ± 0.6	113.6 ± 0.4	283.6 ± 3.3	240.8 ± 2.6
	b	126 ± 1	0.27 ± 0.01	59.8 ± 1.7	107.6 ± 2.6	290.5 ± 0.2	229.3 ± 3.5
	c	125 ± 2	0.28 ± 0.01	nd			

^a Formulation code: Liposome (100) = plain liposomes extruded through a 100 nm membrane; LipoTHP–C11 (400) and LipoTHP–C11 (100) = drug-loaded liposomes extruded through only a 400 nm and through both a 400 and 100 nm membrane, respectively.

^b Measured after preparation.

^c Measured about 2 months (batch a) or 3 weeks (batch b and c) after preparation.

Appendix 12

Reproduced from Ref. G.N. Kaluđerović, A. Dietrich, H. Kommera, J. Kuntsche, K. Mäder, T. Muller, R. Paschke, *Europ. J. Med. Chem.* 2012, 54, 567 with permission from Elsevier Masson SAS.

G.N. Kaluđerović et al. / *European Journal of Medicinal Chemistry* 54 (2012) 567–572

569

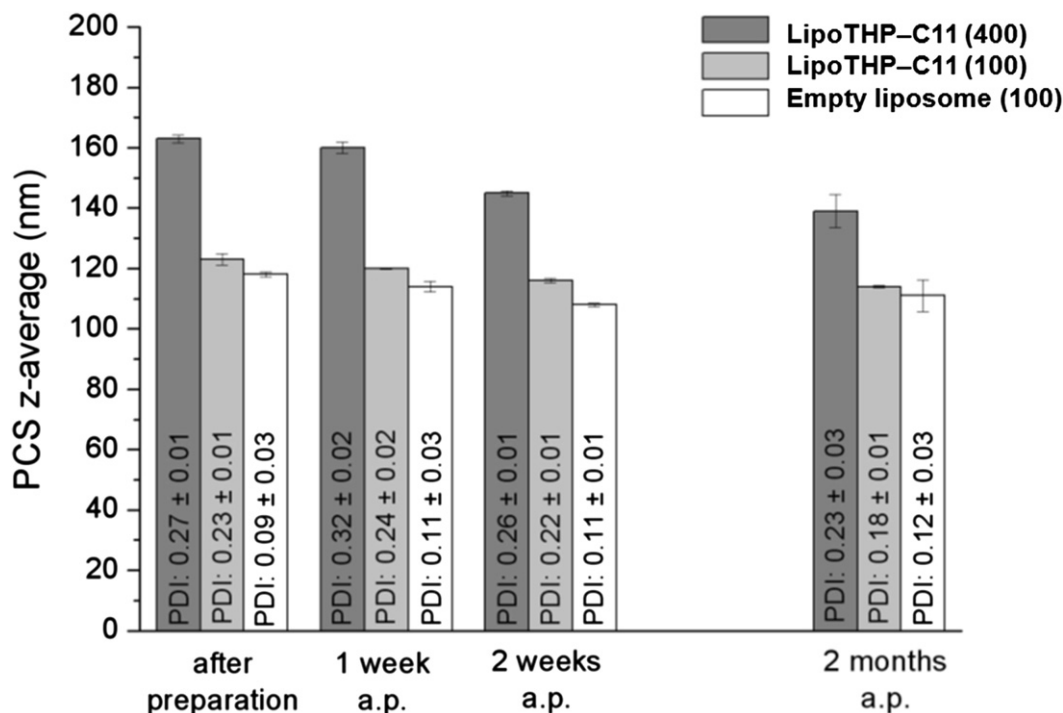


Fig. 2. PCS z-averages and polydispersity indices of the different formulations (Batch a) over a storage time of 2 months. Results are given as averages of 3 repeated measurements.

formulation has been carried out. The motivation for liposomal formulation will be shortly explained. THP-C11 is soluble in chloroform and dimethyl formamide (DMF), but not soluble in water and because of that not suitable for *in vivo* experiments. On the other hand, structural variations (search for analog compound soluble in water) led to *in vitro* deactivation of the THP-C11 [25].

The formed liposomes have a particle size of around 120 nm and are stable for more than two months at 4 °C. Empty liposomes were tested in order to evaluate its influence on the final cytotoxicity of LipoTHP-C11. Cisplatin and THP-C11 were used for comparison. As shown in our previous paper THP-C11 is able to overcome cisplatin resistance in TGCT cells and at first, the antiproliferative activity was tested against cisplatin sensitive H12.1 and cisplatin resistant 1411HP TGCT cell lines.

Liposomes alone are not toxic after 2 and 6 h of action in investigated concentration range against selected TGCT cells (Table 2). Following 96 h of treatment liposomes are also found to show low toxicity. After 2 h of action LipoTHP-C11 formulation has been found to exhibit higher cytotoxicity in both cisplatin sensitive and resistant TGCT cells than cisplatin, namely 1.5 and 9.0 times lower concentration is needed for 50% inhibition of the cell growth on H12.1 and 1411HP, respectively. On the other hand liposomal formulation of THP-C11 is less active up to 96 h than drug dissolved in DMF. At 96 h of treatment THP-C11 is 2.4 (1411HP) and 3.1 times

(H12.1) more active than LipoTHP-C11, but LipoTHP-C11 expressed higher cytotoxicity than cisplatin on cisplatin resistant 1411HP TGCT cells. The lower activity of liposomal formulation in comparison to that of THP-C11 (DMF) can be caused by many effects and one reasonable might be slow release of the drug from liposomes.

Furthermore, the liposomal formulations and platinum(II) complexes have been tested against cell lines from different tumor entities: 518A2 (melanoma), A549 (lung carcinoma), HT-29 (human colonic adenocarcinoma), MCF-7 (human breast adenocarcinoma) and SW1736 (human anaplastic thyroid carcinoma). The results are presented in Table 3. Empty liposomes were found to be not active. THP-C11 showed better activity than cisplatin against MCF-7 and SW1736, comparable against 518A2 and A549, but lower on colonic adenocarcinoma HT-29. LipoTHP-C11 expressed similar *in vitro* antiproliferative activity as THP-C11 on A549 and SW1736. In case on other cell lines (518A2, HT-29 and MCF-7) LipoTHP-C11 was found to be less active. Compared to cisplatin, LipoTHP-C11 exhibited similar activity against A549 and MCF-7, but lower on 518A2 and HT-29 cell lines. Outstandingly, LipoTHP-C11 was found to be 2.9 times more active than cisplatin on anaplastic thyroid carcinoma SW1736.

Beside cytotoxicity on several tumor cell lines, herein is reported activity of formulations as well as THP-C11 and cisplatin on fibroblast normal cells (NF). Toxicity after 96 h treatment with

Table 2

IC₅₀ [μM or pcm]^a for the 2, 6 and 96 h of action of investigated drugs and liposomes on H12.1 and 1411HP TGCT cell lines determined by SRB assay.

Compound/ Formulation	1411HP			H12.1			
	2 h	6 h	96 h	2 h	6 h	6 h	96 h
THP-C11	1.12 ± 0.02	0.94 ± 0.12	0.88 ± 0.03	1.39 ± 0.10	1.10 ± 0.07	1.02 ± 0.13	
LipoTHP-C11	3.50 ± 0.36 (4.4) ^b	2.27 ± 0.06 (2.9)	2.14 ± 0.04 (2.7)	5.03 ± 0.49 (6.3) ^b	3.17 ± 0.27 (4.0)	3.15 ± 0.21 (4.0)	
Liposome	> 120 ^b	> 120	87.2 ± 4.4	> 120 ^b	> 120	44.0 ± 5.6	
cisplatin	31.7 ± 2.9	–	2.8 ± 0.4	7.7 ± 1.6	–	0.8 ± 0.1	

^a Given are values for THP-C11 in μM and for liposomes in pcm (per cent mille).

^b 95 μM LipoTHP-C11 ↔ 120 pcm liposome.

Appendix 12

Reproduced from Ref. G.N. Kaluderović, A. Dietrich, H. Kommera, J. Kuntsche, K. Mäder, T. Muller, R. Paschke, *Europ. J. Med. Chem.* 2012, 54, 567 with permission from Elsevier Masson SAS.

570

G.N. Kaluderović et al. / *European Journal of Medicinal Chemistry* 54 (2012) 567–572

Table 3

IC₅₀ [μM or pcm]^a for the 96 h of action of investigated drugs and liposome on 518A2, A549, HT-29, MCF-7 and SW1736 determined by SRB assay.

Compound/ Formulation	518A2	A549	HT-29	MCF-7	SW1736
THP–C11	1.31 ± 0.08	1.32 ± 0.20	1.16 ± 0.19	0.53 ± 0.01	1.18 ± 0.04
LipoTHP–C11	2.37 ± 0.41	1.45 ± 0.15	2.48 ± 0.03	2.02 ± 0.95	1.11 ± 0.07
Liposome	> 120 ^b	> 120	> 120	> 120	> 120
cisplatin	1.52 ± 0.19	1.51 ± 0.15	0.63 ± 0.03	2.03 ± 0.11	3.20 ± 0.24

^a Given are values for THP–C11 in μM and for liposomes in pcm (per cent mille).

^b 95 μM LipoTHP–C11 ↔ 120 pcm liposome.

Table 4

Selectivity index.

Compound/ Formulation	IC ₅₀ (NF)/IC ₅₀ (cell line)						
	1411HP	H12.1	518A2	A549	HT-29	MCF-7	SW1736
THP–C11	2.43 ± 0.33	2.10 ± 0.51	1.63 ± 0.24	1.63 ± 0.33	1.84 ± 0.39	4.04 ± 0.53	1.81 ± 0.25
LipoTHP–C11	1.45 ± 0.35	1.04 ± 0.24	1.26 ± 0.36	2.06 ± 0.52	1.21 ± 0.28	1.48 ± 0.34	2.70 ± 0.64
Cisplatin	0.63 ± 0.09	2.21 ± 0.11	1.18 ± 0.16	1.18 ± 0.12	2.95 ± 0.18	0.89 ± 0.06	0.55 ± 0.05

LipoTHP–C11 and platinum(II) complexes has been evaluated (IC₅₀: 2.14 ± 0.28, THP–C11; 3.29 ± 0.75, LipoTHP–C11; 1.77 ± 0.06 μM, cisplatin) and in Table 4 selectivity indices of the investigated compounds/formulation are presented. Cisplatin expressed higher selectivity than LipoTHP–C11 and THP–C11 on cisplatin resistant 1411HP and cisplatin sensitive HT-29 cell lines. Both liposomal formulation and THP–C11 possesses higher selectivity than cisplatin on other tumor cell lines than to fibroblasts (exception 518A2: LipoTHP–C11 and cisplatin comparable selectivity). The highest selectivity was found between SW1736 and fibroblast with both LipoTHP–C11 and THP–C11. On the other hand, cisplatin showed higher tendency to kill normal than SW1736 tumor cells. With cytotoxicity testings is shown that it is likely that water insoluble drugs may be released *in vitro*, namely transfer of lipophilic drugs between liposomal membranes and biological interfaces might occur [28].

3. Conclusions

Herein, the formulation of new liposomes loaded with very promising antitumoral compound against TGCT cells has been described. The LipoTHP–C11 was characterized by light microscopy, dynamic light scattering and asymmetrical flow field-flow fractionation. The particle sizes of LipoTHP–C11 were found to be around 120 nm. Liposomal formulation of THP–C11 was stable at 4 °C for more than two months. Cytotoxicity was investigated on seven tumor cell lines (H12.1, 1411HP, 518A2, A549, HT-29, MCF-7 and SW1736) and toxicity against normal fibroblasts. LipoTHP–C11 was found to be more effective than cisplatin against cisplatin resistant TGCT 1411HP and anaplastic thyroid carcinoma SW1736 cell lines. The highest selectivity was found between SW1736 and fibroblast with both LipoTHP–C11 and THP–C11, where cisplatin showed higher tendency to kill normal than SW1736 tumor cells. Results from this study indicates that the promising water insoluble compound THP–C11 with potent antitumor activity may be used as liposomal formulation and in this form is an attractive candidate for further assessment *in vivo* as antitumor agent.

4. Experimental

4.1. Material and methods

THP–C11 was prepared by the method described in literature. ¹H and ¹³C NMR (Varian Gemini 400 MHz) were used for structure confirmation. Lipoid S75 was obtained as kind gift from Lipoid

GmbH Ludwigshafen, Germany. Polycarbonate membranes with 400 and 100 nm were obtained from Avestin, Mannheim, Germany.

4.1.1. Preparation of the liposomes

Liposomes were prepared by conventional well established lipid film method followed by extrusion [29]. 300 mg lecithin (Lipoid S75) were accurately weighted into a round bottom flask and dissolved in 5 ml of chloroform and 15 ml of a solution of THP–C11 (1 mg/ml) in chloroform was added. After gentle shaking to assure homogeneity of the solution, the organic solvent was evaporated under reduced pressure under constant rotation over 1 h and room temperature and for additional 1 h at 50 °C. The dry lipid film containing the drug was dispersed in 5 ml of distilled water by manual shaking until all of the film completely hydrated. Afterwards the crude suspensions were extruded through polycarbonate membranes with 400 and 100 nm pore size 21-times each with a Liposofast Basic Extruder (Avestin, D-Mannheim). After extrusion, liposomes were filled into plastic tubes (Eppendorf) and stored at 4 °C. Liposomes without the drug were prepared for comparison. For all formulations, three independent liposomes batches were prepared.

4.1.2. Determination of platinum concentration in LipoTHP–C11

The platinum content in LipoTHP–C11 was determined by inductively coupled plasma optical emission spectrometry at 214.4 and 203.6 nm (Wessling Laboratorien GmbH, Umweltanalytik Oppin, Germany).

4.1.3. Light microscopy

Selected formulations were frequently examined under a light microscope (DMRXP, Leica, D-Wetzlar) with crossed polarizers and a λ-sheet as well as in the differential interference contrast mode with 100- to 1000-fold magnification for the presence of larger aggregates and drug precipitates.

4.1.4. Size determinations

Photon Correlation Spectroscopy (PCS): Dynamic light scattering was measured with an HPPS instrument (Malvern) at 25 °C in back scattering mode (173°) and at fixed measurement position in the middle of the cuvette. Prior measurements, liposomes were appropriately diluted with filtered (Rotilabo Syringe Filter, regenerated cellulose, pore size 0.2 μm, Carl Roth GmbH & Co., D-Karlsruhe) purified water resulting in a laser attenuation of 7. Each sample was measured 3 times with 10–15 runs over 10 s each. Z-average diameters and the polydispersity indices were determined

using the instruments cumulant analysis software (Dispersion Technology Software version 4.20, Malvern Instr.) assuming a sample viscosity of 0.890 mPa s.

Asymmetrical flow field-flow fractionation (A4F): Samples were analyzed by an Eclipse A4F separation system (Wyatt Technology Europe, D-Dernbach) coupled with a multi-angle laser light scattering detector (DAWN EOS, Wyatt) as described earlier [30]. The separation channel was equipped with a trapezoidal-shaped spacer (Wyatt, height 350 μm , length 265 mm, largest width 21 mm) and a membrane of regenerated cellulose (MWCO 5 kDa, Microdyn-Nadir, D-Wiesbaden) served as accumulation wall. Bi-distilled and filtered (pore size 0.1 μm , VVLP, Millipore) water preserved with 0.02% w/v sodium azide (Fluka/Sigma) was used as eluent and for sample dilution. 100 μl of the diluted liposome suspension (1:50 v/v) were injected (injection flow 0.2 ml/min) into the channel during focusing (focus flow 2 ml/min) over 2 min. After further focusing for 1 min the samples were eluted with a constant detector flow rate of 1 ml/min. A high cross flow gradient of 0.30 ml/min (cross flow decreased from 2.0 to 0.5 ml/min within 5 min) was used in the beginning of elution to assure baseline separation of the liposomes from the void peak. The liposomes were then eluted with a cross flow decreasing from 0.5 ml/min to 0 ml/min over 40 min. Data analysis was done by the Astra software 4.90 using the particle mode and assuming hollow spheres. The RMS (root mean square) radius (being equal to the geometric radius for hollow spheres [31]) at each elution time was calculated applying the Rayleigh-Gans-Debye (RGD) approximation [32]. Size results are given as mean diameters (calculated from the mass weighted RMS radii determined over the defined peak areas) and mass weighted size distributions were calculated using the binning method (sigma spread factor of 20 [32]). The error of the RMS radii calculated by MALLS over the peak areas was $\leq 5\%$ in all measurements.

4.2. In vitro study

4.2.1. Preparation of drug solutions

Stock solutions of THP-C11 and cisplatin were prepared in dimethyl formamide (DMF, Sigma Aldrich) at a concentration of 20 mM, filtered through Millipore filter, 0.22 μm , before use, and diluted by nutrient medium to various working concentrations. Empty (6%) and loaded liposomes ($c_{\text{THP-C11}} = 4.75 \text{ mM}$) were used as prepared and diluted by nutrient medium to various working concentrations. Nutrient medium was RPMI-1640 (PAA Laboratories) supplemented with 10% fetal bovine serum (Biochrom AG) and penicillin/streptomycin (PAA Laboratories).

4.2.2. Cell lines and culture conditions

The malignant cell lines 518A2 (melanoma), A549 (lung carcinoma), HT-29 (colonic adenocarcinoma), MCF-7 (breast adenocarcinoma), SW1736 (anaplastic thyroid carcinoma), cisplatin sensitive H12.1 and cisplatin resistant 1411HP (testicular germ tumor) as well as normal fibroblasts were included in this study. Cultures were maintained as monolayer in RPMI 1640 (PAA Laboratories, Pasching, Germany) supplemented with 10% heat inactivated fetal bovine serum (Biochrom AG, Berlin, Germany) and penicillin/streptomycin (PAA Laboratories) at 37 °C in a humidified atmosphere of 5% (v/v) CO₂.

4.2.3. Cytotoxicity assay

The cytotoxic activities of the compounds were evaluated using the sulforhodamine-B (SRB, Sigma Aldrich) microculture colorimetric assay [33]. In short, exponentially growing cells were seeded into 96-well plates on day 0 at the appropriate cell densities to prevent confluence of the cells during the period of experiment. After 24 h, the cells were treated with serial dilutions of the studied compounds for 96 h or 2, 6 and 96 h in case of 1411HP and H12.1 cell

lines. Each concentration was tested in triplicates on each cell line. The final concentration of DMF solvent never exceeded 0.5%, which was non-toxic to the cells. The percentages of surviving cells relative to untreated controls were determined 96 h after the beginning of drug exposure. After 96 h treatment, the supernatant medium from the 96 well plates was thrown away and the cells were fixed with 10% TCA. For a thorough fixation plates were then allowed to stand at 4 °C. After fixation the cells were washed in a strip washer. The washing was carried out four times with water using alternate dispensing and aspiration procedures. The plates were then dyed with 100 μl of 0.4% SRB for about 45 min. After dyeing the plates were again washed to remove the dye with 1% acetic acid and allowed to air dry overnight. 100 μl of 10 mM Tris base solutions were added to each well of the plate and absorbance was measured at 570 nm using a 96 well plate reader (Tecan Spectra, Crailsheim, Germany). The IC₅₀ value, defined as the concentrations of the compound at which 50% cell inhibition was observed, was estimated from the dose–response curves.

Acknowledgments

We gratefully acknowledge financial support from Ministerium für Wirtschaft und Arbeit des Landes Sachsen-Anhalt, Deutschland (Grant No. 6003368706) and BioSolutions Halle GmbH for cell culture facilities.

References

- [1] T.W. Hambley, A.R. Battle, G.B. Deacon, E.T. Lawrenz, G.D. Fallon, B.M. Gatehouse, L.K. Webster, S. Rainone, *J. Inorg. Biochem.* 77 (1999) 3–12.
- [2] S. Arandelović, Z.L. Tešić, S.S. Radulović, *Med. Chem. Rev.* 2 (2005) 415–422.
- [3] L. Kelland, *Nat. Rev. Cancer* 7 (2007) 573–584.
- [4] R. Paschke, J. Kalbitz, C. Paetz, M. Luckner, T. Mueller, H.J. Schmoll, H. Mueller, E. Sorkau, E. Sinn, *J. Inorg. Biochem.* 94 (2003) 335–342.
- [5] T. Servidei, C. Ferlini, A. Riccardi, D. Meco, G. Scambia, G. Segni, C. Manzotti, R. Riccardi, *Europ. J. Cancer* 37 (1990) 930–938.
- [6] G.N. Kaluderović, R. Paschke, *Curr. Med. Chem.* 18 (2011) 4738–4752.
- [7] G. Natile, M. Coluccia, *Coord. Chem. Rev.* 216–217 (2001) 383–410.
- [8] T. Boulikas, M. Vougiouka, *Oncol. Rep.* 10 (2003) 1663–1682.
- [9] J. Zhang, D. Liu, Y. Li, J. Sun, L. Wang, A. Zang, *Mini Rev. Med. Chem.* 9 (2009) 1357–1366.
- [10] J.T. Hartmann, H.P. Lipp, *Expert Opin. Pharmacother.* 4 (2003) 889–901.
- [11] V.K. Yellepeddi, A. Kumar, D.M. Maher, S.C. Chauhan, K.K. Vangara, S. Palakurthi, *Anticancer Res.* 31 (2011) 897–906.
- [12] I. Ali, U. Rahis, K. Salim, M.A. Rather, W.A. Wani, A. Haque, *Curr. Cancer Drug Targets* 11 (2011) 135–146.
- [13] A. Kowalczyk, E. Stoyanova, V. Mitova, P. Shestakova, G. Momekov, D. Momekova, N. Koseva, *Int. J. Pharm.* 404 (2011) 220–230.
- [14] I. Winer, S. Wang, Y.E. Lee, W. Fan, Y. Gong, D. Burgos-Ojeda, G. Spahlinger, R. Kopelman, R.J. Buckanovich, *Cancer Res.* 70 (2010) 8674–8683.
- [15] Y. Min, C. Mao, D. Xu, J. Wang, Y. Liu, *Chem. Commun.* 46 (2010) 8424–8426.
- [16] R. Guo, L. Zhang, H. Qian, R. Li, X. Jiang, B. Liu, *Langmuir* 26 (2010) 5428–5434.
- [17] B. Thierry, F. Al-Ejeh, A. Khatri, Z. Yuan, P.J. Russell, S. Ping, M.P. Brown, P. Majewski, *Chem. Commun.* (2009) 7348–7350.
- [18] M.J. de Jonge, M. Slingerland, W.J. Loos, E.A. Wiemer, H. Burger, R.H. Mathijssen, J.R. Kroep, M.A. den Hollander, B.D. van der, M.H. Lam, J. Verweij, H. Gelderblom, *Eur. J. Cancer* 46 (2010) 3016–3021.
- [19] B.W. Harper, A.M. Krause-Heuer, M.P. Grant, M. Manohar, K.B. Garbutcheon-Singh, J.R. Drich-Wright, *Chemistry* 16 (2010) 7064–7077.
- [20] T. Tippayamontri, R. Kotb, B. Paquette, L. Sanche, *Invest. New Drugs* 29 (2011) 1321–1327.
- [21] G.C. dos Santos, E.C. de Oliveira Reis, T.G. Ribeiro Rocha, E.A. Leite, R.G. Lacerda, G.A. Ramaldes, M.C. De Oliveira, *J. Liposome Res.* 21 (2011) 60–69.
- [22] M.L. Krieger, N. Eckstein, V. Schneider, M. Koch, H.D. Royer, U. Jaehde, G. Bendas, *Int. J. Pharm.* 389 (2010) 10–17.
- [23] R. Schobert, B. Biersack, A. Dietrich, A. Grote-meier, T. Muller, B. Kalinowski, S. Knauer, W. Voigt, R. Paschke, *J. Med. Chem.* 50 (2007) 1288–1293.
- [24] H. Kommera, G.N. Kaluderović, J. Kalbitz, B. Drager, R. Paschke, *Eur. J. Med. Chem.* 45 (2010) 3346–3353.
- [25] A. Dietrich, T. Mueller, R. Paschke, B. Kalinowski, T. Behlendorf, F. Reipsch, A. Fruehauf, H.J. Schmoll, C. Kloft, W. Voigt, *J. Med. Chem.* 51 (2008) 5413–5422.
- [26] A. Schädlich, C. Rose, J. Kuntsche, H. Caysa, T. Mueller, A. Göpferich, K. Mäder, *Pharm. Res.* 28 (2011) 1995–2007.

Appendix 12

Reproduced from Ref. G.N. Kaluđerović, A. Dietrich, H. Kommera, J. Kuntsche, K. Mäder, T. Muller, R. Paschke, *Europ. J. Med. Chem.* 2012, 54, 567 with permission from Elsevier Masson SAS.

572

G.N. Kaluđerović et al. / European Journal of Medicinal Chemistry 54 (2012) 567–572

- [27] A. Schädlich, H. Caysa, T. Mueller, F. Tenambergen, C. Rose, A. Göpferich, J. Kuntsche, K. Mäder, *ACS Nano* 5 (2011) 8710–8720.
- [28] A. Fahr, P. van Hoogevest, S. May, N. Bergstrand, M.L.S. Leigh, *Eur. J. Pharm. Sci.* 26 (2005) 251–265.
- [29] A.D. Sezer, A.L. Bas, J. Akbuga, *J. Liposome Res.* 14 (2004) 77–86.
- [30] J. Kuntsche, K. Klaus, F. Steiniger, *J. Biomed. Nanotechnol.* 5 (2009) 384–395.
- [31] O. Stauch, R. Schubert, G. Savin, W. Burchard, *Biomacromolecules* 3 (2002) 565–578.
- [32] P.J. Wyatt, *J. Colloid Interface Sci.* 197 (1998) 9–20.
- [33] P. Skehan, R. Storeng, D. Scudiero, A. Monks, J. McMahon, D. Vistica, J.T. Warren, H. Bokesch, S. Kenney, M.R. Boyd, *J. Natl. Cancer Inst.* 82 (1990) 1107–1112.

DOI: 10.1002/chem.200900151

Reproduced from Ref. D. Pérez-Quintanilla, S. Gómez-Ruiz, Ž. Žižak, I. Sierra, S. Prashar, I. del Hierro, M. Fajardo, Z.D. Juranić, G.N. Kaluderović, Chem. - Eur. J. 2009, 15, 5588 with permission from John Wiley and Sons.

A New Generation of Anticancer Drugs: Mesoporous Materials Modified with Titanocene Complexes

Damian Pérez-Quintanilla,^[a] Santiago Gómez-Ruiz,^{*[a]} Željko Žižak,^[b] Isabel Sierra,^[a] Sanjiv Prashar,^[a] Isabel del Hierro,^[a] Mariano Fajardo,^[a] Zorica D. Juranić,^[b] and Goran N. Kaluderović^{*[c, d]}

Abstract: Dehydroxylated MCM-41 and SBA-15 surfaces were modified by the grafting of two different titanocene complexes ($[\text{Ti}(\eta^5\text{-C}_5\text{H}_4\text{Me})_2\text{Cl}_2]$ and $[\text{Ti}\{\text{Me}_2\text{Si}(\eta^5\text{-C}_3\text{Me}_4)(\eta^5\text{-C}_5\text{H}_4)\}\text{Cl}_2]$) to give new materials, which have been characterized by powder X-ray diffraction, X-ray fluorescence, nitrogen gas sorption, MAS-NMR spectroscopy, thermogravimetry, SEM, and TEM. The toxicity of the resulting materials toward human adenocarcinoma HeLa, human myelogenous leukemia K562, human malignant melanoma Fem-x, and normal immunocompetent cells, such as peripheral blood mononuclear cells PBMC has been studied. Estimation of the number of particles per gram of material led to the calculation of Q_{50} values for these samples, which is the number of particles required to inhibit normal cell growth by 50%. In

addition, M_{50} values (quantity of material needed to inhibit normal cell growth by 50%) of the studied surfaces is also reported. Nonfunctionalized MCM-41 and SBA-15 did not show notable antiproliferative activity, whereas functionalization of these materials with different titanocene based anticancer drugs led to very promising antitumoral activity. The best Q_{50} values correspond to titanocene functionalized MCM-41 surfaces (MCM-41/ $[\text{Ti}(\eta^5\text{-C}_5\text{H}_4\text{Me})_2\text{Cl}_2]$ (**1**) and MCM-41/ $[\text{Ti}\{\text{Me}_2\text{Si}(\eta^5\text{-C}_3\text{Me}_4)(\eta^5\text{-C}_5\text{H}_4)\}\text{Cl}_2]$ (**2**)) with Q_{50} values between $3.8 \pm 0.6 \times 10^8$ and $24.5 \pm 3.0 \times 10^8$ particles. Titanocene functionalized SBA-15 surfaces

(SBA-15/ $[\text{Ti}(\eta^5\text{-C}_5\text{H}_4\text{Me})_2\text{Cl}_2]$ (**3**) and SBA-15/ $[\text{Ti}\{\text{Me}_2\text{Si}(\eta^5\text{-C}_3\text{Me}_4)(\eta^5\text{-C}_5\text{H}_4)\}\text{Cl}_2]$ (**4**)) gave higher Q_{50} values, showing lower activity from $73.2 \pm 9.9 \times 10^8$ to $362 \pm 7 \times 10^8$ particles. The best response of the studied materials in terms of M_{50} values was observed against Fem-x ($309 \pm 42 \mu\text{g}$ for **4**) and K562 ($338 \pm 18 \mu\text{g}$ for **2**), whereas moderate activities were observed in HeLa cells (from $508 \pm 63 \mu\text{g}$ of **2** to $912 \pm 10 \mu\text{g}$ of **1**). In addition, the analyzed surfaces presented only marginal activity against unstimulated and stimulated PBMC, showing a slight selectivity on human cancer cells. Comparison of the in vitro cytotoxicity in solution of the titanocene complexes $[\text{Ti}(\eta^5\text{-C}_5\text{H}_4\text{Me})_2\text{Cl}_2]$ and $[\text{Ti}\{\text{Me}_2\text{Si}(\eta^5\text{-C}_3\text{Me}_4)(\eta^5\text{-C}_5\text{H}_4)\}\text{Cl}_2]$ and the corresponding titanocene functionalized materials is also described.

Keywords: antitumor agents • bio-inorganic chemistry • cytotoxicity • mesoporous materials • titanium

[a] Dr. D. Pérez-Quintanilla, Dr. S. Gómez-Ruiz, Dr. I. Sierra, Dr. S. Prashar, Dr. I. del Hierro, Prof. M. Fajardo
Departamento de Química Inorgánica y Analítica, E.S.C.E.T.
Universidad Rey Juan Carlos
28933 Móstoles, Madrid (Spain)
Fax: (+34)914888143
E-mail: santiago.gomez@urjc.es

[b] Dr. Ž. Žižak, Prof. Z. D. Juranić
Institute of Oncology and Radiology of Serbia
11000 Belgrade (Serbia)

[c] Dr. G. N. Kaluderović
Institut für Chemie
Martin-Luther-Universität Halle-Wittenberg
Kurt-Mothes-Strasse 2, 06120 Halle (Germany)

[d] Dr. G. N. Kaluderović
Department of Chemistry
Institute of Chemistry, Technology and Metallurgy
University of Belgrade
Studentski trg 14, 11000 Belgrade (Serbia)
E-mail: goran.kaluderovic@chemie.uni-halle.de
goran@chem.bg.ac.yu

Supporting information for this article is available on the WWW under <http://dx.doi.org/10.1002/chem.200900151>.

Reproduced from Ref. D. Pérez-Quintanilla, S. Gómez-Ruiz, Ž. Žižak, I. Sierra, S. Prashar, I. del Hierro, M. Fajardo, Z.D. Juranić, G.N. Kaluđerović, Chem. - Eur. J. 2009, 15, 5588 with permission from John Wiley and Sons.

Introduction

Mesoporous materials are a new generation of substances that show different geometric arrangements of channels and cavities built up from SiO₂ units. The pore size (from 2 to 50 nm) can be controlled and modified reasonably well by various methods.^[1,2] Very extended examples of these materials are the 2D-hexagonal MCM-41^[3] and SBA-15^[4] silicas, which have pore sizes between 2 and 10 nm.

One of the main properties of mesoporous materials is their capability of adsorbing small molecules.^[5,6] Thus, drug delivery using nanomaterials is one of the most studied applications in recent years.^[7–16] The adsorption and release of molecules with pharmacological interest has opened new directions in medical research into drug release from mesoporous matrices.^[17–32]

However, only very recently, modified mesoporous materials have been used in anticancer therapy tests.^[33,34] Modification of these materials by grafting with anticancer organic drugs led to moderate cytotoxic activity of MCM-41 and spherical silica.^[34]

As many of the most potent drugs used in cancer chemotherapy are based on metal complexes,^[35–38] we used the experience that our research group has in the preparation of new mesoporous materials with important applications,^[39–44] and in the design and applications of organometallic complexes as anticancer drugs,^[45–49] for the synthesis, characterization, and in vitro evaluation of the cytotoxic activity of titanocene-modified MCM-41 and SBA-15. Thus, we measured the cytotoxicity of nonfunctionalized and functionalized MCM-41 and SBA-15 towards human adenocarcinoma HeLa, human myelogenous leukemia K562, human malignant melanoma Fem-x, and normal immunocompetent cells, such as peripheral blood mononuclear cells PBMC. As these materials are not soluble, we report the cytotoxicity using a recently estimated *Q*₅₀ scale (number of particles needed to inhibit normal cell growth by 50 %).^[34]

Results and Discussion

Preparation of modified surfaces: Dehydroxylated (at 500 °C) MCM-41 or SBA-15 mesoporous silica were used in this study, and titanocene complexes were immobilized by direct anchoring on the support. MCM-41 and SBA-15 contain silanol groups and siloxane bridges, which are relatively inert, with the exception of siloxanes in very strained four-membered rings. The concentration of hydroxy groups of the mesoporous materials is expected to decrease substantially at high temperatures. The surfaces were modified by grafting of titanocene complexes [Ti(η⁵-C₅H₄Me)₂Cl₂] and [Ti{Me₂Si(η⁵-C₃Me₄)(η⁵-C₅H₄)}Cl₂] (Figure 1). The dehydroxylated surfaces were treated for 24 h with a solution of the corresponding titanocene complex in toluene. Possible reactions between one of the chlorine atoms of the corresponding titanocene complexes with either the acidic silanol groups or the reactive siloxane bridges may lead to μ-oxido

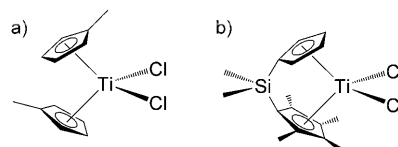


Figure 1. Titanocene complexes used in the study: a) [Ti(η⁵-C₅H₄Me)₂Cl₂]; b) [Ti{Me₂Si(η⁵-C₃Me₄)(η⁵-C₅H₄)}Cl₂].

surface species;^[50,51] however, adsorbed titanocene complexes may also be located in the pores of the corresponding materials.

In previous studies, it was observed that the maximum loading of metallocene complexes on MCM-41 and SBA-15 surfaces was close to 1.6 % metal, even when starting from high metal/SiO₂ ratios.^[52] In addition, treatment of the surfaces with higher concentrations of metallocene saturated the surface, and the maximum load was always very low, probably because of the weak basicity of the chlorido ligands and the weak acidity of the Si–OH groups.^[53] In this context, we performed reactions using 3 % Ti, and the X-ray fluorescence data revealed a Ti wt % of 1.32 and 1.43 % for MCM-41/[Ti(η⁵-C₅H₄Me)₂Cl₂] (**1**) and MCM-41/[Ti{Me₂Si(η⁵-C₃Me₄)(η⁵-C₅H₄)}Cl₂] (**2**), respectively. These values are even lower in SBA-15/[Ti(η⁵-C₅H₄Me)₂Cl₂] (**3**) and SBA-15/[Ti{Me₂Si(η⁵-C₃Me₄)(η⁵-C₅H₄)}Cl₂] (**4**) (0.65 and 0.76 % Ti, respectively), probably because of the lower superficial area of SBA-15 relative to MCM-41. Table 1 shows the wt % of Ti grafted on the silica support.

Table 1. Ti content (wt %) grafted on the silica support.

Surface	Ti ₀ [wt %] ^[a]	Ti _{exptl} [wt %] ^[b]
1	3	1.32
2	3	1.43
3	3	0.65
4	3	0.76

[a] Theoretical Ti content. [b] Experimental Ti content determined by X-ray fluorescence.

Characterization of the modified MCM-41 and SBA-15 supports:

The new materials have been characterized extensively. MAS-NMR spectroscopy has proven to be a useful tool in monitoring surface reactions of organometallic reagents.^[54] All the new surfaces were characterized by ¹H-CP MAS NMR studies. The spectra showed signals corresponding to the protons of the grafted titanocene complexes. For the surfaces functionalized with [Ti(η⁵-C₅H₄Me)₂Cl₂] (**1** and **3**) signals attributed to the protons of the methyl substituents of the cyclopentadienyl ligand were observed between δ = 1.7 and 4.1 ppm. In addition, signals of the protons of the cyclopentadienyl ligand were recorded between δ = 6 and 9 ppm. Materials containing the *ansa*-titanocene complex [Ti{Me₂Si(η⁵-C₃Me₄)(η⁵-C₅H₄)}Cl₂] (**2** and **4**) gave ¹H CP MAS NMR spectra with signals at δ = 1.64 ppm, attributed to the protons of the methyl substituents of the silicon *ansa* bridge. Protons of the methyl groups of the substi-

Reproduced from Ref. D. Pérez-Quintanilla, S. Gómez-Ruiz, Ž. Žižak, I. Sierra, S. Prashar, I. del Hierro, M. Fajardo, Z.D. Juranić, G.N. Kaluđerović, Chem. - Eur. J. 2009, 15, 5588 with permission from John Wiley and Sons.

tuted cyclopentadienyl ligand were observed between $\delta = 3.3$ and 6.3 ppm, and the signals of the protons of the cyclopentadienyl ligand were recorded between $\delta = 6.3$ and 8.9 ppm. Figure 2 shows the ^1H MAS NMR spectra of **1** and **4**.

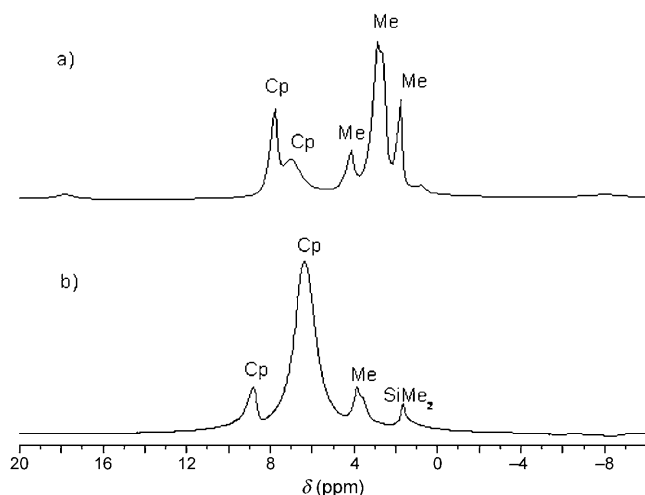


Figure 2. ^1H MAS NMR spectra of a) MCM-41/[Ti($\eta^5\text{-C}_5\text{H}_4\text{Me}_2$) $_2\text{Cl}_2$] (**1**) and b) SBA-15/[Ti(Me $_2$ Si($\eta^5\text{-C}_5\text{Me}_4$)($\eta^5\text{-C}_5\text{H}_4$))Cl $_2$] (**4**).

The ^{13}C CP MAS NMR spectra of MCM-41/[Ti($\eta^5\text{-C}_5\text{H}_4\text{Me}_2$) $_2\text{Cl}_2$] (**1**) (Figure 3a) and SBA-15/[Ti($\eta^5\text{-C}_5\text{H}_4\text{Me}_2$) $_2\text{Cl}_2$] (**3**) showed three sets of signals, one in the

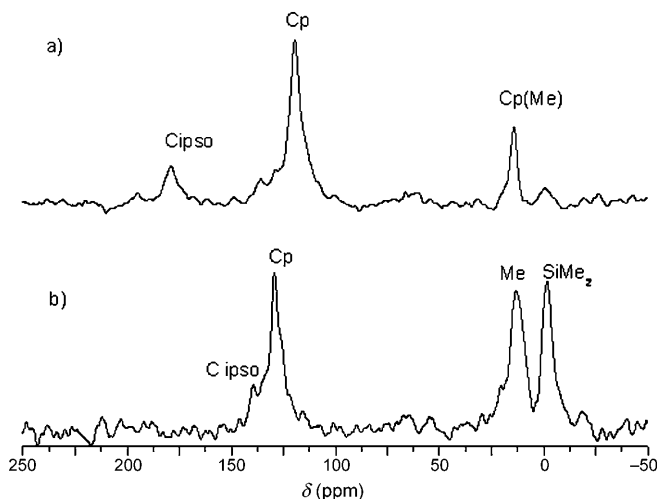


Figure 3. ^{13}C CP MAS NMR spectra of a) MCM-41/[Ti($\eta^5\text{-C}_5\text{H}_4\text{Me}_2$) $_2\text{Cl}_2$] (**1**) and b) SBA-15/[Ti(Me $_2$ Si($\eta^5\text{-C}_5\text{Me}_4$)($\eta^5\text{-C}_5\text{H}_4$))Cl $_2$] (**4**).

region $\delta = 15\text{--}22$ ppm corresponding to the carbon atoms of the methyl substituents, a second attributed to the carbon atoms of the cyclopentadienyl ligand in the region $\delta = 120\text{--}130$ ppm, and a third set of signals corresponding to the substituted carbon atoms of the cyclopentadienyl ligand between $\delta = 175$ and 200 ppm.

In case of the ^{13}C CP MAS NMR spectrum of MCM-41/[Ti(Me $_2$ Si($\eta^5\text{-C}_5\text{Me}_4$)($\eta^5\text{-C}_5\text{H}_4$))Cl $_2$] (**2**), four signals at $\delta = -2.1$, 12.8, 76.6, and 85.1 ppm were observed. The signals at $\delta = 76.6$ and 85.1 ppm were assigned to the carbon atoms of the C_5 rings (C_5Me_4 and C_5H_4 , respectively) and the signal observed at $\delta = 12.8$ ppm to the carbon atoms of the methyl groups of the C_5Me_4 moiety. Finally, the peak at $\delta = -2.1$ ppm refers to the carbon atoms of the SiMe_2 group. A similar spectral pattern with different chemical shifts was observed in the ^{13}C CP MAS NMR spectrum of SBA-15/[Ti(Me $_2$ Si($\eta^5\text{-C}_5\text{Me}_4$)($\eta^5\text{-C}_5\text{H}_4$))Cl $_2$] (**4**) (Figure 3b).

^{29}Si MAS NMR spectra of all the synthesized surfaces were also recorded. The spectra show silicon atoms with hydroxy-bound groups, such as [Si(OSi) $_2$ (OH) $_2$] (Q_2 , at $\delta = -91.6$ ppm), [Si(OSi) $_2$ (OH)] (Q_3 , at $\delta = -100.6$ ppm), and [Si(OSi) $_2$] (Q_4 , at $\delta = -110$ ppm). After grafting the metallocene complex, a modification in the Q_3 and Q_2 sites was observed; as a consequence of the functionalization, the intensity of these peaks clearly decreases (Figure 4).

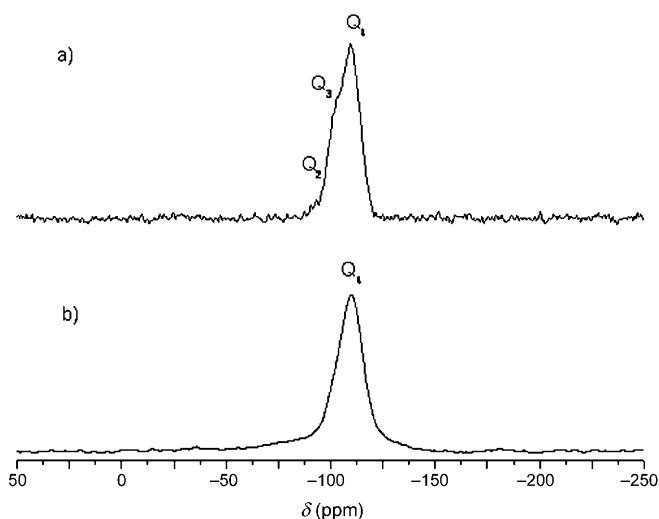


Figure 4. ^{29}Si MAS NMR spectra of a) MCM-41 and b) MCM-41/[Ti(Me $_2$ Si($\eta^5\text{-C}_5\text{Me}_4$)($\eta^5\text{-C}_5\text{H}_4$))Cl $_2$] (**2**).

Structural features of the modified MCM-41 and SBA-15 supports:

The main structural feature of MCM-41 and SBA-15 gives rise to XRD reflections that are typical for hexagonally ordered mesoporous materials.^[55] MCM-41 displayed a well-resolved pattern at low 2θ values with a very sharp diffraction peak at 2.54° and an additional weak peak at 4.77° . These characteristic Bragg peaks, with d -spacings of 34.75 and 18.51 Å, correspond to reflections from the (100) and (110) planes, respectively (Table 2). Unmodified SBA-15 displayed a well-resolved pattern at low 2θ values with a very sharp (100) diffraction peak at 0.93° . This system can be indexed as a hexagonal lattice with d -spacing values of 94.70 Å (Table 2).

No notable alterations were observed in the XRD pattern after the grafting of the titanocene complexes. MCM-41/[Ti($\eta^5\text{-C}_5\text{H}_4\text{Me}_2$) $_2\text{Cl}_2$] (**1**) and MCM-41/[Ti(Me $_2$ Si($\eta^5\text{-C}_5\text{Me}_4$)-

Reproduced from Ref. D. Pérez-Quintanilla, S. Gómez-Ruiz, Ž. Žižak, I. Sierra, S. Prashar, I. del Hierro, M. Fajardo, Z.D. Juranić, G.N. Kaluđerović, Chem. - Eur. J. 2009, 15, 5588 with permission from John Wiley and Sons.

Table 2. XRD data.

Material	Index (<i>hkl</i>)	2θ [°]	<i>d</i> -spacing [Å]
MCM-41	100	2.54	34.75
	110	4.77	18.51
SBA-15	100	0.93	94.70
	100	2.54	34.75
1	110	4.90	18.02
	100	2.52	35.11
2	110	4.91	17.98
	100	0.92	95.44
4	100	0.92	95.54

($\eta^5\text{-C}_5\text{H}_4$)Cl₂) (**2**) displayed a well-resolved pattern at low 2θ value with a very sharp (100) diffraction peak at 2.54° for **1** and 2.52° for **2** and an additional weak peak at 4.90° for **1** and 4.91° for **2** corresponding to 110 (Table 2 and Figure 5a). These peaks can be indexed as a hexagonal lattice with *d*-spacing values of 34.75 and 18.02 Å, respectively, for **1** and 35.11 and 17.98 Å for **2**. Unit cell parameters, *a*₀, of 40.12 Å for **1** and 40.54 Å for **2** were obtained from Equation (1).^[56]

$$a_0 = \frac{2d_{100}}{\sqrt{3}} \quad (1)$$

The XRD pattern of the functionalized SBA-15/[Ti($\eta^5\text{-C}_5\text{H}_4\text{Me}_2$)Cl₂] (**3**) and SBA-15/[Ti{Me₂Si($\eta^5\text{-C}_5\text{Me}_4$)($\eta^5\text{-C}_5\text{H}_4$)}Cl₂] (**4**) suggests that the structural order of the syn-

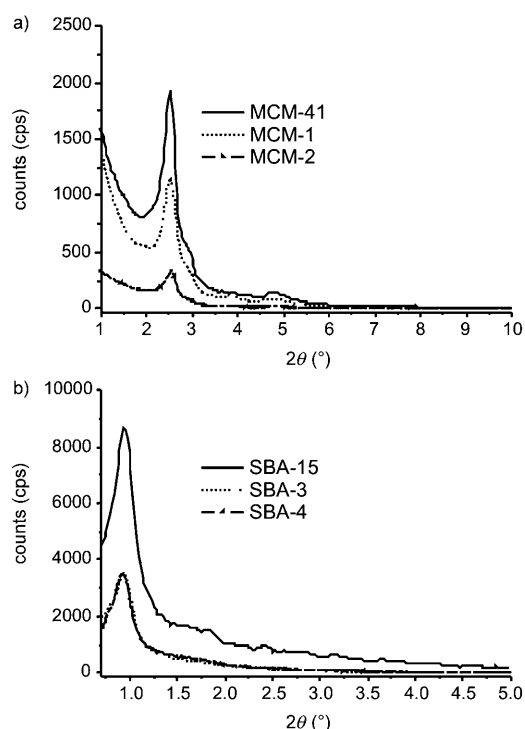


Figure 5. Low-angle powder XRD patterns of a) MCM-41, MCM-41/[Ti($\eta^5\text{-C}_5\text{H}_4\text{Me}_2$)Cl₂] (**1**), and MCM-41/[Ti{Me₂Si($\eta^5\text{-C}_5\text{Me}_4$)($\eta^5\text{-C}_5\text{H}_4$)}Cl₂] (**2**); b) SBA-15, SBA-15/[Ti($\eta^5\text{-C}_5\text{H}_4\text{Me}_2$)Cl₂] (**3**), and SBA-15/[Ti{Me₂Si($\eta^5\text{-C}_5\text{Me}_4$)($\eta^5\text{-C}_5\text{H}_4$)}Cl₂] (**4**).

thesized material is maintained after functionalization. Values for *a*₀ of 110.2 Å for **3** and 110.3 Å for **4** were obtained (Figure 5b). The cell parameters for **1–4** are given in Table 2.

Nitrogen adsorption/desorption isotherms are an efficient tool for characterizing the nature of porous host systems. The isotherms for the unmodified systems MCM-41 and SBA-15 and all the modified mesoporous materials **1–4** are of type IV according to the IUPAC classification^[57] and have an H1 hysteresis loop that is representative of mesopores. The volume adsorbed for all isotherms increased sharply at a relative pressure (*P/P*₀) of approximately 0.3 for (**1–2**) and 0.4 for (**3–4**), which represents capillary condensation of nitrogen within the uniform mesopore structure. The inflection position shifted slightly toward lower relative pressures and the volume of nitrogen adsorbed decreased with functionalization, which is indicative of a reduction in pore size (Figure 6).

Table 3 shows the physical parameters of nitrogen isotherms, such as BET surface area (*S*_{BET}), (BJH) average pore diameter, and wall thickness for the unmodified MCM-41, SBA-15, and the modified surfaces **1–4**. The effective mean pore diameters of MCM-41/[Ti($\eta^5\text{-C}_5\text{H}_4\text{Me}_2$)Cl₂] (**1**) and MCM-41/[Ti{Me₂Si($\eta^5\text{-C}_5\text{Me}_4$)($\eta^5\text{-C}_5\text{H}_4$)}Cl₂] (**2**) were 21.2 and 21.0 Å, respectively (Table 3), whereas for SBA-15/[Ti($\eta^5\text{-C}_5\text{H}_4\text{Me}_2$)Cl₂] (**3**) and SBA-15/[Ti{Me₂Si($\eta^5\text{-C}_5\text{Me}_4$)($\eta^5\text{-C}_5\text{H}_4$)}Cl₂] (**4**) the values were 57.8 and 59.0 Å, respectively. As expected, the pores become slightly smaller as a result of immobilization of the titanocene complexes.

The incorporation of molecules inside the pores of the MCM-41 and SBA-15 may also be justified by the increase in wall thickness (calculated data in Table 3) observed for these surfaces relative to unmodified MCM-41 and SBA-15.

From these results, it seems plausible that some of the titanocene complexes in the surfaces are located within the pores. To determine whether the size of the titanocene complexes is appropriate to fit in the pore cavity, DFT calculations of the complexes [Ti($\eta^5\text{-C}_5\text{H}_4\text{Me}_2$)Cl₂] and [Ti{Me₂Si($\eta^5\text{-C}_5\text{Me}_4$)($\eta^5\text{-C}_5\text{H}_4$)}Cl₂] were carried out (see the Supporting Information). According to the obtained geometrical parameters, titanocene derivatives exhibit, in both cases, distances of less than 8 Å between the most remote atoms of the structures, indicating that they are small enough to be located inside the pore. In addition, the volume of these complexes (0.6 nm³ for [Ti($\eta^5\text{-C}_5\text{H}_4\text{Me}_2$)Cl₂] and 0.73 nm³ for [Ti{Me₂Si($\eta^5\text{-C}_5\text{Me}_4$)($\eta^5\text{-C}_5\text{H}_4$)}Cl₂]) is smaller than the pores of MCM-41 and SBA-15. Therefore, these surfaces would provide more than enough space for the metallocene molecule to bind to the surface OH groups inside the cavities. The wall thickness for MCM-41 and SBA-15 were 18.8 and 43.0 Å, respectively, and 18.3, 19.5, 52.4, and 51.3 Å, for surfaces **1–4**, respectively. These values were calculated from Equation (2).^[56]

$$\text{Wall thickness} = \frac{2d_{100}}{\sqrt{3}} - \text{BJH average pore diameter} \quad (2)$$

Reproduced from Ref. D. Pérez-Quintanilla, S. Gómez-Ruiz, Ž. Žižak, I. Sierra, S. Prashar, I. del Hierro, M. Fajardo, Z.D. Juranić, G.N. Kaluđerović, *Chem. - Eur. J.* 2009, 15, 5588 with permission from John Wiley and Sons.

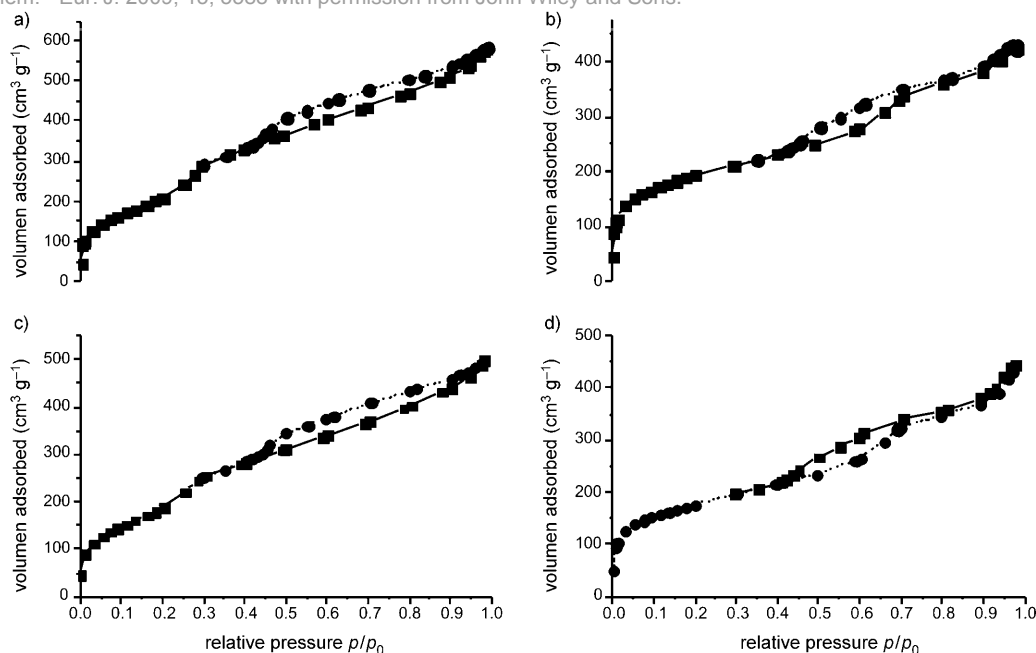


Figure 6. Nitrogen adsorption (■)/desorption (●) isotherms: a) MCM-41, b) SBA-15, c) MCM-41/[Ti(η⁵-C₅H₄Me)₂Cl₂] (**1**), and d) SBA-15/[Ti{Me₂Si(η⁵-C₅Me₄)(η⁵-C₅H₄)Cl₂] (**4**).

Table 3. Physical parameters measured by N₂ adsorption–desorption isotherms.

Sample	BET surface area [m ² g ⁻¹]	Total pore volume [cm ³ g ⁻¹]	Pore diameter (BJH) ^[a] [Å]	Wall thickness [Å]
MCM-41	776	0.87	21.3	18.8
SBA-15	700	0.65	66.0	43.0
1	700	0.75	21.2	18.9
2	770	0.79	21.0	19.5
3	623	0.61	57.8	52.4
4	637	0.64	59.0	51.3

[a] Barrett, Joyner, and Halenda

Moreover, the pore size distribution of the studied surfaces is homogeneous, leading to a narrow distribution (see the Supporting Information).

The thermogravimetric curves (TGA) for the modified mesoporous silica samples (**1–4**) reveal information about the thermal stability and also confirm the amount of immobilized ligand (see TGA curves of the MCM-41, MCM-41/[Ti(η⁵-C₅H₄Me)₂Cl₂] (**1**), SBA-15, and SBA-15/[Ti(η⁵-C₅H₄Me)₂Cl₂] (**3**) in the Supporting Information). The profiles indicate that unmodified silica shows a loss in mass (ca. 3%) in a first step between room temperature and 100 °C attributed to the loss of physically adsorbed water (endothermic process). A second decrease in mass of 0.2% (between 600 and 800 °C) is attributed to the increase in the number of siloxane bridges (Si-O-Si) as a result of isolated silanol condensation (exothermic process).

The TGA curves of the modified material (**1–4**) show an initial loss of mass of approximately 1.5 and 6% attributed to water physically adsorbed on the surface to modified

MCM-41 materials (**1–2**) and modified SBA-15 materials (**3–4**), respectively. In addition, a second loss of mass is observed, which indicates a degradation process that occurs between 250 and 500 °C. The weight losses are of about 4.16, 3.5, 10, and 5.75% for surfaces **1–4**, respectively. This phenomenon is due to the decomposition of titanocene complexes anchored on the silica surface (exothermic process).

Scanning electron microscopy (SEM) and transmission electron microscopy (TEM) were employed to assess morphological differences on the studied surfaces. However, all of the samples can be considered clusters of spheres with average diameters of 845.1, 733.1, 291.4, and 365.8 nm for **1–4**, respectively. Figures 7 (SEM) and 8 (TEM) show the images of unmodified SBA-15 and modified surface **4**.

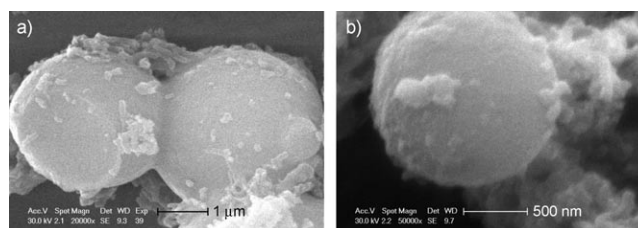


Figure 7. Scanning electron microscope images of a) SBA-15 and b) SBA-15/[Ti{Me₂Si(η⁵-C₅Me₄)(η⁵-C₅H₄)Cl₂] (**4**).

Number of particles per gram of surface: SEM and TEM provided information on the general shape and dimensions of particles and BET-N₂ adsorption measurements gave the surface area per gram of surface as well as the diameter of its adsorptive pores. This information allowed calculation of

Reproduced from Ref. D. Pérez-Quintanilla, S. Gómez-Ruiz, Ž. Žižak, I. Sierra, S. Prashar, I. del Hierro, M. Fajardo, Z.D. Juranić, G.N. Kaluđerović, Chem. - Eur. J. 2009, 15, 5588 with permission from John Wiley and Sons.

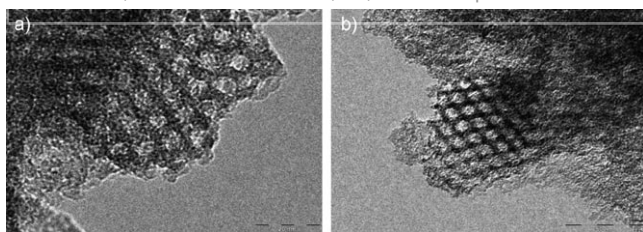


Figure 8. Transmission electron microscope images of a) SBA-15 and b) SBA-15/[Ti{Me₂Si(η⁵-C₅Me₄)(η⁵-C₅H₄)Cl₂] (**4**).

the number of particles per gram weight of MCM-41 using the method of Di Pasqua et al.^[34]

The studied particles were in all cases quasi spherical and were idealized to the spherical geometry to facilitate the calculations. According to all the necessary parameters such as average of the diameter of particle, particle surface, unit cell parameters, wall thickness, and external surface, the number of particles per gram of surface were 6.86×10^{11} , 4.82×10^{12} , 4.20×10^{13} , and 2.37×10^{13} for **1–4**, respectively.

Cytotoxicity studies: Titanocene-modified surfaces **1–4** and unmodified MCM-41 and SBA-15 were used to understand the possible relationship between the different surfaces and titanocene complexes and the corresponding cytotoxic activity. The in vitro cytotoxicities of surfaces **1–4** and MCM-41 and SBA-15 against human adenocarcinoma HeLa, human myelogenous leukemia K562, human malignant melanoma Fem-x, and normal immunocompetent cells, that is, on human peripheral blood mononuclear cells, were determined by MTT-based assays (MTT = 3-(4,5-dimethylthiazol-2-yl)-2,5-diphenyltetrazolium bromide). Table 4 shows the Q_{50} values of these materials. Whereas the unmodified MCM-41 and SBA-15 materials were not active, the functionalized surfaces (**1–4**) showed a dose-dependent antiproliferative effect towards all tumor cell

lines (Figure 9). MCM-41/[Ti(η⁵-C₅H₄Me)₂Cl₂] (**1**) is the best of the studied materials against all the cancer cells in terms of particles, showing Q_{50} values from $3.8 \pm 0.6 \times 10^8$ to $6.3 \pm 0.1 \times 10^8$, whereas its analogue **2** has slightly lower activity against the same cancer cells. As the cytotoxic activity of [Ti(η⁵-C₅H₄Me)₂Cl₂]^[58] (IC₅₀ from 173.3 ± 6.0 to $>200 \mu\text{M}$) in solution is lower than that of [Ti{Me₂Si(η⁵-C₅Me₄)(η⁵-C₅H₄)Cl₂]^[46] (IC₅₀ from 66 ± 6 to $135 \pm 6 \mu\text{M}$), and the present quantity of titanium in the surface is very similar (1.32% for **1** and 1.43% for **2**), it seems plausible that the release of [Ti(η⁵-C₅H₄Me)₂Cl₂] is easier than that of [Ti{Me₂Si(η⁵-C₅Me₄)(η⁵-C₅H₄)Cl₂], which would favor the high cytotoxic activity of **1**. However, for modified SBA-15 surfaces, the release of complex [Ti(η⁵-C₅H₄Me)₂Cl₂] may not be

Table 4. Cytotoxicity values (Q_{50} [particles] for surfaces and IC₅₀ [μM] for titanocene complexes) of the studied samples on various cell lines.^[a]

Sample	Q_{50} ($\times 10^{-8}$) [particles]				
	HeLa	K562	Fem-x	PBMC-PHA	PBMC+PHA
1	6.3 ± 0.1	4.7 ± 0.3	3.8 ± 0.6	>6.86 (NA)	>6.86 (NA)
2	24.5 ± 3.0	16.3 ± 0.1	15.9 ± 0.1	>48.2 (NA)	22.0 ± 1.9
3	362 ± 7	225 ± 20	195 ± 22	>420 (NA)	386 ± 55
4	159 ± 11	108 ± 10	73.2 ± 9.9	>237 (NA)	221 ± 42
MCM-41	NA	NA	NA	ND	ND
SBA-15	NA	NA	NA	ND	ND
[Ti(η ⁵ -C ₅ H ₄ Me) ₂ Cl ₂]	>200	173.3 ± 6.0	198.6 ± 4.3	>200	180.9 ± 4.3
[Ti{Me ₂ Si(η ⁵ -C ₅ Me ₄)(η ⁵ -C ₅ H ₄)Cl ₂]	135 ± 6	66 ± 6	96 ± 4	112 ± 7	77 ± 6

[a] NA = no activity detected in the studied range. ND = not determined.

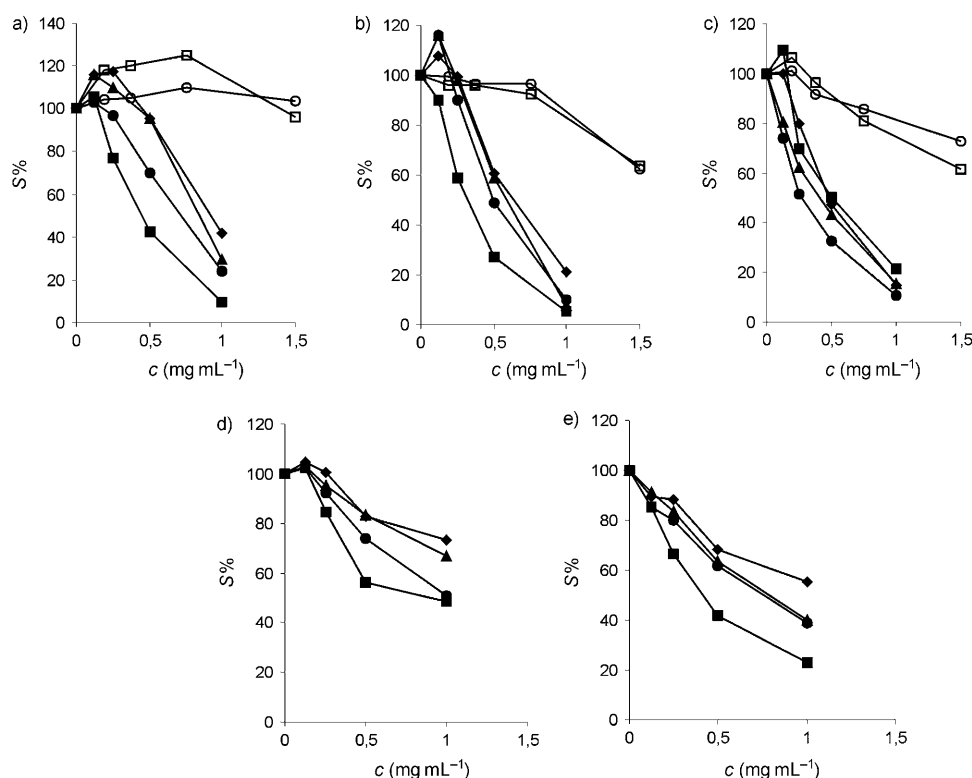


Figure 9. Representative graphs of the survival of a) HeLa, b) K562, c) Fem-x, d) PBMC, and e) PBMC+PHA (PBMC stimulated with PHA) cells grown for 72 h in the presence of increasing amounts of the studied surfaces (**1**: \blacklozenge , **2**: \blacksquare , **3**: \blacktriangle , **4**: \bullet , MCM-41: \square , and SBA-15: \circ).

Reproduced from Ref. D. Pérez-Quintanilla, S. Gómez-Ruiz, Ž. Žižak, I. Sierra, S. Prashar, I. del Hierro, M. Fajardo, Z.D. Juranić, G.N. Kaluđerović, Chem. - Eur. J. 2009, 15, 5588 with permission from John Wiley and Sons.

3 relative to that of 4.

With reference to the different cancer cells, all the studied surfaces show the best activities on Fem-x cells, whereas lower activities were observed on K562 and HeLa cells. The cytotoxic activity of the studied surfaces on normal immunocompetent cells (stimulated PBMC) is marginal for 2–4, and none of the complexes showed activity against unstimulated PBMC in the examined range of concentrations. This phenomenon indicates a good degree of selectivity of the studied materials 1–4.

Furthermore, the studied surfaces led to a higher cytotoxic activity (Q_{50} more than 100 times greater) of MCM-41 surfaces than those reported recently for mesoporous materials modified with organic drugs.^[34]

As the Q_{50} values are the consequence only of the correlation between the calculated number of particles per gram, which depends on the imprecise estimation of the average particle size by SEM, we decided to discuss the anticancer tests also in terms of mass by using an M_{50} scale (quantity of material needed to inhibit normal cell growth by 50%; Table 5).

Table 5. Cytotoxicity values on the M_{50} scale (quantity of material needed to inhibit normal cell growth by 50%) of the studied surfaces on various cell lines.^[a]

Material	M_{50} [μg]				
	HeLa	K562	Fem-x	PBMC-PHA	PBMC+PHA
1	912 ± 10	683 ± 50	555 ± 77	> 1000 (NA)	> 1000 (NA)
2	508 ± 63	338 ± 18	328 ± 18	> 1000 (NA)	457 ± 40 (NA)
3	861 ± 18	536 ± 51	464 ± 52	> 1000 (NA)	918 ± 130
4	671 ± 48	456 ± 36	309 ± 42	> 1000 (NA)	934 ± 178
MCM-41	NA	NA	NA	ND	ND
SBA-15	NA	NA	NA	ND	ND

[a] NA=no activity detected in the studied range. ND=not determined.

The best response of the studied materials was observed against Fem-x (with M_{50} values from 309 ± 42 μg for 4 to 555 ± 77 μg for 1) and K562 cells (with M_{50} values from 338 ± 18 μg for 2 to 683 ± 50 μg for 1). Moderate activities were observed in HeLa cells (from 508 ± 63 μg of 2 to 912 ± 10 μg of 1).

A slight selectivity on all the studied surfaces for human cancer cells was observed, especially in material 4, which is able to kill approximately 3 Fem-x cells per normal immunocompetent cell (Table 5).

Thus, we observed a different tendency in the anticancer activity to that found using the Q_{50} scale. Surfaces 2 and 4 are the most active on all the human cancer cells, whereas 1 and 3 are always less active than 2 or 4. This phenomenon suggests that the anticancer activity is most likely due to the release of the more active titanocene complex $[\text{Ti}\{\text{Me}_2\text{Si}(\eta^5\text{-C}_5\text{Me}_4)(\eta^5\text{-C}_5\text{H}_4)\}\text{Cl}_2]$, taking into account that the grafted titanium content (Ti%) is quite similar in 1 and 3 relative to 2 and 4, respectively.

Conclusions

The cytotoxic activity and selectivity of titanocene-functionalized MCM-41 and SBA-15 is reported. This is the first study of cytotoxicity of mesoporous materials functionalized with biologically active metal complexes. We observed that unmodified MCM-41 and SBA-15 are only marginally active, and therefore the cytotoxicity of the modified surfaces is due to either the release of the grafted titanocene complexes or the action of the functionalized particles. We studied the cytotoxicity in terms of the recently reported Q_{50} system (the number of particles required to reduce normal cell growth by 50%).^[34] Modification of these materials by grafting with anticancer organometallic drugs such as titanocene complexes, led to a higher cytotoxic activity of MCM-41 surfaces relative to that reported previously for mesoporous materials modified with organic drugs.^[34]

As the estimation of the Q_{50} values may lead to a slight uncertainty, we also discussed the anticancer activity of all the studied surfaces in terms of M_{50} values (quantity of material needed to inhibit normal cell growth by 50%), which seems to be a more precise comparative scale.

Surfaces 2 and 4 are the most active on all the human cancer cells, whereas unmodified MCM-41 and SBA-15 materials were not active in the studied range. We observed a slight selectivity of surface 4 for human cancer cells, suggesting that the anticancer activity may be due to the release of the more active titanocene complex $[\text{Ti}\{\text{Me}_2\text{Si}(\eta^5\text{-C}_5\text{Me}_4)(\eta^5\text{-C}_5\text{H}_4)\}\text{Cl}_2]$ and not to the particle as was reported by Di Pasqua et al.^[34]

Future work, already in progress, will now focus on the mechanism of action of the functionalized mesoporous materials with the aim to observe whether the grafted anticancer drug or the mesoporous particle is responsible for the cell death. Until this problem is solved, reports on anticancer tests using this very novel method should include and discuss both Q_{50} and M_{50} scales when comparing the different studied materials.

We will also focus on improving the cytotoxic nature of these surfaces by the grafting of many different anticancer drugs based on titanocene complexes to increase the percentage of titanium in the surface and study the influence of the different amounts of titanium on the final cytotoxicity. Furthermore, modification of the surfaces with titanocene complexes bearing alkenyl groups, which have proved to be very active as antitumoural agents in solution,^[45,46] will be investigated. The introduction of other functional groups at the cyclopentadienyl ligand will also be studied.

In conclusion, this work opens up the possibility of studying many promising organometallic complexes that because of their lack of solubility have been disregarded in this field. In addition, the support onto mesoporous materials may avoid the problems associated with water solubility in the application of organometallic complexes in biological media. Finally, taking into account the observed tendency of the accumulation of some macromolecules in tumor regions,^[59–61] modification of surfaces with metal anticancer drugs may

Reproduced from Ref. D. Pérez-Quintanilla, S. Gómez-Ruiz, Ž. Žižak, I. Sierra, S. Prashar, I. del Hierro, M. Fajardo, Z.D. Juranić, G.N. Kaluđerović, Chem. - Eur. J. 2009, 15, 5588 with permission from John Wiley and Sons.

lead to better delivery and accumulation of the active species in the cellular target.

Experimental Section

Materials and methods: All manipulations were performed under dry nitrogen gas using standard Schlenk techniques and a dry box. Solvents were distilled from the appropriate drying agents and degassed before use. Methylcyclopentadiene, $C_5H_2Me_4$, $[TiCl_4(thf)_2]$, $SiMe_2Cl_2$, and Li^iBu (1.6 M in hexane) were purchased from Aldrich and used without further purification.

Preparation of mesoporous materials: MCM-41 was prepared according to the method of Landau et al. using hydrothermal crystallization, dehydroxylated under vacuum (10^{-2} mmHg) for 16 h at 500 °C, cooled, and stored under dry nitrogen.^[62] SBA-15 was prepared using a poly(alkaline oxide) triblock copolymer surfactant in an acidic medium according to the method of Zhao et al.^[56]

Synthesis of titanocene complexes: $[Ti(\eta^5-C_5H_4Me)_2Cl_2]$ was prepared by the reaction of $[TiCl_4(thf)_2]$ and $Na(C_5H_4Me)^{[63]}$ (1:2) in toluene. $[Ti\{Me_2Si(\eta^5-C_5Me_4)(\eta^5-C_5H_4)\}Cl_2]$ was prepared according to literature procedures.^[64]

Characterization of the materials: 1H , ^{13}C CP, and ^{29}Si MAS NMR spectra were recorded on a Varian-Infinity Plus Spectrometer at 400 MHz operating at 100.52 MHz proton frequency (4 μ s 90° pulse, 4000 transients, spinning speed of 6 MHz, contact time 3 ms, pulse delay 1.5 s). X-ray diffraction (XRD) pattern of the silica samples were obtained on a Phillips Diffractometer model PW3040/00 X'Pert MPD/MRD at 45 kV and 40 mA using the wavelength of Cu K α ($\lambda = 1.5418$ Å). The thermal stability of the modified mesoporous silica samples was studied using a SetSYS 18 A (Setaram) thermogravimetric analyzer with a 100 μ L platinum crucible. A synthetic air atmosphere was used and the temperature increased from 25 °C to 800 °C at a speed of 10 °C per minute. N_2 gas adsorption-desorption isotherms were recorded on a Micromeritics TriStar 3000 analyzer. Scanning electron micrographs and morphological analysis were carried out on a XL30 ESEM Philips with an energy-dispersive spectrometry system (EDS).

The samples were treated with a sputtering method with the following parameters: sputter time 100 s, sputter current 30 mA, and film thickness 20 nm using sputter coater BAL-TEC SCD 005. Conventional transmission electron microscopy (TEM) was carried out on a TECNAI 20 Philips microscope operating at 200 kV.

Preparation of modified surfaces: MCM-41/ $[Ti(\eta^5-C_5H_4Me)_2Cl_2]$ (1): A solution of $[Ti(\eta^5-C_5H_4Me)_2Cl_2]$ (105 mg, 0.37 mmol) (to obtain a theoretical level of 3% Ti/SiO $_2$) in toluene (30 mL) was added to dehydroxylated MCM-41 (0.60 g) and the mixture was stirred at 60 °C for 16 h. The slurry was filtered through fritted disks, and the solid residue was washed with toluene (3 \times 200 mL). The resultant solid was dried under vacuum at room temperature for 16 h to give a pale brown free flowing powder. 1H CP MAS NMR: $\delta = 1.78, 2.88, 4.08$ (Me), 7.02, 7.73 ppm (Cp); ^{13}C CP MAS NMR: $\delta = 14.0$ (Me), 119.5, 178.8 ppm (Cp).

MCM-41/ $[Ti\{Me_2Si(\eta^5-C_5Me_4)(\eta^5-C_5H_4)\}Cl_2]$ (2): The modified mesoporous surface **2** was prepared by following the procedure described for **1**, but using MCM-41 (0.60 g) and $[Ti\{Me_2Si(\eta^5-C_5Me_4)(\eta^5-C_5H_4)\}Cl_2]$ (131 mg, 0.37 mmol). 1H CP MAS NMR: $\delta = 1.64$ (SiMe $_2$), 3.37 (Me of Cp), 8.16 ppm (Cp); ^{13}C CP MAS NMR: $\delta = -2.1$ (SiMe $_2$), 12.8 (Me of Cp), 76.6, 85.1 ppm (Cp).

SBA-15/ $[Ti(\eta^5-C_5H_4Me)_2Cl_2]$ (3): The modified mesoporous surface **3** was prepared by following the procedure described for **1**, but using SBA-15 (0.60 g) and $[Ti(\eta^5-C_5H_4Me)_2Cl_2]$ (105 mg, 0.37 mmol). 1H CP MAS NMR: $\delta = 1.78, 2.88, 4.08$ (Me), 7.02, 7.73 ppm (Cp); ^{13}C CP MAS NMR: $\delta = 15.5, 21.4$ (Me), 120.3, 128.8, 179.3 ppm (Cp).

SBA-15/ $[Ti\{Me_2Si(\eta^5-C_5Me_4)(\eta^5-C_5H_4)\}Cl_2]$ (4): The modified mesoporous surface **4** was prepared by following the procedure described for **1**, but using SBA-15 (0.60 g) and $[Ti\{Me_2Si(\eta^5-C_5Me_4)(\eta^5-C_5H_4)\}Cl_2]$ (131 mg, 0.37 mmol). 1H CP MAS NMR: $\delta = 1.64$ (SiMe $_2$), 3.86 (Me of

Cp), 6.34, 8.82 ppm (Cp); ^{13}C CP MAS NMR: $\delta = -1.5$ (SiMe $_2$), 13.4 (Me of Cp), 129.3, 139.4 ppm (Cp).

In vitro studies: Drug preparation: Stock suspensions of the mesoporous materials modified with titanocene complexes were prepared in dimethyl sulfoxide (DMSO) at a proportion of 50 mg mL $^{-1}$ (**1-4**) or 75 mg mL $^{-1}$ (MCM-41 and SBA-15), diluted by nutrient medium to various working concentrations, and used immediately. The nutrient medium was RPMI 1640 medium, without phenol red, supplemented with L-glutamine (3 mM), streptomycin (100 μ g mL $^{-1}$), penicillin (100 IU mL $^{-1}$), 10% fetal bovine serum (FBS), and 25 mM HEPES (2-[4-(2-hydroxyethyl)-1-piperazinyl]ethanesulfonic acid) and adjusted to pH 7.2 with bicarbonate solution. MTT (3-(4,5-dimethylthiazol-2-yl)-2,5-diphenyltetrazolium bromide) was dissolved (5 mg mL $^{-1}$) in phosphate buffered saline pH 7.2 and filtered through a millipore filter (0.22 μ m) before use. All reagents were purchased from Sigma Chemicals.

Cell culture: Human cervix adenocarcinoma HeLa and malignant melanoma Fem-x cells were cultured as monolayers in the nutrient medium, whereas human myelogenous leukemia K562 cells were maintained as suspension culture. The cells were grown at 37 °C in 5% CO $_2$ and humidified air atmosphere. Peripheral blood mononuclear cells (PBMC) were separated from whole heparinized blood from healthy volunteers by Lymphoprep (Nycomed, Oslo, Norway) gradient centrifugation. Interface cells, washed three times with Haemacel (aqueous solution supplemented with 145 mM Na $^+$, 5.1 mM K $^+$, 6.2 mM Ca $^{2+}$, 145 mM Cl $^-$, and 35 g L $^{-1}$ gelatine polymers, pH 7.4) were counted and resuspended in nutrient medium.

Cell sensitivity analysis: HeLa and Fem-x (2000 cells per well) were seeded into 96-well microtiter plates. After the cell adherence (20 h later), four different proportions of the investigated compounds were added to the wells. Final proportions were in the range 125–1000 μ g mL $^{-1}$ for **1-4** and 187.5–1500 μ g mL $^{-1}$ for MCM-41 and SBA-15. The studied compounds were added to a suspension of leukemia K562 cells (3000 cells per well) 2 h after cell seeding in the same final concentrations applied to HeLa and Fem-x cells. All experiments were carried out in triplicate. PBMC samples were seeded (150 000 cells per well) in nutrient medium only or in nutrient medium enriched with phytohaemagglutinin (PHA; 5 μ g mL $^{-1}$; Wellcome Diagnostics, England) in 96-well microtiter plates and 2 h later, the studied compounds were added to the wells, in triplicate, to five final proportions. Only nutrient medium was added to the cells in the control wells. Nutrient medium with corresponding concentrations of compounds, but void of cells was used as a blank.

Determination of target cell survival: Cell survival was determined by an MTT test according to the method of Mosmann^[65] and modified by Ohno and Abe.^[66] MTT solution (20 μ L; 5 mg mL $^{-1}$ in phosphate buffered saline) was gently added to each well. Samples were incubated for a further 4 h at 37 °C in a humidified atmosphere with 5% CO $_2$. Then, 10% SDS (100 μ L) was added to the wells. The absorbance was measured at 570 nm the next day. Cell survival percentages were determined by the absorbance at 570 nm of a sample of cells grown in the presence of various concentrations of agent divided by the absorbance of a control sample (the absorbance of cells grown only in nutrient medium), after subtracting the absorbance of the blank from the absorbance of the corresponding sample with target cells.

Computational details: DFT calculations were performed with the Gaussian03 program package^[67] using the B3LYP functional.^[68-71] The 6-31G** basis set was used for all atoms.^[72-75] The appropriateness of the chosen functional and basis set for titanium complexes have been stated elsewhere.^[76] All systems were optimized without symmetry restrictions. The resulting geometries were characterized as equilibrium structures by analysis of the force constants of normal vibrations (see the Supporting Information). The radii of complexes were estimated by calculating the molecular volume as defined by the contour of constant electron density, equating this (nonspherical) molecular volume to the radius of an (ideally spherical) cavity, and adding a constant increment for the closest possible approach of solvent molecules as implemented in Gaussian03.^[67]

Reproduced from Ref. D. Pérez-Quintanilla, S. Gómez-Ruiz, Ž. Žižak, I. Sierra, S. Prashar, I. del Hierro, M. Fajardo, Z.D. Juranić, G.N. Kaluderović, *Chem. - Eur. J.* 2009, 15, 5588 with permission from John Wiley and Sons.

Acknowledgements

We gratefully acknowledge financial support from the Ministerio de Educación y Ciencia, Spain (Grant no. CTQ2005-07918-C02-02/BQU), Comunidad de Madrid-URJC (CCG07-URJC/PPQ-149), and the Ministry of Science and Environmental Protection of the Republic of Serbia (Grant Nos. 142010 and 145006).

- [1] J. S. Beck, J. C. Vartuli, W. J. Roth, M. E. Leonowicz, C. T. Kresge, K. D. Schmitt, C. T.-W. Chu, D. H. Olson, E. W. Sheppard, S. B. Higgins, J. L. Schlenker, *J. Am. Chem. Soc.* **1992**, *114*, 10834–10843.
- [2] X. S. Zhao, G. Q. Lu, X. Hu, *Chem. Commun.* **1999**, 1391–1392.
- [3] A. Firouzi, F. Atef, A. G. Oertly, G. D. Stucky, B. Chmelka, *J. Am. Chem. Soc.* **1997**, *119*, 3596–3610.
- [4] D. Zhao, J. P. Feng, Q. S. Huo, N. Melosh, G. H. Fredrickson, B. F. Chmelka, G. D. Stucky, *Science* **1998**, *279*, 548–552.
- [5] C. T. Kresge, M. E. Leonowicz, W. J. Roth, J. C. Vartuli, J. S. Beck, *Nature* **1992**, *359*, 710–712.
- [6] M. Vallet-Regí, *Chem. Eur. J.* **2006**, *12*, 5934–5943.
- [7] C. Y. Lai, B. G. Trewyn, D. M. Jeftinija, K. Jeftinija, S. Xu, S. Jeftinija, V. S. Lin, *J. Am. Chem. Soc.* **2003**, *125*, 4451–4459.
- [8] V. Chupin, A. I. de Kroon, B. de Kruljff, *J. Am. Chem. Soc.* **2004**, *126*, 13816–13821.
- [9] Z. Yinghuai, A. T. Peng, K. Carpenter, J. A. Maguire, N. S. Hosmane, M. Takagaki, *J. Am. Chem. Soc.* **2005**, *127*, 9875–9880.
- [10] M. Conti, V. Tazzari, C. Baccini, G. Pertici, L. P. Serino, U. De Giorgi, *In Vivo* **2006**, *20*, 697–701.
- [11] Q. Tang, Y. Xu, D. Wu, Y. Sun, *J. Solid State Chem.* **2006**, *179*, 1513–1520.
- [12] J. Andersson, J. Rosenholm, S. Areva, M. Lindén, *Chem. Mater.* **2004**, *16*, 4160–4167.
- [13] I. Slowing, B. G. Trewyn, V. S. Lin, *J. Am. Chem. Soc.* **2006**, *128*, 14792–14793.
- [14] J. Gao, G. Liang, B. Zhang, Y. Kuang, X. Zhang, B. Xu, *J. Am. Chem. Soc.* **2007**, *129*, 1428–1433.
- [15] R. P. Feazell, N. Nakayama-Ratchford, H. Dai, S. L. Lippard, *J. Am. Chem. Soc.* **2007**, *129*, 8438–8439.
- [16] G. Han, P. Ghosh, V. M. Rotello, *Nanomedicine* **2007**, *2*, 113–123.
- [17] C. Charnay, S. Begu, C. Tourne-Peteilh, L. Niolle, D. A. Lerner, J. M. Devoisselle, *Eur. J. Pharm. Biopharm.* **2004**, *57*, 533–540.
- [18] Q.-L. Tang, Y. Xu, D. Wu, Y.-H. Sun, J. Wang, J. Xu, F. Deng, *J. Controlled Release* **2006**, *114*, 41–46.
- [19] M. Vallet-Regí, A. Rámila, R. P. del Real, J. Pérez-Pariente, *Chem. Mater.* **2001**, *13*, 308–311.
- [20] B. Muñoz, A. Rámila, I. Díaz, J. Pérez-Pariente, M. Vallet-Regí, *Chem. Mater.* **2003**, *15*, 500–503.
- [21] A. Rámila, B. Muñoz, J. Pérez-Pariente, M. Vallet-Regí, *J. Sol-Gel Sci. Technol.* **2003**, *26*, 1199–1202.
- [22] A. L. Doadrio, E. M. B. Sousa, J. C. Doadrio, J. Pérez-Pariente, I. Izquierdo-Barba, M. Vallet-Regí, *J. Controlled Release* **2004**, *97*, 125–132.
- [23] M. Vallet-Regí, J. C. Doadrio, A. L. Doadrio, I. Izquierdo-Barba, J. Pérez-Pariente, *Solid State Ionics* **2004**, *172*, 435–439.
- [24] C. Charnay, S. Bégu, C. Tourné-Péteilh, L. Nicole, D. A. Lerner, J. M. Devoisselle, *Eur. J. Pharm. Biopharm.* **2004**, *57*, 533–540.
- [25] P. Horcajada, A. Rámila, J. Pérez-Pariente, M. Vallet-Regí, *Microporous Mesoporous Mater.* **2004**, *68*, 105–109.
- [26] J. Andersson, J. Resenholm, S. Arev, M. Linden, *Chem. Mater.* **2004**, *16*, 4160–4167.
- [27] B. G. Trewyn, C. M. Whitman, V. S.-Y. Lin, *Nano Lett.* **2004**, *4*, 2139–2143.
- [28] C.-Y. Lai, B. G. Trewyn, D. M. Jeftinifa, K. Jeftinifa, S. Xu, S. Jeftinifa, V. Lin, *J. Am. Chem. Soc.* **2003**, *125*, 4451–4459.
- [29] W. Zeng, X.-F. Qian, Y. B. Zhang, J. Yin, Z. K. Zhu, *Mater. Res. Bull.* **2005**, *40*, 766–772.
- [30] M. Vallet-Regí, L. Ruiz-González, I. Izquierdo-Barba, J. M. González-Calbet, *J. Mater. Chem.* **2006**, *16*, 26–31.
- [31] W. Zeng, X.-F. Qian, J. Yin, Z.-K. Zhu, *Mater. Chem. Phys.* **2006**, *97*, 437–441.
- [32] W. Zeng, X.-F. Qian, J. Yin, Z.-K. Zhu, *Mater. Res. Bull.* **2005**, *40*, 766–772.
- [33] J. Lu, M. Liong, J. I. Zink, F. Tamanoi, *Small* **2007**, *3*, 1341–1346.
- [34] A. J. Di Pasqua, K. K. Sharma, Y.-L. Shi, B. B. Toms, W. Ouellette, J. C. Dabrowiak, T. Asefa, *J. Inorg. Biochem.* **2008**, *102*, 1416–1423.
- [35] M. A. Jakupcic, M. Galanski, V. B. Arion, C. G. Hartinger, B. K. Keppler, *Dalton Trans.* **2008**, 183–194.
- [36] S. K. Hadjikakou, N. Hadjiliadis, *Coord. Chem. Rev.* **2009**, *253*, 235–249.
- [37] K. Strohfeldt, M. Tacke, *Chem. Soc. Rev.* **2008**, *37*, 1174–1187.
- [38] P. M. Abeyasinghe, M. M. Harding, *Dalton Trans.* **2007**, 3474–3482.
- [39] D. Pérez-Quintanilla, I. del Hierro, M. Fajardo, I. Sierra, *Microporous Mesoporous Mater.* **2006**, *89*, 58–68.
- [40] D. Pérez-Quintanilla, I. del Hierro, M. Fajardo, I. Sierra, *J. Environ. Monit.* **2006**, *8*, 214–222.
- [41] D. Pérez-Quintanilla, I. del Hierro, M. Fajardo, I. Sierra, *J. Hazard. Mater.* **2006**, *134*, 245–256.
- [42] D. Pérez-Quintanilla, I. del Hierro, M. Fajardo, I. Sierra, *J. Mater. Chem.* **2006**, *16*, 1757–1764.
- [43] D. Pérez-Quintanilla, A. Sánchez, I. del Hierro, M. Fajardo, I. Sierra, *J. Sep. Sci.* **2007**, *30*, 1556–1567.
- [44] D. Pérez-Quintanilla, A. Sánchez, I. del Hierro, M. Fajardo, I. Sierra, *J. Colloid Interface Sci.* **2007**, *313*, 551–562.
- [45] S. Gómez-Ruiz, G. N. Kaluderović, D. Polo-Cerón, S. Prashar, M. Fajardo, Ž. Žižak, Z. D. Juranić, T. J. Sabo, *Inorg. Chem. Commun.* **2007**, *10*, 748–752.
- [46] S. Gómez-Ruiz, G. N. Kaluderović, S. Prashar, D. Polo-Cerón, M. Fajardo, Ž. Žižak, T. J. Sabo, Z. D. Juranić, *J. Inorg. Biochem.* **2008**, *102*, 1558–1570.
- [47] M. E. Kelly, A. Dietrich, S. Gómez-Ruiz, B. Kalinowski, G. N. Kaluderović, T. Müller, R. Paschke, J. Schmidt, D. Steinborn, C. Wagner, H. Schmidt, *Organometallics* **2008**, *27*, 4917–4927.
- [48] S. Gruric-Šipka, M. A. M. Alshetwi, D. Jeremić, G. N. Kaluderović, S. Gómez-Ruiz, Ž. Žižak, Z. D. Juranić, T. J. Sabo, *J. Serb. Chem. Soc.* **2008**, *73*, 619–630.
- [49] S. Gómez-Ruiz, G. N. Kaluderović, S. Prashar, E. Hey-Hawkins, A. Erić, Ž. Žižak, Z. D. Juranić, *J. Inorg. Biochem.* **2008**, *102*, 2087–2096.
- [50] C. Alonso, A. Antiñolo, F. Carrillo-Hermosilla, P. Carrión, A. Otero, J. Sancho, E. Villaseñor, *J. Mol. Catal. A* **2004**, *220*, 285–295.
- [51] C. Alonso-Moreno, A. Antiñolo, F. Carrillo-Hermosilla, P. Carrión, I. López-Solera, A. Otero, S. Prashar, J. Sancho, *Eur. J. Inorg. Chem.* **2005**, 2924–2934.
- [52] C. Alonso-Moreno, D. Pérez-Quintanilla, D. Polo-Cerón, S. Prashar, I. Sierra, I. del Hierro, M. Fajardo, *J. Mol. Catal. A* **2009**, in press, DOI: 10.1066/j.molcata.2009.01.034.
- [53] H. Rahiala, I. Beurroies, T. Eklund, K. Hakala, R. Gougeon, P. Trens, J. B. Rosenholm, *J. Catal.* **1999**, *188*, 14–23.
- [54] L. Reven, *J. Mol. Catal.* **1994**, *86*, 447–477.
- [55] G. Engelhardt, D. Michel, *High-resolution Solid-State NMR of Silicates and Zeolites*, Wiley, New York, **1987**.
- [56] D. Zhao, Q. Huo, J. Feng, B. F. Chmelka, G. D. Stucky, *J. Am. Chem. Soc.* **1998**, *120*, 6024–6036.
- [57] K. S. W. Sing, D. H. Everett, R. A. W. Haul, L. Moscou, R. A. Pierotti, J. Rouquérol, T. Siemieniowska, *Pure Appl. Chem.* **1985**, *57*, 603–620.
- [58] S. Gómez-Ruiz, G. N. Kaluderović, Ž. Žižak, I. Besu, Z. D. Juranić, S. Prashar, M. Fajardo, *J. Organomet. Chem.* **2009**, DOI: 10.1016/j.jorganchem.2009.01.05.
- [59] M. R. Dreher, W. Liu, C. R. Michelich, M. W. Dewhirst, F. Yuan, A. Chilkoti, *J. Natl. Cancer Inst.* **2006**, *98*, 335–344.
- [60] D. Garmann, A. Warnecke, G. V. Kalayda, F. Kratz, U. Jaehde, *J. Controlled Release* **2008**, *131*, 100–106.
- [61] Y. W. Cho, Y.-S. Kim, I.-S. Kim, R.-W. Park, S. J. Oh, D. H. Moon, S. Y. Kim, I. C. Kwon, *Macromol. Res.* **2008**, *16*, 15–20.
- [62] M. V. Landau, S. P. Varkey, M. Herskowitz, O. Regev, S. Pevzner, T. Sen, Z. Luz, *Microporous Mesoporous Mater.* **1999**, *33*, 149–163.

Reproduced from Ref. D. Pérez-Quintanilla, S. Gómez-Ruiz, Ž. Žižak, I. Sierra, S. Prashar, I. del Hierro, M. Fajardo, Z.D. Juranić, G.N. Kaluđerović, *Chem. - Eur. J.* 2009, 15, 5588 with permission from John Wiley and Sons.

- [63] T. K. Panda, M. T. Gamer, P. W. Roesky, *Organometallics* **2003**, 22, 877–890.
- [64] G. Tian, B. Wang, X. Dai, S. Xu, X. Zhou, J. Sun, *J. Organomet. Chem.* **2001**, 634, 145–152.
- [65] T. Mosmann, *J. Immunol. Methods* **1983**, 65, 55–63.
- [66] M. Ohno, T. Abe, *J. Immunol. Methods* **1991**, 145, 199–203.
- [67] Gaussian 03, Revision C.02, Gaussian, M. J. Frisch, G. W. Trucks, H. B. Schlegel, G. E. Scuseria, M. A. Robb, J. R. Cheeseman, J. A. Montgomery, Jr., T. Vreven, K. N. Kudin, J. C. Burant, J. M. Millam, S. S. Iyengar, J. Tomasi, V. Barone, B. Mennucci, M. Cossi, G. Scalmani, N. Rega, G. A. Petersson, H. Nakatsuji, M. Hada, M. Ehara, K. Toyota, R. Fukuda, J. Hasegawa, M. Ishida, T. Nakajima, Y. Honda, O. Kitao, H. Nakai, M. Klene, X. Li, J. E. Knox, H. P. Hratchian, J. B. Cross, V. Bakken, C. Adamo, J. Jaramillo, R. Gomperts, R. E. Stratmann, O. Yazyev, A. J. Austin, R. Cammi, C. Pomelli, J. W. Ochterski, P. Y. Ayala, K. Morokuma, G. A. Voth, P. Salvador, J. J. Dannenberg, V. G. Zakrzewski, S. Dapprich, A. D. Daniels, M. C. Strain, O. Farkas, D. K. Malick, A. D. Rabuck, K. Raghavachari, J. B. Foresman, J. V. Ortiz, Q. Cui, A. G. Baboul, S. Clifford, J. Cioslowski, B. B. Stefanov, G. Liu, A. Liashenko, P. Piskorz, I. Komaromi, R. L. Martin, D. J. Fox, T. Keith, M. A. Al-Laham, C. Y. Peng, A. Nanayakkara, M. Challacombe, P. M. W. Gill, B. Johnson, W. Chen, M. W. Wong, C. Gonzalez, J. A. Pople, Inc., Wallingford CT, **2004**.
- [68] A. D. Becke, *J. Chem. Phys.* **1993**, 98, 5648–5652.
- [69] C. Lee, W. Yang, R. G. Parr, *Phys. Rev. B* **1988**, 37, 785–789.
- [70] S. H. Vosko, L. Wilk, M. Nusair, *Can. J. Phys.* **1980**, 58, 1200–1211.
- [71] P. J. Stephens, F. J. Devlin, C. F. Chabalowski, M. J. Frisch, *J. Phys.-Chem.* **1994**, 98, 11623–11627.
- [72] W. J. Hehre, R. Ditchfield, J. A. Pople, *J. Chem. Phys.* **1972**, 56, 2257–2261.
- [73] J. D. Dill, J. A. Pople, *J. Chem. Phys.* **1975**, 62, 2921–2923.
- [74] M. M. Francl, W. J. Pietro, W. J. Hehre, J. S. Binkley, M. S. Gordon, D. J. DeFrees, J. A. Pople, *J. Chem. Phys.* **1982**, 77, 3654–3665.
- [75] V. Rassolov, J. A. Pople, M. A. Ratner, T. L. Windus, *J. Chem. Phys.* **1998**, 109, 1223–1229.
- [76] C. Pampillón, J. Claffey, M. Hogan, M. Tacke, *BioMetals* **2008**, 21, 197–204.

Received: January 19, 2009
Published online: April 15, 2009

Improvement of cytotoxicity of titanocene-functionalized mesoporous materials by the increase of the titanium content†

Goran N. Kaluđerović,^{*a,b} Damián Pérez-Quintanilla,^{*c} Željko Žižak,^d Zorica D. Juranić^d and Santiago Gómez-Ruiz^{*c}

Received 25th September 2009, Accepted 30th November 2009

First published as an Advance Article on the web 27th January 2010

DOI: 10.1039/b920051g

The reaction of $[\text{Ti}(\eta^5\text{-C}_5\text{H}_5)_2\text{Cl}_2]$ (**1**), with 3-mercaptopropyltrimethoxysilane or 3-mercaptopropyltriethoxysilane in the presence of triethylamine leads to the formation of the thiolate complexes $[\text{Ti}(\eta^5\text{-C}_5\text{H}_5)_2\{\text{SCH}_2\text{CH}_2\text{CH}_2\text{Si}(\text{OMe})_3\}_2]$ (**2**) and $[\text{Ti}(\eta^5\text{-C}_5\text{H}_5)_2\{\text{SCH}_2\text{CH}_2\text{CH}_2\text{Si}(\text{OEt})_3\}_2]$ (**3**), respectively. Complexes **2** and **3** have been characterized by traditional methods, in addition, structural studies based on DFT calculations are reported. **1–3** have been grafted onto dehydroxylated MCM-41 to give the novel materials MCM-41/ $[\text{Ti}(\eta^5\text{-C}_5\text{H}_5)_2\text{Cl}_2]$ (**S1**), MCM-41/ $[\text{Ti}(\eta^5\text{-C}_5\text{H}_5)_2\{\text{SCH}_2\text{CH}_2\text{CH}_2\text{Si}(\text{OMe})_3\}_2]$ (**S2**) and MCM-41/ $[\text{Ti}(\eta^5\text{-C}_5\text{H}_5)_2\{\text{SCH}_2\text{CH}_2\text{CH}_2\text{Si}(\text{OEt})_3\}_2]$ (**S3**) which have been characterized by powder X-ray diffraction, X-ray fluorescence, nitrogen gas sorption, multinuclear MAS NMR spectroscopy, thermogravimetry, UV spectroscopy, SEM and TEM. Materials **S2** and **S3** present much higher values of Ti wt% (ca. 3%) than **S1** (ca. 1%), indicating the higher functionalization rate induced by the substitution of the chloro ligands by the thiolato ligands in the starting titanocene derivatives. The cytotoxicity of the non-functionalized MCM-41 and **S1–S3** toward human cancer cell lines such as adenocarcinoma HeLa, human myelogenous leukemia K562 and human malignant melanoma Fem-x has been studied. In addition the cytotoxicity of these materials on normal immunocompetent cells such as stimulated (PBMC+PHA) and non-stimulated (PBMC-PHA) peripheral blood mononuclear cells have been also studied. M_{50} values (quantity of material needed to inhibit normal cell survival by 50%) of the studied surfaces show that non-functionalized MCM-41 was not active against any of the studied cells, while the functionalized surfaces **S1–S3** were active against all the tested human cancer cells. The cytotoxic activity of surfaces **S2** and **S3** were very similar, however, **S1** showed lower cytotoxic activity. This phenomenon indicates that the cytotoxicity of the titanocene-functionalized materials strongly depends on the titanium content.

1. Introduction

Drug delivery systems based on biomaterials is a new research field which has been developed during the last 20 years.^{1–3} In this context, nano-sized surfaces have been widely used to maximize the efficacy of several anticancer drugs.⁴ Nanostructured materials such as mesoporous silica have been extensively studied, observing their bioactive behaviour in simulated body fluids,⁵ which included, in some cases, an appearance of a carbonate

hydroxyapatite layer⁶ that supported their ability to be used for possible medical applications.⁷ In addition, their capability of adsorbing small molecules of pharmacological interest have attracted the attention of many research groups.^{8–30}

One of the possible applications of these nanostructured mesoporous materials is the fight against cancer, especially against bone tumors, due to the observed bioactivity on bone regeneration.^{31–34} Thus, Asefa and coworkers modified MCM-41 by grafting with organic compounds, obtaining new materials with a moderate cytotoxic activity,⁹ attributed to the cytotoxic activity of the functionalized nanostructured particles.

Recent studies carried out by our research group on titanocene-functionalized MCM-41 and SBA-15, have shown a dependence of the grafted titanocene complex on the final cytotoxicity on several human cancer cell lines.^{29–30} In addition, our studies showed a marginal cytotoxic activity of unmodified MCM-41 and SBA-15. In spite of the observations of Asefa and coworkers, we implied the cytotoxic nature of the functionalized materials to be due to the metal complex action, after a controlled release in the biological medium.³⁰ However, many other parameters such as particle size or pore diameter may also be influencing the cytotoxic activity of this novel class of materials. Additionally, an increase of the functionalization rate may also be essential for the improvement of the anticancer activity and subsequent use of these materials

^aInstitut für Chemie, Martin-Luther-Universität Halle-Wittenberg, Kurt-Mothes-Straße 2, D-06120, Halle, Germany. E-mail: goran.kaluderovic@chemie.uni-halle.de

^bDepartment of Chemistry, Institute of Chemistry, Technology and Metallurgy, University of Belgrade, Studentski trg 14, 11000, Belgrade, Serbia. E-mail: goran@chem.bg.ac.rs

^cDepartamento de Química Inorgánica y Analítica, E.S.C.E.T., Universidad Rey Juan Carlos, 28933, Móstoles, Madrid, Spain. E-mail: santiago.gomez@urjc.es, damian.perez@urjc.es; Fax: 34 914888143; Tel: 34 914888527

^dInstitute of Oncology and Radiology of Serbia, 11000, Belgrade, Serbia

† Electronic supplementary information (ESI) available: Solid-state ¹H MAS NMR spectra of **S1–S3**, ¹³C CP MAS NMR spectrum of **S1**, ²⁹Si MAS NMR spectrum of **S1**, UV-vis spectra of **S1–S3**, FT-IR of **S1–S3**, pore distribution of **S1–S3**, thermogravimetric curve of **S1** and full details and figures of the DFT calculations of titanocene derivatives **2** and **3**. See DOI: 10.1039/b920051g

as bone fillers for *in situ* treatment of bone tumors such as osteosarcoma or chondroblastoma upon local implantations which may avoid recurrence of the tumor.

As in previous studies carried out by our research group, a relatively low titanium content (between 0.8 and 1.4% wt) of the titanocene-functionalized MCM-41 or SBA-15 was observed,²⁹⁻³⁰ we decided to study other functionalization reactions starting from different titanocene derivatives containing ligands with $-\text{Si}(\text{OMe})_3$ or $-\text{Si}(\text{OEt})_3$ moieties, in order to achieve a higher titanium content on the final surface.

Thus, we present herein the synthesis and characterization of new titanocene(IV) thiolate complexes which have been used in the preparation of novel mesoporous MCM-41 materials with higher titanium contents of *ca.* 3%. All the surfaces with higher functionalization rates, showed higher cytotoxic activity on all the studied cancer cells indicating a dependence of the grafted titanocene complex content on the final anticancer activity.

2. Materials and methods

All manipulations were performed under dry nitrogen gas using standard Schlenk techniques and a dry box. Solvents were distilled from the appropriate drying agents and degassed before use.

2.1 General remarks on the characterization of the titanocene complexes

^1H and $^{13}\text{C}\{^1\text{H}\}$ NMR spectra were recorded on a Varian Mercury FT-400 spectrometer and referenced to the residual deuterated solvent. Microanalyses were carried out with a Perkin-Elmer 2400 microanalyzer. IR spectra (KBr pellets were prepared in a nitrogen-filled glove box) were recorded on a Nicolet Avatar 380 FTIR spectrometer in the range 300–4000 cm^{-1} . FAB-MS spectra were recorded on a MASPEC II spectrometer with 3-nitrobenzyl alcohol as matrix.

2.2 General remarks on the characterization of the materials

^1H , ^{13}C -CP and ^{29}Si MAS NMR spectra, were recorded on a Varian-Infinity Plus Spectrometer at 400 MHz operating at 100.52 MHz proton frequency ($4\mu\text{s}$ 90° pulse, 4000 transients, spinning speed of 6 MHz, contact time 3 ms, pulse delay 1.5 s). X-ray diffraction (XRD) patterns of the silicas were obtained on a Phillips Diffractometer model PW3040/00 X'Pert MPD/MRD at 45 KV and 40 mA, using a wavelength $\text{Cu-K}\alpha$ ($\lambda = 1.5418 \text{ \AA}$). Ti and S wt% determination by X-ray fluorescence were carried out with a X-ray fluorescence spectrophotometer Phillips MagiX with an X-ray source of 1 kW and a Rh anode using a helium atmosphere. The quantification method is able to analyze from 0.0001% to 100% titanium and sulfur.

The thermal stability of the modified mesoporous silicas was studied using a Setsys 18 A (Setaram) thermogravimetric analyzer, using a platinum crucible of 100 μL . A synthetic air atmosphere was used and the temperature increased from 25 °C to 800 °C at a speed of 10 °C per minute. N_2 gas adsorption-desorption isotherms were performed using a Micromeritics TriStar 3000 analyzer. Scanning electron micrographs and morphological analysis were carried out on a XL30 ESEM Philips with an energy dispersive spectrometry system (EDS).

The samples were treated with a sputtering method with the following parameters: Sputter time 100 s, Sputter current 30 mA, film thickness 20 nm using a Sputter coater BAL-TEC SCD 005. Conventional transmission electron microscopy (TEM) was carried out on a TECNAI 20 Philips, operating at 200 kV.

2.3 Preparation of mesoporous materials

MCM-41 was prepared according to the method of Landau *et al.* using a hydrothermal crystallization.³⁵ The surface was dehydroxylated under vacuum (10^{-2} mmHg) for 16 h at 500 °C, cooled and stored under dry nitrogen.

2.4 Synthesis of titanocene complexes

3-mercaptopropyltrimethoxysilane or 3-mercaptopropyltriethoxysilane and triethylamine were purchased from Alfa Aesar and used without further purification. $[\text{Ti}(\eta^5\text{-C}_5\text{H}_5)_2\text{Cl}_2]$ was prepared with slight modifications to the literature procedures.³⁶⁻³⁷

Synthesis of $[\text{Ti}(\eta^5\text{-C}_5\text{H}_5)_2\{\text{SCH}_2\text{CH}_2\text{CH}_2\text{Si}(\text{OMe})_3\}_2]$ (2). A solution of 3-mercaptopropyltrimethoxysilane (1.18 g, 6.02 mmol) in toluene (15 mL) was added dropwise over 15 min to a solution of $[\text{Ti}(\eta^5\text{-C}_5\text{H}_5)_2\text{Cl}_2]$ (0.75 g, 3.01 mmol) in toluene (15 mL) at room temperature. The reaction mixture was stirred for 20 min, subsequently NEt_3 (0.87 mL, 6.02 mmol) was added dropwise. The reaction mixture, which then turned violet, was stirred overnight. The mixture was decanted and filtered and the filtrate concentrated (5 mL) and cooled to -30 °C to give purple crystals of the title complex which were isolated by filtration. Yield: 0.89 g, 52%. FT-IR: $\nu(\text{Ti-S}) = 387 \text{ cm}^{-1}$; ^1H NMR (400 MHz, CDCl_3 , 25 °C): δ 0.74, 1.61 and 3.05 (m, 4H each, $-\text{CH}_2$); 3.56 (s, 18H, OMe), 6.13 (s, 10H, C_5H_5); $^{13}\text{C}\{^1\text{H}\}$ NMR (100.6 MHz, CDCl_3 , 25 °C): δ 8.8, 26.4 and 47.9 (CH_2), 50.6 (OMe), 111.4 (C_5H_5); FAB-MS (m/z (relative intensity)): 568.7 (2) $[\text{M}^+]$, 373.1 (30) $[\text{M}^+ - \text{SCH}_2\text{CH}_2\text{CH}_2\text{Si}(\text{OMe})_3]$, 297.0 (100) $[\text{M}^+ - \text{SCH}_2\text{CH}_2\text{CH}_2\text{Si}(\text{OMe})_3 - \text{Cp} - \text{Me}]$; $\text{C}_{22}\text{H}_{40}\text{O}_6\text{S}_2\text{Si}_2\text{Ti}$ (568.72); calc. C, 46.46; H, 7.09; found C, 46.27; H, 7.01%.

Synthesis of $[\text{Ti}(\eta^5\text{-C}_5\text{H}_5)_2\{\text{SCH}_2\text{CH}_2\text{CH}_2\text{Si}(\text{OEt})_3\}_2]$ (3). The synthesis of **3** was carried out in an identical manner to **2**. 3-mercaptopropyltriethoxysilane (1.43 g, 6.02 mmol) and $[\text{Ti}(\eta^5\text{-C}_5\text{H}_5)_2\text{Cl}_2]$ (0.75 g, 3.01 mmol). Yield: 1.22 g, 62%. FT-IR: $\nu(\text{Ti-S}) = 382 \text{ cm}^{-1}$; ^1H NMR (400 MHz, CDCl_3 , 25 °C): δ 0.74, 1.63 and 3.04 (m, 4H each, $-\text{CH}_2$); 1.22 (t, 18H, CH_3 of ethoxy), 3.82 (q, 12H, CH_2 of ethoxy), 6.12 (s, 10H, C_5H_5); $^{13}\text{C}\{^1\text{H}\}$ NMR (100.6 MHz, CDCl_3 , 25 °C): δ 10.2, 26.6 and 48.0 (CH_2), 18.1 and 58.1 (OEt), 111.2 (C_5H_5); FAB-MS (m/z (relative intensity)): 652.8 (5) $[\text{M}^+]$, 415.0 (5) $[\text{M}^+ - \text{SCH}_2\text{CH}_2\text{CH}_2\text{Si}(\text{OEt})_3]$, 321.0 (93) $[\text{M}^+ - \text{SCH}_2\text{CH}_2\text{CH}_2\text{Si}(\text{OEt})_3 - \text{Cp} - \text{Et}]$, 223.1 (100) $[\text{M}^+ - \text{Cp}_2\text{TiSCH}_2\text{CH}_2\text{CH}_2\text{Si}(\text{OEt})_3 - \text{Me}]$; $\text{C}_{28}\text{H}_{52}\text{O}_6\text{S}_2\text{Si}_2\text{Ti}$ (652.88); calc. C, 51.51; H, 8.03; found C, 51.33; H, 7.89%.

2.5 Preparation of modified surfaces

Preparation of MCM-41/ $[\text{Ti}(\eta^5\text{-C}_5\text{H}_5)_2\text{Cl}_2]$ (S1). A solution of $[\text{Ti}(\eta^5\text{-C}_5\text{H}_5)_2\text{Cl}_2]$ (**1**) (260 mg, 1.04 mmol) (to obtain a theoretical level of 5% Ti/SiO_2) in toluene (100 mL) was added to dehydroxylated MCM-41 (1.00 g) and the mixture was stirred overnight at 80 °C. The slurry was filtered through fritted discs and the solid residue washed three times with toluene ($5 \times 200 \text{ mL}$).

The resultant solid was dried under vacuum at room temperature for 16 h to give a pale red free flowing powder. ^1H -MAS NMR: $\delta = 4.18, 4.81$ (Cp); ^{13}C -MAS NMR: $\delta = 120.7, 180.8$ (Cp). ^{29}Si -MAS NMR: $\delta = -109.1$ (Q_4).

Preparation of MCM-41/[Ti(η^5 -C₅H₅)₂{SCH₂CH₂CH₂Si(OMe)₃}₂] (S2). The modified mesoporous surface **2** was prepared following the procedure described for **1**, using MCM-41 (1.00 g) and [Ti(η^5 -C₅H₅)₂{SCH₂CH₂CH₂Si(OMe)₃}₂] (**2**) (591 mg, 1.04 mmol). ^1H -MAS NMR: $\delta = -1.73, 0.32$ and 0.94 (-CH₂), 3.77 (OMe), 4.58 (Cp); ^{13}C -MAS NMR: $\delta = 11.2$ and 30.2 (-CH₂), 52.8 (OMe), $115.7, 131.1$ and 176.3 (Cp). ^{29}Si -MAS NMR: $\delta = -109.1$ (Q_4), -60.4 (T_2), -52.0 (T_3).

Preparation of MCM-41/[Ti(η^5 -C₅H₅)₂{SCH₂CH₂CH₂Si(OEt)₃}₂] (S3). The modified mesoporous surface **3** was prepared following the procedure described for **1**, using MCM-41 (1.00 g) and [Ti(η^5 -C₅H₅)₂{SCH₂CH₂CH₂Si(OEt)₃}₂] (**3**) (647 mg, 1.04 mmol). ^1H -MAS NMR: $\delta = -1.43$ and -0.37 (-CH₂), 1.20 and 3.62 (OEt), 4.48 (Cp); ^{13}C -MAS NMR: $\delta = 13.5, 27.8$ and 46.8 (-CH₂), 18.2 and 61.0 (OEt), $116.9, 131.1$ and 176.3 (Cp). ^{29}Si -MAS NMR: $\delta = -109.1$ (Q_4), -60.4 (T_2), -54.8 (T_3).

2.6 In vitro studies

Drug preparation. Stock suspensions of the mesoporous materials modified with titanocene complexes, were prepared in dimethyl sulfoxide (DMSO) at a proportion of 50 mg mL^{-1} (**S1**–**S3**) or 75 mg mL^{-1} (MCM-41), and diluted by nutrient medium to various working concentrations which were used immediately.

In all cases, nutrient medium was RPMI 1640 medium, without phenol red, supplemented with L-glutamine (3 mM), streptomycin ($100 \text{ } \mu\text{g mL}^{-1}$), and penicillin (100 IU/mL), 10% fetal bovine serum (FBS) and 25 mM Hepes, and was adjusted to pH 7.2 by bicarbonate solution. MTT (3-(4,5-dimethylthiazol-2-yl)-2,5-diphenyl tetrazolium bromide) was dissolved (5 mg mL^{-1}) in phosphate buffer saline pH 7.2, and filtered through Millipore filter, $0.22 \text{ } \mu\text{m}$, before use. All reagents were purchased from Sigma Chemicals.

Cell culture. Human cervix adenocarcinoma HeLa and malignant melanoma Fem-x cells were cultured as monolayers in the nutrient medium, while human myelogenous leukemia K562 cells were maintained as suspension culture. The cells were grown at $37 \text{ }^\circ\text{C}$ in 5% CO₂ and humidified air atmosphere. Peripheral blood mononuclear cells (PBMC) were separated from whole heparinized blood from healthy volunteers by Lymphoprep (Nycopmed, Oslo, Norway) gradient centrifugation. Interface cells, washed three times with Haemacel (aqueous solution supplemented with 145 mM Na^+ , 5.1 mM K^+ , 6.2 mM Ca^{2+} , 145 mM Cl^- and 35 g L^{-1} gelatine polymers, pH 7.4) were counted and resuspended in nutrient medium.

Cell sensitivity analysis. HeLa, Fem-x (2000 cells per well) were seeded into 96-well microtitre plates and 20 h later, after the cell adherence, four different proportions of investigated surfaces were added to the wells. Final proportions were in the range from $125 \text{ } \mu\text{g mL}^{-1}$ to $1000 \text{ } \mu\text{g mL}^{-1}$ for **S1**–**S3** and from $187.5 \text{ } \mu\text{g mL}^{-1}$ to $1500 \text{ } \mu\text{g mL}^{-1}$ for MCM-41. The studied surfaces were added to a suspension of leukemia K562 cells (3000 cells per well) 2 h after cell seeding, in the same final concentrations applied to HeLa

and Fem-x cells. All experiments were carried out in triplicate. PBMC were seeded (150000 cells per well) in nutrient medium enriched with ($5 \text{ } \mu\text{g mL}^{-1}$) phytohaemagglutinin (PHA - Welcome Diagnostics, England) in 96-well microtitre plates and 2 h later, the studied compounds or surfaces were added to the wells, in triplicate, to five final proportions. Only nutrient medium was added to the cells in the control wells. Nutrient medium with corresponding concentrations of compounds, but void of cells was used as blank.

Determination of target cell survival. Cell survival was determined by the MTT test according to the method of Mosmann³⁸ and modified by Ohno and Abe.³⁹ Gently, $20 \text{ } \mu\text{L}$ of MTT solution (5 mg mL^{-1} in phosphate buffered saline) was added to each well. Samples were incubated for a further four hours at $37 \text{ }^\circ\text{C}$ in a humidified atmosphere with 5% CO₂. Then, $100 \text{ } \mu\text{L}$ of 10% SDS was added to the wells. Absorbance was measured at 570 nm the next day. To achieve cell survival percentages, absorbance at 570 nm of a sample with cells grown in the presence of various concentrations of agent was divided with absorbance of control sample (the absorbance of cells grown only in nutrient medium), having subtracted from absorbance of a corresponding sample with target cells the absorbance of the blank.

2.7 DNA-binding studies

Fish sperm-deoxyribonucleic acid (FS-DNA) was purchased from Aldrich. The stock solution of FS-DNA was prepared by dissolving an appropriate amount of FS-DNA in phosphate buffer (pH = 7.4) and storing at $4 \text{ }^\circ\text{C}$ in the dark. The concentration of the DNA stock solution ($2.4 \times 10^{-4} \text{ M}$) was determined from the UV absorption spectrum at 260 nm using the molar absorption coefficient $\epsilon_{260} = 6600 \text{ M}^{-1} \text{ cm}^{-1}$. The purity of the DNA was checked by the measurement of the ratio of the absorbance at 260 nm to that at 280 nm . The resulting ratio indicated that the DNA was sufficiently free from protein.⁴⁰⁻⁴¹

UV absorption spectroscopy experiments were conducted by adding different concentrations ($15, 20$ and 25 mg mL^{-1}) of suspensions of **S2** and **S3** in a mixture of DMSO/phosphate buffer, to the DNA solution (the final DMSO concentration was always lower than 0.5%). The final suspensions were shaken during 30 min at $35 \text{ }^\circ\text{C}$ and used immediately for the measurements. The changes in the absorbance observed in the spectra were not due to the experimental error, because baseline corrections were done for all measurements. All measurements were performed at room temperature with an Analytik Jena Specord 200 spectrophotometer between 190 and 900 nm .

2.8 Computational details

All DFT calculations were performed by employing the Gaussian 03 program package⁴² using the B3LYP functional.⁴³⁻⁴⁶ The 6-31G** basis set was used for all atoms.⁴⁷⁻⁵⁰ The appropriateness of the chosen functional and basis set for titanium complexes has been stated elsewhere.⁵¹ All systems have been optimized without symmetry restrictions. The resulting geometries were characterized as equilibrium structures by the analysis of the force constants of normal vibrations (see ESI†). Calculating the molecular volume as defined through the contour of constant electron density, equating this (non-spherical) molecular volume

to the radius of an (ideally spherical) cavity, and adding a constant increment for the closest possible approach of solvent molecules as implemented in Gaussian 03 was used to estimate the radii of the complexes.⁴²

3. Results and discussion

3.1 Preparation of titanocene thiolate complexes

The titanocene thiolate complexes $[\text{Ti}(\eta^5\text{-C}_5\text{H}_5)_2\{\text{SCH}_2\text{CH}_2\text{-CH}_2\text{Si}(\text{OMe})_3\}_2]$ (**2**) and $[\text{Ti}(\eta^5\text{-C}_5\text{H}_5)_2\{\text{SCH}_2\text{CH}_2\text{CH}_2\text{Si}(\text{OEt})_3\}_2]$ (**3**) have been prepared by the reaction of 3-mercaptopropyltrimethoxysilane or 3-mercaptopropyltriethoxysilane, respectively with $[\text{Ti}(\eta^5\text{-C}_5\text{H}_5)_2\text{Cl}_2]$ (**1**), in the presence of triethylamine (Scheme 1).

The NMR, mass and IR spectra showed that **2** and **3**, isolated as crystalline solids, were of high purity. In the ^1H NMR spectra of these complexes three multiplets at *ca.* 0.7, 1.6 and 3.0 ppm corresponding to the methylene protons of the thiolato ligand, and a singlet at *ca.* 6.1 ppm assigned to the cyclopentadienyl protons were observed. In addition, the ^1H NMR spectrum of **2** shows a singlet at 3.56 ppm corresponding to the protons of the methoxy groups, while in the ^1H NMR spectrum of **3** a triplet and a quadruplet at 1.22 ppm and 3.82 ppm, respectively, attributed to the protons of the ethoxy groups, were recorded. $^{13}\text{C}\{^1\text{H}\}$ NMR spectra for **2** and **3** showed the expected signals for the cyclopentadienyl rings, as well as the signals corresponding to the different thiolato ligands. The infrared spectra of the free thiolato ligands show a band between 2480 and 2550 cm^{-1} corresponding to the vibration frequency $\nu(\text{S-H})$ of thiol groups.⁵² After reaction, and formation of the Ti-S bonds, these bands are replaced by others between 360–390 cm^{-1} , which correspond to the vibrations

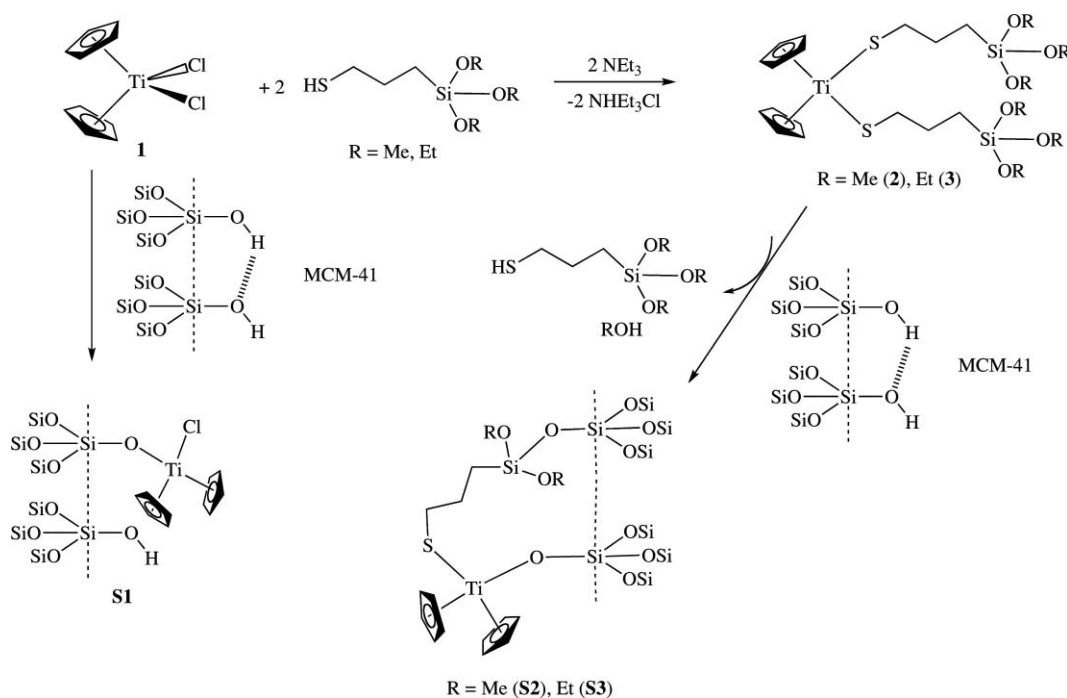
of the Ti-S bonds. **2** and **3** were also characterized by FAB-MS and elemental analysis (see Section 2.4).

3.2 Preparation of modified materials

Grafting of all the studied titanocene compounds $[\text{Ti}(\eta^5\text{-C}_5\text{H}_5)_2\text{Cl}_2]$ (**1**), $[\text{Ti}(\eta^5\text{-C}_5\text{H}_5)_2\{\text{SCH}_2\text{CH}_2\text{CH}_2\text{Si}(\text{OMe})_3\}_2]$ (**2**) and $[\text{Ti}(\eta^5\text{-C}_5\text{H}_5)_2\{\text{SCH}_2\text{CH}_2\text{CH}_2\text{Si}(\text{OEt})_3\}_2]$ (**3**) on a dehydroxylated MCM-41 mesoporous silica have been carried out by overnight treatment of the surfaces with a solution of the corresponding titanocene complex in toluene at 80 °C.

For the reaction of **1** with MCM-41, a limited number of possible reactions between one of the chlorine atoms of the corresponding titanocene complexes, either with the acidic silanol groups or with the reactive siloxane bridges, may lead to μ -oxo surface species (Scheme 1, see synthesis of **S1**), due to the low concentration of hydroxyl groups present on the dehydroxylated MCM-41.^{29-30,53-55} However, in the functionalization reaction of **2** and **3** with MCM-41, elimination of 3-mercaptopropyltrimethoxysilane and methanol or 3-mercaptopropyltriethoxysilane and ethanol, respectively, was observed. These reactions resulted in the functionalization of the surfaces by the binding of the trimethoxysilyl or triethoxysilyl groups to the surface. In addition, the formation of Ti-O-Si bonds due to the elimination of one of the thiolato ligands was also possible (Scheme 1).

Thus, **S2** and **S3** may consist of a mixture of functionalization possibilities which may include elimination of both thiolato ligands and formation of “ $\text{Cp}_2\text{Ti}(\text{O-MCM-41})_2$ ” species (Fig. 1a), elimination of one thiolato ligand to give “ $\text{Cp}_2\text{Ti}\{\text{SCH}_2\text{CH}_2\text{CH}_2\text{Si}(\text{OEt})_2\text{O-MCM-41}\}(\text{O-MCM-41})$ ” fragments (Fig. 1b), or direct functionalization leading to “ $\text{Cp}_2\text{Ti}\{\text{SCH}_2\text{CH}_2\text{CH}_2\text{Si}(\text{OEt})_2\text{O-MCM-41}\}_2$ ” species (Fig. 1c). However, elemental analysis data obtained by X-ray fluorescence,



Scheme 1

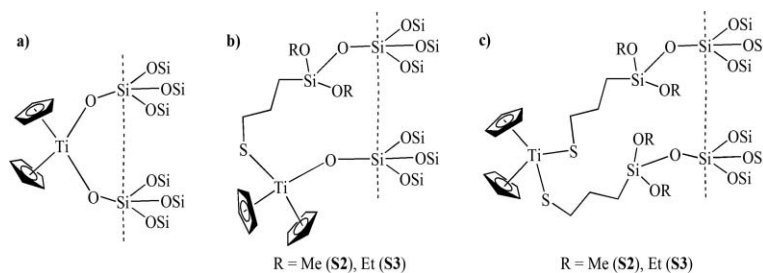


Fig. 1 Different titanium-containing species in **S2** and **S3**, obtained after functionalization.

Table 1 % of Ti and S grafted on the silica support

Surface	Ti _{exp} (wt%) ^a	S _{exp} (wt%) ^a
MCM-41/[Ti(η ⁵ -C ₅ H ₅) ₂ Cl ₂] (S1)	1.11	—
MCM-41/[Ti(η ⁵ -C ₅ H ₅) ₂ -{SCH ₂ CH ₂ CH ₂ Si(OMe) ₃ } ₂] (S2)	3.02	1.72
MCM-41/[Ti(η ⁵ -C ₅ H ₅) ₂ -{SCH ₂ CH ₂ CH ₂ Si(OEt) ₃ } ₂] (S3)	3.27	2.09

^a Experimental Ti and S determined by X-ray fluorescence (wt%)

showed an atomic Ti : S ratio of *ca.* 1 (Table 1) indicating that the predominant species may be the one in which only one thiolato ligand was eliminated (Fig. 1b).

This phenomenon was confirmed by the analysis of the mother liquor and the washing fractions of the functionalization reactions by ¹H NMR spectroscopy. The spectra showed the signals corresponding to 3-mercaptopropyltrimethoxysilane and methanol or 3-mercaptopropyltriethoxysilane and ethanol, respectively.

Additionally, adsorbed titanocene complexes may also be located in the pores of the corresponding materials.

The functionalization reactions were carried out using a theoretical 5% Ti wt%. According to the data obtained by X-ray fluorescence, the value of Ti wt% for the functionalized surface **S1** was 1.11, which is in agreement with previous studies on MCM-41. These analyses have shown a maximum loading of metallocene complexes on the mesoporous surfaces lower than 2.0% of metal. This low functionalization rate was due either to the saturation of the surface or to the weak basicity of both chloro ligands of the titanocene complexes and the Si-OH groups of the MCM-41.^{29-30,53-55} However, following previously reported functionalization procedures, which showed higher functionalization rates with ligands with trimethoxysilyl or triethoxysilyl moieties,⁵⁶⁻⁶¹ **S2** and **S3** were prepared by the reaction of **2** and **3** with MCM-41. These surfaces showed much higher Ti content than **S1** with values of 3.02 and 3.27%. Table 1 shows the Ti and S wt% grafted on to the silica support.

3.3 Characterization of the modified materials

The new materials have been characterized by multinuclear MAS NMR spectroscopy which is a useful tool in monitoring surface reactions of organometallic complexes.⁶² The ¹H-MAS NMR spectra of **S1–S3** showed the signals corresponding to the protons of the grafted titanocene complexes. Thus, surfaces **S1–S3** show broad signals corresponding to the protons of the cyclopentadienyl rings at *ca.* 4.5 ppm. In addition, protons of the thiolato ligands attached to the titanocene complexes of the surfaces **S2** and **S3**

were also observed. Furthermore, protons of the trimethoxysilyl and triethoxysilyl groups gave intense broad signals in the ¹H-MAS NMR spectrum between *ca.* -2.0 and 2.0 ppm, which clearly obscured the less intense signals of the methylene protons of the alkylic chain which appeared in the same spectral region.

The ¹³C-CP MAS NMR spectra of **S1–S3** presented two or three signals between 100–200 ppm corresponding to the carbon atoms of the cyclopentadienyl ligands of the grafted titanocene derivatives. In addition, surfaces **S2** and **S3** showed a set of two (for **S2**, due to the obscuration of an expected third signal by the intense broad peak corresponding to the carbon atoms of the methoxy groups) or three signals (for **S3**) at *ca.* 12, 28 and 47 ppm corresponding to the three carbon atoms of the alkylic chain of the thiolato ligand. The ¹³C-CP MAS NMR spectrum of **S2** also gave a broad signal at 52.8 ppm due to the carbon atoms of the methoxy groups (Fig. 2a). On the other hand, the

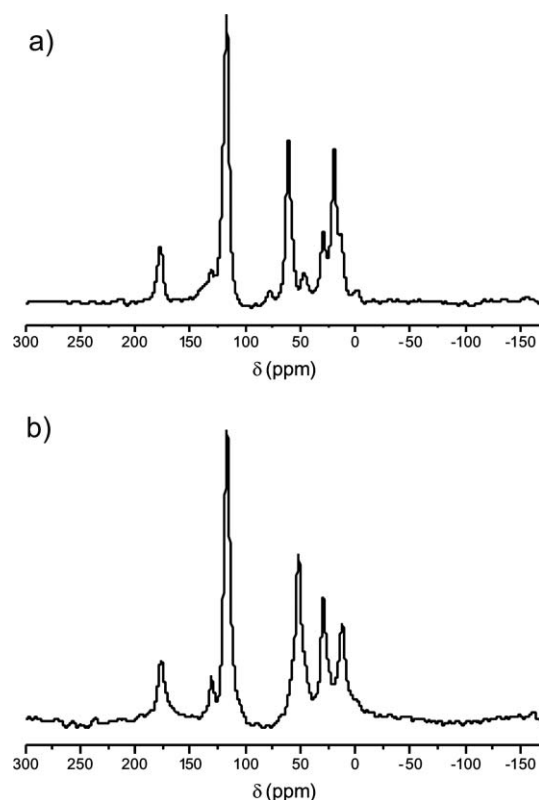


Fig. 2 ¹³C-MAS NMR spectrum of (a) MCM-41/[Ti(η⁵-C₅H₅)₂-{SCH₂CH₂CH₂Si(OMe)₃}₂] (**S2**) and (b) MCM-41/[Ti(η⁵-C₅H₅)₂-{SCH₂CH₂CH₂Si(OEt)₃}₂] (**S3**).

Reproduced from Ref. G.N. Kaluđerović, D. Pérez-Quintanilla, Ž. Žižak, Z.D. Juranić, S. Gómez-Ruiz, Dalton Trans. 2010, 39, 2597 with permission from The Royal Society of Chemistry.

^{13}C -CP MAS NMR spectrum of **S3** gave two broad signals at 18.2 and 61.0 ppm corresponding to the carbon atoms of the ethoxy moieties (Fig. 2b).

In addition, ^{29}Si MAS NMR spectra of all the synthesized surfaces were recorded. The spectra of the non functionalized MCM-41 show silicon atoms with hydroxyl bound groups, such as $[\text{Si}(\text{OSi})_2(\text{OH})_2]$ (Q_2 , at -91.6 ppm), $[\text{Si}(\text{OSi})_2(\text{OH})]$ (Q_3 , at -100.6 ppm) and $[\text{Si}(\text{OSi})_2]$ (Q_4 , at -110 ppm). After grafting the titanocene derivatives, a modification in Q_3 and Q_2 sites was observed, as a consequence of the functionalization the intensity of these peaks clearly decreases (see Fig. 3). In addition, the spectrum of the functionalized MCM-41 **S2** and **S3** showed, two new peaks of low intensity at *ca.* -53 and -60 ppm, which were assigned to T_2 ($(\text{SiO})_2\text{SiOH-R}$) and T_3 ($(\text{SiO})_3\text{Si-R}$) sites, respectively (Fig. 3).⁶³

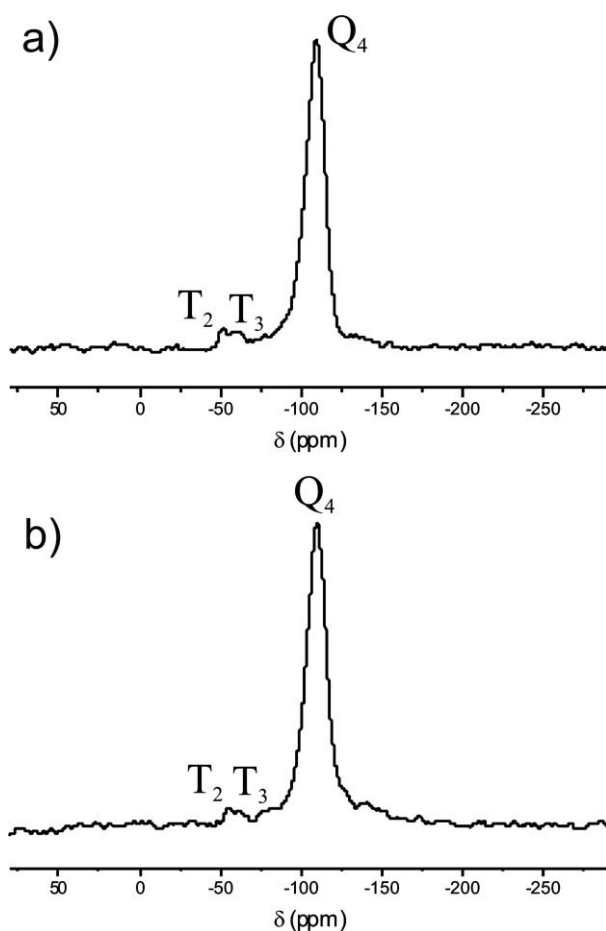


Fig. 3 ^{29}Si -MAS NMR spectrum of (a) MCM-41/ $[\text{Ti}(\eta^5\text{-C}_5\text{H}_5)_2\text{-}\{\text{SCH}_2\text{CH}_2\text{CH}_2\text{Si}(\text{OMe})_3\}_2]$ (**S2**) and (b) MCM-41/ $[\text{Ti}(\eta^5\text{-C}_5\text{H}_5)_2\text{-}\{\text{SCH}_2\text{CH}_2\text{CH}_2\text{Si}(\text{OEt})_3\}_2]$ (**S3**).

UV-vis spectra of the studied surfaces **S1–S3**, and the non-functionalized MCM-41 were recorded. In the functionalized surfaces, a broad peak at *ca.* 250 nm with a shoulder between *ca.* 300–350 nm, corresponding to the supported titanocene complex were observed (see ESI†).

FT-IR spectra of the non-functionalized MCM-41 and the titanocene-functionalized materials **S1–S3** were also measured. The main features of the non-functionalized MCM-41 spectra included a large broad band between 3400 and 3200 cm^{-1} , which

Table 2 XRD data of MCM-41, MCM-41/ $[\text{Ti}(\eta^5\text{-C}_5\text{H}_5)_2\text{Cl}_2]$ (**S1**), MCM-41/ $[\text{Ti}(\eta^5\text{-C}_5\text{H}_5)_2\{\text{SCH}_2\text{CH}_2\text{CH}_2\text{Si}(\text{OMe})_3\}_2]$ (**S2**) and MCM-41/ $[\text{Ti}(\eta^5\text{-C}_5\text{H}_5)_2\{\text{SCH}_2\text{CH}_2\text{CH}_2\text{Si}(\text{OEt})_3\}_2]$ (**S3**)

Material	(<i>hkl</i>)	$2\theta/\text{degrees}$	<i>d</i> -spacing/Å
MCM-41	100	2.54	34.75
	110	2.86	30.87
	200	4.77	18.51
S1	100	2.57	34.33
	200	4.88	18.10
S2	100	2.54	34.75
S3	100	2.51	35.17

was attributed to O–H stretching of the silanol groups of the surface and the remaining adsorbed water molecules. The signal corresponding to the siloxane (Si–O–Si) groups appeared as a broad strong band at *ca.* 1100 cm^{-1} . The stretching band of the Si–O bonds of the silanol groups was observed at *ca.* 900 cm^{-1} . An additional band at *ca.* 1630 cm^{-1} due to deformation vibrations of adsorbed water molecules was also observed.⁶⁴ Surfaces **S1–S3** showed characteristic bands for aliphatic C–H stretching vibrations due to pendant alkyl chains at around $3000\text{--}2800\text{ cm}^{-1}$ and bands at *ca.* 1600 for the cyclopentadienyl ligands (see ESI†).

3.4 Structural features of the modified materials

XRD spectrum of the non functionalized MCM-41 displayed typical reflections for a hexagonally ordered mesoporous material,⁶⁵ that is, a well-resolved pattern at low 2θ with a very sharp diffraction peak at 2.54° and an additional weak peak at 4.77° . These characteristic Bragg peaks, with *d*-spacing 34.75 and 18.51 Å, are due to reflections from the (100) and (200) planes, respectively (Table 2). For the titanocene-functionalized materials **S1–S3** a substantial decrease in the intensity of the (100) peak was observed. In addition, the (200) peak was only observed for **S1**, while for **S2** and **S3**, the high degree of functionalization strongly decreased the intensity of this peak, which was not observed (Table 2, Fig. 4). Thus, the X-ray spectrum of **S1** showed two peaks at 2.57 and 4.88 degrees, while X-ray spectra of **S2** and **S3** showed only the (100) peak at 2.54 and 2.51 degrees, respectively (Table 2, Fig. 4). These parameters can be indexed as hexagonal lattices with *d*-spacing values of 34.33 and 18.10 Å for **S1**, 34.75 Å for **S2** and 35.17 Å for **S3**. The unit cell parameters, a_0 , for

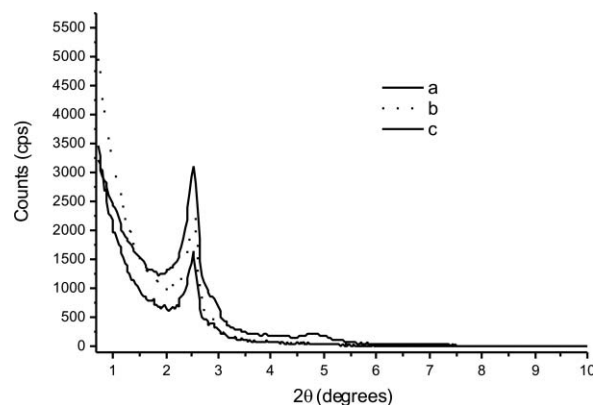


Fig. 4 Powder low-angle XRD patterns of (a) non-functionalized MCM-41; (b) MCM-41/ $[\text{Ti}(\eta^5\text{-C}_5\text{H}_5)_2\{\text{SCH}_2\text{CH}_2\text{CH}_2\text{Si}(\text{OMe})_3\}_2]$ (**S2**) and (c) MCM-41/ $[\text{Ti}(\eta^5\text{-C}_5\text{H}_5)_2\{\text{SCH}_2\text{CH}_2\text{CH}_2\text{Si}(\text{OEt})_3\}_2]$ (**S3**).

Table 3 Physical parameters of MCM-41, MCM-41/Ti(η^5 -C₅H₅)₂Cl₂ (**S1**), MCM-41/[Ti(η^5 -C₅H₅)₂{SCH₂CH₂CH₂Si(OMe)₃}₂] (**S2**) and MCM-41/[Ti(η^5 -C₅H₅)₂{SCH₂CH₂CH₂Si(OEt)₃}₂] (**S3**) measured by N₂ adsorption-desorption isotherms

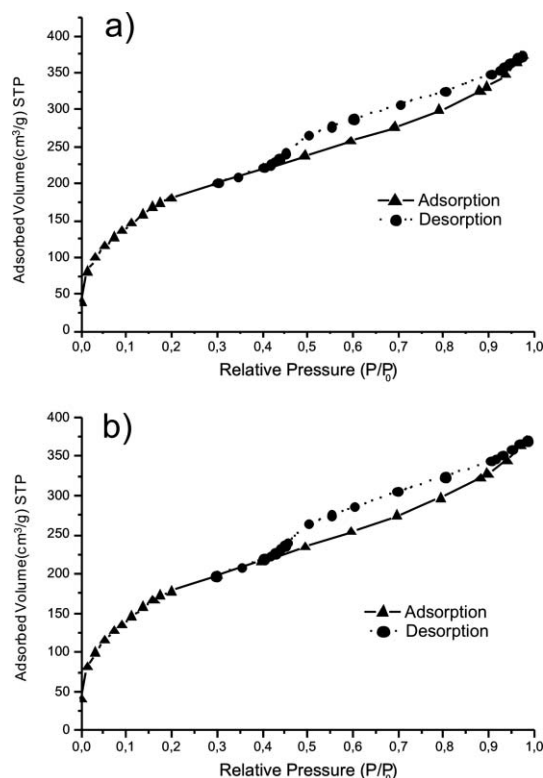
Sample	BET surface area/m ² g ⁻¹	Total pore volume/cm ³ g ⁻¹	Pore diameter (BJH) ^a /Å	Wall thickness/Å
MCM-41	776	0.87	21.3	18.8
S1	645	0.73	20.8	18.9
S2	704	0.56	12.0	28.1
S3	691	0.56	13.9	26.7

^a Barrett, Joyner and Halenda.

S1–S3 were 39.64, 40.12, and 40.61 Å, respectively. These parameters were calculated using the following equation:⁶⁵

$$a_0 = \frac{2d_{100}}{\sqrt{3}}$$

Nitrogen adsorption/desorption isotherms were also recorded for both unmodified MCM-41 and titanocene-functionalized materials S1–S3 observing the formation of type IV isotherms (according to the IUPAC classification)⁶⁶ which have an H1 hysteresis loop indicating the mesoporous nature of all the studied surfaces (Fig. 5). Table 3 shows the physical parameters of nitrogen isotherms, such as the BET surface area (S_{BET}), BJH average pore diameter and wall thickness for the unmodified MCM-41 and the modified surfaces S1–S3.

**Fig. 5** Nitrogen adsorption/desorption isotherms of (a) MCM-41/[Ti(η^5 -C₅H₅)₂{SCH₂CH₂CH₂Si(OMe)₃}₂] (**S2**) and (b) MCM-41/[Ti(η^5 -C₅H₅)₂{SCH₂CH₂CH₂Si(OEt)₃}₂] (**S3**).

Capillary condensation of nitrogen within the uniform mesopore structure, indicated by the increase of the adsorbed volume at a relative pressure (P/P_0) of *ca.* 0.4, was observed for all the studied surfaces. The inflection position shifted slightly toward lower relative pressures and the volume of adsorbed nitrogen decreased in S1–S3 relative to non-functionalized MCM-41. This phenomenon indicates a reduction in pore size, which may be due to the location of titanocene complexes inside those pores. The effective mean pore diameters of S1–S3 were 20.8, 12.0 and 13.9 Å, respectively, while that of non-functionalized MCM-41 was 21.3 Å. As expected, the pores become substantially smaller as a result of functionalization of the surfaces with the titanocene complexes. Comparing all the studied functionalized surfaces, S1 has a much higher pore size than S2 and S3 (*ca.* 7 Å higher) as corresponds to a lower functionalization rate. In addition, the increase of the wall thickness of the modified surfaces S1–S3 (18.9, 28.1 and 26.7, respectively) compared to that of non-functionalized MCM-41 (18.8 Å) indicated that the functionalization reaction took place. The wall thickness was calculated using the following equation:⁶⁵

$$\text{Wall thickness} = \frac{2d_{100}}{\sqrt{3}} - \text{BJH average pore diameter}$$

Furthermore, the pore size distributions of the studied surfaces S1–S3 are homogeneous, giving a narrow distribution (see ESI†).

With all the above results, one can envisage that titanocene complexes in the surfaces, may be located into the pores. DFT calculations of the complexes [Ti(η^5 -C₅H₅)₂{SCH₂CH₂CH₂Si(OMe)₃}₂] (**2**) and [Ti(η^5 -C₅H₅)₂{SCH₂CH₂CH₂Si(OEt)₃}₂] (**3**) were carried out in order to determine whether the size of the titanocene complexes is appropriate to fit into the pore cavity (see ESI†). The geometrical parameters showed that titanocene derivatives have distances of less than 6.75 Å (**3**) between the most remote atoms of the structures, indicating, in both cases, that they are small enough to be located inside the pore. The volume of these complexes (1.13 nm³ for [Ti(η^5 -C₅H₅)₂{SCH₂CH₂CH₂Si(OMe)₃}₂] (**2**) and 1.29 nm³ for [Ti(η^5 -C₅H₅)₂{SCH₂CH₂CH₂Si(OEt)₃}₂] (**3**)) is much smaller than MCM-41 pores. These calculations indicate that MCM-41 provides enough space for the metallocene molecule to bind to the surface OH groups inside the cavities.

The TGA curves of the modified materials (S1–S3) showed an initial loss of mass of approximately 1.5% due to water physically adsorbed on the surface. Subsequently, a second loss of mass of *ca.* 3% for S1 and *ca.* 11% for S2 and S3 is observed between 250–500 °C. This loss of mass indicates the degradation of the titanocene complexes anchored on the silica surface (exothermic process). In addition, this loss of mass is, as expected, much higher for materials S2 and S3 compared to S1, as corresponds to their higher functionalization rate. Finally, a loss in mass of about 1% between 500 and 800 °C attributed to the increase in the number of siloxane bridges (Si–O–Si) due to isolated silanol condensation (exothermic process), was also observed in the thermogravimetric curves of S1–S3 (Fig. 6).

Scanning electron microscopy (SEM) and transmission electron microscopy (TEM) were used for the exploration of morphology of the studied surfaces observing that S1–S3 consists of clusters of “quasi” spheres with uniform average diameters of *ca.* 900 nm. TEM images of all materials demonstrated a clear arrangement of

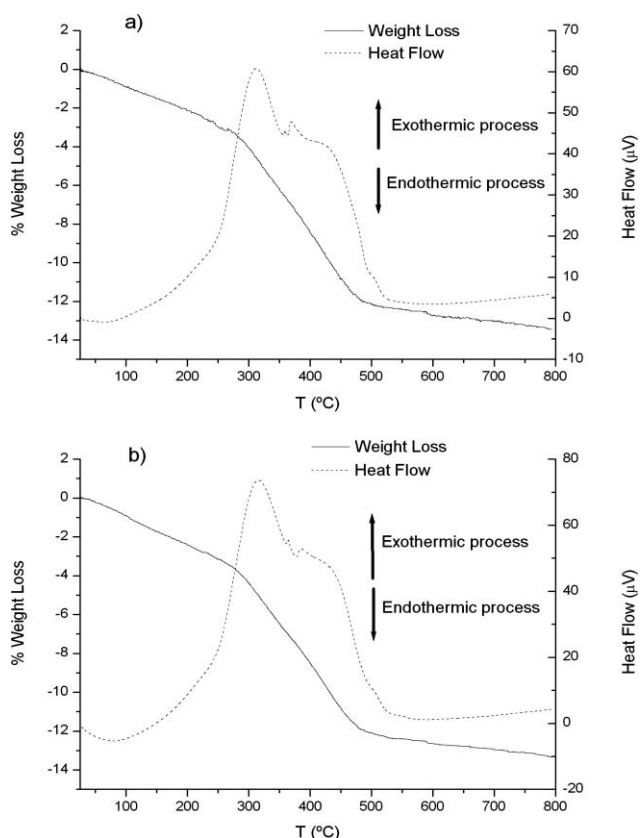


Fig. 6 Thermogravimetric curves and heat flow of MCM-41/[Ti(η^5 -C₅H₅)₂{SCH₂CH₂CH₂Si(OMe)₃}₂] (S2) and MCM-41/[Ti(η^5 -C₅H₅)₂{SCH₂CH₂CH₂Si(OEt)₃}₂] (S3).

hexagonal pores with uniform size. Fig. 7a (SEM) and 7b (TEM) shows the pictures of S2.

3.5 Cytotoxic studies

The functionalized materials S1–S3 have been prepared in order to study the influence of the titanium content on the cytotoxic activity. Taking into account that after release of the titanocene derivatives by the functionalized surfaces, the titanium content species may be converted into similar species with the same “Cp₂Ti” moiety, if there is an influence of the titanium content,

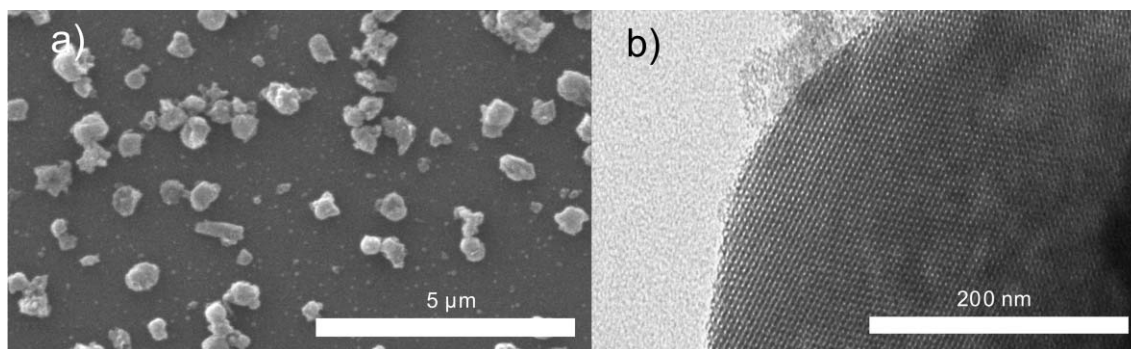


Fig. 7 (a) Scanning electron microscope picture and (b) transmission electron microscope picture of MCM-41/[Ti(η^5 -C₅H₅)₂{SCH₂CH₂CH₂Si(OMe)₃}₂] (S2).

Table 4 Cytotoxicity values (M_{50} in μg) on HeLa, K562, Fem-x, PBMC and PBMC stimulated with PHA of the nanostructured materials MCM-41, MCM-41/[Ti(η^5 -C₅H₅)₂Cl₂] (S1), MCM-41/[Ti(η^5 -C₅H₅)₂{SCH₂CH₂CH₂Si(OMe)₃}₂] (S2) and MCM-41/[Ti(η^5 -C₅H₅)₂{SCH₂CH₂CH₂Si(OEt)₃}₂] (S3)

Sample	$M_{50}/\mu\text{g}$ for S1–S3 and MCM-41					
	$IC_{50}/\mu\text{M}$ for titanocene complex 1					
	HeLa	K562	Fem-x	PBMC-PHA	PBMC+PHA	
S1	897 ± 21	874 ± 42	977 ± 63	>1000 NA	670 ± 68	
S2	743 ± 44	784 ± 19	631 ± 51	>1000 NA	>1000 NA	
S3	685 ± 60	704 ± 30	573 ± 76	>1000 NA	>1000 NA	
MCM-41	>1000 NA	>1000 NA	>1000 NA	ND	ND	
1	>200 NA	>200 NA	177.7 ± 4.9	>200 NA	>200 NA	

NA = not active in the studied range. ND = not determined.

surfaces S2 and S3 (with ca. 3% Ti) should present a much higher activity than S1 (with ca. 1% Ti).

Thus, the cytotoxicity of S1–S3 toward human cancer cell lines such as adenocarcinoma HeLa, human myelogenous leukemia K562 and human malignant melanoma Fem-x has been studied. Additional studies on the toxicity of these materials on normal immunocompetent cells such as stimulated (PBMC+PHA) and non-stimulated (PBMC-PHA) peripheral blood mononuclear cells has been also carried out. The final cytotoxicity of the studied surfaces has been discussed in terms of mass, using an M_{50} scale (quantity of material needed to inhibit normal cell survival by 50%) (Table 4), since the Q_{50} values, reported by Asefa and coworkers,⁹ are only the consequence of the correlation between the calculated particle number/gram, which depends on the estimation of the particle average size by SEM, which is not very precise. The M_{50} values show that all the functionalized materials S1–S3 showed a dose-dependent antiproliferative effect towards all cancer cell lines (Fig. 8), while the unmodified MCM-41 was unactive.

As expected, S2 and S3 are more active than S1 in all the studied cancer cell lines with M_{50} values for S2 and S3 from 150 up to 400 μg lower than S1, indicating a clear dependence of the titanium content on the final anticancer activity.

All the studied modified surfaces, presented no activity against unstimulated immunocompetent cells PBMC and stimulated PBMC (except S1 which is unexpectedly active against PBMC+PHA), indicating a slight selectivity of S1–S3 on the studied human cancer cells, however, these results are only of

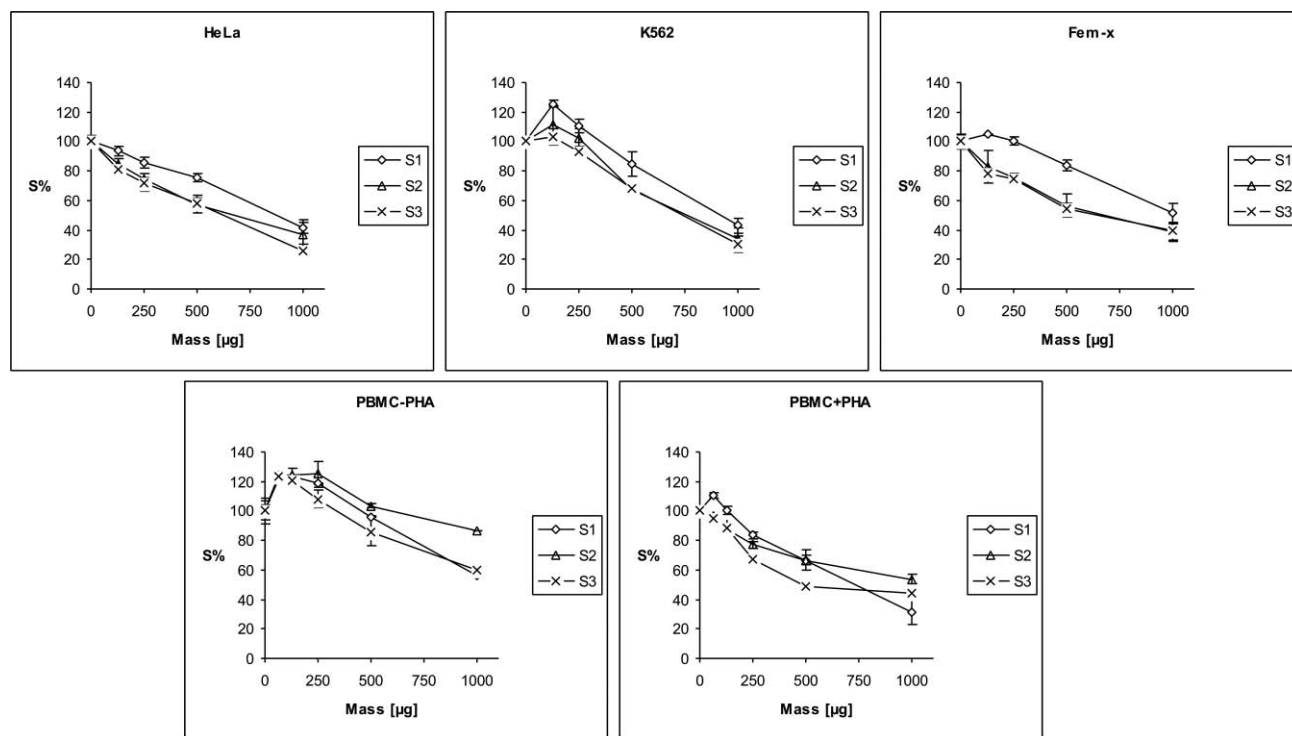


Fig. 8 Representative graphs showing survival of HeLa, K562, Fem-x, PBMC and PBMC+PHA (PBMC stimulated with PHA) cells grown for 72 h in the presence of increasing amounts of the mesoporous materials MCM-41/ $\text{Ti}(\eta^5\text{-C}_5\text{H}_5)_2\text{Cl}_2$ (S1), MCM-41/ $[\text{Ti}(\eta^5\text{-C}_5\text{H}_5)_2\{\text{SCH}_2\text{CH}_2\text{CH}_2\text{Si}(\text{OMe})_3\}_2]$ (S2) and MCM-41/ $[\text{Ti}(\eta^5\text{-C}_5\text{H}_5)_2\{\text{SCH}_2\text{CH}_2\text{CH}_2\text{Si}(\text{OEt})_3\}_2]$ (S3).

in vitro tests and the behaviour of these surfaces in *in vivo* tests may be different.

The most active material on all the cells is S3 with M_{50} values from $573 \pm 76 \mu\text{g}$ (on Fem-x) to $704 \pm 30 \mu\text{g}$ (on K562), while the M_{50} values of the less cytotoxic material (S1) are between $977 \pm 63 \mu\text{g}$ (on Fem-x) and $874 \pm 42 \mu\text{g}$ (on K562).

Interestingly, the cytotoxicity of S1–S3 could not be compared to that of compounds 2 and 3, which due to their lack of solubility in DMSO, DMF or water were not available for *in vitro* anticancer tests, however, the same titanocene complexes supported onto mesoporous materials (surfaces S2 and S3) were tested and showed antiproliferative activity.

The proposed anticancer mechanism of these materials may be similar to that suggested for titanocene complexes in solution, with DNA the biological target^{67–69} of Ti(IV) ions which resulted from the release from the titanocene complexes by the mesoporous nanoparticles and the subsequent hydrolysis of the titanium-containing species.

After hydrolysis reactions of the free titanocene compounds and elimination of the ligands, titanium ions may reach the cells assisted by transferrin, as was previously proposed by Sadler and coworkers.^{70–73} Endosome action may release Ti(IV) ions, which assisted probably by ATP would reach the DNA regions of the cell nucleus (Fig. 9).⁷⁴

3.6 Qualitative DNA-binding studies

The absorption spectra of DNA in the absence and presence of S2 and S3 at various increasing concentrations has been recorded (Fig. 10). In the presence of the surfaces, the absorbance of DNA

increases notably, without notable changes in the location of the peaks. This may indicate that the addition of the materials to the DNA solution, leads to the adsorption of the DNA on the surface of the studied particles forming ground state adducts DNA-particles. These adducts give an absorption peak at 260 nm. This may be the reason for the increase in absorbance of DNA with the addition of the studied materials, as supported by similar observations in other reports.⁷⁵

These results may indicate a possible electrostatic interaction between titanocene-functionalized materials and DNA. A qualitative increase of the absorbance at increasing concentration of the surfaces was recorded, indicating the interaction of materials with DNA, however, the apparent equilibrium constant for the formation of the complex between DNA and the materials could not be satisfactorily calculated due to problems of quantification of the absorbance of the suspensions.

Conclusions

Two novel titanocene(IV) thiolate complexes $[\text{Ti}(\eta^5\text{-C}_5\text{H}_5)_2\{\text{SCH}_2\text{CH}_2\text{CH}_2\text{Si}(\text{OMe})_3\}_2]$ (2) and $[\text{Ti}(\eta^5\text{-C}_5\text{H}_5)_2\{\text{SCH}_2\text{CH}_2\text{CH}_2\text{Si}(\text{OEt})_3\}_2]$ (3) have been synthesised, characterized and grafted onto MCM-41 mesoporous silica. In addition, the simplest titanocene compound $[\text{Ti}(\eta^5\text{-C}_5\text{H}_5)_2\text{Cl}_2]$ (1) has also been anchored onto MCM-41. We have observed an increase of the functionalization rate by the incorporation of thiolato ligands with $-\text{Si}(\text{OMe})_3$ or $-\text{Si}(\text{OEt})_3$ groups in their structure. While unmodified MCM-41 is not active against the studied human cancer and immunocompetent cells, the functionalized surfaces S1–S3 were active against all the studied cancer cells. The cytotoxicity of

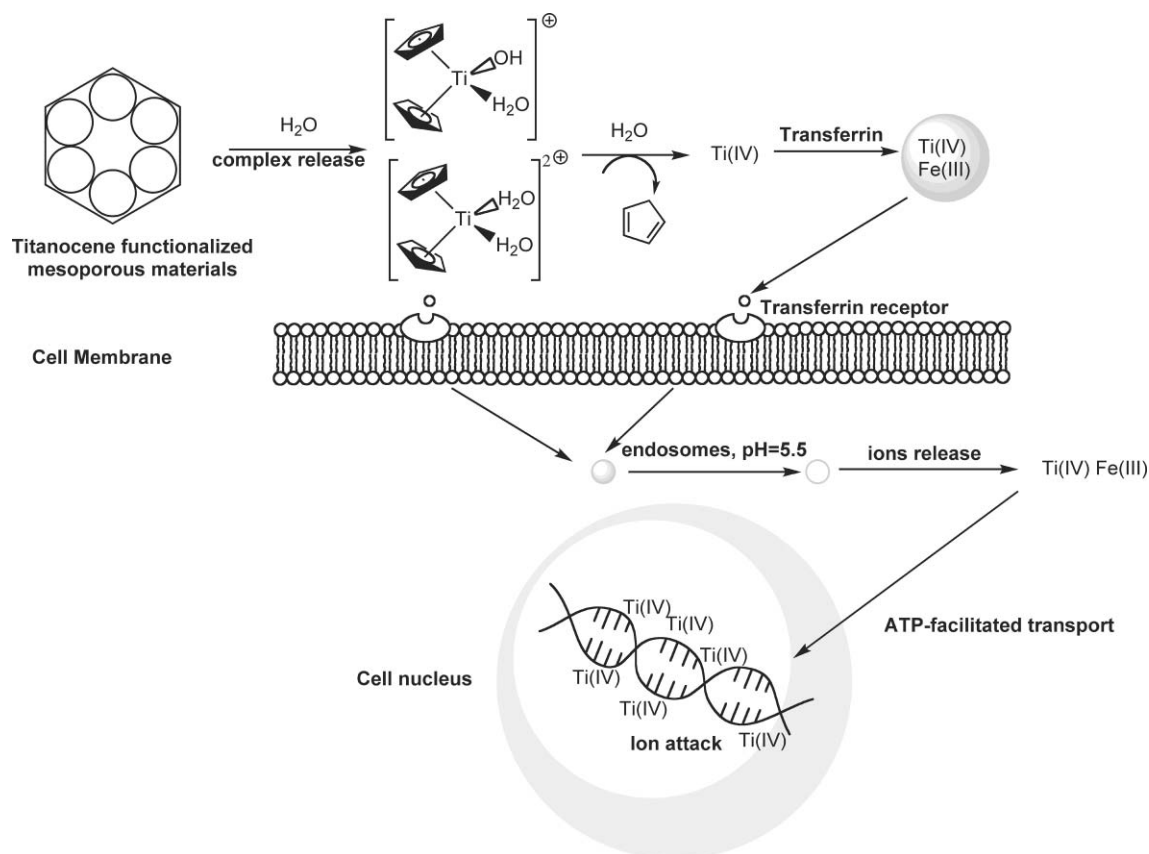


Fig. 9 Proposed mechanism for the cellular action of S1-S3.

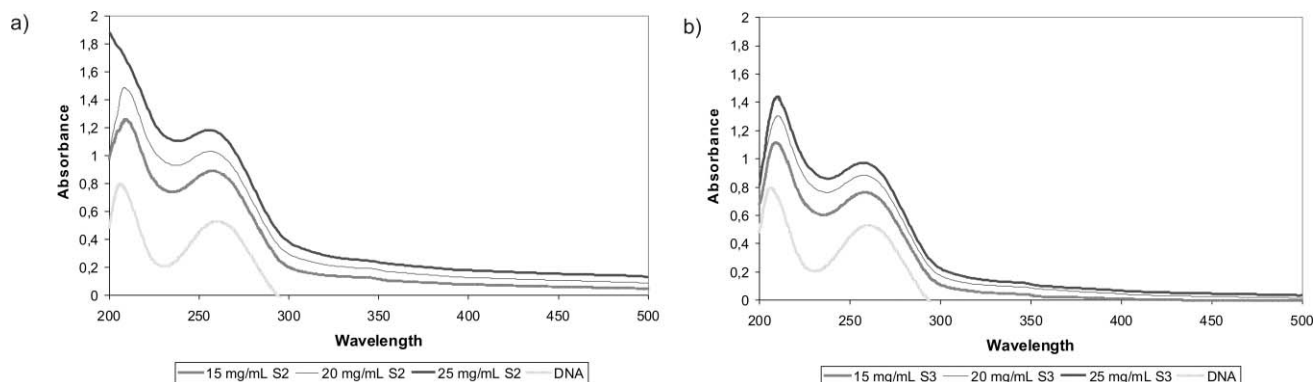


Fig. 10 UV-vis spectra of DNA-material adducts S2-DNA (left), S3-DNA (right).

surfaces **S2** and **S3** (with *ca.* 3% wt Ti) were very similar on all the studied cancer cells, however, **S1** (1.1% wt Ti) showed M_{50} values that indicated the lowest activity of all the analyzed materials on all the studied cells. Thus, a clear dependence of the titanium content of the functionalized MCM-41 on the cytotoxic activity on human cancer cell lines has been reported.

This work has also shown the possibility of studying many promising organometallic complexes which because of their lack of solubility have been disregarded in this field.

Future work, already in progress, will now focus on the study of the influence of the particle size and type of mesoporous surfaces on the final anticancer activity of titanocene-functionalized materials. In addition, the possibility of applying this new class of

materials as bone fillers or additives for bone implants, will also be biologically explored.

Acknowledgements

We gratefully acknowledge financial support from the Ministerio de Educación y Ciencia, Spain (Grant no. CTQ2008-05892/BQU), Comunidad de Madrid-URJC (CCG07-URJC/PPQ-149) and Ministry of Science and Environmental Protection of the Republic of Serbia (Grant Nos. 142010 and 145006). We would also like to thank Prof. D. Steinborn (Universität Halle-Wittenberg), Dr I. Sierra, Dr S. Prashar, Dr I. del

Hierro, Prof. M. Fajardo and C. Forcé (Universidad Rey Juan Carlos) for useful discussions.

Notes and references

- G. D. Prestwich and Y. Luo, *Expert Opin. Ther. Pat.*, 2001, **11**, 1395–1410.
- J. Park, R. S. Lakes, *Biomaterials: An Introduction*. 3rd Ed. Springer, New York, 2007.
- B. D. Ratner, *Biomaterials science: an introduction to materials in medicine*, Elsevier Academic Press, London, 2004.
- K. T. Oh, H. Yin, E. S. Lee, Y. H. Bae and J. Mat, *J. Mater. Chem.*, 2007, **17**, 3987–4001.
- M. Vallet-Regí, L. Ruiz-González, I. Izquierdo-Barba and J. M. González-Calbet, *J. Mater. Chem.*, 2006, **16**, 26–31.
- I. Izquierdo-Barba, L. Ruiz-González, J. C. Doadrio, J. M. González-Calbet and M. Vallet-Regí, *Solid State Sci.*, 2005, **7**, 983.
- M. Vallet-Regí and D. Arcos, Mesoporous materials for biomedical applications, in: *Trends in Biomaterial Research*, pp 109–142, Nova Publishers, Hauppauge, 2007.
- J. Lu, M. Liang, J. I. Zink and F. Tamanoi, *Small*, 2007, **3**, 1341–1346.
- A. J. Di Pasqua, K. K. Sharma, Y.-L. Shi, B. B. Toms, W. Ouellette, J. C. Dabrowiak and T. Asefa, *J. Inorg. Biochem.*, 2008, **102**, 1416–1423.
- Z. Chen, H. Meng, G. Xing, C. Chen and Y. Zhao, *Int. J. Nanotechnol.*, 2007, **4**, 179–196.
- E. C. Gryparis, M. HatziaPOSTOLOU, E. Papadimitriou and K. Avgoustakis, *Eur. J. Pharm. Biopharm.*, 2007, **67**, 1–8.
- P. Xu, E. A. Van Kirk, W. J. Murdoch, Y. Zhan, D. D. Isaak, M. Radosz and Y. Shen, *Biomacromolecules*, 2006, **7**, 829–835.
- C. Charnay, S. Begu, C. Tourne-Peteilh, L. Niolle, D. A. Lerner and J. M. Devoisselle, *Eur. J. Pharm. Biopharm.*, 2004, **57**, 533–540.
- Q.-L. Tang, Y. Xu, D. Wu, Y.-H. Sun, J. Wang, J. Xu and F. Deng, *J. Controlled Release*, 2006, **114**, 41–46.
- M. Vallet-Regí, A. Rámila, R. P. del Real and J. Pérez-Pariente, *Chem. Mater.*, 2001, **13**, 308–311.
- B. Muñoz, A. Rámila, I. Díaz, J. Pérez-Pariente and M. Vallet-Regí, *Chem. Mater.*, 2003, **15**, 500–503.
- A. Rámila, B. Muñoz, J. Pérez-Pariente and M. Vallet-Regí, *J. Sol-Gel Sci. Technol.*, 2003, **26**, 1199–1202.
- A. L. Doadrio, E. M. B. Sousa, J. C. Doadrio, J. Pérez-Pariente, I. Izquierdo-Barba and M. Vallet-Regí, *J. Controlled Release*, 2004, **97**, 125–132.
- M. Vallet-Regí, J. C. Doadrio, A. L. Doadrio, I. Izquierdo-Barba and J. Pérez-Pariente, *Solid State Ionics*, 2004, **172**, 435–439.
- G. Wang, A. N. Otuonye, E. A. Blair, K. Denton, Z. Tao and T. Asefa, *J. Solid State Chem.*, 2009, **182**, 1649–1660.
- P. Horcajada, A. Rámila, J. Pérez-Pariente and M. Vallet-Regí, *Microporous Mesoporous Mater.*, 2004, **68**, 105–109.
- J. Andersson, J. Resenholm, S. Arev and M. Linden, *Chem. Mater.*, 2004, **16**, 4160–4167.
- B. G. Trewyn, C. M. Whitman and V. S.-Y. Lin, *Nano Lett.*, 2004, **4**, 2139–2143.
- C.-Y. Lai, B. G. Trewyn, D. M. Jettinifa, K. Jettinifa, S. Xu, S. Jettinifa and V. Lin, *J. Am. Chem. Soc.*, 2003, **125**, 4451–4459.
- W. Zeng, X. F. Qian, Y. B. Zhang, J. Yin and Z. K. Zhu, *Mater. Res. Bull.*, 2005, **40**, 766–772.
- M. Vallet-Regí and F. Balas, *Open Biomed. Eng. J.*, 2008, **2**, 1–9.
- W. Zeng, X.-F. Qian, J. Yin and Z.-K. Zhu, *Mater. Chem. Phys.*, 2006, **97**, 437–441.
- Q. Tang, Y. Xu, D. Wu and Y. Sun, *J. Solid State Chem.*, 2006, **179**, 1513–1520.
- D. Pérez-Quintanilla, S. Gómez-Ruiz, Ž. Žižak, I. Sierra, S. Prashar, I. del Hierro, M. Fajardo, Z. D. Juranić and G. N. Kaluderović, *Chem.–Eur. J.*, 2009, **15**, 5588–5597.
- G. N. Kaluderović, D. Pérez-Quintanilla, I. Sierra, S. Prashar, I. del Hierro, Ž. Žižak, Z. D. Juranić, M. Fajardo and S. Gómez-Ruiz, *J. Mater. Chem.*, 2010, 806–814.
- M. Vallet-Regí, M. Colilla and I. Izquierdo-Barba, *J. Biomed. Nanotechnol.*, 2008, **4**, 1–15.
- F. Balas, M. Manzano, M. Colilla and M. Vallet-Regí, *Acta Biomater.*, 2008, **4**, 514–522.
- I. Izquierdo-Barba, D. Arcos, Y. Sakamoto, O. Terasaki, A. López-Noriega and M. Vallet-Regí, *Chem. Mater.*, 2008, **20**, 3191–3198.
- M. Colilla, I. Izquierdo-Barba and M. Vallet-Regí, *Expert Opin. Ther. Pat.*, 2008, **18**, 639–656.
- M. V. Landau, S. P. Varkey, M. Herskowitz, O. Regev, S. Pevzner, T. Sen and Z. Luz, *Microporous Mesoporous Mater.*, 1999, **33**, 149–163.
- G. Wilkinson and J. G. Birmingham, *J. Am. Chem. Soc.*, 1954, **76**, 4281–4284.
- S. Gómez-Ruiz, G. N. Kaluderović, S. Prashar, D. Polo-Cerón, M. Fajardo, Ž. Žižak, T. J. Sabo and Z. D. Juranić, *J. Inorg. Biochem.*, 2008, **102**, 1558–1570.
- T. Mosmann, *J. Immunol. Methods*, 1983, **65**, 55–63.
- M. Ohno and T. Abe, *J. Immunol. Methods*, 1991, **145**, 199–203.
- J. Marmur, *J. Mol. Biol.*, 1961, **3**, 208–218.
- M. E. Reichmann, S. A. Rice, C. A. Thomas and P. Doty, *J. Am. Chem. Soc.*, 1954, **76**, 3047–3053.
- M. J. Frisch, G. W. Trucks, H. B. Schlegel, G. E. Scuseria, M. A. Robb, J. R. Cheeseman, J. A. Montgomery, Jr., T. Vreven, K. N. Kudin, J. C. Burant, J. M. Millam, S. S. Iyengar, J. Tomasi, V. Barone, B. Mennucci, M. Cossi, G. Scalmani, N. Rega, G. A. Petersson, H. Nakatsuji, M. Hada, M. Ehara, K. Toyota, R. Fukuda, J. Hasegawa, M. Ishida, T. Nakajima, Y. Honda, O. Kitao, H. Nakai, M. Klene, X. Li, J. E. Knox, H. P. Hratchian, J. B. Cross, V. Bakken, C. Adamo, J. Jaramillo, R. Gomperts, R. E. Stratmann, O. Yazyev, A. J. Austin, R. Cammi, C. Pomelli, J. Ochterski, P. Y. Ayala, K. Morokuma, G. A. Voth, P. Salvador, J. J. Dannenberg, V. G. Zakrzewski, S. Dapprich, A. D. Daniels, M. C. Strain, O. Farkas, D. K. Malick, A. D. Rabuck, K. Raghavachari, J. B. Foresman, J. V. Ortiz, Q. Cui, A. G. Baboul, S. Clifford, J. Cioslowski, B. B. Stefanov, G. Liu, A. Liashenko, P. Piskorz, I. Komaromi, R. L. Martin, D. J. Fox, T. Keith, M. A. Al-Laham, C. Y. Peng, A. Nanayakkara, M. Challacombe, P. M. W. Gill, B. G. Johnson, W. Chen, M. W. Wong, C. Gonzalez and J. A. Pople, *GAUSSIAN 03 (Revision C.02)*, Gaussian, Inc., Wallingford, CT, 2004.
- A. D. Becke, *J. Chem. Phys.*, 1993, **98**, 5648–5652.
- C. Lee, W. Yang and R. G. Parr, *Phys. Rev. B: Condens. Matter*, 1988, **37**, 785–789.
- S. H. Vosko, L. Wilk and M. Nusair, *Can. J. Phys.*, 1980, **58**, 1200–1211.
- P. J. Stephens, F. J. Devlin, C. F. Chabalowski and M. J. Frisch, *J. Phys. Chem.*, 1994, **98**, 11623–11627.
- W. J. Hehre, R. Ditchfield and J. A. Pople, *J. Chem. Phys.*, 1972, **56**, 2257–2261.
- J. D. Dill and J. A. Pople, *J. Chem. Phys.*, 1975, **62**, 2921–2923.
- M. M. Francl, W. J. Pietro, W. J. Hehre, J. S. Binkley, M. S. Gordon, D. J. DeFrees and J. A. Pople, *J. Chem. Phys.*, 1982, **77**, 3654–3665.
- V. Rassolov, J. A. Pople, M. A. Ratner and T. L. Windus, *J. Chem. Phys.*, 1998, **109**, 1223–1229.
- C. Pampillón, J. Claffey, M. Hogan and M. Tacke, *BioMetals*, 2008, **21**, 197–204.
- L. J. Bellamy, in *The Infra-red Spectra of Complex Molecules*, 3rd ed., Wiley, New York, 1975.
- C. Alonso, A. Antiñolo, F. Carrillo-Hermosilla, P. Carrión, A. Otero, J. Sancho and E. Villasenor, *J. Mol. Catal. A: Chem.*, 2004, **220**, 286–295.
- C. Alonso-Moreno, A. Antiñolo, F. Carrillo-Hermosilla, P. Carrión, I. López-Solera, A. Otero, S. Prashar and J. Sancho, *Eur. J. Inorg. Chem.*, 2005, 2924–2934.
- C. Alonso-Moreno, D. Pérez-Quintanilla, D. Polo-Cerón, S. Prashar, I. Sierra, I. del Hierro and M. Fajardo, *J. Mol. Catal. A: Chem.*, 2009, **304**, 107–116.
- D. Pérez-Quintanilla, I. del Hierro, M. Fajardo and I. Sierra, *Microporous Mesoporous Mater.*, 2006, **89**, 58–68.
- D. Pérez-Quintanilla, I. del Hierro, M. Fajardo and I. Sierra, *J. Environ. Monit.*, 2006, **8**, 214–222.
- D. Pérez-Quintanilla, I. del Hierro, M. Fajardo and I. Sierra, *J. Hazard. Mater.*, 2006, **134**, 245–256.
- D. Pérez-Quintanilla, I. del Hierro, M. Fajardo and I. Sierra, *J. Mater. Chem.*, 2006, **16**, 1757–1764.
- D. Pérez-Quintanilla, A. Sánchez, I. del Hierro, M. Fajardo and I. Sierra, *J. Sep. Sci.*, 2007, **30**, 1556–1567.
- D. Pérez-Quintanilla, A. Sánchez, I. del Hierro, M. Fajardo and I. Sierra, *J. Colloid Interface Sci.*, 2007, **313**, 551–562.
- L. Reven, *J. Mol. Catal.*, 1994, **86**, 447–477.
- G. Engelhardt, D. Michel, *High-resolution Solid-State NMR of Silicates and Zeolites*, Wiley, Chichester, 1987.
- D. Pavia, G. Lampman and G. Kriz, *Introduction to spectroscopy*, Harcourt College Publishers, USA, 2001.
- D. Zhao, Q. Huo, J. Feng, B. F. Chmelka and G. D. Stucky, *J. Am. Chem. Soc.*, 1998, **120**, 6024–6036.

Appendix 14

Reproduced from Ref. G.N. Kaluđerović, D. Pérez-Quintanilla, Ž. Žižak, Z.D. Juranić, S. Gómez-Ruiz, *Dalton Trans.* 2010, 39, 2597 with permission from The Royal Society of Chemistry.

- 66 K. S. W. Sing, D. H. Everett, R. A. W. Haul, L. Moscou, R. A. Pierotti, J. Rouquérol and T. Siemienińska, *Pure Appl. Chem.*, 1985, **57**, 603–620.
- 67 P. Köpf-Maier and D. Krahl, *Chem.-Biol. Interact.*, 1983, **44**, 317–328.
- 68 P. Köpf-Maier and D. Krahl, *Naturwissenschaften*, 1981, **68**, 273–274.
- 69 P. Köpf-Maier, *J. Struct. Biol.*, 1990, **105**, 35–45.
- 70 H. Sun, H. Li, R. A. Weir and P. J. Sadler, *Angew. Chem., Int. Ed.*, 1998, **37**, 1577–1579.
- 71 M. Guo and P. J. Sadler, *J. Chem. Soc., Dalton Trans.*, 2000, 7–10.
- 72 M. Guo, H. Sun, S. Bihari, J. A. Parkinson, R. O. Gould, S. Parsons and P. J. Sadler, *Inorg. Chem.*, 2000, **39**, 206–215.
- 73 M. Guo, H. Sun, H. J. McArdle, L. Gambling and P. J. Sadler, *Biochemistry*, 2000, **39**, 10023–10033.
- 74 P. M. Abeysinghe and M. M. Harding, *Dalton Trans.*, 2007, 3474–3482.
- 75 A. Kathiravan and R. Renganathan, *Polyhedron*, 2009, **28**, 1374–1378.

ACKNOWLEDGMENTS

The results presented in this habilitation thesis could not have been conquered without support from people from different research areas and the open exchange of ideas with them.

First of all, I would like to thank my mentor Prof. Dr. Dirk Steinborn for his confidence and a lasting impact on me and my career. I am very grateful to him for the opportunity to try my hand at teaching as well as for giving me the possibility to develop special topic “Metals in Medicine” within Bioinorganic Chemistry course, and for his constant support.

Interdisciplinary work in the area of Bioinorganic Chemistry is impossible to conduct alone. By this time, many people have helped and supported me throughout my academic career that it would be impossible to acknowledge them all here. Out of all my collaborators, I want to highlight and send an especially big thank you to Harry, Santi, Danijela and Sanja. Harry never hesitated to share not only his great professional expertise in many fields, but also much essentially his life experience. Santi created a healthy long-lasting friendship and fruitful scientific cooperation. Beside numerous *in vitro* and *in vivo* experiments, the best result of research with Danijela and Sanja is the friendship we made.

My special thanks are dedicated to all my students Bojana, Christian, Jelena, Till, Denise and Thomas who helped to finish this thesis, and also to former and current members of the AG Steinborn for hospitality and friendship.

My thanks also go to Reinhard and Valentina for wonderful cooperation. Working in BioSolutions GmbH gave me opportunity to gain knowledge in cell biology and to learn different techniques for *in vitro* tests.

For English corrections, I would like to thank Mrs. H. Felgner for her valuable help.

Finally, a warm and heartfelt thank you to my wife Milena and for her support, understanding and patience with me and her never-ending love. She gave me the energy and everything I needed to complete my habilitation process.

CURRICULUM VITAE

Personal details:

Name: Goran Kaluđerović
Address: Moscheles Str. 8, 04109 Leipzig, Germany
Date of birth: 8. November 1975
Place of birth: Cetinje (Montenegro)
Marital status: Married (Milena Kaluđerović)

Education:

1982–1990 Primary school „Orjenski bataljon“ Bijela, Yugoslavia
1990–1994 Gymnasium „Ivan Goran Kovačić“ Herceg–Novi, Yugoslavia
1994–1999 Study of chemistry, Faculty of Chemistry, Belgrade University, Belgrade, Yugoslavia
07/1999 Diploma, Faculty of Chemistry, Belgrade University, Yugoslavia
05/2002 Magister, Faculty of Chemistry, Belgrade University, Serbia and Montenegro
„Synthesis und Characterization of mixed cobalt(III) and platinum(IV) complexes with ethylenediamine-*N,N'*-di-3-propionato derived ligands“
03/2005 Dissertation, Faculty of Chemistry, Belgrade University, Serbia and Montenegro
„Synthesis, Structure und *in vitro* antitumor activity of platinum(II) and platinum(IV) complexes with ethylenediamine-*N,N'*-di-3-propionato ligands and its esters “

Employment:

1999–2003 Assistant, Faculty of Chemistry, Belgrade University, Belgrade, Yugoslavia
2003–2005 Scientific Assistant, Hemofarm Concern, Pharmaceutical company, Vršac, Serbia and Montenegro
2005–2011 Research Assistant, Institute of Chemistry, Technology and Metallurgy, Belgrade University, Belgrade, Serbia
2006–2008 Alexander von Humboldt–Fellow, Institute of Chemistry, Martin Luther University Halle–Wittenberg, Germany
2008–2012 Research Assistant, BioSolutions Halle GmbH, An–Institute of Martin Luther University Halle–Wittenberg, Germany
2009–2012 Leader of Cell culture lab, BioSolutions Halle GmbH, An–Institute of Martin Luther University Halle–Wittenberg, Germany
2012–2013 Research Assistant, Institute of Inorganic Chemistry, Faculty of Chemistry and Mineralogy, Leipzig University, Germany

CURRICULUM VITAE

- since 2012 Research Assistant, Leibniz Institute for Plant Biochemistry, Halle, Germany
- since 2012 Associate Professor, Faculty of Pharmacy, European University, Novi Sad, Serbia

Awards:

- 2006–2008 Alexander von Humboldt–Fellow
- 2007 Scientific prize Martin–Luckner–Stiftung for the work on the development of platinum-based antitumour drugs
- 2008 Medal for the scientific zeal and success of the Serbian Chemical Society



Goran Kaluđerović

Halle (Saale), 23.09.2013.

TEACHINGS

- 1999–2003 Seminars and practical courses (Inorganic Chemistry I, II, Qualitative Chemical Analysis), Faculty of Chemistry, Belgrade University, Serbia and Montenegro
- 2010 Practical course ACII, Institute of Chemistry, Martin Luther University Halle–Wittenberg, Germany
- 2011 Practical course ACIII, Institute of Chemistry, Martin Luther University Halle–Wittenberg, Germany
- from 2009 Lectures Bioinorganic Chemistry (part: „Metals in Medicine“), Institute of Chemistry, Martin Luther University Halle–Wittenberg, Germany
- 05/2010 Ring–lecture „Smart molecules – Biomolecules“ (part: „Medicinal inorganic chemistry“), Institute of Inorganic Chemistry, Faculty of Chemistry and Mineralogy, Leipzig University, Germany

Until 2012 supervised 3 Bachelor, 2 Master and 2 Doctoral students.

STATEMENT OF ORIGINALITY

I hereby declare in lieu of an oath that presented thesis I wrote independently, without the help of another person and that I have not used any other media or materials than the ones referred to in this thesis.

The work was presented only in the Faculty of Natural Sciences II of the Martin-Luther University of Halle-Wittenberg.

This work has not been previously submitted for a degree at any University.



Goran Kaluđerović

Halle (Saale), 23.09.2013.